Construction Materials

Their nature and behaviour

Third edition

Edited by

J.M. Illston and
P.L.J. Domone

London and New York

Also available as a printed book
see title verso for ISBN details

Construction Materials

Third edition

Construction Materials

Their nature and behaviour

Third edition

Edited by

J.M. Illston and
P.L.J. Domone

SPON PRESS
Taylor & Francis Group
London and New York

First published 2001 by Spon Press
11 New Fetter Lane, London EC4P 4EE

Simultaneously published in the USA and Canada
by Spon Press
29 West 35th Street, New York, NY 10001

This edition published in the Taylor & Francis e-Library, 2002.

Spon Press is an imprint of the Taylor & Francis Group

© 2001 Spon Press

All rights reserved. No part of this book may be reprinted or reproduced or utilised in any form or by any electronic, mechanical, or other means, now known or hereafter invented, including photocopying and recording, or in any information storage or retrieval system, without permission in writing from the publishers.

The publisher makes no representation, express or implied, with regard to the accuracy of the information contained in this book and cannot accept any legal responsibility or liability for any errors or omissions that may be made.

British Library Cataloguing in Publication Data
A catalogue record for this book is available from the British Library

Library of Congress Cataloging in Publication Data
Construction materials : their nature and behaviour/edited by J.M. Illston and P.L.J.
Domone, – 3rd ed.
p. cm.
Includes bibliographical references and index.
1. Building materials. I. Illston, J.M. II. Domone, P.L.J.
TA403 .C636 2001
624.1'8–dc21
2001020094

ISBN 0-419-25860-4 (pbk)
ISBN 0-419-25850-7 (hb)
ISBN 0-203-47898-3 Master e-book ISBN
ISBN 0-203-78722-6 (Glassbook Format)

The biggest thing university taught me was that with ambition, perseverance and a book you can do anything you want to.

It doesn't matter what the subject is; once you've learnt how to study, you can do anything you want.

George Laurer, inventor of the bar code

Contents

Part One Fundamentals W.D. Biggs, revised and updated by I.R. McColl and J.R. Moon 1

Part Two Metals and alloys W.D. Biggs, revised and updated by I.R. McColl and J.R. Moon 53

Part Three Concrete P.L.J. Domone 89

Contributors

Professor D.G. Bonner
Department of Aerospace, Civil and
Environmental Engineering
University of Hertfordshire
Hatfield Campus
College Lane
Hatfield
Herts AL10 9AB
(Bituminous materials)

Professor J.M. Dinwoodie OBE
16 Stratton Road
Princes Risborough
Nr Aylesbury
Bucks HP17 9BH
(Timber)

Dr P.L.J. Domone
Department of Civil and Environmental
Engineering
University College London
Gower Street, London WC1E 6BT
(Editor and concrete)

Professor D.J. Hannant
Department of Civil Engineering
University of Surrey
Guildford
Surrey GU2 5XH
(Fibre reinforced cements and concrete)

Professor L. Hollaway
Department of Civil Engineering
University of Surrey
Guildford
Surrey GU2 5XH
(Polymers and polymer composites)

Professor J.M. Illston
10 Merrifield Road
Ford
Salisbury
Wiltshire SP4 6DF
(Previous editor)

Dr I.R. McColl
School of Mechanical, Materials, Manufacturing
Engineering and Management
University of Nottingham
University Park
Nottingham NG7 2RD
(Fundamentals and metals)

Dr J.R. Moon
School of Mechanical, Materials, Manufacturing
Engineering and Management
University of Nottingham
University Park
Nottingham NG7 2RD
(Fundamentals and metals)

Dr R.C. de Vekey
Building Research Establishment
Garston
Watford
Herts WD2 7JR
(Brickwork and blockwork)

D.G. Bonner

Professor David Bonner graduated in Civil Engineering from the University of Leeds where he later gained a PhD in Traffic Engineering. Following a period working in the Highways Department of Lincolnshire County Council, he joined the University of Hertfordshire (then Hatfield Polytechnic) where he became Reader in Construction Materials. He subsequently became Head of Civil Engineering and is presently Associate Dean (Academic Quality) for the Faculty of Engineering and Information Sciences.

J.M. Dinwoodie

Professor John Dinwoodie graduated in Forestry from Aberdeen University, and was subsequently awarded his MTech in Non-Metallic Materials from Brunel University, and both his PhD and DSc in Wood Science subjects from Aberdeen University. He carried out research at the UK Building Research Establishment for a period of 35 years on timber and wood-based panels with a special interest in the rheological behaviour of these materials. For this work he was awarded with a special merit promotion to Senior Principal Scientific Officer. Since his retirement from BRE in 1995, he has been employed as a consultant to BRE to represent the UK in the preparation of European standards for wood-based panels. In 1985 he was awarded the Sir Stuart Mallinson Gold Medal for research on creep in particleboard and was for many years a Fellow of the Royal Microscopical Society. In 1994 he was appointed an Honorary Professor in the Department of Forest Sciences, University of Wales, Bangor, and in the same year was awarded an OBE. He is author, or co-author, of over one hundred and thirty technical papers and author of three text books on wood science and technology.

P.L.J. Domone

Dr Peter Domone graduated in civil engineering from University College London, where he subsequently completed a PhD in concrete technology. After a period in industrial research with Taylor Woodrow Construction Ltd, he was appointed to the academic staff at UCL, first as lecturer and then as senior lecturer in concrete technology. He teaches all aspects of civil engineering materials to undergraduate students, and his principle research interests have included non-destructive testing, the rheology of fresh concrete, high-strength concrete and most recently, self-compacting concrete.

D.J. Hannant

Professor David Hannant is a Professor in Construction Materials at the University of Surrey and has been researching and teaching in the field of fibre-reinforced cement and concrete since 1968. He has authored a book, patents and many publications on steel, glass and polypropylene fibres and has been active in commercialising thin sheet products to replace asbestos cement.

L.C. Hollaway

Professor Len Hollaway is Professor of Composite Structures at the University of Surrey and has been engaged in the research and teaching of composites for more than 30 years. He is the author and editor of a number of books and has written many research papers on the structural and material aspects of fibre matrix composites.

J.M. Illston

Professor John Illston spent the early part of his career as a practising civil engineer before entering higher education. He was involved in teaching and researching into concrete technology and structural engineering as Lecturer and Reader at King's College, London and then Head of Department of Civil Engineering at Hatfield Polytechnic. His interest in his discipline took second place when he became Director of the Polytechnic, but, on retirement he undertook preparation of the second edition of this book. He has acted as passive editor of this edition.

I.R. McColl

Dr Ian McColl is a senior lecturer at the University of Nottingham. His first degree is in physics and after receiving his PhD from Nottingham he was involved in industrially sponsored research and development work at the university before taking up a lecturing post in 1988. He teaches mainly in the areas of engineering materials and engineering design. His research interests centre around the fretting and fatigue properties of engineering materials, components and assemblies, and the use of surface engineering to improve these properties.

J.R. Moon

Dr Bob Moon is a metallurgist married to the first woman to study civil engineering at the University of Nottingham. His PhD was awarded by the University of Wales (Cardiff) in 1960. He has worked in the steel industry in South Wales, researched into titanium and other new metals at IMI in Birmingham and into superconductors, magnetic materials and materials for steam turbines at C.A. Parsons on Tyneside. He joined the staff of the University of Nottingham over 30 years ago and has taught materials to civil engineers for the majority of that time. He is now reader in materials science and researches into the triangle connecting processing, microstructure and properties of materials made from powders.

R.C. de Vekey

Dr Bob de Vekey studied chemistry at Hatfield Polytechnic and graduated with the Royal Society of Chemistry. He subsequently gained a DIC in materials science and a PhD from Imperial College, London on the results of his work at the Building Research Establishment (BRE) on materials. At BRE he has worked on many aspects of building materials research and development and between 1978 and 2000 led a section concerned mainly with structural behaviour, testing, durability and safety of brick and block masonry buildings. From September 2000 he has relinquished his previous role and become an associate to the BRE. He has written many papers and advisory publications and has contributed to several books on building materials and masonry and has been involved in the development of UK and international standards and codes for building.

Acknowledgements

I first of all want to express my thanks to John Illston for his tremendous work and vision that resulted in the first two editions of this book, and for his encouragement and helpful advice in the early stages of preparing this edition. My thanks also go to all the contributors who have willingly revised and updated their text despite many other commitments. They have all done an excellent job, and any shortfalls in the book are entirely my responsibility. I greatly appreciate the advice and inspiration provided by my students at UCL and my colleagues at UCL and elsewhere, who have suffered due to my neglect of other duties whilst preparing and editing the manuscript.

Finally, but most importantly, I must acknowledge the support given to me by my wife and children, who I have neglected most of all, but who have borne with good grace the many hours I have spent in my study.

P.L.J. Domone

I wish to express my appreciation to the Building Research Establishment (BRE) and in particular to Dr A.F. Bravery, Director of the Centre for Timber Technology and Construction, not only for permission to use many plates and figures from the BRE collection, but also for providing laboratory support for the production of the figures from both existing negatives and from new material.

Thanks are also due to several publishers for permission to reproduce figures.

To the many colleagues who have so willingly helped me in some form or other in the production of this revised text I would like to record my very grateful thanks. In particular, I would like to record my appreciation to Dr P.W. Bonfield and Dr Hilary Derbyshire, BRE; Dr J.A. Petty, University of Aberdeen; Dr D.G. Hunt, University of the South Bank for all their valuable and helpful advice. I would also like to thank colleagues at BRE for assistance on specific topics: C.A. Benham, J. Boxall, Dr J.K. Carey, Dr V. Enjily, C. Holland, J.S. Mundy, Dr R.J. Orsler, J.F. Russell, E.D. Suttie and P.P. White. Lastly, my deep appreciation to both my daughter, who did much of the word processing, and my wife for her willing assistance in editing my text and in proof reading.

J.M. Dinwoodie

Preface

This book is an updated and extended version of the second edition, which was published in 1994. This has been extremely popular and successful, but the continuing recent advances in many areas of construction materials technology have resulted in the need for this new edition.

The first edition was published under the title *Concrete, Timber and Metals* in 1979. Its scope, content and form were significantly changed for the second edition, with the addition of three further materials – bituminous materials, masonry and fibre composites – with a separate part of the book devoted to each material, following a general introductory part on 'Fundamentals'.

This overall format has been retained. One new small part has been added, on polymers, which was previously subsumed within the section on polymer composites. The other significant changes are, first, in the section on concrete, where Portland cement, admixtures, cement replacement materials and aggregates now have their own chapters, and new chapters on mix design, non-destructive testing and high performance concrete have been added; and, second, in the section on fibre reinforced cement and concrete, which has been rearranged so that each type of composite is considered in full in turn.

All of the contributors to the second edition were able and willing to contribute again, with two exceptions. First, the co-author of the first edition and editor and inspiration for the second edition, John Illston, is enjoying a well-earned retirement from all professional engineering and academic activities, and did not wish to continue as editor for this edition. This role was taken over by Peter Domone, with considerable apprehension about following such an illustrious predecessor and the magnitude of the task. Fortunately, John Illston provided much needed encouragement, advice and comments, particularly in the early stages,

Second, one of the contributors, Bill Biggs, had sadly died in the intervening period, but two new contributors have revised, extended and updated his 'Fundamentals' and 'Metals' sections. The most significant addition is a consideration of equilibrium phase diagrams.

Objectives and scope

As before, the book is addressed primarily to students taking courses in civil or structural engineering, where there is a continuing need for the unified treatment of the kind that we have again attempted. We believe that the book provides most if not all of the information required by students for at least the first two years of three- or four-year degree programmes. More specialist project work in the third or fourth years may require recourse to the more detailed texts that are listed in 'Further reading' at the end of each section. We also believe that our approach will continue to provide a valuable source of interest and stimulation to both undergraduates and graduates in engineering generally, materials science, building, architecture and related disciplines.

The objective of developing an understanding of the behaviour of materials from a knowledge of their structure remains paramount. Only in this way can information from mechanical testing, experience in processing, handling and placing, and materials science, i.e. empiricism, craft and science, be brought together to give the sound foundation for materials technology required by the practitioner.

The 'Fundamentals' section provides the necessary basis for this. Within each of the subsequent sections on individual materials, their structure and composition from the molecular level upwards is discussed, and then the topics of deformation, strength and failure, durability, and manufacture and processing are considered. A completely unified treatment for each material is not possible due to their different nature and the different requirements for manufacture, processing and handling, but a look at the contents list will show how each topic has been covered and how the materials can be compared and contrasted. Cross-references are given throughout the text to aid this, from which it will also be apparent that there are several cases of overlap between materials, for example concrete and bituminous composites use similar aggregates, and Portland cement is a component of masonry, some fibre composites and concrete.

It is impossible in a single book to cover the field of construction materials in a fully comprehensive manner. Not all such materials of construction are included, nor has the attempt been made to introduce design criteria or to provide a compendium of materials data. Neither is this book a manual of good practice. Nevertheless we hope that we have provided a firm foundation for the application and practice of materials technology.

Levels of information

The structure of materials can be described on dimensional scales varying from the smallest, atomic or molecular, through materials structural to the largest, engineering.

The molecular level

This considers the material at the smallest scale, in terms of atoms or molecules or aggregations of molecules. It is very much the realm of materials science and a general introduction for all materials is given in Part One of the book. The sizes of the particles are in the range of 10^{-7} to 10^{-3} mm. Examples occurring in this book include the crystal structure of metals, cellulose molecules in timber, calcium silicate hydrates in hardened cement paste and the variety of polymers, such as polyvinyl chloride, included in fibre composites.

As shown in Part One consideration of established atomic models leads to useful descriptions of the forms of physical structure, both regular and disordered, and of the ways in which materials are held together. Chemical composition is of fundamental importance in determining this structure. This may develop with time as chemical reactions continue; for example, the hydration of cement is a very slow process and the structure and properties show correspondingly significant changes with time. Chemical composition is of especial significance for durability which is often determined, as in the cases of timber and metals, by the rate at which external substances such as oxygen or acids react with the chemicals of which the material is made.

Chemical and physical factors also come together in determining whether or not the material is porous, and what degree of porosity is present. In materials such as bricks, timber and concrete, important properties such as strength and rigidity are inversely related to their porosities. Similarly, there is often a direct connection between permeability and porosity.

Some structural phenomena such as dislocations in metals are directly observable by microscopic and diffractometer techniques, but more often mathematical and geometrical models are employed to deduce both the structure of the material and the way in which it is likely to behave. Some engineering analyses, like fracture mechanics, come straight from molecular scale considerations, but they are the exception. Much more often the information from the molecular level serves to provide mental pictures which aid the engineers' understanding so that they can deduce likely behaviour under anticipated conditions. In the hands of specialists, knowledge of the chemical and physical structure may well offer a route to the development of better materials.

Materials structural level

This level is a step up in size from the molecular level, and the material is considered as a composite of different phases, which interact to realise the behaviour of the total material. This may be a matter of separately identifiable entities within the material structure as in cells in timber or grains in metals; alternatively, it may result from the deliberate mixing of disparate parts, in a random manner in concrete or asphalt or some fibre composites, or in a regular way in masonry. Often the material consists of particles such as aggregates distributed in a matrix like hydrated cement or bitumen. The dimensions of the particles differ enormously from the wall thickness of a wood cell at 5×10^{-3} mm to the length of a brick at 225 mm. Size itself is not an issue; what matters is that the individual phases can be recognised independently.

The significance of the materials structural level lies in the possibility of developing a more general treatment of the materials than is provided from knowledge derived from examination of the total material. The behaviours of the individual phases can be combined in the form of multiphase models which allow the prediction of behaviour outside the range of normal experimental observation. In formulating the models consideration must be given to three aspects:

1. Geometry: the shape, size and concentration of the particles and their distribution in the matrix or continuous phase.
2. State and properties: the chemical and physical states and properties of the individual phases influence the structure and behaviour of the total material.
3. Interfacial effects. The information under (1) and (2) may not be sufficient because the interfaces between the phases may introduce additional modes of behaviour that cannot be related to the individual properties of the phases. This is especially true of strength, the breakdown of the material often being controlled by the bond strength at an interface.

To operate at the materials structural level requires a considerable knowledge of the three aspects described above. This must he derived from testing the phases themselves, and additionally from interface tests. While the use of the multiphase models is often confined to research in the interest of improving understanding, it is sometimes taken through into practice, albeit mostly in simplified form. Examples include the estimation of the elastic modulus of concrete, and the strength of fibre composites.

The engineering level

At the engineering level the total material is considered; it is normally taken as continuous and homogeneous and average properties are assumed throughout the whole volume of the material body. The materials at this level are those traditionally recognised by construction practitioners, and it is the behaviour of these materials that is the endpoint of this book.

The minimum scale that must be considered is governed by the size of the representative cell, which is the minimum volume of the material that represents the entire material system, including its regions of disorder. The linear dimensions of this cell varies considerably from, say, 10^{-3} mm for metals to 100 mm for concrete and 1000 mm for masonry. Properties measured over volumes greater than the unit cell can be taken to apply to the material at large. If the properties are the same in all directions then the material is isotropic and the representative cell is a cube, while if the properties can only be described with reference to orientation, the material is anisotropic, and the representative cell may be regarded as a parallelepiped.

Most of the technical information on materials used in practice comes from tests on specimens of the total material, which are prepared to represent the condition of the material in the engineering structure. The range of tests, which can be identified under the headings used throughout this book, includes strength and failure, deformation, and durability. The test data is often presented either in graphical or mathematical form, but the graphs and equations may neither express the physical and chemical processes within the materials, nor provide a high order of accuracy of prediction. However, the graphs or equations usually give an indication of how the property values are affected by significant variables; such as the carbon content of steel, the moisture content of timber, the fibre content and orientation in composites or the temperature of asphalt. It is extremely important to recognise that the quality of information is satisfactory only within the ranges of the variables used in the tests. Extrapolation beyond those ranges is very risky; this is a common mistake made not only by students, but also often by more experienced engineers and technologists who should know better.

Comparability and variability

Throughout this book we have tried to excite comparison of one material with another. Attention has been given to the structure of each material, and although a similar scientific foundation applies to all, the variety of physical and chemical compositions gives rise to great differences in behaviour. The differences are carried through to the engineering level of information and have to be considered by practitioners engaged in the design of structures who first have to select which material(s) to use, and then ensure that they are used efficiently, safely and economically.

Selection of materials

The engineer must consider the fitness of the material for the purpose of the structure being designed. This essential fitness-for-purpose is a matter of ensuring that the material will perform adequately both during construction and in subsequent service. Strength, deformation and durability are likely to be the principal criteria that must be satisfied, but other aspects of behaviour will be important for particular applications, for example water-tightness or speed of construction. In addition, aesthetics and environmental impact should not be forgotten.

Table 0.1 gives some properties of a number of individual and groups of materials. These are mainly structural materials, with some others added for comparison. The mechanical properties listed – stiffness, strength (or limiting stress) and work to fracture (or toughness) – are all defined and discussed in this book. It is immediately apparent that there is a wide variety of each property that the engineer can select from (or cope with, if it is not ideal). It is also interesting to note the overall range of each property. Density varies by about two orders of magnitude from the least to the most dense (timber to metals). Stiffness varies by nearly three orders of magnitude (nylon to diamond), strength by about four orders (concrete to diamond) and work to fracture by the greatest of all, five orders (glass to ductile metals). The great range of the last property is perhaps the most significant of all. It is a measure of how easy it is to break a material, particularly under impact loading, and how well it copes with minor flaws, cracks, etc.; it should not be confused with strength. Low values are extremely difficult for engineers to deal with – low strength and stiffness can be accommodated by bigger section sizes and structural arrangements (within limits), but low toughness is much more difficult to handle. It is one reason why fibre composites have become so popular.

Clearly, in many circumstances more than one material satisfies the criterion of fitness-for-purpose; for instance, members carrying tension can be made of steel or timber, facing panels can be fabricated from fibre composite, metal, timber or masonry. The matter may be resolved by the engineer making a choice based on his or her judgement, with often some help from calculations. For example, comparisons of minimum weight or minimum cost options for a simple structure with different materials, obtained with some fairly elementary structural mechanics, with different materials gives some interesting results.

Consider the cantilever shown in Figure 0.1. For linear elastic behaviour, the deflection at the free end is given by:

$$\delta = Fl^3/3EI$$

where E is the elastic modulus of the material and

TABLE 0.1 Selected properties of a range of materials

Material	*Density (tonne/m^3)*	*Stiffness (E) (GPa)*	*Strength or limiting stress (MPa)**	*Work to fracture (toughness) (kJ/m^2)*	*Relative cost (£) per unit:*	
					mass	*volume*
Diamond	3.5	1000	50 000	–	2×10^6	8.9×10^5
Common pure metals	5–19	20–200	20–80	100–1000	–	–
Structural steel	7.85	195–205	235–450	100–130	1.0	1.0
High strength steel	7.85	205	260–1300	15–120	–	–
Cast iron	6.9–7.8	170–190	220–1000	0.2–0.3	–	–
Silica glass	2.6	94	50–200	0.01	3.4	1.1
Titanium and alloys	4.5	80–130	180–1320	25–115	27.5	16
Aluminium and alloys	2.7	69–79	40–630	8–30	5.0	1.7
Timber	0.17–0.98 (dry)	0.6–1.0 perp grain 9–16 par grain	90–200 (tens) 15–90 (comp)**	8–20 Crack perp grain 0.5–2 crack par grain	–	–
Spruce (par. to grain)	0.5	13	40–80	0.5–1	1.0	0.06
Concrete	1.8–2.5	20–45	4–10 (tens) 20–150 (comp)	0.03	0.7	0.12
Epoxy resin	1.1–1.4	2.6–3	30–100	0.1–0.3	3.8	0.53
Glass fibre comp (grp)	1.4–2.2	35–45	100–300	10–100	–	–
Carbon fibre composite		180–200	600–700	5–30	–	–
Nylon	1.1–1.2	2–4	50–90	2–4	7.5	1.1
Rubber	0.95–1.15	2–10	15–30	–	–	–

*in tension unless stated; yield stress for metals, otherwise ultimate stress.

**on clear specimens.

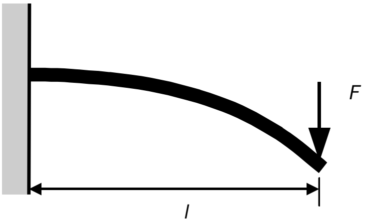

FIGURE 0.1 A simple cantilever.

I is the second moment of area. For a rectangular beam $I = bd^3/12$, where b is the width of the beam and d is its depth. Usually, the width is a design constant, e.g. a bridge for four carriageways, but the depth can be altered to meet the loading and deflection requirements. The depth is:

$$d = (4Fl^3/Eb\delta)^{1/3}$$

The weight is:

$$W = \rho lA = \rho lbd = \rho lb(4Fl^3/Eb\delta)^{1/3}$$

where ρ is the density.

Rearranging, we have:

$$W = l^2 b^{2/3}(4F/\delta)^{1/3}(\rho/E^{1/3}) \qquad (0.1)$$

so that, for a given set of design conditions (F, l, b, δ), W is minimised by maximising $E^{1/3}/\rho$. It turns out that the same condition applies for any type of beam, of any shape or of any loading configuration. The parameter $E^{1/3}/\rho$ is therefore the selection criterion for stiffness at minimum weight.

A similar approach can be taken to derive a selection criterion for the strength of the beam. For the cantilever in Figure 0.1, the maximum tension stress generated is:

$$\sigma_{\max} = 6Fl/bd^2$$

Following the argument through as before gives:

$$W = l^{3/2} b^{1/2}(6F)^{1/2}(\rho/\sigma_{\text{limit}}^{1/2}) \qquad (0.2)$$

So, for strength at minimum weight, we want to maximise $\sigma_{\text{limit}}^{1/2}/\rho$. Note the use of σ_{limit}, the maximum useful stress that the material can tolerate in tension. In defining this, we must take into account the variability of materials, discussed below.

The cost of a beam is simply $W£_M$, where $£_M$ is the cost of the material per unit mass. Working the arguments through again give criteria for stiffness and for strength at minimum cost. These turn out to be similar to those used before, i.e. $E^{1/3}/£_V$ and $\sigma^{1/2}/£_V$, where $£_V$ is the material cost per unit volume = density × cost per unit mass.

Table 0.2 shows how these four factors relative to those for structural steel work out for some of the materials listed in Table 0.1. Where appropriate the mid-range properties have been used, together with the prices given in Table 0.2. Remembering that we are looking for maximum values, the most obvious result is that timber is outstanding in terms of stiffness and strength at both minimum weight and minimum cost – nature clearly got things right without any help from us. Thinking only about weight and neglecting cost points to the efficiency of diamond (not a realistic option!), titanium, aluminium, epoxy resin and nylon. But when it comes to minimising costs, the highest scoring materials other than timber are steel and concrete.

Table 0.2 does not, of course, give a complete picture. Prices will vary from time to time, and other properties, such as ease of construction, durability and toughness have not been taken into account. Also, composite systems, such as reinforced concrete and fibre reinforced systems have not been considered. Nevertheless, it does give food for thought.

The cost of the energy used in manufacturing the material and its transport and fabrication must also not be overlooked, either in simple economic or in environmental terms. High-strength versions of all the materials covered in this book are often sought with the intention of reducing the volume of material for a given structure, normally with a commensurate saving in energy; and, conversely, lower grade materials are sometimes introduced to replace higher grades as, for example, in the partial replacement of cement by the waste material, pulverised fuel ash (fly ash).

Variability and characteristic strength

An important issue facing engineers is the variability of the properties of the material itself, which clearly depends on the uniformity of its structure and composition.

The strength or maximum allowable stress is of particular concern. In tension, for ductile materials this can be taken as the yield strength or the proof stress (see Chapter 9), but for brittle materials it may have to be chosen on the basis of the approach described in Chapter 6. In compression, brittle materials have a well defined maximum stress, but ductile materials may not fail at all, they just continue being squashed.

The variability can be assessed by a series of tests on nominally similar specimens from either the same or successive batches of a material; this usually gives a variation of strength or maximum stress with a normal or Gaussian distribution as shown in Figure 0.2. This can be represented by the bell-shaped mean curve given by the equation

$$y = \frac{1}{s\sqrt{2\pi}} \exp\left[-\frac{(\sigma-\sigma_m)^2}{2s^2}\right] \qquad (0.3)$$

where y is the probability density, and σ is the variate, in this case the strength. The strength results are therefore expressed in terms of two numbers:

1. the mean strength, σ_m, where for n results:

$$\sigma_m = \Sigma\sigma/n \qquad (0.4)$$

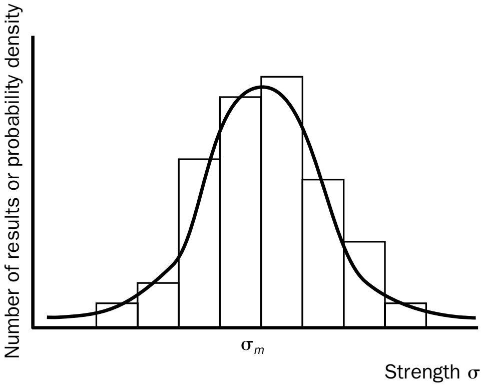

FIGURE 0.2 Histogram and normal distribution of strength.

2. the range or variability, expressed as the standard deviation, s, given by

$$s^2 = \Sigma[(\sigma - \sigma_m)^2/(n-1)] \qquad (0.5)$$

The standard deviation has the same units as the variate.

For comparison of different materials or different kinds of the same material the non-dimensional coefficient of variation c_v is used, given by

$$c_v = s/\sigma_m \qquad (0.6)$$

c_v is often expressed as a percentage.

TABLE 0.2 Weight and cost comparisons for the use of alternative materials for the cantilever of Figure 0.1 (all figures relative to mild steel = 1, material properties as in Table 0.1)

Material	*Cost*	*Minimum weight*		*Minimum cost*	
	(£/tonne)	*Stiffness criterion* $E^{1/3}/\rho$	*Strength criterion* $\sigma_{max}^{1/2}/\rho$	*Stiffness criterion* $E^{1/3}/\rho.\text{£/tonne}$	*Strength criterion* $\sigma_{max}^{1/2}/\rho.\text{£/tonne}$
Diamond	2×10^6	3.8	31.8	1.9×10^{-6}	1.6×10^{-5}
Structural steel	1.0	1.0	1.0	1.0	1.0
Silica glass	3.4	2.4	2.1	0.8	0.7
Titanium and alloys	27.5	1.4	3.0	0.05	0.1
Aluminium and alloys	5.0	2.1	3.4	0.4	0.7
Spruce (par. to grain)	1.0	6.4	7.7	6.4	7.7
Concrete	0.7	1.8	0.6	2.6	0.8
Epoxy resin	3.8	1.5	3.2	0.4	0.8
Nylon	7.5	1.7	3.6	0.2	0.5

TABLE 0.3 Comparison of strengths of construction materials and their coefficients of variation. c = compression, t = tension

Material	*Mean strength MPa*	*Coefficient of variation (%)*	*Comment*
Steel	460 t	2	Structural mild steel
Concrete	40 c	15	Typical concrete cube strength at 28 days
Timber	30 t	35	Ungraded softwood
	120 t	18	Knot free, straight grained softwood
	11 t	10	Structural grade chipboard
Fibre cement composites	18 t	10	Continuous polypropylene fibre with 6% volume fraction in stress direction
Masonry	20 c	10	Small walls, brick on bed

Values of typical mean strengths and their coefficients of variation for materials in this book are given in Table 0.3. Steel and ungraded timber at the two ends of the scale. The manufacture of steel is a well developed and closely controlled process so that a particular steel can be readily reproduced and the variability of properties such as strength is small; conversely, ungraded or unprocessed timber, which in its natural form is full of defects such as knots, and inevitably exhibits a wide variation in property values. The variability can, however, be reduced by processing so that the coefficient of variation for chipboard or fibreboard is appreciably lower than that for ungraded timber.

Engineers need to take both the mean strength and the strength variation into account in determining a 'safe' strength at which the possibility of failure is reduced to acceptable levels. If the mean stress alone is used, then by definition half of the material will fail to meet this criterion, which is clearly unacceptable. The statistical nature of the distribution of results means that a minimum strength below which no specimen will ever fail cannot be defined, and therefore a value known as the *characteristic strength* (σ_{char}) is used, which is set at a distance below the mean, called the

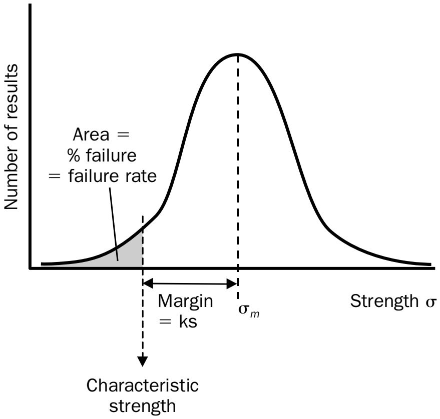

FIGURE 0.3 Failure rate, margin and characteristic strength.

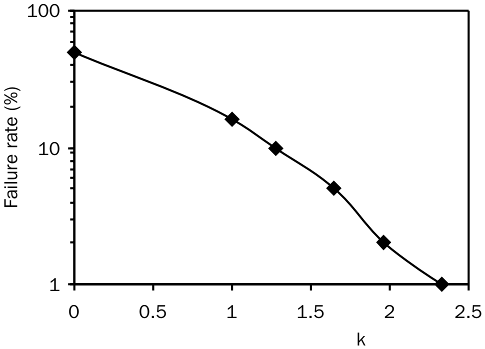

FIGURE 0.4 Relationship between k and failure rate for normally distributed results

margin, below which an acceptably small number of results will fall.

The total area under the normal distribution curve of Figure 0.2 represents 100 per cent of the results, and the area below any particular strength is the number of results that will occur below that strength, or in other words the *failure rate* (Figure 0.3). The greater the margin, the lower the failure rate. Clearly, if the margin is zero, then the failure rate is 50 per cent. It is a property of the normal distribution curve that if the value of the margin is expressed as ks where k is a constant, then k is related to the failure rate as in Figure 0.4. Hence

$$\sigma_{char} = \sigma_m - ks \qquad (0.7)$$

Engineering judgement and consensus is used to choose an acceptable failure rate. In practice, this is not always the same in all circumstances; for example, 5 per cent is typical for concrete (i.e. $k = 1.64$), and 2 per cent for timber (i.e. $k = 1.96$).

As we have said, this analysis uses values of s obtained from testing prepared specimens of the material concerned. In practice it is also necessary to consider likely differences between these and the bulk properties of material, which may vary due to size effects, manufacturing inconsistencies, etc., and therefore further materials safety factors will need to be applied to the characteristic strength. It is beyond the scope of this book to consider these in any detail – guidance can be obtained from relevant design codes and design text books.

Concluding remarks

We hope that this preface has encouraged you to read on. It has described the general content, nature and approach of the book, and sets the scene for the level and type of information on the various materials that is provided. It has also given an introduction to some ways of comparing materials, and discussed how the unavoidable variability of properties can be taken into account by engineers. You will probably find it useful to refer back to these latter two sections from time to time.

Enjoy the book.

A note on units

In common with all international publications, and with national practice in many countries, the SI system of units has been used throughout this text. Practice does however vary between different parts of the engineering profession and between individuals over whether to express quantities which have the dimensions of [force]/[length]^2 in the units of its constituent parts, e.g. N/m^2, or with the internationally recognised combined unit of the Pascal (Pa). In this book, the latter is used in Parts 1 to 7, and the former in Part 8, which reflects the general practice in other publications on the materials concerned.

The following relationships may be useful whilst reading:

$$1 \text{ Pa} = 1 \text{ N/m}^2$$
$$1\text{kPa} = 10^3 \text{ Pa} = 10^3 \text{ N/m}^2 = 1 \text{ kN/m}^2$$
$$1\text{MPa} = 10^6 \text{ Pa} = 10^6 \text{ N/m}^2 = 1 \text{ N/mm}^2$$
$$1\text{GPa} = 10^9 \text{ Pa} = 10^9 \text{ N/m}^2 = 1 \text{ kN/mm}^2$$

The magnitude of the unit for a particular property is normally chosen such that convenient numbers are obtained e.g. MPa (or N/mm^2) for strength and GPa (or kN/mm^2) for modulus of elasticity of structural materials.

Part One

Fundamentals

W.D. Biggs

Revised and updated
by I.R. McColl and
J.R. Moon

Introduction

As engineers our job is to design, but any design remains just that and no more until we start to use materials to convert it into a working artefact. There are, basically, three things we need to know about materials:

1. How do they behave in service?
2. Why do they behave in the way that they do?
3. Is there anything we can do to alter their behaviour?

This first section of the book is primarily concerned with (2). We include consideration of the fundamental elements of which all matter is composed and the forces which hold it together. The concept of 'atomistics' is not new. The ancient Greeks – and especially Democritus (*c*.460 BC) – had the idea of a single elementary particle but their science did not extend to observation and experiment. For that we had to wait nearly 22 centuries until Dalton, Avogadro and Cannizzaro formulated atomic theory as we know it today. Even so, very many mysteries remain unresolved, a fact which is as pleasing as it is provoking. So in treating the subject in this way we are reaching a long way back into the development of thought about the universe and the way in which it is put together.

One other important concept is more recent. Engineering is much concerned with change – the change from the unloaded to the loaded state, the consequences of changing temperature, environment, etc. The first scientific studies of change can be attributed to Sadi Carnot (1824), later extended by such giants as Clausius, Joule and others to produce such ideas as the conservation of energy, momentum, etc. Since the early studies were carried out on heat engines it became known as the science of thermodynamics, but if we take a broader view it is really the art and science of managing, controlling and using the transfer of energy – whether the energy of the atom, the energy of the tides or the energy of, say, a lifting rig.

In many engineering courses thermodynamics is treated as a separate topic, or, in many civil engineering courses, not considered at all. But, because its applications set rules which no engineer can ignore, a brief discussion is included. What are these rules? In summary (and rather jocularly) they are:

1. You cannot win, i.e. you cannot get more out of a system than you put in.
2. You cannot break even – in any change something will be lost or, to be more precise, it will be useless for the purpose you have in mind.

All this may be unfamiliar ground so you may skip past the sections relating to this on first reading. But come back to it because it is important.

We shall not, in the present part, deal specifically with item (3) above; later parts will deal with this in more specific terms. But what every engineer should remember is that engineering is all about compromise and trade-off. Some properties can be varied – strength is one such – but some, such as density, cannot be varied. If we were designing aircraft we could, in principle, choose between maximum strength and minimum weight, and minimum weight would win because it would ensure a higher payload (we must not forget that engineering is also about money*).

---

*An engineer has been defined as a person who can do for £100 what any fool could do for £1000.

But, of course, compromise must be sought and engineering is about finding optimal solutions, not necessarily a ‘best’ solution.

So good luck with your reading. If you really understand the principles much of what follows will be clearer to you. But, in a few short chapters we can do little more than describe the highlights of materials science, and a list of suggestions for further reading is given at the end of this part.

We should add a simple philosophy – engineering is much too important to be left to engineers.

Chapter one

States of matter

We conventionally think of matter (material) as being in one of two states, fluid or solid. We recognise these 'states of matter' based on the response of the matter to an applied force. Fluids, i.e. gases and liquids, flow easily when a force is applied, whereas solids resist an applied force.

1.1 Fluids

Consider first the observable characteristics of a gas.

1. Gases are of low mass density, expand to fill a container, are easily compressed and have low viscosity.
2. Gases exert a uniform pressure on the walls of their container.
3. Gases diffuse readily into each other.

The first set of observations suggests that the gas particles are not in direct contact with each other, the second and third that they are in constant motion in random directions and at high speeds.

Liquids exhibit most of the above properties; most diffuse into each other readily and their viscosities, although some orders of magnitude higher than those of gases, are still low, so that they flow irreversibly under small forces. However, there are two significant differences. The first is that liquids are a condensed state and have much higher mass densities, which are not very different from solids. The second is that they are almost incompressible (hydraulic braking systems depend on this).

All this suggests that the particles of fluids are in contact but are free to move relative to each other. We shall consider the nature of the interaction between the particles in Chapter 3. Meanwhile, we can think of a liquid as being similar to people at a well-run party in which the guests keep circulating from one group to another.

Since the particles are free to move, the application of even a small force causes irreversible flow. Strictly, this is a shear deformation in which parts of the material slide past other parts (see Figure 1.3(c)). In an ideal (Newtonian) liquid the rate of shear flow, $d\gamma/dt$, is proportional to the applied shear stress:

$$d\gamma/dt = \beta\tau \qquad (1.1)$$

where β = fluidity.

This is generally written in the inverse form:

$$\tau = \eta d\gamma/dt \qquad (1.2)$$

where η is the coefficient of dynamic viscosity. As might be expected, the viscosities of gases and liquids differ markedly. For air at 20°C, $\eta \approx 18 \times 10^{-5}$ Pa.s, for water at 20°C, $\eta \approx 1.5 \times 10^{-3}$ Pa.s. At higher temperatures the particles possess more energy of their own and the stress required to move them is reduced, i.e. viscosity reduces rapidly as temperature is increased (e.g. lubricating oil, treacle, asphalt).

1.1.1 Diffusion

We noted above that both gases and liquids diffuse into each other. Here, for simplicity, we consider the diffusion of one gas into another, but the same arguments apply broadly to liquids and even to solids under the appropriate conditions.

Diffusion is caused by countless haphazard wanderings of individual atoms or molecules which continually bump into each other. The atoms or molecules can rebound in any direction and the path of any individual atom or molecule is unpredictable but, if enough make such movements, the result is a steady and systematic flow.

Imagine a box containing a partition (plane), on one side there are C_1 particles of gas/unit volume and on the other C_2, where $C_1 > C_2$. The particles are moving randomly and exerting pressures of P_1 and P_2, respectively, on the partition, with $P_1 > P_2$. Now remove the partition. Both sets of particles will move across the plane into the space formerly occupied solely by the other. However, because of the higher concentration more will move in the direction $C_1 \rightarrow C_2$ and, eventually, a totally random mixture is formed and pressure is equalised.

Provided certain simplifying assumptions are made it is easy to show that the total flux J of particles (i.e. the number of particles flowing in the x-direction per unit time per unit cross-sectional area) through the plane is:

$$J = -D\mathrm{d}C/\mathrm{d}x \tag{1.3}$$

which is Fick's first law of diffusion. The constant D is known as the diffusion coefficient and is proportional to the average distance travelled by a particle before colliding with another and the frequency at which the collisions occur. Thus, the rate of diffusion is proportional to the concentration gradient $\mathrm{d}C/\mathrm{d}x$, and is directed down the gradient, hence the minus sign above. Both of these follow directly from the statistical nature of the process.

It does not take much imagination to see that temperature will play an important role. At higher temperatures the particles are more active and jump more frequently so that the rate of diffusion increases exponentially as the temperature rises and vice versa. This has many important technological consequences, e.g. in modifying the properties of metals and alloys by heat treatment.

1.1.2 Vapour–liquid transition

Understanding of the vapour–liquid transition derives from the work of Van der Waals. He pointed out that the perfect gas law $PV = RT$ which relates pressure P, volume V and temperature T, via a constant R, neglected two important factors:

1. the volume of the particles themselves;
2. the forces of attraction between the particles.

The first is fairly obvious and can be corrected by deducting from the volume a term representing the volume of the particles. Thus:

$$P(V - b) = RT \tag{1.4}$$

The second is less obvious, the forces of attraction between the particles will have the effect of drawing them closer together, just as if additional pressure were applied. So a correction must be added to P. Consider a single particle about to strike the wall of the chamber containing the gas. It will be subjected to an attractive force due to the adjacent particles, proportional to the number of particles n per unit volume. Furthermore, the number of particles striking the wall is also proportional to n. So that the total attractive force experienced by the particles about to strike the wall is proportional to n^2. Now, for a chamber containing a fixed number of particles n is inversely proportional to the volume of the chamber V, so that the attractive force is proportional to $1/V^2$. Thus, the Van der Waals equation is:

$$(P + a/V^2)(V - b) = RT \tag{1.5}$$

where a is a constant. The consequences of this are noteworthy. If P is plotted against V for different values of T we obtain a set of isotherms as shown in Figure 1.1. Note that at low temperatures each curve has a maximum and minimum, at higher temperatures they become smooth.

The minimum and maximum on each curve are connected by the dotted line. The point C where the minimum and maximum coincide at a point of inflection is the *critical point* and denotes the conditions where liquid and vapour can coexist in equilibrium.

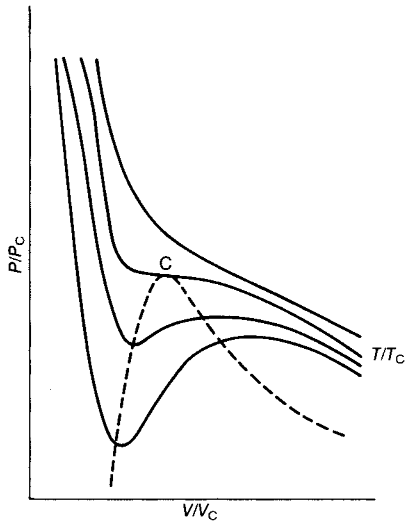

FIGURE 1.1 Isotherms from Van der Waals equation. The values for P, V and T are expressed in terms of their values at the critical point C. In this form they are dimensionless and independent of their actual values.

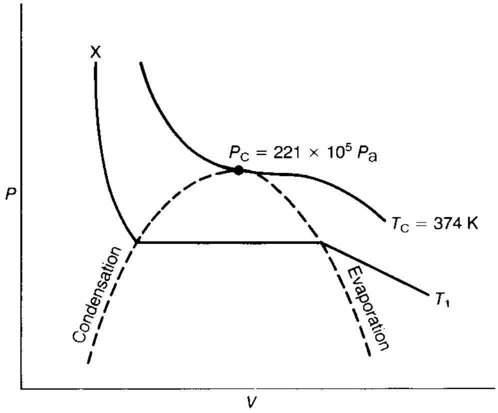

FIGURE 1.2 P–V–T curves for water vapour.

Real materials, however, behave as shown in Figure 1.2 where we note that starting with a liquid at X at some constant temperature T_1 the volume increases as the pressure is reduced. Eventually the liquid becomes saturated with vapour and the volume increases with no change of pressure, as a saturated vapour, i.e. a vapour saturated with liquid, forms. With further decreases in pressure a true vapour is formed and the liquid is said to have evaporated. The reverse happens if we start with a gas and increase the pressure while keeping temperature constant.

The particles within a liquid (at constant temperature and pressure) may or may not have sufficient thermal energy to escape. Those which escape constitute the vapour and the pressure they exert is the *vapour pressure*. In a closed container equilibrium is set up between those particles escaping from the liquid and those returning, this is the saturation vapour pressure. When the *saturation vapour pressure* is equal to or greater than the external pressure the liquid boils. Thus the boiling point is conventionally defined as the temperature to which the liquid must be raised in order for this to occur at atmospheric pressure. As the atmospheric pressure decreases so does the boiling point.

1.2 Solids

Intuitively the first thing that we notice about a solid is that it resists the application of a force. A liquid will also resist a force provided that it is applied equally in all directions. The essential difference is that, unlike gases and liquids, a solid does not appear to change shape except by a tiny amount when a modest load is applied in just one direction. We shall see later that this is not strictly true; under appropriate conditions all materials will flow, but the definition is good enough for our purpose and accords with normal experience.

The reason for no apparent shape change is simple, the mechanism quite complex. First, we must note what mechanics tells us. Any combination of forces can be thought of as a combination of a hydrostatic pressure (Figure 1.3 (d)) and a shear (Figure 1.3 (c)). Flow in any circumstances

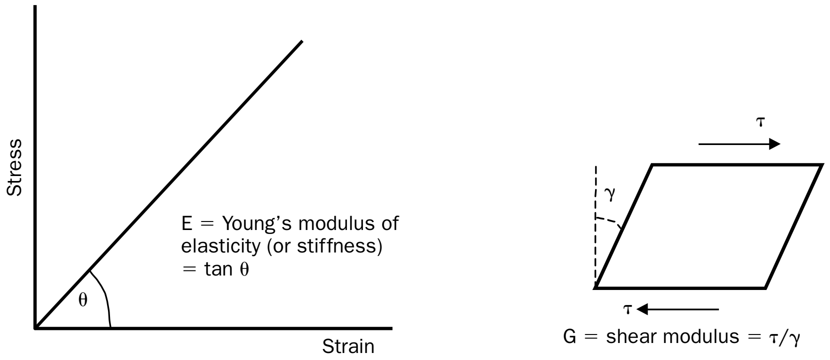

(a) Linear behaviour under direct stress

(c) Behaviour under shear stress

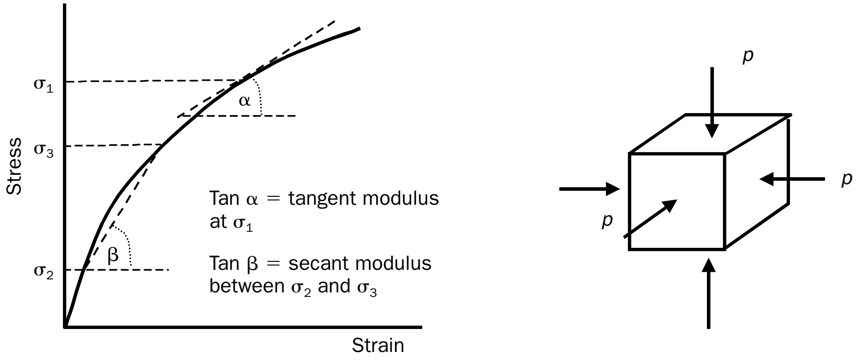

(b) Non-linear behaviour under direct stress

(d) Hydrostatic loading

FIGURE 1.3 Elastic stress–strain behaviour.

other than under pure hydrostatic pressure is really a response to the shear component. The atoms of which the solid is composed are physically bonded together into patterns that must be maintained. When we first apply a force we displace all the atoms of which the solid is composed in a way that nearest neighbour atoms in the pattern remain nearest neighbours (provided, of course, that the force is not sufficient to break any bonds). This is quite unlike a liquid in which the individual particles move past each other.

1.2.1 The elastic constants

Before discussing the mechanics and consequences of bonding we should digress a little to define some of the properties that are used to characterise solids.

When a solid is extended or compressed by a modest external force the dimensions change a little. Conventionally we express the force F in terms of the area A over which it acts, this is known as stress σ:

$$\sigma = F/A \tag{1.6}$$

Under simple uniaxial tension or compression the material either extends or shortens. Conventionally we express this as an increment of strain $\Delta\epsilon = \Delta l/l$, i.e. change in length per unit length. Strain is therefore a ratio and has no dimensions. Integrating the expression for strain between the original length, l_0 and the final length, l_1, gives $\epsilon = \ln(l_1/l_0) = \ln(1 + \Delta l/l_0)$, where $\Delta l = l_1 - l_0$. This rather cumbersome expression for strain is used for analytical purposes when thinking about large strains, but for most engineering purposes where $\Delta l/l_0 \ll 1$, it reduces to the much more convenient and familiar definition:

$$\epsilon = \Delta l/l_0 \tag{1.7}$$

When solids are not strained very much, say up to about $\epsilon \approx 0.001$, or 0.1 per cent, the material reverts to its original dimensions when the load is released, i.e. the strain is reversible. The relationship between stress and strain is often linear or, at least, linear to a first approximation (Figure 1.3a). This is known as Hooke's law, i.e.:

$$\sigma = E\epsilon \tag{1.8}$$

where E is a material constant known as *Young's modulus of elasticity*, or simply the *elastic modulus*, and has units of stress, e.g. N/m^2 (or Pa) or, more commonly, GPa. Table 1.1 includes some typical values.

In many materials the stress–strain relationship is not sufficiently linear for this definition. For such materials, a modulus value can be defined as either the slope of the tangent to the stress–strain curve at a particular value of stress – giving the *tangent modulus* – or as the slope of the line joining two points on the curve at two values of stress – giving the *secant modulus* (Figure 1.3b). When quoting either value, clearly the corresponding level of stress must also be quoted, e.g. the tangent modulus at the origin. Values of secant modulus are often given for a zero lower value of stress, i.e. it is the slope of the line from the origin to a point on the curve.

Modulus values arising from similar relationships apply for other forms of stress. Thus, in shear (Figure 1.3c) the shear stress τ produces a

TABLE 1.1 Typical mass densities, elastic constants and Poisson's ratios for a range of materials

Material	*Mass density* *Mgm*$^{-3}$	*E* *GPa*	*G* *GPa*	*K* *GPa*	ν
Diamond	3.5	1000	417	556	0.20
Alumina	4.0	530	217	315	0.22
Tungsten carbide	15.8	720	300	400	0.20
Iron	7.9	210	79	206	0.33
Silica glass	2.5	70	30	35	0.17
Titanium	4.5	120	46	105	0.31
Spruce (parallel to grain)	0.5	13	500	–	0.38
Aluminium	2.7	69	26	68	0.33
Concrete (lightweight)	1.4	15	6	8	0.20
Concrete (normal weight)	2.4	25	10	14	0.20
Epoxy resin	1.1	4.5	–	–	–
Nylon	1.14	3	1.1	4.5	0.39

shear strain γ which, when small, is conveniently measured as an angle (in radians). For linear behaviour

$$\tau = G\gamma \tag{1.9}$$

where G is known as the *shear modulus*.

Under hydrostatic pressure (Figure 1.3d) the volume changes. As before this is expressed non-dimensionally as $\Delta V/V$ and

$$p = -K(\Delta V/V) \tag{1.10}$$

where p is the hydrostatic pressure and K is the *bulk modulus*. The minus sign arises as a consequence of the fact that as pressure increases, volume decreases.

Young's modulus is a measure of the stress required to produce a given deformation, and engineers often refer to it as the stiffness of the material, for that is what it is. It will be apparent that whereas a liquid can display a bulk modulus it does not possess a shear modulus since it cannot resist shear. Solids, on the other hand, display a bulk modulus and a shear modulus. It is the resistance to shear that is the fundamental difference between solids and liquids.

1.2.2 Elastic resilience – stored energy

We noted that a linearly elastic (Hookean) material deforms reversibly, i.e. it returns to its original length when the load is removed. When a bar of material experiences an extension of δl under an applied force F, mechanical work $F\delta l$ is done. This work is stored in the material as a slight stretching of the atomic bonds. The total energy stored is obtained by integrating this equation. The energy per unit volume of material U, which is called the *strain energy density*, is then obtained by dividing by the volume of material Al_0:

$$U = \int \frac{F\delta l}{Al_0} \tag{1.11}$$

Now, as previously defined, $\sigma = F/A$ and $\epsilon = \int \frac{\delta l}{l_0} = \frac{\Delta l}{l_0}$, and therefore, for elastic deformation:

$$U = \sigma\epsilon/2 = \sigma^2/2E = \epsilon^2 E/2 \tag{1.12}$$

We can use this to estimate, in a few simple cases, the stresses generated by impact. Figure 1.4 shows a simple wire suspended from a support

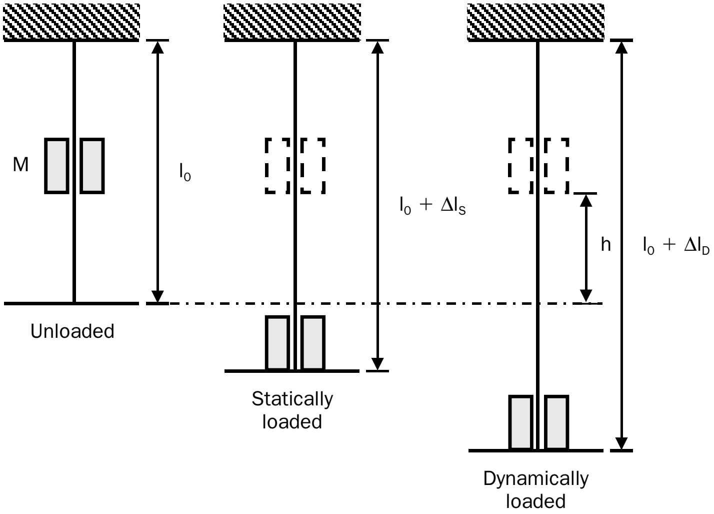

FIGURE 1.4 Simple arrangement for comparing static and dynamic loads.

and carrying a small tray at its lower end. If a weight of mass M were to be gently lowered onto the tray, the wire would experience a static force Mg, where g is the acceleration due to gravity, and a stress of $\sigma_s = Mg/A$, and would strain by $\sigma_s/E = Mg/AE$. If now, the weight were lifted and allowed to fall onto the tray from a height h, the impact would cause the wire to stretch by more than the static strain, after which it would oscillate until it settled at the static strain. Taking the maximum dynamic stretch to be Δl_D, the weight would lose potential energy $Mg(h + \Delta l_D)$, all of which would be converted into strain energy of the wire. Now the wire has a volume of Al_0 and so the strain energy at maximum dynamic strain is $(\sigma_D \epsilon_D/2)(Al_0)$. Equating the two energies and remembering that $\epsilon_D = \Delta l_D/l_0$, gives after some manipulation:

$$\sigma_D = \sigma_s + \sqrt{\sigma_s^2 + \sigma_s \frac{2hE}{l_0}} \tag{1.13}$$

Typically, $E/\sigma_s \sim 10^3$ and if $h = l_0/2$, we have $\sigma_D/\sigma_s \approx 34$. No wonder things can snap when hit with a hammer!

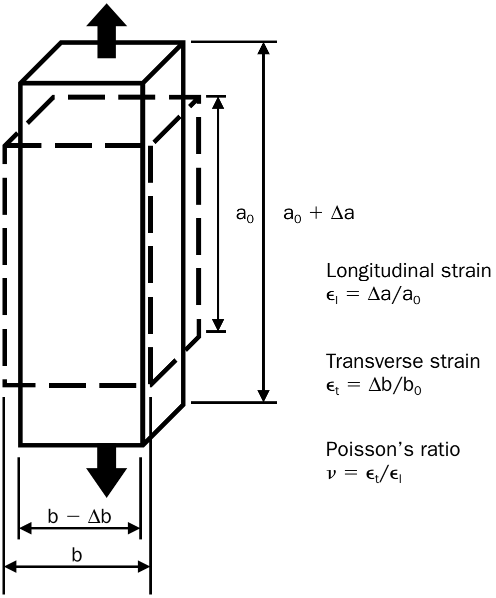

FIGURE 1.5 Poisson effect under a uniaxial tensile load.

1.2.3 Poisson's ratio

Clearly the application of a force displaces the atoms from their normal positions. Thus, in an elastic solid, the application of a longitudinal tension force causes a transverse contraction, as in Figure 1.5.

Poisson's ratio ν relates the longitudinal and transverse strains:

$$\nu = -\text{transverse strain/longitudinal strain}$$

1.2.4 Relation between elastic constants

We now have all four elastic constants, and typical values for these are given in Table 1.1. It is not too difficult using linear elastic analysis to show that they are not independent, and that they are related to one another as follows:

$$K = \frac{E}{3(1 - 2\nu)} \tag{1.14}$$

$$G = \frac{E}{2(1 + \nu)} \tag{1.15}$$

Thus if any two are known, or measured, the other two can be calculated, which makes the engineer's life easier.

It is interesting and instructive to calculate the change of volume that is brought about by a uniaxial stress. If a cube of side a is stressed in the z direction, it will extend by:

$$\delta_z = a\epsilon_z$$

and in accordance with Poisson's ratio:

$$\delta_x = \delta_y = -a\nu\epsilon_z$$

The final volume is:

$$V = (a + \delta_x)(a + \delta_y)(a + \delta_z)$$

Expanding and neglecting second and higher order terms in δ which are vanishingly small:

$$V = a^3 + a^2(\delta_x + \delta_y + \delta_z) = a^3 + a^3(\delta_x + \delta_y + \delta_z)$$

the change of volume is:

$$\Delta V = a^3(\epsilon_x + \epsilon_y + \epsilon_z) = a^3\epsilon_z(1 - 2\nu)$$

and:

$$\Delta V/V = \epsilon_z(1 - 2\nu) \qquad (1.16)$$

For a liquid, the volume remains constant during deformation, i.e. the material is incompressible, and $\Delta V = 0$. K is therefore infinite, and, from equation 1.14, $\nu = 0.5$. In most other materials there is a small volume increase when stretched elastically and a volume decrease when compressed. This means that K is finite and positive – if it were negative the volume would increase when the material is compressed, which does not bear thinking about. Since E is also a positive number, then equation 1.14 tells us that $1 - 2\upsilon$ must be positive, and hence $\nu < 0.5$. Combining the two conditions gives

$$\nu \leq 0.5 \qquad (1.17)$$

Table 1.1 shows that for many common materials ν lies between 0.2 and 0.35. Soft rubber is unusual in having a Poisson's ratio close to 0.5, which means that it behaves very like a stiffish fluid.

1.3 Intermediate behaviour

We have already emphasised the lack of any dividing line between solids and liquids, the reason being that the response of materials to shear can vary over a wide range. Solids may be either crystalline or amorphous (Figure 1.6). In a crystalline solid (and metals are an important group) the atoms are arranged in a regular, three-dimensional array or lattice. Amorphous solids do not possess this regularity of structure and we can further subdivide them into glassy and molecular solids.

True glasses are obtained by cooling liquids which, because of their elaborate molecular configuration, lack the necessary activation energy (see Chapter 2) at the melting temperature to rearrange themselves in an ordered crystalline array.

The material then retains, even when rigid, a typically glassy structure involving short range order only and resembling, except for its immobility, the structure of the liquid form. Silica gives rise to the commonest form of glass. If cooled sufficiently slowly from the melt it can be obtained in the crystalline form which is more stable thermodynamically than the vitreous state. In nature, cooling over long time spans gives rise to beautiful crystals of quartz and other crystalline forms.

At ordinary cooling rates crystallisation does not take place, and the amorphous nature of the solid gives rise to its most important physical property, its transparency. Most non-metallic single crystals are transparent, but in the polycrystalline state light is scattered from internal reflections at flaws and internal boundaries, the material then becomes translucent in thin sections and completely opaque in the mass, as with naturally occurring rocks. If it is amorphous, there are no internal boundaries. Polymers may be totally amorphous and transparent, but most contain small crystalline regions (spherulites) within their structure that act as light scatterers, giving the rather milky appearance that we are familiar with, that is if they do not contain deliberately added colouring matter.

Molecular solids are of two types. So-called *thermoplastic polymers* are best exemplified by soft polymers such as polyethylene, which consist of long, highly convoluted molecules. The bulk strength depends upon the entanglement of the molecular chains rather than upon three-dimensional bonding. *Thermosets*, such as Bakelite, have genuine extended three-dimensional molecules. Mostly, these are harder and stronger than thermoplastics but tend to be rather brittle.

There are, however, more complex structures involving both solid and liquid phases. One of the most familiar of these is the gel, known to most of us from childhood in the form of jellies and lozenges.

Gels are formed when a liquid contains a fairly concentrated suspension of very fine particles, usually of colloidal dimensions (<1 μm). The particles bond into a loose structure, trapping liquid

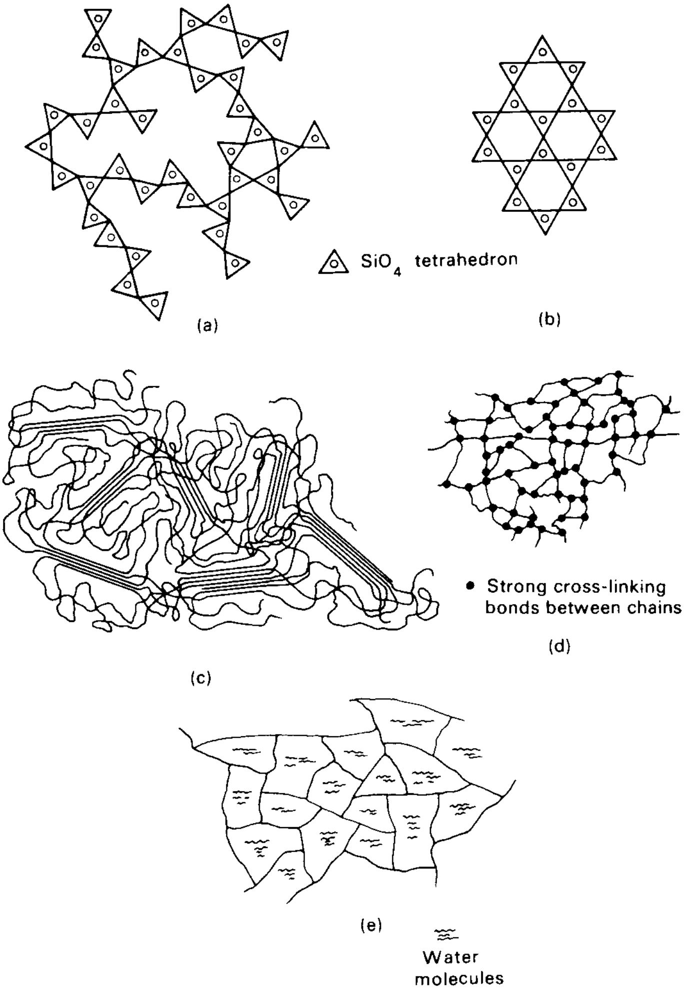

FIGURE 1.6 Schematic structures of some covalent materials: (a) vitreous silica (glass); (b) crystalline silica; (c) thermoplastic polymer showing crystalline regions (spherulites); (d) thermosetting polymer; (e) gel – by comparison with (d), the links between the chains are weak and easily broken.

in its interstices. Depending on the number of links formed, gels can vary from very nearly fluid structures to almost rigid solids. If the links are few or weak, the individual particles have considerable freedom of movement around their points of contact, and the gel deforms easily. A high degree of linkage gives a structure that is hard and rigid in spite of all its internal pores. The most important engineering gel is undoubtedly cement, which develops a highly rigid structure (which we will discuss in some detail in Chapter 13). When water is added to the cement powder, the individual particles take up water of hydration, swell and link up with each other to give rise to a high-strength but permeable gel of complex calcium silicates. A feature of many gels is their very high specific surface area; if the gel is permeable as well as porous, the surface is available for adsorbing large amounts of water vapour, and such a gel is an effective drying agent. Adsorption is a reversible process (see pages 42–3); when the gel is saturated it may be heated to drive off the water and its drying powers regained. Silica gel is an example of this.

If a gel sets by the formation of rather weak links, the linkages may be broken by vigorous stirring so that the gel liquefies again. When the stirring ceases, the bonds will gradually link up and the gel will thicken and return to its original set. Behaviour of this sort, in which an increase in the applied shear rate causes the material to act in a more fluid manner, is known as *thixotropy*. Not all gels behave in this manner or, if they do, it is only at a certain stage of their setting procedure. Hardened concrete, alas, will not heal itself spontaneously after it has cracked, although it exhibits a marked degree of thixotropy at an early state of setting.

The most familiar application of thixotropy is in non-drip paints, which liquefy when stirred and spread easily when being brushed on, but which set as a gel as soon as brushing is completed so that dripping or streaks on vertical surfaces are avoided. Clays can also exhibit thixotropy. This is turned to advantage on a potter's wheel and in the mixing of drilling muds for oil exploration. The thixotropic mud serves to line the shaft with an impermeable layer, whilst in the centre it is kept fluid by the movement of the drill and acts as a medium for removing the rock drillings. On the other hand, a thixotropic clay underlying major civil engineering works could be highly hazardous.

The reverse effect to thixotropy occurs when an increase in the applied shear rate causes a viscous material to behave more in the manner of a solid, and is known as *dilatancy*. It is a less familiar but rather more spectacular phenomenon. Cornflour–water mixtures demonstrate the effect over a rather narrow range of composition, when the viscous liquid will fracture if stirred vigorously. It is of short duration, however, since fracture relieves the stress, and the fractured surfaces immediately liquefy and run together again.

Silicone putty is also a dilatant; it flows very slowly if left to itself, but fractures if pulled suddenly, and will bounce like a rubber ball if thrown against a hard surface. So far, no engineering applications of dilatancy have been developed.

Chapter two

Energy and equilibrium

Although the engineer conventionally expresses his findings in terms of force, deflection, stress, strain and so on, these are simply the convention. Fundamentally, what he is really dealing with is energy. Any change, no matter how simple, involves an exchange of energy. The mere act of lifting a beam involves a change in the potential energy of the beam, a change in the strain energy held in the lifting cables, an input of mechanical energy from the lifting device which is itself transforming electrical or other energy into kinetic energy. The harnessing and control of energy is at the heart of all engineering.

Thermodynamics teaches us about energy, and draws attention to the fact that every material possesses an *internal* energy associated with its structure. In this section we examine some of the thermodynamic principles which are of importance to understanding the behaviour patterns.

We begin by recognising that all systems are always seeking to minimise their energy, i.e. to become more stable. We also note that although thermodynamically correct, some changes towards a more stable condition proceed so slowly that the system appears to be stable even though it is not. For example, a small ball sitting in a hollow at the top of a hill will remain there until it is lifted out and rolled down the hill. The ball is in a *metastable* state and requires a small input of energy to start it on its way down the main slope.

Figure 2.1 shows a ball sitting in a depression, its potential energy is P_1. It will roll to a lower energy state P_2, but only if it is first lifted to the top of the hump between the two hollows. Some energy has to be lent to the ball to do this. Of course, the ball returns the energy when it rolls down the hump to its new position. This borrowed energy is known as the *activation energy* for the process. Thereafter it possesses free energy as it rolls down to P_2. However, it is losing potential energy all the time and eventually (say, at sea level) it will achieve a stable equilibrium. However, note two things. At P_1, P_2, etc. it is 'stable', actually metastable because there are other more stable states available to it, given the necessary activation energy. Where does the activation energy come from? In materials science it is extracted mostly (but not exclusively) from

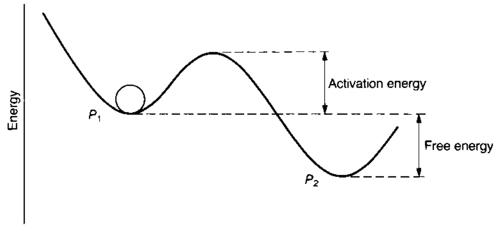

FIGURE 2.1 Schematic illustration of activation energy and free energy.

heat. As things are heated to higher temperatures the atomic particles react more rapidly and can break out of their metastable state into one where they can now lose energy.

2.1 Mixing

If whisky and water are placed in the same container, they mix spontaneously. The internal energy of the solution so formed is less than the sum of the two internal energies before they were mixed. There is no way that we can separate them except by distillation, i.e. by heating them up and collecting the vapours and separating these into alcohol and water. We must, in fact, put in energy to separate them. But, since energy can neither be created nor destroyed, the fact that we must use energy, and quite a lot of it, to restore the status quo must surely pose the question, 'Where does the energy come from initially?' The answer is by no means simple but, as we shall see, every particle, whether water or whisky, possesses kinetic energies of motion and of interaction.

When a system such as a liquid is left to itself, its internal energy remains constant, but when it interacts with another system it will either lose or gain energy. The transfer may involve work or heat or both and the first law of thermodynamics, 'the conservation of energy and heat', requires that:

$$dE = dQ - dW \qquad (2.1)$$

where E = internal energy, Q = heat and W = work done by the system on the surroundings.

What this tells us is that if we raise a cupful of water from 20°C to 30°C it does not matter how we do it. We can heat it, stir it with paddles or even put in a whole army of gnomes each equipped with a hot water bottle, but the internal energy at 30°C will always be above that at 20°C by exactly the same amount. The first law says nothing about the sequences of changes that are necessary to bring about a change in internal energy.

2.2 Entropy

Classical thermodynamics, as normally taught to engineers, regards entropy S as a capacity property of a system which increases in proportion to the heat absorbed (dQ) at a given temperature (T). Hence the well-known relationship:

$$dS \geq dQ/T$$

which is a perfectly good definition but does not give any sort of picture of the meaning of entropy and how it is defined. To a materials scientist entropy has a real physical meaning, it is a measure of the state of disorder in the system. Whisky and water combine; this simply says that, statistically, there are many ways that the atoms can get mixed up and only one possible way in which the whisky can stay on top of, or, depending on how you pour it, at the bottom of, the water. Boltzmann showed that the entropy of a system could be represented by:

$$S = k \ln N \qquad (2.2)$$

where N is the number of ways in which the particles could be distributed and k is a constant (Boltzmann's constant $k = 1.38 \times 10^{-23} J/K$). The logarithmic relationship is important; if the molecules of water can adopt N_1 configurations and those of whisky N_2 the number of possible configurations open to the mixture is not $N_1 + N_2$ but $N_1 \times N_2$. It follows from this that the entropy of any closed system will tend to a maximum since this represents the most probable array of configurations. You should be grateful for this. As you read these words, you are keeping alive by breathing a randomly distributed mixture of oxygen and nitrogen. Now it is statistically possible that at some instant all the oxygen atoms will collect in one corner of the room while you try to exist on pure nitrogen, but only statistically possible. There are so many other possible distributions involving a random arrangement of the two gases that it is most likely that you will continue to breathe the normal random mixture.

2.3 Free energy

It must be clear that the fundamental tendency for entropy to increase, that is, for systems to become more randomised, must be stopped somewhere and somehow. For, if not, the entire universe would break down into chaos. As we shall see, the reason for the existence of liquids and solids is that atoms and molecules are not totally indifferent to each other and, under certain conditions and with certain limitations, will associate with each other in a non-random way.

As we stated above, from the first law of thermodynamics the change in internal energy is given by:

$$dE = dQ - dW$$

From the second law of thermodynamics the entropy change in a reversible process is:

$$TdS = dQ$$

Hence:

$$dE = TdS - dW \qquad (2.3)$$

In discussing a system subject to change, it is convenient to use the concept of free energy. For irreversible changes, the change in free energy is always negative and is a measure of the driving force leading to equilibrium. Since a spontaneous change must lead to a more probable state (or else it would not happen) it follows that, at equilibrium, energy is minimised while entropy is maximised.

The Helmholtz free energy is defined as:

$$H = E - TS \qquad (2.4)$$

and the Gibbs free energy as:

$$G = pV + E - TS \qquad (2.5)$$

and, at equilibrium, both must be a minimum. We shall later in Chapter 4 apply these ideas to the elastic deformation of materials.

2.4 Equilibrium and equilibrium diagrams

So far, we have seen that materials can exist as gases, liquids and crystalline or amorphous solids. We need a scheme that allows us to summarise the influences of temperature and pressure on the relative stability of each state and on the transitions that can occur between these. Thermodynamics tells us that we must seek the internal condition of a material that minimises its internal energy.

The time-honoured approach is through the medium of the *equilibrium diagram*. Note the word ‘equilibrium’. As we have seen at the start of this chapter, it takes a finite time for a transition to occur from one state to another or for a chemical reaction to take place. Sometimes, this time is vanishingly small, as when dynamite explodes. At other times, it can be a few seconds, days or even centuries. Glass made in the Middle Ages is still glass and shows no sign of crystallising. Not every substance or mixture has reached a state of thermodynamic equilibrium, i.e. where its internal energy is lowest. Nevertheless, we have to begin from a knowledge of what the equilibrium condition would be.

Although there is a great wealth of fundamental theory underlying the forms of equilibrium diagrams, we shall only dip our toes into it. We will think of them as useful maps. Until recently, these maps were established by experiment, but the theory and the computational power to do the calculations have now reached the stage where the diagrams can be predicted if the necessary basic data is in place.

2.4.1 Single component diagrams

There are two commonly used types of diagram. We have met one already, the P–V–T diagram for water shown in Figure 1.2. An alternative and more helpful way of looking at the same data is shown in Figure 2.2. We need to look at this in some detail in order to establish some ground rules and language for use later.

The diagram is in ‘temperature–pressure space’, i.e. the axes are of temperature and pressure. A number of lines are marked which represent boundary conditions between differing ‘phases’, i.e. states of H_2O. The line *AD* represents combinations of temperature and pressure at which

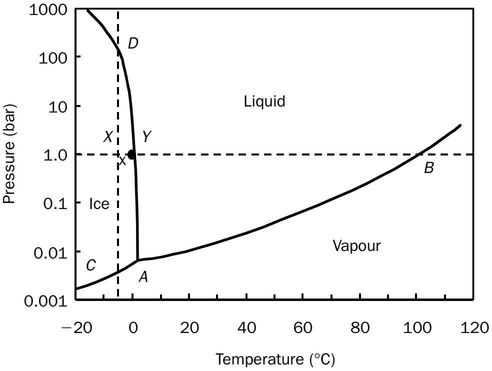

FIGURE 2.2 Pressure–temperature diagram for water (from W.D. Kingery (1976) Introduction to ceramics, Wiley, New York).

liquid water and solid ice are in equilibrium, i.e. can coexist. A small heat input will alter the proportions of ice and water by melting some of the ice. However, it is absorbed as a change in internal energy of the mixture, the latent heat of melting. The temperature is not altered.

What happens if we put in large amounts of heat, so that all the ice is melted and we have some heat left over? Of course, the temperature rises and now we have just slightly warmed water.

By the same token, line *AB* represents the equilibrium between liquid water and gaseous steam, and line *AC* the equilibrium between solid ice and rather cold water vapour.

It is helpful to go on one or two journeys within the diagram. To begin with, let us start at point *X*, representing −5°C at atmospheric pressure. We know we should have ice and, indeed, the point *X* lies within the phase field labelled ice. Adding heat at constant pressure takes the temperature along the broken line. This crosses the phase boundary, *AD*, at 0°C and the ice begins to melt as further heat is added. Not until all the ice has melted does the temperature continue to rise. We now have liquid water until we reach 100°C. Now, again, heat has to be added to boil the water but there is no temperature increase until all the liquid water has gone. We now have steam and its temperature can be increased by further heat input.

Now think of keeping temperature constant and increasing pressure, again starting at point *X*. If the pressure is raised enough, to about 100 atmospheres (≈10 MPa) we reach the ice water equilibrium and the ice can begin to melt. It is thought in some quarters that this accounts for the low friction between, for example, an ice skate and the ice itself: local pressures cause local melting. It is a factor which no doubt enters the minds of engineers when contemplating the use of locally refrigerated and frozen ground as coffer dams or as foundations for oil rigs in Alaska.

Now consider starting with steam at say 200°C and 1 atmosphere. Increasing pressure to the liquid–vapour equilibrium will cause it to condense to water. Wet steam at high pressures is a familiar bugbear of mechanical engines which use steam as their working fluid. It should be noted though that when the temperature is taken above a critical temperature, 374.14°C, no amount of pressure will cause the steam to condense. The pressure at the critical point is ≈221 atmospheres (22.1 MPa) and the mass density of the steam is $\approx 0.32\,\mathrm{Mg\,m^{-3}}$, about 1/3 of that of liquid water at 0°C!

There is a formal way of summarising the relationship between the number of phases (*P*) that can coexist at any given point in the diagram and the changes brought about by small changes in temperature or pressure. It is the famous phase rule, first enunciated by J.W. Gibbs:

$$P + F = C + 2 \qquad (2.6)$$

Here, C is the number of *components* in the system; in this case we have only H_2O so $C = 1$. F is the number of degrees of freedom allowed to change. To illustrate, at point X (Figure 2.2) there is just one phase, ice, so $P = 1$ and $F = 2$. This means that both temperature and pressure can be changed independently without bringing about a significant change to the material. At Y, both ice and liquid can coexist, $P = 2$ and $F = 1$. To maintain the equilibrium, temperature and pressure must be changed in a co-ordinated way so that the point Y moves along the boundary AD. At A, all three phases can coexist and $F = 0$, i.e. any change at all will disturb the equilibrium.

One further point needs to be made before moving on. The slope of each phase boundary curve is given by the Clausius–Clapeyron equation:

$$dp/dT = \Delta H/T\Delta V \qquad (2.7)$$

where ΔH is the heat of transformation (fusion, boiling) per mole of the substance, T is the absolute temperature and ΔV is the volume change accompanying the transformation (per mole). ΔH and ΔV refer to changes from the low temperature condition to the higher temperature one. Now, ΔH is always positive and ΔV on boiling is large and positive. Thus, AB has a low slope. Usually, ΔV on melting is also positive, but we know that water is unusual in that it contracts when it melts. In this case, ΔV is small and negative, giving AD a steep and negative slope.

Transformations can also occur between solid phases. For example, silica can exist in four crystalline forms, each stable over a different temperature range. ΔV on going from one form to another is very small and so dp/dT is steep. The equilibrium diagram is shown in Figure 2.3. In silica the transformation rates are extremely slow and so high temperature phases can be retained at low temperatures even though they are not thermodynamically stable. Extensions of each curve in the manner shown in Figure 2.4 can be useful in thinking about such circumstances. The phase with the lowest vapour pressure is the most stable. Figure 2.4 shows clearly that (amorphous) silica glass is unstable with respect to cristobalite, tridymite and quartz at low temperatures. Silica glass remains technologically useful only because the transformation rates are extremely slow.

2.4.2 Two component diagrams

We now go on to look at two component diagrams, such as we get when carbon is alloyed into iron to make steels and cast irons. We now have an extra variable, composition, and, strictly, we should consider the joint influences of this variable in addition to temperature and pressure. We need three-dimensional diagrams. To simplify things we usually take pressure to be constant. After all, most engineering materials are prepared and used at atmospheric pressure, unless you work for NASA! This leaves us with a composition–temperature diagram, the lifeblood of materials scientists.

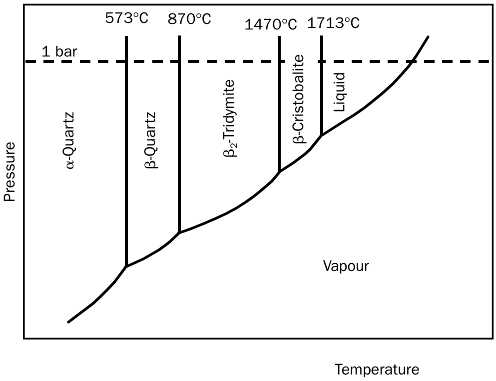

FIGURE 2.3 Equilibrium phase diagram for silica (SiO_2) (from W.D. Kingery (1976) Introduction to ceramics, Wiley, New York).

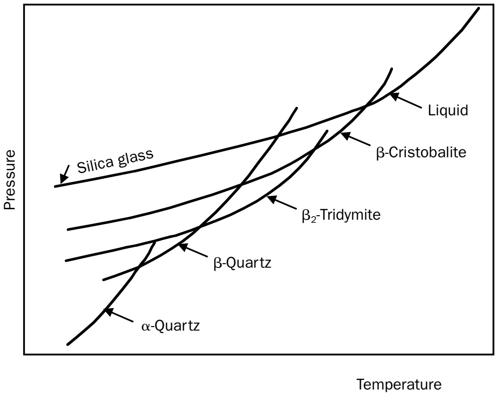

FIGURE 2.4 Equilibrium phase diagram from Figure 2.3 extended to include the metastable (amorphous) silica glass phase of SiO_2 (from W.D. Kingery (1976) Introduction to ceramics, Wiley, New York).

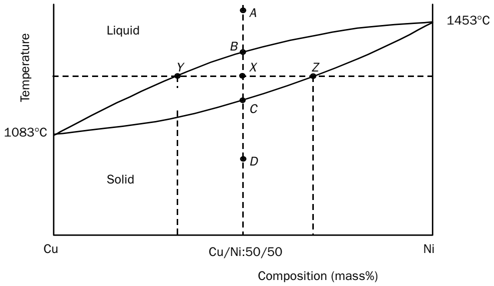

FIGURE 2.5 Equilibrium phase diagram for Cu–Ni.

We begin with the simplest example, Figure 2.5. This is for alloys formed between copper (Cu) and nickel (Ni). The diagram is drawn with composition as the horizontal axis, one end representing pure Cu, the other pure Ni. The vertical axis is temperature.

Let us think about an alloy which is 50%Cu:50%Ni by mass. At high temperatures, e.g. at *A*, the alloy is totally molten. On cooling, we move down the composition line until we arrive at *B*. At this temperature, a tiny number of small crystals begin to form. Further reduction in temperature brings about an increase in the amount of solid in equilibrium with a diminishing amount of liquid. On arriving at *C*, all the liquid has gone and the material is totally solid. Further cooling brings no further changes. Before moving on, note the important difference between this alloy and the pure metals of which it is composed. Both Cu and Ni have well-defined unique melting (or freezing) temperatures. The alloy solidifies over the temperature range *BC*; metallurgists often speak of the 'pasty range'.

We now need to examine several matters in more detail. First, the solid crystals that form are what is known as a 'solid solution'. Cu and Ni are chemically similar elements and both, when pure, form face-centred cubic crystals (see Chapter 8). In this case, a 50:50 alloy is also composed of face-centred cubic crystals but each lattice site has a 50:50 chance of being occupied by a Cu atom or an Ni atom.

How does the phase rule work? Consider point *A*. Here we have two components (Cu and Ni) and one phase (liquid). This leaves us with three degrees of freedom. We can independently alter composition, temperature and pressure and the structure remains liquid. But remember, we have taken pressure to be constant and so we are left with two practical degrees of freedom, composition and temperature. The same argument holds at point *D*, but, of course, the structure here is the crystalline solid solution of Cu and Ni.

At a point between *B* and *C* we have liquid and solid phases coexisting, $P = 2$ and $F = 2$. As before we must discount one degree of freedom because pressure is taken as constant. This leaves us with $F = 1$, which means that the status quo can be maintained only by a coupled change in composition and temperature. What is the status quo in this case? It is not only that the structure is two phase, but also that the proportions of liquid and solid phases remain unaltered.

The next trick is to find the proportions of liquid and solid corresponding to any point in the two-phase field. To do this we draw the constant temperature line through the point *X*, Figure 2.5. This intersects the phase boundaries at *Y* and *Z*. The solid line containing *Y* represents the lower limit of 100 per cent liquid, and is known as the *liquidus*. The solid line containing *Z* is the upper limit of 100 per cent solid and is known as the *solidus*.

Neither the liquid nor solid phases corresponding to point *X* have a composition identical with that of the alloy as a whole. The liquid contains more Cu and less Ni, the solid less Cu and more Ni. The composition of each phase is given by the points *Y* and *Z* respectively. The proportions of the phases balance so that the weighted average is the same as the overall composition of the alloy. It is easy to show that:

$$(\text{Weight of liquid of composition } Y) \times YX = (\text{Weight of solid of composition } Z) \times XZ$$

This is similar to what would be expected of a mechanical lever balanced about *X* and consequently is known as the *Lever rule*.

One consequence of all this can be seen by

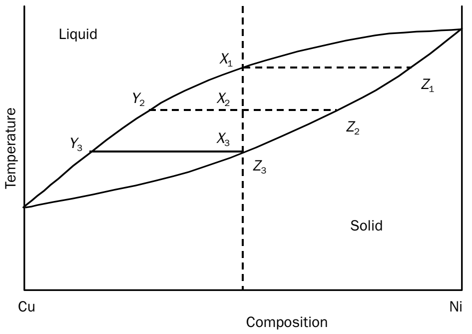

FIGURE 2.6 Equilibrium phase diagram for Cu–Ni (Figure 2.5) redrawn to emphasise composition variations with temperature.

re-examining the cooling of the 50:50 alloy from the liquid phase. Consider Figure 2.6. At point X_1 on the liquidus, solidification is about to begin. At a temperature infinitesimally below X_1 there will be some crystals solidifying out of the liquid; their composition is given by Z_1. At a temperature about halfway between solidus and liquidus (X_2), we have a mixture of solid and liquid of compositions Z_2 and Y_2. In general, the proportion of liquid to solid halfway through the freezing range need not be ≈50:50, but in this case it is. Finally, at a temperature infinitesimally above X_3, which is on the solidus, we have nearly 100 per cent solid of composition Z_3 together with a vanishingly small amount of liquid of composition Y_3. When the temperature falls to just below X_3, the alloy is totally solid and Z_3 has become identical with X_3.

Note two important features. First, Z_3 is the same as the average composition we started with, X_1. Second, solidification takes place over a range of temperatures, and as it occurs the compositions of liquid and solid phases change continuously. For this to actually happen, substantial amounts of diffusion must occur in both liquid and solid. That in solids is very much slower than that in liquids, and is the source of some practical difficulty. Either solidification must occur slowly enough for diffusion in the solid to keep up or strict equilibrium conditions are not met. The kinetics of phases transformations is something to which we will return. However, for the moment, we continue to confine attention to very slowly formed, equilibrium or near equilibrium structures.

2.4.3 Eutectic systems

Let us now examine another diagram, that for aluminium–silicon (Al–Si) alloys (Figure 2.7.) Pure Al forms face-centred crystals, but Si has the same crystal structure as diamond. These are incompatible and extensive solid solutions like those for Cu:Ni cannot be formed. Si crystals can dissolve only tiny amounts of Al. For our purposes, we can ignore this solubility, although we might recognise that the semiconductor industry makes great use of it, small as it is. Al crystals can dissolve a little Si, but again not very much, and we will ignore it. Thus, two solid phases are possible, Al and Si.

When liquid, the elements dissolve readily in the melt in any proportions.

Consider the composition Y. On cooling to the liquidus line at A, pure (or nearly pure) crystals

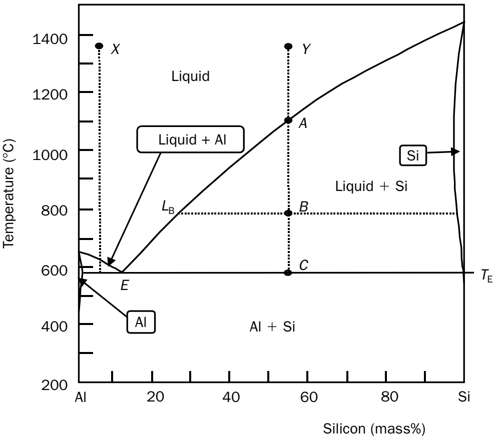

FIGURE 2.7 Equilibrium phase diagram for Al–Si.

of Si begin to form. At *B* we have solid Si coexisting with liquid of composition L_B in proportions given by the Lever rule. At *C* we have solid Si in equilibrium with liquid of composition nearly at *E*.

Now consider alloy *X*. The sequence is much the same except the first solid to form is now crystals of Al. When the temperature has fallen to almost T_E we have solid Al in equilibrium with liquid of composition close to *E*.

Note that both alloy *X* and alloy *Y*, when cooled to T_E, contain substantial amounts of liquid of composition *E*. An infinitesimal drop of temperature below T_E causes this liquid to solidify into a mixture of solid Al and solid Si. At *E* we have three phases which can coexist: liquid, solid Al and solid Si. The system has two components and thus the phase rule gives us no degrees of freedom once we have discounted pressure. *E* is an invariant point; any change in temperature or composition will disturb the equilibrium.

The point *E* is known as the eutectic point and we speak of the eutectic composition and the eutectic temperature, T_E. This is the lowest temperature at which liquid can exist and the eutectic alloy is that which remains liquid down to T_E. It solidifies at a unique temperature, quite unlike Cu–Ni or Al–Si alloys of other compositions. Alloys close to the eutectic composition (Al – 13%Si) are widely used because they can be easily cast into complex shapes, and the Si dispersed in the Al strengthens it. Eutectic alloys in other systems find similar uses (cast-iron is of near eutectic composition) as well as uses as brazing alloys, etc.

2.4.4 Intermediate compounds

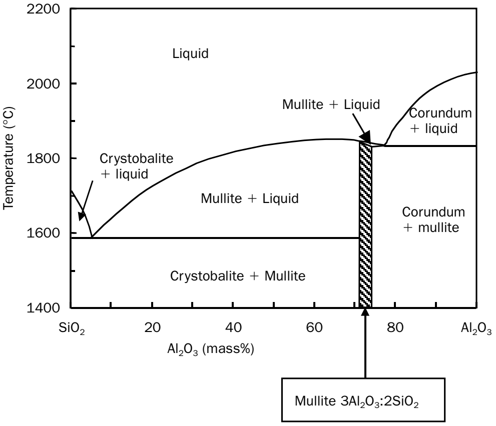

FIGURE 2.8 Equilibrium phase diagram for SiO_2–Al_2O_3.

Often, the basic components of a system can form compounds. For example, lime, CaO, and silica, SiO_2, can form the compounds $2(CaO)SiO_2$, $3(CaO)SiO_2$ and others, which have great technological significance as active ingredients in Portland cement (to be discussed in detail in Chapter 13). Similarly, SiO_2 and corundum, Al_2O_3, form mullite, $3(Al_2O_3)2(SiO_2)$, an important constituent of fired clays, pottery and bricks. In metals we can have $CuAl_2$, Fe_3C and many more.

Figure 2.8 shows the SiO_2–Al_2O_3 diagram. It can be thought of as two diagrams, one for 'SiO_2–mullite' and the other for 'mullite–Al_2O_3', joined together. Each part diagram is a simple eutectic system like Al–Si. In a similar way, the lime (CaO) silica (SiO_2) diagram, Figure 2.9, can

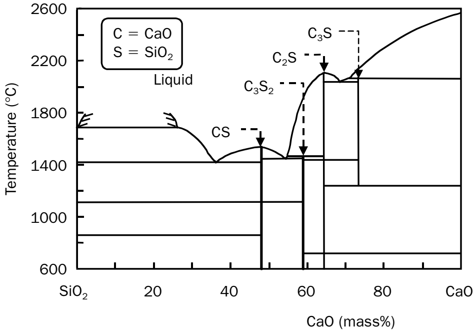

FIGURE 2.9 Equilibrium phase diagram for lime (CaO) – silica (SiO_2).

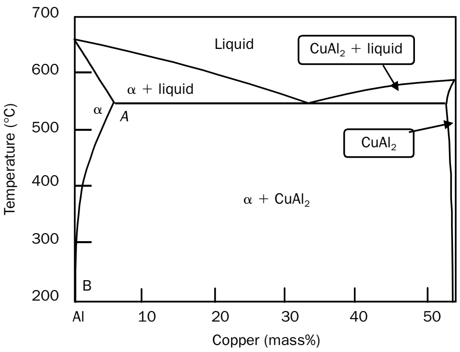

FIGURE 2.10 Equilibrium phase diagram for Al–CuAl$_2$.

be thought of as a series of joined together eutectic systems.

In many cases we do not have to think about the whole diagram. Figure 2.10 shows the Al–CuAl$_2$ diagram, again a simple eutectic system. A notable feature is the so-called *solvus* line, AB, which represents the solubility of CuAl$_2$ in solid crystals of Al. This curves sharply, so that very much less CuAl$_2$ will dissolve in Al at low temperatures than will at high temperatures. This is a fortunate fact that underlies our ability to alter the microstructures of some alloys by suitable heat treatments. Details will be taken up later.

2.4.5 The Fe–C diagram

When I was a student, my tutor told me that I could consider myself a true metallurgist when I had dreamed about the Fe–C diagram! Such is its importance to the metallurgy of steels and cast irons, both of which are of prime interest to civil engineers.

A section of the diagram for carbon contents up to ≈5 per cent is shown in Figure 2.11. It has a eutectic at ≈4.3%C and 1150°C. This low melting temperature allows such alloys to be melted with relative ease and to be cast into complex shapes. Cast irons have carbon contents usually above 2 per cent. Sometimes the products of solidification are Fe and Fe$_3$C, sometimes Fe and graphite, and sometimes Fe, Fe$_3$C and graphite. Graphite containing cast-irons are relatively soft and easy to machine. Cast-irons containing no graphite but with all the carbon as Fe$_3$C are very hard and wear resistant. They often turn up as wear resistant facings on earth moving

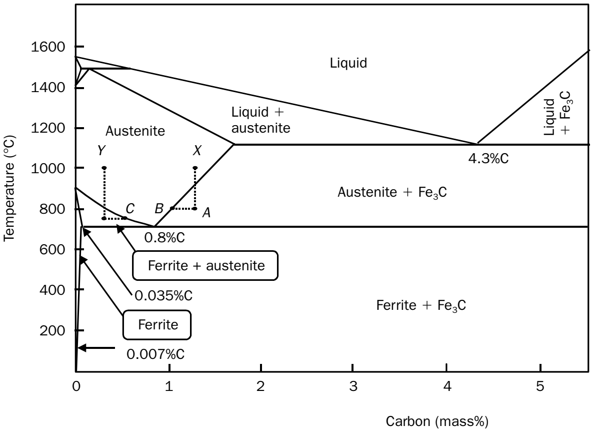

FIGURE 2.11 Equilibrium phase diagram for iron–carbon.

machinery. Both types are easily cast into complex shapes.

At lower carbon contents, less than ≈1 per cent, the liquidus climbs to temperatures which make melting more tricky. But by far the most important feature of the diagram arises from the allotropy of iron. At temperatures below 910°C, pure Fe forms into body-centred cubic crystals, known as ferrite. At higher temperatures, the crystals have face-centred cubic structures and are known as austenite. Up to 2%C can dissolve in austenite at 1150°C, but this rapidly reduces and Fe_3C is precipitated as the temperature falls to 723°C, at which a maximum of 0.8 per cent carbon can dissolve in austenite. Almost no carbon will dissolve in ferrite, but that which does has very profound effects. Transitions from austenite to lower temperature forms of the alloys give rise to a part of the diagram that is reminiscent of a eutectic diagram. To emphasise the fact that it represents transitions from one solid condition to another solid condition, it is referred to as a *eutectoid*.

Consider the alloy *X* at 1000°C (Figure 2.11). It is fully austenitic; on cooling to the point *A* some Fe_3C is precipitated and the composition of the austenite in equilibrium with the Fe_3C is given by point *B*. Similarly, on cooling alloy *Y* from 1000°C to say 750°C, ferrite is precipitated and the composition of the austenite in equilibrium with it is *C*. At 723°C, we have the eutectoid point and the austenite contains 0.8%C. Further cooling causes the austenite to decompose into a mixture of ferrite and Fe_3C. It consists of alternating lamellae (lathes) of Fe and Fe_3C, arranged in colonies within which the lamellae are nearly parallel. The scale is such that the structure acts as a diffraction grating to light and gives the microstructures an iridescent and pearly appearance. Consequently, the mixture is known as pearlite. The consequences of all this to the metallurgy of steels and cast irons will be dealt with in Chapter 12.

Chapter three

Atomic structure and interatomic bonding

It will be clear that the differences between solids and liquids, indicated earlier, are a consequence of the bonding forces between the atoms of which they are composed. In order to discuss these forces some understanding of the structure of the atom is required. The following uses a simplified model.

The atoms of all elements can be visualised as a positively charged nucleus, comprising of one or more positively charged protons and electrically neutral neutrons, surrounded by orbiting negatively charged electrons. The electrical charges on the proton (+e) and electron (−e) are equal and opposite. All atoms, in their normal state, contain equal numbers of protons and electrons and are electrically neutral. The mass of the proton is about 2000 times that of the electron. Except in the case of hydrogen, the incorporation of neutrons in the nucleus is essential for stability; however, for our purposes we can disregard their presence. The nucleus of hydrogen, the simplest atom, comprises a single proton, about which a single electron orbits (Figure 3.1 (a)). Helium has a nucleus containing two protons, with two electrons in orbit about it (Figure 3.2 (b)). The next element, lithium, has a nucleus containing three protons, with three electrons arranged in orbits about it, the third electron being in a separate

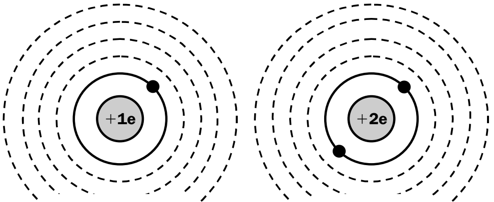

(a) Hydrogen (b) Helium

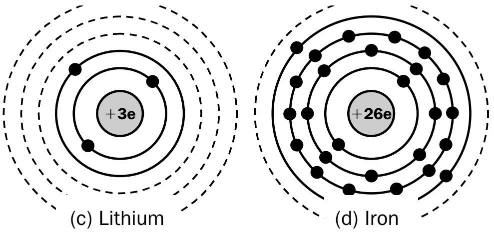

(c) Lithium (d) Iron

FIGURE 3.1 Schematic of the atomic structures of the first three elements of the periodic table and iron.

shell from the first two (Figure 3.1 (c)). Heavier atoms, of course, contain increasing numbers of protons (and neutrons) and electrons (Figure 3.1 (d)).

In order to emphasise how the electronic structure of the elements affects their properties, listings of all the known elements are usually arranged in a form called the *periodic table*. This table enables predictions to be made regarding which elements will form compounds and what the properties of the compounds will be. An atomic structure of particular stability arises whenever the outermost shell contains eight electrons. These *octets*, as they are known, are found in neon, argon, krypton, xenon, etc.; that is, the *inert gases*, so-called because they are just that.

Consider now the atom of sodium. It contains eleven electrons arranged in shells as 2–8–1 (Figure 3.2). Clearly it can realise the octet configuration by losing an electron. In doing so it is left with a net positive charge and is known as an *ion*, in this case a positive ion. Chlorine, on the other hand, contains seventeen electrons arranged as 2–8–7 (Figure 3.2) and the octet configuration can be achieved if it accepts an electron to become a negative ion. The electrons in the outer shell of an atom are responsible for bonding with other atoms and are called valence electrons. The number of these outermost electrons determines the *valency*, i.e. the number of bonds which can be formed with other atoms. Sodium has a valency of 1 and the chemical formula for sodium chloride is NaC1, since chlorine, being able to accept one electron, also has a valency of 1. Oxygen, however, has six valence electrons and needs to borrow two. Since sodium can only donate one electron, the chemical formula for sodium oxide is Na_2O. Magnesium has two valence electrons and so the chemical formula for magnesium chloride is $MgCl_2$ and for magnesium oxide MgO. Hence, it can be seen how the number of valence electrons determines how atoms combine to form compounds. The number of valence electrons also strongly influences the nature of the interatomic bonds.

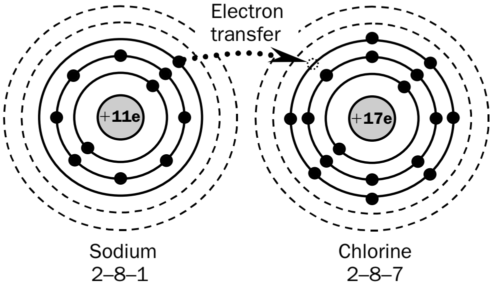

FIGURE 3.2 Schematic of ionic bonding.

3.1 Ionic bonding

If an atom (*A*) with one electron in the outermost shell reacts with an atom (*B*) with seven electrons in the outermost shell, then both can attain the octet structure if atom *A* donates its valence electron to atom *B*. However, the electrical neutrality of the atoms is disturbed and *B*, with an extra electron, becomes a negatively charged ion, whereas *A* becomes a positively charged ion. The two ions are then attracted to each other by the electrostatic force between them and an ionic compound results, the strength of the bond is proportional to e_Ae_B/r where e_A and e_B are the charges on the ions and r is the interatomic separation. The bond is strong, as shown by the high melting point of ionic compounds, and its strength increases, as might be expected, where two or more electrons are donated. Thus the melting point of sodium chloride, NaCl, is 801°C; that of magnesium oxide, MgO, where two electrons are involved, is 2640°C; and that of zirconium carbide, ZrC, where four electrons are involved, is 3500°C. Although ionic bonding involves the transfer of electrons between different atoms, the overall neutrality of the material is maintained.

The ionic bond is always non-directional; that is, when a crystal is built up of large numbers of ions, the electrostatic charges are arranged symmetrically around each ion, with the result that *A* ions tend to surround themselves with *B* ions and vice versa (Figure 3.3). The pattern adopted

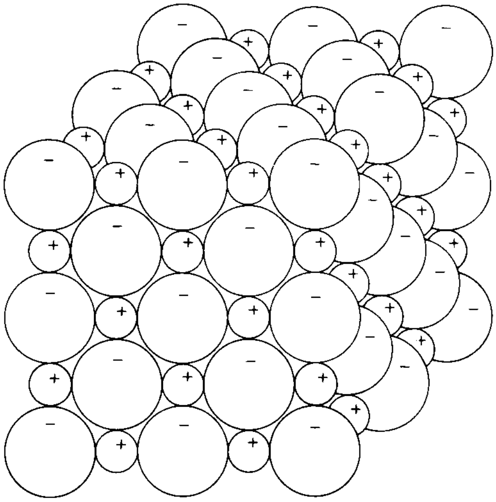

FIGURE 3.3 Non-directional nature of the ionic bond: A^- ions surrounded by B^+ ions, B^+ ions surrounded by A^- ions. This particular arrangement, where each species of ion taken by itself lies on the sites of a face-centred cubic structure, is known as the sodium chloride (NaCl) or rock salt structure.

depends on the relative sizes of the *A* and *B* ions, i.e. how many *B* ions can be comfortably accommodated around *A* ions whilst preserving the correct ratio of *A* to *B* ions.

3.2 Covalent bonding

An obvious limitation of the ionic bond is that it can only occur between atoms of different elements, and therefore it cannot be responsible for the bonding of any of the solid elements. Where both atoms are of the electron acceptor type, i.e. with close to eight outermost electrons, octet structures can be built up by the sharing of two or more valence electrons between the atoms.

Thus, two chlorine atoms can bond together and achieve the octet structure by each contributing one electron to share with the other atom. The interaction may be written:

$$:\overset{\cdot\cdot}{\underset{\cdot\cdot}{\mathrm{Cl}}}\cdot + :\overset{\cdot\cdot}{\underset{\cdot\cdot}{\mathrm{Cl}}}\cdot \rightarrow :\overset{\cdot\cdot}{\underset{\cdot\cdot}{\mathrm{Cl}}}:\overset{\cdot\cdot}{\underset{\cdot\cdot}{\mathrm{Cl}}}: \tag{3.1}$$

Where two electrons are required to make up the octet, the interaction may either be:

$$:\overset{\cdot}{\underset{\cdot}{\mathrm{O}}}: + :\overset{\cdot}{\underset{\cdot}{\mathrm{O}}}: \rightarrow :\overset{\cdot}{\underset{\cdot}{\mathrm{O}}}\vdots\overset{\cdot}{\underset{\cdot}{\mathrm{O}}}: \tag{3.2}$$

as in the oxygen molecule, or:

$$:\overset{\cdot}{\underset{\cdot}{\mathrm{S}}}: + :\overset{\cdot}{\underset{\cdot}{\mathrm{S}}}: + :\overset{\cdot}{\underset{\cdot}{\mathrm{S}}}: + :\overset{\cdot}{\underset{\cdot}{\mathrm{S}}}: + \ldots \rightarrow \overset{\cdot\cdot}{\underset{\cdot\cdot}{\mathrm{S}}}:\overset{\cdot\cdot}{\underset{\cdot\cdot}{\mathrm{S}}}:\overset{\cdot\cdot}{\underset{\cdot\cdot}{\mathrm{S}}}:\overset{\cdot\cdot}{\underset{\cdot\cdot}{\mathrm{S}}}: \tag{3.3}$$

as in one form of sulphur, where there is an obvious tendency for the atoms to form up in long chains.

Structurally, the elements showing covalent bonding obey what is known as the $(8-N)$ Rule. This states that the number of nearest neighbours to each atom is given by $8-N$ where N is the number of electrons in the outermost shell. Thus chlorine ($N=7$) has only one nearest neighbour and the atoms pair off as diatomic molecules; with sulphur, selenium and tellurium ($N=6$) long chains occur; with arsenic, antimony and bismuth ($N=5$) sheets of atoms occur, and with carbon ($N=4$) a three-dimensional network can form, as in diamond. Atoms with values of N less than 4 cannot show covalent bonding with their own species. They would require at least five nearest neighbours, whilst only having three or fewer electrons available for making up the shared bonds.

The possible arrangements of atoms are shown schematically in Figure 3.4, and it will be seen that only carbon can achieve a three-dimensional pattern in which all the bonds are covalent. This reveals the major structural difference between ionic and covalent bonding: the covalent bond, unlike the ionic bond, is saturated by the individual atoms participating in it.

The chlorine molecule, which consists of two chlorine atoms, is structurally self-sufficient and there is no extension of the covalent bonding between molecules. Similarly, the chains of sulphur and the sheets of bismuth are really large molecules but there is little bonding between the chains or sheets. The result is that the covalent

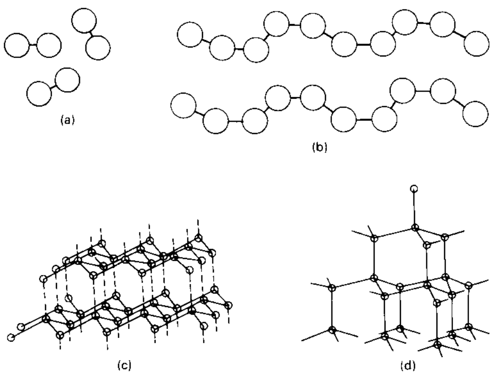

FIGURE 3.4 Schematic structures of elements conforming to the $8-N$ rule. (a) Chlorine ($N=7$): individual molecules; (b) tellurium ($N=6$): spiral chains; (c) antimony ($N=5$): corrugated sheets; (d) diamond ($N=4$): three-dimensional crystal.

elements (which effectively means the non-metallic elements) have poor physical strength, not because the covalent bond itself is weak, but because, with the exception of diamond (one form of carbon), they do not form a three-dimensional lattice. In fact, the hardness and high melting point of diamond (3500°C) show that the covalent bond is extremely strong. Covalent bonding is not limited to elements; many compounds are covalent, some simple examples being HCl, H_2O, CH_4 and NH_3. A large number of compounds show partly ionic and partly covalent bonding, e.g. sulphates such as Na_2SO_4 in which the sulphate ion is covalently bonded whilst the bond to the sodium is ionic.

The vast field of industrial polymers is also predominantly concerned with covalent compounds. Individual bonds may exhibit hybrid qualities akin to both ionic and covalent bonding; although in the pure form the two bond types represent different modes of linkage, there is in fact no sharp line of demarcation between them. When elements of high valency combine to form ionic compounds (e.g. the nitrides and carbides of the transition elements), the donor ion may lose three, or even four, electrons to the acceptor ion. The result is a strong polarising pull (electrostatic force) exerted by the donor ion on the electrons of the acceptor ion, so that the electrons are sucked back towards the donor and spend more time between the two ions than circling each individually. The bond thus acquires some of the characteristics of the covalent linkage. Compounds of this sort are usually extremely hard and have very high melting points, since they combine to some extent the strength of the covalent bond and the non-directionality of the ionic bond.

3.3 Metallic bonding

Metallic atoms possess few valence electrons and thus cannot bond with themselves covalently, rather, they obey what is termed the *free-electron theory*. In a metallic crystal the valence electrons are detached from their atoms and can move freely between the positive metallic ions (Figure 3.5). The positive ions are arranged regularly in a crystal lattice, and the electrostatic attraction between the positive ions and the free negative electrons provides the cohesive strength of the metal. The metallic bond may thus be regarded as

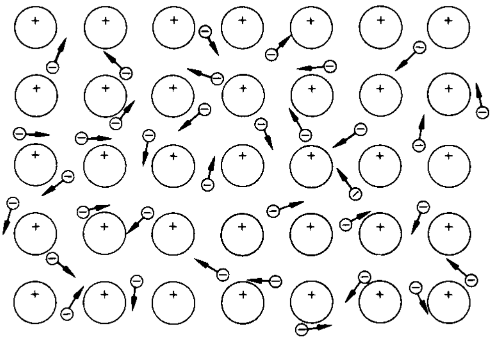

FIGURE 3.5 Schematic 'free-electron' structure for a monovalent metal. In the absence of an electric field the electrons are in ceaseless random motion, but the overall distribution remains uniform over any period of time.

a very special case of covalent bonding, in which the octet structure is satisfied by a generalised donation of the valence electrons to form a 'cloud' which permeates the whole crystal lattice, rather than by electron sharing between specific atoms (true covalent bonding) or by donation to another atom (ionic bonding).

Since the electrostatic attraction between ions and electrons is non-directional, i.e. the bonding is not localised between individual pairs or groups of atoms, metallic crystals can grow easily in three dimensions, and the ions can approach all neighbours equally to give maximum structural density.

Crystallographically, these structures are known as 'close-packed' (see Section 8.2). They are geometrically simple by comparison with the structures of ionic compounds and naturally occurring minerals, and it is this simplicity that accounts in part for the ductility (ability to deform non-reversibly) of the metallic elements.

Metallic bonding explains the high thermal and electrical conductivity of metals. Since the valence electrons are not bound to any particular atom, they can move through the lattice under the application of an electric potential, causing a current flow, and can also, by a series of collisions with neighbouring electrons, transmit thermal energy rapidly through the lattice (see Chapter 7). Optical properties are also explained by the theory. If a ray of light falls on a metal, the electrons (being free) can absorb the energy of the light beam, thus preventing it from passing through the crystal and rendering the metal opaque. The electrons which have absorbed the energy are excited to high energy levels and subsequently fall back to their original values with the emission of the light energy. In other words, the light is reflected back from the surface of the metal, and the high reflectivity of metals can be accounted for.

The ability of metals to form alloys (of extreme importance to engineers) is also explained by the free-electron theory. Alloys are discussed in Chapter 8.

Since the electrons are not bound, when two metals are alloyed there is no question of electron exchange or sharing between atoms in ionic or covalent bonding, and hence the ordinary valency laws of combination do not apply. The principal limitation then becomes one of atomic size, and providing there is no great size difference (see Section 2.4.2), two metals may be able to form a continuous series of alloys or solid solutions from 100 per cent A to 100 per cent B.

3.4 Van der Waals bonds

The three strong primary types of atomic bond (ionic, covalent and metallic) all occur because of the need for atoms to achieve a stable electron configuration. However, even when a stable configuration exists already, as in the case of the inert gases, some form of bonding force between the molecules must be present since these elements will all liquefy and ultimately solidify at sufficiently low temperatures.

Bonds of this nature are universal to all atoms and molecules, but are normally so weak that their effect is overwhelmed when primary bonds are present. They are known as *Van der Waals bonds*, and are one reason why real gases deviate from the ideal gas laws. They arise as follows. Although in Figure 3.1 we represented the orbiting electrons in discrete shells, the true picture is that of a cloud, the density of the cloud at any point being related to the probability of finding an electron there. Such a picture implies that the electron charge is 'spread' around the atom, and, over a period of time, the charge may be thought of as symmetrically distributed within its particular cloud.

However, the electronic charge is moving, and this means that on a scale of nanoseconds the electrostatic field around the atom is continuously fluctuating, resulting in the formation of a dynamic electric dipole, i.e. the centres of positive charge and negative charge are no longer coincident. When another atom is brought into proximity, the dipoles of the two atoms may interact co-operatively with one another (Figure 3.6) and the result is a weak non-directional electrostatic bond.

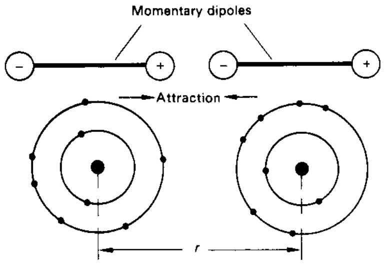

FIGURE 3.6 Weak Van der Waals linkage between atoms arising from fluctuating electronic fields.

The attractive force between two atoms is given by the expression:

$$F = \frac{\alpha_1 \alpha_2}{r^6} \qquad (3.4)$$

where α_1 and α_2 are the polarisabilities of the two atoms, i.e. the ease with which their electronic fields can be distorted by a unit electric field to form a dipole, and r is the distance between them. Polarisability increases with atomic number, since the outermost electrons, which are responsible for the effect, are further removed from the nucleus and therefore more easily pulled towards neighbouring atoms. This is shown by a comparison of the freezing points of the inert gases He (1 K) and Xe (133 K), or the halogens, fluorine (51 K) and iodine (387 K).

As well as this fluctuating dipole, many molecules have permanent dipoles as a result of bonding between different species of atoms. These can play a considerable part in the structure of polymers and organic compounds, where side chains and radical groups of ions can lead to points of predominantly positive or negative charges. These will exert an electrostatic attraction to other oppositely charged groups.

The strongest and most important example of dipole interaction occurs in compounds between hydrogen and nitrogen, oxygen or fluorine. It occurs because of the small and simple structure of the hydrogen atom and is known as the hydrogen bond. When, for example, hydrogen links covalently with oxygen to form water, the electron contributed by the hydrogen atom spends the greater part of its time between the two atoms. The bond acquires a definite dipole with hydrogen becoming virtually a positively charged ion.

Since the hydrogen nucleus is not screened by any other electron shells, it can attract to itself other negative ends of dipoles, and the result is the hydrogen bond. It is considerably stronger (roughly ×10) than other Van der Waals linkages, but is much weaker (by 10 to 20 times) than any of the primary bonds. Figure 3.7 shows the resultant structure of water, where the hydrogen bond forms a secondary link between the water molecules, and acts as a bridge between two electronegative oxygen ions. Thus, this relatively insignificant bond is one of the most vital factors for the benefit and survival of mankind. It is responsible for the abnormally high melting and boiling points of water and for its high specific heat, which affords an essential global temperature control. In the absence of the hydrogen bond, water might well be gaseous at ambient temperatures like ammonia or hydrogen sulphide.

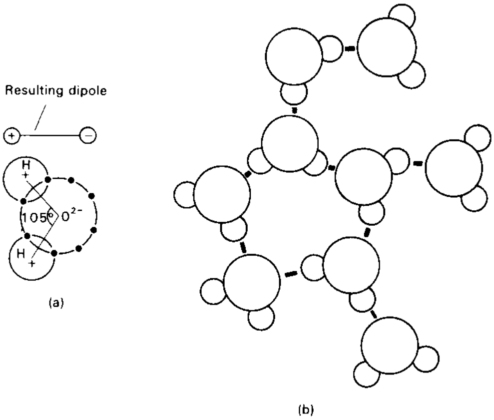

FIGURE 3.7 The hydrogen bond: (a) individual water molecule showing dipole resulting from bond angle; (b) structure of water.

Chapter four

Elasticity and plasticity

We noted in Chapter 1 that the product of stress and strain has the dimensions of energy per unit volume. Since thermodynamics teaches us about energy it is convenient to start with the thermodynamics of a deformation process. From the first law, the internal energy is (equation (2.1)):

$$dE = dQ - dW$$

We can write the second law of thermodynamics as:

$$dQ = TdS$$

and hence:

$$dE = TdS - dW$$

Let us consider a bar in which an applied tensile force F results in an extension dL. The work done on the bar is FdL and so the work done by the bar in resisting the force is

$$dW = -FdL$$

$$\therefore dE = TdS + FdL$$

The Helmholtz free energy (equation (2.4)) is:

$$H = E - TS$$

so that the change in free energy is:

$$dH = dE - TdS - SdT$$

However, if the conditions are such that temperature remains constant, then $SdT = 0$ and the change is:

$$dH = dE - TdS = FdL$$

so that:

$$F = (\delta H/\delta L)_T = (\delta E/\delta L)_T - T(\delta S/\delta L)_T \quad (4.1)$$

where the subscript T indicates that the equation is valid for constant temperature.

This is the thermodynamic equation of state for deformation and shows that the force is distributed between a change in internal energy and a change in entropy. We now examine these changes.

4.1 Linear elasticity

The first term of equation (4.1) implies that at least part of the response to an applied force involves a change in internal energy. In crystalline solids, where the atoms are arranged in orderly ranks in space, the capacity for independent movement is limited and the bulk of the internal energy is to be found in the interaction energies between the atoms.

To keep things simple, let us consider the energies involving a pair of atoms. There are both attractive and repulsive forces which balance one another when the atoms are in equilibrium. Whatever the cause of the energies, they tend to vary as the inverse of the distance between the atoms, raised to some power. So, if the distance between the atoms is r, and A, B, m and n are constants that vary with the material and its structure, then:

The attractive energy is Ar^{-n}
The repulsive energy is Br^{-m}
The resultant energy is $U = Br^{-m} - Ar^{-n}$

These energies, as a function of interatomic spacing, are sketched in Figure 4.1 (a). Figure 4.1 (b) presents the same information, but in terms of the force between adjacent atoms, F. There are three things to note:

1. The bond energy U is a continuous function of r. Thus we can express the energy as a series:

$$U_{(r)} = U_{(r_0)} + r(\mathrm{d}U/\mathrm{d}r)_{r_0} + (r^2/2)(\mathrm{d}^2U/\mathrm{d}r^2)_{r_0} + \ldots\ldots$$

   where $U_{(r_0)}$ is the energy at $r = r_0$, i.e. the interatomic separation at which the attractive and repulsive forces balance, and the differential is taken at $r = r_0$.
2. The minimum in the curve at r_0 allows the second term to be eliminated, since $(\mathrm{d}U/\mathrm{d}r) = 0$ at a minimum.
3. The displacement from r_0 is small, so ignore terms higher than r^2. Then we find that:

$$U_{(r)} = U_{(r_0)} + (r^2/2)(\mathrm{d}^2U/\mathrm{d}r^2)_{r_0}$$

   hence:

$$F = \mathrm{d}U/\mathrm{d}r = r(\mathrm{d}^2U/\mathrm{d}r^2)_{r_0}$$

   i.e. force is proportional to displacement via a constant $(\mathrm{d}^2U/\mathrm{d}r^2)$.

   In other words, the constant of proportionality is the slope of the F:r graph at the equilibrium position where $r = r_0$.

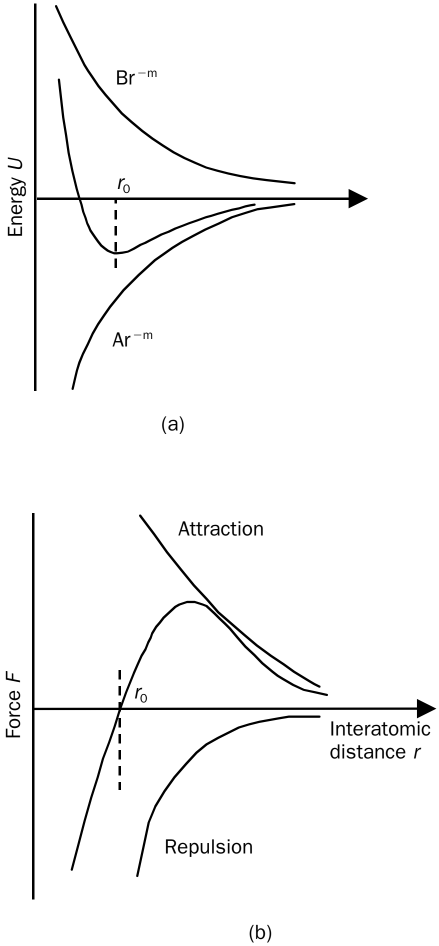

FIGURE 4.1 (a) Condon Morse curves of energy versus interatomic spacing, r (b) the force acting on an ion as a function of r. r_0 is the interatomic spacing.

4.2 Consequences of the theory

Having established some mathematical facts about the graphs of force and energy against distance, we can use them to predict some consequences and tie them up with the real world. To a materials scientist there are a great many consequences but only eight of the most noteworthy are given below.

1. When a material is extended or compressed a little, the force is proportional to the extension (from equation (1.8)). This is Hooke's law. The slope of the F:r curve at $r = r_0$ is the fundamental origin of the elastic constant (or stiffness).

2. Since the *F*:*r* curve is nearly symmetrical about the equilibrium position, the stiffness of a material will be nearly the same in tension and compression. This is, in fact, the case.
3. At large strains, greater than about 10 per cent, the *F*:*r* curve can no longer be considered straight and so Hooke's law should break down. It does.
4. There should be a limit to the tensile strength, since the attractive force between the atoms has a maximum value. This is so. It turns out that the maximum strength corresponding to the maximum in Figure 4.1 (b) is about E/10. For steel this would be at ≈20 000 MPa, but we know only too well that steels are nowhere near this strong. We will see why later. For the moment we note that the strain corresponding to maximum load is ≈1 (100 per cent). Something else happens before we get there.
5. There should be no possibility of failure in compression since the repulsive force between the atoms increases *ad infinitum*. This is so. A uniaxial compressive stress always gives rise to shear stresses which are maximised on planes at 45° to the compression direction. It is these shear stresses that cause failure.
6. If the atoms vibrate about their equilibrium positions, then their mean separation will increase the more they vibrate. This follows from the trough of the *U*:*r* curve being asymmetrical. In fact, in materials at any temperature above absolute zero (−273°C), the atoms do vibrate in proportion to the temperature. It follows then that as a material is heated it should expand in all directions. This is so.
7. If the heating process is continued the atoms should reach a degree of vibration that causes them to separate, i.e. the bond is broken. This is what happens when a solid evaporates.
8. Any degree of vibration by the atoms should reduce the extra amount of energy required to break the bond. In other words the tensile strength should decrease as the temperature increases. This does happen.

There is another point to make, which the reader may have noticed already. Points 4 and 5 both contain intimations that other things are going on in materials when they are strained. Later, we shall find out what.

4.3 Long-range elasticity

We now consider the second term in equation (4.1). Specific polymers will be discussed in Chapter 34, but meanwhile we will consider the basic nature of polymer structure. In its simplest form this consists of a chain of atoms, often many units long and generally, though not necessarily, of carbon, each of which is covalently bonded to another atom. The structure of polyethylene is shown diagrammatically in Figure 4.2 (a).

However, things are not quite so simple. Two adjacent carbon bonds must be at a fixed angle to one another (Figure 4.2 (b)), but there is no constraint about which plane the angle lies in. The consequence is that over a distance of tens or hundreds of carbon bonds the chain tends to get twisted. Second, the long chain is a complete molecular entity and, in the simplest case, is not bonded to another chain. We therefore have a structure which looks rather like a tangle of wet spaghetti, or a can of worms. In addition, at temperatures above a certain level, which is a characteristic property of the polymer, the chains are in constant motion as a result of thermal fluctuations. It is intuitively obvious that the application of a force will cause changes in the internal configuration. A given atom in the molecular chain will not change its neighbours within the chain

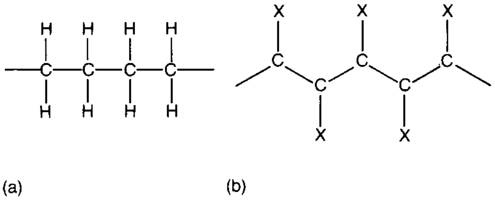

FIGURE 4.2 Polyethylene. (a) Diagrammatic. In (b) X represents two hydrogen atoms, one above and one below the plane of the carbon chain.

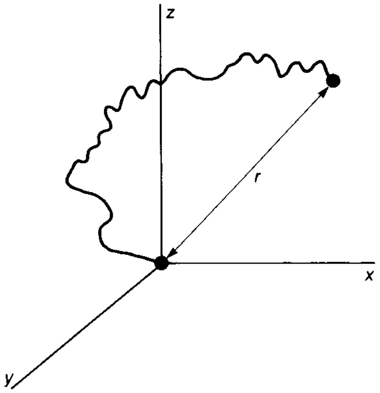

FIGURE 4.3 Schematic representation of a randomly convoluted molecular chain.

but it will change its neighbours in adjacent chains several times during the loading–unloading cycle. Think of the worms wriggling about.

Expressed in thermodynamic terms we may say that the unloaded configuration is, or is close to being, the most probable one, in other words this is the equilibrium configuration of maximum entropy. Under load the configuration changes to one that is the most probable for the loaded condition and the entropy changes. A straight chain is only one of many possible configurations, and it can be shown that the number of possible configurations, whether convoluted or not, is a function of its end-to-end length, r. The number of possible configurations N_c decreases as r increases. This is known as the *configurational entropy* S_c and is given by Boltzmann's equation (equation (2.2)) here rewritten as:

$$S_c = k \ln N_c \tag{2.2a}$$

i.e. the entropy decreases as r increases.

We shall not pursue here the statistical arguments describing the probability of a particular configuration being obtained. This is done fully in standard texts (Treloar, 1949) and here we state only the principles.

1. If the ends of the molecule are moved from their most probable positions, the change in entropy causes a force to act along the line joining the ends of the molecule (Figure 4.3).
2. The entropy force is proportional to the absolute temperature. The magnitude of the force is a function of the end-to-end length as represented by a straight line joining the ends. In this it behaves as though it were an elastic spring.

The spring analogy should not, however, be taken too literally. Being statistical in origin the tension in a chain whose endpoints are fixed will be subject to continual fluctuations like the pressure exerted by a gas on the walls of a container. Similarly, if the molecule is subjected to a constant tension its length will fluctuate. But we see that rubber elasticity is long range and is quite a different thing from the short-range forces which determine Hookean elasticity. For rubbers we often speak of the entropy spring.

4.4 Viscoelasticity

We have already indicated that it is not possible to draw a sharp dividing line between the mechanical behaviour of liquids and solids. There is a large group of materials, known as *viscoelastics*, whose behaviour is part liquid and part solid. Many natural materials, tendon, plant fibres and wood all behave in this way. Of engineering materials, rubbers are the archetype and so are many soft polymers as well as substances like tar and asphalt.

Two cases at least are of importance to engineers. If the strain remains constant, as in a tension bolt clamping two girders together, stress relaxation may occur without dimensional change. When the material is under constant stress it will respond by steadily increasing strain and, under prolonged loading, many normally rigid materials such as cement and concrete are prone to this process, i.e. to creep.

If an instantaneous stress is applied to a Hookean material (Figure 4.4(a)), a corresponding strain is produced. As long as the load is maintained the strain remains constant (Figure 4.4(b)) and is fully recovered when the load is

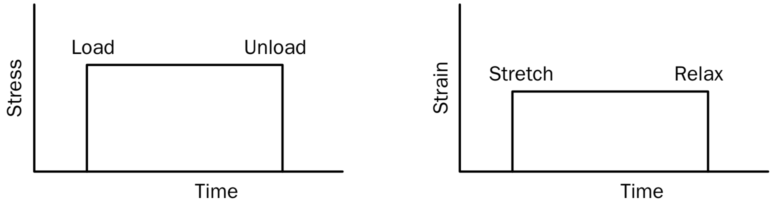

(a) Load history: constant applied stress

(d) Strain history: constant applied strain

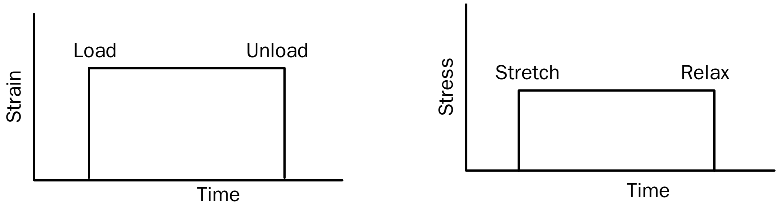

(b) Elastic (Hookean) strain response

(e) Elastic (Hookean) stress response

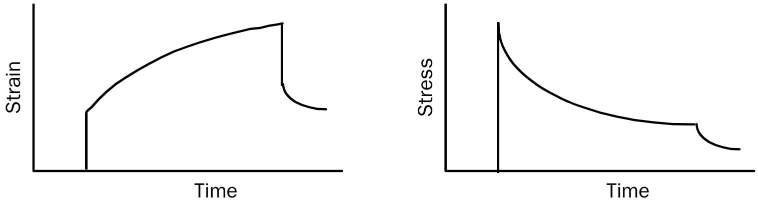

(c) Viscoelastic (creep) response

(f) Viscoelastic response – stress relaxation

FIGURE 4.4 Types of materials' response to constant stress (a–c) and constant strain (d–f).

removed. The corresponding strain behaviour of a viscoelastic material is illustrated in Figure 4.4 (c). The strain builds up over a period of time and, when the load is removed, the strain takes time to relax. This behaviour is known as *creep*. A similar phenomenon occurs if a material is subjected to a fixed strain (Figure 4.4 (d)). In a Hookean material stress remains constant for as long as the strain is maintained (Figure 4.4 (e)); in a viscoelastic material the stress diminishes over a period of time, as shown in Figure 4.4 (f). This is *stress relaxation*.

The structural reasons for this behaviour need not delay us here as they will be discussed in later chapters dealing with specific materials, cements, polymers and timber especially. Meanwhile we

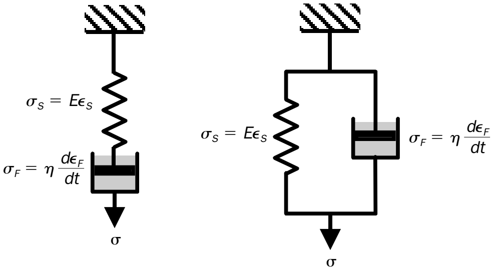

(a) Maxwell (b) Voigt

FIGURE 4.5 Viscoelastic models.

note that the behaviour is usually modelled using mechanical analogues consisting of arrays of springs which behave according to Hooke's law and viscous elements which behave as an ideal Newtonian liquid.

One such array is shown in Figure 4.5 (a). It consists of an elastic spring *s* of modulus *E* in series with a dash pot, i.e. a piston moving in a fluid *F* of viscosity η contained in a cylinder. Now think of suddenly applying a constant strain. At first all the strain is taken up by stretching of the spring and the load required to do this is calculated from the strain of the spring. Later, the spring shortens by pulling the piston up through the fluid in the dash pot. Some of the total strain is now taken up by the movement of the piston and less by the stretch in the spring. The load required is now less than before, and thus the system is exhibiting stress relaxation. Mathematical analysis gives:

$$\sigma_t = \sigma_0 \exp(-t/\tau) \tag{4.3}$$

where σ_0 is the stress sustained at time = 0, σ_t is the stress sustained at time t and $\tau = E/\eta$ is the so-called *relaxation time*. Under constant strain the stress decays exponentially.

Now think of doing things differently. Apply a constant stress. The spring stretches and remains at that strain as long as the load remains. At the same time the dash pot slowly extends as the piston is pulled through the fluid in it. The total extension increases linearly with time. This model represents stress relaxation very well, but is less successful at representing creep.

To get a good representation of creep, we use a model (Figure 4.5 (b)) in which the spring and dash pot are arranged in parallel. Both elements must experience the same strain but load can be transferred over time from one element to the other. Unfortunately, this gives a poor representation of stress relaxation.

To get out of these difficulties, the two types are combined into what is known as the four element model. This and its responses are shown in Figure 4.6. In this, τ_M is the relaxation time for stress at constant strain and τ_V is the relaxation time for strain at constant stress.

The concept of relaxation times is important for two reasons. First because it helps us to distinguish between solids and liquids. A perfect solid will support the stress indefinitely, i.e. $\tau = \infty$, but for a liquid, relaxation is virtually instantaneous (for water $\tau = \approx 10^{-11}$s). In between there is a grey area where stress relaxation may occur over a few seconds or centuries.

Then we have the relationship between the relaxation time and the time scale of the loading *t*. If the load is applied so fast that the relaxation cannot occur ($t < \tau$) the material will effectively behave elastically, but under slow loading ($t > \tau$) it will flow. This is well shown by 'potty putty' which bounces under impact loading but collapses into a puddle under its own weight when left alone. Many polymeric materials show a similar sensitivity to loading speed.

To model a real material, we would need to combine large numbers of simple elements, each having its own relaxation time, to achieve a *relaxation spectrum* in which different elements relax at different times.

There are a number of important consequences of viscoelasticity. The first is that the stress–strain relationship is non-linear. We noted that in a Hookean solid the strain energy stored on loading is completely recovered when we unload. Figure 4.7 shows that for a viscoelastic material the energy recovered on unloading is less than that stored during loading. Where has the energy gone? It has gone into heat, which explains why,

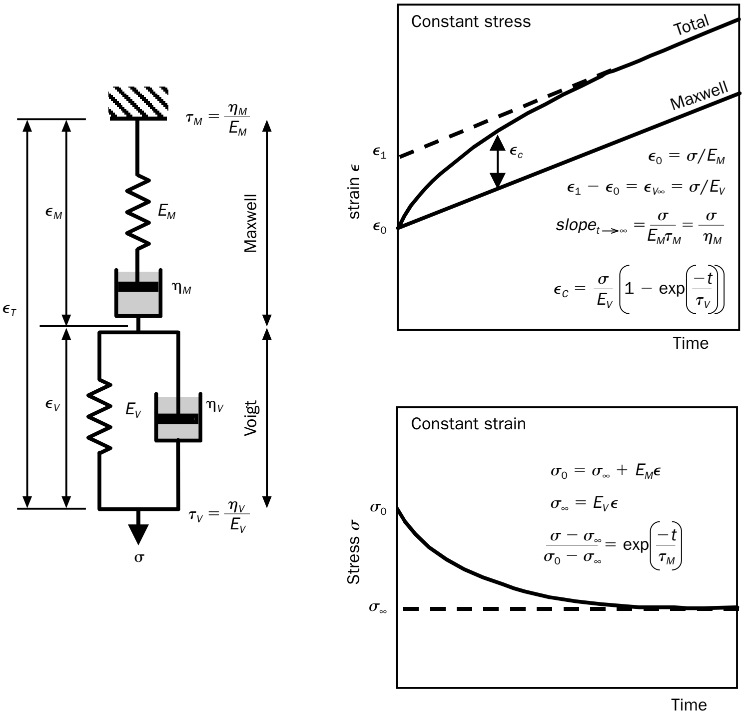

FIGURE 4.6 Four element model of viscoelasticity and its response.

after a few miles in which they are repeatedly loaded and unloaded, car tyres get hot.

The second consequence is known as Boltzmann's superposition theory. This states that each increment of load makes an independent and additive contribution to the total deformation. Thus, under the loading programme shown in Figure 4.8, the creep response is additive and the total creep is the sum of all the units of incremental creep. This has certain consequences when we apply it to the creep behaviour of concrete and soils.

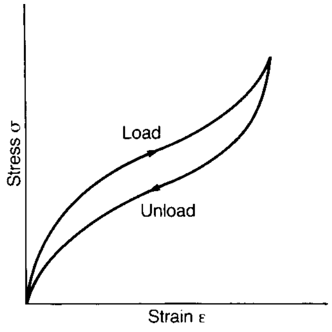

FIGURE 4.7 Loading/unloading curves for a viscoelastic solid.

4.5 Plasticity

Many materials display *plasticity*; that is to say, when they are deformed the change in shape is permanent and the original dimensions can only be restored by applying a force in the opposite

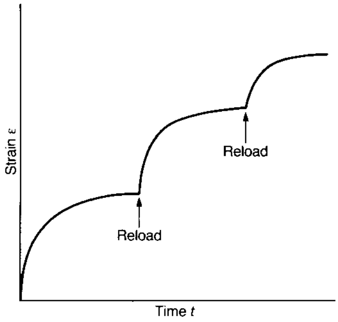

FIGURE 4.8 Boltzmann's superposition principle.

direction. This is a particularly valuable attribute of metals and we shall discuss the reasons in Chapter 9. Meanwhile we consider the more general case as exhibited, for instance, by clays.

We have noted already that the ideal (Newtonian) fluid flows according to:

$$\tau = \eta(\delta\gamma/\delta t) \tag{4.4}$$

where η is the viscosity. When the fluid contains dispersed particles these perturb the pattern of flow and, for dispersed spheres, the viscosity is now given by Einstein's equation:

$$\eta = \eta_0[1 + 5V_f/2] \tag{4.5}$$

where η_0 is the viscosity of the pure fluid and V_f the volume fraction of particles.

The actual viscosities of suspensions are usually much higher than this because the particles are non-spherical. Thus, for randomly oriented dumb-bells,

$$\eta = \eta_0(1 + 3p^2V_f/2) \tag{4.6}$$

where p is the ratio of dumb-bell length to diameter.

The above equations break down still further when the volume fraction of the particles increases to the point where the perturbed regions in the liquid begin to overlap and we find terms in V_f^2 appearing. We are now in the region of pastes, clays, sand, gravel, etc., where the volume fraction of grains is high. Typically, $V_f = 0.65$ for a sand bed and $V_f = 0.95$ for a mixed sand/gravel bed where the sand can fill the spaces between the grains of gravel.

Clearly the mechanical properties are sensitive to the volume fraction of grains, dry clay becomes plastic when water is added to it. At 30 per cent water content, each clay particle is separated by a film of water and it can be modelled into shapes. With more water added the grains float apart to form a slurry.

Pastes and modelling clays, however, are plastic solids rather than viscous fluids. They deform, more or less elastically, up to a certain *yield stress* and can preserve their shape against gravity. This is important to the moulding of bricks and clay pottery. Above this stress, however, they behave like liquids and deform rapidly. This behaviour is described, approximately, by the Bingham equation:

$$(\delta\gamma/\delta t) = (\tau - \tau_y)/\eta \tag{4.7}$$

where τ_y is the yield stress as shown in Figure 4.9. Tattersall and Banfill (1983) have shown that fresh concrete can be considered as a so-called 'Bingham solid' and instance the difference between two concrete mixes having the flow curves shown in Figure 4.9. At low rates of flow, *B* is less workable than *A*; the reverse is true at high rates of flow. At *X* both would be classed as having the same workability.

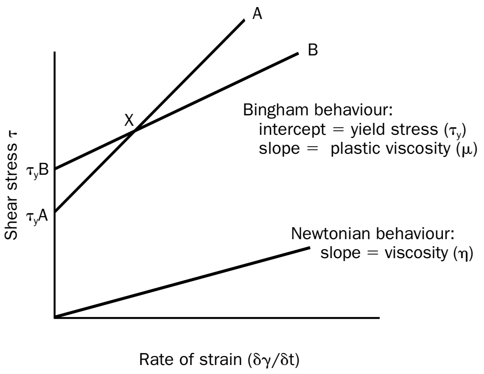

FIGURE 4.9 Newtonian and Bingham fluid behaviour.

Chapter five

Surfaces

All materials are bounded by interfaces of varying nature. For the engineer the most important are the liquid–vapour, solid–vapour, solid–liquid and solid–solid interfaces. The latter exists as the boundary between two differing solid phases in a material, e.g. cement gel and aggregate in concrete, or between two similar crystals which differ only in orientation, e.g. the grain boundaries in a pure metal, or, at the macroscopic level, as the interface between structural components, e.g. concrete and steel. Surfaces owe their interest and importance to two simple features: they are areas of abnormality in relation to the structure that they bound, and they are the only part of the material accessible to chemical change, i.e. all chemical change and, for that matter, most temperature changes take place through the media of surfaces. The importance of surfaces in determining the bulk behaviour of materials naturally depends on the ratio of surface area to the total mass. This, in turn, depends partly on the size and partly on the shape of the individual particles making up the bulk material.

Surface influence on bulk behaviour may reach its zenith with clays, which are composed of platelets that may be as small as 0.01 μm thick by 0.1 μm across. These platelets have a high surface area/volume ratio by comparison with spheres of equal volume. One gram of montmorillonite clay, rather smaller than a sugar cube, may contain a total surface area of over 800 m^2! Porous structures such as cement and wood also contain enormous internal surface areas that exercise a considerable effect on their engineering properties.

5.1 Surface energy

All surfaces have one thing in common: the atoms or ions in the surface are subjected to asymmetric or unsaturated bonding forces; this is particularly the case with solid–vapour and liquid–vapour interfaces. Since bonding is taken to lower their energy (Figure 4.1) the surface atoms or ions will be in a state of higher energy than interior ones. This excess energy is known as the surface energy of the material. In solids the presence of the *surface energy* is not immediately apparent, since the atoms in the surface are held firmly in position. However, with liquids the mobile structure permits the individual atoms to respond, and the result is the well-known surface tension effect. Since surfaces are high-energy regions they will always act to minimise their area, and thus lower their energy, when possible. If a soap film is stretched across a frame with a movable wire as in Figure 5.1, the force required to hold the wire in place is:

$$F = 2\gamma l \tag{5.1}$$

where l is the length of the wire, γ is the surface tension of the soap film/air interface and the factor 2 is introduced because the film has two surfaces. The surface tension is in the plane of the soap film/air interface and has units of force per unit length (N/m). It is important to note that

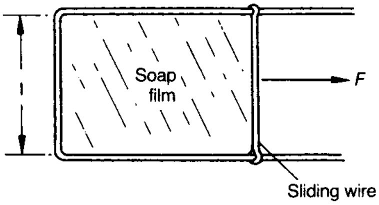

FIGURE 5.1 Equilibrium between soap film and applied force *F*.

surface tension differs from an elastic force acting between the surface atoms in that it remains constant whether the film is forced to expand or allowed to contract. This is because the work done in expanding the film is used to bring additional atoms to the surface rather than to increase the interatomic spacing in the surface. Only when the film has become so thin that the two surfaces interact with each other will the force show partial elastic behaviour, by which time the film is on the point of rupture.

If the film is stretched by pulling the movable wire through a distance d, the work done on it $2l\gamma d$ is stored as surface energy of the newly created surface of area $2ld$, therefore the surface energy per unit area σ is:

$$\sigma = \frac{2l\gamma d}{2ld} = \gamma \tag{5.2}$$

Surface tension and surface energy are numerically equal. The unit of surface energy is $\mathrm{Jm^{-2}}$ ($=\mathrm{Nm^{-1}}$). It should be noted that γ tends to be used interchangeably for both surface tension and energy.

5.2 Water of crystallisation

It is well known that many ionic crystals contain water molecules locked up in their structure as water of crystallisation; such crystals are known in general as hydrates, and their formation can be very important in the development of bulk strength. Both cement and 'plaster of Paris' owe their commercial importance to their ability to take up water and form a rigid mass of interlocking crystals. However, in the case of cement the crystals are so small that it is difficult to decide whether to classify the structure as a crystalline hydrate or a hydrated gel.

Water and ammonia are the only two molecules that can be taken up as a structural part of crystals, and both for the same reasons: they are small molecules which are strongly polar. The small size permits them to penetrate into the interstices of crystal structures where close packing of ions is not possible. This is particularly the case where the negative ion is large, such as SO_4 (sulphate), SiO_4 (silicate) or B_4O_7 (borate). It must be emphasised that this process is not to be thought of as a capillary action, analogous to the take-up of large amounts of water by clays. The water molecules are bonded into definite sites within the crystal structure, and the crystal will only form a stable hydrate if ions of the appropriate signs are available and correctly placed to form bonds with the positively and negatively charged regions of the water molecule. We have already mentioned (page 30) the abnormal properties of water arising from the ability of the molecules to link up by means of hydrogen bonds; the formation of crystalline hydrates is an extension of the same behaviour.

Normally the water molecules cluster round the positive ions in the crystal-forming hydrated ions. This has the effect of making the small positive ion behave as if it were a good deal larger. As a result, the size difference between the positive and negative ions is effectively reduced, thus making possible simpler and more closely packed crystal structures. Water bonded in this manner is very firmly held, in many instances, so that hydration becomes virtually irreversible. Cement, for example, retains its water of crystallisation up to temperatures of ≈900°C.

5.3 Wetting

There are other ways besides reduction in area by which a system of interfaces may reduce its total surface energy. One of the most important technological aspects concerns the behaviour of liquids on solids.

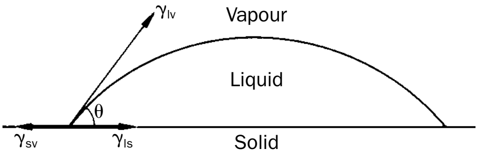

FIGURE 5.2 Surface forces acting at the periphery of a droplet.

If a droplet of liquid is placed on a solid, the immediate behaviour of the liquid depends on the relative magnitudes of three surface tensions (energies): liquid–solid γ_{ls}, liquid–vapour γ_{lv}, and solid–vapour γ_{sv}. At the periphery of the droplet the three tensions operate as depicted in Figure 5.2 and the final contour of the droplet will result when they are in equilibrium, resolved parallel to the solid surface, that is when:

$$\gamma_{sv} = \gamma_{ls} + \gamma_{lv} \cos\theta \tag{5.3}$$

The difference:

$$\gamma_{sv} - (\gamma_{ls} + \gamma_{lv}) \tag{5.4}$$

is termed the *spreading force* and if it is positive then $\theta = 0°$, and complete wetting of the solid surface occurs. The energy of such a system is obviously lowered when the solid–vapour interface is replaced by a solid–liquid and a liquid–vapour interface.

When $\gamma_{sv} - (\gamma_{ls} + \gamma_{lv})$ is negative then $\theta > 0°$ and partial or no wetting occurs. If $\gamma_{sv} > \gamma_{ls}$ then $\gamma_{lv} \cos\theta$ (equation 5.3) is positive and $\theta < 90°$ giving partial wetting. If $\gamma_{sv} < \gamma_{ls}$ (this is comparatively rare, provided the surfaces are clean) then $\gamma_{lv} \cos\theta$ (equation 5.3) is negative and $\theta > 90°$ giving little or no tendency to wetting.

The rise of water in a capillary tube is a consequence of the ability of water to wet glass. If, in Figure 5.3, θ is the angle of contact between water and glass, the water is drawn up the tube by a circumferential force $2\pi r \gamma_{lv} \cos\theta$, so that:

$$2\pi r \gamma_{lv} \cos\theta = \pi r^2 h \rho \tag{5.5}$$

where $\pi r^2 h \rho$ is the mass of water in the capillary, neglecting the mass of water contained in the curve of the meniscus. It follows that the height of the water in the capillary is:

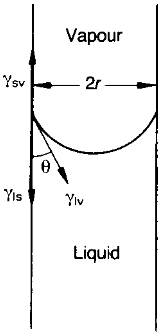

FIGURE 5.3 Capillary rise of liquid up a tube.

$$h = \frac{2\gamma_{lv} \cos\theta}{\rho r} \tag{5.6}$$

If r is small, h can be very large. If all the pores in brick or concrete were continuous, $h \approx 10\,\text{m}$ is possible. Rising damp indeed! Fortunately the pores are not continuous and evaporation keeps the level lower than this.

5.4 Adhesives

The ability of adhesives to spread and thoroughly wet surfaces is highly important, e.g. where glue, molten solder or brazing alloy has to penetrate into a thin joint. Furthermore, the adhesion of a liquid to a solid surface is relevant to the performance of adhesives. The work to break away the adhesive (which may be considered as a viscous liquid) from the solid is the work required to create a liquid–vapour and a solid–vapour interface from an equivalent area of liquid–solid interface, i.e. it is the work to totally 'de-wet' the solid surface. Hence the work to cause breakage at the interface, per unit area, is given by:

$$W = \gamma_{lv} + \gamma_{sv} - \gamma_{ls} \tag{5.7}$$

But from equation (5.3):

$$\gamma_{sv} - \gamma_{ls} = \gamma_{lv} \cos\theta \tag{5.8}$$

and therefore:

$$W = \gamma_{lv}(1 + \cos\theta) \tag{5.9}$$

Thus, the liquid–solid adhesion increases with the ability of the adhesive to wet the solid, reaching a maximum, when $\theta = 0°$ and wetting is complete, given by:

$$W = 2\gamma_{lv} \tag{5.10}$$

For this to be the case $\gamma_{sv} > \gamma_{lv}$ (equation 5.8) and under these conditions fracture will occur within the adhesive, since the energy necessary to form two liquid–vapour interfaces is less than that to form a liquid–vapour and a solid–vapour interface.

Surface tension is also the cause of the adhesion between two flat surfaces separated by a thin film of fluid. Where the surface of a liquid is curved (as for example in Figure 5.4) there will be a pressure difference p across it; if the curvature is spherical of radius r, then:

$$p = \frac{2\gamma}{r} \tag{5.11}$$

In the case of two circular discs, however, the surface of the film has two radii of curvature, as shown in Figure 5.4; r_1 is approximately equal to the radius of the discs and presents a convex surface to the atmosphere whilst $r_2 \approx d/2$, where d is the thickness of the film between the plates, and presents a concave surface to the atmosphere. The pressure difference between the liquid film and its surroundings is now given by:

$$p = \gamma\left(\frac{1}{r_1} - \frac{1}{r_2}\right) = \gamma\left(\frac{1}{r_1} - \frac{2}{d}\right) \tag{5.12}$$

If $d \ll r_1$ then:

$$p = -\frac{2\gamma}{d} \tag{5.13}$$

the negative sign indicating that the pressure is lower within the liquid than outside it.

Since the pressure acts over the whole surface of the discs, the force to overcome it and separate the discs is given by:

$$F = \frac{2\pi r_1^2 \gamma}{d} \tag{5.14}$$

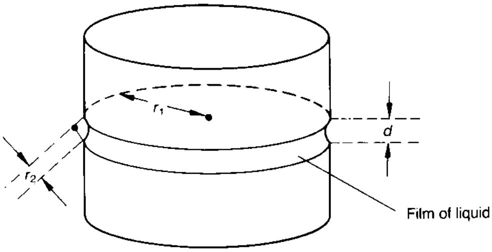

FIGURE 5.4 Adhesive effect of a thin film of liquid between two flat plates. If the liquid wets the surfaces of the discs, then $r_2 \simeq d/2$.

The magnitude of F thus depends on the factor r_1^2/d, and it is therefore important that surfaces to be joined should be as flat and closely spaced as possible. Any reader who has tried to pull apart two wet beer glasses will confirm how tenaciously they cling to each other; by contrast, however, they can easily be slid apart since liquid films have little resistance to shear. If $d = 0.01\,\text{mm}$, $r = 100\,\text{mm}$ and γ (water) $= 0.073\,\text{Nm}^{-1}$ then $F \approx 460\,\text{N}$. This value of F for a liquid film gives some idea of the potential of adhesives that gain additional strength and rigidity by setting to highly viscous materials on polymerisation or solvent evaporation.

5.5 Adsorption

The ability of liquids to wet solids depends very much on the cleanliness of the solid, as anyone with any experience of soldering will appreciate. The presence of any dirt, such as oxide or grease films, will totally alter the balance of surface tensions discussed above and usually prevents wetting.

Clean surfaces, in fact, are so rare as to be virtually non-existent, since the broken surface bonds will readily attract to themselves any foreign atoms or molecules that have a slight affinity for the surface material. This effect is known as *adsorption*, and by satisfying or partially satisfying the unsaturated surface bonds it serves to lower surface energy. Adsorption is a dynamic process, i.e. molecules are constantly alighting on and taking off from the surface.

Different molecules adsorb with varying degrees of intensity, depending on the nature of the bond that is able to form at the interface, and the strength of the bond may be expressed in terms of ϕ_a, the energy of adsorption. As in the case of interatomic bonds, a negative value of ϕ_a is taken to indicate positive adsorption, i.e. the molecules are attracted to the interface, and the surface energy (tension) is lowered thereby. A positive value of ϕ_a indicates a repulsive interaction and the molecules avoid the surface. Typical plots of ϕ_a against the distance of the adsorbed layer from the surface are given in Figure 5.5. They closely resemble the Condon–Morse curves (Figure 4.1) and their shape is due to the same circumstance of equilibrium between attractive and repulsive forces, although the attraction is far weaker than that of the principal interatomic bonds.

If the molecule being adsorbed is non-polar and does not react chemically with the surface, adsorption, if it occurs, will be by Van der Waals bonds, and the minimum value of ϕ_a is small (curve 2 in Figure 5.5). If on the other hand the molecule is strongly polar, as is the case with water or ammonia, the electrostatic forces between the surface and the charged portion of the molecule give rise to stronger bonding. If a chemical reaction occurs as part of the bonding mechanism, e.g. when fatty acid in a lubricant forms an adsorbed layer of metallic soap on a metal surface, the bonding is still stronger (curve 1) and the effect is referred to as *chemisorption.*

The behaviour of water is of particular importance in this context. Because of its ability to form hydrogen bonds with neighbouring molecules, water adsorbs rapidly and strongly on most solid surfaces. Despite the tenacity with which such a layer is held (clay does not lose all its adsorbed water until heated to 300°C), the interaction cannot be thought of as chemisorption; rather it is, in a sense, a halfway stage to solution or alternatively to the taking up of crystalline water of hydration. Bonding is strong enough to maintain a surface layer perhaps several molecules thick, but the affinity is not sufficient for the molecules to penetrate into the interstices of the structure.

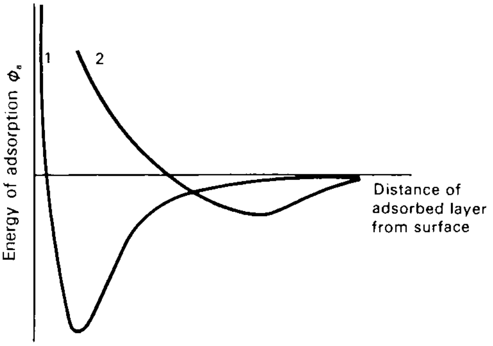

FIGURE 5.5 Energies of adsorption for different adsorption mechanisms: curve 1, chemisorption; curve 2, physical adsorption.

The physical nature of such a film is difficult to visualise; it cannot be thought of as a fluid in the accepted sense of the term even when more than one molecule thick, as in the case of the clays and cements. Yet the molecules are mobile in this situation. They will not desorb readily, but they can diffuse along the surface under the impetus of pressure gradients.

Such movements, occurring over the vast internal surface area of cement gels, are primarily responsible for the slow creep of concrete under stress. The ability of water molecules to penetrate solid–solid interfaces in clays and build up thick adsorbed layers results in the swelling of clays and has caused, and may well continue to cause, considerable structural damage to buildings erected on clays that are liable to behave in this manner. The readiness with which water will adsorb on surfaces is turned to account in the use of porous silica gel and molecular sieves as drying agents.

Chapter six

Fracture and fatigue

The term 'fracture' is often used synonymously with the term 'failure' but the two are not necessarily describing the same process. Failure, in the sense that a component is rendered unfit for further service, can occur without fracture; as, for instance, by excessive deformation or by reduction of load-supporting area due to wear or corrosion. Fracture is the separation of a component into two or more pieces under the action of a static or slowly changing imposed load, at temperatures that are low compared with the melting temperature of the material.

Separation of a component into two or more pieces can also occur under the action of an *impact* (suddenly applied) load; a fluctuating load, *fatigue*; a static load with the component at a temperature above one-half of its melting temperature, *creep rupture*; or the combined action of an imposed load and a chemical reaction, *stress corrosion cracking*.

Brittle fracture occurs when a material absorbs little or no energy prior to fracture. Ductile fracture requires a material that can experience appreciable plastic (i.e. irreversible) deformation and energy absorption prior to fracture. The tensile stress–strain behaviour for brittle and ductile fractures is shown in Figure 6.1. The area under the stress–strain curve up to fracture is a measure of the energy absorbed per unit volume of material, and is termed the *toughness* of the material. Ductile materials exhibit much higher values of toughness than do brittle materials. Figure 6.2 illustrates the extent of deformation associated with brittle and ductile fractures. In the case of ductile fracture, the specimen can experience a considerable change in shape prior to fracture.

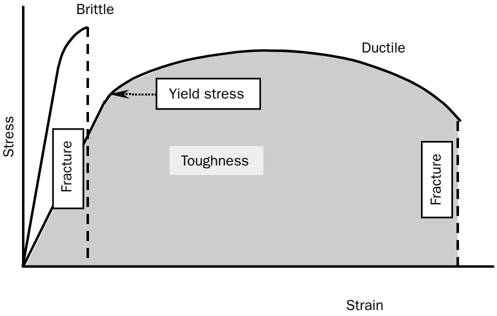

FIGURE 6.1 Schematic of tensile stress–strain curves for brittle and ductile materials taken to fracture.

We shall confine our attention here to ductile and brittle fractures, and to the process of fatigue. Furthermore, we shall only consider uniaxial stressing, although the theory can be extended to cover the case of multiaxial stressing.

The strength of a material is expected to be a function of the interatomic bonding forces. As we have seen in Chapter 4, various approaches based

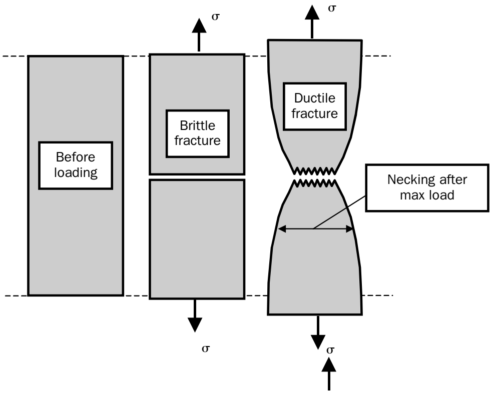

FIGURE 6.2 Schematic of brittle and ductile fractures.

on the Condon–Morse curves (Figure 4.1) predict that the strengths of materials should be of the order of 10 per cent of their elastic modulus values, i.e. ≈*E*/10. However, real materials exhibit very much lower values than this. Brittle materials, i.e. glasses and ceramics, under most conditions, fracture at stresses in the region of *E*/1000, with little deformation. Ductile materials, i.e. most metallic alloys and many polymers, start to deform irreversibly at stresses around *E*/1000 and fracture at stresses between ≈*E*/1000 and *E*/100.

6.1 Brittle fracture

In order to explain the low observed strengths of brittle materials, A.A. Griffith, working on glasses, proposed that the presence of small cracks in such materials controlled their strength. The effect of the cracks is to concentrate stress in the regions around their crack tips so that, although the average stress is very much lower than *E*/10, the stress at the tips is ≈*E*/10 when fracture occurs.

Griffith adopted a thermodynamics approach, i.e. for a crack to grow under a remotely applied uniform static stress, the rate of release of strain energy accompanying crack growth must exceed the rate of absorption of energy. The inference being that when the thermodynamic criterion is satisfied for crack growth the forces carried by the atomic bonds at the crack tips are sufficient for them to rupture. For brittle materials, energy is absorbed in the creation of additional fracture surfaces.

Consider a thin plate of unit thickness containing a central crack of length 2*a* under an applied uniform stress σ (Figure 6.3). The strain energy released by an elliptical region of semi-axes *a* and 2*a* (Figure 6.3) if completely relaxed (unstressed) due to the presence of the crack is:

$$U_R = \frac{\sigma^2}{2E}(2\pi a^2) \qquad (6.1)$$

and the energy absorbed by a crack of length 2*a* is:

$$U_A = 4\gamma a \qquad (6.2)$$

where γ is the surface energy. The factor of 4 takes account of the two crack tips and the two fracture faces. Although the concept of an elliptical region being completely relaxed by the presence of the crack is unrealistic, it turns out that the values predicted by equation (6.1) are quite reasonable.

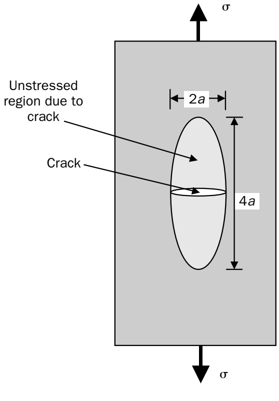

FIGURE 6.3 Schematic of a crack in a uniformly stressed plate.

For crack growth to be possible requires:

$$\frac{dU_R}{da} \geq \frac{dU_A}{da} \qquad (6.3)$$

i.e. the rate of release of strain energy to exceed the rate of absorption. Differentiating equations (6.1) and (6.2) and substituting in equation (6.3) gives:

$$\frac{2\pi\sigma^2 a}{E} \geq 4\gamma \qquad (6.4)$$

and

$$\sigma = \sqrt{\frac{2\gamma E}{\pi a}} \qquad (6.5)$$

Inspection of equation (6.4) shows that for a given applied stress there is a critical value of crack length for crack growth to commence. Furthermore, once crack growth commences the rate of release of strain energy increases continuously with increasing crack length, whereas the rate of absorption of energy remains unchanged. Consequently, crack growth can become very rapid approaching the speed of sound in the material. The large excess of energy released may also result in crack splitting and branching. The minimum value of applied stress required for a crack of length $2a$ to grow is given by equation (6.5). As might have been expected, this predicts that the 'brittle tensile fracture strength' decreases with increasing crack length.

Brittle materials do not exhibit a single value of tensile strength. Real materials contain many flaws (cracks), the size and distribution of which are random, so that the fracture stress is determined by the size and location of the largest defect in the sample. Since no two samples are exactly alike, if fifty samples are tested the measured strengths will show an approximate Gaussian distribution (Figure 6.4(a)). The concept of a mean strength is sometimes useful, but it must be remembered what it actually means. If the data is replotted as a cumulative probability curve (Figure 6.4(b)) the mean stress simply means the stress at which 50 per cent of the samples may be expected to fail. Not a very good design parameter! There are ways of dealing with the problem but, of course, the safest thing to do would be to never subject these materials to tension forces.

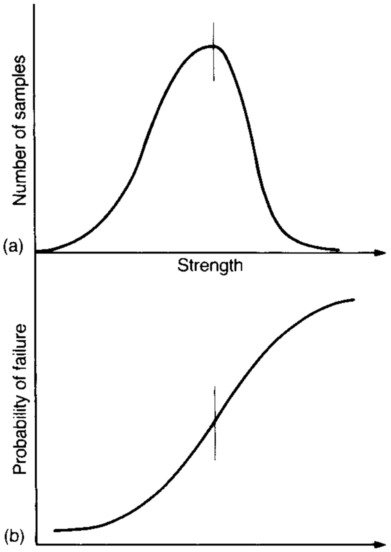

FIGURE 6.4 Strength of brittle solids: (a) distribution of measured strengths; (b) cumulative probability of failure under load.

Fracture in the way described above cannot occur in compression since the applied forces would tend to close the cracks rather than open them. The mechanism is much more complicated and many materials such as glass, stone, brick and concrete are strong in compression, although they are weak in tension. The classical arched and domed styles of architecture testify to the strength of brittle materials in compression.

6.2 Ductile fracture

As indicated earlier, ductile fracture involves appreciable plastic (irreversible) deformation before fracture occurs. Plastic deformation commences at stresses around $E/1000$, or greater, and failure occurs at stresses between $\approx E/1000$ and $E/100$, i.e. at stresses still appreciably less than

$E/10$. Why is this? The crystalline, i.e. periodic, structure of ductile crystalline metals and polymers exhibit many local disruptions at the atomic scale, known formally as dislocations (see Chapter 8). These dislocations are able to move relatively easily under applied stresses of $\approx E/1000$. This movement allows the shape of a material, not its volume, to change relatively easily, i.e. it enables plastic deformation. The stress at which plastic deformation first occurs is termed the *yield stress* or *yield strength* (Figure 6.1).

Ductile fracture occurs when a particular region of a material suffers excessive plastic deformation and necks down sufficiently for the necked region to no longer be able to sustain the applied force (Figure 6.2). The process of necking is aided by the formation of internal necks around impurity particles, which lead to the type of fracture surface indicated schematically in Figure 6.2.

6.3 Fracture mechanics

It was generally thought at one time that the Griffith approach applied only to elastic materials containing flaws, i.e. glass, concrete, fired clay products, ceramics, etc. However, doubts started to arise when structures, including welded steel ships, oil rigs, pressure vessels and aircraft, manufactured from ductile materials, fractured in a brittle manner.

For ductile materials the work involved with plastic deformation as the crack grows is considerably greater than the surface energy term, i.e. 2γ per crack tip. Hence, it is necessary to replace γ in equations (6.2), (6.4) and (6.5) by another term G_c, the *fracture energy*, also known simply as the *toughness*. This is the total energy absorbed per unit increment of crack growth and has units of J/m². Table 6.1 gives some typical values and it will at once be apparent why copper, say, is tough and glass is not.

TABLE 6.1 Fracture energy G_c and fracture toughness K_c for common construction materials

Material	*G_c(J/m²)*	*K_c(MN/m$^{3/2}$)*
Pure, ductile metals	100–1000	100–350
High-strength steels	15–120	50–150
0.2% C plain carbon steel	100	150
Glass fibre reinforced polymers	10–100	20–50
Polyethylene	6–8	1
Reinforced concrete	0.2–4.0	10–15
Common timbers*	0.5–2.0	0.5–1.0
Concrete	0.03	0.2
Glass	0.01	0.8

*Crack parallel to grain.

Equation (6.5) becomes:

$$\sigma = \sqrt{\frac{EG_c}{\pi a}}$$

or, as it is more generally written:

$$\sqrt{EG_c} = \sigma\sqrt{\pi a} \qquad (6.6)$$

The left-hand side of this equation is materials dependent and the right-hand side includes the engineering factors. It is clear that the critical combination of crack length and stress at which fast fracture occurs is a material constant.

The term $\sigma\sqrt{\pi a}$ is abbreviated to a single symbol K, having units of N/m$^{3/2}$, and is called the *stress intensity factor*. Fast fracture occurs when K reaches a critical value K_c, known as the *fracture toughness*.

In the case of ductile materials, G_c is tens of times larger than surface energy γ, so that the crack sizes necessary for the brittle fracture of ductile materials to occur are generally very much larger than for brittle materials. However, such sizes can be realised due to the presence of large impurity particles, holes, notches and, as we will see in the next section, fatigue cracks. Also, service conditions and manufacturing processes can embrittle otherwise ductile materials. Carbon steels are ductile at room temperatures and above, but as the temperature is lowered they experience a transition from ductile to brittle fracture behaviour. The temperature at which this transition occurs depends on carbon content and grain size, but can occur at temperatures above 0°C, so it can have serious engineering consequences. The welding of steels can alter their structure at the grain level and increase the temperature of the ductile to brittle transition temperature.

6.4 Fatigue

Failure by fatigue may occur when a component is subjected to repetitive or cyclically varying stresses. It may occur after the stress has been applied for a thousand cycles or after many millions of cycles, at stresses appreciably below those which the component could sustain under a static stress. Indeed, in the case of a metal, failure may occur at stresses below the yield strength.

Fatigue failure usually originates from a region of concentrated stress, such as an impurity particle in the material or at an engineering feature, such as a hole or notch. Once a fatigue crack has initiated it grows under the action of the cyclic stress until its length is such that its associated stress intensity factor equals the fracture toughness of the material (equation 6.6) when fast fracture occurs. The crack growth region of the fatigue fracture face is relatively smooth whereas, in the case of a ductile metal, the fast fracture region is rougher and characteristic of local plastic deformation. Fatigue failure does not normally involve gross plastic deformation and hence shows similarities with brittle fracture. Ductile metals are particularly prone to fatigue failure, but ceramics and polymers can also suffer from the same phenomenon.

Fatigue performance, in its simplest form, is characterised in the laboratory by plotting experimental stress range versus number of cycles to failure (Figure 6.5). As the stress range is increased the number of cycles to failure decreases. Such curves show considerable scatter and are affected by the environment and surface finish of the test pieces (or components).

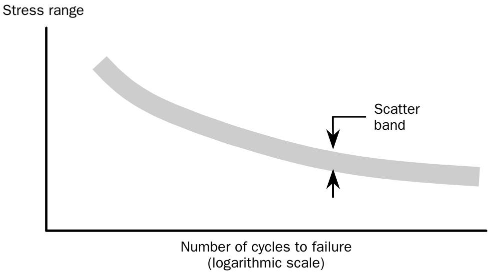

FIGURE 6.5 Schematic of stress range versus fatigue life (number of cycles to failure).

With some reservation it may be stated that, in most buildings, the designer has little to fear from fatigue in the structure itself, though such cases as the collapse of the oil rig Alexander Keilland in 1980, due to fatigue failure in one of the legs, cannot be ignored. Welded joints, if not carefully made, are particularly at risk because of the adventitious introduction of stress raisers in the form of unwelded regions and changes to the material structure. Certainly individual components such as bolts may be at risk under cyclic loading conditions. Fatigue is an important consideration in bridge design.

Chapter seven

Electrical and thermal conductivity

Although electrical conductivity is not a constraint in structural design, thermal conductivity is important and perhaps nowhere more so than in the shell of a building. Nonetheless, we shall briefly consider electrical conductivity since it provides a basis for the more complex ideas of thermal conductivity.

Some typical values of electrical and thermal conductivity are given in Table 7.1. Electrical conductivity is defined as the current per unit cross-sectional area of conductor, per unit voltage gradient along the conductor. Thermal conductivity is defined similarly. It can be seen that:

- metals are good conductors of heat and electricity;
- non-metals are poor conductors;
- there is an approximate relationship between electrical and thermal conductivity in metals. This is not true of non-metals.

The structure of the metallic bond was described earlier as an 'electron cloud' and as long as no electrostatic field is applied, the free electrons in a metal behave in much the same way as the particles in a gas, i.e. they move around randomly and collide elastically with each other and with the

TABLE 7.1 Electrical and thermal conductivities of a range of materials. Gases are at STP, other substances are at 0°C (273 K)

	Electrical conductivity $(\Omega m)^{-1}$	*Thermal conductivity* $W/m-K$	*Wiedemann–Franz ratio* $\Omega - W/K^2$
Air		24.1×10^{-3}	–
Oxygen		24.4×10^{-3}	–
Nitrogen		24.3×10^{-3}	–
Brick	5×10^{-7}	1	7.3×10^{3}
Concrete (dry)	1×10^{-9}	1.4	5.1×10^{6}
Glass	1×10^{-10}	1.0	3.7×10^{7}
Polyethylene	1×10^{-16}	0.5	1.8×10^{13}
Aluminium alloys	2.1×10^{7}	150	2.6×10^{-8}
Copper	6.0×10^{7}	390	2.4×10^{-8}
Lead	0.6×10^{7}	35	2.1×10^{-8}
Silver	6.8×10^{7}	420	2.3×10^{-8}
Steel	0.9×10^{7}	50	2.0×10^{-8}

stationary ions in the lattice. However, when an electrostatic field is applied, the electrons drift preferentially and, being negatively charged, they 'drift' towards the positive 'pole', though the random motion still remains. In drifting, they collide more frequently with the 'stationary' ions. This provides a resistance to drift, which increases with temperature.

The force F tending to accelerate each electron is:

$$F = Ee \tag{7.1}$$

where e is the charge on the electron and E is the electrostatic field.

The bodily movement of the electrons J, i.e. current per unit cross-sectional area, can be expressed as:

$$J = neV_a \tag{7.2}$$

where n is the concentration of free electrons and V_a is the *drift velocity*. Since metals contain a large concentration of free electrons the flux is high. Thus, as Ohm's law states, current is directly proportional to voltage (potential difference) and inversely proportional to resistance, $I = V/R$. Since non-metals are either ionically or covalently bonded there are few free electrons, hence their low conductivities.

Thermal conductivity in metals follows much the same general argument, though here it is not the bodily movement of electrons but rather the transference of heat energy by collision. The analysis is, however, much more complicated but it is intuitively obvious that the higher the temperature, the greater the excitation of the electrons and the larger the number of collisions. Since, in metals, both thermal and electrical conductivities have their origins in the same structural features the proportionality apparent in Table 7.1 is not surprising. It is known as the Wiedemann–Franz ratio and has a theoretical constant value of $2.44 \times 10^{-8}\,\Omega - \mathrm{W/K^2}$, which should be independent of temperature if heat flow is entirely by free electrons.

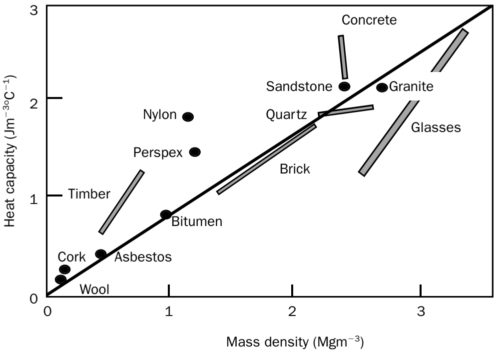

FIGURE 7.1 Thermal capacities of various substances.

The thermal conductivity of non-metals is more complex still, since it involves energy transfer between the atoms which make up the material. Heating of the material manifests itself as increasing vibration of the nominally stationary atoms. What is important to note, however, is that the thermal conductivity is controlled largely by the product of the mass density and the specific heat at constant volume C_v. This is called the *heat capacity*. Specific heat is the heat energy required to increase the temperature of unit mass of the material by one degree. Figure 7.1 shows that light materials with an open structure are better insulators than heavy, compact materials.

Moisture has a significant effect on the thermal conductivity of porous materials. If the pores are filled, the water acts as a bridge and since the conductivity of water is many times greater than that of air, the resulting conductivity is greater. At the same time, water is denser and has a higher specific heat so that the heat capacity also increases.

Further reading

General

Ashby, M.F. and Jones, D.R.H. *Engineering Materials*, Pergamon Press, Oxford.

- Vol. 1 (2nd edn, 1996) An introduction to their properties and applications.
- Vol. 2 (1986) An introduction to microstructures, processing and design.
- Vol. 3 (1993) Materials failure analysis.

Certainly books to be dipped into. Perhaps a little detailed for easy reading but with a set of excellent case studies which illustrate the engineer's approach.

Callister, Jr, W.D. (2000) *Materials Science and Engineering, An introduction*, 5th edn, John Wiley & Sons Inc., New York.

A comprehensive introduction to the science and engineering of materials.

Gordon, J.E. (1976) *The New Science of Strong Materials – or Why You Don't Fall Through the Floor*. Penguin Books, Harmondsworth, Middlesex.

Gordon, J.E. (1978) *Structures – or Why Things Don't Fall Down*. Penguin Books, Harmondsworth, Middlesex.

Excellent and very readable. Read them on the bus or in the bath. They will tell you more than many hours of library study.

Petrowski, H. (1982) *To Engineer is Human,* Macmillan, London.

Petrowski considers what it is like to be an engineer in the twentieth century and lays some emphasis on the things that have gone wrong. Not a book for those lacking in self-confidence but good (and easy) reading.

Van Vlack, L.H. (1989) *Elements of Materials Science and Engineering,* 6th edn, Addison Wesley, New York.

Fairly elementary but expands upon matters dealt with in this part.

The symposium *Design Life of Buildings* (Institution of Civil Engineers, 1985, Thomas Telford, London).

Scarcely a textbook but the papers cover many aspects of the engineer's profession. Well worth a glance at those papers that may interest you.

Specialist

Angrist, S.W. and Hepler, L. (1973) *Order and Chaos,* Harmondsworth, Middlesex.

A helpful (and non-mathematical) introduction to thermodynamics. Recommended as bedtime reading.

Cottrell, A.H. (1964) *The Mechanical Properties of Matter,* John Wiley, New York.

First class, scientific and of much wider coverage than the title suggests. Essential reading for any student wishing to follow up the concepts herein and highly desirable reading for all students of all branches of engineering.

Freudenthal, A.M. (1950) *The Inelastic Behaviour of Engineering Materials and Structures,* John Wiley, New York.

Old now but still very readable in the way it deals with materials in relation to their structures. Not easy to read, but good.

Houwink, R. and De Decker, H.K. (eds) (1973) *Elasticity, Plasticity and Structure of Matter,* 3rd edn, Cambridge University Press, Cambridge.

You need to be pretty strong-minded for this, but where else could you find out about the rheology of baker's dough or of liquid paints, gelatins and glues or soaps? They may not be 'engineering' as defined by your average university lecturer but they are all materials and it never does to assume that the findings of one discipline are inapplicable to another.

Treloar, L.R.G. (1949) *The Physics of Rubber Elasticity,* Clarendon Press, Oxford.

Old now and pretty hard going, but the classic work on the subject. Perhaps overtaken by Aklonis, J.J. and MacKnight, W.J.L. (1983) *Introduction to Polymer Viscoelasticity*, 2nd edn, John Wiley, New York.

Part Two

Metals and alloys

W.D. Biggs

Revised and updated
by I.R. McColl and
J.R. Moon

Introduction

Useful metals have been known to mankind for a long time and probably came into service very gradually. Stone tools were adequate for many purposes in early cultures, but when metals became available they offered many advantages. Metals could be strong and hard, but their chief advantages were in their ductility. This enabled them to withstand a blow and the range of shaping procedures and products that became possible. The significance to us all is encapsulated in the ideas of the Stone Age, Bronze Age and Iron Age. Metals and their differences have even been the subject of poetry. Thus, from Rudyard Kipling:

> Gold is for the mistress – silver for the maid,
> Copper for the craftsman – cunning at his trade,
> 'Good!' said the Baron, sitting in his hall,
> 'But iron – cold iron – is master of them all.'

Most metals are found in nature as ores, oxides, sulphides, carbonates, etc. *Extraction metallurgy* is that aspect of the art concerned with extracting the metals from these compounds. The basic chemistry is generally fairly simple. The industrial problem is to do the job on a big enough scale to make it economically worthwhile. The converse problem also exists. When a metal is exposed to a working environment it will tend to revert to the appropriate compound, i.e. it corrodes. Rust on steel is almost the same as the ore from which iron is extracted. Thus, the metallurgist has two tasks, to get the metal extracted from its ore and then to keep it that way.

The origins of extraction metallurgy are in prehistory and it is supposed that early discoveries were made accidentally: a piece of rather special rock when heated in the reducing atmosphere of a fire gave up some metal. Copper, lead and tin were amongst the earliest to be produced this way, and alloys such as bronze (copper and tin) and brass (copper and zinc) followed. Bronze was much prized for its ability to be cast into shapes or mechanically formed, as well as for its combination of strength, hardness and toughness.

Unaided fires can reach temperatures of about 1100–1200°C on a good day. This is sufficient to melt all the metals referred to so far, but cannot cope with iron, which melts at about 1550°C. The early history of iron involved extraction processes which gave rise to solid lumps of very porous and friable metal, mixed with a glassy slag. This was formed into useful articles by hammering at temperatures high enough to melt the slag. The slag was partially squeezed out and the pores closed. The product is *wrought iron*, a technical term with a specific meaning in metallurgy. There were later improvements, particularly in the eighteenth century, but iron remained an expensive and precious material until the technology for reaching higher temperatures evolved.

The eighteenth and nineteenth centuries saw the development of a forced air blast to raise the temperatures in blast furnaces enough to make liquid iron possible. In the furnace, this picked up about 4 mass per cent of carbon from the fuel, which had the advantage of also lowering the melting temperature of the alloy. The product, pig iron or cast iron, was brittle but easily cast into moulds and found a wide range of uses in engineering and as household articles.

The problem was that to make tough iron or steel required a much lower carbon content and, consequently, a higher melting temperature. It was Henry Bessemer who worked out how to do this on a large scale. A Bessemer converter blew cold air through a molten bath of pig iron to oxidise the impurities, including carbon, to leave relatively pure liquid iron. The oxidation process generated enough heat to raise the melt temperature enough to keep the material molten as it became purer. The whole process, from start to finish, took about an hour and produced about 10 to 20 tonnes of steel, not much by today's standards, but revolutionary at the time. A slower, but more easily controlled process also came into use. Large pools of metal were melted in shallow hearths and oxidation achieved by reactions with a covering slag and controlled additions of iron oxide.

Both processes have been superseded by more efficient methods. The basic oxygen converter is based on Bessemer's principle, but uses oxygen rather than air. No heat is wasted in heating the 80 per cent of air that is nitrogen. The oxygen is blown in from the top through a lance. Several hundred tonnes per hour are possible from modern furnaces. Much steel is also produced from remelted scrap, for which purpose electric arc furnaces are often used: good control over material quality is possible using well-characterised scrap.

The development of freely available supplies of electricity in the late nineteenth century allowed aluminium to be extracted on a commercial scale: this metal has to be extracted electrolytically from molten salts.

Many other metals, magnesium being one, are produced electrolytically and the process is exploited in the refinement of still more metals, copper for instance. Electrical power is also essential to the production of the 'modern metals', such as titanium.

Physical metallurgy (Chapter 8) deals with the structure of metals with the aim of designing and producing internal structures to meet the properties desired. This provides a basis for understanding the properties of metals and alloys which are subsequently described.

We should emphasise that metals need to be shaped into a great range of artifacts if they are to fulfil the needs of the engineer. This is the area of *mechanical metallurgy*, dealt with in Chapter 10, involving understanding and control of processes such as hot working, cold working and joining. Many of these processes remained small scale until the advent of steam power in the Industrial Revolution. The rolling mill, developed in the eighteenth century, revolutionised the speed of production of long shapes. One of the most important features of these processes and perhaps the least understood is that they allow metallurgists to control the internal microstructures of the materials and through that their properties.

Chapter eight

Physical metallurgy

8.1 Grain structure

Probably the greatest single breakthrough in our understanding of the properties of metals was made by Henry Clifton Sorby in the latter part of the nineteenth century. He developed a technique by which the structure of metals could be examined using an optical microscope. Despite many advances since that time, *metallography*, as it is known, remains the most widely used tool of the metallurgist. Figure 8.1 shows the structure of a pure metal. It consists of an assembly of minute, interlocked grains. There are a number of ways by which such a structure can develop. Here we consider one of them, the solidification of a pure metal.

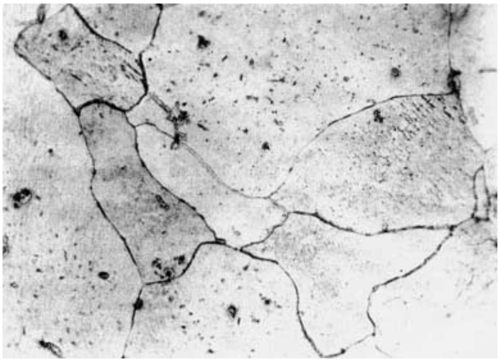

FIGURE 8.1 The microstructure of Armco iron.

We noted in Chapter 1 that, in a liquid, the atoms are in a state of constant motion and change positions frequently. As a liquid cools the motion of the atoms becomes more sluggish and, sooner or later, the atoms arrange themselves into a pattern that forms the nucleus of the solid material. The kinetics of nucleation are quite complex. We note here only that nucleation of the solid almost always begins from an impurity particle in the melt. Let us not worry too much about the conditions for nucleation of a solid crystal, but rather concern ourselves with the growth thereafter. Suppose we assume that a solid nucleus has formed within a liquid melt and that it has the geometrical configuration of an elementary cube of atoms. As the metal solidifies it must give up the latent heat of solidification. The corners of the cube lose heat faster than the edges so that atoms from the melt attach themselves to the corners first, then to the edges and last of all to the faces of the elementary cube. Thus a branching pattern or *dendrite* is built up from each nucleation site (Figure 8.2) and dendrites will grow from each site until they are stopped by interference from other dendrites.

Eventually the liquid is used up by infilling between the arms of the dendrites and the characteristic polycrystalline structure results (Figure 8.2(f)). There are three important facts to note here:

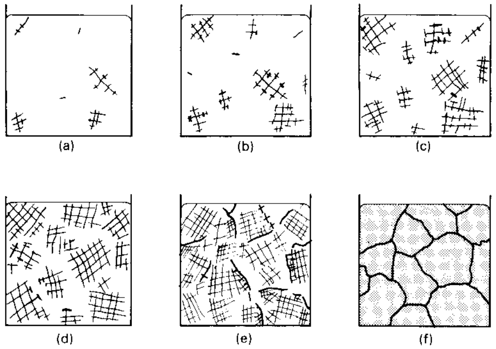

FIGURE 8.2 Solidification of a metal by dendritic growth (schematic).

1. within each grain the atoms are arranged in a regular lattice;
2. the orientation of the crystal lattice differs from grain to grain;
3. at each grain boundary there is a line of mismatch in the atomic arrangement.

In practice few metals are really pure and it would be prohibitively expensive to make them so. Most, of course, are deliberately alloyed. In these cases compositional changes accompany the solidification process, as described in Chapter 2, and the microstructural developments are more complex.

8.2 Crystal structures of metals

It will be recalled from Chapter 3 that the nature of the metallic bond allows development of crystalline structures in which each metal ion is bound in a non-directional way to all its immediate neighbours. Metal ions, therefore, tend to pack as closely as possible in order to achieve as high a density as possible. This requirement means that most metals have, at any given temperature, one of only three crystal structures. Compare this with the enormous range of structures met in ionic and covalent solids. What structures are most likely? We will think of the ions as being equally sized and incompressible, like billiard balls, and find how these might be packed together to achieve maximum density. We begin with one ball. The maximum number of others that can be packed around it in one plane is six (Figure 8.3). By continuing the plane, a close-packed plane is built up.

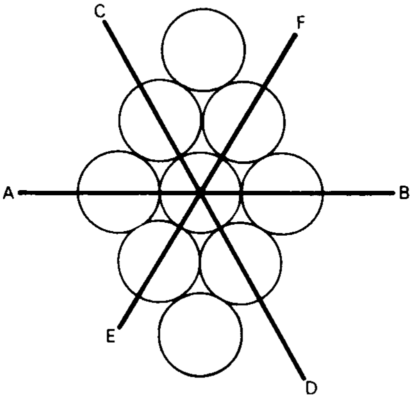

FIGURE 8.3 Close-packed directions in a close-packed plane of spheres.

There are now two possible arrangements for the next plane provided that each sphere is in contact with three spheres below (Figure 8.4). The second layer is placed in the dimples at BBBB…, etc. But putting a third plane in place offers two options about where to put it. The spheres may be placed either in positions vertically above the original spheres to give the sequence ABABAB…, or they may be placed in the unoccupied dimples CCCC…, which are vertically aligned with neither the spheres in the first or the second layer, to give ABCABC… (Figure 8.4).

At first sight these differences in stacking may appear to be trifling but they have important consequences. We define these structures in terms of a unit cell and visualise the metal as composed of an *array* of such cells. The ABABAB … arrangement gives us the hexagonal close-packed (hcp) structure (Figure 8.5 (a)). The ABCABC … arrangement gives us the face-centred cubic (fcc)

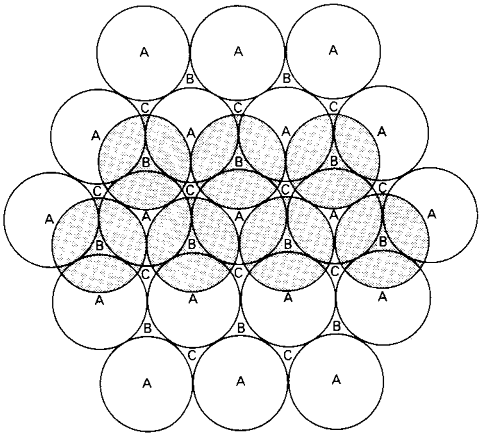

FIGURE 8.4 The B spheres (shaded) rest on the A spheres. A third close-packed layer may then rest on the B spheres either directly above the A spheres or in C positions.

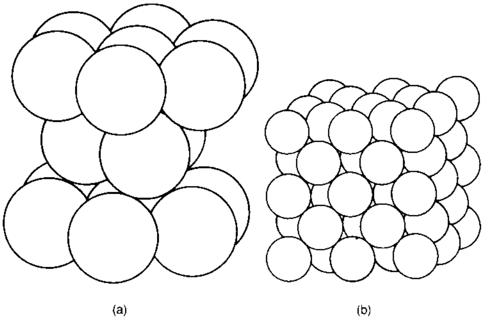

FIGURE 8.5 (a) The close-packed hexagonal structure. (b) The face-centred cubic structure (from W. Hume-Rothery and G.E. Raynor (1956) *The Structure of Metals and Alloys*, by permission of the Institute of Metals).

arrangement (Figure 8.5 (b)). At first sight this does not appear to be close packed, but a view on the diagonal plane XYZ (Figure 8.6) shows that it is. These two structures represent the closest possible packing of spheres of equal size. In each case the spheres occupy 74 per cent of the volume available.

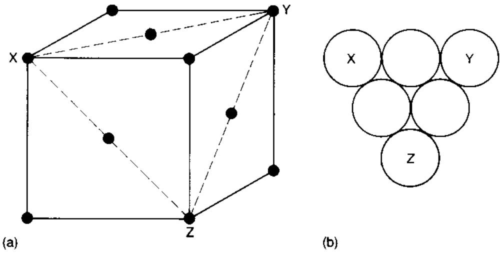

FIGURE 8.6 Face-centred cubic structure: (a) location of atomic sites and (b) view on XYZ plane showing close packing.

There is a third common structure in which the atoms are not quite close packed. This is the body-centred cubic cell (bcc) shown in Figure 8.7.

Metals crystallising in the above forms are:

fcc – aluminium, copper, nickel, iron (above 910°C), lead, silver, gold;
hcp – magnesium, zinc, cadmium, cobalt, titanium;
bcc – iron (below 910°C), chromium, molybdenum, niobium, vanadium.

Why do these differences occur? Why is aluminium fcc and magnesium hcp? We expect that the structure adopted is the one that gives the crystal the least internal energy, although this

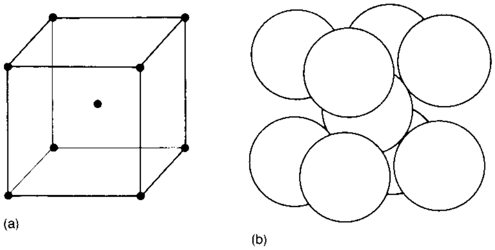

FIGURE 8.7 The body-centred cubic structure: (a) expanded unit cell and (b) sphere model of unit cell (from W. Hume-Rothery and G.E. Raynor (1956) *The Structure of Metals and Alloys*, by permission of the Institute of Metals).

structure need not necessarily be close packed. The energy difference between different structures is often very small and the crystal structure that has the lowest energy at one temperature may not have the lowest energy at another. These various forms are called *allotropes*. Changes from one structure to another, brought about by changes of temperature, are of fundamental importance to metallurgical practice. For example, the change from fcc to bcc as the temperature of iron is reduced through 910°C forms the foundation of the metallurgy of steel.

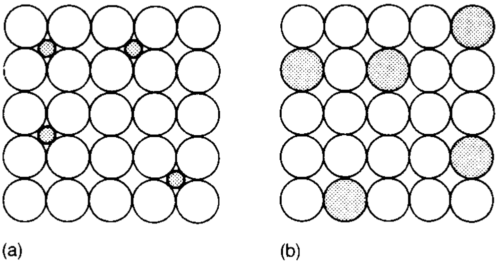

FIGURE 8.8 Solid solutions: (a) interstitial and (b) substitutional.

8.3 Solutions and compounds

Very few metals are used in the pure state, they are nearly always *alloyed* with other elements to obtain better mechanical properties. The phases that can form in any given alloy system and the ranges of composition and temperature for which they are stable are summarised in equilibrium diagrams, which we discussed in some detail in Chapter 2. We saw there that some alloying elements can dissolve in the basis metal to form *solid solutions*. Some elements dissolve readily, some with more difficulty. Iron can only dissolve 0.007 mass per cent carbon at room temperature, but copper can dissolve 30 per cent zinc to make brass. In the copper–nickel system, including Monel metal, cupronickel, etc., there is complete solubility of nickel in copper and of copper in nickel.

There are two principal classes of solid solution. In one, small atoms, such as carbon and nitrogen, fit into the spaces between the larger atoms. This is an *interstitial solid solution* (Figure 8.8 (a)). The solubility of the small atoms is generally limited, but the effects on properties can be dramatic. In the other class, the dissolved atoms are similar in size and chemistry to those of the host metal and they simply replace some of the host atoms to produce a *substitutional solid solution* (Figure 8.8 (b)). The classic example is copper–nickel, which are similar chemically and where the sizes of the ions are 0.127 nm and 0.125 nm, respectively. Substitutional solid solutions may be random (they mostly are) or ordered depending upon what sort of neighbours the ions find most comfortable in energy terms.

However, some atoms do not fit comfortably into the host lattice. At some limit, the energy of the lattice is increased to a critical value and the surplus atoms are rejected, usually as an *interme-*

FIGURE 8.9 Relatively coarse pearlite in a plain carbon steel (×200) (from A.R. Bailey (1967) *The Structure and Strength of Metals*, by permission of Metallurgical Services Laboratories Ltd).

diate compound, such as iron carbide (Fe_3C) in steel, or $CuAl_2$ in some of the heat treatable aluminium alloys (see Chapter 12). Generally such compounds are hard and brittle and exert a 'reinforcing' effect upon the matrix of softer metal in which they are dispersed. Figure 8.9 shows Fe_3C in carbon steel and it will be noted that the 'reinforcement' occurs at the microscopic level of resolution. Some intermediate compounds are used in their own right, such as tungsten carbide for cutting tools.

The metallurgist refers to these solid solutions and compounds as 'phases'. A phase is simply a material, or part of a material, which has the same structure and properties. Much of the science and technology of physical metallurgy is concerned with organising manufacturing schedules to get the right phases together in the most appropriate geometrical dispersion. This *microstructure* of the material is what controls its strength and the properties related to strength. The interplay between manufacturing, microstructure and properties is what modern materials science and engineering is all about. In doing these things, the equilibrium diagrams for the particular alloy systems are uppermost in the mind. A full discussion is beyond the scope of this chapter and the reader is referred to the standard texts such as Cottrell (1967).

Chapter nine

Mechanical properties of metals

Materials scientists tend to divide properties into two groups – *structure insensitive* and *structure sensitive*. Structure insensitive properties are wholly invariant, they are associated with the properties of the atoms themselves and the primary forces between them. They do not depend on the microstructure. The principal properties here are mass, density, elastic modulus, specific heat, thermal expansion coefficient and, to a lesser extent, some chemical and electrical characteristics. On the other hand, structure sensitive properties are wholly dependent upon the microstructure of the material, which in turn is generated by its past history; whether hot rolled or cold rolled, whether heated and cooled, and, if so, how. All of these processes influence the final microstructure, and, through that, can be used to manipulate the properties of the material. From the designer's point of view, the most important structure sensitive properties are the *yield strength, fracture strength (or energy), ductility and the performance in fatigue.*

9.1 Stress–strain behaviour

The most commonly used form of tension test uses an arrangement in which the test piece is elongated in series with a device to measure the load generated by the stretching. It gives rise to behaviour like that in Figure 9.1.

Up to *A*, the behaviour is essentially elastic (see Chapter 1) but at *A* it changes. This point is variously called the *yield point* (YP), the *yield stress* or *strength* (YS), the *limit of proportionality* (LP) or the *elastic limit* (EL). We shall generally use the first, yield point, not because it is the most descriptive but because it (or yield stress) is most widely used in specifications. Below the yield point the material returns to its original dimensions on unloading. Beyond the yield point it is permanently deformed. Try squeezing a beer can, first lightly, and it takes no notice, then squeeze it hard and it stays deformed.

The yield stress is of particular importance for structural designers as it is often chosen to be the level which the stresses in service should not exceed, or even approach. In Figure 9.1, the yield stress is easily defined as there is a distinct change of slope at point *A*, but this is not the case with many materials. An equivalent, the *proof stress*, is then used, which is obtained as shown in Figure 9.2. A small strain is chosen, typically 0.1 or 0.2 per cent, and a line drawn through this value on the strain axis parallel to the initial linear part of

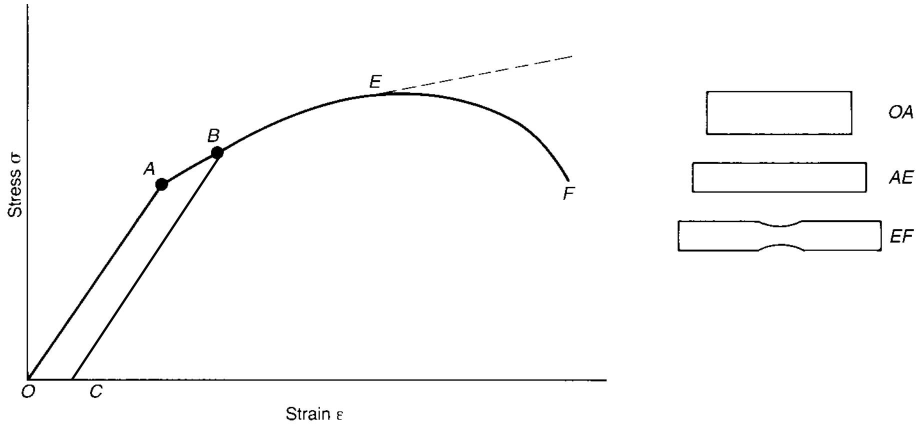

FIGURE 9.1 Tensile stress–strain curve (schematic). From *O* to *A* the bar remains substantially constant in shape; from *A* to *E* it lengthens but reduces uniformly; at *E* it forms a 'neck' at which fracture eventually occurs.

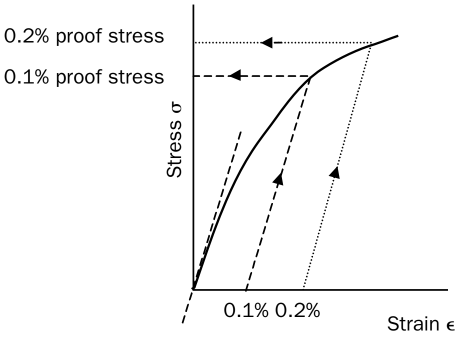

FIGURE 9.2 Determination of proof stress when the yield point is not well defined.

the stress–strain curve (or to a tangent to the curve at the origin if it is entirely non-linear). The point of intersection with the stress–strain curve then gives the 0.1 per cent or 0.2 per cent proof stress.

Once the yield stress is passed, reversing the direction of stretch gives an unloading line like *BC*. There is a permanent deformation *OC*, known as plasticity. But here is the interesting fact. Once you reload it to *B* it goes on as before. In other words, if we took a new beer can it would start to deform at stress *A*. If we take another, loaded it to *B* and then unloaded it, it will not start to deform again until the stress *B* is reached. What an interesting phenomenon! Overload a metal and it gets stronger. We call this *strain* or *work hardening*. It was the principal method used by early blacksmiths to produce harder, stronger bronze and iron by cold hammering. It is of importance (and comfort) to the structural engineer since it forms the basis of what is known as 'plastic design' of structural steelwork. If parts of structural steelwork are 'overloaded', they deform plastically and the imposed stresses are redistributed away from the overloaded parts.

9.2 Tensile strength

At point *E* in Figure 9.1 the load falls away. This occurs because, as the material starts to deform locally, a waist or neck is produced. In this neck the material is continuing to get stronger but its cross-sectional area is decreasing faster, and the load that can be sustained decreases. Fracture will eventually occur in the necked region. This does not always happen. Sometimes, failure occurs before the necking process can begin. Service fractures in such materials can be sudden and unexpected (Chapter 6).

In the early days of testing, the change in behaviour at *E* was readily observed and was described as the *ultimate tensile strength*, a term which is still in use. Its value is of little concern to the designers of structures and artifacts, but is of appreciable interest to those who have to shape the parts by deforming them.

If the reduction in area is measured in the neck region when it has formed, and the true stress, that is, load/actual area, is calculated, the dashed curve is obtained (Figure 9.1), i.e. increasing stress up to failure, which is a much more logical behaviour than reducing stress. This curve can be described by simple mathematics, although this is rarely done except for research purposes.

9.3 Ductility

The reduction in cross-sectional area of the test piece at the site of fracture, and the total elongation at fracture, are both conventionally used as measures of ductility. Unfortunately, elongation to fracture is a function not only of material behaviour but also of test piece geometry. Long test pieces will appear to be less ductile than short ones of the same diameter. This is a consequence of necking, which is concentrated into a length equal to about two or three diameters. Reduction in area does not suffer as markedly from this problem, although round and square section test pieces may give differing results. It is for these and other reasons that test piece geometries are subject to rigorous standards.

As yield strength and tensile strength increase, ductility and fracture toughness decrease (Figure 9.3). For example, cold working a material will raise its yield strength ever closer to the tensile strength, but at the same time the reserve of ductility is diminished and, in the limit, the material will snap under heavy cold working. This is familiar to anyone who has broken a piece of wire by continually bending and rebending it.

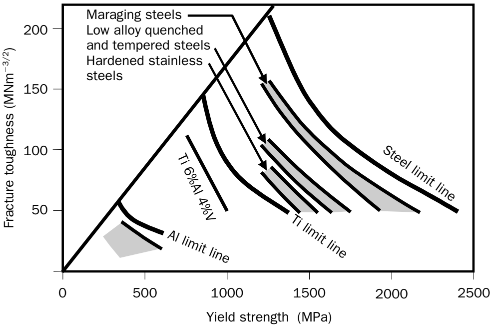

FIGURE 9.3 Relationship between fracture toughness and yield strength for a range of alloys (after Dieter 1988, Mechanical Metallurgy, McGraw-Hill, London)

9.4 Plasticity

This is one of the most important properties of metals and one that we should all be grateful for. If you run your car into a tree, the wing, etc., will be seriously deformed, but in doing so will absorb energy. Careful design, based on this idea, underlies the use of crumple zones to improve safety. It also makes possible a wide range of shaping methods.

Clearly, at the yield stress (see Figure 9.1), the behaviour changes from recoverable (elastic) deformation to one which adds permanent deformation. Early observations on specially prepared samples showed that at the yield stress, whole rows of atoms slide bodily past each other rather like a pack of cards (Figure 9.4). This is known as *slip*. It is a shear deformation produced by a shear stress. Further theoretical consideration showed that the energy required to shear a whole plane of atomic bonds was far greater than the strain energy applied at yield, and an alternative mechanism was sought. Suppose you want to move a heavy carpet lying on a rough floor. The way not to do it is to try to move it bodily; the frictional forces over the whole area are considerable. The more economical way is to create a small ripple in the carpet and then to work it across to the other edge. The force required is

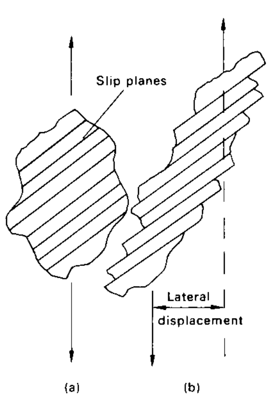

FIGURE 9.4 (a) Crystal under stress. (b) Free unconstrained yielding results in considerable lateral displacement. (c) Rotation of slip planes during deformation permits elongation with very little overall lateral movement.

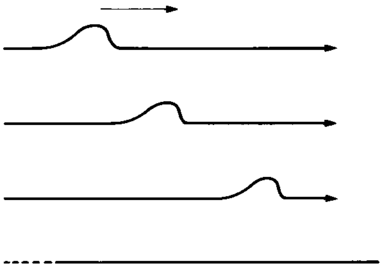

FIGURE 9.5 How to move a heavy carpet.

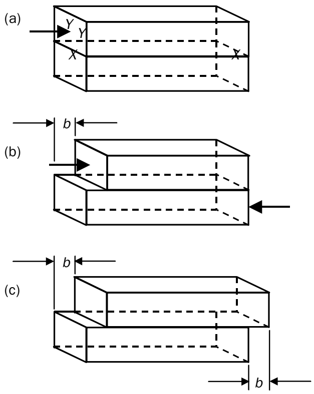

FIGURE 9.6 Illustration of the slip process.

small because the friction between the carpet and floor is easily overcome locally (Figure 9.5).

This is a good analogy for the mechanism that exists in metals, and which provides the answer to a puzzle met in Chapter 6. There, the theoretical strength of a material was estimated to be ≈E/10, but we know the practical strengths to be ≈1/100 of this. Think about Figure 9.6. We want to shear the top half of the metal over the bottom half along the shear plane *XX*. We hold the bottom half rigidly and push hard over the surface *YY* so that the material is displaced by one atom spacing (Figure 9.6 (b)). The opposite surface at the other end of the slip plane has not moved. This means that we have more atoms per unit length along the slip plane in the top half than in the bottom. The atoms do not squeeze up evenly all along the plane.

Somewhere along the plane the picture looks like Figure 9.7. On either side the crystal appears to be perfect, even across the slip plane. But we have generated a *dislocation*. Because only one interatomic bond, that at *X*, is unsatisfied, it takes only a small shear stress to move the site of the dislocation to the left or the right. If it continues on its way from left to right it will eventually reach the opposite surface and produce one unit of slip (Figure 9.6 (c)). You will see that the dislocation represents a boundary; to the left, the material has slipped, to the right it has not. Three-dimensionally, the dislocation can be thought of as a small core which extends perpendicular to the plane of Figure 9.7. Looked at from a distance it looks like a line and for this reason it is known as a *line defect*.

The slip produced by one dislocation is an interatomic distance, typically ≈0.2 nm. Imagine now taking a cube of metal, 50 mm edge, and

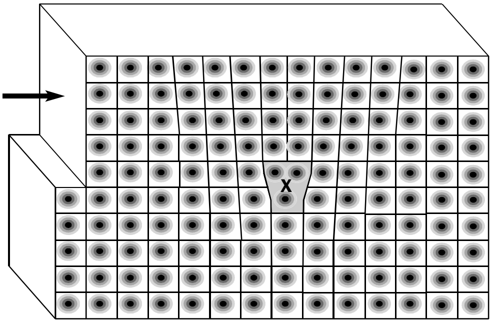

FIGURE 9.7 Illustration of one type of dislocation – an edge dislocation.

deforming it between two parallel plates so that its height is halved. A simple calculation concludes that this requires the movement of ≈100 million dislocations. If it is all done in about one second, as in drop forging, the average dislocation speed has to be about 90 km/h. We need lots of them, moving fast, to give us plasticity on a practical scale. They arise in the manner described above and also from errors in assembling crystals during solidification and other ways.

It is important to note that dislocations can move only along certain atomic planes within the lattice. These are the *slip planes* and generally are the close-packed planes in the crystal. The hcp metals have a fairly restricted number of slip planes; the bcc and fcc metals have many.

9.5 Dislocation energy

The atoms at the core of the dislocation are displaced from their proper positions. We can express this in terms of a strain. It is approximately 1/2 so that the corresponding stress is of the order of $G/2$, where G is the shear modulus, and the strain energy per unit volume is about $G/8$. If we now assume that the radius of the core is about the size of the atom b, the cross-sectional area of the core is πb^2 and its total volume is $\pi b^2 l$, where l is the length of the dislocation line. Hence, the total dislocation energy per unit length is:

$$U/l = \pi G b^2/8 \approx G b^2/2 \tag{9.1}$$

which has units of J/m or N.

In order to minimise the energy, the dislocation line tries to be as short as possible. It behaves as if it were an elastic band under a tension T, the value of which is identical with U/l.

$T \approx Gb^2/2$ is actually very small, but, relative to the size of the dislocation, it is large and it plays an important role in determining the way in which obstacles of one sort or another can obstruct the movement of dislocations.

9.6 Strengthening of metals

Although we must take care not to lose too much ductility and toughness, the critical property in design is the yield stress. If the material requires a higher stress to produce yield then the safe working stress is correspondingly increased. In using the term ‘strengthening’, we are concerned with the various ways by which we can make the start of slip more difficult. We now consider some of the ways in which this is done.

9.6.1 Grain boundaries

In a single crystal of a pure metal the shear stress required to move a dislocation is small, in some cases maybe only ≈1 MPa. However, most materials are polycrystalline. It was noted above that, within a single grain, the atomic arrangement is regular but there is a discontinuity at a grain boundary. A dislocation that has reached a grain boundary cannot produce a slip step there, unless the neighbouring grain also deforms to accommodate the shape change. A dislocation in the second grain cannot move until the shear stress, resolved onto the new slip plane and in the new slip direction, reaches the value needed to continue movement. Back in the first grain, the dislocation is stuck and other dislocations will pile up behind it in a traffic jam, exerting a force on it, until, ultimately, the push is too great and it is forced to the grain boundary. The stress on the leading dislocation is a simple function of the number of dislocations in the pile-up. In a coarse-grained structure many dislocations can pile up and the critical stress is reached early, whereas in a fine-grained structure the length of the pile-up is smaller and more stress must be applied from external forces, i.e. the yield point is raised. The outcome is summarised in the famous Hall–Petch equation:

$$\sigma_y = \sigma_0 + kd^{-1/2} \tag{9.2}$$

where σ_y is the yield strength of our polycrystalline material, σ_0 is the yield strength of one crystal on its own, k is a proportionality constant and d is the grain size of the material. Mild steel with a grain size of 250 μm has $\sigma_y \approx 100$ MPa, but when $d = 2.5$ μm, $\sigma_y \approx 500$ MPa. The incentive for making fine-grained steels is clear.

Control of grain size in castings is generally achieved by 'inoculating' the liquid metal with substances which can react with ingredients in the metal to form small solid particles that act as nucleation sites for crystal growth. In wrought products, the thermal and mechanical history of the working process can be controlled to give fine grains. Rolling and forging are used not only to shape materials but also, perhaps more importantly, to control their microstructures and hence their properties.

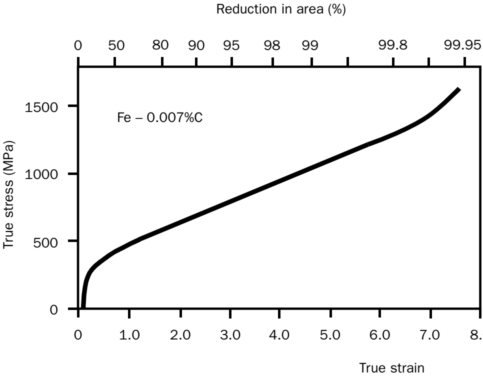

FIGURE 9.8 Work hardening in wire drawing to strains beyond those available in tension testing.

9.6.2 Strain hardening

In a tension test, we can stretch a reasonably ductile metal by only about 30 per cent or so before it becomes unstable and begins to form a neck. But when we roll the same metal or form it into wire by drawing, the deformation in the local area being worked is essentially compressive. This allows us, for example, to draw a wire to many times its original length with relative ease. The work hardening is extended beyond what can be achieved in a tension test (Figure 9.8).

Metals, especially those in the fcc and bcc systems, have many different planes on which dislocations can move to produce slip. But none of these are markedly different from the others and, under increasing stress, all dislocations try to move at once. If the slip planes intersect each other, as indeed they do, the dislocations on one slip plane act as a barrier to dislocations trying to move across them. As we have seen, many millions of dislocations are on the move, the traffic pile-up is considerable, and the dislocations get jammed. Very much more stress needs to be applied to get things moving again, and strain hardening is the result. It is one of the most effective ways of raising the yield strength of a metal, though, if carried too far, it results in fracture as we have seen.

9.6.3 Annealing

Since each dislocation is a region of high strain in the lattice, they are not thermodynamically stable and comparatively little energy is required to cause a redistribution and cancellation of the trapped dislocation arrays. The energy is most conveniently supplied in the form of heat, which gives the atoms enough energy to move spontaneously, and to form small areas which are relatively free of dislocations. This is called *recovery* but, since the dislocation density is only slightly reduced, the yield strength and ductility remain

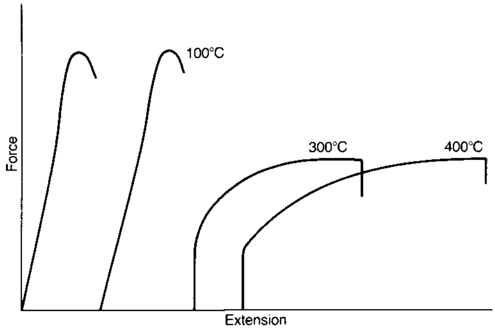

FIGURE 9.9 Load–extension curves for heavily cold worked copper reheated to various temperatures (after K.J. Pascoe (1978) *An Introduction to the Properties of Engineering Materials*, Van Nostrand Reinhold).

almost unchanged. The major change involves *recrystallisation*. New grains nucleate and grow, the material is restored to its original dislocation density and the yield point returns to its original value. This process (Figure 9.9) involves heating to temperatures of around 0.6 T_m (where T_m is the melting point in degrees K) and is known as *annealing*. In addition to overcoming the effects of work hardening, this is an important way of controlling grain size. We shall later see (Section 10.3 pp. 70 and 71) the importance of annealing in the preparation of metals and alloys for commercial use.

9.6.4 Dispersion hardening

One of the most powerful ways of impeding dislocation movement, and hence of increasing the yield strength, is to disperse hard and often brittle particles throughout the structure, so that the dislocations in the softer matrix are stopped and then must find a way round. But there are limitations and perhaps the following analogy will help to explain what these are.

Bitumen is a soft substance which, if left alone, will flow under its own weight and will most certainly flow under load. And yet it is used for roads. This is possible only because it is mixed with a hard aggregate. Let us suppose that the aggregate is supplied as a fine ‘flour’. This will offer little or no resistance to flow since it will be carried along by the bitumen matrix, rather as fine sand is carried along by water. At the other extreme, assume that the same amount of aggregate is supplied in the form of a few large boulders. The bitumen will simply flow in between them. Between these two extremes there lies a region where the particles are small enough and sufficiently close together to restrict flow.

So it is in metals. By various means, the metallurgist is able to produce dispersions of hard particles of such a size and of such a spacing that the movement of dislocations is impeded with a consequent increase in yield strength. This facility is used in certain aluminium alloys, where the dispersion is brought about by suitable heat treatment, and increasingly in steel metallurgy.

9.7 Unstable microstructures

Many of us know that if you take a piece of steel containing, say, 0.5%C, heat it to glowing red (≈900°C) and then quench it by placing it in a bath of water, the outcome is a very hard but brittle substance. Indeed, it could be used to cut a piece of steel that had not been so treated. The quenching of steel is an example in which an unstable microstructure is generated when there is no time for diffusion to keep up with the requirements of thermodynamic equilibrium. The procedure generates a new and unexpected structure, and in which there are large, internal locked-in stresses. It is called *martensite*. In the as-quenched condition it is too brittle to be useful, but if heated to just a few hundred degrees C a number of subtle changes come about. The steel is softened a little, not much, but a useful degree of toughness is restored. This second heating is called *tempering*, and gives us tempered steel. In this state it finds many uses as components in machinery, gears, cranks, etc.

One difficulty with this method of obtaining strength is that it works well only for certain types of steel!

Chapter ten

Forming of metals

We now look at the various ways in which metals and alloys may be prepared for industrial use. There are many ways available to the metal producer and the treatment here is of necessity brief, and will concentrate on only a few of the more important ones. Further information may be found in, for example, Thomas (1970).

Before looking at some of the processes in more detail, it must be emphasised that metallurgists look on them not only as ways of shaping materials but also as ways of controlling microstructures and, consequently, properties.

Figure 10.1 outlines the processing routes for most of the more common metals and alloys used in structural engineering.

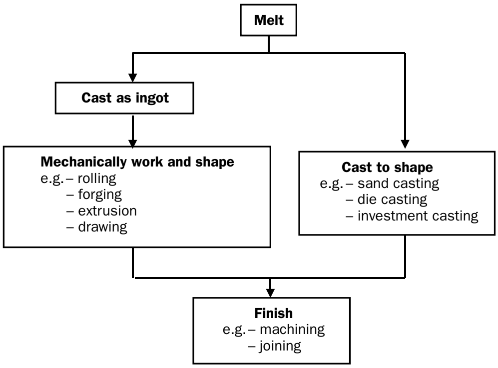

FIGURE 10.1 Processing of the more common engineering materials.

10.1 Castings

Most common metals can be produced by melting and casting into moulds. By casting, the metal may be shaped and dimensioned according to the required component geometry, or a prism of material may be produced for further processing.

The general process of solidification of a molten pure metal has already been described. Solidification of alloys is more complicated and often gives rise to compositional variations from place to place in a casting and on a microstructural scale within dendrites. When intended for further processing, little attempt is made to control grain size and the metal often solidifies to a rather coarse grain structure and will contain a number of casting defects, such as porosity, compositional variations and shrinkage. These are not disastrous because further processing will rectify them. Shaped castings need more care. They are normally degassed, the grain size carefully controlled by means available to the foundryman, and compositional variations minimised by attention to solidification patterns within the mould, if the desired mechanical properties are to be achieved.

10.2 Hot working

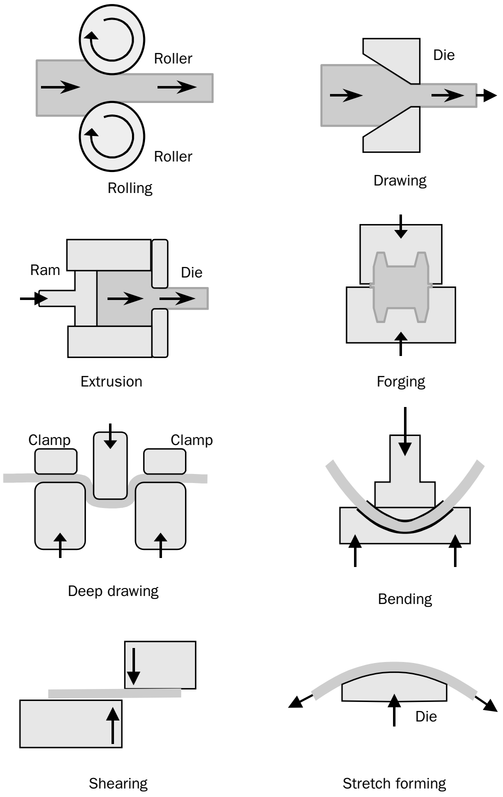

FIGURE 10.2 Some metal-forming methods.

The working of metals and alloys by rolling, forging, extrusion, etc., depends upon plasticity which is usually much greater at high temperatures, i.e. temperatures above their recrystallisation temperature. This allows all the common metals to be heavily deformed, especially in compression, without breaking. For steel structural members, the most usual method is by hot rolling between simple cylindrical or shaped rolls at temperatures around 1000°C or more. After rolling, the members are left to cool naturally and end up with annealed microstructures and grain sizes which depend on how heavy was the deformation, at what temperature, and how fast was the cooling rate. It follows that all these process variables need to be controlled to give products with consistent properties. Another feature of hot working processes is that the exposure to air at high temperatures causes a heavy film of oxide to form on the surface. Thus steel sections delivered 'as rolled' are covered with iron oxide (mill scale) and need to be shot blasted or sand blasted before receiving any protective coating.

Many familiar articles, e.g. engine crankshafts, are forged into shape. This involves placing a hot blank into one half of a shaped mould and then impressing the other half of the mould onto the blank. This is done under impact using such methods as drop forging, die stamping, etc., or more slowly using large hydraulic presses.

Many metals can be extruded. This has the advantage that very long lengths with complex sections can be produced. Aluminium glazing bars are a familiar example.

One disadvantage of hot forming arises from the contraction of dimensions on cooling and from such problems as oxidation. These and other factors conspire to limit the precision of the product. In some cases the tolerances of hot formed parts are acceptable. In other cases, further cold forming or machining may be employed to meet more demanding tolerances.

10.3 Cold working

Because of their cold ductility, many metals and alloys can be cold worked, that is to say, shaped at temperatures below the recrystallisation temperature of the alloy. This creates an immense number of dislocations and, as a consequence, the metal work hardens and its yield point is raised. Indeed, for pure metals and some alloys it is the only way of increasing the yield strength.

There are many processes. Cold rolling is extensively used to produce sheet material, while high-strength wire, as used for cables, is cold drawn by pulling through a tapered die. Metal sheets can be shaped into cups, bowls or motor car body panels by deep drawing or stretch forming (Figure 10.2).

Clearly there comes a limit beyond which the ductility is exhausted and the metal will fracture. If further cold work is required the metal must be annealed by heating it to a temperature where recrystallisation occurs when the original ductility is restored and further working is possible. Some metals can be cold extruded.

Cold working using well-designed tools and a little thought about how to go about it is capable of delivering to demanding tolerances. From the metallurgist's point of view, control over rolling and annealing schedules is a very effective way of controlling the grain size of the product.

10.4 Joining

Although adhesive bonding is being used increasingly for joining metal parts, the commonest methods are still welding, brazing, soldering or by mechanical fasteners, such as rivets and bolts.

10.4.1 Welding

It is beyond the scope of this book to list the various welding processes that are available (see, for example, Houldcroft (1977)). All welding involves essentially the same sequence of operations at the joint. The material is heated locally to its melting temperature, additional metal may or may not be added and the joint is then allowed to cool naturally. Whatever the material or process all welds should comply with the two following ideal requirements:

1. There should be complete continuity between the parts to be joined and every part of the joint should be indistinguishable from the parent metal. In practice this is not always achieved, although welds giving satisfactory performance can be made.
2. The joining material should have metallurgical properties that are no worse than those of the parent metal. This is largely the concern of the supplier of welding consumables though poor welding practice can significantly affect the final product.

The weld itself is a small and rapidly formed casting, but is surrounded by a heat-affected zone (HAZ). During welding, a temperature gradient is created in the parent material. This gradient ranges from the melting temperature at the fusion zone to ambient temperature at some distant point. In the regions that have been exposed to high temperature and fast cooling rates, metallurgical changes can occur. The quality of the joint is affected by:

1. the structure and properties of the weld metal;
2. the structure and properties of that part of the parent material which has undergone a significant thermal cycle (the HAZ).

Both of these are significantly affected by the rate of cooling after welding; the slower the rate of cooling, the closer the structure is to equilibrium. Cooling occurs, principally, by conduction in the parent material and since the thermal conductivity of a metal is a fixed property, the controlling factor is the thermal mass, i.e. the thickness and size of the material to be welded. The greater the thermal mass the faster the cooling rate. Responses to rapid cooling differ markedly from metal to metal, not only from, say, aluminium to steel but also from one steel to another. Structural steels are designed to be weldable, i.e. they are able to be welded without serious loss of performance in the weld and heat-affected zone. Nevertheless, the job must be carried out with thought, care and skill. The best way of coping with these sorts of problems is to get advice from a good welding specialist.

10.4.2 Brazing, soldering and gluing

Brazing and soldering, and in some cases gluing, involve joining by means of a thin film of a material which has a melting temperature lower than that of the parent material and which, when melted, flows into the joint, often by capillary action, to form a thin film which subsequently solidifies. A good brazed or soldered joint should have a strength that is not too different from that of the parent material. Quite high forces are needed to break a film of liquid provided the film is thin enough (Chapter 5) and the same applies to thin solid films. This is not quite the whole explanation but is a very significant part of it. The rest is associated with the behaviour of materials under complex stress conditions, biaxial and triaxial, and is beyond the scope of this chapter. See, for instance, Cottrell (1964).

Although it may seem strange to say so, gluing works in a very similar way. Thin layers of modern adhesives bond well to the substrate material and are strong in shear.

Design of joints to be made by gluing, soldering or brazing should avoid potential failure by peeling and aim to use the adhesive in shear.

10.4.3 Pinning

Some materials (such as cast iron) do not lend themselves to joining by welding. Gluing and brazing are valid options but require thought about the joint design. Bolting or riveting are by far the most common ways of making joints involving such materials. Both bolting and riveting rely on friction. A tightened bolt forces the two members together and the friction between nut and bolt at the threads holds it in place. In riveting, the hot rivet is hammered into prepared holes. As it cools it contracts and develops a tensile stress which effectively locks the members together. High-strength friction grip (HSFG) bolts used in structural steelwork combine both aspects, the nut is tightened to place the bolt into tension, and this tensile pre-stress acts in the same way as the tensile stress in a rivet.

Chapter eleven

Oxidation and corrosion

Corrosion can be divided into two areas: dry oxidation and wet corrosion.

11.1 Dry oxidation

The earth's atmosphere is an oxidising one, and of the metals, only gold and silver are widely found in the native, i.e. unoxidised, state. The general oxidising reaction is often written:

$$\mathrm{M} + \mathrm{O} \rightarrow \mathrm{MO} \qquad (11.1)$$

where M is the metal and O is oxygen. Most usually, this takes place in two steps. First, the metal forms an ion, releasing electrons, and the electrons are accepted by oxygen to form an ion. Second, the ions attract one another to form the compound:

$$\mathrm{M} \rightarrow \mathrm{M}^{++} + 2\mathrm{e} \;\&\; \mathrm{O} + 2\mathrm{e} \rightarrow \mathrm{O}^{--} \text{ and then}$$
$$\mathrm{M}^{++} + \mathrm{O}^{--} \rightarrow \mathrm{MO} \qquad (11.2)$$

At the surface, the oxygen ions attach themselves to the surface to form a thin layer of oxide. Thereafter the metal ions M^{++} and electrons must diffuse outwards through the oxide to meet O^{--} at the outer surface, or the oxygen ions must diffuse inwards. The rate of oxidation is determined by whichever reaction can proceed the faster and, largely, this is controlled by the thickness and structure of the oxide skin.

On some metals the oxide occupies less volume than the metal from which it was formed. If it is brittle (and oxides usually are), it will crack and split, exposing fresh metal. On other metals, the oxide occupies more volume and it will tend to wrinkle and spring away, again exposing fresh metal.

In some cases, however, the oxide volume matches the metal volume and thin adherent films form that act as barriers to further oxidation. This is true of aluminium, chromium and nickel, the last two metals being essential components of so-called 'stainless steel' for that very reason.

11.2 Wet corrosion

In the presence of moisture, the situation changes drastically and the loss of metal by corrosion becomes appreciable. It has been estimated that, in the UK, the annual corrosion bill for either replacement or prevention is around £5000 million.

As in dry oxidation, the basic mechanism involves ionisation but, if the ions are soluble in the corroding medium, which is usually, but not necessarily, water, the metal steadily corrodes. Consider a simple cell in which two electrodes, both of the same metal, are connected via a battery and placed in a suitable electrolyte (Figure 11.1). The battery pumps out electrons which increase the negativity of the cathode while, at the same time, electrons are leaving the anode in order to maintain the flow of current. The electrolyte completes the circuit and the metal ions go

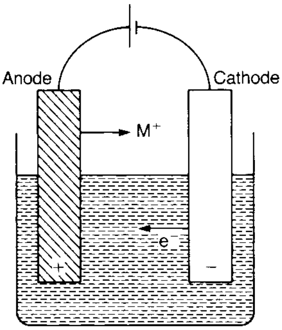

FIGURE 11.1 A simple cell.

into solution and flow across to try to neutralise the surplus negative charge on the cathode. Thus the anode corrodes and the metal ions collect on the cathode. This is, in fact, a simple electroplating cell and is used to produce metals of a high degree of purity. 'Electrolytic' copper used for its high electrical conductivity is one example.

However, in some cases, the metal ions react with the electrolyte. Iron is one example, and if we were to set up a cell similar to that in Figure 11.1 we would obtain the following reactions:

at the anode:

$$\begin{gathered} Fe \rightarrow Fe^{++} + 2e^- \text{ or } Fe \rightarrow Fe^{+++} + 3e^- \\ H_2O \rightarrow H^+ + (OH)^- \\ \text{and } 2H^+ + 2e^- \rightarrow H_2 \end{gathered} \tag{11.3}$$

and, at the cathode:

$$\begin{gathered} Fe^{++} + 2(OH)^- \rightarrow Fe(OH)_2 \text{ or} \\ Fe^{+++} + 3(OH)^- \rightarrow Fe(OH)_3 \end{gathered} \tag{11.4}$$

Iron hydroxides $Fe(OH)_2$ and $Fe(OH)_3$ either deposit away from the cathode or, if they deposit on the cathode, they do so as a loose deposit giving no protection. It is, in fact, the orange slimy oxide often seen on, say, sheet piling in stagnant water. But, since, for example:

$$2Fe(OH)_3 \rightarrow Fe_2O_3 + 3H_2O \tag{11.5}$$

evaporation of water to the air leaves the more conventionally recognised rust, a mixture of iron hydroxides and, principally, Fe_2O_3.

For the above a battery was used to drive the reactions along; however, the reinforcing bars in structural concrete are not connected to a battery and yet they rust. Why?

In these circumstances, the whole subtlety of the process often makes it difficult to establish what is happening, and many large books have been written about it. This is not surprising, as nearly every case of corrosion involves some departures from the ideal but here we can only consider a few of the more general phenomena.

11.2.1 Electrochemical series

The process of ionisation itself produces a change in electric potential and this can be measured relative to some convenient reference value. The reference value usually selected is that of the ionisation of hydrogen:

$$H \rightarrow H^+ + e^- \tag{11.6}$$

and the emf produced by a given metal relative to this reaction gives the *electromotive series*. An abbreviated version is given in Table 11.1. Metals which are more positive than the reference value are anodic and will corrode, metals which are relatively cathodic will not.

One of the first batteries for generating electric-

TABLE 11.1 Standard electrode potentials

Electrode	Voltage	
Na^{++}	+2.71	base, anodic, corrodes
Al^{++}	+1.66	
Zn^{++}	+0.76	
Fe^{++}	+0.46	
Ni^{++}	+0.25	
Sn^{++}	+0.14	
H^+	0.0	reference
Cu^{++}	−0.34	
Ag^{++}	−0.80	
Pt^{++}	−1.20	
Au^{++}	−1.50	noble, cathodic

Note: Conventions differ as to which are negative and which are positive in the series. This does not matter too much since it is the relative position that is important. The convention used here is more directly associated with the text.

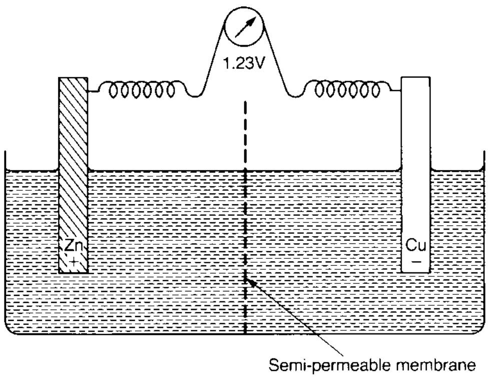

FIGURE 11.2 A Daniell cell.

ity was the Daniell cell (Figure 11.2) containing a zinc anode which corroded and a copper cathode which did not. With zinc at +0.76 V and copper at −0.47 V, the cell produced an output of 1.23 V.

The electromotive series given in Table 11.1 was developed under laboratory conditions. In the real world the nature of the electrolyte, sea water, boiler water, etc., may change the order of merit. Table 11.2 gives an example. When pairs of metals are immersed in sea water one will become the cathode and unreactive, the other will become the anode and react (i.e. corrode). Table 11.2 indicates that brass and stainless steel fittings would form a cell in which the brass would corrode. Other situations which are more commonly found in construction are listed in Blyth (1990). These also include metal–non-metal cells, such as steel–concrete, etc.

TABLE 11.2 Galvanic series in sea water

magnesium	anodic, corrodes
zinc	
aluminium	
mild steel	
cast iron	
lead	
tin	
60–40 brass	
70–30 brass	
copper	
nickel	
silver	
stainless steel (18Cr 8Ni)	
monel metal (70Ni 30Cu)	cathodic, noble

11.2.2 Cells

The above is an extreme example of a composition cell, i.e. a galvanic cell which arises as a result of the energy difference between two metals. But there are ways in which a composition cell can be used to advantage.

The most familiar is the use of zinc to galvanise steel. Table 11.2 shows that zinc is more anodic than iron and on exposure to the atmosphere the zinc corrodes first, thereby protecting the steel. The same system is used for buried pipelines where zinc slabs are connected to the steel pipe and are periodically replaced when they corrode. The converse occurs with chromium plating. Chromium is more cathodic than iron so that, if a small pit appears in the chromium, the steel underneath rusts away quite rapidly. The phenomenon will be familiar to the owners of elderly cars.

There are, however, some variations whose origins are, at first sight, less obvious. In the so-called *concentration cell* preferential corrosion is a consequence of a difference in the constitution of the electrolyte itself. For example, consider water containing dissolved oxygen to differing concentrations in different regions. The reaction:

$$2H_2O + O_2 + 4e^- \rightarrow 4(OH)^- \qquad (11.7)$$

removes electrons and these must be supplied from adjacent areas which are deficient in oxygen. These act as the anode and hence corrode. Thus, in a riveted or bolted connection, corrosion will occur in the inaccessible (i.e. oxygen-poor) areas as indicated in Figure 11.3. A classic case is the ‘waterline’ corrosion of steel piling in stagnant water. Here the surface layers of the water are richer in oxygen and become the cathode. The lower, oxygen-deficient layers are anodic and corrosion occurs locally. Much the

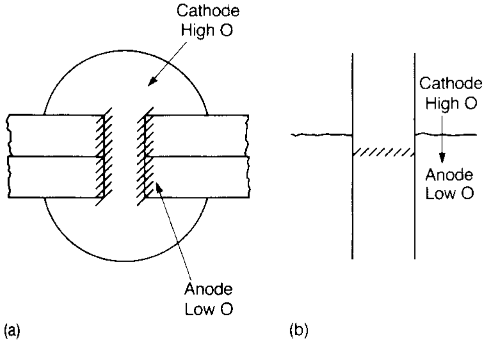

FIGURE 11.3 Concentration cells: (a) at riveted connection; (b) waterline corrosion.

same mechanism applies to pitting corrosion where the oxygen-poor region at the bottom of the pit is anodic and the pit therefore tends to deepen, often leading to premature failure by fatigue or brittle fracture.

Note that water line corrosion can be confused with a different phenomenon. We are all familiar with the enhanced corrosion that is seen on steel supports of seaside piers, etc. Here we have a region that is washed by wave and tidal action. The region is alternately wetted and dried and it is this that accelerates corrosion.

11.3 Control of corrosion

Of all the problems facing the design engineer, the management and control of corrosion is one of the most difficult. But it cannot be stressed too firmly that the problems start at, and must be tackled at, the design stage. There are three requirements, all easy in theory but difficult in practice.

1. Understand the environment in which the metal must work, whether polluted or not, whether facing or away from pervading sources of corrosion, whether wet and/or humid or dry, whether these conditions are stable or variable. Thus, given adequate cover and 'normal' working conditions, steel reinforcement in concrete should not corrode. But it does, often because of sloppy workmanship and poor inspection leading to inadequate and over-porous cover. Furthermore, if it is a motorway bridge, a combination of the excessive use of de-icing salts with inadequate drainage will speed up corrosion.
2. Consider the 'design life'. How long before the first major maintenance? Are you designing a throw-away structure like a modern motor car or are you designing a bridge for a century of service? If the component is not expected to outlive the structure as a whole, how easy is it to inspect and replace?
3. Select the most appropriate method of control. You will, of course, be excused for imagining that the 'most appropriate' method is that one which involves the longest life. You will, of course, be wrong. In the commercial world the most appropriate means of control is that one which produces the longest life at the least annual cost. So, on the whole, you would be best to master such matters as payback, rate of return, and discounted cash flow before deciding upon an appropriate technology.

11.4 Protection against corrosion

11.4.1 Design

At ambient temperatures corrosion occurs only if moisture is present. Thus, surfaces should be exposed as little as possible to moisture and arranged so that they dry out quickly after wetting. In practice all surfaces are at risk, vertical surfaces suffer 'run off', flat surfaces retain moisture on their top side and can attract dew and condensation on the under side. Water retention by 'V', 'H' and other channel sections is obvious and drain holes should be provided, if mechanically acceptable. Overlaps and joints should be arranged to avoid the formation of water channels (Figure 11.4). Porous materials, which can retain moisture, should not be in contact with metals.

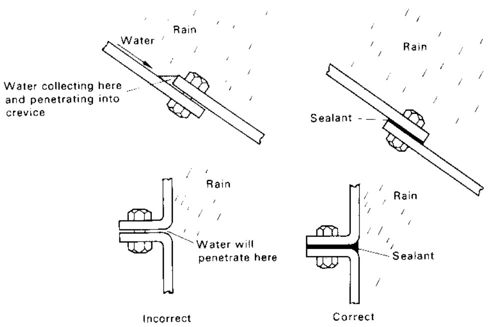

FIGURE 11.4 Design of joints to minimise corrosion risks. Note that small relative movements at joints can quickly abrade away any protective coatings of primer or paint.

Steel which has been allowed to rust on site poses a threat, for the methods available to clean the steel are usually less than adequate and some rust will inevitably remain at the bottom of the pits formed during rusting. These will contain sufficient active material for rusting to continue below any paint film. The only real remedy is not to let rusting start by protecting the steel by priming coats as an integral part of the manufacturing process and, if these are damaged during erecting, to repair the damage as soon as possible.

Remember also that structures need maintenance and the design should ensure that this can be carried out effectively.

11.4.2 Isolation from the environment

This is done by applying one or more protective coatings to a suitably prepared surface. Some metallic coatings simply form a protective barrier, e.g. nickel or chromium on steel. Other coatings, e.g. zinc, cadmium and aluminium, are anodic with respect to steel and provide sacrificial protection.

Organic coatings, such as paints, pitch, tar, etc., form a protective barrier and are commonly used, often in conjunction with a metallic primer. There are now so many different types of paint available that it would be impossible to summarise the virtues and limitations here. For steelwork the publications of the British Constructional Steelwork Association provide excellent guidance for the practising engineer.

It must be emphasised that all paint coatings even of the highest quality and meticulous application are only as good as the quality of the preceding surface preparation. Application, whether by brushing or spraying, should always be carried out on dry surfaces and in conditions of low humidity.

11.4.3 Cathodic protection

In addition to the use of sacrificial anodes, cathodic protection can be achieved by the use of an external power source to make the metal cathodic to its surroundings. Inert anodes are used, commonly carbon, titanium, lead or platinum. The procedure is not without its problems. Thus, in many cases, the cost of replacement anodes is greater than the cost of the impressed power supply.

In buried structures, secondary reactions with other nearby buried structures may enhance, rather than control, corrosion and there is the possibility of hydrogen evolution at the cathode. This can diffuse into the metal and embrittle it. Nonetheless, this method of cathodic protection has been quite widely used in marine environments, especially on offshore oil rigs. Similarly, considerable attention has also been paid to the application of cathodic protection to concrete reinforcement.

Chapter twelve

Metals, their differences and uses

Metals are divided into ferrous (based on iron) and non-ferrous (based on metals other than iron). The principal ferrous alloys in use today are those of iron and carbon, i.e. cast iron and steel. The cast irons contain more than 1.7%C, steels contain up to about 1.5%C with structural steels containing only about 0.25%C or less. The main non-ferrous alloys of interest in civil and structural engineering are those based on aluminium and copper.

12.1 The extraction of iron

Like all metals, iron is extracted from naturally occurring ores. These are actually quite complex chemical compounds but, for simplicity, we shall assume that the starting material is iron oxide. High temperatures (≈1600°C) are needed to allow the reaction:

$$FeO + C \rightarrow Fe + CO \qquad (12.1)$$

The CO is collected and used as a fuel in the steelworks. The *pig iron,* which contains about 4 per cent of carbon, is industrially useless unless processed further. It is remelted, often with scrap iron or steel, and by controlled oxidation using an air blast, the carbon content may be reduced to 2–4 per cent. This is cast iron which, as its name implies, is cast directly into sand moulds. It can be produced in a tough form (SG iron), but usually it is a brittle material and is best used in compression rather than in tension.

12.2 Cast irons

These are used in a variety of applications, the major consumption being in pipes and fittings for services. In civil engineering, an important use is for tunnel segments and mine shaft tubing. The engineer should, however, be aware that cast iron was one of the dominant structural materials in the nineteenth century and will be found as beams, columns and arches in many rehabilitation and refurbishment projects. As we shall see, it should be treated with respect. There are four principal types, whose properties are summarised in Table 12.1.

12.2.1 White cast iron

The carbon here is combined as hard brittle iron carbide, Fe_3C, and the cast iron overall is hard and very brittle. This makes it structurally undesirable and its main use is for applications where high resistance to wear and abrasion is required. Typical applications in the civil engineering field include hard facings to earth-moving machinery.

TABLE 12.1 Representative properties of cast irons

Material	*Young's modulus (GPa)*	*Compressive strength (MPa)*	*Yield strength (MPa)*	*Tensile strength (MPa)*	*%E*	*Brinell hardness (kgm^{-2})*	*Impact energy (J)*
White	170	–	–	275	0	500	4 CU
Grey	100–145	600–1200	–	150–400	0.2–0.7	130–300	8–50 IU
Ferritic SG	165	–	240–400	400–600	18–6	115–215	5–15 CN
Pearlitic SG	170	–	270–530	450–700	7–2	140–300	2–10 CN

%E = % Elongation to fracture, CU = Charpy unnotched, CN = Charpy notched, IU = Izod unnotched.

12.2.2 Grey cast iron

Old cast iron structures are almost certainly of this type and it is still the form of cast iron most commonly met. Most of the carbon is present in the form of free graphite flakes, which can be quite large. The graphite makes it softer than white cast iron and allows it to be machined. Nevertheless, it is still a brittle material and its use in tension is inadvisable, but it has good strength in compression.

12.2.3 Spheroidal graphite (SG), nodular or ductile irons

The flakes in grey cast iron act as internal notches and the metal is brittle in tension. Graphite may be induced to form spherulites by the addition of certain alloying elements and correct casting procedure. These irons have good strength, toughness and ductility. Modern tunnel linings and many other applications are of this type of iron.

12.2.4 Malleable irons

These used to be produced from white irons by annealing which results, again, in nodules of graphite. Depending on the process used, and the composition, they may be described as whiteheart or blackheart (this derives from the appearance of the fracture surface). Both have good strength and resistance to impact. The procedure has been superseded in recent years by the production of SG irons.

12.2.5 Joining of cast irons

All cast irons are extremely difficult to weld and, all too often, the welds are unreliable and of poor strength. Unless specialist advice is available the engineer should use brazing rather than welding. Riveting is possible, but again needs care for fear of cracking the iron. Bolting is the safest method of joining.

12.3 Steel

Steel making involves some very complex thermochemistry, but the basic reaction is simply that of reducing the carbon content still further (for structural steels down to about 0.2 per cent or lower) by a process of controlled oxidation:

$$2Fe[C] + O_2 \leftrightarrow 2Fe + 2CO \qquad (12.2)$$

To keep the reaction moving to the right a considerable amount of oxygen must be used. Some dissolves in the liquid steel. If not removed this would form hard, brittle iron oxide, FeO, and we would be back at square one. Thus, when the desired carbon content is reached the residual oxygen is 'fixed' as an oxide which, after a period of resting, rises to the surface and is removed as slag. The metals commonly used to fix the oxygen in this way are manganese and silicon, and steels treated in this way are known as killed steels. Manganese is added for another reason also. One of the most persistent impurities, and one that is difficult to eliminate economically, is sulphur. This could form iron sulphide, FeS. If FeS is present, even in small quantities, it can cause a defect known as *hot shortness*, in which the steel cracks disastrously if it is stressed when hot. Even contraction stresses on cooling can lead to irredeemable cracking. The manganese addition counteracts this by forming relatively innocuous MnS, and so even the simplest steels contain silicon and manganese.

The terminology used to describe steels is traditional and far from exact. With up to about 0.25 per cent carbon they are ‘mild steel’ or ‘low carbon steel’ (structural steels come into this category). Between about 0.3 per cent and 0.6 per cent carbon they are ‘medium carbon steels’ or often ‘carbon steels’. Above about 0.6 per cent they are ‘high carbon steels’. If elements, other than the normal Mn and Si, are added they become ‘alloy steels’ and, if certain elements, notably chromium and nickel, are added in quantity, ‘stainless steels’.

We discussed the iron–carbon equilibrium phase diagram in Chapter 2 (Figure 2.11) and it is worthwhile having a look at this and re-reading the accompanying text before reading on.

12.3.1 Structural steels

Structural steels are processed into the required section shapes and lengths by hot rolling and their microstructures are effectively those of a normalised steel. They consist of two phases, ferrite and Fe_3C. The Fe_3C does not appear as large isolated particles, but combines with ferrite into laminar regions of alternating layers of ferrite and Fe_3C (see Figure 8.9). These layers are generally about 0.5 μm thick and act as a diffraction grating for natural light. Thus, a steel containing only such regions and properly prepared has a coloured pearly appearance and is known throughout the world as *pearlite*. The overall composition of pearlite is close to 0.8 per cent carbon. Steels containing less carbon are mixtures of ferrite and regions of pearlite, as illustrated in Figure 12.1. To a working approximation, ferrite contains no carbon and so the proportions of ferrite:pearlite depend linearly on the carbon content between 100 per cent ferrite at 0 per cent carbon to 100 per cent pearlite at 0.8 per cent carbon. It follows that at high carbon contents (say 0.7 per cent) the properties of the steel are dominated by those of pearlite, high hardness, high strength and poor ductility and toughness. Conversely, at say 0.15 per cent carbon, the pro-perties are dominated by those of the ferrite. This is a typical metallic substance and its properties are governed by its grain size and whether or not it has been strain (work) hardened.

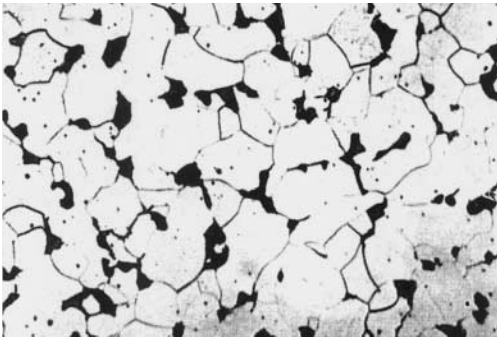

FIGURE 12.1 Typical microstructure of a low-carbon (structural) steel.

From all of this it might be expected that the properties of steels are affected strongly by how much pearlite they contain, or to put it another way, by their carbon content. Figure 12.2 illustrates this.

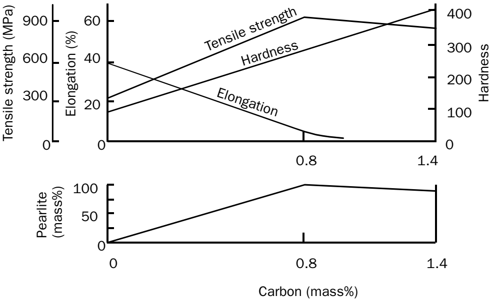

FIGURE 12.2 The influence pearlite content, or carbon content, on the strength and ductility of steels (adapted from Rollason, Metallurgy for Engineers, 1961, Arnold, by permission Butterworth-Heinemann, a division of Reed Educational & Professional Publishing Ltd.).

The tensile strength increases approximately linearly from about 300 MPa at 0 per cent carbon to about 900 MPa at 100 per cent pearlite (0.8 per cent carbon). Over the same range, the elongation to fracture decreases from about 40 per cent to nearly zero. This is a bit of an oversimplification, because the properties of low carbon steels are affected by the grain size of the ferrite that occupies the greater part of the microstructure. However, before going into this, we need to note another very important feature of the behaviour of steels.

Steels, especially structural steels, can go through a ductile to brittle transition as the temperature of use changes over ranges which are typical of those due to variations in weather, season and climate. This phenomenon is usually shown up most clearly by impact tests, which give results like those in Figure 12.3. The method normally used is the Charpy test in which a notched bar is struck by a hammer of known momentum and the energy used up in causing fracture is deduced from the follow through of the pendulum. Even though this phenomenon appears to have been first noted by I.K. Brunel in 1847, it still brings about its fair share of failures.

The trick is to formulate steels for which the ductile to brittle transition temperature (DBTT) is low and which can also be joined successfully by welding. To do this, we want the carbon content to be low, a high ratio of manganese to carbon and a small grain size of the ferrite. When we recall that the yield strength is increased by reducing grain size, we have a powerful argument in favour of fine-grained steels. These are summarised in Table 12.2. To produce and maintain fine grain sizes, careful control must be exercised over the temperatures of hot rolling, the amounts of deformation imposed and cooling rates. As might be expected, so-called controlled rolled steels are more expensive than less carefully controlled products.

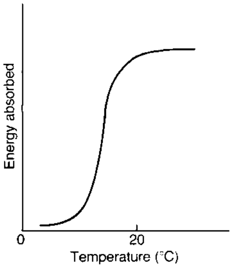

FIGURE 12.3 Energy absorption of structural steel (schematic).

Prior to 1990, the relevant British standard was BS 4360 ‘Weldable structural steels’ and much steel made to that specification is still in use. It is now superseded by BS EN 10025: 1993 ‘Hot rolled products of non alloy structural steels’ and BS EN 10113: 1993 ‘Hot rolled products in weldable fine grain structural steels’. This division into two standards emphasises once again the importance of grain size. Generally these steels contain ≈0.16% C, 0.1 to 0.5% Si and 1.5 to 1.6% Mn. They are all designed to be weldable. Extracts from these standards and equivalents between them are given in Table 12.3.

In essence, there are four strength grades. The 1993 standards identify them by numbers that are the same as the minimum yield strength of the steel: the older schemes referred to the tensile strength. A number of points arise from these standards:

1. The specified minimum yield strength in grades 235 and 275 (40 and 43) can be obtained by various combinations of carbon and manganese.
2. Sulphur and phosphorous are both deleterious. Maximum permissible values are always specified.

TABLE 12.2 Illustrating the importance of grain size to the properties of low carbon structural steels

Grain size (μm)	*σ_y (MPa)*	*Ductile to brittle transition temperature (°C)*
25	255	0
10	400	−40
5	560	−60

TABLE 12.3 Extracts and approximate equivalents from British Standards for structural steels

BS EN 10025: 1993	*BS EN 10113: 1993*	*Previous description*	*BS 4360: 1990*	*%C*	*%Mn (Max)*	*%Si (Max)*	*Other (%)*	*Yield strength (MPa)*	*Tensile strength (MPa)*
S 235		Fe 360	40	0.06–0.22	1.5–1.6	0.5		235	340–500
S 275		Fe 430	43	0.06–0.22	1.5–1.6	0.5		275	430–580
S 355		Fe 510	50	0.06–0.22	1.5–1.6	0.5	0.1Nb, 0.1V	355	490–640
	S 460		55	0.06–0.22	1.5–1.6	0.5	0.1Nb, 0.1V	450	550–700

BS EN 10025: 1993	*BS EN 10113: 1993*	*Previous description*	*BS 4360: 1990*	*Temperature (°C) at which impact energy is:*		*%P*	*%S*	*Examples*
				27 J	*40 J*			
JR			B	20		0.05	0.05	BS EN 10025 S275JO BS 4360 43C $\sigma_y = 275\,\text{MPa}$ $\sigma_{max} = 430\text{–}580\,\text{MPa}$ 27 J at 0°C
JO			C	0		0.04	0.04	
J2			D	−20		0.04	0.04	
K2	N or M*		DD*		−20			BS EN 10025 S355K2 BS 4360 50DD $\sigma_y = 355\,\text{MPa}$ $\sigma_{max} = 490 - 640\,\text{MPa}$ 40 J at −20°C
			E*	−40				
	NL or ML*		EE*	−50	−30	0.04	0.03	
			F*	−60		0.025	0.025	

N = normalised or normalised rolled; M = thermomechanical rolled; L = low temperature (−50°C) impacts; * = a grain-refined steel; % ≡ mass%.

3. The lower grade structural steels are normally delivered normalised (cooled in air). The term 'as rolled' implies no further treatment. Frequently, a steel which had been rolled at high temperatures, above ≈950°C and just left to cool naturally, is effectively a normalised steel.
4. The specified yield strength decreases with size of section. This size effect arises from the fact that thick sections cool more slowly than thin ones and, consequently, the grain size is larger and the Fe_3C ends up differently distributed.
5. The higher grade steels, 355 and 460 (50 and 55) achieve their enhanced strengths not by increasing the carbon content but by attention to their grain sizes. This is done by adding niobium and/or vanadium to the steel, in small amounts, and by careful control of rolling schedules, i.e. thermomechanical treatment. The small grain size is also required to give a low ductile to brittle transition temperature. To give information about the low temperature performance of steels, a letter code is added according to Table 12.3.
6. All structural steels are designed to be readily weldable, although some care is needed with the higher, grain refined grades if the low temperature performance is to be retained (see below).

12.3.2 Cold rolled steels

Many lightweight sections are produced from cold rolled steel of very low carbon content. Strength is derived from work hardening of the ferrite, and good control over section sizes and shapes is possible. Examples of applications include lightweight lintels, angle sections, hollow square sections made by welding two angles together and so forth. Welding, of course, will locally anneal the material, with consequent changes to properties in the heat-affected zone.

Sheet and other sections are available in a special steel (Cor Ten) which contains a small quantity of copper, in addition to the usual alloying elements. When exposed to rainwater it rusts to produce a hard, adherent and subsequently protective oxide layer of an attractive brown colour. It is finding an increasing range of architectural applications as cladding for buildings.

12.3.3 Heat treated steels

With a carbon content greater than about 0.3 per cent, the properties of steel can be varied by heat treatment, that is to say, by fast cooling (generally by quenching in oil or water) from a high temperature, followed by reheating to temperatures not exceeding about 650°C (tempering). The fast cooling produces a hard brittle microstructure, known as *martensite,* in which all the carbon is trapped and which is of little use, except for a few applications such as cutting tools or cutlery. The structure is, however, metastable and the reheating causes the carbon to be precipitated as tiny particles of carbides throughout the matrix. The loss of carbon from the martensite in this way allows it to become softer and more ductile. By varying the tempering temperature and controlling the amount of carbon left in the martensite, great control over the properties can be achieved (Figure 12.4).

Such steels do not, however, find great application in structural engineering. High strength friction grip (HSFG) bolts are one. These are supplied in the hardened and tempered condition. It follows that these should not be reheated (e.g. by welding or flame cutting) or the effects of the heat treatment may well be cancelled. The bolt could easily be embrittled.

It is, however, important to note that the higher strength structural steels can also harden in the same way, not to the same extent but enough to compromise their properties. Welding, and especially flame cutting, of these grades should be undertaken with caution and due respect for the specification and any recommendations by the manufacturer of the welding consumables. Better still, consult an expert welding engineer.

12.3.4 Stainless steel

The term 'stainless steel' covers a wide range of ferrous alloys, all of which contain at least 12 per cent of chromium which produces a stable passive oxide film. Other alloying elements, notably nickel and molybdenum, may also be present. There are three basic types, grouped according to metallurgical structure (Table 12.4):

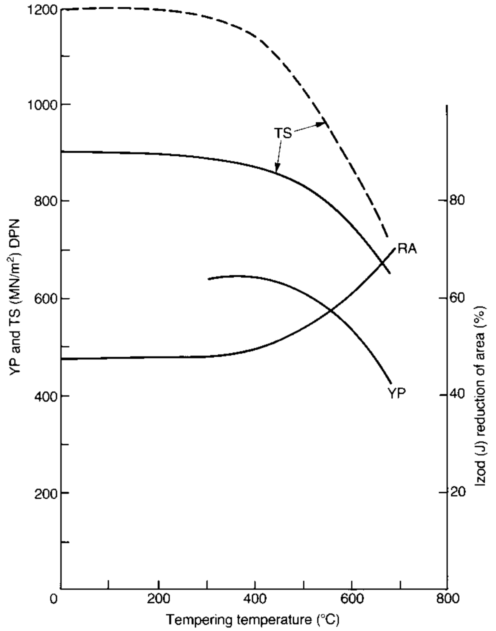

FIGURE 12.4 Variation in properties of 1 per cent Ni steel with varying tempering temperatures. TS: tensile strength; RA: reduction in area; YP: yield point (from O.H. Wyatt and D. Dew-Hughes (1974) *Metals, Ceramics and Polymers*, by permission of Cambridge University Press).

1. Martensitic. The 410 series are low carbon steels containing 13 per cent chromium. They are heat treatable and can be made very hard. Since they retain a keen cutting edge they are particularly used for cutlery.
2. Ferritic. These (the 430 series) also contain 13 per cent chromium but with very low carbon. They are not heat treatable. They are reasonably ductile middle strength steels.
3. Austenitic. The 300 series are low carbon with a basic composition of 18 per cent Cr and 8 per cent Ni though other additions may be made. Like ferritic steels, they are not heat treatable, are reasonably ductile and have good strength.

All these steels offer good resistance to corrosion as long as the passive film can be maintained. All will corrode in solutions low in oxygen and this has been the cause of some embarrassing disasters. The austenitic steels are the most resistant to pitting corrosion, though they may suffer from stress corrosion cracking in chloride solutions at slightly elevated temperatures. Type 316 (18 Cr 10 Ni 3 Mo) is recommended for all external applications. Ferritic steels should be limited to internal uses.

For all practical purposes, martensitic and ferritic stainless steels should be regarded as unweldable, since both undergo significant changes in structure and properties as a result of the thermal cycle. Ordinarily, austenitic stainless steels can be welded (BS 2926: 1984). However, they can suffer from a form of intergranular attack (weld decay), and grades recommended for welding, i.e. stabilised by the use of titanium, should be specified.

TABLE 12.4 Representative properties of stainless steels

Type	*Yield strength (MPa)*	*Tensile strength (MPa)*	*% elongation to fracture*	*Hardness*	*Izod impact energy/J*
Martensitic	350–1360	600–1800	33–3	170–450	7–130
Ferritic	280	420	20	170	–
Austenitic	200	510	40	185	–

Note: the wide range of properties for the martensitic type reflects its ability to be heat treated.

12.4 Aluminium and alloys

Aluminium and its alloys are used both structurally and decoratively. Pure aluminium and some alloys can be readily rolled and extruded into long lengths with complex cross sectional shapes. Typical applications include cladding, roofing, window frames, window and door furniture, etc. Other alloys are designed to be used as castings and are generally fairly strong but not tough. Some alloys can be heat-treated to give high strengths.

The high cost, however, is still a limiting factor and aluminium can compete with steel only where the inherent properties of the material, i.e. lightness, strength, durability and appearance, can be exploited. The most economical use of lightweight materials is in structures that have a high ratio of self-weight to live-load, i.e. roofs, footbridges and long span structures, and where the lightness of the material offers advantages in transport, handling and erection. The comparatively good durability of aluminium makes it attractive in polluted and coastal areas where its high initial cost may be offset by reduced maintenance. Aluminium alloys may be cast or wrought while structural sections are produced almost exclusively by extrusion.

Because the modulus is significantly lower than that of steel, 70 GPa compared with 210 GPa, the deflection under a given load is correspondingly greater and, for deflection limited designs, deeper beams must be used. At the same time, of course, the density of aluminium is significantly lower than that of steel (2.7 against 7.9 $\mathrm{Mgm^{-3}}$) so that specific moduli E/ρ are very similar, $\approx 26\,\mathrm{GPa/Mgm^{-3}}$.

The thermal expansion of aluminium and its alloys is nearly twice that of steel, but the lower modulus means that the thermal stress developed by a given rise in temperature is less in aluminium than in steel.

Unlike mild steel, aluminium and its alloys do not show a definitive yield stress and, for design purposes, the working stress is usually defined as that stress at which a small, but acceptable, amount of plastic deformation has occurred. This is known as the proof stress, generally defined as the stress corresponding to a plastic deformation of 0.1 or 0.2 per cent.

The term ‘aluminium’ is normally used to include aluminium alloys. There are three general types of alloy, those designed for casting, wrought non-heat-treatable alloys and age hardenable alloys. Examples of each are given in Table 12.5.

Casting alloys are generally based on a eutectic alloy system, aluminium–silicon being a widely used example. Solidification is over a narrow temperature range, which makes them very

TABLE 12.5 Representative properties of aluminium alloy types

Alloy and treatment	*Yield strength (MPa)*	*Tensile strength (MPa)*	*% elongation to fracture*	*hardness* kgm^{-2}
Pure aluminium:				
annealed	28	70	43	19
work-hardened	125	130	6	35
Al–11.5%Si, as-cast, modified	–	190	7	–
Al–2.5%Mg, non-heat-treatable, work hardened	270	330	10	80
Al–5.5%Cu, naturally aged	310	405	15	100
Al–5.5%Zn, 2.5%Mg, 1.6%Cu, artificially aged to best strength	505	570	11	150

suitable for casting into moulds that cause rapid solidification.

Wrought, non-heat-treatable alloys are available in a wide range of forms: sheet, rod, extruded sections, etc. Their properties are controlled by how much they have been strain (work) hardened.

Age hardenable alloys are those whose properties can be changed by heat treatment. Earlier we noted that plastic flow, by dislocation movement, can be impeded by suitable barriers. The classic example here is the original alloy, first developed in 1906, Al–4% Cu, Duralumin, upon which the whole of the aircraft industry depended, and, in more sophisticated form, still depends.

When heated to around 550°C the copper dissolves into solid solution in the aluminium and remains in solution when the alloy is rapidly cooled. Thereafter, even at room temperature, a fine dispersion of a hard, intermediate compound $CuAl_2$ forms slowly. Because the particles are small, actually sub-microscopic, and evenly dispersed throughout the matrix, they offer maximum resistance to dislocation movement and the yield stress is consequently considerably higher than that of pure aluminium (Figure 12.5).

This process, known as *ageing*, can be speeded up by reheating to temperatures of about 150°C. But, if reheated to too high a temperature (≈250°C) the minute particles of $CuAl_2$ coalesce and clump together. They are then more widely separated, the dislocations can pass easily through the matrix and the yield strength is correspondingly reduced. This is known as *overageing*. This phenomenon places a restriction on the temperatures the alloy can be used at if the properties are not to deteriorate during use. Modern alloys are more sophisticated and capable of use at higher temperatures, but the same principles apply.

The durability of aluminium alloys is, generally, greater than that of steel, but their corrosion resistance depends upon their composition and heat treatment. The fully heat treated alloys generally being the most susceptible to corrosion and needing, therefore, some protection.

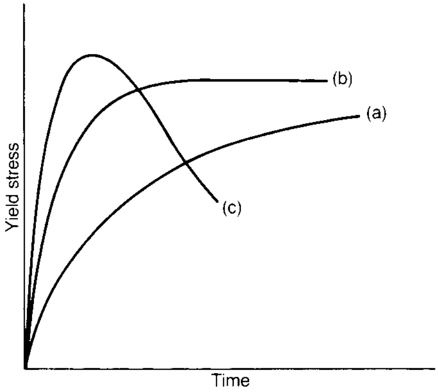

FIGURE 12.5 Effects of ageing on the strength of an Al–Cu alloy: (a) naturally aged at room temperature; (b) accelerated ageing at ~150°C; (c) over-ageing at higher temperature.

It will be clear that welding of casting alloys and non-heat-treatable alloys is possible with the usual care. However, the welding of heat treated aluminium alloys is not without its problems, since the thermal cycle will, inevitably, produce an over-aged structure in the parent metal. Although techniques for welding are now well established, bolting, and to a lesser extent riveting, are preferred, especially for joints made on site.

Steel bolts may be used but should be protected by a zinc coating. Cold riveting, using rivets up to 22 mm diameter, is often used and there are many varieties, some solid, some hollow, but limitations of size and the lower shear strength of aluminium require that, compared with steel, more rivets are used. In both bolting and riveting, arrangements must be made to keep the bolts or rivets (if not themselves aluminium) electrically isolated from the aluminium. Otherwise the phenomenon of bimetallic corrosion can lead to rapid attack of the aluminium.

Most normal structural forms are available and special sections can be produced by extrusion more readily than in steel, though at some cost, and these are really only justified when large quantities are needed. On the other hand, the use of special sections perhaps allows the designer more freedom and scope, the classic example is extruded window frame sections.

12.5 Copper and alloys

Copper finds its main uses in applications where its compatibility with water, high thermal conductivity and high electrical conductivity are important, e.g. domestic water services, heating, sanitation, etc. Also, its high resistance to corrosion combined with the pleasing colour of its oxide film has seen much demand for roofs, cladding and flashing. Decorative schemes make considerable use of the wide range and variety of colours available in copper alloys. In addition to pure copper, two alloy families are widely used.

12.5.1 Brasses

These are alloys of copper and zinc with other additions to produce enhanced strength. Two main classes are used: alpha brasses, nominally 70 Cu:30 Zn, and alpha-beta, nominally 60 Cu:40 Zn. Both are stronger than pure copper and 70:30 brass is extremely ductile. Neither are heat treatable, both are difficult to weld and are better soldered or brazed. Neither is as resistant as pure copper to corrosion. Brasses are, however, generally cheaper than pure copper.

12.5.2 Bronzes

These are basically alloys of copper and tin, but with a whole range of possible other additions to produce alloys with specific properties, e.g. phosphor–bronze, aluminium–bronze, silicon–bronze, etc. *Gunmetal* is bronze containing zinc. Many of the compositions are tractable to forming only by casting, although some of the less highly alloyed bronzes are ductile enough to enable sheet metal working. All are stronger and harder than copper and brasses, have high corrosion resistance, and many are weldable by inert gas processes. All are expensive.

Further reading

Properties of a wide range of engineering materials and their codings according to both British and American Standards are given in:

Bolton, W. (1996) *Engineering Materials Pocket Book,* Newnes, Oxford.

Other information which expands on the subject matter of this part can be found in:

Blyth, A. (ed.) (1990) *Specification,* Architectural Press and Building Publications, London.
Very straightforward and oversimplified but extremely useful as reference.

Brandon, D. and Kaplan, W.D. (1997) *Joining Processes – An Introduction*, John Wiley and Sons, Chichester.
Aimed at students, this includes more detailed sections on surface science and welding than we have room for in this book.

British Constructional Steelwork Association (1986) *Guides for Protection Against Corrosion in Steelwork,* Brit Const Steelwork Ass.

Brunel, I.K., in evidence to the Royal Commission appointed to inquire into the application of iron to railway structures. Report, HMSO, 1849.

Chilton, J.P. (1963) *Principles of Metallic Corrosion,* Royal Institute of Chemistry, London.

Cottrell, A.H. (1964) *The Mechanical Properties of Matter,* John Wiley, London.
Particularly good for the treatment of multiaxial stressing and for plastic design.

Cottrell, A.H. (1967) *An Introduction to Metallurgy,* Edward Arnold, London.
Thorough but probably more detailed than required. Worth dipping into.

Evans, U.R. (1960) *The Corrosion and Oxidation of Metals,* Edward Arnold, London.
Size and cost also make this a reference book, but it is the classic textbook on the subject.

Honeycomb, R.W.K. (1981) *Steels, Microstructure and Properties,* Edward Arnold, London.

Houldcroft, P.T. (1977) *Welding Process Technology,* Cambridge University Press, Cambridge.

Llewellyn, D.T. (1994) *Steels, Metallurgy and Applications,* Butterworth–Heinemann, Oxford.

Pascoe, K.J. (1978) *An Introduction to the Properties of Engineering Materials,* Van Nostrand Reinhold, New York.
Very much a beginner's text.

Polmear, I.J. (1981) *Light Alloys, Metallurgy of the Light Metals,* Edward Arnold, London.

Thomas, G.G. (1970) *Production Technology,* Oxford University Press, Oxford.

Part Three

Concrete

P.L.J. Domone

Introduction

Concrete is a ubiquitous material and its versatility, comparative cheapness and energy efficiency have ensured that it is of great and increasing importance for all types of construction throughout the world. Many structures have concrete as their principal material, albeit as a composite with steel to give either reinforced or prestressed concrete, but even in those structures where other materials such as steel or timber form the principal structural elements, concrete will normally still have an important role, for example in the foundations.

In its simplest form, concrete is a mixture of cement, water and aggregates in which the cement and water have combined to bind the aggregate particles together to form a monolithic whole. The hardened properties are obviously of paramount importance, and depend on a very complex structure. However, as we shall see, the study of concrete is further complicated by other factors, including:

- Many concretes also contain other materials, in small or large quantities, which modify the properties, generally to advantage, but often with undesirable side effects.
- The properties in the newly mixed, fresh (or fluid) state must be such that the concrete can be transported from the mixer, handled, placed in the moulds or formwork and compacted satisfactorily. This requirement can be demanding, for example with in-situ concrete being placed in extreme weather conditions in parts of a structure with difficult access. The responsibility for ensuring that these operations are carried out satisfactorily rests with civil engineers; in this respect concrete is different to most other structural materials which are supplied in a ready-to-use state.
- Even when hardened, the concrete's structure and properties are not static, but continue to change with time. For example, about 50–60 per cent of the ultimate strength may be developed in 7 days, 80–85 per cent in 28 days, and small but measurable increases in strength have been found in 30-year-old concrete.
- The concrete, and any steel contained within it, can deteriorate for a variety of reasons, and so ensuring adequate durability as well as mechanical properties such as strength and stiffness is a major consideration.

A look at the contents list will show that all of these issues are covered in this part of the book. We start by describing the constituent materials of concrete, and then discuss the fresh and early properties before going on to consider the hardened properties of deformation and strength. The principles of mix design, the process of selecting the relative proportions of the constituents to give the required properties, are then presented. We then discuss some non-destructive test methods, following which various aspects of durability are then considered. Finally, we come right up-to-date by describing some aspects of recent developments in high performance concrete which are extending the properties and uses of the material in exciting ways. This is a logical sequence of presentation, but not all courses in concrete technology follow this order, and the chapters and sections within them are written so that they need not be read consecutively.

Historical background

Even though our knowledge and understanding of the material is far from complete, and research continues apace, concrete has been successfully used in many cultures and in many civilisations. It is not just a modern material; various forms of it have been used for several millennia. The oldest concrete discovered so far is in southern Israel, and dates from about 7000 BC. It was used for flooring, and consists of quicklime, made by burning limestone, mixed with water and stone which set into a hardened material. Mortars and concretes made from lime, sand and gravels dating from about 5000 BC have been found in Eastern Europe, and similar mixtures were used by the ancient Egyptians and Greeks some three to four thousand years later. Early concretes produced by the Romans were also of this type, but during the second century BC, it was the Romans who first made concrete with a *hydraulic cement*, i.e. one which reacts chemically with the mix water, and is therefore capable of hardening under water and is subsequently insoluble. The cement was a mixture of lime and volcanic ash from a source near Pozzuoli. This ash contained silica and alumina in an active form which combined chemically with the lime; the term *pozzolana* is still used to describe such materials. Concretes produced by combining this cement with aggregates were used in many of the great Roman structures, for example in the foundations and columns of aqueducts, and, in combination with pumice, a lightweight aggregate, in the arches of the Colosseum and in the dome of the Pantheon in Rome.

Lime concretes were used in some structures in the Middle Ages and after, particularly in thick walls of castles and other fortifications, but it was not until the early stages of the Industrial Revolution in the second half of the eighteenth century that a revival of interest in the material led to any significant developments. In 1756, John Smeaton required a mortar for use in the foundations and masonry of the Eddystone Lighthouse, and, after many experiments, he found that a mixture of burnt Aberthaw blue lias, a clay-bearing limestone from South Wales, and an Italian pozzolana produced a suitable hydraulic cement.

In the 1790s, James Parker developed and patented 'Roman cement' (a confusing name since it bore little resemblance to the cement of Roman times). This was made from nodules of a calcareous clay from North Kent, which were broken up, burnt in a kiln or furnace, and then ground to a powder to produce the cement. Alternative sources of suitable clay were soon identified, and production of significant quantities continued until the 1860s. The cement was used in many of the pioneering civil engineering structures of the period, such as Brunel's Thames Tunnel and the foundation of Stephenson's Britannia Bridge over the Menai Straits.

Roman cement, and some others of a similar type developed at about the same time, relied on using a raw material which was a natural mixture of clay and calcareous minerals. Methods of producing an 'artificial' cement from separate clay- and lime-bearing materials were therefore sought, resulting in the patenting by Joseph Aspdin in 1824 of Portland cement. A mixture of clay and calcined (or burnt) limestone was further calcined until carbon dioxide was expelled, and the product was then ground into the fine cement powder. This had hydraulic cementitious properties when mixed with water, and was called Portland cement because Aspdin considered the hardened product to have a resemblance to Portland stone. In 1828, Brunel found the hardened mortar to be three times stronger than that made from Roman cement, and he used it for repairs in the Thames Tunnel. However, Portland cement was relatively expensive, and it did not become widespread in use until larger scale production processes were developed. In particular, the replacement of single-shaft kilns by continuous-process rotary kilns in the 1890s was critical. Increasingly larger capacity kilns have met the enormous world-wide demand of the twentieth century. A measure of the importance of Portland cement is that it was the subject of one of the first British Standards (BS 12) in 1904, subsequently revised several times. Although the constituent materials have remained essentially the same, refinements in the production processes, in particular higher burning temperatures and finer grinding, and a greater knowledge of cement chemistry and physics have led to steadily increasing quality and uniformity of the cement.

For at least the last 100 years, the vast majority of concrete has been made with Portland cement. However, as we will see in the next chapter, this is not a single material, and there are a considerable number of varieties and types, with an ever more increasing number of international standards.

Over the last 50 years or so, there has also been increasing use of other materials incorporated either to replace some of the Portland cement (*cement replacement materials*) or added to enhance the fresh and/or hardened properties (*admixtures*). These are described in their own chapters.

Definitions

Concrete is a mixture of cement, water, fine aggregate (sand) and coarse aggregate (gravel or crushed rocks) in which the cement and water have hardened by a chemical reaction – *hydration* – to form a *binder* for the (nearly) non-reacting aggregate. Other materials in addition to the above are often incorporated, such as cement replacement materials and admixture mentioned above.

Grout is a mixture of cement and water only; it will hydrate and gain strength, but it is rarely used for structural purposes since it is subject to much higher dimensional changes than concrete under loading or in different environments, and it is more expensive. *Mortar*, a mixture of cement, water and fine aggregate or sand, is more commonly used for small volume applications, for example in brickwork (see Chapter 30).

Mix proportions

The aggregates form the bulk of the concrete volume, typically 70–80 per cent. Most of the remainder is the hydrated cement and water binder, often called the *hardened cement paste* (hcp). There is also a small quantity of air voids (typically 1–3 per cent of the volume) which has not been expelled when the concrete was placed.

The aggregate is divided at a particle size of 5 mm, all particles with a diameter smaller than this being the fine aggregate, and all particles larger being the coarse aggregate. The maximum particle size of the coarse aggregate can be either 10, 20 or 40 mm. In most concrete, the fine aggregate is somewhere between 30 and 45 per cent of the total aggregate. On mixing, the volume of water is normally in the range of 50–75 per cent of the cement and therefore, assuming no air, the freshly mixed concrete comprises, by volume:

6–16% cement
12–20% water
20–30% fine aggregate
40–55% coarse aggregate.

We will see that nearly all of the properties of the concrete are affected by the amounts of the constituents, i.e. the mix proportions. Therefore, to ensure that satisfactory properties are achieved, the mix proportions must be carefully chosen and controlled. Measuring exact volumes of the materials is difficult, and the weights required are normally specified and used for concrete production; the mix proportions are therefore expressed as the weight of each material required in a unit volume of the concrete, e.g. in kg/m^3. The relative density of Portland cement is about 3.15, and most aggregates used for concrete have a relative density of 2.55 to 2.65 (the exceptions being lightweight and high density aggregate used for more specialised concrete). A few calculations using these figures and the volumes given above show that the ranges of the mix proportions by weight are:

cement	150–600 kg/m^3
water	110–250 kg/m^3
aggregates (coarse + fine)	1600–2000 kg/m^3

The total of these for any particular mix gives, of course, the concrete density, which can vary from 2200–2450 kg/m^3. As we will see, the ratio of the weights of water to cement, normally referred to just as the *water/cement ratio*, is an important factor influencing many of the concrete's properties. Values are typically in the range 0.3 to 1.0.

Chapter thirteen

Portland cements

13.1 Manufacture

The crucial ingredients of Portland cement are calcium oxide (CaO) and silicon dioxide or silica (SiO_2). Both of these occur in large quantities, the former in various forms of calcareous calcium carbonate ($CaCO_3$), e.g. chalk and limestone, and the latter in a variety of mineral forms in argillaceous clay or shale. Cement production is a large-scale operation requiring huge quantities of the raw materials, and the plants are therefore normally sited close to a suitable source of one or both of these, which occasionally even occur in a single source such as marl. The raw materials all contain some other components, and in particular clays contain oxides of aluminium, iron, magnesium, sodium and potassium. These cannot be avoided; the first two have a significant effect on the manufacture and composition of the resulting cement, and as we shall see when discussing durability, some of the others can have significant effects even though they are present in small quantities.

The manufacturing process is basically simple, although high temperatures are involved. Initially the chalk and clay are reduced to particle sizes of 75 μm or less, and then intimately mixed in the required proportions. The composition of the mixture is critical, and it may be necessary to add small quantities of other materials such as ground sand or iron oxide. The mixture can be either mixed with water to form a slurry (for the *wet process*) or dried and transported as a powder (in the *dry process*). The most important part of converting the raw material mixture into Portland cement takes place in a rotary kiln. This is an inclined steel cylinder lined with refractory bricks, it can be up to 200 m long and 6 m in diameter, and it is rotated about its longitudinal axis which is set at a slope of about 3 degrees (Figure 13.1). The kiln is heated at its lower end to about 1500°C by the combustion of a fuel–air mixture; the most common fuel is powdered coal, but oil, natural gas and organic waste materials are also used. In the wet process, the slurry is fed into the higher end of the kiln, which is at about ambient temperature, and it is heated as it passes down under the combined action of rotation and gravity. The mixture takes a few hours to pass through the kiln, but the process is continuous, and kilns are only stopped for maintenance from time to time. The mixture experiences increasing temperature as it passes down the kiln, and four physical and chemical changes occur at progressively higher temperatures – drying, preheating, calcining and burning or clinkering; the basic elements of each stage are included in Figure 13.1.

The dry process requires less energy than the wet process since the raw materials do not need

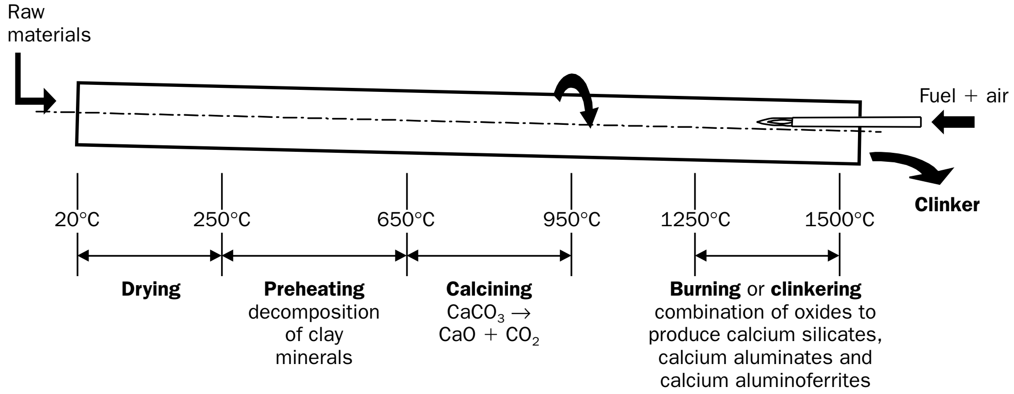

FIGURE 13.1 The processes taking place in a Portland cement kiln in the wet process.

drying, and the heat transfer to the powdered materials is more efficient. The general arrangement of the plant is somewhat different, with the preheating and some calcining being carried out in heat exchangers before the materials enter the kiln about 800°C. A dry process kiln is therefore shorter than a wet process kiln. There are also intermediate semi-dry and semi-wet processes, but in all processes great attention is given to efficiency in terms of energy use and to the environmental issues of exhaust gas discharge.

The heart of all of the processes is the formation of the calcium silicates and aluminates and smaller amounts of other compounds in the burning zone. The reactions take place in a semi-molten state, and the oxides of iron, aluminium and magnesium from the clay assist by acting as a flux enabling the calcium silicates to be formed at considerably lower temperatures than would otherwise be possible. The material emerges from the kiln as a clinker with particle sizes of the order of a few millimetres. This is cooled and a few per cent of gypsum (calcium sulfate dihydrate, $CaSO_4.2H_2O$) is added before the mixture is then ground to a fine powder. The ground clinker and gypsum are often the sole constituents of the final Portland cement, although in many countries the addition of up to 5 per cent of an inert filler such as limestone dust is allowed.

13.2 Physical properties

Portland cements are fine grey powders. The particles have a specific gravity of about 3.14, and most have a size between 2 and 80 μm. The particle size is, of course, dependent on the grinding process, and it can be and is varied depending on the requirements of the cement, as will be discussed in Section 13.3. The particles are too small for their distribution to be measured by sieve analysis (as used for aggregates), and instead the specific surface (SSA), the surface area per unit weight, is normally used as an alternative measurement. This increases as the particle size reduces, i.e. a higher value means smaller average particle size. There are a number of ways of measuring this, but unfortunately they all give somewhat different values. It is therefore necessary to define the method of measurement when specifying, quoting or using a value. The Blaine method, which is the most commonly used, is based on measuring the flow rate of air under a constant pressure through a small compacted sample of the cement. Values of SSA measured with this method range from about 300 to 500 m^2/kg for most cements in common use.

13.3 Chemical composition

We have seen that Portland cement consists of a mixture of compounds formed from a number of oxides at the high temperatures in the burning zone of the kiln. For convenience, a shorthand notation for the principal oxides present is often used:

$$\begin{gathered} CaO \text{ (lime)} = C \\ SiO_2 \text{ (silica)} = S \\ Al_2O_3 \text{ (alumina)} = A \\ Fe_2O_3 \text{ (iron oxide)} = F. \end{gathered}$$

The four main compounds, sometimes called *phases,* in the cement are:

Tricalcium silicate	$3CaO.SiO_2$	in short C_3S
Dicalcium silicate	$2CaO.SiO_2$	in short C_2S
Tricalcium aluminate	$3CaO.Al_2O_3$	in short C_3A
Tetracalcium aluminoferrite	$4CaO.Al_2O_3.Fe_2O_3$	in short C_4AF

Strictly, C_4AF is not a true compound, but represents the average composition of a solid solution.

Each grain of cement consists of an intimate mixture of these compounds, but it is difficult to determine the amounts of each by direct analysis; instead the oxide proportions are determined, and the compound composition then calculated from these using a set of equations developed by Bogue (1955), which, in the shorthand form, are:

$$(C_3S) = 4.07(C) - 7.60(S) - 6.72(A) - 1.43(F) - 2.85(\bar{S}) \quad (13.1)$$

$$(C_2S) = 2.87(S) - 0.754(C_3S) \quad (13.2)$$

$$(C_3A) = 2.65(A) - 1.69(F) \quad (13.3)$$

$$(C_4AF) = 3.04(F) \quad (13.4)$$

Where $\bar{S} = SO_3$, and (C_3S), (C_2S) etc. are the percentages by weight of the various compounds, and (C), (S) are the percentages by weight of the oxides from the oxide analysis. The value of (C) should be the total from the oxide analysis less the free lime, i.e. that not compounded.

The Bogue equations do not give exact values of the compound composition, mainly because these do not occur in a chemically pure form, but contain some of the minor oxides in solid solution. (The impure forms of tricalcium and dicalcium silicates, C_3S and C_2S, are called *alite* and *belite* respectively). However, the values obtained are sufficiently accurate for most purposes, including consideration of the variations in the composition for different types of Portland cement, and their effect on its behaviour.

The approximate range of oxide composition that can be expected for Portland cements is given in the first column of figures in Table 13.1. It can be seen that CaO and SiO_2 are the principal oxides, with the ratio of CaO and SiO_2 normally being about three to one by weight. The composition of any one cement will depend on the quality and proportions of the raw materials, and will therefore vary from one cement works to another, and even with time from a single works. All four cements A, B, C and D are typical individual cements, for which the compound composition has been calculated with the above Bogue formulae. In each case, the principal compounds are C_3S and C_2S, and these together normally amount to about three-quarters of the cement. However, it is immediately clear that the relative proportions of each compound vary considerably, and that these large differences are caused by very small variations in the oxide composition. As we will see, such variations have considerable effects on the hydration process and hardened cement properties, and therefore careful control of the raw materials and manufacturing processes is vital if cement of uniform quality is to be produced. Cement A can be considered to have a 'typical' or 'average' composition for Portland cement; cements B, C and D are common and useful variations of this, i.e. higher early strength, low heat and sulfate-resisting properties respectively, all of which are discussed in more detail in Section 13.3. (Note: the compound compositions in Table 13.1 do not add up to 100 per cent – the remainder comprises the minor compounds, which include the gypsum added to the clinker before grinding)

TABLE 13.1 Compositions of Portland cements

		Cement			
	Range	*A*	*B*	*C*	*D*
Oxides (% by weight)					
CaO	60–67	66	67	64	64
SiO_2	17–25	21	21	22	23
Al_2O_3	3–8	7	5	7	4
Fe_2O_3	0.5–6	3	3	4	5
$Na_2O + K_2O$	0.2–1.3				
MgO	0.1–4				
Free CaO	0–2	1	1	1	1
SO_3	1–3	2	2	2	2
Compounds (% by weight)					
C_3S		48	65	31	42
C_2S		24	11	40	34
C_3A		13	8	12	2
C_4AF		9	9	12	15

13.4 Hydration

For an initial period after mixing, the fluidity or consistency of a paste of cement and water appears to remain relatively constant. In fact, a small but gradual loss of fluidity occurs, which can be partially recovered on remixing. At a time called the *initial set*, normally between two and four hours after mixing at normal temperatures, the mix starts to stiffen at a much faster rate. However, it still has little or no strength, and hardening, or strength gain, does not start until after the *final set*, which occurs some hours later. The rate of strength gain is rapid for the next few days, and continues, but at a steadily decreasing rate, for at least a few months.

The cement paste also gets warm, particularly during the setting and early hardening period. In other words, the hydration reactions are exothermic, and measurement of the rate of heat output at constant temperature is a direct indication of the rate of reaction. Figure 13.2 shows a typical variation of this with time after mixing. Immediately on mixing, there is a high but very short peak (A), lasting only a few minutes. This quickly declines to a low constant value for the so-called *dormant period*, when the cement is relatively inactive; this may last for up to two or three hours. The rate then starts to increase rapidly, at a time corresponding roughly to the initial set, and reaches a broad peak (B), some time after the final set. The reactions then gradually slow down, with sometimes a short spurt after one or two days giving the further narrow peak (C)

The hydration reactions causing this behaviour involve all four main compounds simultaneously. The physical and chemical processes which result in the formation of the solid products of the hardened cement paste are complex, but the following simplified description, starting by considering the chemical reactions of each of the compounds individually, is nevertheless valuable.

The main contribution to the short, intense first peak (A) is rehydration of calcium sulphate hemihydrate, which arises from the decomposition of the gypsum in the grinding process. Gypsum is reformed:

$$2C\bar{S}0.5H + 3H = 2C\bar{S}H_2$$
$$[H = H_2O \text{ in shorthand form}] \qquad (13.5)$$

Additional contributions to this peak come from the hydration of the free lime, the heat of wetting, heat of solution and the initial reactions of the aluminate phases.

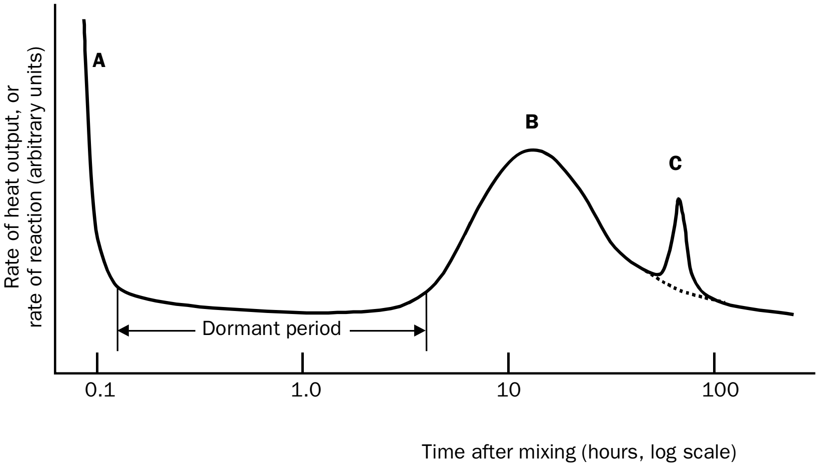

FIGURE 13.2 Typical rate of hydrating cement paste at constant temperature (Forester, 1970).

The behaviour of the aluminates is particularly important in the early stages of hydration. In a pure form, C_3A reacts very violently with water, resulting in an immediate stiffening of the paste. This must be prevented, which is why the gypsum is added to the clinker. The initial reaction of the gypsum and C_3A is

$$C_3A + 3C\bar{S}H_2 + 26H \rightarrow C_3A3C\bar{S}H_{32} \quad (13.6)$$

The product, calcium sulfoaluminate, is also known as *ettringite*. Although the ettringite is insoluble and crystallises out, the reaction is much slower than that of the C_3A alone, and so the problems of flash set are avoided.

Usually about 5–6 per cent of gypsum by weight of the cement is added and, as this is consumed, the ettringite is gradually transformed to calcium monosulfoaluminate, which has a lower sulfate content, and eventually, if all the gypsum is consumed before all the C_3A, the direct hydrate, C_3AH_6 is formed. This causes the short third peak C, which can occur some 2 or 3 days after hydration starts. Whether this peak occurs at all depends on the relative amount of gypsum and C_3A in the unhydrated cement, and it follows that it tends to be a feature of high C_3A content cements.

The C_4AF phase reacts over similar timescales, and the reaction also involves an intermediate compound with the gypsum. The products have an imprecise and variable composition, but include high and low sulfate forms approximating to $C_3(A.F).3C\bar{S}.H_{32}$ and $C_3(A.F).C\bar{S}.H_{16}$ respectively, i.e. similar to the C_3A products. The reactions of products contribute little of significance to the overall cement behaviour.

As we have seen, the two calcium silicates C_3S and C_2S form the bulk of unhydrated cement, and it is their hydration products that give the hardened cement most of its significant engineering properties such as strength and stiffness; their reactions and reaction rates therefore dominate the properties of the hcp (and concrete), and are extremely important.

The C_3S (or, more accurately, the alite) is the faster to react, producing a tricalcium disilicate hydrate and calcium hydroxide:

$$2C_3S + 6H \rightarrow C_3S_2H_3 + 3CH \qquad (13.7)$$

Most of the main peak B in the heat evolution curve (Figure 13.2) results from this reaction, and it is the calcium silicate hydrate (often simply referred to as C—S—H) that is responsible for the strength of the hardened cement paste (hcp).

The C_2S (or, strictly, the belite) reacts much more slowly, but produces identical products:

$$2C_2S + 4H \rightarrow C_3S_2H_3 + CH \qquad (13.8)$$

This reaction contributes little heat in the timescales of Figure 13.2, but it does make an important contribution to the long-term strength of hcp.

The cumulative amounts of individual products formed over timescales a few days longer than those of Figure 13.2 are shown in Figure 13.3. The dominance of the C—S—H after a day or so is readily apparent; this is accompanied by an increase in calcium hydroxide, which, together with some of the minor oxides, results in the hcp being highly alkaline with a pH between 12.5 and 13. As we will see in Chapter 23, this alkalinity has significant influences on some aspects of the durability of concrete construction.

The timescales and the contributions of the reactions of the individual compounds to the development of the cement strength are shown in Figure 13.4. This further emphasises the long-term nature of the strength-giving reactions of the calcium silicates, particularly of the C_2S (or, more correctly, the belite). In fact the reactions can never be regarded as complete, and the extent of their completeness is called *the degree of hydration.*

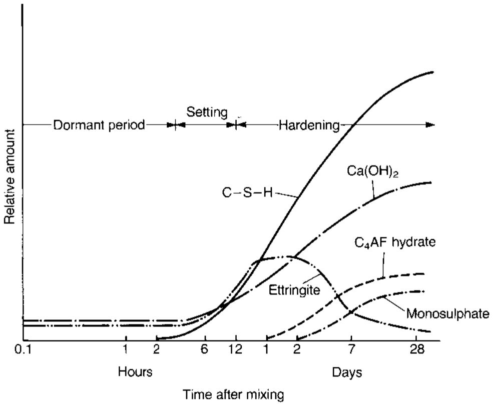

FIGURE 13.3 Typical hydration product development in Portland cement paste (Soroka, 1979).

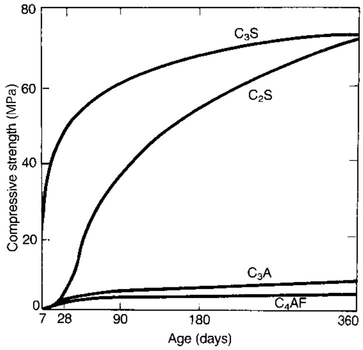

FIGURE 13.4 Development of strength of pure compounds from Portland cement (Bogue, 1955).

In common with most chemical processes, increasing temperature accelerates all of the above reactions. With decreasing temperature, hydration will continue even below 0°C, but stops completely at about −10°C. We will be discussing the effect of temperature in relation to cement and concrete strength development in Chapter 17.

The physical processes during hydration and the resulting microstructure of the hardened cement paste are equally, if not more, important than the chemical reactions, and numerous studies have been made of these by scanning, transmission and analytical electron microscopy. Figure 13.5 illustrates the hydration of a single grain of cement in a large volume of water. The important features are:

- the processes take place at the solid–liquid interface, with solid products being deposited in the region around a diminishing core of unhydrated cement in each cement grain;
- the very early products form a surface layer

on the cement grain which acts as a barrier to further reactions during the dormant period;

- the dormant period ends when this layer is broken down by either a build-up of internal pressure by osmosis, or by calcium hydroxide crystals, or both, enabling hydration to proceed more rapidly;
- the hydration products (known as the *gel*) consist of:
  - an amorphous mass, mainly C—S—H, of small, irregular fibrous particles, some solid, some hollow and some flattened, typically 0.5–2 μm long and less than 0.2 μm diameter, with a very high surface area estimated to be of the order of 200 000 m^2/kg, i.e. approaching a thousand times greater than the fresh cement grains from which it has been formed;
  - large hexagonal crystals of calcium hydroxide interspersed in the fibrous matrix;
- the gel contains many small *gel pores*, typically between 0.5 and 0.5 nm wide, in between the fibrous particles, and as hydration continues, new product is deposited within the existing matrix, decreasing the gel porosity;
- the rate of hydration reduces over a long period after peak B due to the increased difficulty of diffusion of water through the hydration products to the unhydrated cement. It has been estimated that, for this reason, complete hydration is not possible for cement grains of more than 50 μm in diameter – even after many years there is a residual core of the unhydrated cement;
- the products deposited near the fresh cement/water interface (*inner product*) are denser than those deposited further away (*outer product*);
- at complete hydration:
  - the gel porosity reaches a lower limit of about 28 per cent;
  - the volume of the products of hydration is a little more than twice that of the unhydrated cement, but about two-thirds of the combined initial volume of the unhydrated cement and the water which it consumes.

In reality, of course, the hydration is occurring simultaneously in a mass of cement grains in the mix water, and so the hydration productions interact and compete for the same space. An important and vital feature of hydration is that it occurs at a (nearly) constant overall volume, i.e. the mixture does not swell or contract and the hardened cement paste or concrete is the same size and shape when hardened as the mould in which was placed after mixing. Using this fact,

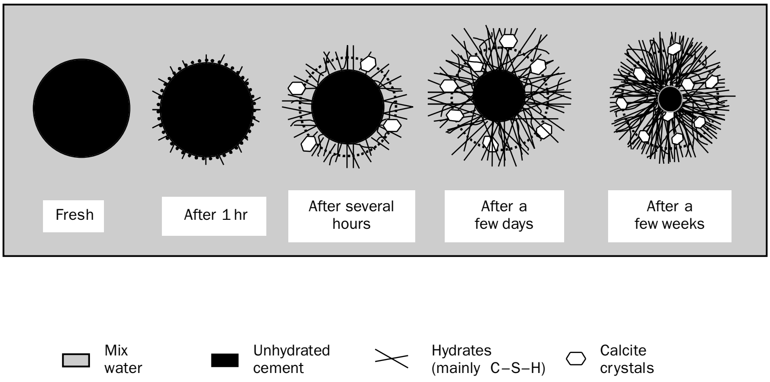

FIGURE 13.5 Illustration of the hydration of a single cement grain.

and the measured properties of the fresh and hydrated materials[1] it can be shown that:

- at a water/cement ratio of about 0.43, there is just sufficient mix water to hydrate all the cement and fill all of the resulting gel pores. Therefore at water/cement ratios lower than this, full hydration can never occur unless there is an available external source of water, for example if the cement or concrete is immersed in water. This is the *condition of insufficient water*, and the paste is subject to *self-desiccation*. In practice, in a sealed specimen the hydration will cease somewhat before all of the available water is consumed, and an initial water/cement ratio of about 0.5 is required for full hydration. As we will see in Chapter 19, self-desiccation can also have other effects.
- at a water/cement ratio of about 0.38, the volume of hydration products, i.e. the gel, exactly matches that of the fresh cement and water. At values lower than this, hydration will be stopped before completion, even if an external source of water is available. This is called the *condition of insufficient volume*. At water/cement ratios higher than this there is an increasing amount of unfilled space between the original grains in the form of *capillary pores*, which are on average about a hundred times larger than gel pores within the gel itself. Calculations give the relative volumes of unhydrated cement, gel and capillary pores at complete hydration shown in Figure 13.6. In reality, for the reasons discussed above, hydration is never complete and therefore the volumes in Figure 13.6 are never achieved, but may be approached. However, at any stage of hydration, the volume of capillary pores will increase with water/cement ratio.

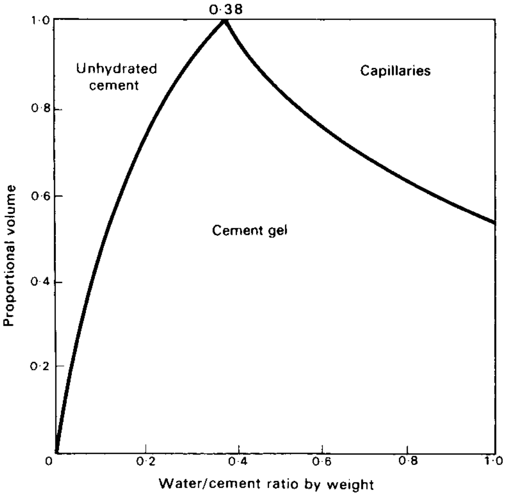

FIGURE 13.6 Volumetric composition of fully-hydrated hardened cement paste after storage in water (Hansen, 1970).

The diagrams in Figure 13.7 provide a visual illustration of this. These show an idealised structure of two cement pastes with high and low water/cement ratios, say of the order of 0.8 and 0.4 respectively, on mixing and when mature, say after several months. In the high water/cement ratio paste the grains are initially fairly widely dispersed in the mix water and, when mature, there is still a significant capillary pore volume. On the other hand, in the low water/cement ratio paste, the grains are initially much more closely packed, and the hydrates occupy a greater volume of the mature paste, which therefore has a greater volume of capillary pores (but which, if the water/cement ratio is low enough, may eventually disappear altogether).

Although it is important to distinguish between the capillary and gel pores, in practice there is a near continuous distribution of pore sizes. Figure 13.8 shows typical measurements which illustrate this, and also provides direct evidence of the reduction in both overall pore volume and pore

---

[1] Relative densities: unhydrated cement 3.15, gel solids 2.61, saturated gel 2.16, unsaturated gel 1.88.

Gel porosity 28 per cent.

1 gm of cement chemically combines with 0.23 gm of water during hydration.

The analysis derives from the work of Powers in the 1950s; a full treatment can be found in Neville (1995).

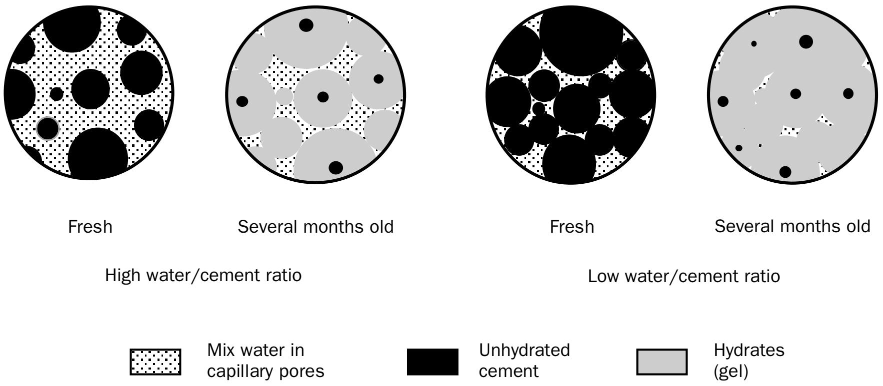

FIGURE 13.7 Structure of cement pastes.

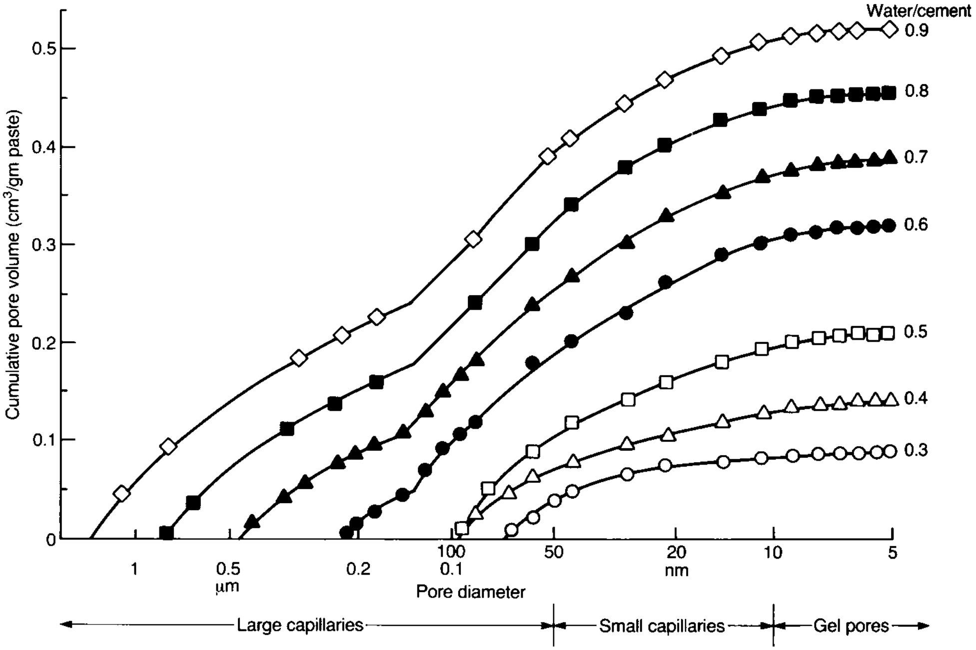

FIGURE 13.8 Pore size distribution in 28-day-old hydrated cement paste (Mehta, 1986).

size with reducing water/cement ratio for pastes of similar age, in this case 28 days.

13.5 Structure and strength of hardened cement paste

We have therefore seen that, at any stage of hydration, the hardened cement paste (hcp) consists of:

1. a residue of unhydrated cement, at the centre of the original grains;
2. the hydrates, chiefly calcium silicates (C—S—H) but also some calcium aluminates, sulfoaluminates and ferrites, which have a complex fibrous form containing gel pores;
3. crystals of calcium hydroxide (sometimes called calcite);
4. the unfilled residues of the spaces between the cement grains – the capillary pores.

The strength of hcp derives from Van der Waals type forces between the hydrate fibres. Although these forces are of relatively low magnitude, the integrated effect over the enormous surface area is considerable. The unhydrated cement is, in itself, strong and is not detrimental to strength. Indeed it is even beneficial in that it is exposed if the paste or concrete is subsequently cracked or fractured, and can therefore form new hydrates to seal the crack and restore some structural integrity provided, of course, some water is present. No other common structural materials have this self-healing property.

For any particular cement, the compressive strength of specimens stored at constant temperature and humidity increases with age and decreasing water/cement ratio; Figure 13.9 shows typical behaviour. We should note here that the strength continues to increase at water/cement ratios below 0.38, even though Figure 13.6 shows that there is an increasing volume of unhydatred cement in the 'end state'. This is further evidence that unhydrated cement is not detrimental to strength – it is the quality of the hydrates that is the governing factor (there are, however, lower practical limits to water/cement ratio, which we will discuss in Chapter 20).

We have seen that both the size and volume of the capillary pores are also influenced by age and water/cement ratio (Figures 13.6 and 13.8) and it is therefore not surprising that the strength and porosity are closely linked. In simple terms – less porosity, due to either increasing age or lower water/cement ratio or both, means higher

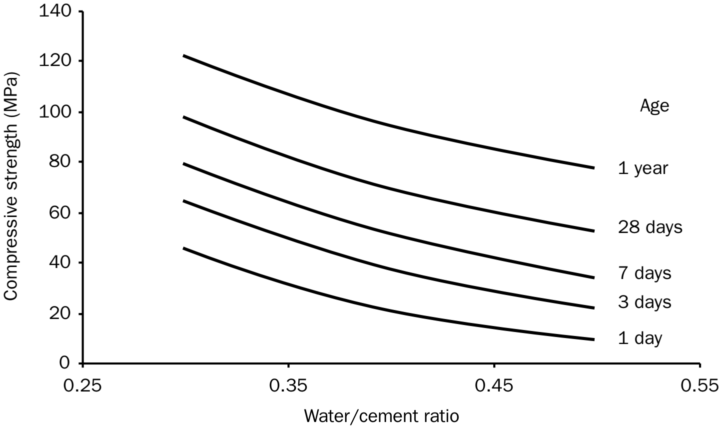

FIGURE 13.9 Compressive strength development of Portland cement paste stored in water at 20°C (Domone and Thurairatnam, 1986).

strength. The relationship between the two was shown by Powers (1958) to be of the form

$$\sigma = k.(1 - P^3) \qquad (13.9)$$

where k is a constant
σ = compressive strength
and P = porosity = pore volume/total paste volume

Note that in this expression the porosity is raised to power three, showing its great significance.

Powers' experiments were on 'normally' cured pastes, i.e. kept in water at ambient temperatures and pressures, with variations in porosity obtained by varying the water/cement ratio. This resulted in porosities ranging from about 25 to 50 per cent. Porosities down to about 2 per cent were obtained by Roy and Gouda (1975) by curing pastes with water/cement ratios down to 0.093 at higher temperatures (up to 250°C) and pressures (up to 350 MPa). Figure 13.10 shows that, at these very low porosities, they achieved compressive strengths of more than 600 MPa, with Powers' results being consistent with their overall relationship of the form

$$\sigma = A \log (P/P_{\text{crit}}) \qquad (13.10)$$

where A is a constant and P_{crit} is a critical porosity giving zero strength, shown by Figure 13.10 to be about 55 per cent.

The size of the pores rather than their total volume has also been shown to be an important factor. Birchall *et al.* (1981) reduced the volume of the larger pores (greater than about 15 μm diameter) by incorporating a polymer in pastes of water/cement ratios of about 0.2 and curing initially under pressure. The resulting 'macrodefect-free' (MDF) cement had compressive strengths of 200 MPa and above, with flexural strengths of 70 MPa, a much higher fraction of compressive strength than in 'normal' pastes or concrete.

Clearly, the extremes of low porosities or high strengths cannot be achieved in concretes produced on a large scale by conventional civil engineering practice, but they have possible applications in factory-produced small units as an alternative to extruded plastics, etc. However, results such as those shown in Figure 13.10 are useful *per se* in helping to understand the behaviour of hardened cement paste.

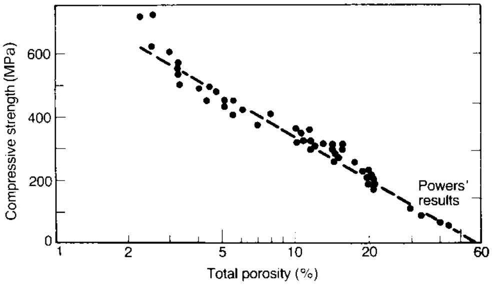

FIGURE 13.10 The dependence of strength of hardened cement paste on porosity (Roy and Gouda, 1975).

We will discuss concrete strength in detail in Chapter 20, and in Chapter 23 we will see that porosity is also a significant factor influencing the durability of concrete.

13.6 Water in hcp and drying shrinkage

The large surface areas in the gel give the hcp a considerable affinity for water, and make its overall dimensions water-sensitive, i.e. loss of water results in shrinkage, which is largely recoverable on regain of water. We will discuss the magnitude of these effects and their consequences in Chapter 19, but for the moment we will consider the various ways in which the water is contained in the paste and how its loss can lead to shrinkage. The possible sites of the water are illustrated in the diagram of the gel structure shown in Figure 13.11.

1. Water vapour. The larger voids may only be partially filled with water, and the remaining space will contain water vapour at a pressure in equilibrium with the relative humidity and temperature of the surrounding environment.
2. Capillary water. This is located in the capillary and larger gel pores (wider than about 5 nm). Water in the voids larger than about

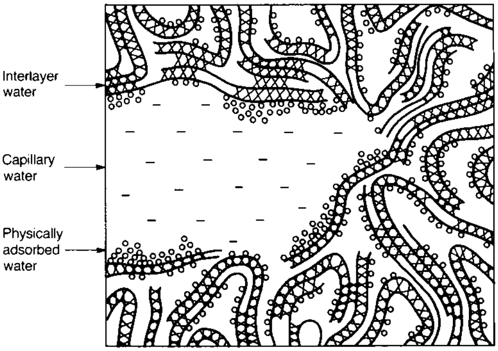

FIGURE 13.11 Schematic of types of water within calcium silicate hydrate (Feldman and Sereda, 1970).

50 nm can be considered as free water as it is beyond the reach of any surface forces (see Chapter 5), and its removal does not result in any overall shrinkage; however, the water in pores smaller than about 50 nm is subject to capillary tension forces, and its removal at normal temperatures and humidities may result in some shrinkage.

3. Adsorbed water. This is the water that is close to the solid surfaces, and under the influence of surface attractive forces. Up to five molecular layers of water can be held, giving a maximum total thickness of about 1.3 nm. A large proportion of this water can be lost on drying to 30 per cent relative humidity, and this loss is the main contributing factor to drying shrinkage.
4. Interlayer water. This is the water in gel pores narrower than about 2.6 nm; it follows from (3) that such water will be under the influence of attractive forces from two surfaces, and will therefore be more strongly held. It can be removed only by strong drying, for example, at elevated temperatures and/or relative humidities less than 10 per cent, but its loss results in considerable shrinkage, the Van der Waals forces being able to pull the solid surfaces closer together.
5. Chemically combined water. This is the water that has combined with the fresh cement in the hydration reactions discussed in Section 13.1.3. This is not lost on drying, but is only evolved when the paste is decomposed by heating to high temperatures in excess of 900–1000°C.

The above divisions should not be thought of as having distinct boundaries, but the removal of the water does become progressively more difficult. An arbitrary but often useful division is sometimes made between *evaporable* and *non-evaporable* water. There are a number of ways of defining this, the simplest being that the evaporable water is that lost on drying at 105°C. This encompasses all the water in (1) to (3) above, and some of (4). The non-evaporable water includes the rest of (4) and all of (5); its amount expressed as a proportion of the total water content increases as hydration proceeds, and this can be used to assess the progress of the hydration reactions.

13.7 Modifications of Portland cement

When discussing the properties and composition of cements in Sections 13.2 and 13.3, we pointed out that these can be altered either by variations in the composition of the raw material or by changes in the manufacturing process. In this section we will discuss ways in which the cement can be altered from ‘average’ or ‘normal’ to obtain properties that are more useful for specific purposes.

13.7.1 Setting, strength gain and heat output

The relative timescales of the dormant period, setting and strength gain govern some of the critical operations in concrete practice, for example the transport and placing of the concrete, and the time at which formwork can safely be removed. One way of modifying these properties is to alter the compound composition by varying the type and relative proportions of the raw materials used in the cement manufacture. For example, if a cement with a higher C_3S and lower C_2S content is produced, as in cement B in Table 13.1, this will have a higher rate of strength gain than cement A (but it should be noted that this does not mean rapid setting). Figure 13.12 shows that rapid hardening properties can also be achieved by finer grinding of the cement, which gives an increased surface area exposed to the mix water, and therefore faster hydration reactions.

Since the hydration reactions are exothermic, a consequence of the rapid hardening is a higher rate of heat output in the early stages of hydration, which will increase the risk of thermal cracking in large pours from substantial temperature differentials at early ages, i.e. during the first few days after casting. To reduce the rate of heat of hydration output a low-heat cement with a lower C_3S and higher C_2S content may be used, i.e. as in cement C in Table 13.1. The disadvantage is a lower rate of gain of strength.

13.7.2 Sulfate resistance

If sulfates from external sources, such as groundwater, come into contact with the hcp, reactions can take place with the hydration products of the calcium aluminate phases, forming calcium sulfoaluminate, *ettringite,* or, strictly, reforming since it was also formed very early in the hydration process (as described in Section 13.4). Crucially the reaction is expansive and can therefore lead to disruption, cracking and loss of strength in the relatively brittle, low tensile strength hcp. (Its earlier formation did not have this effect as the paste was still fluid, or at least soft.) The solution is a low C_3A content cement such as cement D in Table 13.1 which is, therefore, an example of a sulfate resisting cement. We will return to this when discussing sulfate attack in more detail in Chapter 23.

13.7.3 White cement

The grey colour of most Portland cements is largely due to ferrite in the C_4AF phase, which derives from the ferrite compounds in the clay or shale used in the cement manufacture. The use of non-ferrite-containing material, such as china clay, results in a near zero C_4AF content cement, which is almost pure white, and therefore attractive to architects for exposed finishes. White cement is significantly more expensive than normal Portland cements due to the increased cost of the raw materials, and the greater care needed during manufacture to avoid discoloration.

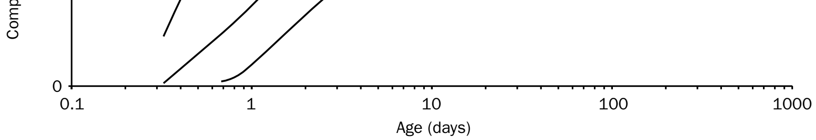

FIGURE 13.12 Effect of specific surface area on the strength gain of Portland cement concrete with a water/cement ratio of 0.4 (Bennett and Collings, 1969).

As we shall see in the next two chapters, it is also possible to modify the concrete properties by other means, involving the use of admixtures and/or cement replacement materials.

13.8 Cement standards and nomenclature

The first edition of the UK standard for ordinary Portland cement was issued in 1904, since when there have been a further fourteen editions, the last being in 1996. A unified European standard, BS–EN 197–1: 2000,[2] has now replaced this. Each edition of BS 12 was increasingly complex and rigorous in its detailed requirements for chemical composition and properties such as setting time and strength production. The 1989 edition was a move towards the European standard, the two most significant changes introduced being:

- the cement could contain up to 5 per cent of material additional to the Portland cement clinker and the gypsum. This additional material is of similar particle size to the cement, and is often an inert filler such as limestone powder. This had been a common practice in many countries before 1989
- the classifications of Ordinary Portland Cement (opc), with the composition, properties and behaviour corresponding to those described as 'normal' throughout this chapter, and Rapid Hardening Portland Cement (rhpc), with a higher early strength gain, as more briefly described above, were dropped in favour of a more extensive strength classification system. The strength characteristics of a cement are determined by measuring the compressive strength of prisms made of a standard mortar with a sand:cement:water ratio of 3:1:0.5 by weight, which has been mixed, cast and stored under defined and carefully controlled conditions. A cement is then given a number, either 32.5, 42.5, 52.5 or 62.5, which corresponds to the strength in MPa achieved at 28 days, and a letter, either N or R (N for normal and R for rapid), depending on the strength at either 2 or 7 days. The requirements of the strength classes are set out in Table 13.2. The previous Ordinary Portland Cement roughly corresponds to class 42.5N, and although it is strictly not now correct to use the term 'opc', it will take a long time before it dies out.

The complexity of the subject is illustrated by the fact that BS-EN 197–1: 2000 includes five main cement types, denoted CEM I to V. CEM I is Portland cement, and CEM II to V are composite cements (i.e. blends with other cementitious materials such as those described in Chapter 15), with, in all, 26 subtypes, only five of which are currently manufactured in the UK.

Sulfate Resisting Portland Cement has a separate standard (BS 4027) for which there is no European equivalent; the most significant difference to other Portland cements is the requirement for a C_3A content of less than 3.5 per cent. There is no standard for white cement.

Many other countries have their own standards. For example, in the USA, the American Society for Testing and Materials (ASTM) classifies Portland cement in their specification C–150–94 by type number:

TABLE 13.2 BS 12: 1996 strength requirements for Portland cement

Class	*Compressive strength from mortar prisms (MPa)*			
	2 days	*7 days*	*28 days*	
32.5N		≥16	≥32.5	<52.5
32.5R	≥10			
42.5N	≥10		≥42.5	<62.5
42.5R	≥20			
52.5N	≥20		≥52.5	<72.5
62.5N	≥20		≥62.5	

---

[2] A list of all standards referred to in the text is included in 'Further reading' on p. 222.

Type I is ordinary Portland cement;
Type II is moderate sulfate-resistant or moderate-heat cement;
Type III is a rapid-hardening cement;
Type IV is low-heat cement;
Type V is sulfate-resistant cement.

It is beyond the scope of this book, and very boring for its readers, to go into further details about these standards. They can be found in most libraries when necessary.

13.9 References

Bennett, E.W. and Collings, B.C. (1969) High early strength concrete by means of very fine Portland cement. *Proc. Inst. Civil Engineers* July, 1–10.

Birchall, J.D., Howard, A.J. and Kendall, K. (1981) Flexural strength and porosity of cements. *Nature* 289, 5796, Jan., 388–90.

Bogue, R.H. (1955) *Chemistry of Portland Cement,* Van Nostrand Reinhold, New York.

Domone, P.L. and Thurairatnam, H. (1986) Development of mechanical properties of ordinary Portland and Oilwell B cement grouts. *Magazine of Concrete Research* 38, 136, Sept., 129–38.

Feldman, R.F. and Sereda, P.J. (1970) A new model for hydrated Portland cement paste and its practical implications. *Eng. J. (Canada)* 53, 8/9, 53–9.

Forester, J. (1970) A conduction calorimeter for the study of cement hydration. *Cement Technology* 1, 3, May/June, 95–9.

Hansen, T.C. (1970) Physical composition of hardened Portland cement paste. *Proc. Amer. Conc. Inst.* 67, 404.

Mehta, P.K. (1986) *Concrete: Structure, Properties and Materials,* Prentice-Hall, New Jersey, p. 450

Neville, A.M. (1995) *Properties of Concrete*, 4th edn, Pearson Education, Harlow, p. 844.

Powers, T.C. (1958) Structure and physical properties of hardened cement paste. *J. Amer. Ceramic Soc.* 41, 1, 1–6.

Roy, D.M. and Gouda, G.R. (1975) Optimization of strength in cement pastes. *Cement and Concrete Research* 5, 2, March, 153–62.

Soroka, I. (1979) *Portland Cement Paste and Concrete,* Macmillan, London.

Chapter fourteen

Admixtures

Admixtures are chemicals that are added to the concrete immediately before or during mixing and significantly change its fresh, early age or hardened state to economic or physical advantage. Only small quantities are required, typically 1 to 2 per cent by weight of the cement. Their popularity and use have increased considerably in recent years; estimates for the UK are that about 12 per cent of all concrete produced in 1975 contained an admixture, and that this increased to 50 per cent by 1991. In some places, notably parts of Europe, North America, Australia and Japan, the proportion is even higher.

An extremely large number of commercial products are available, which are usually classified or grouped according to mode of action rather than chemical type. We shall consider the five distinct types, namely plasticisers, superplasticisers, accelerators, retarders and air entraining agents, and briefly mention others.

14.1 Plasticisers

Plasticisers, also called *workability aids*, increase the fluidity or workability of a cement paste or concrete. They are long chain polymers, the main types being based on either lignosulfonic acids or hydroxycarboxylic acids and their salts. They are relatively inexpensive but can contain significant impurities. Their plasticising action is due to the surface active nature of the component polymer molecules, which are adsorbed onto the surface of the cement grains with an ionic group pointing outwards. This gives the surface a uniform negative charge of the order of a few millivolts, causing mutual repulsion of the cement particles, thereby breaking up the flocs of particles formed in a neat water/cement system, and releasing entrapped water, as illustrated in Figure 14.1. The particles also become surrounded by a sheath of oriented water molecules which prevent close approach of the cement grains, a phenomenon known as *steric hindrance*. The overall effect is one of greater lubrication and hence increased fluidity of the paste or concrete.

Plasticisers are also known as *water-reducers*, since they can produce a concrete with the same workability at a lower water/cement ratio, hence increasing the strength or durability with the same cement content. Their use has been increasingly widespread since their development in the 1950s, and the quantitative benefits that can be obtained are discussed when considering mix design in Chapter 21.

Significant, and sometimes undesirable, secondary effects with some plasticisers are that they act as retarders, delaying the set and decreasing the early strength gain, and/or that they entrain air in the form of small bubbles. They may also contain impurities which have other undesirable side-effects at increasing doses, and therefore the magnitude of the primary effects that can be satisfactorily achieved with plasticisers are relatively modest, though nevertheless useful and cost effective.

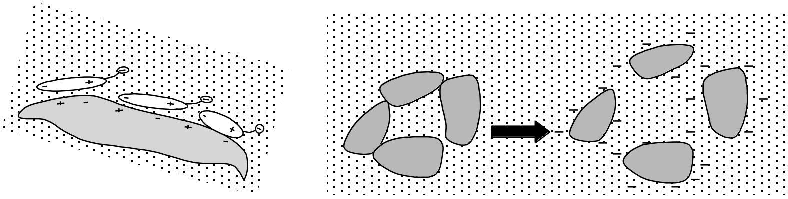

(a) Adsorption on to cement particle surface

(b) Dispersion of particles and release of entrapped water to give greater fluidity

FIGURE 14.1 Mode of action of plasticisers.

14.2 Superplasticisers

As the name implies superplasticisers are more powerful than plasticisers and are used to achieve increases in fluidity and workability of a much greater magnitude than those obtainable with plasticisers. They are also known as *high-range water reducers*. They were first marketed in the 1960s, since when they have been continually developed and increasingly widely used. They have higher molecular weights and are manufactured to higher standards of purity than plasticisers, and can therefore be used to achieve substantially greater primary effects without significant undesirable side-effects. They are a crucial ingredient of many of the so-called 'high performance' concretes, which are discussed in Chapter 24.

Currently four main types can be distinguished (Edmeades and Hewlett, 1998; Ramachandran *et al.*, 1998):

1. modified lignosulfonates (MLSs), essentially purified lignosulfonate plasticisers with the higher molecular weight fractions selected to give greater efficiency;
2. sulfonated melamine formaldehyde condensates (SMFs), normally a sodium salt;
3. sulfonated naphthalene formaldehyde condensates (SNFs), again normally a sodium salt;
4. polymers containing carboxylic acid groups, e.g. polycarboxylates (PCLs). These include polyacrylates, acrylic esters and sulfonated polystyrenes. These have been the most recently developed, and are sometimes referred to as 'new generation' superplasticisers.

The mode of action of superplasticisers is similar to that of plasticisers, i.e. they cause a combination of mutual repulsion and steric hindrance between the cement particles. Opinions differ about the relative magnitude and importance of these two effects with different superplasticisers, but the general consensus (Collepardi, 1998; Edmeades and Hewlett, 1998) is that:

- with MLSs, SMFs and SNFs, electrostatic repulsion is the dominant mechanism;
- with PCLs, steric hindrance is equally if not more important. This is due to a high density of polymer side chains on the polymer backbone which protrude from the cement particle surface (Figure 14.2). This leads to greater efficiency, i.e. similar increases in fluidity require lower admixture dosages. The term 'comb polymer' has been used to describe this molecular structure.

Some typical fluidity effects of admixtures of different types, measured by spread tests on a mortar, are shown in Figure 14.3. The limited range and effectiveness of a lignosulfonate-based plasticiser and the greater efficiency of a PCL superplasticiser (in this case a polyacrylate) compared to an NFL-based material are apparent.

Some of the more important features of the

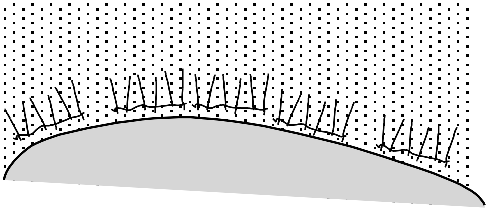

FIGURE 14.2 ‘Comb’ molecules of polycarboxylic superplasticisers on the surface of a cement grain leading to steric hindrance between grains.

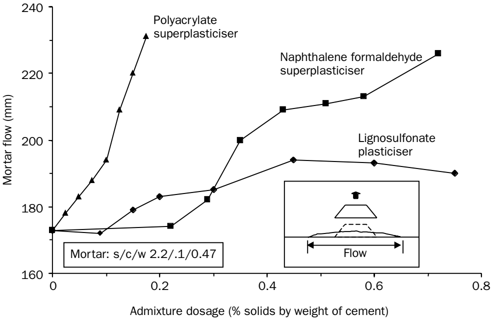

FIGURE 14.3 Typical effects of plasticising and superplasticising admixtures on flow of mortars (Jeknavarian *et al.*, 1997 by permission, American Concrete Institute).

behaviour of superplasticisers which directly effect their use in concrete are:

- The behaviour of any particular combination of superplasticiser and cement will depend on several factors other than the admixture type, including the cement composition, the cement fineness and the water/cement ratio (Aitcin *et al.*, 1994)
- Substantially increased performance can be obtained if the superplasticiser is added a short time (1–2 minutes) after the first contact of the mix water with the cement. It appears that if the superplasticiser is added at the same time as the mix water, a significant amount is incorporated into the rapid C_3A/gypsum reaction, hence reducing that available for workability increase. This effect has been clearly demonstrated for MLS-, SMF- and SNF-based admixtures, but has been reported as being less significant for at least some PCLs, which are therefore more tolerant of variations in mixing procedures.
- The superplasticising action occurs for only a limited time, which may be less than that required if, for example, the concrete has to be transported by road from mixing plant to site. Methods of overcoming this include:
  - blending a retarder with the superplasticiser;
  - addition of the superplasticiser on site just before discharge from the mixer truck;
  - repeated additions of small extra doses of the admixture.

  The losses with some PCLs have been shown to be lower than with other types, at least over the critical first hour after mixing.
- For any particular binder/superplasticiser combination there is a ‘saturation point’ or optimum dosage beyond which no further increases in fluidity occur (Figure 14.4). At dosages higher than this, not only is there no increase in fluidity, but detrimental effects such as segregation, excessive retardation or air entrapment during mixing which is subsequently released, can occur.

We will comment on the quantitative benefits that can be obtained in Chapter 21.

14.3 Accelerators

An accelerator is used to increase the rate of hardening of the cement paste, thus enhancing the early strength, perhaps thereby allowing early removal of formwork, or reducing the curing time for concrete placed in cold weather. They may also reduce the setting time.

Calcium chloride ($CaCl_2$) has historically been very popular as it is readily available and very effective. Figure 14.5 (a) shows that it accelerates both the initial and final set, and Figure 14.5 (b)

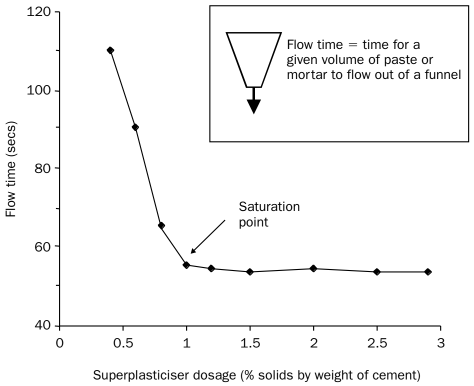

FIGURE 14.4 The saturation point for a cement/superplasticiser combination (Aitcin, *et al.*, 1994 by permission, American Concrete Institute).

shows that a 2 per cent addition by weight of cement can result in very significant early strength increases. This effect diminishes with time, and the long-term strength is similar to that of non-accelerated concrete.

The $CaCl_2$ becomes involved in the hydration reactions involving C_3A, gypsum and C_4AF, but the acceleration is caused by it acting as a catalyst in the C_3S and C_2S reactions (Edmeades and Hewlett, 1998). There is also some modification to the structure of the C—S—H produced.

Of great significance is the increased vulnerability of embedded steel to corrosion due to the presence of the chloride ions. This has led to the use of $CaCl_2$ being prohibited in reinforced and prestressed concrete, and to the development of a number of alternative chloride-free accelerators, most commonly based on either calcium formate, sodium aluminate or triethanolamine. However, as with plasticisers and superplasticisers the magnitude of the effects of these depends on the cement composition and fineness and cannot be predicted with certainty, and so should be established by testing. We shall discuss the corrosion of steel in concrete in some detail when considering durability in Chapter 23.

14.4 Retarders

Retarders delay the setting time of a mix, and examples of use include:

1. counteracting the accelerating effect of hot weather, particularly if the concrete has to be transported over a long distance;

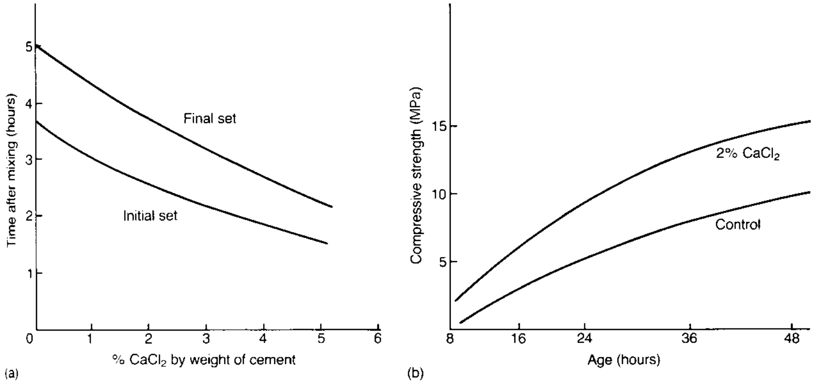

FIGURE 14.5 Typical effects of calcium chloride admixture on (a) setting times, and (b) early strength of concrete (Dransfield and Egan, 1988).

2. controlling the set in large pours, where concreting may take several hours, to achieve concurrent setting of all the concrete, hence avoiding cold joints and discontinuities, and achieving uniform strength development.

The retardations resulting from varying doses of three different retarding chemicals are shown in Figure 14.6. Sucrose and citric acid are very effective retarders, but it is difficult to control their effects, and lignosulfonates, often with a significant sugar content, are preferred. The retarding action of normal plasticisers, such as some lignosulfonates and carboxylic acids, has already been mentioned; most commercial retarders are based on these compounds, and therefore have some plasticising action as well.

The mode of action of retarders involves modification of the formation of the early hydration products, including the calcite crystals. As with other admixtures, temperature, mix proportions, fineness and composition of the cement and time of addition of the admixture all affect the degree of retardation, and it is therefore difficult to generalise.

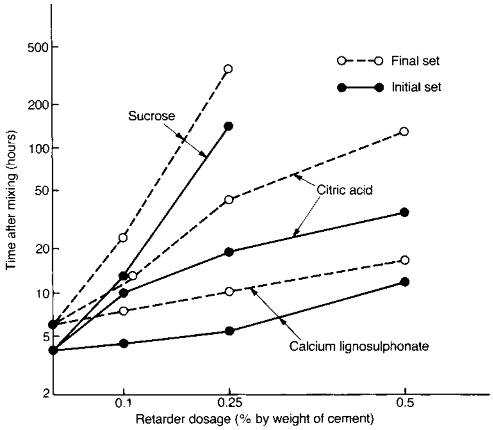

FIGURE 14.6 Influence of retarders on the setting times of cement paste (Ramachandran *et al.*, 1981).

14.5 Air entraining agents

Air entraining agents (AEAs) are organic materials which, when added to the mix water, entrain a controlled quantity of air in the form of microscopic bubbles in the cement paste component of the concrete. The bubble diameters are generally in the range 0.02–0.1 mm, with an average spacing of about 0.25 mm. They are sufficiently stable to be unchanged during the placing, compaction, setting and hardening of the concrete. Entrained air should not be confused with entrapped air which is normally present as the result of incomplete compaction of the concrete, and usually occurs in the form of larger irregular cavities.

AEAs are powerful surfactants which act at the air–water interface within the cement paste. Their molecules have a hydrocarbon chain or backbone terminated by a hydrophilic polar group, typically of a carboxylic or sulfonic acid. This becomes orientated into the aqueous phase, with the hydrocarbon backbone pointing inwards towards the air, thus forming stable, negatively charged bubbles which become uniformly dispersed. This is illustrated in Figure 14.7. Only a limited number of materials are suitable, including vinsol resins extracted from pinewood and synthetic alkylsulfonates and alkylsulfates.

The major reason for entraining air is to provide freeze–thaw resistance to the concrete. Moist concrete contains free water in entrapped and capillary voids, which expands on freezing, setting up disruptive internal bursting stresses.

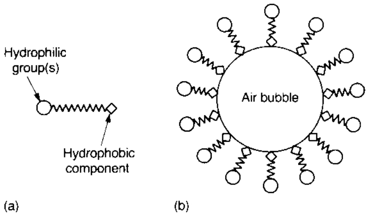

FIGURE 14.7 Schematic of air entrainment by surface-active molecules: (a) surface-active molecule; (b) stabilised air bubble (Mindess and Young, 1981).

Successive freeze–thaw cycles, say, over a winter, may lead to a progressive deterioration. Entrained air voids, uniformly dispersed throughout the hcp, provide a reservoir for the water to expand into when it freezes, thus reducing the disruptive stresses. Entrained air volumes of only about 4–7 per cent by volume of the concrete are required to provide effective protection, but the bubble diameter and spacing are important factors. We will consider freeze–thaw damage in more detail when discussing durability of concrete in Chapter 23.

Air entrainment has two important secondary effects:

1. There is a general increase in the workability of the mix, the bubbles seeming to act like small ball-bearings. The bubbles' size means that they can compensate for the lack of fine material in a coarse sand, which would otherwise produce a concrete with poor cohesion. (Aggregate gradings will be discussed in Chapter 16.)
2. The increase in porosity results in a drop in strength, by a factor of about 6 per cent for each 1 per cent of air. This must therefore be taken into account in mix design, but the improvement in workability means the loss can at least be partly offset by reducing the water content and hence the water/cement ratio.

Air entraining agents have little influence on the hydration reactions, at least at normal dosages, and therefore have no effect on the resulting concrete properties other than those resulting from the physical presence of the voids, as described above.

14.6 Classification of admixtures

We said at the start of this section that admixtures are grouped by mode of action, and as well as those described, there are a number that have dual actions, such as acceleration or retardation together with either plasticising or superplasticising. These can be either single materials, or, more often, blends of two or more materials. They are recognised in standards in several countries, but sometimes with differing terminology; the British and ASTM (American) Standards classification given in Table 14.1 provides a good example of this.

Other admixtures include pumping aids, waterproofers, anti-bacterial agents, bonding agents, viscosity agents or thickeners, foaming agents, corrosion inhibitors, wash water systems and pigments for producing coloured concrete; some selected texts that contain information on these, and give a more detailed treatment of the admixtures we have described, are included in 'Further reading' on page 221.

TABLE 14.1 Classification of admixtures in British and American standards

British Standards	*ASTM Standards*
BS 5075–1: 1982	ASTM C-494
Accelerating	Type A: Water-reducing
Retarding	Type B: Retarding
Water-reducing: normal, accelerating, retarding	Type C: Accelerating
BS 5075–2: 1982	Type D: Water-reducing and retarding
Air-entraining	Type E: Water-reducing and accelerating
BS 5075–3: 1985	Type F: Water-reducing, high range
Superplasticising	Type G: Water-reducing, high range and retarding
	ASTM C-260
	Air-entraining admixtures

A list of relevant standards is included in 'Further reading' on page 222.

14.7 References

Aitcin, P.-C., Jolicoeur, C. and MacGregor, J.G. (1994) Superplasticisers: how they work and why they occasionally don't. *Concrete International* 16, 5, May, 45–52.

Collepardi, M. (1998) Admixtures used to enhance placing characteristics of concrete. *Cement and Concrete Composites* 20, 103–12.

Dransfield, J.M. and Egan, P. (1988) Accelerators. In *Cement Admixtures: Use and Applications* (ed. P.C. Hewlett), Longman, Essex (2nd edn), pp. 102–29.

Edmeades, R.M. and Hewlett, P.C. (1998) Cement admixtures. In *Lea's Chemistry of Cement and Concrete* (ed. P.C. Hewlett), Arnold, London, pp. 837–901.

Jeknavorian, A.A., Roberts, L.R., Jardine, L., Koyata, H. and Darwin, D.C. (1997) *Condensed polyacrylic acid-aminated polyether polymers as superplasticisers for concrete*. ACI SP – 173. Proceedings of Fifth CANMET/ACI International Conference on Superplasticisers and Other Chemical Admixtures in Concrete. Rome, Italy (ed. V.M. Malhotra), American Concrete Institute, Detroit, USA, 55–81.

Mindess, S. and Young, J.F. (1981) *Concrete,* Prentice-Hall, New Jersey.

Ramachandran, V.S., Feldman, R.F. and Beaudoin, J.J. (1981) *Concrete Science,* Heyden and Sons, London.

Ramachandran, V.S., Malhotra, V.M., Jolicoeur, C. and Spiratos, N. (1998) *Superplasticisers: Properties and Applications in Concrete*, CANMET, Ottawa, p. 404.

Chapter fifteen

Cement replacement materials

Cement replacement materials (CRMs) are used as a substitute for some of the Portland cement in a concrete; *partial* cement replacement materials is therefore a more accurate but less convenient name. Confusingly, there are also a number of other names for this group of materials, including supplementary cementitious materials, cement extenders, mineral admixtures, mineral additives, latent hydraulic materials or, simply, cementitious materials.

Several types of materials are in common use, some of which are by-products from other industrial processes, and hence their use may have economic advantages. However, the main reason for their use is that they can give a variety of useful enhancements of or modifications to the concrete properties. All the materials have two common features:

- their particle size range is similar to or smaller than that of Portland cement;
- they become involved in the hydration reactions.

They can be supplied either as individual materials and added to the concrete at mixing, or as pre-blended mixtures with the Portland cement. The former case allows choice of the rate of addition, but means that an extra material must be handled at the batching plant; a pre-blended mixture overcomes the handling problem but the addition rate is fixed. Pre-blended mixtures have the alternative names of extended cements, Portland composite cements or blended Portland cements. Generally, only one material is used in conjunction with the Portland cement, but there are an increasing number of examples of the combined use of two or even three materials for particular applications.

The incorporation of CRMs leads to a rethink about the definition and use of the water/cement ratio, which is an important controlling factor for many properties of hardened cement paste and concrete. It is generally accepted that this should remain as the ratio of the amount of mix water to that of the Portland cement, and the term *water/binder ratio* should be used for the ratio of the amount of mix water to the sum of the amounts of all of the cementitious materials, i.e. the Portland cement *plus* the CRMs.

15.1 Pozzolanic behaviour

A common feature of nearly all CRMs is that they exhibit pozzolanic behaviour to a greater or lesser extent, and so we will define this before discussing the individual materials. A pozzolanic material is one which contains active silica (SiO_2)

and is not cementitious in itself but will, in a finely divided form and in the presence of moisture, chemically react with calcium hydroxide at ordinary temperatures to form cementitious compounds. The key to the pozzolanic behaviour is the structure of the silica; this must be in a glassy or amorphous form with a disordered structure, which is formed in rapid cooling from a molten state. A uniform crystalline structure which is formed in slower cooling, such as is found in silica sand, is not chemically active.

Naturally occurring pozzolanic materials were used in early concretes, as mentioned in the Introduction to this part of the book, but when a pozzolanic material is used in conjunction with a Portland cement, the calcium hydroxide that takes part in the pozzolanic reaction is that produced from the cement hydration (see equations (13.7) and (13.8)). Further quantities of calcium silicate hydrate are produced:

$$2S + 3CH \rightarrow C_3S_2H_3 \qquad (15.1)$$

The reaction is clearly secondary to the hydration of the Portland cement, which has lead to the name 'latent hydraulic material' in the list of alternatives above. The products of the pozzolanic reaction cannot be distinguished from those of the primary cement hydration, and therefore make their own contribution to the strength and other properties of the hardened cement paste and concrete.

15.2 Types of material

The main cement replacement materials in use world-wide are:

1. pulverised fuel ash (pfa), called fly ash in several countries:
   the ash from pulverised coal used to fire power stations, collected from the exhaust gases before discharge to the atmosphere; only selected ashes have a suitable composition and particle size range for use in concrete;
2. ground granulated blast furnace slag (ggbs):
   slag from the 'scum' formed in iron smelting in a blast furnace, which is rapidly cooled in water and ground to a similar fineness to Portland cement;
3. condensed silica fume (csf), often called microsilica:
   extremely fine particles of silica condensed from the waste gases given off in the production of silicon metal;
4. calcined clay or shale:
   a clay or shale heated, rapidly cooled and ground;
5. rice husk ash:
   ash from the controlled burning of rice husks after the rice grains have been separated;
6. natural pozzolans; some volcanic ashes and diatomaceous earth.

We should also mention fine fillers. These are also materials which are ground to a similar fineness to that of the Portland cement before adding to the cement and/or concrete, but they are chemically inert, or nearly so, and so do not conform to the definition of CRMs given above. Limestone powder is a common example and, as we mentioned in Chapter 13, up to 5 per cent addition of this to Portland cement is permitted in many countries. Higher additions are also used in cement for specific applications. There is some reaction between the calcium carbonate in the limestone with the aluminate phases in the cement, but the main enhancement of properties is physical – the fine powder particles can improve the workability and cohesiveness of the fresh paste or concrete, and can act as nucleation sites for the cement hydration products.

We will now discuss the first four of the materials in the above list in more detail, using metakaolin (also known as HRM – high reactivity metakaolin) as the example of a calcined clay. All these four are somewhat different in their composition and mode of action, and therefore in their uses in concrete. Rice husk ash has similarities with microsilica, and natural pozzolans are not extensively used.

15.3 Chemical composition and physical properties

Typical chemical compositions and physical properties are given in Table 15.1, together with typical equivalent properties of Portland cement for comparison. Two types of pfa are included, high- and low-lime, which result from burning different types of coal. High-lime pfa is not available in many countries, where only the low-lime form is marketed. It is normally safe to assume that when pfa is referred to in text books, papers etc, it is the low-lime version unless specifically stated otherwise.

The following features arise from the table.

- All of the materials contain substantially greater quantities of silica than does Portland cement, but crucially, most of this is in the active amorphous or glassy form required for the pozzolanic action.
- The csf is almost entirely active silica.
- The alumina in the pfa, ggbs and metakaolin are also in an active form, and become involved in the pozzolanic reactions, forming complex products. The metakaolin comprises nearly all active silica and alumina.
- Two of the materials, high-lime pfa and ggbs, also contain significant quantities of CaO. This also takes part in the hydration reactions, and therefore neither material is a true pozzolan, and both are to a certain extent self-cementing. The reactions are very slow in the neat material, but they are much quicker in the presence of the cement hydration, which seems to act as a form of catalyst.
- The above considerations lead to maximum effective Portland cement replacement levels of about 90 per cent for high-lime pfa and ggbs, 40 per cent for low-lime pfa and metakaolin and 25 per cent for csf. At higher levels than these, there is insufficient Portland cement to produce the required quantities of calcium hydroxide for the secondary reactions. However, as we will see, levels less than these maxima are normally used, to good effect.
- Pfa and ggbs have particle sizes similar to those of the Portland cement, whereas the metakaolin particles are, on average, nearly ten times smaller and the csf particles 100 times smaller (although the ggbs and metakaolin are both ground specifically for use in concrete, and so their fineness can be varied). The consequences of the associated differences in surface area are:

TABLE 15.1 Typical composition and properties of cement replacement materials

	pfa		*ggbs*	*csf*	*metakaolin*	*Portland cement*
	Low lime (class F)	*High lime (class C)*				
Oxides (% by wt)						
SiO_2	48	40	36	97	52	20
CaO	3	20	40	<1	<1	64
Al_2O_3	27	18	9	<1	41	5
Fe_2O_3	9	8	1	<1	5	4
MgO	2	4	11	<1	<1	1
Pozzolan reactivity (mg CH/gm)	875		400	427	1050	
Particle size range (microns)	1–100		3–100	0.03–0.3	0.2–15	0.5–100
Specific surface area (m^2/kg)	350		400	20 000	12 000	350
Particle relative density	2.3		2.9	2.2	2.5	3.15
Particle shape	spherical		irregular	spherical	irregular	angular

Materials with these properties will conform to the relevant standards for use in concrete, where these exist. A list of these is included in 'Further reading' on page 222.

  - The rate of reaction of the metakaolin is higher than that of pfa and ggbs, and that of csf highest of all (but remember that all are still secondary to that of the Portland cement).
  - Both metakaolin and csf result in a loss of fluidity of the cement paste and concrete if no other changes are made to the mix, with again the effect of csf being greater than that of metakaolin. To maintain fluidity, either the water content must be increased, or a plasticiser or superplasticiser added (see admixtures above). The latter is the preferred option, since other properties such as strength are not compromised. With a sufficient dosage of superplasticiser to disperse the fine particles, a combination of excellent workability with good cohesion and low bleed can be obtained.
- The spherical shape of the pfa particles leads to an increase in fluidity if no other changes are made to the mix. Some increase is also obtained with ggbs.
- All the materials have lower specific gravities than Portland cement, and therefore substitution of the cement on a weight-for-weight basis will result in a greater volume of paste.

All the above effects have led to an increasing use of the various CRMs in all types of concrete in the latter part of the twentieth century, and we will discuss their effect on several aspects of concrete behaviour in the subsequent chapters.

15.4 Supply and specification

As we said earlier, CRMs can be supplied as separate materials or preblended with Portland cement. Blends with ggbs are called Portland Blast Furnace cement, and blends with pfa Portland Pozzolanic cement. There are a bewildering array of relevant standards throughout the world, made all the more complicated by the recent emergence of unified European standards. As with Portland cements, it is beyond the scope of this book to list and discuss these. Standards for the individual materials are listed in 'Further reading' on page 222.

Chapter sixteen

Aggregates for concrete

In Chapter 13 we saw that hardened cement paste (hcp) has strength and other properties that could make it suitable for use as a construction material in its own right, but it suffers from two main drawbacks – high dimensional changes, in particular low modulus, high creep and shrinkage, and cost. Both of these disadvantages are overcome, or at least modified, by adding aggregates to the cement paste, thus producing concrete. The objective is to use as much aggregate as possible, binding the particles together with the hcp. This means that the largest possible aggregate size should be used, with a continuous range of particle sizes from the fine sand up to the coarse stones; this minimises the void content of the aggregate mixture and therefore the amount of hcp required, and helps the fresh concrete to flow more easily. Normally the aggregates occupy about 65–80 per cent of the total concrete volume.

With one or two notable exceptions, the aggregates can be thought of as being inert fillers; for example, they do not hydrate, and they do not swell or shrink. They are distributed throughout the hcp, and it is sometimes useful to regard concrete as a two-phase material of either coarse aggregate dispersed in a mortar matrix, or coarse and fine aggregate dispersed in an hcp matrix. Models based on this two-phase material are of value in describing deformation behaviour, as discussed in Chapter 15, but, when cracking and strength are being considered, a three-phase model of aggregate, hcp and the transition or interfacial zone between the two (about 30–50 μm wide) is required, since the transition zone is often the weakest phase, and cracking initiates within it. This will be discussed in more detail when considering concrete strength in Chapter 20. In this section we shall first describe the various types of most commonly used aggregates and how they are classified, and then consider some of their most important properties when used in concrete.

16.1 Types of aggregate

Aggregates can be obtained either from natural sources, such as gravel deposits and crushed rocks, or specifically manufactured for use in concrete. It is convenient to group them in terms of their density.

16.1.1 Normal density aggregates

Many different natural materials are used for making concrete, including gravels, igneous rocks such as basalt and granite and the stronger sedimentary rocks such as limestone and sandstone. They should have sufficient integrity to maintain their shape during the concrete mixing, and be sufficiently strong to withstand the stresses imposed on the concrete. The latter becomes a particular consideration with high-strength concrete (Chapter 24). The mineral constituents are not generally of great importance, the notable exceptions being those that can participate in alkali–silica reaction and thaumasite damage, both of which will be discussed in Chapter 23.

All of the above rock types have relative densities within a limited range of approximately 2.55–2.75, and therefore all produce concretes with similar densities, normally in the range 2250–2450 kg/m^3, depending on the mix proportions.

Gravels from suitable deposits in river valleys or shallow coastal waters have particles which, for the most part, are of a suitable size for direct use in concrete, and therefore only require washing and grading, i.e. subdividing into various sizes, before use. Bulk rock sources, e.g. granite, require crushing to produce suitable size material. The particles are therefore sharp and angular, distinctly different from the naturally rounded particles in a gravel; we will see later that particle shape has a significant effect on fresh and hardened concrete properties.

16.1.2 Lightweight aggregates

Lightweight aggregates are used to produce lower density concretes, which are advantageous in reducing the self-weight of structures and also have better thermal insulation than normal weight concrete. The reduced relative density is obtained from air voids within the aggregate particles. Pumice, a naturally occurring volcanic rock of low density, has been used since Roman times, but it is only available at a few locations, and artificial lightweight aggregates are now widely available. They are of three main types:

1. sintered pulverised fuel ash, formed by heating the pelletised ash from pulverised coal used in power stations until partial fusion and hence binding occurs;
2. expanded clay or shale, formed by heating suitable sources of clay or shale until gas is given off and trapped in the semi-molten mass;
3. foamed slag, formed by directing jets of water, steam and compressed air on to the molten slag from blast furnaces.

In each case, both fine and coarse aggregates can be produced, and many different products are available, particularly in industrialised countries. Because they all achieve lower specific gravity by increased porosity, they are all weaker than the normal density aggregates, and their use results in an overall lowering in the concrete strength – the penalty to be paid for the lower density. The quality and properties of different aggregates vary considerably, and therefore produce different strength/density relationships, illustrated in Figure 16.1.

Lightweight aggregates are not as rigid as normal weight aggregates, and therefore produce concrete with a lower elastic modulus and higher creep and shrinkage. As with strength, the properties depend on the lightweight aggregate type and source, and also whether lightweight fines or natural sands are used.

16.1.3 Heavyweight aggregates

Where concrete of high density is required, for example in radiation shielding, heavyweight

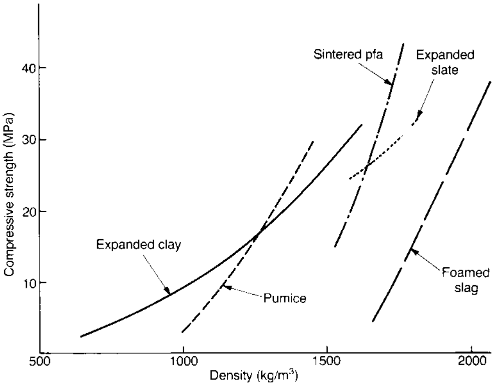

FIGURE 16.1 Typical strength versus density relationships for concretes containing selected lightweight aggregates (from aggregate supplier's information).

aggregates can be used. Densities of 3500 to 4500 kg/m^3 are obtained by using barytes (a barium sulphate ore), and about 7000 kg/m^3 by using steel shot.

16.2 Aggregate classification: shape and size

Within each of the types described above, aggregates are classified principally by shape and particle size.

Normal-density aggregates in particular may contain a range of particle shapes, from well rounded to angular, but it is usually considered sufficient to classify the aggregate as uncrushed, i.e. coming from a natural gravel deposit, with most particles rounded or irregular, or crushed, i.e. coming from a bulk source, with all particles sharp and angular.

The principal size division is that between fine and coarse aggregate at a particle size of 5 mm (although some countries use 4, 6 or 8 mm). The coarse aggregate can have a maximum size of 10, 14, 20 or 40 mm (although, again some countries use different values). The distribution of particle sizes within each of these major divisions is also important both for classification and for determining the optimum combination for a particular mix (a part of the mix design process, discussed in Chapter 21). To measure this, a *sieve analysis* is carried out using a series of standard sieves with apertures ranging from 75 µm to 37.5 mm, each sieve having approximately twice the aperture size of the previous one, i.e. in a logarithmic progression, with the exception of a 14 mm sieve.

The analysis starts with drying and weighing a representative sample of the aggregate, and then passing this through a stack or nest of the sieves, starting with that with the largest aperture. The weights of aggregate retained on each sieve are then measured. These are converted first to percentage retained and then to cumulative, i.e. total, per cent passing, which are then plotted against the sieve size to give a *grading curve*.

Standards for aggregate for use in concrete contain limits inside which the grading curves for coarse and fine aggregate must fall. In the UK standard (BS 882[1]), the coarse aggregate can be either *single size* where all (or, strictly, nearly all) of the particles are within two successive sizes, e.g. 5 to 10 mm, 10 to 20 mm or 20 to 40 mm, or *graded*, where the smallest size is 5 mm in each case, e.g. 5 to 14 mm, 5 to 20 mm or 5 to 40 mm (10 mm graded material is obviously the same as 10 mm single size). The range for suitable fine aggregate is wide, and the UK standard subdivides this into three overlapping divisions of fine, medium and coarse fine aggregate. The various limits are given in Table 16.1, and the grading curves for the mid-points of the ranges for each aggregate division are plotted in Figure 16.2.

A single number, the *fineness modulus*, is sometimes also calculated from the sieve analysis results. The cumulative per cent passing figures are converted to cumulative per cent retained, and the fineness modulus is defined as the sum of all of these starting with that for the 150 µm sieve, divided by 100. A higher fineness modulus indicates a coarser material; the values for the grading curves in Figure 16.2 are given in Table 16.2. It is important to remember that the definition applies to the standard sieve sizes only (with the 14 mm sieve excluded), and that for coarse aggregate with all particles larger than, say, 5 mm the cumulative per cent retained on all sieves smaller than 5 mm should be entered as 100.

During the process of mix design, the individual subdivisions or *fractions* of aggregate are combined in proportions to give a suitable overall grading for good workability and stability. This should be continuous and uniform. Examples for maximum coarse aggregates sizes of 10, 20 and 40 mm that are produced by the mix design process to be discussed in Chapter 21 are shown in Figure 16.3. These result from using aggregates with ideal gradings, and in practice it is normally not possible to achieve these exactly, but they are good 'targets'.

Sieve analysis and grading curves take no account of particle shape, but this does influence the voids content of the aggregate sample – more

---

[1] A list of all standards referred to in the text is included in 'Further reading' on page 222.

TABLE 16.1 British Standard grading requirements for aggregates for concrete (BS 882: 1992)

	Coarse aggregate							*Fine aggregate*			
Sieve size (mm)	*Single size*				*Graded*			*Overall limits*	*Additional limits*		
	40 mm	*20 mm*	*14 mm*	*10 mm*	*40–5 mm*	*20–5 mm*	*14–5 mm*		*Coarse*	*Medium*	*Fine*
	Per cent by weight passing										
37.5	85–100	100	–	–	90–100	100	–				
20	0–25	85–100	100	–	35–70	90–100	100				
14	–	0–70	85–100	100	25–55	40–80	90–100				
10	0–5	0–25	0–50	85–100	10–40	30–60	50–85	100			
5	–	0–5	0–10	0–25	0–5	0–10	0–10	89–100			
2.36		–	–	0–5	–	–	–	60–100	60–100	65–100	80–100
1.18				–				30–100	30–90	45–100	70–100
0.6								15–100	15–54	25–80	55–100
0.3								5–70	5–40	5–48	5–70
0.15								0–15			

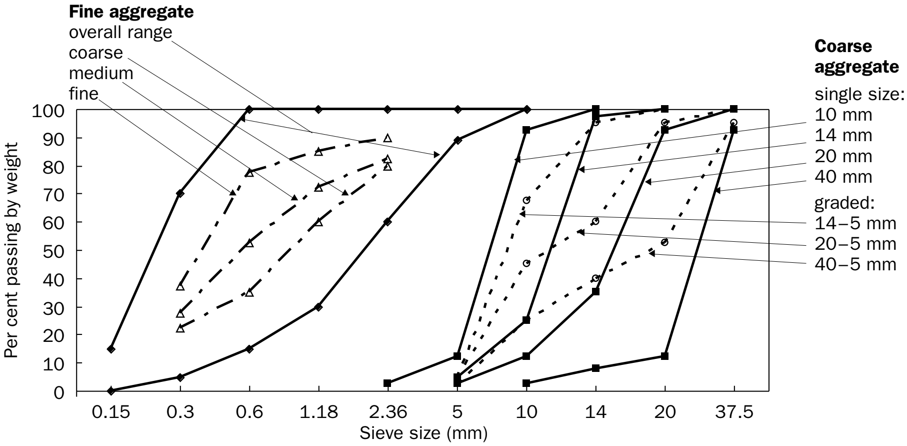

FIGURE 16.2 Grading curves of aggregates at mid-range of BS 882 limits.

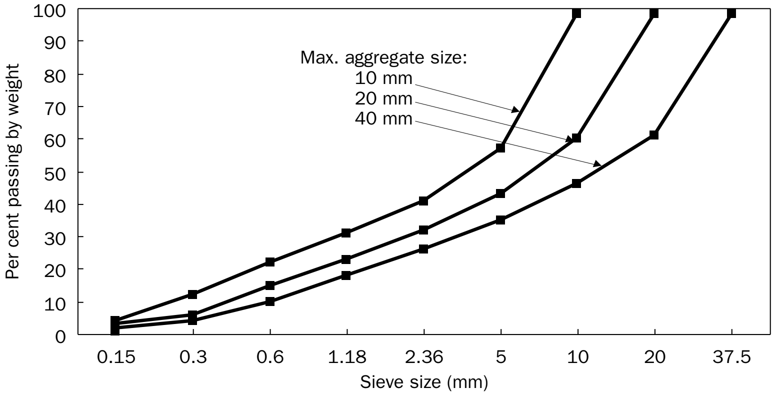

FIGURE 16.3 Examples of good combined aggregate grading curves for use in concrete.

rounded particles will pack more efficiently and will therefore have a lower voids content. According to Dewar (1983) it is sufficient to use only three numbers to characterise an aggregate for mix design purposes – specific gravity (or particle relative density), mean particle size and voids content in the loosely compacted state.

We should also mention here the *bulk density*. This is the weight of aggregate occupying a unit overall volume of both the particles and the air voids between them. It is measured by weighing a container of known volume filled with aggregate. The value will clearly depend on the grading which will govern how well the particles fit together, and also on how well the aggregate is compacted. Unlike the particle relative density, which is more useful, it is not therefore a constant for any particular aggregate type.

TABLE 16.2 Fineness modulus (fm) values for aggregates with the gradings in Figure 16.2

Coarse aggregate				*Fine aggregate*	
Single size	*fm*	*Graded*	*fm*	*Grading*	*fm*
40 mm	7.93	40–5 mm	7.25	coarse	3.03
20 mm	6.93	20–5 mm	6.55	medium	2.65
14 mm	6.70	10–5 mm	6.28	fine	2.10
10 mm	5.93				

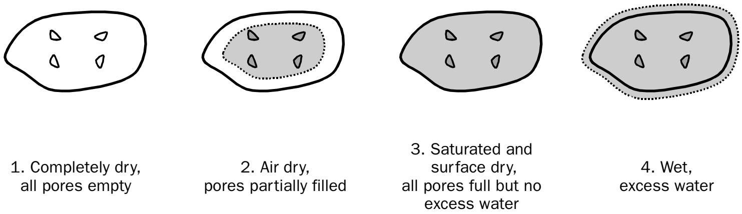

FIGURE 16.4 Possible moisture conditions of aggregate.

16.3 Other properties of aggregates

Other properties of aggregates that effect their use in concrete include porosity and absorption, elasticity, strength and surface characteristics.

16.3.1 Porosity and absorption

We have mentioned the high porosity of lightweight aggregates, but normal weight aggregates also contain some pores (typically 1–3 per cent by volume) which can absorb and hold water. Before concrete mixing, the aggregate can therefore be in one of the four moisture conditions shown in Figure 16.4. In the fresh concrete, aggregate that is in either of conditions (1) or (2) will absorb some of the mix water, and aggregate in condition (4) will contribute water to it. Condition (3), saturated surface dry, is perhaps most desirable, but is difficult to achieve except in the laboratory. Of prime importance to the subsequent concrete properties is the amount of water available for cement hydration, i.e. the amount that is non-absorbed or ‘free’; therefore, to ensure that the required free water/cement ratio is obtained, it is necessary to allow for the aggregate moisture condition when calculating the amount of mix water. If the aggregate is drier than saturated surface dry, extra water must be added; if it is wetter, then less mix water is required.

16.3.2 Elastic properties and strength

Since the aggregate occupies most of the concrete volume, its elastic properties have a major influence on the elastic properties of the concrete, as we shall discuss in Chapter 19. The reduction in strength of the concrete resulting from the use of the porous, lower strength lightweight aggregate has been discussed above. Normal weight aggregates are generally considerably stronger than the hcp, and therefore do not have a major influence on the strength of most concretes. However, in high-strength concrete (with strengths in excess of, say, 80 MPa – see Chapter 24) more careful aggregate selection is important.

16.3.3 Surface characteristics

The surface texture of the aggregate depends on the mineral constituents and the degree to which the particles have been polished or abraded. It seems to have a greater influence on the flexural strength than on the compressive strength of the concrete, probably because a rougher texture results in a better adhesion to the hardened cement paste. This adhesion is also greatly affected by the cleanliness of the surface – which must therefore not be contaminated by mud, clay or other similar materials. The interface or transition zone between the aggregate surface and the hardened cement paste has a major influence on the properties of the concrete, particularly strength, and is discussed in some detail in Chapter 20.

16.4 Reference

Dewar J.D. (1999) *Computer Modelling of Concrete Mixtures*, E & FN Spon, London, p. 272.

Chapter seventeen

Properties of fresh concrete

Civil engineers are responsible for the production, transport, placing, compacting and curing of fresh concrete. Without adequate attention to all of these the potential hardened properties of the mix, such as strength and durability, will not be achieved in the finished structural element. It is important to recognise that it is not sufficient simply to ensure that the concrete is placed correctly; the behaviour and treatment of the concrete during the period before setting, typically some six to ten hours after casting, and during the first few days of hardening, have a significant effect on the long-term performance.

It is beyond the scope of this book to discuss the operations and equipment used to batch, mix, handle, compact and finish the concrete. The aim of these practices is to produce a homogeneous structure with minimum air voids as efficiently as possible; it is also necessary to ensure that the concrete is then stable and achieves its full, mature properties. We therefore need to consider the properties when freshly mixed, between placing and setting, and during the early stages of hydration. We will discuss the former in this chapter, and the latter two in the next chapter. We will see that much of the technology is based on empiricism, but that an understanding can be achieved by applying the principles of *rheology* – the science of the deformation and flow of materials.

17.1 General behaviour

Experience in mixing, handling and placing fresh concrete quickly gives concrete workers (and students) a subjective understanding of the behaviour, and an ability to recognise ‘good’ and ‘bad’ concrete. A major problem is that a wide variety of subjective terms are used to describe the concrete, e.g. harsh, cohesive, lean, stiff, rich, which can mean different things to different people, and do not quantify the behaviour in any way. However, the main properties of interest can be described as follows:

1. Fluidity or consistency. It must be capable of being handled and of flowing into the formwork and around any reinforcement, with the assistance of whatever equipment is available. For example, concrete for a lightly reinforced, shallow floor slab need not be as fluid as that for a narrow, heavily reinforced column.
2. Compactability. All, or nearly all, of the air entrapped during mixing and handling should be capable of being removed by the compacting system being used, such as poker vibrators.
3. Stability or cohesiveness. The concrete should remain as a homogeneous uniform mass. For example, the mortar should not be so fluid that it segregates from the coarse aggregate.

The first two of these properties, fluidity and compactability, are generally combined into the property called *workability*. Although this might seem a fairly obvious property, engineers and concrete technologists have struggled since concrete construction became popular early in the last century to produce an adequate definition. Two fairly recent examples illustrate the difficulty. These are:

- 'that property of freshly mixed concrete or mortar which determines the ease and homogeneity with which it can be mixed, placed, consolidated and finished' (ACI Committee, 116, 1990).
- 'that property determining the effort required to manipulate a freshly mixed quantity of concrete with minimum loss of homogeneity' (American Society for Testing and Materials, 1993).

These relate to the requirements in very general terms only, but the biggest problem is that neither makes any reference to a quantitative measurable property, which engineers need and have for most other properties, e.g. elastic modulus, fracture toughness, etc. As we will see, measurement of workability is by no means straightforward.

In general, higher workability concretes (however defined or measured) are easier to place and handle, but if this high workability is obtained, for example, by an increased water content, then a lower strength and/or durability will result. Plasticisers and superplasticisers (Chapter 14) will help, but in most cases it is normal practice to use the lowest workability consistent with efficient handling and placing in the particular application, thereby increasing the need for a proper understanding of the fresh properties and the factors that effect them. (Achieving the balance between workability and strength is part of the mix design process, which we will be discussing in Chapter 21.)

As mentioned in the Introduction, most of the concrete (about 65–80 per cent of the volume) consists of fine and coarse aggregate. The remainder is cement paste, which in turn consists of 30–50 per cent by volume of cement, the rest being water. Cement paste, mortar and concrete are all therefore concentrated suspensions of particles of varying sizes, but all considerably denser than the mix water. Surface-attractive forces are significant in relation to gravitational forces for the cement particles, but less so for the aggregate particles, and the main resistance to flow comes from interference and friction between them. The behaviour is therefore far from simple.

17.2 Measurement of workability

17.2.1 Rheological properties

Rigorous definition of the flow behaviour of any fluid requires the application of rheological principles, and in particular the measurement of the relationship between shear stress and rate of shear strain (or shear rate), normally called the *flow curve*. This is normally carried out in a rheometer or viscometer of some sort. There are several types of these, perhaps the most common being a concentric cylinder viscometer in which an inner cylinder or bob is rotated in an outer cylinder or cup of the fluid. Any respectable undergraduate textbook in fluid mechanics will describe such instruments. Several such tests have been developed for concrete, involving either a mixing or shearing action, and which are of sufficient size to cope with coarse aggregate particles of up to 20 mm (RILEM, 2000). There is general agreement that the behaviour of fresh paste, mortar and concrete all approximate reasonably closely to the Bingham model illustrated in Figure 17.1. Flow only starts when the applied shear stress reaches a *yield stress* (τ_y) sufficient to overcome the interparticle interference effects, and at higher stresses the shear rate varies approximately linearly with shear stress, the slope defining the *plastic viscosity* (μ). Thus the two Bingham constants, τ_y and μ, are required to define the behaviour, unlike the simpler and very common case of a Newtonian fluid which does not have a yield stress, and which therefore requires only a single constant, *viscosity* (Chapter 4). Because at least two data points are required to define the flow curve, the first satisfactory test that was devised to measure this on concrete was called the *two- point workability test* (Tattersall and Banfill, 1983; Tattersall, 1991; Domone *et al.*, 1999).

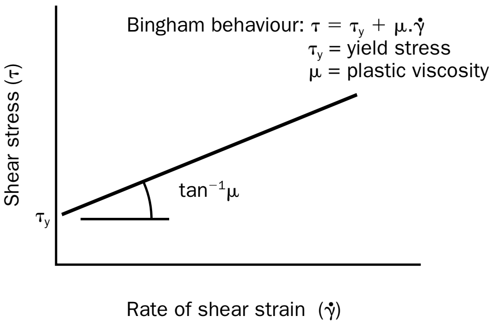

FIGURE 17.1 Flow curve of fresh concrete and the definitions of yield stress and plastic viscosity.

17.2.2 Single-point tests

Measurement of the two Bingham constants for concrete is a relatively recent development and involves the use of sophisticated and expensive apparatus. A large number of simpler and more convenient tests have been devised over many years, some only being used by their inventors. These all give only one number or test value, and can therefore be called *single point tests*; they clearly give a limited, but nevertheless useful, description of the concrete. Four have been adopted as 'standard tests' in many countries, and we will now consider these in some detail.[1]

The simplest, and crudest, is the *slump test* (Figure 17.2). The concrete is placed in the frustum of a steel cone and hand tamped in three layers. The cone is lifted off, and the slump is defined as the downward movement of the concrete. A true slump in which the concrete retains the overall shape of the cone and does not collapse is preferred, which gives a limit to the slump measurement of about 180 mm. A shear slump invalidates the test, and may indicate a mix prone to segregation due to lack of cement or paste. A collapsed slump is not ideal, but there has been a trend to the increasing use of superplasticised high workability mixes which produce collapsed slumps with little or no segregation, and slump values up to, and even above, 250 mm are regularly measured and quoted. For such very high workability mixes an alternative is to measure the final diameter or 'flow' of the concrete, which is more sensitive to changes in the mix than the change in height. Indeed, for self-compacting mixes (see Chapter 24) the *slump-flow test* is carried out without any initial compaction when filling the cone.

As a general guide, mixes with slumps ranging from about 10 mm upwards can be handled with conventional site equipment, with higher slumps (100 mm and above) being required to ensure full compaction of the concrete in areas with limited access or congested reinforcement. However, some zero slump mixes have sufficient workability for some applications. A recent European standard (ENV 206) classifies slump in four classes:

S1: slump = 10–40 mm
S2: slump = 50–90 mm
S3: slump = 100–150 mm
S4: slump ≥ 160 mm

and recommends using a mix in class S3 unless there is particular reason otherwise.

The *compacting factor test* (Figure 17.3) is able to distinguish between low slump mixes. Concrete is placed in an upper hopper, dropped into a lower hopper to bring it to a standard state, and then allowed to fall into a cylinder. The resulting degree of compaction of the concrete is then measured by comparing its weight with the weight of concrete in the cylinder when fully compacted. The compacting factor is defined as the former divided by the latter; values in the range 0.7 to 1 are obtained. The closer the value approaches 1, the higher the workability.

In the *Vebe test* (Figure 17.4), the response of the concrete to vibration is determined. The Vebe time is defined as the time taken to completely remould a sample of concrete from a slump test carried out in a cylindrical container. Standard vibration is applied, and remoulding times from 1 to about 25 secs are obtained, with higher values indicating decreased workability. It is often difficult to define the end point of complete remoulding with a sufficient degree of accuracy.

---

[1] A list of relevant standards is included in 'Further reading' on page 222.

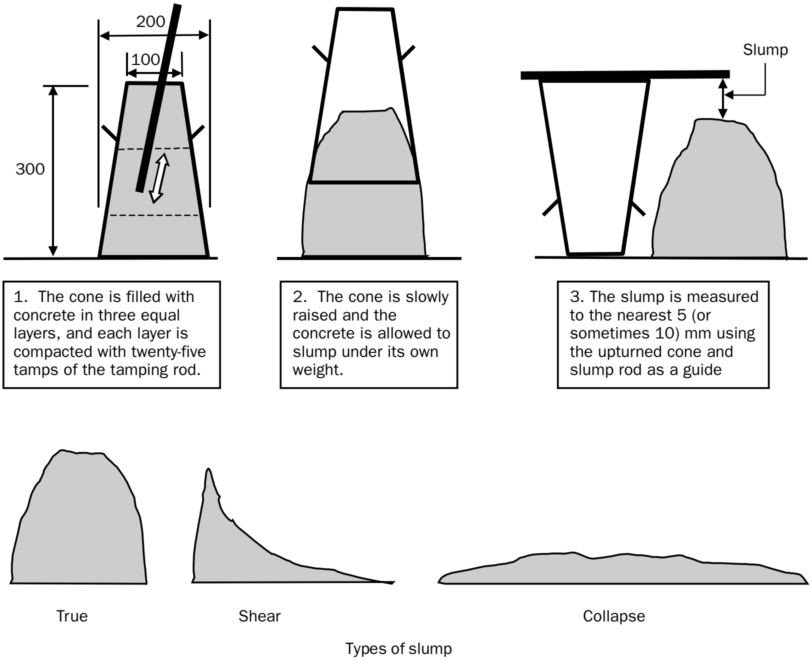

FIGURE 17.2 The slump test.

To differentiate between high workability mixes, the *flow table test* has been devised (Figure 17.5). It is essentially a slump test with a lower volume of concrete in which, after lifting the cone, some extra work is done on the concrete by lifting and dropping one edge of the board (or table) on which the test is carried out. A flow or spread of 400 mm indicates medium workability, and 500 mm high workability.

Apart from only giving a single test value, these four tests (or five if we consider the slump–flow test to be distinct from the slump test) all measure the response of the concrete to specific, but arbitrary and different, test conditions. The slump, slump–flow, Vebe and flow table tests provide a measure of the consistency or mobility of the concrete; the slump test after a standard amount of compaction work has been done on the concrete, the slump–flow test after the minimal amount of work of pouring into the cone, the Vebe test during a standard energy input, and the flow table with a combination of compaction work and energy input. The compacting factor test comes closest to assessing the compactability of the concrete, but the amount of work done on the concrete in falling into the cylinder is much less than the energy input from practical compaction equipment such as a poker vibrator.

There is some degree of correlation between the results of these tests, as illustrated in Figure 17.6, but as each of the tests measures the response to different conditions the correlation is quite broad. It is even possible for the results to be conflicting – e.g. for, say, the slump test to rank Mix A to be more workable than Mix B, and for the Vebe test to give the opposite

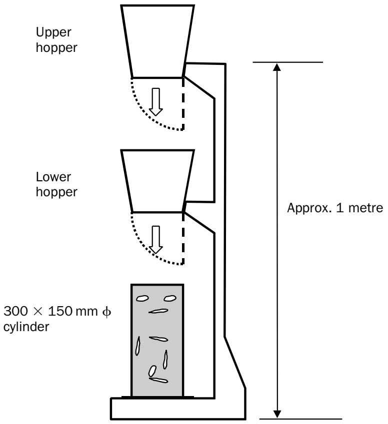

1. Concrete is loaded into the upper hopper.
2. The trap door is opened, and the concrete falls into the lower hopper.
3. The trap door is opened, and the concrete falls into the cylinder.
4. The concrete is struck off level with the top of the cylinder.
5. The cylinder + concete is weighed, to give the partially compacted weight of concrete.
6. The concrete is fully compacted, and extra concrete added to fill the cylinder.
7. The cylinder + concrete is weighed, to give the fully compacted weight of concrete.

$$\textbf{Compacting factor} = \frac{\textbf{weight of partially compact concrete}}{\textbf{weight of fully compact concrete}}$$

FIGURE 17.3 The compacting factor test.

ranking. The result therefore depends on the choice of test, which is far from satisfactory.

The slump and slump–flow tests clearly involve very low shear rates, and therefore, not surprisingly, reasonable correlations are obtained with yield stress. No correlation is obtained with plastic viscosity.

Despite there limitations, single point tests, particularly the slump test and, to a somewhat lesser extent, the flow table and slump–flow tests, are popular and in regular use. Perhaps the main reason for this is their simplicity and ease of use both in the laboratory and on site, but specifiers and users must be aware of the potential pitfalls of over-reliance on the results.

17.3 Factors affecting workability

Lower values of yield stress (τ_y) and plastic viscosity (μ) indicate a more fluid mix; in particular, reducing τ_y lowers the resistance to flow at low shear stresses, e.g. under self-weight when being poured, and reducing μ results in less cohesive or less 'sticky' mixes and increased response during compaction by vibration, when the localised shear rates can be high. Some of the more important

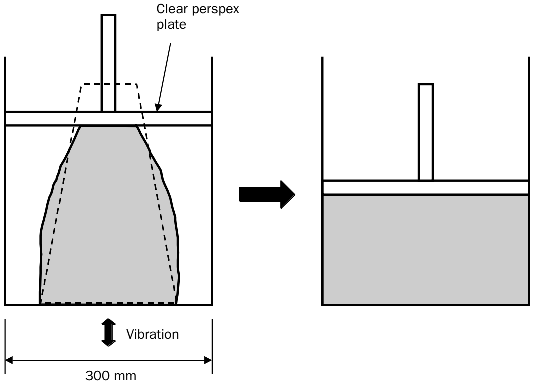

1. A slump test is performed in a container.
2. A clear perspex disc, free to move vertically, is lowered onto the concrete surface.
3. Vibration at a standard rate is applied.

Vebe degrees is the time (in seconds) to complete covering of the underside of the disc with concrete.

FIGURE 17.4 The Vebe test.

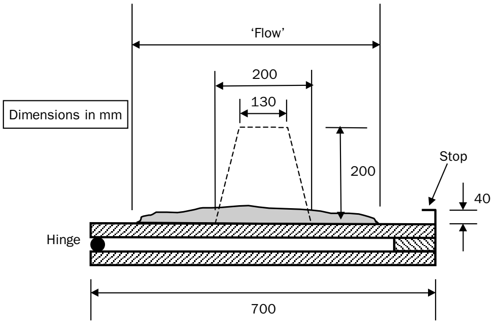

1. A conical mould (smaller than that of the standard slump test) is used to produce a sample of concrete in the centre of a 700 mm square board, hinged along one edge.
2. The free edge of the board is lifted against the stop and dropped 15 times.

Flow = final diameter of the concrete
(mean of two measurements at right angles)

FIGURE 17.5 The flow table test.

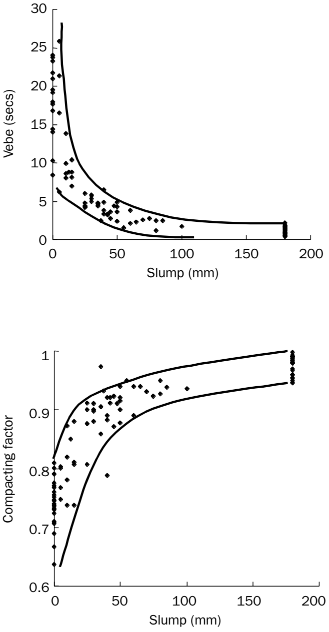

FIGURE 17.6 Typical relationship between results from single point workability tests (data from Ellis, 1977).

effects of variation of mix proportions and constituents on τ_y and μ, shown schematically in Figure 17.7, are as follows:

- Increasing the water content whilst keeping the proportions of the other constituents constant decreases τ_y and μ in approximately similar proportions.
- Adding a plasticiser or superplasticiser decreases τ_y but leaves μ relatively constant. In essence, the admixtures allow the particles to flow more easily but in the same volume of water. The effect is more marked with superplasticisers, which can even increase μ, and can therefore be used to give greatly increased flow properties under self-weight, whilst maintaining the cohesion of the mix. This is the basis for whole range of high workability or *flowing concretes*.
- Increasing the paste content will normally increase μ and decrease τ_y, i.e. the mix may start to flow more easily but will be stickier, and vice versa.
- Replacing some of the cement with pfa or ggbs will generally decrease τ_y, but may either increase or decrease μ, depending on the nature of the CRM and its interaction with the cement.
- The small bubbles of air produced by air-entraining agents provide lubrication to reduce the plastic viscosity, but at relatively constant yield stress.

There is a great deal of information available on the effect of mix constituents and proportions on workability measurements using single point tests, particularly slump. Since the specification and achievement of a slump value is the basis for the mix design method that we will describe in Chapter 21, to avoid unnecessary duplication we will leave discussion of these relationships until then.

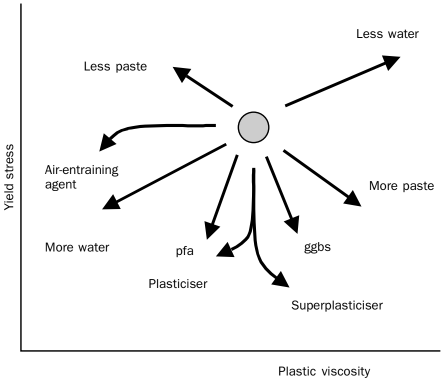

FIGURE 17.7 Summary of the effect of varying the proportions of concrete constituents on the Bingham constants.

17.4 Loss of workability

Although cement remains sufficiently workable for handling and placing for some time after it has been mixed, its workability continually decreases. This is due to:

- mix water being absorbed by the aggregate if this not in a saturated state before mixing;
- evaporation of the mix water;
- early hydration reactions (but this should not be confused with cement setting);
- interactions between admixtures (particularly plasticisers and superplasticisers) and the cementitious constituents of the mix.

Absorption of water by the aggregate can be avoided by ensuring that saturated aggregate is used, for example by spraying aggregate stockpiles with water and keeping them covered in hot/dry weather, although this may be difficult in some regions. It is also difficult, and perhaps undesirable, with lightweight aggregates. Evaporation of mix water can be reduced by keeping the concrete covered during transport and handling as far as possible.

Most available data relates to loss of slump, which increases with higher temperatures, higher initial slump, higher cement content and higher alkali and lower sulfate content of the cement. Figure 17.8 shows data from two mixes differing in water content only which illustrate the first two factors.

The rate of loss of workability can be reduced by continued agitation of the concrete, e.g. in a readymix truck, or modified by admixtures (Chapter 14). In principle, retempering, i.e. adding water to compensate for slump loss, should not have a significant effect on strength if only that water which has been lost by evaporation is replaced. Also, studies have shown that water can be added during retempering to increase the initial water/cement ratio by up to 5 per cent without any loss in 28-day strength

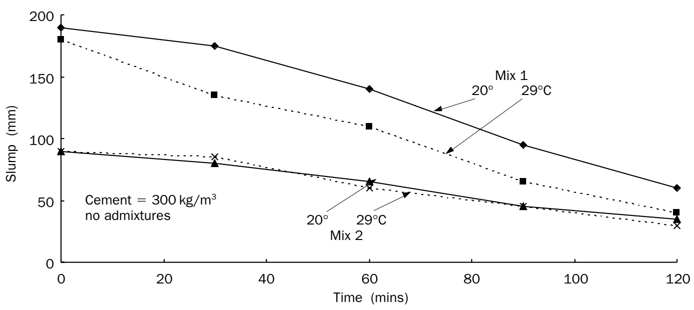

FIGURE 17.8 Typical slump loss behaviour of mixes differing in water content only (Previte, 1977).

(Cheong and Lee, 1993). However, except in very controlled circumstances, retempering can lead to unacceptably increased water/cement ratio and hence lower strength, and is therefore best avoided.

17.5 References

ACI (1990) *Cement and Concrete Terminology*. ACI 116R-90. American Concrete Institute, Detroit, USA.

ASTM (1993) *Specification C 125–93: Standard definitions and terms relating to concrete and concrete aggregates*.

Cheong, H.K. and Lee, S.C. (1993) Strength of retempered concrete. *ACI Materials Journal* 90, 3, 203–6.

Domone, P.L., Xu, Y. and Banfill, P.F.G. (1999) Developments of the two-point workability test for high-performance concrete. *Magazine of Concrete Research* 51, 171–9.

Ellis, C. (1977) *Some Aspects of pfa in Concrete*, MPhil thesis, Sheffield City Polytechnic.

Previte, R.W. (1977) Concrete slump loss. *ACI Materials Journal* 74, 8, 361–7.

RILEM (2000) TC 145-WSM. *Compendium of Concrete Workability Tests*, RILEM, Paris.

Tattersall, G.H. (1991) *Workability and Quality Control of Concrete*, E & FN Spon, London.

Tattersall, G.H. and Banfill, P.F.G. (1983), *The Rheology of Fresh Concrete*, Pitman, London.

Chapter eighteen

Early age properties of concrete

Successful placing of concrete is not enough. It is necessary to ensure that it comes through the first few days of its life without mishap, so that it goes on to have the required mature properties.

Immediately after placing, the concrete is still in a plastic and at least semi-fluid state, and the component materials are relatively free to move. During setting, it changes into a material which is stiff and unable to flow, but which has no strength. Clearly it must not be disturbed during this period. At some stage, hardening starts and the concrete develops strength, initially quite rapidly.

In this chapter we will discuss the behaviour of the concrete during each of these stages and how they affect construction practice. The hydration processes and the timescales involved have been described in some detail in Chapter 14, and their modification by admixtures and cement replacement materials in Chapter 15. In particular, we discussed the exothermic nature of the hydration reactions, and we will see that this has some important consequences.

18.1 Behaviour after placing

The constituent materials of the concrete are of differing relative density (cement 3.15, normal aggregates approx. 2.6, etc.) and therefore whilst the concrete is in its semi-fluid, plastic state the aggregate and cement particles tend to settle and the mix water has a tendency to migrate upwards. This may continue for several hours, until the time of final set and the onset of strength gain. Interparticle interference reduces the movement, but the effects can be significant. There are four inter-related phenomena – bleeding, segregation, plastic settlement and plastic shrinkage.

18.1.1 Segregation and bleeding

Segregation involves the larger aggregate particles falling towards the lower parts of the pour, and *bleeding* is the process of the upward migration or upward displacement of water. They often occur simultaneously (Figure 18.1).

The most obvious manifestation of bleeding is the appearance of a layer of water on the top surface of concrete shortly after it has been placed; in extreme cases this can amount to 2 per cent or more of the total depth of the concrete. In time this water either evaporates or is re-absorbed into the concrete with continuing hydration, thus resulting in a net reduction of the original concrete volume. This in itself may not

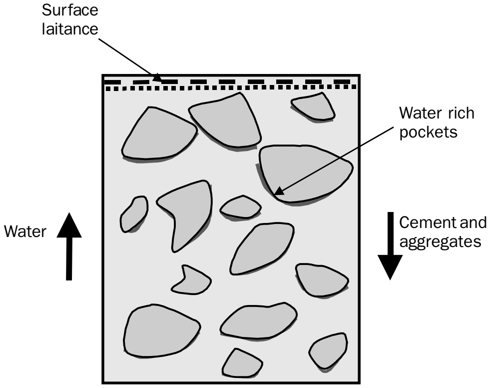

FIGURE 18.1 Segregation and bleed in freshly placed concrete.

be of concern, but there are two other effects of bleeding that can give greater problems, illustrated in Figure 18.1. Firstly, the cement paste at or just below the top surface of the concrete becomes water rich and therefore hydrates to a weak structure, a phenomenon known as surface laitance. This is a problem in, for example, floor slabs which are required to have a hard wearing surface. Secondly, the upward migrating water can be trapped under aggregate particles, causing a local enhanced weakening of the transition zone between the paste and the aggregate, which may already be a relatively weak part of the concrete, and hence an overall loss of concrete strength. However, in most concrete, some bleed may be unavoidable, and may not be harmful. We will discuss the transition zone and its effects in more detail in Chapter 20.

The combined effects of bleed and particle settlement are that after hardening the concrete in the lower part of a pour of any significant depth is stronger than that in the upper part. This effect is illustrated in Figure 18.2, which shows test data from trial columns made with three different mixes. Even though these are of a modest height of 500 mm, the strength differences between the top and bottom are of the order of 10 per cent

18.1.2 Plastic settlement

Overall settlement of the concrete will result in greater movement in the fresh concrete near the top surface of a deep pour. If there is any local restraint to this movement from, say, horizontal reinforcing bars, then plastic settlement cracking can occur, in which vertical cracks form along the line of the bars, penetrating from the surface to the bars (Figure 18.3 (a)).

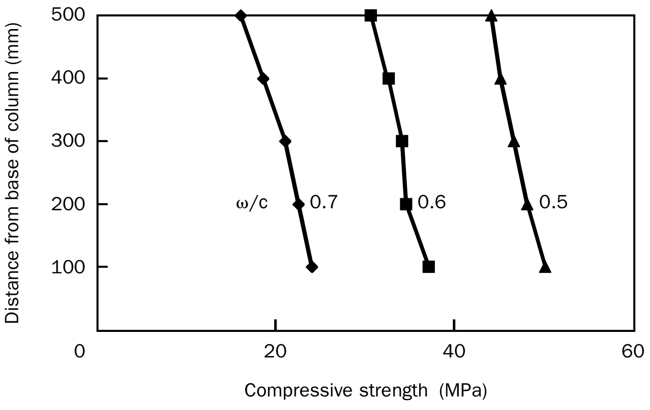

FIGURE 18.2 Variation of strength in a concrete column after full compaction (Hoshino, 1989).

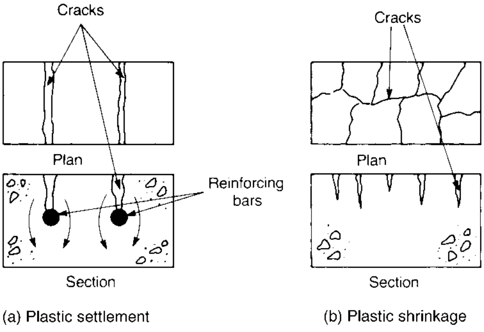

FIGURE 18.3 Causes of cracking in freshly placed concrete.

18.1.3 Plastic shrinkage

Bleed water arriving at an unprotected concrete surface will be subject to evaporation; if the rate of evaporation is greater than the rate of arrival of water at the surface, then there will be a net reduction in water content of the surface concrete, and plastic shrinkage, i.e. drying shrinkage whilst the concrete is still plastic, will occur. The restraint of the mass of concrete will cause tensile strains to be set up in the near-surface region, and as the concrete has near zero tensile strength, plastic shrinkage cracking may result. The cracking pattern, illustrated in Figure 18.3 (b) is a fairly regular 'crazing', and is therefore distinctly different from that resulting from plastic settlement.

Any tendency to plastic shrinkage cracking will be encouraged by greater evaporation rates of the surface water which occurs, for example, with higher concrete or ambient temperatures, or if the concrete is exposed to wind.

18.1.4 Methods of reducing segregation and bleed and their effects

A major cause of excessive bleed is the use of a poorly graded aggregate, with a lack of fine material below a particle size of 300 μm being most critical. This can be remedied by increasing the sand content, but if this is not feasible for other reasons, or if a particularly coarse sand has to be used, then air entrainment can be an effective substitute for the fine particles.

Higher bleeds may also occur with higher workability mixes, and if very high workabilities are required, it is preferable to use superplasticisers rather than high water contents, as discussed in Chapter 14. Condensed silica fume, with its very high surface area, is also an effective bleed control agent.

Bleed, however, cannot be entirely eliminated, and so measures must be taken in practice to reduce its effects if these are critical. Plastic settlement and plastic shrinkage cracks that occur soon after placing the concrete can be eliminated by revibrating the surface region, particularly in large flat slabs.

18.2 Curing

All concretes, no matter how great or small their tendency to bleed, must be protected from moisture loss from as soon after placing as possible, and for the first few days of hardening. This will not only reduce or eliminate plastic shrinkage cracking, but also ensure that there is an adequate supply of water for continued hydration and strength gain. This protection is called *curing*, and is an essential part of any successful concreting operation, although often overlooked. Curing methods include:

- spraying or ponding the surface of the concrete with water;
- protecting exposed surfaces from wind and sun by windbreaks and sunshades;
- covering surfaces with wet hessian and/or polythene sheets;
- applying a curing membrane, usually a spray-applied resin seal, to the exposed surface; this prevents moisture loss, and weathers away in a few weeks.

Extended periods of curing are required for mixes that gain strength slowly, such as those containing CRMs, particularly pfa and ggbs, and in conditions of low ambient temperatures.

18.3 Strength gain and temperature effects

18.3.1 Effect of curing temperature

We mentioned in Chapter 13 that the hydration reactions between cement and water are temperature-dependent and their rate increases with curing temperature. Typical effects of curing temperature on concrete strength development are shown in Figure 18.4, in which the following features can be seen.

1. At early ages the rate of strength gain increases with curing temperature, as would be expected.
2. At later ages, however, higher strengths are obtained from the concrete cured at lower temperatures. Explanations of this behaviour have been conflicting, but it would seem that, as similar behaviour is obtained with cement paste, the C—S—H gel more rapidly produced at the higher temperatures is less uniform and hence weaker than that produced at the lower temperatures. There also appears to be an optimum temperature for maximum long-term strength, in this case 13°C; this optimum has been found to vary for different types of cement.
3. The hydration reactions proceed at temperatures below the freezing point of water, 0°C. In fact they only cease completely at about −10°C. However, the concrete must only be exposed to such temperatures after a significant amount of the mix water has been incorporated in the hydration reactions, since the expansion of free water on freezing will disrupt the immature, weak concrete. A degree of hydration equivalent to a strength of 3.5 MPa is considered sufficient to give protection against this effect.

18.3.2 Maturity

Since the degree of cement hydration depends on both time and temperature, it might be expected that maturity, defined as the product of time and curing temperature, would show some correlation with strength. For the reasons given above, −10°C is taken as the datum point for temperature, and hence

$$\text{maturity} = \Sigma t(T + 10)$$

where t and T are the time (normally in hours) and curing temperature (in °C) respectively. Figure 18.5 shows maturity plotted against

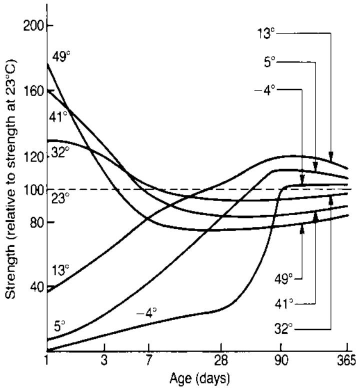

FIGURE 18.4 Effect of curing temperature on concrete strength (Portland cement, w/c = 0.4) (Klieger, 1958 by permission, American Concrete Institute).

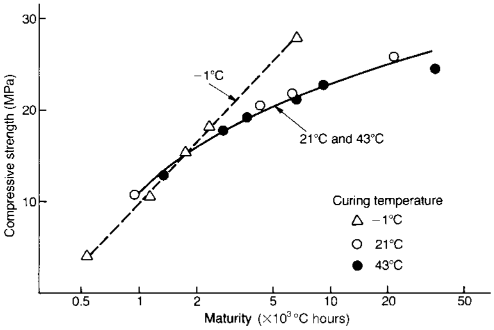

FIGURE 18.5 Strength versus maturity relationship for a concrete cured at three different temperatures (Carino *et al.*, 1983).

strength for three different but constant curing temperatures, −1, 21 and 43°C. It can be seen that concrete at all three temperatures has similar strength/maturity values at low maturities, but subsequently the maturities for the lowest temperature give higher strength values. In addition, initial curing for even a few hours at temperatures higher or lower than that for subsequent curing alters the strength/maturity relationship.

The maturity concept is useful when estimating the strength of concrete in a structure from the strength of laboratory samples cured at a different temperature. However, the limitations of the temperature range, as illustrated in Figure 18.5, must be borne in mind.

18.3.3 Heat of hydration effects

As well as being temperature-dependent, cement hydration is exothermic, and in Chapter 13 we discussed in some detail the rate of heat output at constant temperature (i.e. isothermal) conditions in relation to the various hydration reactions. The opposite extreme to the isothermal condition is adiabatic (i.e. perfect insulation or no heat loss), and in this condition the exothermic reactions result in heating of a cement paste, mortar or concrete. This leads to progressively faster hydration, heat output rate and temperature rise, the result being substantial temperature rises in relatively short timescales (Figure 18.6). The temperature rise in concrete is less than that in cement paste as the aggregate acts as a heat sink and there is less cement to react. An average rise of 13°C per 100 kg of cement per m^3 of concrete has been suggested for typical structural concretes.

When placed in a structure, the concrete will lose heat to its surrounding environment either directly or through formwork, and it will therefore not be under either truly adiabatic or isothermal conditions, but in some intermediate state. This results in some rise in temperature within the pour followed by cooling to ambient. Typical temperature/time profiles for the centre of pours of varying depths are shown in Figure 18.7; it can be seen that the central regions of a pour with an overall thickness in excess of about 1.5 to 2 m will behave adiabatically for the first few days after casting.

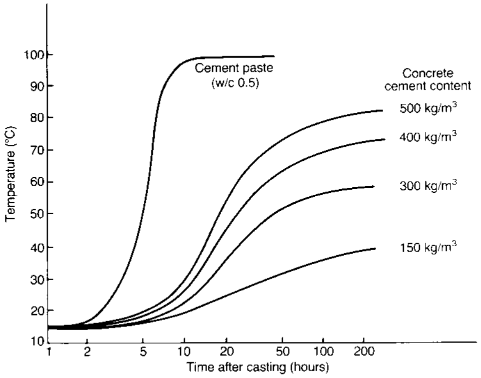

FIGURE 18.6 Typical temperature rise during curing under adiabatic conditions for a neat cement paste and concrete with varying cement content (Bamforth, 1988).

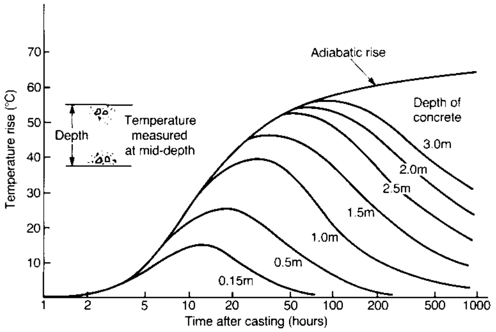

FIGURE 18.7 The effect of depth of a concrete pour on temperature rise at mid-depth during hydration (placing temperature = 20°C, Portland cement content = 400 kg/m^3) (Browne and Blundell, 1973 by permission, Concrete Society).

Such behaviour has two important effects.

1. The cool down from the peak temperature conditions will result in thermal contraction of the concrete, which if restrained will result in tensile stresses which may be sufficiently large to crack the concrete. Restraint can result from the structure surrounding the concrete, e.g. the

soil underneath a foundation, or from the outer regions of the concrete pour itself, which will have been subject to greater heat losses, and therefore will not have reached the same peak temperatures, or from reinforcement within the concrete. The amount of restraint will obviously vary in different structural situations.

As an example, a typical coefficient of thermal expansion for concrete is 10×10^{-6} per °C, and therefore a thermal shrinkage strain of 300×10^{-6} would result from a cool down of 30°C. Taking a typical elastic modulus for the concrete of 30 GPa, and assuming complete restraint with no relaxation of the stresses due to creep, the resulting tensile stress would be 9 MPa, well in excess of the tensile strength of the concrete, which would therefore have cracked.

In structural concrete, a reinforcement system can be designed to control and reduce the effects of any cracking, but it is also necessary in pours of any substantial size to limit the temperature differentials. Insulation by way of increased formwork thickness or thermal blankets will have some beneficial effect, but, more commonly, or in addition, low-heat mixes are used. If strength or durability criteria mean that a sufficiently low cement content cannot be used, then either a low-heat Portland cement (mentioned in Chapter 13) can be used, or, more conveniently, partial cement replacement by pulverised fuel ash (pfa) or ground granulated blast furnace slag (ggbs) is an effective solution, as shown in Figure 18.8. (These materials were described in Chapter 14.)

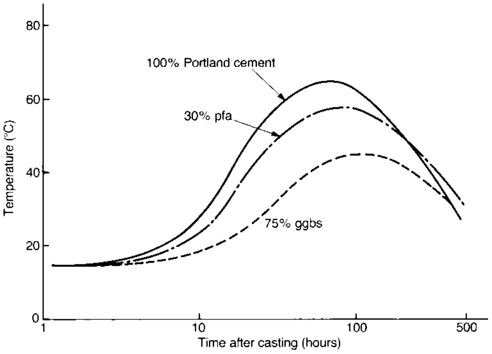

FIGURE 18.8 Temperature variation at mid-height of a 2.5 m deep pour during hydration of concrete made with 100 per cent Portland cement, 70 per cent + 30 per cent pfa and 25 per cent Portland cement + 75 per cent ggbs (Bamforth, 1980 by permission, Institute of Civil Engineers).

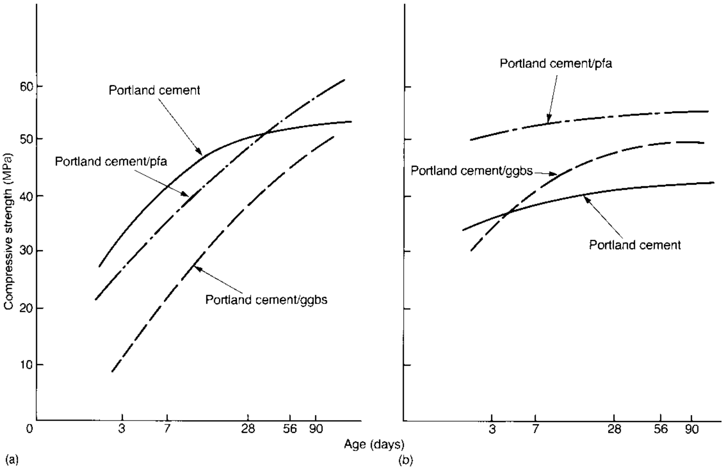

FIGURE 18.9 Strength development of concrete made with 100 per cent Portland cement, 70 per cent Portland cement + 30 per cent pfa and 25 per cent Portland cement + 75 per cent ggbs when subjected to: (a) standard curing at 20°C; and (b) the curing cycle shown in Figure 18.8 (Bamforth, 1980 by permission, Institute of Civil Engineers).

As alternative or additional measures, the temperature of the fresh concrete can be reduced by pre-cooling the mix water or the aggregates, or by injecting liquid nitrogen.

2. Much of the concrete will have hydrated for at least a few days after casting at temperatures higher than ambient, and the long-term strength may therefore be reduced, due to the effects described above. Typical effects of this on strength development are shown in Figure 18.9. By comparing Figure 18.9(a) and (b) it can be seen that pfa and ggbs mixes do not suffer the same strength losses as the 100 per cent Portland cement mixes. Measurement of the concrete properties after being subjected to such 'temperature matched curing' is therefore extremely important if a full picture of the in-situ behaviour is to be achieved.

18.4 References

Bamforth, P.B. (1980) In-situ measurement of the effect of partial Portland cement replacement using either fly ash or ground granulated blast-furnace slag on the performance of mass concrete. *Proc. Instn Civ. Engnrs,* Part 2, 69, Sept., 777–800.

Bamforth, P.B. (1988) Early age thermal cracking in large sections: towards a design approach. Institute for International Research, *Proceedings of Asia Pacific Conference on Roads, Highways and Bridges,* Hong Kong, Sept.

Browne, R.D. and Blundell, R. (1973) Hong Kong. *Proceedings of Symposium on Large Pours for RC Structures*, Concrete Society University of Birmingham, Sept., pp. 42–65.

Carino, N.J., Lew, H.S. and Volz, C.K. (1983) Temperature effect on strength maturity relationships of mortar. *J. Amer. Concrete Inst., 80,* 2, March–April, 93-101.

Hoshino, J. (1989) Relationship between bleeding, coarse aggregate and specimen height of concrete. *ACI Materials Journal* 86, 2, 185–90.

Klieger, P. (1958) Effect of mixing and curing temperature on concrete strength. *Journ. Amer. Concrete Inst.* 54, 12, June, 1063–81.

Chapter nineteen

Deformation of concrete

Deformation of concrete results both from environmental effects, such as moisture gain or loss movement and heat, and from applied stress, both short- and long-term. A general view of the nature of the behaviour is given in Figure 19.1, which shows the strain arising from a uniaxial compressive stress applied to the concrete in a drying environment. The load or stress is applied at a time t_1, and held constant until removal at time t_2. Before applying the stress, there is a net contraction in volume of the concrete, or shrinkage, associated with the drying. The dotted extension in this curve beyond time t_1 would be the subsequent behaviour without stress, and the effects of the stress are therefore the differences between this curve and the solid curves. Immediately on loading there is an instantaneous strain response, which for low levels of stress is approximately proportional to the stress, and hence an elastic modulus can be defined. With time, the strain continues to increase at a decreasing rate. This increase, after allowing for shrinkage, represents the creep strain. Although reducing in rate with time, the creep does not tend to a limiting value.

On unloading, at time t_2, there is an immediate (elastic) strain recovery, which is often less than the initial strain on loading. This is followed by a time-dependent creep recovery, which is less than the preceding creep, i.e. there is a permanent deformation, but, unlike creep, this reaches completion in due course.

In this chapter we shall discuss the mechanisms and the factors influencing the magnitude of all of the components of this behaviour, i.e. shrinkage, elastic response and creep, and also consider thermally induced strains. We shall for the most part be concerned with the behaviour of hardened cement paste and concrete when mature, but some mention of age effects will be made.

19.1 Drying shrinkage

19.1.1 Drying shrinkage of hardened cement paste

In Section 13.6 we described the broad divisions of water in hardened cement paste (hcp) and how their removal led to a net volumetric contraction, or drying shrinkage of the paste. Even though shrinkage is a volumetric effect, it is normally measured in the laboratory or on structural elements by determination of length change, and it is therefore expressed as a linear strain.

A considerable complication in interpreting and comparing drying shrinkage measurements is that specimen size will affect the result. Water can only be lost from the surface and, therefore, the inner core of a specimen will act as a restraint

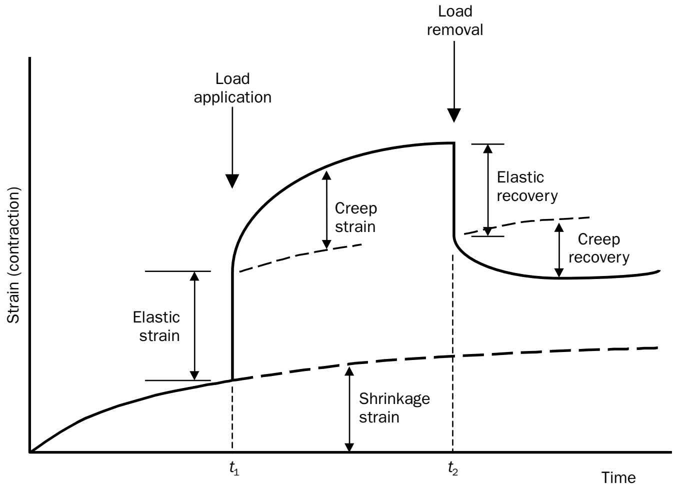

FIGURE 19.1 The response of concrete to a compressive stress applied in drying environment.

against overall movement; the amount of restraint and hence the measured shrinkage will therefore vary with specimen size. In addition, the rate of moisture loss, and hence the rate of shrinkage, will depend on the rate of transfer of water from the core to the surface. The behaviour of hcp discussed in this section is therefore based on experimental data from specimens with a relatively small cross-section.

A schematic illustration of typical shrinkage behaviour is shown in Figure 19.2. Maximum shrinkage occurs on the first drying, and a consid-

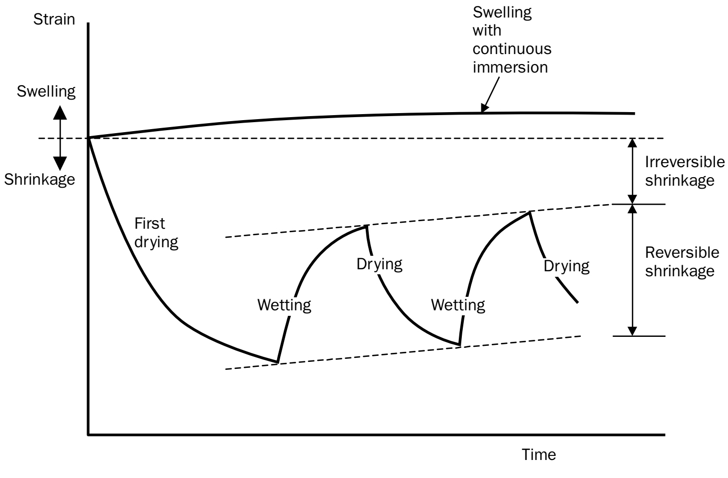

FIGURE 19.2 Strain response of cement paste or concrete to alternate cycles of drying and wetting.

erable part of this is irreversible, i.e. is not recovered on subsequent rewetting. Further drying and wetting cycles result in more or less completely reversible shrinkage; hence there is an important distinction between reversible and irreversible shrinkage.

Also shown in Figure 19.2 is a continuous, but relatively small, swelling of the hcp on continuous immersion in water. The water content first increases to make up for the self-desiccation during hydration (see Section 13.4), and to keep the paste saturated. Second, additional water is drawn into the C—S—H structure to cause the net increase in volume. This is a characteristic of many gels, but in hcp the expansion is resisted by the skeletal structure so that the swelling is small compared to the drying shrinkage strains.

In principle, the stronger the hcp structure, the less it will respond to the forces of swelling or shrinkage. This is confirmed by the results shown in Figure 19.3, in which the increasing total porosity of the paste is, in effect, decreasing strength. It is interesting that the reversible shrinkage appears independent of porosity, and the overall trend of increased shrinkage on first drying is entirely due to the irreversible shrinkage.

The variations in porosity shown in Figure 19.3 were obtained by testing pastes of different water/cement ratios, and in general, increased water/cement ratio will result in increasing shrinkage. As we have seen in Chapter 13, reduction in porosity also results from greater degrees of hydration of pastes with the same water/cement ratio, but the effect of the degree of hydration on shrinkage is not so simple. The obvious effect should be that of reduced shrinkage with age of paste if properly cured; however, the unhydrated cement grains provide some restraint to the shrinkage, and as their volume decreases with hydration, an increase in shrinkage would result. Another argument is that a more mature paste contains more water of the type whose loss causes greater shrinkage, e.g. less capillary water, and so loss of the same amount of water from such a paste would cause more shrinkage. It is thus difficult to predict the net effect of age on the shrinkage of any particular paste.

Since shrinkage results from water loss, the

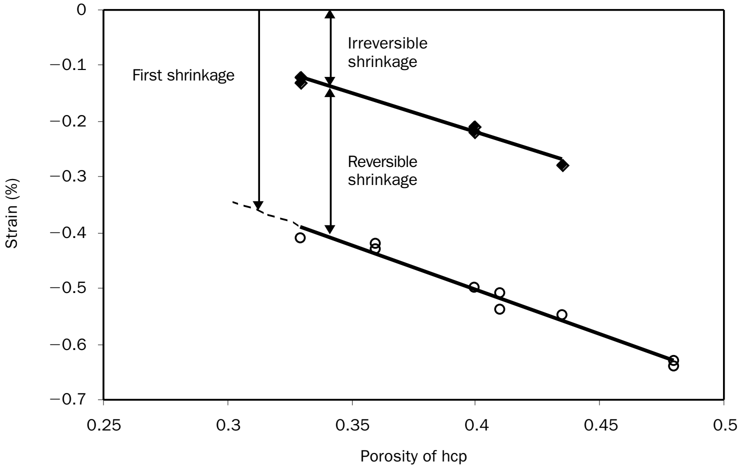

FIGURE 19.3 Reversible and irreversible shrinkage of hcp after drying at 47 per cent relative humidity (Helmuth and Turk, 1967).

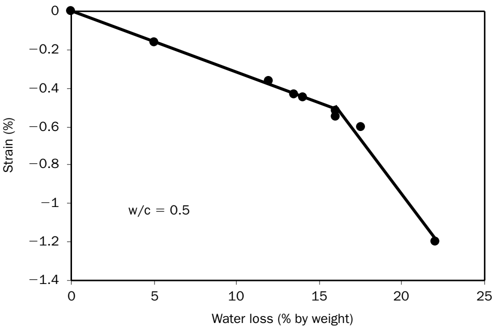

FIGURE 19.4 The effect of water loss on the drying shrinkage of hardened cement paste (Verbeck and Helmuth, 1968).

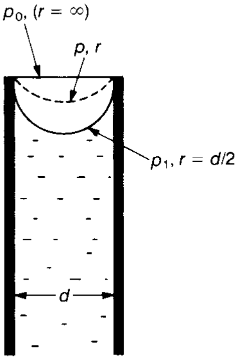

FIGURE 19.5 Relationship between the radius of curvature and vapour pressure for water in a capillary (Soroka, 1979).

relationship between the two is of interest. Typical data are given in Figure 19.4, which shows that there is a distinct change of slope with increased moisture losses, in this case about a 17 per cent loss. This implies that there is more than one mechanism of shrinkage; as other tests have shown two or even three changes of slope, it is likely that, in fact, several mechanisms are involved.

19.1.2 Mechanisms of shrinkage and swelling

Four principal mechanisms have been proposed for shrinkage and swelling in cement pastes, which are now summarised.

Capillary tension

Free water surfaces in the capillary and larger gel pores (see Section 13.6) will be in surface tension, and when water starts to evaporate due to a lowering of the ambient vapour pressure, the free surface becomes more concave and the surface tension increases (Figure 19.5). The relationship between the radius of curvature, r, of the meniscus and the corresponding vapour pressure, p, is given by Kelvin's equation:

$$\ln(p/p_0) = 2T/R\theta\rho r \qquad (19.1)$$

where p_0 is the vapour pressure over a plane surface, T is the surface tension of the liquid, R is the gas constant, θ is the absolute temperature and ρ the density of the liquid.

The tension within the water near the meniscus can be shown to be $2T/r$, and this tensile stress must be balanced by compressive stresses in the surrounding solid. Hence the evaporation which causes an increase in the tensile stress will subject the hcp solid to increased compressive stress which will result in a decrease in volume, i.e. shrinkage. The diameter of the meniscus cannot be smaller than the diameter of the capillary, and the pore therefore empties at the corresponding vapour pressure, p_1. Hence on exposing a cement paste to a steadily decreasing vapour pressure, the pores gradually empty according to their size, the widest first. Higher water/cement ratio pastes with higher porosities will therefore shrink more, thus explaining the general form of Figure 19.3. As a pore empties, the imposed stresses on the surrounding solid reduce to zero, and so full recovery of shrinkage would be expected on complete drying. Since this does not occur, it is generally accepted that other mechanisms become operative at low humidities, and that this mechanism only applies at relative humidities above about 50 per cent.

Surface tension or surface energy

The surface of both solid and liquid materials will be in a state of tension due to the net attractive forces of the molecules within the material. Work, therefore, has to be done against this force to increase the surface area, and the surface energy is defined as the work required to increase the surface by unit area.

Surface tension forces induce compressive stresses in the material of value $2T/r$ (see above) and in the hcp solids, whose average particle size is very small, these stresses are significant. Adsorption of water molecules onto the surface of the particles reduces the surface energy, hence reducing the balancing internal compressive stresses, leading to an overall volume increase, i.e. swelling. This process is also reversible.

Disjoining pressure

Figure 19.6 shows a typical gel pore, narrowing from a wider section containing free water in contact with vapour to a much narrower space between the solid in which all the water is under the influence of surface forces. The two layers are prevented from moving apart by an interparticle Van der Waals type bond force. The adsorbed water forms a layer about five molecules or 1.3 nm thick on the solid surface at saturation, which is under pressure from the surface-attractive forces. In regions narrower than twice this thickness, i.e. about 2.6 nm, the interlayer water will be in an area of hindered adsorption. This results in the development of a swelling or disjoining pressure, which is balanced by a tension in the interparticle bond.

On drying, the thickness of the adsorbed water layer reduces, as does the area of hindered adsorption, hence reducing the disjoining pressure. This results in an overall shrinkage.

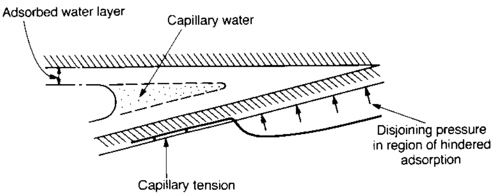

FIGURE 19.6 Water forces in a gel pore in hardened cement paste (Bazant, 1972).

Movement of interlayer water

The mechanisms described above concern the free and adsorbed water. The third type of evaporable water, the interlayer water, may also have a role. Its intimate contact with the solid surfaces and the tortuosity of its path to the open air suggest that a steep hygrometric energy gradient is needed to move it, but also that such movement is likely to result in significantly higher shrinkage than the movement of an equal amount of free or adsorbed water. It is likely that this mechanism is associated with the steeper slope of the graph in Figure 19.4 at the higher values of water loss.

The above discussions apply to the reversible shrinkage only, but the reversibility depends on the assumption that there is no change in structure during the humidity cycle. This is highly unlikely, at least during the first cycle, because:

1. the first cycle opens up interconnections between previously unconnected capillaries, thereby reducing the area for action of subsequent capillary tension effects;
2. some new interparticle bonds will form between surfaces that move closer together as a result of movement of adsorbed or interlayer water, resulting in a more consolidated structure and a decreased total system energy.

Opinion is divided on the relative importance of the above mechanisms and their relative contribution to the total shrinkage. These differences of opinion are clear from Table 19.1, which shows the mechanisms proposed by four main authors, and the suggested humidity levels over which they act.

TABLE 19.1 Summary of suggested shrinkage mechanisms (Soroka, 1979)

Source	*Relative humidity (%)*										
	0	*10*	*20*	*30*	*40*	*50*	*60*	*70*	*80*	*90*	*100*
Powers (1965)	⟵ disjoining pressure ⟶										
							⟵ capillary tension ⟶				
Ishai (1965)	⟵ surface energy ⟶				⟵ capillary tension ⟶						
Feldman and Sereda (1970)	⟵ interlayer water ⟶			⟵ capillary tension and surface energy ⟶							
Wittman (1968)	⟵ surface energy ⟶				⟵ disjoining pressure ⟶						

19.1.3 Drying shrinkage of concrete

Effect of mix constituents and proportions

The drying shrinkage of concrete is less than that of neat cement paste because of the restraining influence of the aggregate, which, apart from a few exceptions, is dimensionally stable under changing moisture states.

The effect of aggregate content is shown in Figure 19.7. It is apparent that normal concretes have a shrinkage of some 10 to 20 per cent of that of neat paste. Aggregate stiffness will also have an effect. Normal density aggregates are stiffer and therefore give more restraint than lightweight aggregates, and therefore lightweight aggregate concretes will tend to have a higher shrinkage than normal density concretes of similar volumetric mix proportions.

The combined effect of aggregate content and stiffness are contained in the empirical equation

$$\epsilon_c/\epsilon_p = (1 - g)^n \qquad (19.2)$$

where ϵ_c and ϵ_p are the shrinkage strains of the concrete and paste respectively, g is the aggregate volume content, and n is a constant which depends on the aggregate stiffness, and has been found to vary between 1.2 and 1.7.

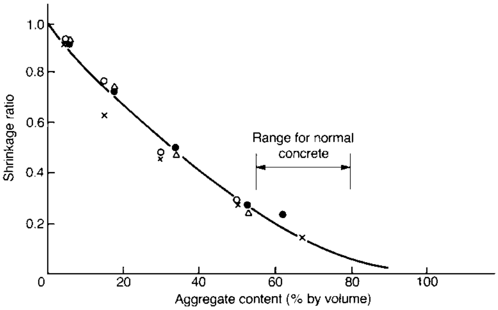

FIGURE 19.7 Influence of aggregate content in concrete on the ratio of the shrinkage of concrete to that of neat cement paste (Pickett, 1956).

The overall pattern of the effect of mix proportions on the shrinkage of concrete is shown in Figure 19.8; the separate effects of increased shrinkage with increasing water content and increasing water/cement ratio can be identified.

The properties and composition of the cement and the incorporation of pfa, ggbs and microsilica all have little effect on the drying shrinkage of concrete, although interpretation of the data is sometimes difficult. Admixtures do not in themselves have a significant effect, but if their use

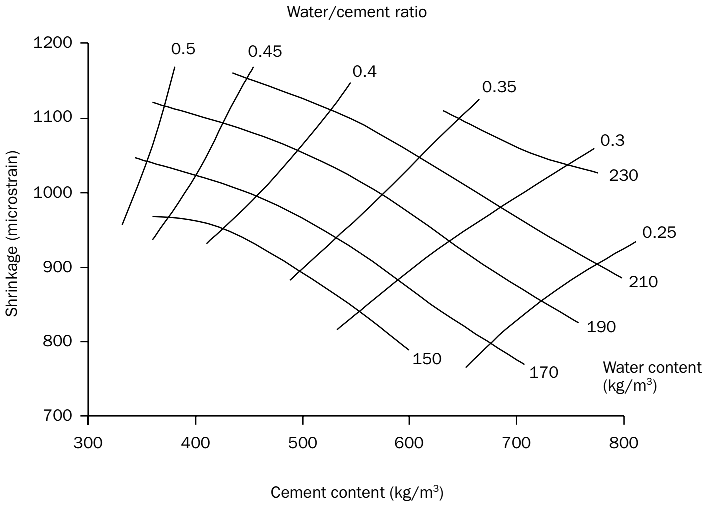

FIGURE 19.8 Typical effects of cement content, water content and water/cement ratio on shrinkage of concrete – moist curing for 28 days followed by drying for 450 days (Shoya, 1979).

results in changes in the mix proportions then, as shown in Figure 19.8, the shrinkage will be affected.

Effect of specimen geometry

The size and shape of a concrete specimen will influence the rate of moisture loss and the degree of overall restraint provided by the central core, which will have a higher moisture content than the surface region. The rate and amount of shrinkage and the tendency for the surface zones to crack are therefore affected.

In particular, longer moisture diffusion paths lead to lower shrinkage rates. For example, a member with a large surface area to volume ratio, e.g. a T-beam, will dry and therefore shrink more rapidly than, say, a beam with a square cross-section of the same area. In all cases, however, the shrinkage process is protracted. In a study lasting 20 years, Troxell *et al.* (1958) found that in tests on 300 × 150 mm diameter cylinders made from a wide range of concrete mixes and stored at relative humidities of 50 and 70 per cent, an average of only 25 per cent of the 20-year shrinkage occurred in the first two weeks, 60 per cent in three months, and 80 per cent in one year.

The non-uniform drying and shrinkage in a structural member will result in differential strains and hence shrinkage-induced stresses – tensile near the surface and compressive in the centre. The tensile stresses may be sufficient to cause cracking, which is the most serious consequence for structural behaviour and integrity. However, as discussed above, the effects in practice occur over a protracted timescale, and the stresses are relieved by creep before cracking occurs. The structural behaviour is therefore complex and difficult to analyse with any degree of rigour.

19.1.4 Prediction of shrinkage

It is clear from the above discussion that, although much is known about shrinkage and the factors that influence its magnitude, it is difficult to estimate its value in a structural situation with any degree of certainty. It has been shown that it is possible to obtain reasonable estimates of long-term shrinkage from short-term tests (Neville *et al.*, 1983), but designers often require estimates long before results from even short-term tests can be obtained. There are a number of methods of varying degrees of complexity for this, often included in design codes, e.g. BSI (1997), ACI (2000a), all of which are based on the analysis and interpretation of extensive experimental data.

19.2 Autogenous shrinkage

Continued hydration with an adequate supply of water leads to slight swelling of cement paste, as shown in Figure 19.2. Conversely, with no moisture movement to or from the cement paste, self-desiccation leads to removal of water from the capillary pores (as described in Section 13.4) and *autogenous shrinkage*. It may be the only form of shrinkage occurring in the centre of large mass of concrete, but its magnitude is normally at least an order of magnitude less than that of drying shrinkage. It can, however, be larger and more significant in concrete with very low water/cement ratios.

19.3 Carbonation shrinkage

Carbonation shrinkage differs from drying shrinkage in that its cause is chemical, and it does not result from loss of water from the hcp or concrete. Carbon dioxide, when combined with water as carbonic acid, attacks most of the components of the hcp, and even the very dilute carbonic acid resulting from the low concentrations of carbon dioxide in the atmosphere can have significant effects. The most important reaction is that with the calcium hydroxide:

$$CO_2 + Ca(OH)_2 \rightarrow CaCO_3 + H_2O \quad (19.3)$$

Thus water is released and there is an increase in weight of the paste. There is an accompanying shrinkage, and the paste also increases in strength and decreases in permeability. The most likely mechanism to explain this behaviour is that the calcium hydroxide is dissolved from more highly stressed regions, resulting in the shrinkage, and the calcium carbonate crystallises out in the pores, thus reducing the permeability and increasing the strength.

The rate and amount of carbonation depend in part on the relative humidity of the surrounding air, and within the concrete. If the pores are saturated, then the carbonic acid will not penetrate the concrete, and no carbonation will occur; if the concrete is dry, then no carbonic acid is available. Maximum carbonation shrinkage occurs at humidities of about 50 per cent and it can be of the same order of magnitude as drying shrinkage (Figure 19.9). The porosity of the concrete is also an important controlling factor. With average strength concrete, provided it is well compacted and cured, the carbonation front will only penetrate a few centimetres in many years, and with high-strength concrete even less. However, much greater penetration can occur with poor quality concrete or in regions of poor compaction, and this can lead to substantial problems if the concrete is reinforced, as we shall see in Chapter 23.

19.4 Thermal expansion

In common with most other materials, cement paste and concrete expand on heating. Knowledge of the coefficient of thermal expansion is needed in two main situations; first to calculate stresses due to thermal gradients arising from heat of hydration effects or continuously varying diurnal temperatures, and second to calculate overall dimensional changes in structures such as bridge decks due to ambient temperature variations.

The measurement of thermal expansions on laboratory specimens is relatively straightforward, provided sufficient time is allowed for thermal equilibrium to be reached (at most a few hours). However, the in situ behaviour is complicated by the observation that, unlike most other materials, the thermal movement is time-dependent, and, as with shrinkage, it is difficult to estimate movement in structural elements from those on laboratory specimens.

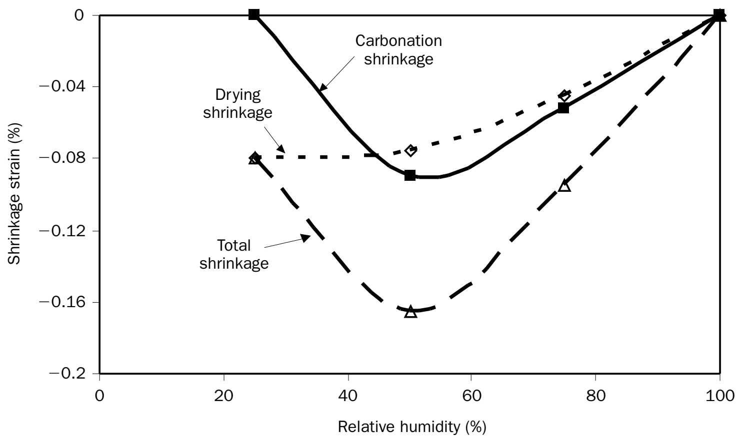

FIGURE 19.9 The effect of surrounding relative humidity on drying and carbonation shrinkage of mortar (Verbeck, 1958).

19.4.1 Thermal expansion of hardened cement paste

The coefficient of thermal expansion of hcp varies between about 10 and 20×10^{-6} per °C, depending mainly on the moisture content. Figure 19.10 shows typical behaviour, with the coefficient reaching a maximum at about 70 per cent rh. The value at 100 per cent rh, i.e. about 10×10^{-6} per °C, probably represents the 'true' inherent value for the paste itself. The time-dependence of the behaviour takes the form of an initial expansion on an increase in temperature showing some reduction over a few hours if the temperature is held constant.

Explanations for this behaviour have all involved the role of water, and relate to the disturbance of the equilibrium between the water vapour, the free water, the freely adsorbed water, the water in areas of hindered adsorption and the forces between the layers of gel solids (see Chapter 13, Section 13.6). Any disturbances will have a greater effect at intermediate humidities, when there is a substantial amount of water present with space in which to move. On an increase in temperature, the surface tension of the capillary water will decrease, and hence its internal tension and the corresponding compression in the solid phases will decrease, causing extra swelling, as observed. However, changes in internal energy with increased or decreased temperature will stimulate internal flow of water, causing the time-dependent volume change in the opposite sense to the initial thermal movement mentioned above.

19.4.2 Thermal expansion of concrete

The thermal expansion coefficients of the most common rock types used for concrete aggregates vary between about 6 and 10×10^{-6} per °C, i.e. lower than either the 'true' or 'apparent' values for cement paste. The thermal expansion coefficient for the concrete is therefore lower than that for cement paste, as shown in Figure 19.10. Furthermore, since the aggregate occupies 70 to 80 per cent of the total concrete volume, there is a considerable reduction of the effects of humidity that are observed in the paste alone, to the extent that a constant coefficient of thermal expansion over all humidities is a reasonable approximation.

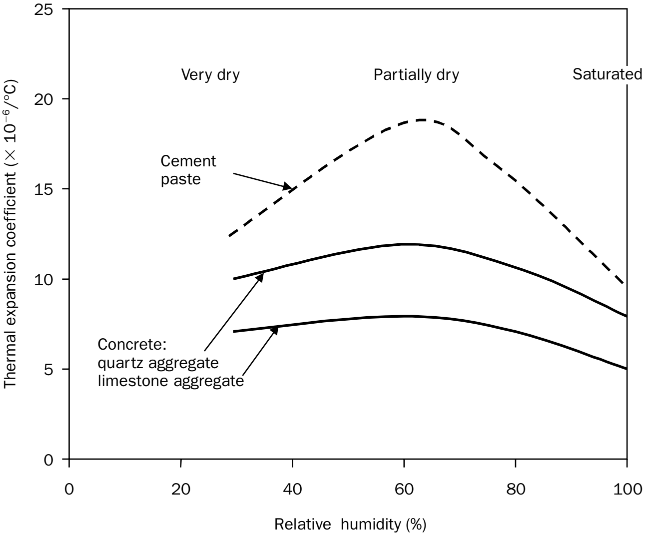

FIGURE 19.10 The effect of dryness on the thermal expansion coefficient of hardened cement paste and concrete (Myers, 1950).

The value depends on the concrete mix proportions, chiefly the cement paste content, and the aggregate type; for normal mixes the latter tends to dominate. The curves for quartz and limestone aggregate concrete shown in Figure 19.10 represent the two extremes of values for most normal aggregate concrete. Such values apply over a temperature range of about 0 to 60°C. At higher temperatures, the differential stresses set up by the different thermal expansion coefficients of the paste and aggregate can lead to internal microcracking and hence non-linear behaviour. We shall discuss this further when considering fire damage in Chapter 24.

19.5 Stress–strain behaviour

19.5.1 Elasticity of the hardened cement paste

Hardened cement paste has a near linear compressive stress–strain relationship for most of its range and therefore a modulus of elasticity can readily be determined from stress–strain data. Water-saturated pastes generally have a slightly higher modulus than dried pastes, indicating that some of the load is carried by the water in the pores. Nevertheless, the skeletal lattice of the paste carries most of the load, and the elastic response is governed by the lattice properties. As might therefore be expected, the elastic modulus (E_p) is highly dependent on the capillary porosity (p_c); the relationship has been found to be of the form

$$E_p = E_g(1 - p_c)^3 \qquad (19.4)$$

where E_g is the modulus when $p_c = 0$, i.e. it represents the modulus of elasticity of the gel itself. This is a similar expression to equation (13.9) for the strength of the paste, and therefore it is to be expected that the same factors will influence both strength and modulus. This is indeed the case; for example, Figure 19.11 shows that decreasing water/cement ratio and increasing age both

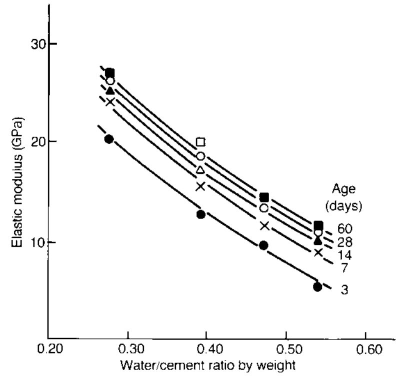

FIGURE 19.11 Effect of water/cement ratio and age on the elastic modulus of hardened cement paste (Hirsch, 1962).

increase the elastic modulus, a directly comparable effect to that on strength shown in Figure 13.9.

19.5.2 Models for concrete behaviour

Concrete is, of course, a composite multiphase material, and its elastic behaviour will depend on the elastic properties of the individual phases – unhydrated cement, cement gel, water, coarse and fine aggregate and their relative proportions and geometrical arrangements. The real material is too complex for rigorous analysis, but if it is considered as a two-phase material consisting of hcp and aggregate, then analysis becomes possible, and instructive.

The model for the concrete behaviour requires the following:

1. The property values for the phases; in this simple analysis, three are sufficient:
   (a) the elastic modulus of the aggregate, E_a;
   (b) the elastic modulus of the hcp, E_p; and
   (c) the volume concentration of the aggregate, g.
2. A suitable geometrical arrangement of the phases; three possibilities are shown in Figure 19.12. All the models consist of unit cubes. Models A and B have the phases arranged as adjacent layers, the difference being that in A the two phases are in parallel, and therefore undergo the same strain, whereas in B the phases are in series and are therefore subjected to the same stress. Model C has the aggregate set within the paste such that its height and base area are both equal to $\sqrt{g}$, thus complying with the volume requirements. This intuitively is more satisfactory in that it bears a greater resemblance to concrete.

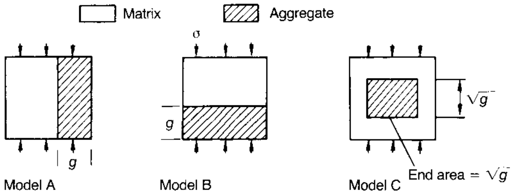

FIGURE 19.12 Simple two-phase models for concrete (Hansen, 1960; Counto, 1964).

Analysis of the models is not intended to give any detail of the actual distribution of stresses and strains within the concrete, but to predict average or overall behaviour. Three further assumptions are necessary:

1. the applied stress remains uniaxial and compressive throughout the model;
2. the effects of lateral continuity between the layers can be ignored;
3. any local bond failure or crushing does not contribute to the deformation.

Model A – phases in parallel

Strain compatibility

The strain in the concrete, ϵ_c is equal to the strain in the aggregate, ϵ_a and the paste, ϵ_p, i.e.

$$\epsilon_c = \epsilon_a = \epsilon_p \tag{19.5}$$

Equilibrium

The total force is the sum of the forces on each of the phases. Expressed in terms of stresses and areas this gives

$$\sigma_c.1 = \sigma_a.g + \sigma_p.(1 - g) \qquad (19.6)$$

Constitutive relations
Both of the phases and the concrete are elastic, hence

$$\sigma_c = \epsilon_c.E_c \quad \sigma_a = \epsilon_a.E_a \text{ and } \sigma_p = \epsilon_p.E_p \qquad (19.7)$$

where E_c, E_a and E_p are the elastic moduli of the concrete, aggregate and paste respectively.

Substituting into equation (19.6) from equation (19.7) gives

$$\epsilon_c.E_c = \epsilon_a.E_a.g + \epsilon_p.E_p.(1 - g)$$

and hence, from equation (19.5)

$$E_c = E_a.g + E_p.(1 - g) \qquad (19.8)$$

Model B – phases in series

Equilibrium
The forces and hence the stresses (since the forces act on equal areas) in both phases and the composite are equal, i.e.

$$\sigma_c = \sigma_a = \sigma_p \qquad (19.9)$$

Strains
The total displacement is the sum of the displacements in each of the phases; expressed in terms of strain this gives

$$\epsilon_c = \epsilon_a.g + \epsilon_p.(1 - g) \qquad (19.10)$$

Substituting from equations (19.7) and (19.9) into (19.10) and rearranging gives

$$\frac{1}{E_c} = \frac{g}{E_a} + \frac{(1 - g)}{E_p} \qquad (19.11)$$

Model C – combined

This is a combination of two layers of hcp alone in series with a third layer of hcp and aggregate in parallel, as in model A. Repetition of the above two analyses with substitution of the appropriate geometry and combination gives:

$$\frac{1}{E_c} = \frac{(1 - \sqrt{g})}{E_p} + \frac{\sqrt{g}}{E_a.g + E_p.(1 - \sqrt{g})} \qquad (19.12)$$

Figure 19.13 shows the predicted results of equations 19.8, 19.11 and 19.12 from the three models for varying aggregate concentrations, with $E_p < E_a$ as is normally the case. Models A and B give upper and lower bounds respectively to the concrete modulus, with model C, not surprisingly, giving intermediate values. The effect of aggregate stiffness is shown in non-dimensional form in Figure 19.14, on which some typical experimental results are also plotted. It is clear that, for concrete in which E_a/E_p is near 1, e.g. with low modulus lightweight aggregates, all three models give a reasonable fit, but for normal aggregates which are stiffer than the paste, i.e. $E_a/E_p > 1$, model C is preferable.

19.5.3 Measured stress–strain behaviour of concrete

The stress–strain behaviour of both the hcp and aggregate is substantially linear over most of the range up to a maximum. However, the composite concrete, although showing intermediate stiffness as predicted from the above analysis, is markedly non-linear over much of its length, as shown in Figure 19.15 (a). Furthermore, successive unloading/loading cycles to stress levels below ultimate show substantial, but diminishing, hysteresis loops, and residual strains at zero load, as in Figure 19.15 (b).

The explanation for this behaviour lies in the contribution of microcracking to the overall concrete strains, i.e. assumption (3) in the above analysis is invalid. As we will see in Chapter 20, the transition zone between the aggregate and the hcp or mortar is a region of relative weakness, and in fact some microcracks will be present in this zone even before loading. The number and width of these will depend on such factors as bleeding characteristics and the amount of drying or thermal shrinkage. As the stress level increases, these cracks will increase in length, width and number, thereby making a progressively increasing contribution to the overall strain, resulting in the non-linear behaviour. The cracking eventually leads to complete breakdown and failure, and therefore we will

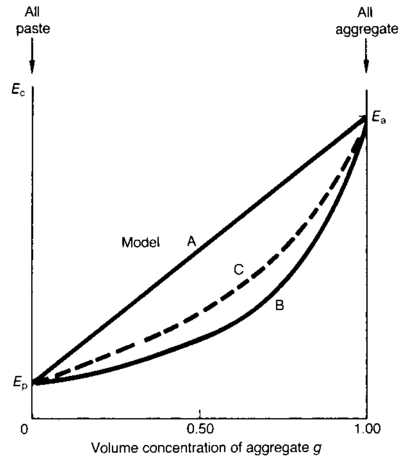

FIGURE 19.13 The effect of volume concentration of aggregate on elastic modulus of concrete calculated from simple two-phase models.

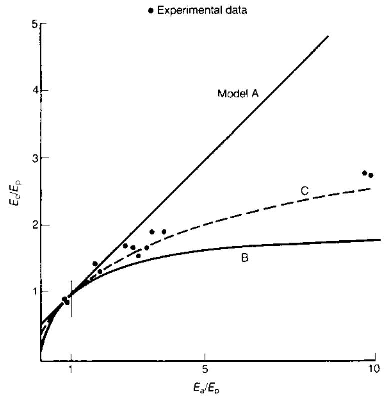

FIGURE 19.14 Prediction of elastic modulus of concrete (E_c) from the modulus of the cement paste (E_p) and the aggregate (E_a) for 50 per cent volume concentration of aggregate.

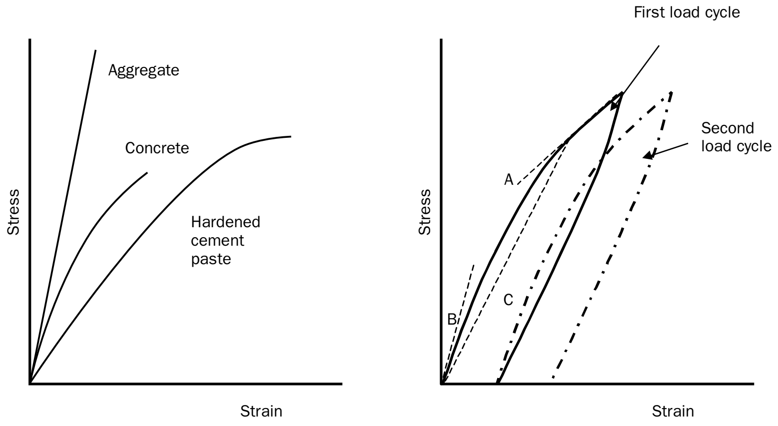

(a) Typical behaviour of hcp, aggregate and concrete

(b) Behaviour of concrete under successive loading cycles

FIGURE 19.15 Stress–strain behaviour of cement paste, aggregate and concrete.

postpone more detailed discussion of cracking until the next chapter.

Subsequent cycles of loading will not tend to produce or propagate as many cracks as the initial loading, provided the stress levels of the first or previous cycles are not exceeded. This explains the diminishing size of the hysteresis loops shown in Figure 19.15 (b).

19.5.4 Elastic modulus of concrete

The non-linear stress–strain curve for concrete means that a number of different elastic modulus values can be defined. These include the slope of the tangent to the curve at any point (giving the *tangent modulus*, A or B in Figure 19.15 (b)) or the slope of the line between the origin and a point on the curve (giving the *secant modulus*, C in Figure 19.15 (b)).

A typical test involves loading to a working stress, say 40 per cent of ultimate, and measuring the corresponding strain. Cylindrical or prism specimens are usually used, loaded longitudinally, and with a length at least twice the lateral dimension. Strain measurements are usually taken over the central section of the specimen to avoid end effects. To minimise hysteresis effects, the specimens are normally subjected to a few cycles of load before the strain readings are taken over a load cycle lasting about five minutes. It is usual to calculate the secant modulus from these readings. This test is often called the static test, and the resulting modulus the static modulus, to distinguish it from the dynamic modulus test which will be described in Chapter 22.

The elastic modulus increases with age and decreasing water/cement ratio of the concrete, for the reasons outlined above, and as with paste, these two factors combine into an increase of modulus with compressive strength, but with progressively smaller increases at higher strength. However, there is no simple relationship between strength and modulus since, as we have seen, the aggregate modulus and its volumetric concentration, which can vary at constant concrete strength, also have an effect. The modulus should therefore be determined experimentally if its value is required with any certainty. This is not always possible, and estimates are often needed, e.g. early in the structural design process, and a number of empirical relationships have been suggested, including

$$E_c = 3.32(f_{cyl})^{0.5} + 6.9$$

for strengths between 21 and 83 MPa (ACI, 2000b) (19.13)

where E_c = elastic modulus (in GPa) and f_{cyl} = cylinder compressive strength (in MPa). (We will discuss the difference between cylinder and cube compressive strength in the next chapter.)

Alternatively:

$$E_c = 9.5\ (f_{ck} + 8)^{0.33} \quad \text{(BSI, 1992)} \quad (19.14)$$

where f_{ck} = characteristic cylinder compressive strength (in MPa).

Both of these expressions apply to concrete of normal density, i.e. made with normal density aggregates. Lightweight concrete will have a lower modulus for the same strength, and ACI (2000a) gives an equation incorporating density:

$$E_c = 4.3 \times 10^{-5} \times \rho^{1.5} \times f_{cyl}{}^{0.5} \qquad (19.15)$$

where ρ = concrete density (in kg/m³).

Although at first glance these expressions (and others that have been suggested) appear conflicting, when plotted they all give largely similar results. The important thing to remember is that they only give not very good estimates of the elastic modulus.

19.5.5 Poisson's ratio

The Poisson's ratio of water-saturated cement paste varies between 0.25 and 0.3; on drying it reduces to about 0.2. It seems to be largely independent of water/cement ratio, age and strength. For concrete, the addition of aggregate again modifies the behaviour, with lower values obtained with increasing aggregate content. For most concrete, values lie within the range 0.17–0.2.

19.6 Creep

The general nature of the creep behaviour of concrete was illustrated in Figure 19.1. The magnitude of the creep strains can be several times higher than the elastic strains on loading, and they therefore often have a highly significant influence on structural behaviour. Also, the creep does not appear to tend to a limit, as shown in Figure 19.16 for tests of 30 years' duration. This figure also shows that the creep is substantially increased when the concrete is simultaneously drying, i.e. creep and shrinkage are interdependent. This leads to the definitions of creep strains shown in Figure 19.17. Free shrinkage (ϵ_{sh}) is defined as the shrinkage of the unloaded concrete in the drying condition, and basic creep (ϵ_{bc}) as the creep of a similar specimen under load but not drying, i.e. sealed so that there is no moisture movement to or from the surrounding environment. The total strain (ϵ_{tot}) is that measured on the concrete whilst simultaneously shrinking and creeping, and, as shown in Figure 19.16, it is found that

$$\epsilon_{tot} > \epsilon_{sh} + \epsilon_{bc} \tag{19.16}$$

The difference, i.e. $\epsilon_{tot} - (\epsilon_{sh} + \epsilon_{bc})$ is called the drying creep (ϵ_{dc}). It follows that the total creep strain (ϵ_{cr}) is given by

$$\epsilon_{cr} = \epsilon_{dc} + \epsilon_{bc} \tag{19.17}$$

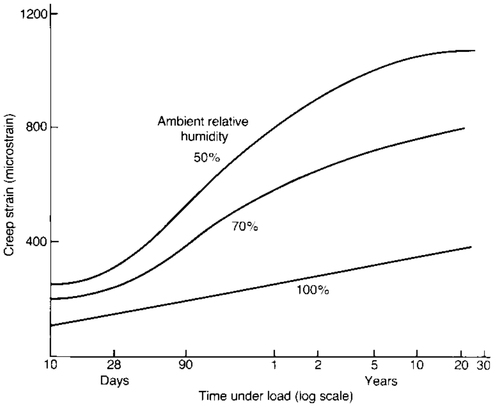

FIGURE 19.16 Creep of concrete moist-cured for 28 days, then loaded and stored at different relative humidities (Troxell *et al.*, 1958).

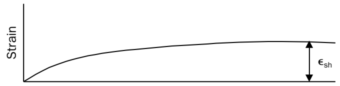

(a) Free shrinkage (no stress)

(b) Basic creep (stress, no loss of moisture)

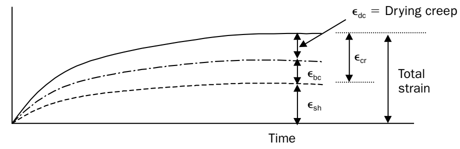

(c) Total creep (stress and drying)

FIGURE 19.17 Definitions of strains due to shrinkage, creep and combined shrinkage and creep of hardened cement paste and concrete.

19.6.1 Factors influencing creep

Apart from the increase in creep with simultaneous shrinkage just described, the following factors have a significant effect on creep.

- A reduced moisture content before loading, which reduces creep. In fact, completely dried concrete has very small, perhaps zero, creep.
- The level of applied stress; for any given concrete and loading conditions, the creep is found to increase approximately linearly with the applied stress up to stress/strength ratios of about 0.4 to 0.6 (different studies have indicated different limits). It is therefore often useful to define the *specific creep* as the creep strain per unit stress in this region. At higher stress levels increased creep is observed, which can ultimately result in failure, as will be discussed in the next chapter.
- Increasing concrete strength, which decreases the creep.
- Increasing temperature, which increases the

creep significantly for temperatures up to about 70°C. Above this, moisture migration effects lead to lower creep.

- The aggregate volume concentration, illustrated in Figure 19.18, which shows that the aggregate is inert as regards creep, and hence the creep of concrete is less than that of cement paste. This is, therefore, directly comparable to the shrinkage behaviour shown in Figure 19.7.

Neville (1964) suggested a relationship between the creep of the concrete (C_c) and that of neat cement paste (C_p) of the form

$$C_c/C_p = (1 - g - u)^n \qquad (19.18)$$

where g and u are the volume fractions of aggregate and unhydrated cement respectively, and n is a constant which depends on the modulus of elasticity and Poisson's ratio of the aggregate and the concrete. This therefore shows that:

- the properties of the aggregate are important, and that they can have a substantial effect of the magnitude of the creep;
- the effect of the water/cement ratio and age of concrete need not be considered separately, since they both effect the elastic modulus;
- the effect of other materials which also effect the rate strength gain, such as admixtures and cement replacement materials, can be treated similarly.

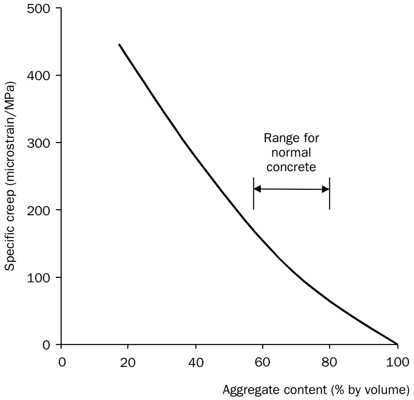

FIGURE 19.18 The effect of aggregate content on creep of concrete (Concrete Society, 1973).

19.6.2 Mechanisms of creep

Since the creep process is occurring within the cement paste, and the moisture content and movement have a significant effect on its magnitude, it is not surprising that the mechanisms proposed for creep have similarities with those proposed for shrinkage and discussed in Section 19.1.2. As with shrinkage, it is likely that a combination of the mechanisms now outlined is responsible.

Moisture diffusion

The applied stress causes changes in the internal stresses and strain energy within the hcp, resulting in an upset to the thermodynamic equilibrium; moisture then moves down the induced free energy gradient, implying a movement from smaller to larger pores, which can occur at several levels:

- in capillary water as a rapid and reversible pressure drop;
- in adsorbed water moving more gradually from zones of hindered adsorption – this movement should be reversible;
- in interlayer water in diffusing very slowly out of the gel pores. Some extra bonding may then develop between the solid layers, and so this process may not be completely recoverable.

In sealed concrete, there are always sufficient voids to allow the moisture movement, hence basic creep can occur with this mechanism. With simultaneous drying, all of the processes are much enhanced, hence explaining drying creep.

Structural adjustment

Stress concentrations arise throughout the hcp structure because of its heterogeneous nature, and consolidation to a more stable state without loss of strength occurs at these points by either:

- viscous flow, with adjacent particles sliding past each other; or
- local bond breakage, closely followed by reconnection nearby after some movement.

Concurrent moisture movement is assumed to disturb the molecular pattern, hence encouraging a greater structural adjustment. The mechanisms are essentially irreversible.

Microcracking

We have seen that hcp and concrete contain defects and cracks before loading, and propagation of these and the formation of new cracks will contribute to the creep strains, particularly at higher levels of stress. This is the most likely explanation of the non-linearity of creep strain with stress at high stress levels. In a drying concrete, the stress gradient arising from the moisture gradient is likely to enhance the cracking.

Delayed elastic strain

The 'active' creeping component of the hcp or concrete, i.e. mainly the water in its various forms in the capillary or gel pores, will be acting in parallel with inert material that will undergo elastic response only. In hcp this will be solid gel particles, the unhydrated cement particles, and the calcium hydroxide crystals, augmented in concrete with the aggregate particles. The stress in the creeping material will decline as the load is transferred to the inert material, which then deforms elastically as its stress gradually increases. The process acts in reverse on removal of the load, so that the material finally returns to its unstressed state; thus the delayed elastic strain would be fully recoverable in this model.

19.6.3 Prediction of creep

As with shrinkage, it is often necessary to estimate the likely magnitude of the creep of a structural element at the design stage, but, again, because of the number of factors involved, prediction of creep with a degree of certainty is problematic. Brooks and Neville (1978) suggest that a satisfactory method is to carry out short-term (28 day) tests, and then estimate creep at a later age by extrapolation using the expressions:

$$\text{basic creep} \quad c_\text{t} = c_{28} \times 0.5t^{0.21} \tag{19.19}$$

$$\text{total creep} \quad c_\text{t} = c_{28} \times (-6.19 + 2.15\log_\text{e} t)^{0.38} \tag{19.20}$$

where t = age at which creep is required (days >28)
c_{28} = measured specific creep at 28 days
c_t = specific creep at t days in microstrain per MPa.

If short-term tests are not feasible, there are, as for shrinkage, a number of empirical methods of varying degrees of complexity for estimating creep, often included in design codes, e.g. BSI (1997), ACI (2000a).

19.7 References

ACI (2000a) ACI 209R-92 Prediction of creep, shrinkage and temperature effects in concrete structures. *ACI Manual of Concrete Practice, Part 1 Materials and General Properties of Concrete*, American Concrete Institute, Michigan, USA.

ACI (2000b) ACI 363R-23 State of the art report on high strength concrete. *ACI Manual of Concrete Practice, Part 1 Materials and General Properties of Concrete*, American Concrete Institute, Michigan, USA.

Bazant, Z.P. (1972) Thermodynamics of hindered adsorption and its implications for hardened cement paste and concrete. *Cement and Concrete Research* 2, 1, January, 1–16.

Brooks, J.J. and Neville, A.M. (1978) Predicting the long-term creep and shrinkage from short-term tests. *Mag. of Concrete Research* 30, 103, 51–61.

BSI (1992) DD ENV 1–1: 1992 *Eurocode 2: Design of Concrete Structures, Part 1 General Rules and Rules for Buildings*, British Standards Institution, London.

BSI (1997) BS 8110–1: 1997 *Structural Use of Concrete. Code of Practice for Design and Construction,* British Standards Institution, London.

Concrete Society (1973) *The Creep of Structural Concrete,* Technical Report No. 101, London.

Counto, U.J. (1964) The effect of the elastic modulus of aggregate on the elastic modulus, creep and creep recovery of concrete. *Magazine of Concrete Research* 16, 48, Sept., 129–38.

Feldman, R.F. and Sereda, P.J. (1970) A new model for hydrated Portland cement and its practical implications. *Engng J.* 53, 8/9, 53–9.

Hansen, T.C. (1960) Creep and stress relaxation of concrete. *Proceedings of Swedish Cement and Concrete Research Institute* 31.

Helmuth, R.A. and Turk, D.M. (1967) The reversible and irreversible drying shrinkage of hardened Portland cement and tricalcium silicate pastes. *Journal of the Portland Cement Association, Research and Development Laboratories* 9, 2, 8–21.

Hirsch, T.J. (1962) Modulus of elasticity of concrete as affected by elastic moduli of cement paste matrix and aggregate. *Proc. Amer. Conc. Inst.* 59, March, 427.

Ishai, O. (1965) The time-dependent deformational behaviour of cement paste, mortar and concrete. *Proceedings of the Conference on Structure of Concrete and its Behaviour Under Load*, Cement and Concrete Association, London, Sept., 345–64.

Meyers, S.L. (1950) Thermal expansion characteristics of hardened cement paste and concrete. *Proceedings of the Highway Research Board* 30, 193.

Neville, A.M. (1964) Creep of concrete as a function of its cement paste content. *Magazine of Concrete Research* 16, 46, March, 21–30.

Neville, A.M., Dilger W.H. and Brooks, J.J. (1983) *Creep of Plain and Structural Concrete*, Construction Press, London, 361 pp.

Pickett, G. (1956) Effect of aggregate on shrinkage of concrete and hypothesis concerning shrinkage. *J. Amer. Conc. Inst.* 52, January, 581–90.

Powers, T.C. (1965) Mechanisms of shrinkage and reversible creep of hardened cement paste. *Proceedings of the Conference on Structure of Concrete and its Behaviour Under, Load*, Cement and Concrete Association, London, Sept., 319–44.

Shoya, M. (1979) Drying shrinkage and moisture loss of superplasticiser admixed concrete of low water/cement ratio. *Transactions of the Japan Concrete Institute II* – 5, 103–10.

Soroka, I. (1979) *Portland Cement Paste and Concrete,* Macmillan, London.

Troxell, G.E., Raphael, J.M. and Davis, R.E. (1958) Long-time creep and shrinkage tests of plain and reinforced concrete. *Proc. Amer. Soc. Test and Mater.* 58, 1101–20.

Verbeck, G.J. (1958) Carbonation of hydrated Portland cement. *ASTM Special Publication* 205, American Society for Testing and Materials, 17–36.

Verbeck, G.J. and Helmuth, R.A. (1968) Structure and physical properties of cement paste. *Proceedings of the Symposium on the Chemistry of Cement*, Tokyo, 3, 1–37.

Wittman, F.H. (1968) Surface tension, shrinkage and strength of hardened cement paste. *Mater. Struct.* 1, 6, 547–52.

Chapter twenty

Strength and failure of concrete

Strength is probably the most important single property of concrete, since the first consideration in structural design is that the structural elements must be capable of carrying the imposed loads. The maximum value of stress in a loading test is usually taken as the strength, even though under compressive loading the test piece is still whole (but with substantial internal cracking) at this stress, and complete breakdown subsequently occurs at higher strains and lower stresses. Strength is also important because it is related to several other important properties which are more difficult to measure directly, and a simple strength test can give an indication of these properties. For example, we have already seen the relation of strength to elastic modulus; we shall discuss durability in the next chapter, but in many cases a low permeability, low porosity concrete is the most durable, and, as discussed when we considered the strength of cement paste in Chapter 13, this also means it has high strength.

In structural situations concrete will be subject to one of a variety of types of loading, resulting in different modes of failure. Knowledge of the relevant strength is therefore important; for example, in columns or reinforced concrete beams, the compressive strength is required; for cracking of a concrete slab the tensile strength is important. Other situations may require torsional strength, fatigue or impact strength or strength under multiaxial loading. As we shall see, most strength testing involves the use of a few, relatively simple tests, generally not related to a particular structural situation. Procedures enabling data from the tests described in this chapter to be used in design have been obtained from empirical test programmes at an engineering scale on large specimens. The reader is referred to texts on structural design for a description of these design procedures.

In this chapter we shall describe the most common test methods used to assess concrete strength, discuss the factors influencing the results obtained from them, and then return to a more detailed consideration of the cracking and fracture processes taking place within the concrete. Finally, we shall briefly discuss strength under multiaxial loading situations.

20.1 Strength tests

20.1.1 Compressive strength

The simplest compressive strength test uses a concrete cube, and this is the standard test in the

UK.[1] The cube must be sufficiently large to ensure that an individual aggregate particle does not unduly influence the result; 100 mm is recommended for maximum aggregate sizes of 20 mm or less, 150 mm for maximum sizes up to 40 mm. The cubes are usually cast in lubricated steel moulds, accurately machined to ensure that opposite faces are smooth and parallel. The concrete is fully compacted by external vibration or hand tamping, and the top surface trowelled smooth. After demoulding when set, the cube is normally cured under water at constant temperature until testing.

The cube-testing machine has two heavy platens through which the load is applied to the concrete. The bottom one is fixed and the upper one has a ball seating which allows rotation to match the top face of the cube at the start of loading. This then locks in this position during the test. The load is applied to a pair of faces which were cast against the mould, i.e. with the trowelled face to one side. This ensures that there are no local stress concentrations which would result in a falsely low average failure stress. A very fast rate of loading gives overhigh strengths, and a rate to reach the ultimate stress in a few minutes is recommended. It is vital that the cube is properly made and stored; only then will the test give a true indication of the properties of the concrete, unaffected by such factors as poor compaction, drying shrinkage cracking, etc.

The cracking pattern within the cube (Figure 20.1 (a)) produces a double pyramid shape after failure. From this it is immediately apparent that the stress within the cube is far from uniaxial. The compressive load induces lateral tensile strains in both the steel platens and the concrete due to the Poisson effect. The mismatch between the elastic modulus of the steel and the concrete, and the friction between the two, result in lateral restraint forces in the concrete near the platen. This concrete is therefore in a triaxial stress state, with consequent higher failure stress than the true, unrestrained strength. This is the major objection to the cube test. The test is, however, relatively simple, and capable of comparing different concretes. (We shall consider triaxial stress states in more detail later in the chapter.)

An alternative test, which at least partly overcomes the restraint problem, uses cylinders; this is popular in North America, most of Europe and in many other parts of the world. Cylinders with a height/diameter ratio of 2, most commonly 300 mm high and 150 mm diameter, are tested vertically; the effects of end restraint are much reduced over the central section of the cylinder, which fails with near uniaxial cracking (Figure 20.1 (b)), indicating that the failure stress is much closer to the unconfined compressive strength. As a rule of thumb, it is often assumed that the cube strength is about 25 per cent higher than the cylinder strength, but this ratio has been found to depend on several factors, and in particular, reduces with increasing strength. For example, CEB-FIP (1990) gives

$$f_{\text{cube}} = 1.25 f_{\text{cyl}} \text{ for } f_{\text{cyl}} \leq 40\,\text{MPa}$$
$$\text{and } f_{\text{cube}} = 1.25 f_{\text{cyl}} \text{ for } 40\,\text{MPa} \leq f_{\text{cyl}} \leq 80\,\text{MPa}$$

A general relationship between the height/diameter ratio (h/d) and the strength of cylinders for low- and medium-strength concrete is shown in Figure 20.2. This is useful in, for example,

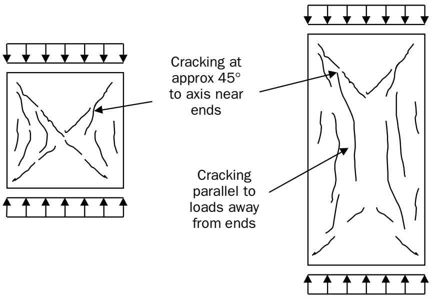

(a) Cube (b) Cylinder with a height/diameter = 2

FIGURE 20.1 Cracking patterns during testing of concrete specimens in compression.

---

[1] A list of relevant standards is included in 'Further reading' on page 222.

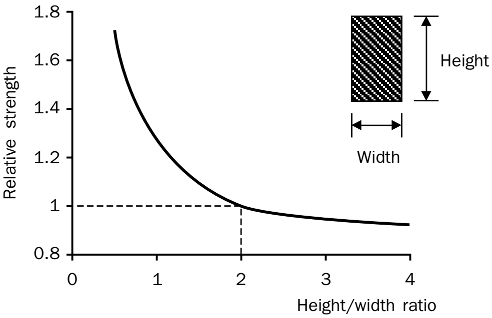

FIGURE 20.2 The relationship between height/width (or diameter) ratio and strength of concrete in compression.

interpreting the results from testing cores cut from a structure, where h/d often cannot be controlled. It is preferable to avoid an h/d ratio of less than 1, where sharp increases in strength are obtained, and high values, although giving closer estimates of the uniaxial strength, result in excessively long specimens which can fail due to slenderness ratio effects.

Testing cylinders has one major disadvantage; the top surface is finished by a trowel and is not plane and smooth enough for testing, and it therefore requires further preparation. It can be ground, but this is very time consuming, and the normal procedure is to cap it with a thin (2–3 mm) layer of high-strength gypsum plaster, molten sulfur or high early strength cement paste, applied a day or two in advance of the test. Alternatively, the end of the cylinder can be set in a steel cap with a bearing pad of an elastomeric material or fine dry sand between the cap and the concrete surface. Apart from the inconvenience of having to carry this out, the failure load is sensitive to the capping method, particularly in high-strength concrete.

20.1.2 Tensile testing

Direct testing of concrete in uniaxial tension, as shown in Figure 20.3 (a), is more difficult than for, say, steel or timber. Relatively large cross-sections are required to be representative of the concrete, and, because the concrete is brittle, it is difficult to grip and align. Eccentric loading and failure at or in the grips is then difficult to avoid. A number of gripping systems have been developed, but these are somewhat complex, and their use is confined to research laboratories. For more routine purposes, one of the following two indirect tests is preferred.

Splitting test

A concrete cylinder, of the type used for compression testing, is placed on its side in a compression testing machine and loaded across its vertical diameter (Figure 20.3 (b)). The size of cylinder used is normally either 300 or 200 mm long (l) by 150 or 100 mm diameter (d). The theoretical distribution of horizontal stress on the plane of the vertical diameter, also shown in Figure 20.3 (b), is a near uniform tension (f_s), with local high compression stresses at the extremities. Hardboard or plywood strips are inserted between the cylinder and both top and bottom platens to reduce the effect of these and ensure even loading over the full length.

Failure occurs by a split or crack along the vertical plane, the specimen falling into two neat halves. The cylinder splitting strength is defined as the magnitude of the near-uniform tensile stress on this plane, which is given by

$$f_s = 2P/\pi \mathrm{ld} \qquad (20.1)$$

where P is the failure load.

The state of stress in the cylinder is biaxial rather than uniaxial, and this, together with the local zones of compressive stress at the extremes, results in the value of f_s being higher than the uniaxial tensile strength. However, the test is very easy to perform with standard equipment used for compressive strength testing, and gives consistent results; it is therefore very useful.

Flexural test

A rectangular prism, of cross-section $b \times d$ (usually 100 or 150 mm square) is simply

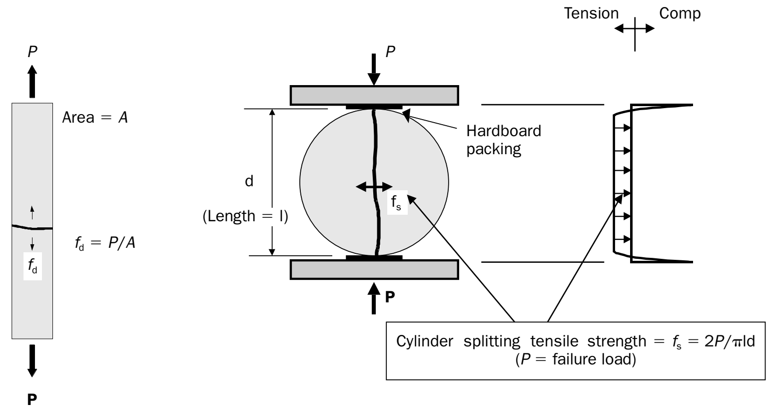

(a) Direct tension

(b) Indirect – cylinder splitting

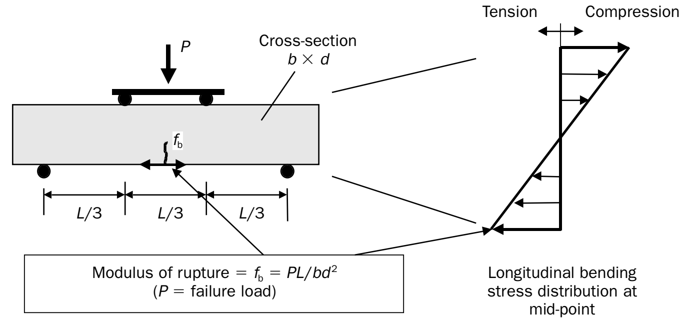

(c) Indirect – modulus of rupture

FIGURE 20.3 Tensile testing methods for concrete.

supported over a span L (usually 400 or 600 mm). The load is applied at the third points (Figure 20.3 (c)), and since the tensile strength of the concrete is much less than the compressive strength, failure occurs when a flexural tensile crack at the bottom of the beam, normally within the constant bending moment zone between the loading points, propagates upwards through the beam. If the total load at failure is P, then analysis based on simple beam-bending theory and linear elastic stress–strain behaviour up to failure gives the stress distribution shown in Figure 20.3 (c) with a maximum tensile stress in the concrete, f_b, as

$$f_b = PL/bd^2 \tag{20.2}$$

f_b is known (somewhat confusingly) as the *modulus of rupture.*

However, as we have seen in the preceding chapter, concrete is a non-linear material and the assumption of linear stress distribution is not valid. The stress calculated from equation (20.2) is therefore higher than that actually developed in the concrete. The strain gradient in the specimen may also inhibit the crack growth. For both of these reasons the modulus of rupture is also greater than the direct tensile strength.

20.1.3 Relationship between strength measurements

We have already discussed the relationship between cube and cylinder compressive strength measurements.

The tensile strength, however measured, is roughly one order of magnitude lower than the compressive strength. The relationship between the two is non-linear, with a good fit being an expression of the form

$$f_t = a(f_c)^b \tag{20.3}$$

where f_t = tensile strength, f_c = compressive strength and a and b are constants. The Eurocode for Design of Concrete Structures (BSI 1996) gives $a = 0.30$ and $b = 0.67$ when f_c is the characteristic cylinder strength and f_t is the design tensile strength. This relationship, converted to actual cube compressive strengths and tensile strengths, is plotted in Figure 20.4 together with equivalent data from cylinder splitting and modulus of rupture tests obtained by UCL undergraduate students in laboratory classes.

It is clear from this figure that, as we have already said, both the modulus of rupture and the cylinder-splitting tests give higher values than the direct tensile test. The modulus of rupture is the higher value, varying between about 10 and 17 per cent of the cube strength (the higher value applies to lower strengths). The cylinder-splitting strength is between about 8 and 11 per cent of the cube strength, and the direct tensile strength between about 6 and 8 per cent of the cube strength. Figure 20.4 also shows that, as with all such relationships, there is a considerable scatter of individual data points about the best-fit line, although in this case some of this may be due to the inexperience of the testers.

20.2 Factors influencing strength of Portland cement concrete

In this section we will consider the strength of concrete with Portland cement as the sole binder. The effect of cement replacement materials will be discussed in the next section.

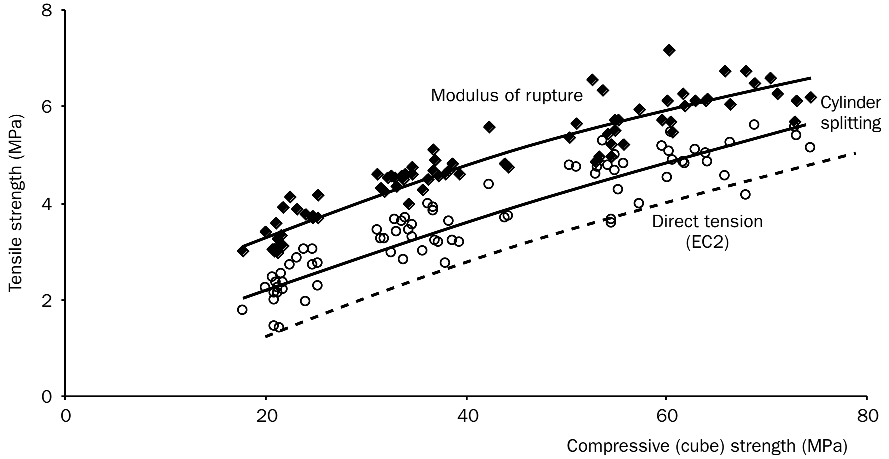

FIGURE 20.4 The relationship between direct and indirect tensile strength measurements and compressive strength (EC2, 1996, and UCL data).

20.2.1 Transition/interface zone

Before looking at the relationships between the strength of concrete and the many factors which influence it, we need to introduce an extremely important aspect of the concrete's structure. In Chapter 13 we described the microstructure of the hardened cement paste that is formed during hydration. Concrete is, of course, a mixture of the paste and aggregate, and it is the interface between these that is of great interest. The paste close to the aggregate surface is substantially different to that of the bulk paste, and crucially this *transition* or *interface zone* is significantly weaker than the rest of the paste. As the load on the concrete increases, cracking will start in this zone, and subsequently propagate into the hcp until crack paths are formed through the concrete, as shown in Figure 20.5, which when sufficiently extensive will result in complete breakdown, i.e. failure.

The formation, structure and consequences of the transition zone have been the focus of much research since the mid-1980s, even to the extent of two major international conferences being dedicated to the subject (Maso, 1992; Katz *et al.*, 1998). Although there are some differences of opinion, there is a general consensus that the zone is between 30 and 50 microns wide, and that its structure in a much simplified form is as shown in Figure 20.6. This shows two main features:

- a very thin surface layer of calcium silicate hydrate on the aggregate, also containing some small calcium hydroxide (calcite) crystals;
- most of the zone consists mainly of larger calcite crystals and fine needles of calcium sulfoaluminate (ettringite – see page 99).

Suggested mechanisms for the zone's formation include an increased water/cement ratio at the paste aggregate/interface due to:

- the 'wall effect', whereby the cement grains cannot pack as efficiently next to the aggregate surface as they can in the bulk paste;
- mix water separation at the interface due to the relative movement of the aggregate particles and cement paste during mixing, compounded by localised bleeding (see page 136).

We should therefore think of concrete as a three-phase material – hardened cement paste, aggregate and the transition zone, and it will be useful to bear this model in mind during the discussion of the more important factors that effect concrete strength that now follows. We will discuss some further aspects of the cracking and failure process later in the chapter.

20.2.2 Water/cement ratio

In Chapter 13 we saw that the strength of cement paste is governed by its porosity, which in turn

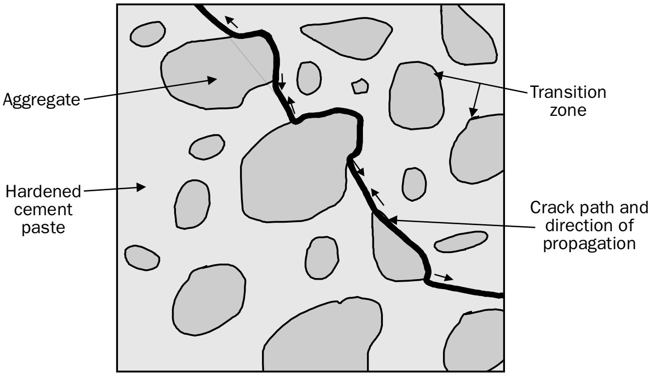

FIGURE 20.5 Cracking pattern in normal strength concrete.

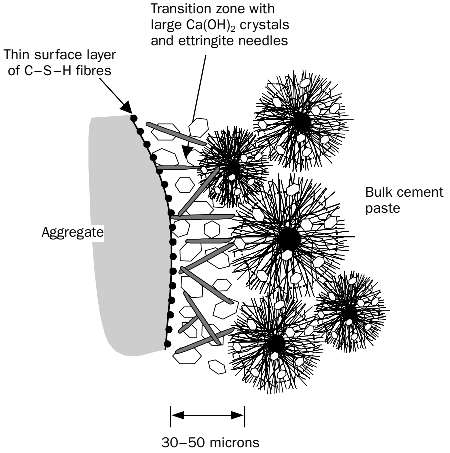

FIGURE 20.6 Features of the transition zone at the paste–aggregate interface (adapted from De Rooij *et al.*, 1998).

depends on the water/cement ratio and degree of hydration. The overall dependence of strength of concrete on the amount of cement, water and air voids within it was recognised by Feret in 1896, who suggested a rule of the form:

$$f_c = K(c/\{c + w + a\})^2 \qquad (20.4)$$

where f_c = strength, c, w and a are the absolute volumetric proportions of cement, water and air respectively, and K is a constant.

Working independently, Abrams, in 1918, demonstrated an inverse relationship with concrete strength of the form:

$$f_c = k_1/(k_2^{w/c}) \qquad (20.5)$$

This has become known as Abrams' law, although strictly, as it based on empirical observations, it is a rule.

The constants K, k_1 and k_2 are empirical and depend on age, curing regime, type of cement, amount of air entrainment, test method and, to a limited extent, aggregate type and size.

Feret's rule and Abrams' law both give an inverse relationship between strength and water/cement ratio for a fully compacted concrete of the form shown in Figure 20.7. It is important to recognise the limitations of such a relationship. First, at low water/cement ratios, the concrete becomes less workable and increasingly more difficult to compact. Feret's rule recognises that increasing air content will reduce the strength, and in general the strength will decrease by 6 per cent for each 1 per cent of included air by volume. This leads to the steep reduction in strength shown by the dashed lines in Figure 20.7. The point of the divergence from the fully compacted line can be moved further up and to the left by the use of more efficient compaction and/or by improvements in workability without increasing the water/cement ratio, for example by using plasticisers or superplasticisers, which were discussed in Chapter 14. Without such admixtures, it is difficult to achieve adequate workability for most normal compaction methods at water/cement ratios much below 0.4; with admixtures this limit can be reduced to 0.25 or even less.

At the other end of the scale, Abrams himself showed that his rule was valid for water/cement ratios of up to 2 or more. However, at these high values the paste itself is extremely fluid, and it is very difficult to achieve a homogeneous, cohesive concrete without significant segregation. In practice, water/cement ratios in excess of 1 are rarely used.

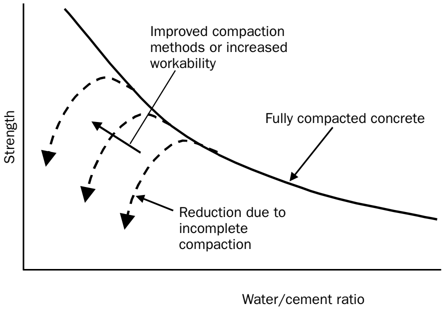

FIGURE 20.7 The general relationship between strength and water/cement ratio of concrete (adapted from Neville, 1995 by permission, Pearson Education).

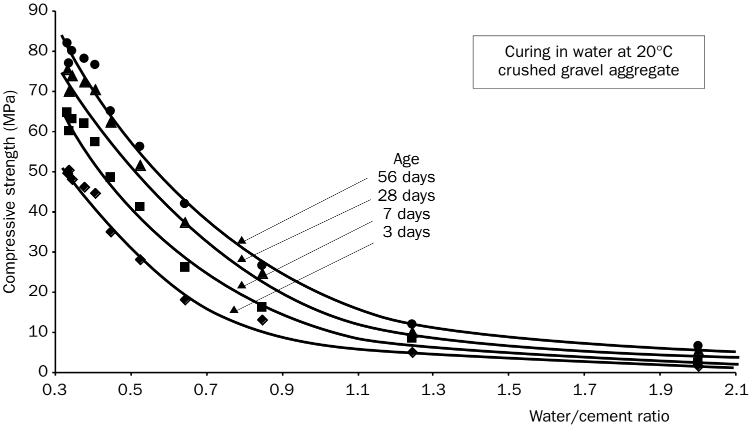

FIGURE 20.8 Compressive strength versus water/cement for concrete made with class 42.5N Portland cement (Balmer, 2000).

Figure 20.8 shows a recent set of results obtained with class 42.5N Portland cement, where good compaction was achieved in laboratory conditions at water/cement ratios down to 0.33. This gives a good idea of typical concrete performance, but we must add our normal proviso that the use of other constituent materials (cement source, aggregate type, etc.) will give different strength levels.

We will be discussing examples of achieving strengths significantly higher than those in Figure 20.7 in Chapter 24 when we consider high performance concrete.

20.2.3 Effect of age

The degree of hydration increases with age, leading to the effect of age on strength apparent from Figure 20.8. The strength at 28 days is often used to characterise the concrete for specification and compliance purposes, probably because it was originally thought to be a reasonable indication of the long-term strength without having to wait too long for test results. The rate of gain of strength varies with water/cement ratio, and, as discussed in Chapter 13, the rate of hydration and therefore the rate gain of strength will vary with cement composition and fineness, and thus it is impossible and futile to generalise.

It is important to remember that, as also discussed in Chapter 13, the hydration reactions are never complete, and, in the presence of moisture, concrete will continue to gain strength for many years, although, of course, the rate of increase after such times will be very small.

20.2.4 Temperature

As we discussed in Chapter 18, a higher temperature maintained throughout the life of a concrete will result in higher short-term strengths but lower long-term strengths. Also, an early age heating/cooling cycle from heat of hydration effects can lead to lower long-term strength, but the effect can be reduced or even eliminated by the incorporation of pulverised fuel ash or ground granulated blast furnace slag. We shall discuss the effect of transient high temperatures when considering the durability of concrete in fire in Chapter 23.

20.2.5 Humidity

The necessity of a humid environment for adequate curing has already been discussed; for this reason concrete stored in water will achieve a higher strength than if cured in air for some or all of its life, as shown in Figure 20.9. Also, specimens cured in water will show a significant increase in strength (5 per cent or more) if allowed to dry out for a few hours before testing.

20.2.6 Aggregate properties, size and volume concentration

As discussed above, for normal aggregate it is the strength of the paste/aggregate bond or transition zone that has a dominant effect on concrete strength; the aggregate strength itself is generally significant only in very-high strength concrete or with the relatively weaker lightweight aggregates. Struble *et al.* (1980) have concluded that with some carbonate and siliceous aggregates there is evidence that the structure and chemistry of the transition zone are influenced by both the aggregate mineralogy and surface. Also, increased surface roughness can improve the bond, probably due to mechanical interlocking. For this reason, and also the increased mechanical interlocking of the aggregate particles themselves, concretes made with crushed rocks are typically some 15 per cent stronger than those made with uncrushed gravels, provided all other mix proportions are the same.

The use of a larger maximum aggregate size reduces the concrete strength, again provided all other mix proportions are the same. The reduction is greater at lower water/cement ratios and larger aggregate sizes (Figure 20.10). The larger aggregates have a lower overall surface area with a weaker transition zone, and this has a more critical effect on the concrete strength at the lower water/cement ratios. In fresh concrete, the decreased surface area with the increased aggregate size leads to increased workability for the same mix proportions, and therefore for mix design at constant workability the water content can be reduced and a compensating increase in strength obtained.

Increasing the volumetric proportion of aggregate in the mix will, at constant water/cement ratio, produce a relatively small increase in concrete strength (Figure 20.11). This has been attributed, at least in part, to the increase in aggregate concentration producing a greater number of

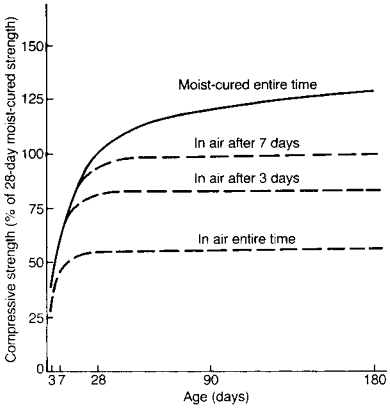

FIGURE 20.9 The influence of curing conditions on concrete strength (Portland Cement Association, 1968).

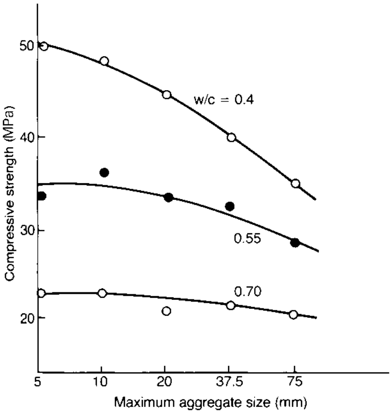

FIGURE 20.10 The effect of aggregate size and water/cement ratio on concrete strength (Cordon and Gillespie, 1963 by permission, American Concrete Institute).

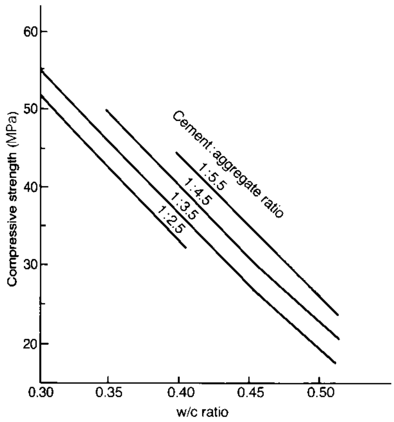

FIGURE 20.11 The effect of aggregate concentration and water/cement ratio on concrete strength (Erntroy and Shacklock, 1954).

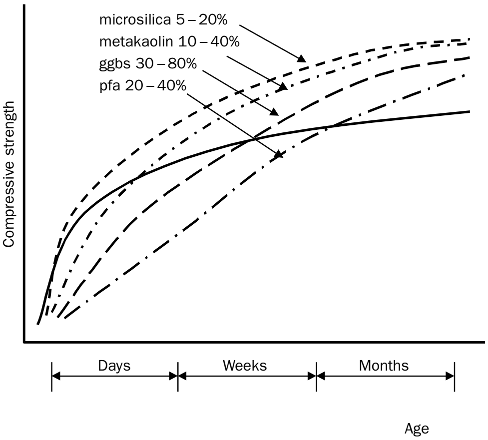

FIGURE 20.12 Schematic of average strength gain characteristics of concrete containing cement replacement characteristics.

secondary cracks prior to failure, which require greater energy, i.e. higher stress, to reach fracture. This effect is only valid if the paste content remains high enough to at least fill the voids in the coarse/fine aggregate system, thereby allowing complete consolidation of the concrete. This therefore imposes a maximum limit to the aggregate content for practical concretes.

20.3 Strength of concrete containing CRMs

We discussed the nature, composition and behaviour of four cement replacement materials – pfa, ggbs, microsilica and metakaolin – in Chapter 15, and in particular we described the supplementary or secondary pozzolanic reaction that leads to the formation of further calcium silicate hydrates. When each CRM is used within its overall replacement level limitation (page 119), the general effect is an increase in long-term strength compared to the equivalent Portland cement mix (i.e. the two mixes being compared differing only in the binder composition). This is due to a combination of:

- better packing of the particles in the fresh state, leading to an overall reduced porosity of the hardened cement paste after hydration;
- preferential enhancement of the transition zone, which, as we have seen, is of higher porosity and is rich in calcite and is therefore a prime target for the secondary reactions.

Not surprisingly, the strength of mixes with CRMs does take some time to reach and overtake that of the equivalent Portland cement mix. Figure 20.12 shows a schematic of the strength development behaviour when each CRM is used within its normal replacement limitation. The 'cross-over' point for the microsilica mixes is very early, sometimes within a day; metakaolin mixes take a few days, ggbs mixes days or weeks, and pfa mixes weeks or months. The reasons for the different rates of strength gain with the four different materials lie in their descriptions given in Chapter 15, which can be summarised as:

- the extremely fine particles, which act as nucleation sites for hydrate deposition, and very high active silica content of the microsilica results in the strength quickly overtak-

ing that of the equivalent Portland cement mix;
- the metakaolin is somewhat coarser so it is a little slower to react, but it contains a high active silica content and is therefore not far behind the microsilica mixes;
- the ggbs and pfa have similar particle sizes to the Portland cement, but the ggbs also contains its own calcium oxide which contributes to the secondary reactions.

If the slower rate of strength gain is a problem, mixes can, of course, be modified accordingly, e.g. by using plasticisers to maintain workability at a reduced water/cement ratio.

The contribution of the CRMs to strength is often expressed in terms of an *activity coefficient* or *cementing efficiency factor* (*k*) which is a measure of the relative contribution of the CRM to strength compared to an equivalent weight of Portland cement. This means that if the amount of CRM is x kg/m^3, then this is equivalent to kx kg/m^3 of cement, and the concrete strength is that that would be achieved with a cement content of $c + kx$, where c is the amount of cement.

If k is greater than 1, then the CRM is more active than the cement, and if less than 1, it is less active. Its value will clearly vary with the age of the concrete, and also with the amount of CRM and other mix proportions. For 28-day-old concrete and proportions of the CRM within the overall limits of Figure 20.12, values of 3 for microsilica, 1 for ggbs and 0.4 for pfa have been suggested (Sedran *et al.,* 1996). These can be used in mix design as will be discussed in Chapter 21.

It is, however, difficult to do more than generalise on the time-scales and magnitude of the strength characteristics, for two reasons:

- the vast amount of published information on the properties of concrete containing CRMs shows that, with each CRM, there is a wide range of performance (not just of strength, but also of all other properties), due mainly to the differences in physical and chemical composition of both the CRM and the Portland cement in the various test programmes;
- each set of tests will have been designed for a different purpose and therefore will have a different set of variables, such as changing the water content to obtain equal workability or equal 28 days' strength, and therefore it is often difficult to compare like with like (indeed, this is a problem facing students in nearly all areas of concrete technology).

20.4 Cracking and fracture in concrete

20.4.1 Development of microcracking

As we discussed in Chapter 19, the non-linear stress–strain behaviour of concrete in compression is largely due to the increasing contribution of microcracking to the strain with increasing load. Four stages of cracking behaviour have been identified, illustrated in Figure 20.13(a). Below 30 per cent of ultimate load, the transition zone cracks remain stable, and the stress–strain curve remains approximately linear (Stage 1). As the stress increases beyond 30 per cent of ultimate, the cracks begin to increase in length, width and number, causing non-linearity, but are still stable and confined to the transition zone (Stage 2). At loads above 50 per cent ultimate (Stage 3), the cracks start to spread into the matrix and become unstable at loads approaching 75 per cent ultimate, resulting in further deviation from linearity. Above 75 per cent ultimate (Stage 4), spontaneous and unstable crack growth becomes increasingly frequent, leading to very high strains. Also at this stage the excessive cracking results in transverse strains increasing at a faster rate than the longitudinal strains, resulting in an overall increase in volume (Figure 20.13(b)).

Complete breakdown, however, does not occur until strains significantly higher than those at maximum load are reached. Figure 20.14 shows stress–strain curves from strain controlled tests on paste, mortar and concrete. The hcp has a small descending branch after maximum stress; with the mortar it is more distinct, but with the concrete it is very lengthy. During the descending

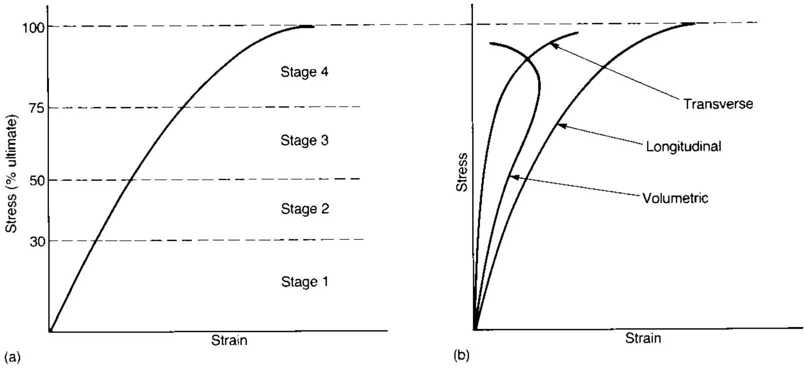

FIGURE 20.13 Stress–strain behaviour of concrete under compressive loading: (a) from Glucklich (1965); (b) from Newman (1966).

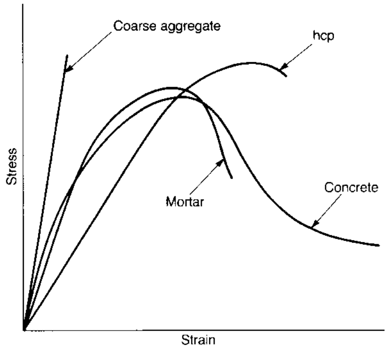

FIGURE 20.14 Typical stress–strain characteristics of aggregate, hardened cement paste, mortar and concrete compressive loading (Swamy and Kameswara Rao, 1973).

region, excess cracking and slip at the paste–aggregate interface are occurring before the cracking through the hcp is sufficiently well developed to cause complete failure.

20.4.2 Creep rupture

We discussed in Chapter 19 the contribution of microcracking to creep. This increases with stress level to the extent that if a stress sufficiently close to the short-term ultimate is maintained then failure will eventually occur, a process known as *creep rupture*. There is often an acceleration in creep rate shortly before rupture. The behaviour can be shown by stress–strain relationships plotted at successive times after loading, giving an ultimate strain envelope, shown for compressive and tensile loading in Figures 20.15 (a) and (b) respectively. The limiting stress below which creep rupture will not occur is about 70 per cent of the short-term maximum for both compression and tension.

20.4.3 The fracture mechanics approach

Griffith's theory for the fracture of materials and its consequent development into fracture mechanics was described in general terms in Chapter 6. Not surprisingly, there have been a number of studies attempting to apply linear fracture mechanics to concrete, with variable results. Three main reasons for the difficulties encountered have been suggested (American Concrete Institute, 1980):

1. Failure in compression, and to a lesser extent in tension, is controlled by the interaction of

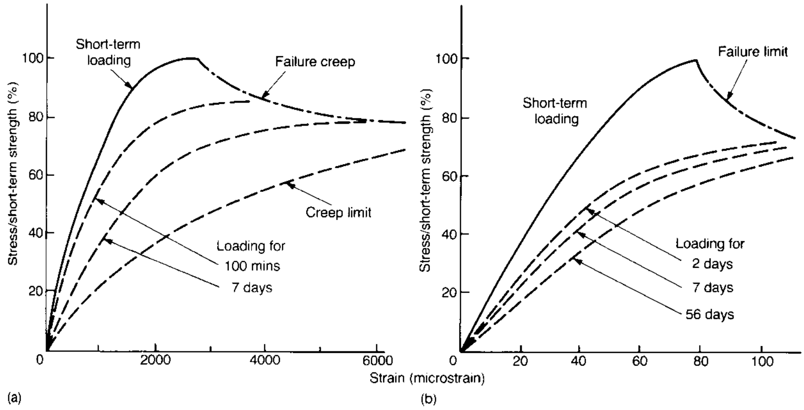

FIGURE 20.15 The effect of sustained compressive and tensile loading on the stress–strain relationship for concrete: (a) compressive loading; (b) tensile loading (Rusch, 1960; Domone, 1974).

many cracks, rather than by the propagation of a single crack.

2. Cracks in cement paste or concrete do not propagate in straight lines, but follow tortuous paths around cement grains, aggregate particles, etc., which both distort and blunt the cracks (Figure 20.5).
3. Concrete is a composite made up of cement paste, the transition zone and the aggregate, and each has its own fracture toughness (K_c), in themselves difficult to measure. There is also disagreement on the size of concrete specimen necessary to determine an overall fracture toughness.

Despite these difficulties, K_c values for cement paste have been estimated as lying in the range 0.1 to 0.5 MN/m$^{3/2}$, and for concrete between about 0.45 and 1.40 MN/m$^{3/2}$ (Mindess and Young, 1981). K_c for the transition zone seems to be smaller, about 0.1 MN/m$^{3/2}$, confirming the critical nature of this zone. Comparison of these values with those for other materials given in Table 6.1 shows the brittle nature of concrete.

20.5 Strength under multiaxial loading

So far in this chapter our discussions on compressive strength have been concerned with the effects of uniaxial loading, i.e. where σ_1 (or σ_x) is finite, and the orthogonal stresses σ_2 (or σ_y) and σ_3 (or σ_z) are both zero. In many, perhaps most, structural situations concrete will be subject to a multiaxial stress state (i.e. σ_2 and/or σ_3 as well as σ_1 are finite). This can result in considerable modifications to the failure stresses, primarily by influencing the cracking pattern.

A typical failure envelope under biaxial stress (i.e. $\sigma_3 = 0$) is shown in Figure 20.16, in which the applied stresses, σ_1 and σ_2 are plotted non-dimensionally as proportions of the uniaxial compressive strength, σ_c. First, it can be seen that concretes of different strengths behave very similarly when plotted on this basis. Not surprisingly, the lowest strengths in each case are obtained in the tension–tension quadrant. The effect of combined tension and compression is to reduce considerably the compressive stress needed for failure even if the tensile stress is significantly less than the uniaxial tensile strength. The cracking pattern over most of this region (Type 1 in Figure 20.16) is a single tensile crack, indicating that the failure criterion is one of maximum tensile strain, with the tensile stress enhancing the lateral tensile strain from the compressive stress. In the region of near uniaxial compressive stress, i.e. close to the compressive stress axes, the cracking pattern (Type 2) is essentially the same as that in the central region of the cylinder shown in Figure 20.1; i.e. the cracks form all around the specimen approximately parallel to the compressive load. In the compression–compression quadrant, the cracking pattern (Type 3) becomes more regular, with the cracks forming in the plane of the applied loads, splitting the specimen into slabs. Under equal biaxial compressive stresses, the failure stress is somewhat larger than the uniaxial strength. Both Type 2 and Type 3 crack patterns also indicate a limiting tensile strain failure criterion, in the direction perpendicular to the compressive stress(es).

With triaxial stresses, if all three stresses are compressive then the lateral stresses (σ_2 and σ_3) act in opposition to the lateral tensile strain produced by σ_1. This in effect confines the specimen, and results in increased values of σ_1 being required for failure, as illustrated in Figure 20.17 for the case of uniform confining stress (i.e. $\sigma_2 = \sigma_3$); the axial strength ($\sigma_{1\text{ult}}$) can be related to the lateral stress by the expression

$$\sigma_{1\text{ult}} = \sigma_c + K\sigma_2 \text{ (or } \sigma_3) \qquad (20.6)$$

where K has been found to vary between about 2 and 4.5.

In describing strength tests in Section 20.1.1, we said that when a compressive stress is applied to a specimen by the steel platen of a test machine, the lateral (Poisson effect) strains induce restraint forces in the concrete near the platen due to the mismatch in elastic modulus between the concrete and the steel. This is, therefore, a particular case of triaxial stress, and the cause of the higher strength of cubes compared to longer specimens such as cylinders.

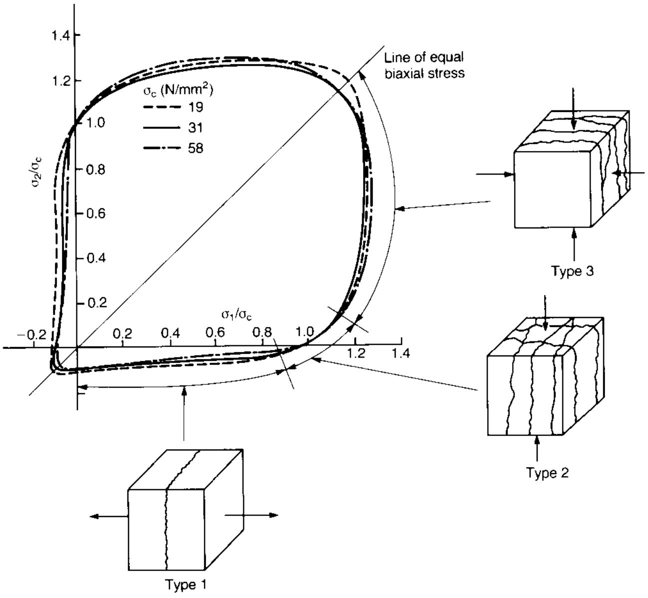

FIGURE 20.16 Failure envelopes and typical fracture patterns for concrete under biaxial stresses σ_1 and σ_2, relative to uniaxial stress σ_c (Kupfer *et al.*, 1969; Vile, 1965).

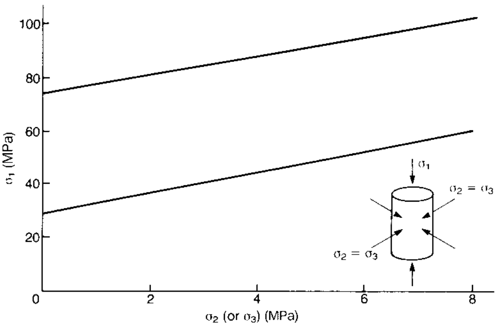

FIGURE 20.17 The effect of lateral confining stress (σ_2, σ_3) on the axial compressive strength (σ_1) of concretes of two different strengths (FIP/CEB, 1990).

20.6 References

Balmer, T. (2000) Investigation into the effects on the main concrete relationship using class 42.5N Portland cement at varying compliance levels. *Association of Concrete Technology Diploma Report*, BCA, Crowthorne.

British Standards Institution (1996) DD ENV: 1992–1–2 Eurocode 2: Design of Concrete Structures.

CEB-FIP (1990) *Model Code for the Design of Concrete Structures*, Thomas Telford, London.

Cordon, W.A. and Gillespie, H.A. (1963) Variables in concrete aggregates and Portland cement paste which influences the strength of concrete. *J. Amer. Conc. Inst.* 60, 8, August 1029–50.

De Rooij, M.R. and Bijen, J.M.J.M. and Frens, G. (1998) Introduction of syneresis in cement paste. *Proc. of Int. RILEM Conf. on the Interfacial Transition Zone in Cementitious Composites* (eds A. Katz, A. Bentur, M. Alexander and G. Arliguie), Israel, March, E & FN Spon, London, pp. 59–67.

Domone, P.L. (1974) Uniaxial tensile creep and failure of concrete. *Magazine of Concrete Research* 26, 88, Sept., 144–52.

Erntroy, H.C. and Shacklock, B.W. (1954) Design of high strength concrete mixes. *Proceedings of the Symposium on Mix Design and Quality Control of Concrete*, Cement and Concrete Association, London, pp. 55–73.

FIP/CEB (1990) *State-of-the-Art Report on High Strength Concrete*, Thomas Telford, London.

Glucklich, J. (1965) The effect of microcracking on time-dependent deformations and the long-term strength of concrete. *Proceedings of the International Conference on Structure of Concrete and its Behaviour Under Load*, Cement and Concrete Association, London, Sept., pp. 176–89.

Katz, A., Bentur, A., Alexander, M. and Arliguie, G. (eds) (1998) *Proc. of Int. RILEM Conf. on the Interfacial Transition Zone in Cementitious Composites*, Israel, March, E & FN Spon, London, p. 342.

Kupfer, H., Hilsdorf, H.K. and Rusch, H. (1969) Behaviour of concrete under biaxial stress. *Proc. Amer. Conc. Inst.* 66, 660.

Maso, J.C. (ed.) (1992) *Proc. of Int. RILEM Conf. on Interfaces in Cementitious Composites,* Toulouse, October, E & FN Spon, London, p. 315.

Mindess, S. and Young, J.F. (1981) *Concrete,* Prentice-Hall, New Jersey.

Neville, A.M. (1995) *Properties of Concrete,* 4th edn, Pearson Education, Harlow, p. 844.

Newman, K. (1966) Concrete systems. In *Composite Materials* (ed. L. Hollaway), Elsevier, London.

Portland Cement Association (1968) *Design and Control of Concrete Mixes,* 11th edn, Stokie, Illinois, USA.

Rusch, H. (1960) Researches towards a general flexural theory for structural concrete. *J. Amer. Conc. Inst.* 57, 1, July, 1–29.

Sedran, T., de Larrard, F., Hourst, F. and Contamines, C. (1996) Mix design of self-compacting concrete (SCC). *Proceedings of Int. RILEM Conf. on Production Methods and Workability of Concrete* (eds P.J.M. Bartos, D.L. Marrs and D.J. Cleland) E & FN Spon, London, pp. 439–50.

Struble, L., Skalny, J. and Mindess, S. (1980) A review of the cement-aggregate bond. *Cement and Concrete Research,* 10, 2, March, 277–86.

Swamy, R.N. and Kameswara Rao, C.B.S. (1973) Fracture mechanism in concrete systems under uniaxial loading. *Cement and Concrete Research* 3, 4, July, 413–28.

Vile, G.W.D. (1965) The strength of concrete under short-term biaxial stress. *Proceedings of the International Conference on Structure of Concrete and its Behaviour Under Load*, Cement and Concrete Association, London, Sept., pp. 275–88.

Chapter twenty-one

Concrete mix design

Mix design is the process of selecting the proportions of cement, water, fine and coarse aggregates and, if to be used, cement replacement materials and admixtures to produce an economic concrete mix with the required fresh and hardened properties. The cement and other binder constituents are usually the most expensive component(s), and 'economic' usually means keeping its/their content as low as possible, without, of course, compromising the resulting properties. There may also be other advantages, such as reduced heat of hydration (Chapter 17) or drying shrinkage (Chapter 19)

21.1 The mix design process

Figure 21.1 shows the stages in the complete mix design process; we will discuss each of these in turn.

21.1.1 Specified concrete properties

The required hardened properties of the concrete result from the structural design process, and are therefore provided to the mix designer. Strength is normally specified in terms of a characteristic strength (or *grade*) at a given age (see Preface). Durability requirements, to be discussed in Chapter 23, may impose a limit on some mix proportions, e.g. a minimum cement content or maximum water/cement ratio, or demand the use of air-entraining agent or a particular aggregate type.

The choice of workability will depend on the methods selected for transporting, handling and placing the concrete (e.g. pump, skip), the size of the section to be filled and the density of reinforcement. The workability must clearly be sufficient at the point of placing, which in the case of ready-mixed concrete transported by road to site, may be some time after mixing.

21.1.2 Constituent material properties

As a minimum, the fine and coarse aggregate size, type and grading, and the cement type must be known. The relative density of the aggregates, the cement composition, and details of any cement replacement materials and admixtures that are to be used or considered may also be needed.

21.1.3 Initial estimate of mix proportions

An initial best estimate of the mix proportions that will give concrete with the required properties is then made. In doing this, as much use as possible is made of previous results from concrete made with the same or similar constituent materials. In some cases, for example in producing a new mix from an established site plant, the behaviour of the materials will be well known. In

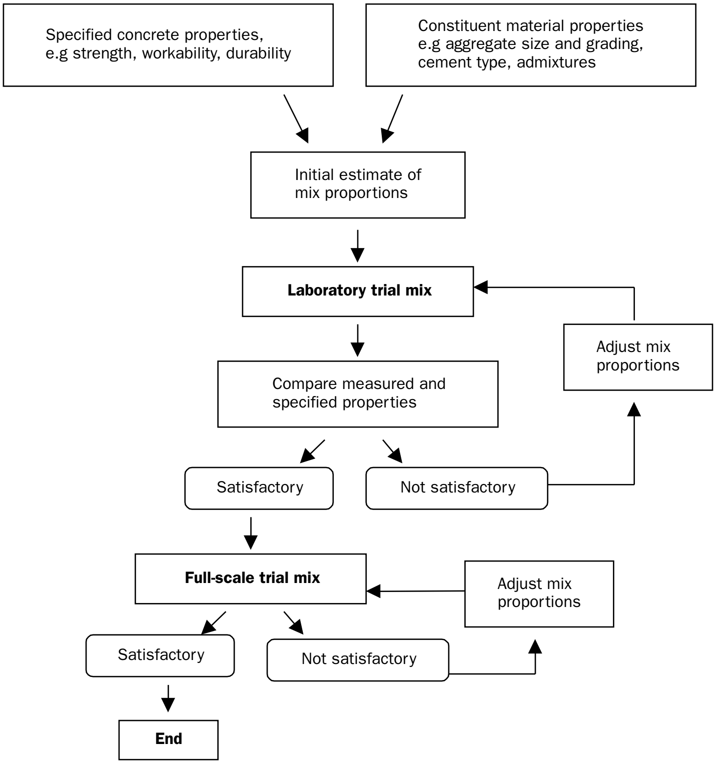

FIGURE 21.1 The mix design process.

other circumstances, there will be no such knowledge, and typical behaviour such as that given in the preceding few chapters has to be used.

There are a considerable number of step-by-step methods of varying complexity that can be used to produce this 'best estimate'. Many countries have their own preferred method or methods, and, as an example, we will describe a current UK method below. Whichever method is used, it is important to recognise that the result is only a best estimate, perhaps even only a good guess. Because the constituent materials will not be exactly as assumed and their interaction cannot be predicted with any great certainty, the concrete is unlikely to meet the requirements precisely.

21.1.4 Laboratory trial mixes

It follows from the above that a trial mix to determine the resulting properties of the 'best guess' mix is essential. This is normally first carried out at a relatively small scale in the laboratory. Some adjustment to the mix portions will probably be necessary when the test results are obtained, e.g. a decrease in the water/cement ratio if the strength is too low. A second trial mix with the revised mix proportions is then carried out, and the process repeated until a satisfactory mix in all respects is obtained.

21.1.5 Full-scale trial mixes

The laboratory trials do not provide the complete answer. The full-scale batching and mixing procedures will not be exactly the same as those in the laboratory, and may cause differences in the concrete properties. Complete confidence in the mix can therefore only be obtained with further trials at full scale, again with adjustments to the mix proportions and re-testing if necessary.

21.2 UK method of 'Design of normal concrete mixes' (BRE, 1997)

This method of mix design provides a good example of the process of making an initial estimate of the mix proportions. It has the advantage of being relatively straightforward and producing reasonable results with the materials most commonly available in the UK. It should be emphasised that it is not necessarily the 'best' method available world-wide, and that it may not give such good results with other materials.

The main part of the method is concerned with the design of mixes incorporating Portland cement, water and normal density coarse and fine aggregates only, and with characteristic strengths of up to about 70 MPa. It encompasses both crushed and uncrushed coarse aggregate. The steps involved can be summarised as follows.

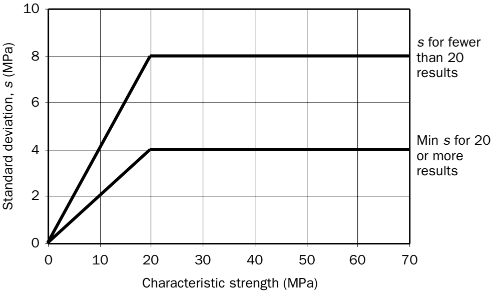

FIGURE 21.2 Standard deviation versus characteristic strength of concrete (BRE, 1997).

21.2.1 Target mean strength

As described in the Preface, the specified *characteristic strength* is a lower limit of strength to be used in structural design. As with all materials, concrete has an inherent variability of strength, and an average cube compressive strength (or *target mean strength*) somewhat above the characteristic strength is therefore required. The difference between the characteristic and target mean strength is called the *margin;* a 5 per cent failure rate is normally chosen for concrete, and the margin should therefore be 1.64 times the standard deviation of the strength test results (Figure 0.4).

This means that a knowledge of the standard deviation is required. For an existing concrete production facility this will be known from previous tests. Where limited or no data are available, the upper values given in Figure 21.2,[1] which has been derived from analysis of the data from many production facilities, can be used. When production is under way, this can be reduced if justified by test results, but not below the lower values in Figure 21.2. The advantage of reducing the variability by good practice is clear.

21.2.2 Free water/cement ratio

For a particular cement and aggregate type, the concrete strength at a given age is assumed to be governed by the free water/cement ratio only. The first step is to obtain a value of strength at water/cement ratio of 0.5 from Figure 21.3 for the relevant age/aggregate type/cement type combination (this figure has been drawn from data in a table in the method document). This value is then plotted on the vertical line in Figure 21.4 to give a starting point for a line which is constructed parallel to the curves as shown. The point of intersection of this line with the horizontal line of the required target mean strength then gives the required free water/cement ratio. The ranges of the axes in Figure 21.4 indicates the limits of validity of the method.

---

[1] Figures 21.2 to 21.7 inclusive have been taken from BRE (1997), and Figures 21.2, 21.4, 21.6 and 21.7 are ©BRE and have been reproduced with the permission of BRE.

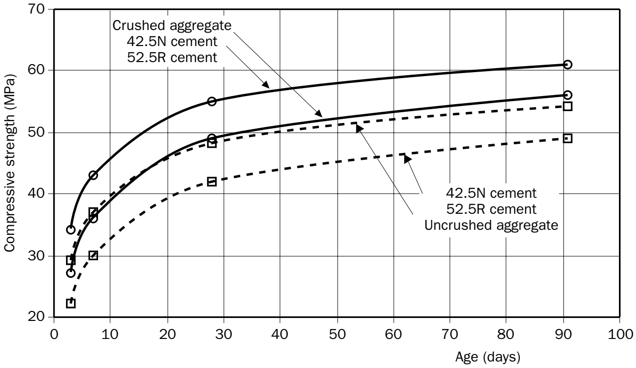

FIGURE 21.3 Compressive strength versus age for concrete with a water/cement ratio of 0.5 (BRE, 1997).

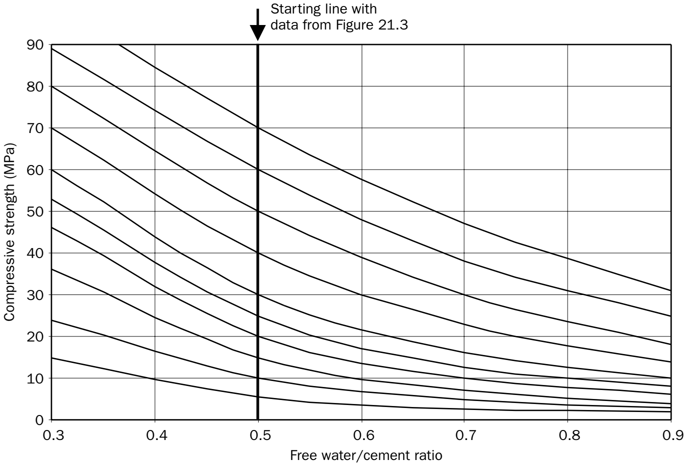

FIGURE 21.4 Compressive strength versus water/cement ratio of concrete (BRE, 1997).

21.2.3 Free water content

It is now assumed that, for a given coarse aggregate type and maximum size, the concrete workability is governed by the free water content only. The workability can be specified in terms of either slump or Vebe time (see Chapter 17), although slump is by far the most commonly used. Figure 21.5 is a graph of data for slump, again drawn from data given as a table in the method document, from which the free water content for the appropriate aggregate can be obtained.

21.2.4 Cement content

This is a simple calculation from the values of free water/cement ratio and free water content just calculated.

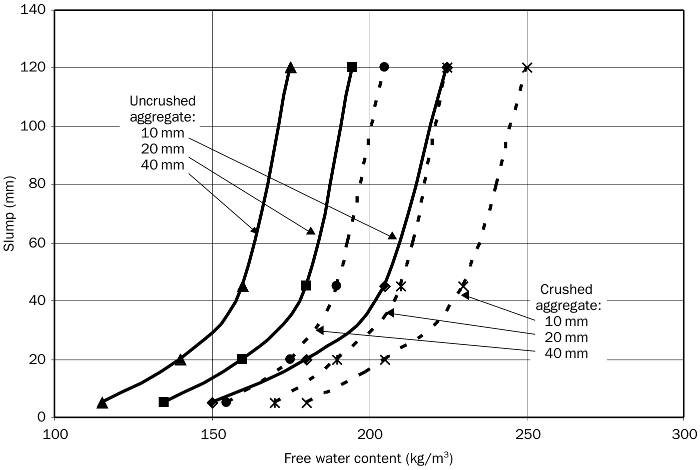

FIGURE 21.5 Slump versus free water content of concrete (BRE, 1997).

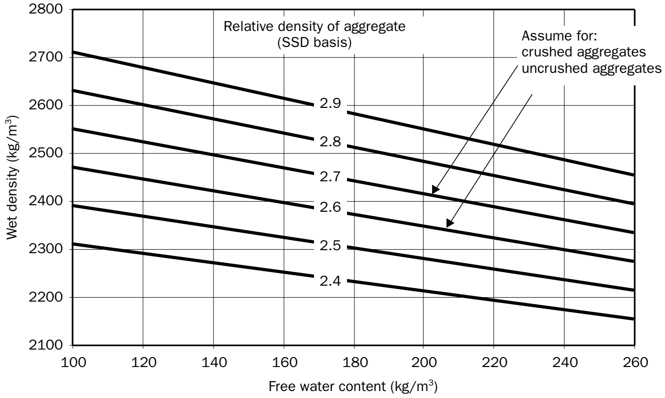

FIGURE 21.6 Wet density of fully compacted concrete versus free water content (BRE, 1997).

21.2.5 Total aggregate content

An estimate of the density of the concrete is now required. This is obtained from Figure 21.6, using known or assumed values of the relative density of the aggregates. A weighted mean value is used if relative densities of the coarse and fine aggregate are different. Subtraction of the free water content and cement content from this density gives the total aggregate content.

21.2.6 Fine and coarse aggregate content

The estimated value of the proportion of fine aggregate in the total aggregate depends on the maximum size of aggregate, the concrete workability, the grading of the fine aggregate (specifically the amount passing a 600 micron sieve) and the free water/cement ratio. Figure 21.7 shows the relevant graphs for obtaining this proportion for a maximum aggregate size of 20 mm. Sufficient

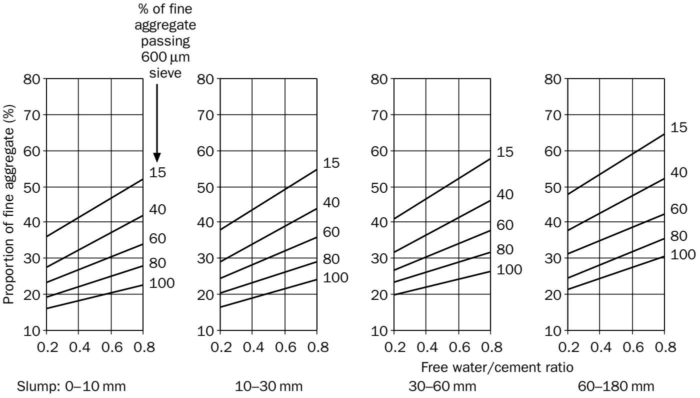

FIGURE 21.7 Proportions of fine aggregate according to percentage passing 600 μm sieve (for 20 mm max. coarse aggregate size) (BRE, 1997).

fine aggregate must be incorporated to produce a cohesive mix that is not prone to segregation, and Figure 2.17 shows that increasing quantities are required with increasing water/cement ratio, increasing slump and if the aggregate itself is coarser. The mix design document also gives equivalent graphs for 10 and 40 mm coarse aggregate; with the former between 5 and 15 per cent more fine aggregate is required, and with the latter between 5 and 10 per cent less.

The fine and coarse aggregate content is now calculated by simple arithmetic, and the amounts (in kg/m^3) of free water, cement, coarse and fine aggregates for the laboratory trial mix have now all been obtained.

It is important to note the simplifying assumptions used in the various stages. These make the method somewhat simpler than many other alternatives, but highlight the importance of trial mixes and subsequent refinements.

21.3 Mix design with cement replacement materials (CRMs)

As we have seen, CRMs effect both the fresh and hardened properties of concrete, and it is often difficult to predict their interaction with the Portland cement with any confidence. The mix design process for concretes including CRMs is therefore more complex, and again, trial mixes are essential.

The mix design method described above (BRE, 1997) includes modifications for mixes containing good quality low-lime pfa or ggbs. With pfa:

- the amount, expressed as a proportion of the total binder, first needs to be selected, for example for heat output, durability or economic reasons, subject to a maximum of 40 per cent;
- the increase in workability is such that the water content obtained from Figure 21.5 can be reduced by 3 per cent for each 10 per cent of pfa;
- the effect upon the strength is allowed for by the use of a *cementing efficiency factor*, k, which we discussed in Chapter 20. This converts the amount of PFA to an equivalent amount of cement. The total equivalent cement content is then $C + kF$, where C = Portland cement content and F = pfa content. The value of k varies with the type of pfa and Portland cement and with the age of the concrete, but a value of 0.30 is taken for 28-day strength with a class 42.5 Portland cement. Thus, if w = water content, a value of the equivalent water/cement ratio $w/(C + kF)$ is obtained from Figure 21.4;

- subsequent calculations follow using $C+F$ when the total binder content is required.

With ggbs:

- again the amount as a proportion of the binder is first chosen, with values of up to 90 per cent being suitable for some purposes;
- the improvements in workability are such that the water contents derived from Figure 21.5 can be reduced by about 5 kg/m^3;
- the cementing efficiency factor approach used for pfa is more difficult to apply as the value of k is dependent on more factors, including the water/equivalent cement ratio, and for 28-day strengths varies from about 0.4 to over 1.0. It is assumed that for ggbs contents of up to 40 per cent there is no change to the strength, i.e. $k=1$, but for higher proportions information should be obtained from the cement manufacturer or the ggbs supplier.

21.4 Design of mixes containing admixtures

21.4.1 Mixes with plasticisers

As we have seen in Chapter 14, plasticisers increase the fluidity or workability of the concrete. This leads to three methods of use:

1. to provide an increase in workability, by direct addition of the plasticiser with no other changes to the mix proportions;
2. to give an increase in strength at the same workability, by allowing the water content to be reduced, with consequent reduction in the water/cement ratio;
3. to give a reduction in cement content for the same strength and workability, by coupling the reduction in water content with a corresponding reduction in cement content to maintain the water/cement ratio.

(1) and (2) change the properties of the concrete, (3) will normally result in a cost saving as the admixture costs much less than amount of cement saved.

Table 21.1 gives typical figures for these effects for an average strength concrete mix and a lignosulfonate-based plasticiser. The figures have been obtained from data provided by the admixture supplier. The admixture amount is a 'standard' dose. The important changes are, in each case:

1. an increase in slump from 75 to 135 mm;
2. an increase in strength from 39 to 45 MPa;
3. a reduction in cement content of 30 kg/m^3.

Plasticisers can have some effect on the setting times, but mechanical properties and durability at later ages appear largely unaffected and are similar to those expected for a plain concrete of the same water/cement ratio, with two relatively minor exceptions:

1. there is some evidence of a slight increase in 28-day strength, attributed to the dispersion of the particles causing an increased surface

TABLE 21.1 Methods of using a plasticiser in average quality concrete (typical data from admixture supplier's information)

Mix	*Cement (kg/m^3)*	*Water*	*w/c*	*Plasticiser dose (% by wt of cement)*	*Slump (mm)*	*28 day strength (MPa)*
control	325	179	0.55	0	75	39
1	325	179	0.55	0.3[1]	135	39.5
2	325	163	0.5	0.3	75	45
3	295	163	0.55	0.3	75	39

Note:
1. A 'standard' dose.

area of cement being exposed to the mix water (Hewlett, 1988);
2. some plasticisers entrain about 1–2 per cent air because they lower the surface tension of the mix water. This will reduce the density and strength of the concrete.

21.4.2 Mixes with superplasticisers

For the reasons explained in Chapter 14, it is very difficult to generalise about the effects and uses of superplasticisers other than to say that they can produce greater increases in workability and/or strength and/or cement reduction than plasticisers. They are more expensive than plasticisers, and therefore the economic advantages of cement reduction may not be as great. The suppliers will provide information for each specific product or formulation, but a mix designer must ensure compatibility with the proposed binder. This can often be judged by tests on paste or mortar in advance of trial mixes on concrete (Aitcin, 1994).

Superplasticisers enable a much greater range of concrete types to be produced than with plasticisers, e.g. high workability flowing concrete, self-compacting mixes and high-strength mixes low water/cement ratios. These will be discussed in Chapter 24.

21.4.3 Mixes with air entraining agents

As discussed in Chapters 14 and 23, air entrainment is used to increase the resistance of concrete to freeze–thaw damage, but the entrained air increases the workability and reduces the subsequent strength. The method of mix design described above (BRE, 1997) includes the following modifications to allow for these effects if the specified air content is within the normal range of 3 to 7 per cent by volume:

- it is assumed that the strength is reduced by 5.5 per cent for each 1 per cent of air; the target mean strength is therefore increased by the appropriate amount;
- the slump is reduced by a factor of about two for the selection of water content from Figure 21.5;
- the concrete density obtained from Figure 21.6 is reduced by the appropriate amount,

21.5 References

Aitcin, P.C., Jolicoeur, C. and MacGregor, J.G. (1994) Superplasticizers: how they work and why they occasionally don't. *Concrete International* 16, 5, 45–52.

BRE (1997) *Design of Normal Concrete Mixes*, 2nd edn, Building Research Establishment, Watford.

Hewlett, P.C. (ed.) (1988) *Cement Admixtures: Use and Applications*, 2nd edn, Longman, Essex.

Chapter twenty-two

Non-destructive testing of hardened concrete

There are a wide variety of available methods and techniques available for the non-destructive testing of structural concrete, which can be broadly divided into those which assess the concrete itself, and those which are concerned with locating and determining the condition of the steel embedded in it. We are going to describe three well-established tests for concrete which are strictly non-destructive, and more briefly discuss others which involve some minor damage to the concrete – the so-called near-to-surface tests. We do not have space to consider tests to assess the location and condition of reinforcing and prestressing, important though these are. Some references to useful selected publications on these and other tests on concrete are included in the 'Further reading' on page 222.

Non-destructive testing of concrete is used for two main purposes:

- in laboratory studies, where it is particularly useful for repeated testing of the same specimen to determine the change of properties time, for example to provide information on degradation in different environments;
- to assess the properties of concrete in a structure, for example for compliance with specifications, after damage due to fire or overload or when a change of use is proposed.

Two of the tests that we will describe, the rebound hammer and ultrasonic pulse velocity, can be used for both these purposes; the third, the resonant frequency test, can only be used on prepared specimens in the laboratory.

An estimation of the strength of the concrete is often required, and therefore the degree of correlation of the non-destructive test measurement(s) with strength is important, and will be discussed in each case. It will be apparent that a single non-destructive test rarely gives a single definitive answer, and engineering judgement is required in interpreting the results. Nevertheless, the usefulness of such tests will become apparent.

22.1 Surface hardness – rebound (or Schmidt) hammer test

This is perhaps the simplest of the commonly available tests, and can be used on laboratory specimens or on in-situ concrete. The apparatus is contained in a hand-held cylindrical tube, and consists of a spring-loaded mass which is fired with a constant energy against a plunger held against the concrete surface (Figure 22.1). The amount of rebound of the mass expressed as the percentage of the initial extension of the spring is shown by the position of a rider on a graduated scale, and recorded as the *rebound number*. Less energy is absorbed by a harder surface, and so the rebound number is higher. A smooth concrete surface is required, but even then there is considerable local variation due to the presence of coarse aggregate particles (giving an abnormally high rebound number) or a void (giving a low number) just below the surface, and therefore a number of readings must be taken and averaged. Typical recommendations are for ten readings over an area of 150 mm diameter, with no two readings being taken within 25 mm of each other.[1] Also, the concrete being tested must be part of an unyielding mass; laboratory specimens such as cubes should therefore be held under a stress of about 7 MPa in a compression testing machine.

The test clearly only measures the properties of the surface zone of the concrete, to a depth of about 25–30 mm. The correlation between rebound number and concrete strength depends on:

- the aggregate type, since the hardness is a function of both strength and elastic modulus of the concrete;
- the moisture condition of the surface;
- the angle of the hammer with the vertical, which will vary since the test must be carried out with the plunger normal to the concrete surface.

There is therefore no single universal correlation. Figure 22.2 shows the relationship between rebound number and strength obtained by students at UCL in laboratory classes over several years. The degree of scatter is somewhat higher than that reported by other workers, the most likely explanation being the inexperience of the operatives. Even with more skilful operatives, strength cannot be predicted with great certainty, but the test is very simple and convenient, and so is often used as a first step in an investigation of in situ concrete, for example to assess uniformity or to compare areas of known good quality and suspect concrete.

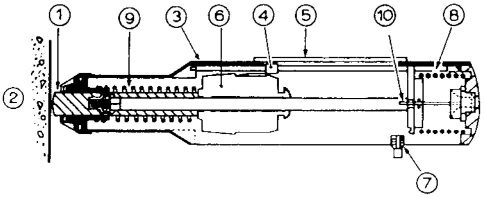

FIGURE 22.1 Rebound hammer: (1) plunger; (2) concrete; (3) tubular housing; (4) rider; (5) scale; (6) mass; (7) release button; (8) spring; (9) spring; (10) catch (Neville, 1995 by permission, Pearson Education).

22.2 Resonant frequency test

This is a laboratory test on prepared specimens, and can be used to assess progressive changes in the specimen due, for example, to freeze/thaw damage or chemical attack. It is therefore particularly useful for generating data in durability testing.

The specimen is in the form of a beam, typically 500 × 100 × 100 mm; the test normally consists of measuring the beam's fundamental longitudinal resonant frequency when it is supported at its mid-point. A value of elastic modulus called the *dynamic elastic modulus* can be obtained from this frequency (n), the length of the beam (l) and its density (ρ) using the relationship:

$$E_d = 4.n^2.l^2.\rho \qquad (22.1)$$

The resonant frequency is measured with the test system shown in Figure 22.3. The vibration is produced by a small oscillating driver in contact with one end of the beam, and the response of the beam is picked up by a similar device at the other end (Figure 22.3(a)). The amplitude of vibration

---

[1] A list of relevant standards is included in 'Further reading' on page 222.

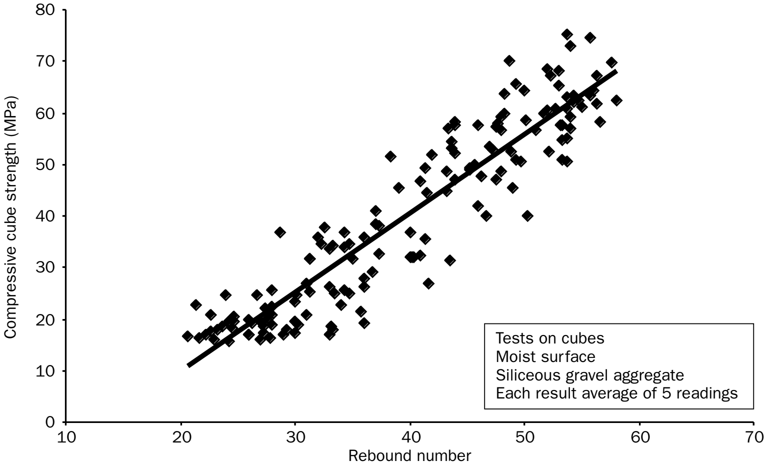

FIGURE 22.2 Relation between strength of concrete and rebound test results (UCL data).

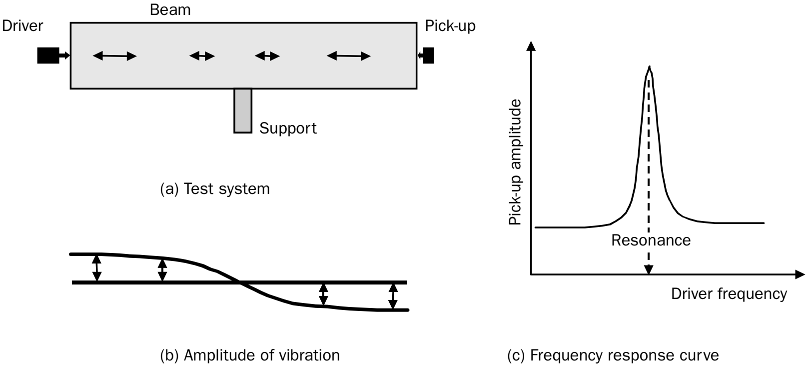

FIGURE 22.3 Measurement of the longitudinal resonant frequency of a concrete beam.

varies along the beam as in Figure 22.3 (b). The frequency of the driver is altered until a maximum amplitude of vibration is detected by the pick-up, indicating resonance (Figure 22.3 (c)). The frequency is normally displayed digitally and manually recorded.

The test involves very small strains, but, as we have seen in Chapter 19, concrete is a non-linear material. The dynamic modulus, E_d, is therefore in effect the tangent modulus at the origin of the stress–strain curve, i.e. the slope of line *B* in Figure 19.15 (a), and it is higher than the static or secant modulus (E_s) measured in a conventional stress–strain test, i.e. the slope of line *C* in Figure 19.15 (b). The ratio of E_s to E_d depends on several factors, including the compressive strength, but is normally between 0.8 and 0.85.

As with the static modulus, for a particular set of constituent materials the dynamic modulus and strength can be related; Figure 22.4 shows data obtained by students at UCL. The amount of scatter is less than that for rebound hammer versus strength (Figure 22.2), mainly because the dynamic modulus gives an average picture of the concrete throughout the beam, not just at localised points. The relationship is clearly non-linear, as with those for static modulus and strength given in equations (19.13) to (19.15). The applicability of relationships such as those in Figure 22.4 to only a restricted range of parameters (aggregate type, curing conditions, etc.) must be emphasised.

22.3 Ultrasonic pulse velocity test (upv)

This is an extremely versatile and popular test for both in-situ and laboratory use. It involves measuring the time taken for an ultrasonic pulse to travel through a known distance in concrete, from which the velocity is calculated. The ultrasonic signal is generated by a piezo-electric crystal housed in a transducer, which transforms an electric pulse into a mechanical wave. The pulse is detected by a second similar transducer, which converts it back to an electrical impulse, and the time taken to travel between the two transducers is measured and displayed by the instrumentation. Various test arrangements, illustrated in Figure 22.5, are possible. Efficient acoustic coupling between the transducers and the concrete is essential, and is usually obtained by a thin layer of grease. The pulse velocity is independent of the pulse frequency, but for concrete fairly low frequencies in the range 20–150 kHz (most commonly 54 kHz) are used to give a strong signal which is capable of passing through several metres of concrete. Transducers which produce longitudinal waves are normally used, although shear wave transducers are available.

The velocity (V) of the longitudinal ultrasonic pulse depends on the material's dynamic elastic modulus (E_d), Poisson's ratio (ν) and density (ρ):

$$V = \sqrt{\frac{E_d(1-\nu)}{\rho(1+\nu)(1-2\nu)}} \qquad (22.2)$$

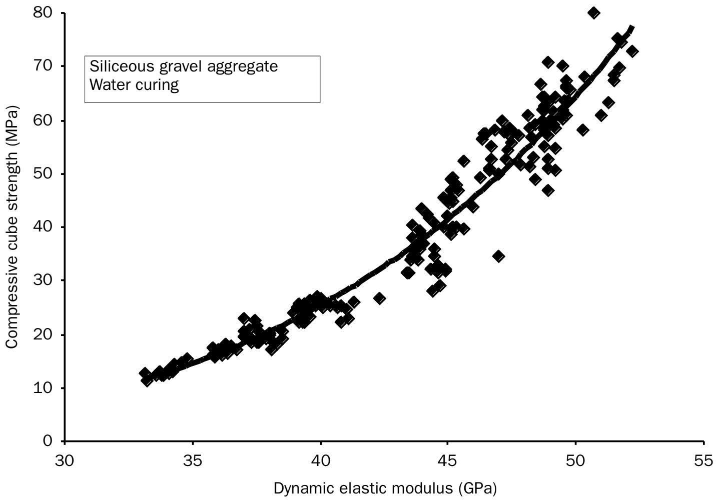

FIGURE 22.4 Relation between strength and dynamic elastic modulus of concrete (UCL data).

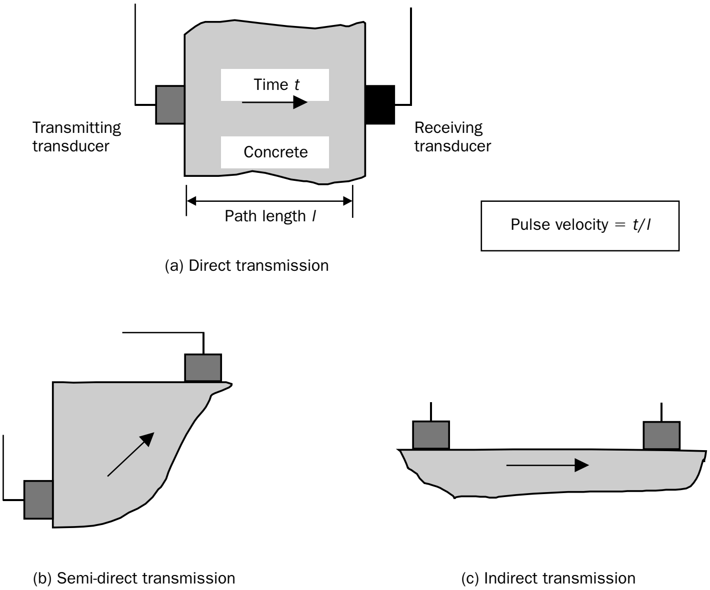

FIGURE 22.5 Measurement of ultrasonic pulse velocity in concrete.

Hence upv is related to the elastic properties, and, as with E_d, can be correlated empirically to strength, but with the similar limitations of dependence on constituent materials and as with the rebound hammer, moisture conditions. Figure 22.6 shows UCL students' data. The relation is clearly non-linear, which is to be expected since upv is related to dynamic modulus, but shows a greater degree of scatter than the strength/E_d relationship in Figure 22.4. Two factors contribute to this. First, the upv test requires a little more skill than the resonant frequency test, e.g. in ensuring good acoustic coupling between the transducer and the concrete. Second, the results were obtained on 100 mm cubes, and therefore a smaller and inherently more variable volume of concrete was being tested. It is extremely important to bear both of these factors in mind when interpreting any non-destructive test data.

The ultrasonic pulse is travelling through both the hardened cement paste and the aggregate, and hence the pulse velocity will depend on the velocity through each and their relative proportions. The velocity through normal density aggregate is higher than that through the paste, which leads to the broad relationships between upv and strength for paste, mortar and concrete shown in Figure 22.7.

The upv test has the great advantage of being able to assess concrete throughout the signal path, i.e. in the interior of concrete element. Direct transmission is preferred, but for in situ measurements, semi-direct or indirect operation can be used if access to opposite faces is limited (Figure 22.5). With in situ testing, it is also very important to ensure that measurements are taken where they are not influenced by the presence of reinforcing steel, through which the pulse travels faster (upv = 5.9 km/sec), and which can therefore result in a falsely low transit time.

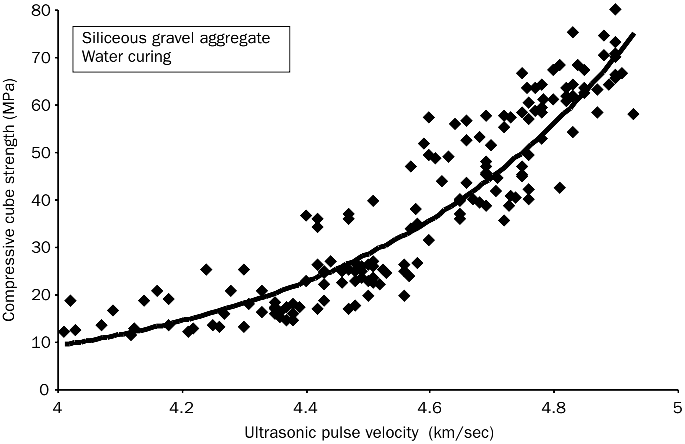

FIGURE 22.6 Relation between strength and ultrasonic pulse velocity (UCL data).

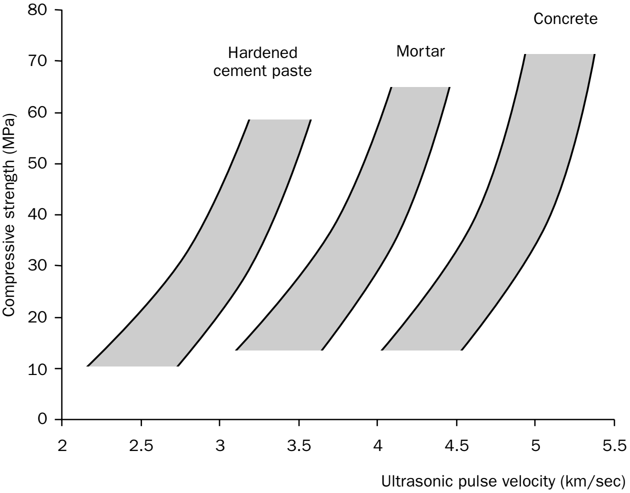

FIGURE 22.7 Envelope of strength and ultrasonic pulse velocity for hardened cement paste, mortar and concrete (based on Sturrup *et al.*, 1984, and UCL data).

22.4 Near-to-surface tests

The specific need to assess the strength of in situ concrete has led to the development of a range of tests in which the surface zone is penetrated or fractured. The limited amount of damage incurred does not significantly affect the structural performance of the concrete elements or members, but it does normally require making good after the test for aesthetic or durability requirements.

The five main types of test are shown in Figure 22.8; there are a number of commercial versions of each test. The penetration resistance test, in

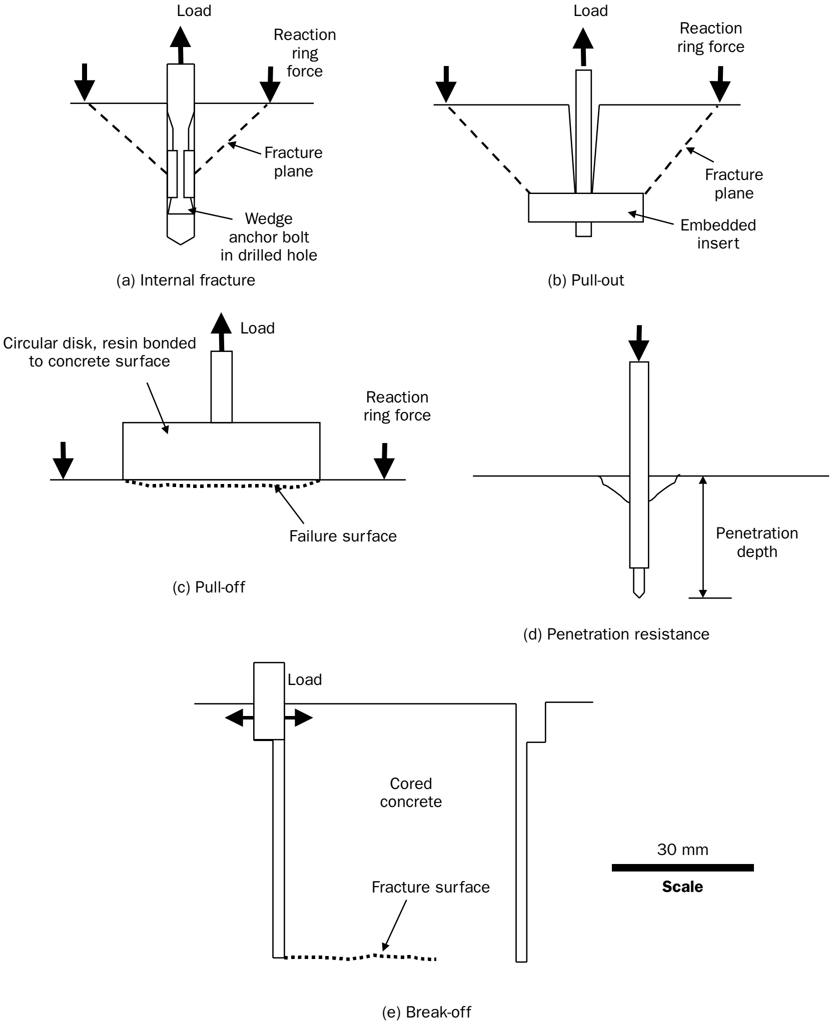

FIGURE 22.8 The main types of near-to-surface tests for concrete (all to same approx. scale).

TABLE 22.1 Required repetitions and accuracy of strength estimation for near-to-surface tests (Bungey, 1992 by permission, Concrete Society)

Test method	*Recommended number of tests for a mean value at each location*	*Likely 95% confidence limit for compressive strength estimation*
Internal fracture	6	±30%
Pull-out	4	±10–20%
Pull-off	6	±15%
Penetration resistance	3	±20%
Break-off	5	±20%

which the depth of penetration of a bolt fired into the concrete with a standard explosive charge is measured, is somewhat different from the others which involve the measurement of the force required to cause a fracture of some form. The force is applied via a device either inserted into a pre-drilled hole, as in the internal fracture and break-off tests, or glued to the concrete surface, as in the pull-off tests, or cast into the concrete, as in the pull-out test. This last type involves preplanning before or during construction, although a version which fits into an under-reamed drilled hole is available.

To give an estimate of compressive strength, prior collaboration in the laboratory is necessary for all tests, and, as with the truly non-destructive tests already described, considerable scatter is obtained. Table 22.1 gives recommendations for the number of test repetitions required to give a satisfactory mean value, and the resulting confidence of the strength estimation. It can be seen that this is of a similar order of magnitude to that in Figures 22.2 and 22.6. All of the correlations are also dependent on a number of factors, particularly the aggregate type.

The non-destructive and near-to-surface tests are often used in advance of taking larger core samples, which after preparation can be tested to give a direct measurement of strength, but which involved a lot more work, and result in more damage to the structure.

22.5 References

Bungey, J. (1992) Near-to-surface strength testing. *Concrete,* Sept–Oct, 34–6.

Neville, A.M. (1995) *Properties of Concrete*, 4th edn, Longman, Essex, p. 625.

Sturrup, V.R., Vecchio, F.J. and Caratin, H. (1984) Pulse velocity as a measure of concrete compressive strength. In *In-situ/Non-destructive Testing of Concrete* (ed. V. Malhotra), *ACI SP-82*, American Concrete Institute, Detroit, USA, pp. 201–7.

Chapter twenty-three

Durability of concrete

Durability can be defined as the ability of a material to remain serviceable for at least the required lifetime of the structure of which it forms a part. The specified design life can typically be 50 or 100 years, but for many structures this is not well defined, and then the durability should be such that the structure remains serviceable more or less indefinitely, given reasonable maintenance. For many years, concrete was regarded as having an inherently high durability, but experiences in recent decades have shown that this is not necessarily the case. Degradation can result from either the environment to which the concrete is exposed, for example frost damage, or from internal causes within the concrete, as in alkali–aggregate reaction. It is also necessary to distinguish between degradation of the concrete itself and loss of protection and subsequent corrosion of the reinforcing or prestressing steel contained within it.

The rate of most of the degradation processes is controlled by the rate at which moisture, air or other aggressive agents can penetrate the concrete. This *penetrability* is a unifying theme when considering durability, and for this reason we shall first consider the various transport mechanisms through concrete – pressure-induced flow, diffusion and absorption – their measurement and the factors which influence their rate. We shall then discuss the main degradation processes, firstly of concrete – chemical attack by sulfates, sea water, acids and alkali–silica reaction, and physical attack by frost and fire – and then the corrosion of embedded steel. This will show how potential problems in all of these areas can be eliminated, or at least minimised, by due consideration to durability criteria in the design and specification of new structures. By way of illustration, some typical recommendations are included. Ignorance of, or lack of attention to, such criteria in the past has led to a thriving and expanding repair industry in recent years; it is to be hoped that today's practitioners will be able to learn from these lessons and reduce the need for such activities in the future. It is beyond the scope of this book to discuss inspection and repair methods; publications on this subject are now extensive, and a useful review is listed in the 'Further reading' on page 222.

23.1 Transport mechanisms through concrete

As we have seen in Chapter 13, hardened cement paste and concrete contain pores of varying types and sizes, and therefore the transport of materials through concrete can be considered as a particular case of the more general phenomenon of flow through a porous medium. The rate of flow will

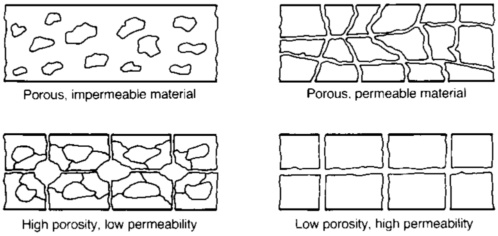

FIGURE 23.1 Illustration of the difference between permeability and porosity (Concrete Society, 1988 by permission).

not depend simply on the porosity, but on the degree of continuity of the pores and their size – flow will not take place in pores with a diameter of less than about 150 nm. The term *permeability* is often loosely used to describe this general property (although we shall see that it also has a more specific meaning); Figure 23.1 illustrates the difference between permeability and porosity.

Flow can occur by one of three distinct processes:

- movement of a fluid under a pressure differential – i.e. permeation;
- movement of ions, atoms or molecules under a concentration gradient, i.e. diffusion;
- capillary attraction of a liquid into empty or partially empty pores, i.e. sorption.

Each of these has an associated 'flow constant', defined as follows:

1. In the flow or movement of a fluid under a pressure differential, the flow passages through concrete and the flow rates are sufficiently small for the flow of either a liquid or gas to be laminar, and hence it can be described by Darcy's law:

   $$u_x = -K\partial h/\partial x \qquad (23.1)$$

   where, for flow in the x-direction, u_x = mean flow velocity, $\partial h/\partial x$ = rate of increase in pressure head in the x-direction, and K is a constant called the *coefficient of permeability*, the dimensions of which are (length)/(time), e.g. m/sec.

   The value of K depends on both the pore structure within the concrete and the properties of the permeating fluid. The latter can, in theory, be eliminated by using the *intrinsic permeability* (k) given by

   $$k = K\eta/\rho \qquad (23.2)$$

   where η = coefficient of viscosity of the fluid and ρ = unit weight of the fluid. k has dimensions of $(\text{length})^2$, and should be a property of the porous medium alone and therefore applicable to all permeating fluids. However, for liquids, it depends on the viscosity being independent of the pore structure, and for hcp with its very narrow flow channels in which a significant amount of the water will be subject to surface forces this may not be the case. Furthermore, comparison of k values from gas and liquid permeability tests has shown the former to be between 5 and 60 times higher than the latter, a difference attributed to the flow pattern of a gas in a narrow channel differing from that of a liquid (Bamforth, 1987). It is therefore preferable to consider permeability in terms of K rather than k, and accept the limitation that the values given apply to one permeating fluid only, normally water.
2. The movement of ions, atoms or molecules under a concentration gradient is a process of diffusion, and is governed by Fick's law:

   $$J = -D\partial C/\partial x \qquad (23.3)$$

   where, for the x-direction, J = transfer rate of the substance per unit area normal to the x-direction, $\partial C/\partial x$ = concentration gradient and D is a constant called the *diffusivity*, which has the dimensions of $(\text{length})^2/(\text{time})$, e.g. m^2/sec.

   Defining the diffusivity in this way treats the porous solid as a continuum, but the complex and confining pore structure within concrete means that D is an effective, rather than a true, diffusion coefficient. We are also interested in more than one type of diffusion process, for example moisture movement during drying shrinkage, or de-icing salt diffusion through saturated concrete road decks.

Furthermore, in the case of moisture diffusion (in, say, drying shrinkage) the moisture content within the pores will be changing throughout the diffusion process. There is, however, sufficient justification to consider D as a constant for any one particular diffusion process, but it should be remembered that, as with the permeability coefficient K, it is dependent on both the pore structure of the concrete and the properties of the diffusing substance.

3. Adsorption and absorption of a liquid into empty or partially empty pores occurs by capillary attraction. Experimental observations show that the relationship between the depth of penetration (x) and the square root of the time (t) is bi- or tri-linear (Figure 23.2), with a period of rapid absorption in which the larger pores are filled, being followed by more gradual absorption (Buenfeld and Okundi, 1998). A constant called the *sorptivity* (S) can be defined as the slope of the relationship (normally over the initial period), i.e.:

$$x = S.t^{0.5} \tag{23.4}$$

As before, S relates to a specific liquid, often water. It has the dimensions of $(\text{length})/(\text{time})^{0.5}$, e.g. $\text{mm/sec}^{0.5}$.

The applicability of these mechanisms in practice is illustrated by the case of an offshore concrete structure, which is exposed to a range of different environments. Figure 23.3 shows the predominant mechanisms in the respective exposure zones.

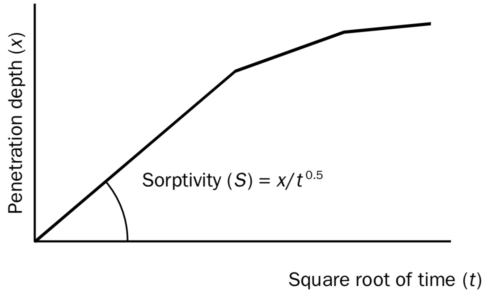

FIGURE 23.2 Typical form of results from sorptivity measurements.

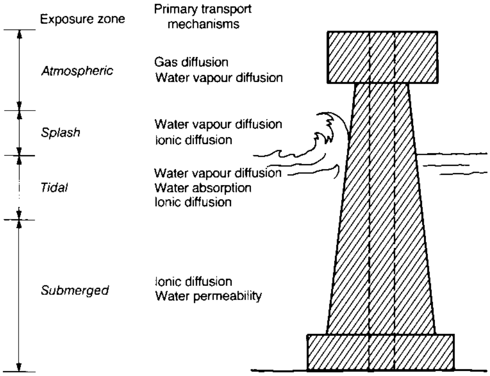

FIGURE 23.3 Primary transport mechanisms in the various exposure zones of a concrete offshore structure (Concrete Society, 1988 by permission).

23.2 Measurements of flow constants for cement paste and concrete

23.2.1 Permeability

Permeability is commonly measured by subjecting the fluid on one side of a concrete specimen to a pressure head, and measuring the steady-state flow rate that eventually occurs through the specimen, as illustrated in Figure 23.4. The specimen is normally a circular disc, the sides of which are sealed to ensure uniaxial flow. If the fluid is incompressible, i.e. it is a liquid such as water, the pressure head gradient through the specimen is linear, and Darcy's equation reduces to:

$$\Delta Q/A = -K.\Delta P/l \tag{23.5}$$

where ΔQ = volumetric flow rate, A = total cross-sectional area of flow perpendicular to the z-direction, ΔP = pressure head and l = flow path length.

Much of the fundamental work on the permeability of cement paste to water was carried out

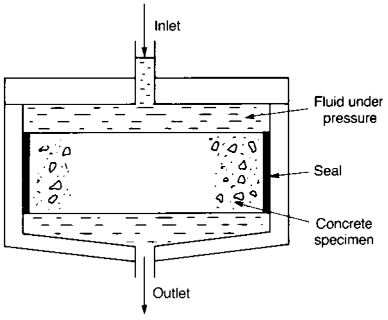

FIGURE 23.4 Typical test system for measurement of concrete permeability under steady-state flow.

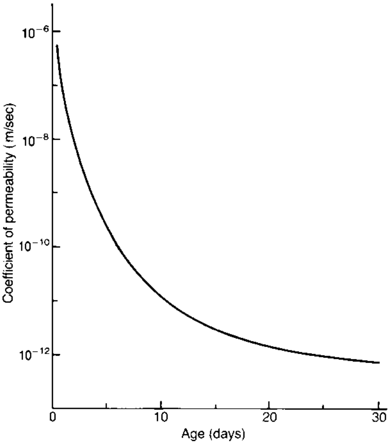

FIGURE 23.5 The effect of hydration on the permeability of cement paste (waste/cement = 0.7) (Powers *et al.*, 1954).

by Powers (1954, 1958). As the cement hydrates, the hydration products infill the skeletal structures, blocking the flow channels and hence reducing the permeability. As might be expected from our earlier description of cement hydration in Chapter 13, the reduction of permeability is high at early ages, when hydration is proceeding rapidly. In fact, as shown in Figure 23.5, it reduces by several orders of magnitude in the first 2–3 weeks after casting.

Although, as we discussed above, permeability and porosity are not necessarily related (Figure 23.1) there is a general non-linear correlation between the two for cement paste, as shown in Figure 23.6. The greatest reduction in permeability occurs for porosities reducing from about 40 to 25 per cent, where increased hydration product reduces both the pore sizes and the flow channels between them. Further hydration product, although still reducing porosity significantly, results in much lower changes in the permeability. This explains the general form of Figure 23.5, and also accounts for the effect of water/cement ratio on permeability shown in Figure 23.7 for a constant degree of hydration. At water/cement ratios above about 0.55 the capillary pores form an increasingly continuous system, with consequent large increases in permeability.

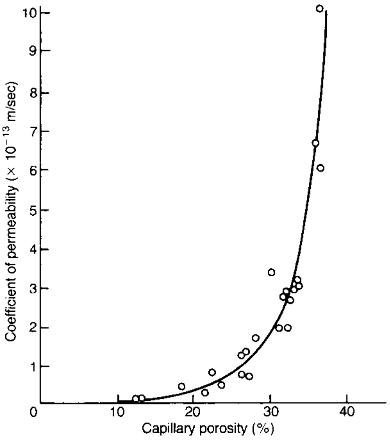

FIGURE 23.6 The relationship between permeability and capillary porosity of hardened cement paste (Powers, 1958).

It is apparent from the above arguments and from those in Chapter 13 that high strength and low permeability both result from low porosity, and in particular a reduction in the volume of the larger capillary pores. In general, higher strength

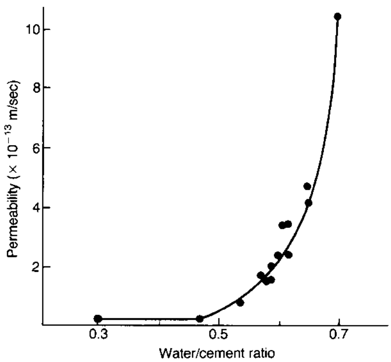

FIGURE 23.7 The relationship between the permeability and water/cement ratio of mature cement paste (93 per cent hydrated) (Powers *et al.*, 1954).

implies lower permeability, although the relationship is not linear, and may be different for different curing histories and cement types.

The permeability of the concrete will also be influenced by the permeability of the aggregate. Many of the rock types used for natural aggregates have permeabilities of the same order as that of cement paste (Table 23.1), despite having relatively low porosities. Lightweight aggregates, which are highly porous, can have much higher permeabilities. However, in practice the permeability of the composite concrete is often found to be substantially higher than that of either the aggregate or the paste, as can be seen by comparing the data for concrete shown in Figure 23.8 with those for aggregate and cement paste in Table 23.1 and Figure 23.7 respectively. This is primarily due to the presence of defects or cracks, particularly in the weaker transition zone at the cement/aggregate interface. Larger aggregates, with larger transition zones, exaggerate the effect.

As with cement paste, similar factors control both the permeability and strength of the concrete, and it is therefore possible to produce low permeability by attention to the same factors required to produce high strength. These include using a low water/cement ratio (Figure 23.8) and

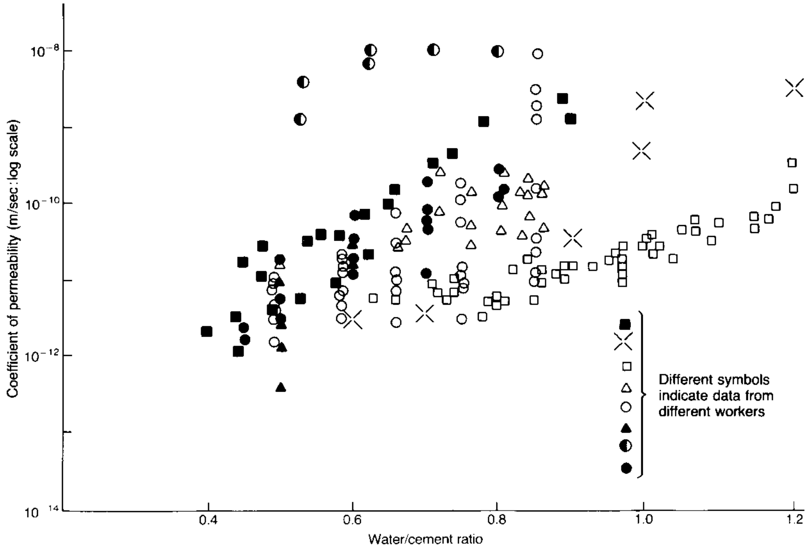

FIGURE 23.8 Comparison between test results of permeability of concrete to water (Lawrence, 1985 by permission, Concrete Society).

TABLE 23.1 Comparison between permeabilities of rocks and cement paste (Powers, 1958)

Type of rock	*Permeability (m/sec)*	*Water/cement ratio of cement paste of same permeability*
Dense trap	2.47×10^{-14}	0.38
Quartz diorite	8.24×10^{-14}	0.42
Marble	2.39×10^{-13}	0.48
Marble	5.77×10^{-12}	0.66
Granite	5.35×10^{-11}	0.70
Sandstone	1.23×10^{-10}	0.71
Granite	1.56×10^{-10}	0.71

an adequate cement content, and ensuring proper compaction and adequate curing; in addition, the properties of the transition zone may be improved by the use of cement replacement materials (see Chapter 20), although longer curing periods are necessary to ensure continuance of the pozzolanic reaction. The avoidance of microcracking from thermal or drying shrinkage strains and premature or excessive loading is also important.

23.2.2 Diffusivity

The principle of diffusivity testing is relatively simple. A high concentration of the diffusant is placed on one side of a suitable specimen (normally a disc) of hcp, mortar or concrete, and the diffusion rate calculated from the increase of concentration on the other side. In the case of gas diffusion, the high concentration side may be an atmosphere of the pure gas; in the case of salts, a high concentration aqueous solution would be used. The test is therefore similar to the permeability test without the complication of high pressure. It is generally found that, after an initial period for the diffusant to penetrate through the specimen, the concentration on the 'downstream' side increases linearly with time. The diffusivity will change if the moisture content of the concrete changes during the test, and so the specimens must be carefully conditioned before testing.

Control of test conditions is important, and diffusivity measurements from different test programmes are not entirely consistent. Table 23.2 shows values of chloride ion diffusivity that have been obtained on mature saturated pastes and concrete. The beneficial effects from lower water/cement ratio and the use of CRMs are clear.

TABLE 23.2 Chloride ion diffusivities of paste and concrete

Binder	*w/c*	*Diffusivity (m^2/sec)*
Paste (Page *et al.*, 1981)		
100%pc	0.4	2.6×10^{-12}
100%pc	0.5	4.4×10^{-12}
100%pc	0.6	12.4×10^{-12}
70%pc + 30%pfa	0.5	1.47×10^{-12}
30%pc + 70%ggbs	0.5	0.41×10^{-12}
Concrete (Buenfeld *et al.*, 1998)		
100%pc	0.4	18×10^{-12}
100%pc	0.5	60×10^{-12}
60%pc + 40%pfa	0.4	2×10^{-12}
25%pc + 75%ggbs	0.4	2×10^{-12}

23.2.3 Sorptivity

Sorptivity can be calculated from measurements of penetration depth, and tests are carried out on samples in which penetration is restricted to one direction only, such as cylinders with the curved surface sealed with a suitable bitumen or resin coating. The penetration depth at a particular time can be measured by splitting a sample open, but this requires a considerable number of samples to obtain a significant number of results. Alternatively, it can be estimated from weight gain, providing the concrete's porosity is known; this can be conveniently found by drying the specimen after the test. Such tests can only be carried out in the laboratory, either on specimens cast for this purpose, or on cores cut from structural concrete.

Values of sorptivity at various distances for the surface of a concrete slab are shown in Figure 23.9. These were obtained on slices of cores cut from concrete slabs 28 days old which had been moist cured for 4 days and then air cured for 24

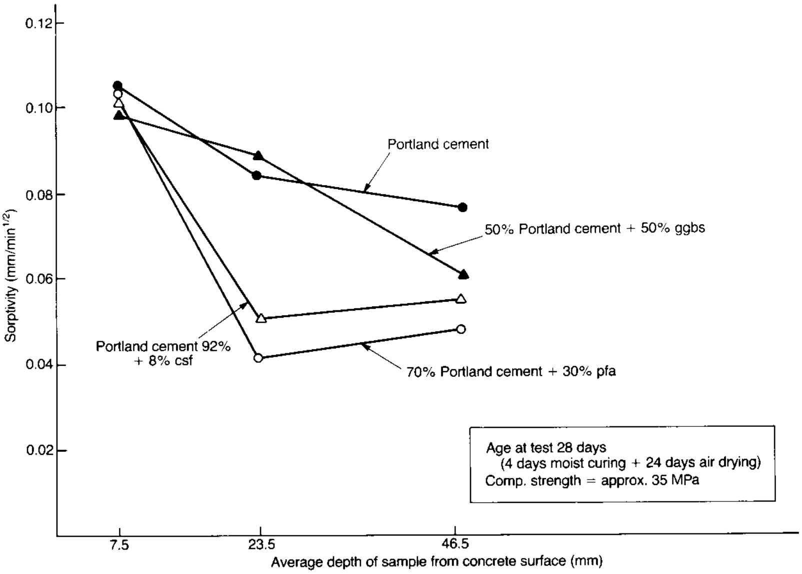

FIGURE 23.9 Variation of sorptivity with distance from cast surface of concrete made with Portland cement and cement replacement materials (Bamforth and Pocock, 1990).

days. The sorptivity decreases with depth, attributed to the air drying causing imperfect curing of the surface zone. However, although the similar strength mixes containing CRMs had similar sorptivities in the 15 mm thick surface zone, they generally had lower values than the plain Portland cement concrete at greater depth, again indicating the advantages to be gained from these materials with sufficient curing.

A number of tests have been developed to measure the absorption and permeability characteristics of in situ concrete whilst still in the structure, i.e. avoiding the need to cut cores. These all measure the penetration rate of a fluid (normally air or water) into the concrete, either through the concrete surface with the fluid contained in a chamber fixed to the concrete (Figure 23.10(a)) or outwards from a hole drilled into the concrete, with the fluid delivered via a small tube or needle inserted in the hole (Figure 23.10(b)). Depending on the fluid pressure, which varies from test to test, estimates are made of either the absorption characteristics of the surface combination of the two.

A commonly used test of this type is the Initial

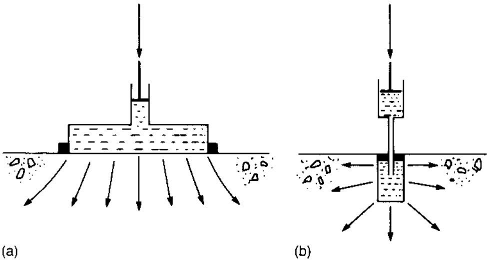

FIGURE 23.10 Techniques for surface permeability and absorption measurements on in situ concrete.

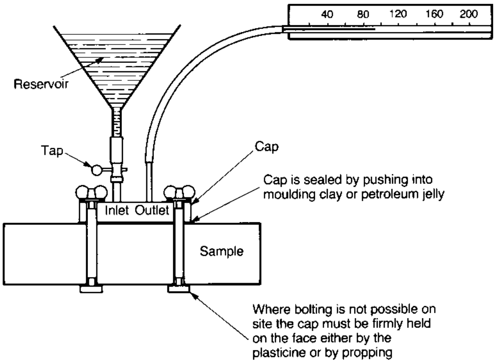

FIGURE 23.11 Initial Surface Absorption Test system (Concrete Society, 1988 by permission).

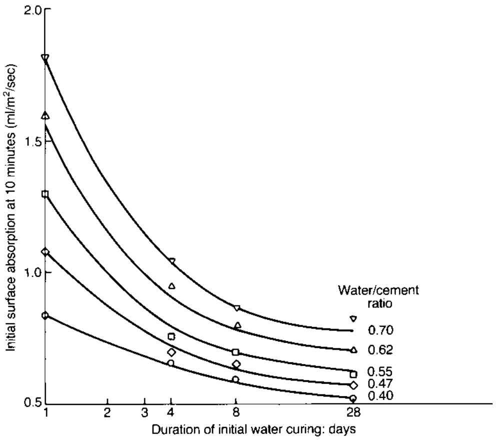

FIGURE 23.12 Effect of water/cement ratio and initial curing on surface absorption measured by the ISAT test (Dhir *et al.*, 1987 by permission, Thomas Telford Ltd).

Surface Absorption Test (ISAT), shown in Figure 23.11. A cap is clamped to the concrete surface and a reservoir of water is set up with a constant head of 200 mm. The reservoir is connected through the cap to a capillary tube set level with the water surface. At the start of the test, water is allowed to run through the cap (thus coming into contact with the concrete surface) and to fill the capillary tube. The rate of absorption is then found by closing off the reservoir and observing the rate of movement of the meniscus in the capillary tube. Readings are taken at standard times after the start of the test (typically 10 mins, 20 mins, 30 mins, 1 hour and 2 hours), and expressed as flow rate per surface area of the concrete, e.g. in units of ml/m^2/sec. The rate drops off with time, and in general increases with the sorptivity of the concrete.

Typical results showing the effect of water/cement ratio of the concrete and the duration of the initial water curing period on the 10 minute ISAT value for tests carried out on concrete 28 days old are shown in Figure 23.12. Not surprisingly, decreasing water/cement ratio and increased curing time both decrease the ISAT values; the results clearly reinforce the importance of curing.

In common with the other tests of this type, the ISAT has two main disadvantages. First, the results depend on the moisture state of the concrete at the start of the test, which is particularly difficult to control if the test is carried out in situ. Second, the flowpath of the fluid through the concrete is not unidirectional but diverges; a fundamental property of the concrete is therefore not measured, and it is difficult to compare results from different test systems.

However, the tests all measure some property of the surface layers of the concrete and, as we shall see, this is all important in ensuring good durability.

23.3 Degradation of concrete

The degradation agencies that affect concrete can be divided into two broad groups:

1. those whose action is initially chemical, before subsequently leading to loss of physical integrity, including sulfates, sea water, acids and alkali–silica reactions;
2. those which directly lead to physical effects, such as frost and fire.

Each of these is now discussed.

23.3.1 Attack by sulfates

We have seen in Chapter 13 that a controlled amount of calcium sulfate, in the form of gypsum, is added to Portland cement during its manufacture to control the setting process. Further sulfates can arise from contaminated aggregates, a particular problem in some Middle Eastern countries, or from ground-water containing sulfates from clay soils, fertilisers or industrial effluent coming into contact with concrete in foundations, retaining walls, etc. Sodium, potassium, magnesium and calcium sulfates are all common; when these are in solution they can attack the hardened cement paste. We briefly described the nature of the problem when discussing sulfate-resisting Portland cement in Chapter 13; specifically, the sulfates and the hydrated aluminate phases in the hardened cement paste react to form ettringite, according to equation (13.12), which in its full chemical notation is::

$$3CaO.Al_2O_3.12H_2O + 3CaSO_4 + 20H_2O \rightarrow 3CaO.Al_2O_3.3CaSO_4.32H_2O \qquad (23.6)$$

This is an expansive reaction, with the solid phases more than trebling in volume, causing disruption.

With sulfates other than calcium sulfate, reactions can also occur with the calcium hydroxide in the hcp, forming gypsum, again with an increase in volume, and a loss of stiffness and strength of the paste, thereby increasing the degradation. For example, the reaction with sodium sulfate is:

$$Ca(OH)_2 + Na_2SO_4.10H_2O \rightarrow CaSO_4.2H_2O + 2NaOH + 8H_2O \qquad (23.7)$$

With magnesium sulfate, a similar reaction takes place, but the magnesium hydroxide formed is relatively insoluble and poorly alkaline; this reduces the stability of the calcium silicate hydrate which is also attacked:

$$3CaO.2SiO_2.3H_2O + 3(MgSO_4.7H_2O) \rightarrow 3(CaSO_4.2H_2O) + 3(Mg(OH)_2) + 2SiO_2.aq \qquad (23.8)$$

Thus the severity of attack depends on the type of sulfate; magnesium sulfate is more damaging than sodium sulfate, which, in turn, is more damaging than calcium sulfate. In each case, attack occurs only when the amount of sulfates present exceeds a certain threshold; the rate of attack then increases with increasing sulfate, but at a reducing rate of increase above about 1 per cent concentration. Also, the rate of attack will be faster if the sulfates are replenished, for example if the concrete is exposed to flowing groundwater.

Concrete which has been attacked has a whitish appearance; damage usually starts at edges and corners, followed by progressive cracking and spalling, eventually leading to complete breakdown. Although this stage can be reached in a few months in laboratory tests, it normally takes several years in the field.

For any given concentration and type of sulfate, the rate and amount of the deterioration decreases with:

- the C_3A content of the cement, hence the low C_3A content of sulfate-resisting Portland cement;
- higher cement content and lower water/cement ratio of the concrete; higher quality concrete is less vulnerable due to its lower permeability. This is a more significant factor than the C_3A content, as shown in Figure 23.13;
- the incorporation of cement replacement materials, which can decrease the permeability, reduce the amount of free lime in the hcp, and effectively 'dilute' the C_3A.

Recommendations for suitable concrete for use in sulfate-containing environments follow from a detailed knowledge of the above factors. As an example, Table 23.3 is an extract of the requirements in the UK (BRE, 1996). Low sulfate levels do not require any special considerations over and above those for all concrete construction. With increasing sulfate levels a number of combinations of sulfate resistance of the binder and overall quality of the concrete are possible, with fewer options with high sulfate levels. In the most severe class 5, the concrete itself cannot be made sufficiently durable, and some form of surface protection or coating is also required.

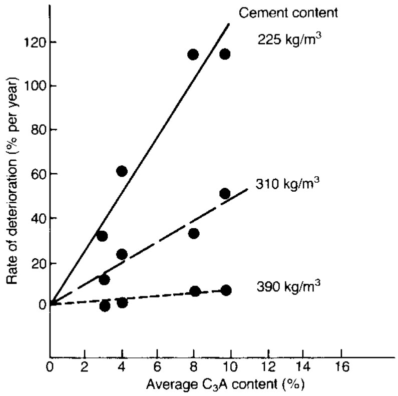

FIGURE 23.13 The effect of C_3A content of cement and cement content of concrete on deterioration in a soil containing 10 per cent Na_2SO_4 (Verbeck, 1968).

23.3.2 The thaumasite form of sulfate attack

This form of attack, known as TSA for short, also involves sulfates, but has distinct differences from the sulfate attack described above, and can have more serious consequences.

Thaumasite is a rare mineral that occurs naturally in some basic rocks and limestones. It is a compound of calcium silicate, carbonate and sulfate with the formula $CaSiO_3.CaCO_3.CaSO_4.15H_2O$. To be formed in concrete and mortar it requires:

- a source of calcium silicate, clearly available from the hydrated or unhydrated Portland cement;
- a source of sulfate ions, for example from soil or groundwater;
- a source of carbonate, usually in the aggregate or inert fillers, or less commonly from carbon dioxide dissolved in the surrounding ground water; and
- a very wet, cold (below 15°C) environment.

Clearly all of these requirements do not often occur together, the most common case where they do being in concrete made with limestone aggregate used for foundations of structures in sulfate-bearing soils in temperate or cold climates. Because the attack involves the calcium silicate

TABLE 23.3 Extract of the requirements for well-compacted concrete exposed to a permeable sulfate soil or fill (BRE, 1996, ©BRE, by permission)

	Concentration in groundwater				
Class	*SO_4 (%)*	*Mg (%)*	*Cement type*	*Minimum cement content (kg/m³)*	*Maximum water/cement ratio*
1	<0.4	–	any	275	0.65
2	0.4–1.4	–	Portland or Portland blended with moderate amounts of ggbs or pfa	330	0.50
			Sulfate-resisting	280	0.55
			Portland blended with 74–90% ggbs or 25–40% pfa	300	0.55
3	1.4–3.0	–	Sulfate-resisting	320	0.50
			Portland blended with 74–90% ggbs or 25–40% pfa	340	0.50
4	3.0–6.0	<1	Sulfate-resisting	360	0.45
			Portland blended with 74–90% ggbs or 25–40% pfa	380	0.45
		>1	Sulfate-resisting	360	0.45
5	>6.0	<1 >1	as for class 4 plus surface protection		

hydrates, it can lead to complete disintegration of the cement paste, which turns into a soft, white, mushy mass.

Incidents of attack are not widespread, the most notable involving buried concrete in house and bridge foundations in the west of England, column building supports in Canada, tunnel linings, sewage pipes and road sub-bases. The incidents in England came to light in the early 1990s and led to a major investigation. TSA has also been found in brickwork where the Portland cement render or mortar has been in contact with sulfate-bearing clay bricks in prolonged wet, cold conditions; the source of the carbonate was thought to be atmospheric carbon dioxide dissolved in surface run-off water (Thaumasite Expert Group, 1999)

Research into the mechanisms, rates and avoidance of TSA is incomplete, but the following factors are apparent:

- As with other forms of attack involving agents external to the concrete, it generally starts at the surface and works inwards at a rate depending on the composition and quality of the concrete and the curing history, all of which, as we have seen, effect the permeability and porosity.
- Although the ultimate outcome of TSA is complete loss of strength, the deterioration will be relatively slow and, even though this may be in buried foundations, visual signs of distress to a structure should become apparent long before its integrity is significantly impaired.
- The expansive disruption associated with other forms of sulfate attack may or may not accompany the formation of thaumasite.
- Thaumasite can form in pre-existing voids and cracks in the concrete along with ettringite and gypsum, or on its own, but this is not necessarily disruptive. Disruption only occurs when the thaumasite replaces some or all of the hardened cement matrix.
- TSA has occurred in concrete which has been designed to resist the other forms of sulfate attack described above. The specifications for this are therefore not sufficient for TSA avoidance.
- In assessing the risk from groundwater and soils, account should be taken of the sulfide as well as the sulfate content. Sulfides often occur as pyrite (FeS_2), which when exposed to atmospheric conditions, when the soil is disturbed during excavation and backfill, will oxidise to form more sulfates, thus increasing the risk of attack.
- An acceptable threshold level of calcium carbonate within either the coarse or fine aggregate has not been rigorously defined, but the likelihood of TSA is reduced when the $CaCO_3$ content of the total aggregate is reduced to a level between 10 per cent and 30 per cent, depending on whether this is in the fine or coarse aggregate fraction respectively.
- A safe limit for the amount of carbonate material within a cement such as Portland limestone cement is difficult to define, but it is considered that the 5 per cent addition of finely divided limestone allowed in Portland cement will not be detrimental.
- Some concrete made with sulfate-resisting Portland cement is more resistant to TSA than others, but C_3A is not involved in the reaction and the reason for this is not clear. In laboratory tests, concrete made with a blended cement of 70 per cent ggbs and 30 per cent Portland cement has given promising results.

The result of a survey of an extreme case of TSA which illustrates the distinctive features of the degradation are shown in Figure 23.14. This was on a high-quality concrete (cement content 370 kg/m^3, w/c about 0.5, estimated in situ cube strength greater than 60 MPa) in a 29-year-old buried highway bridge column, made with a mixture of dolomitic and oolitic limestone coarse aggregate and a quartz sand, and surrounded with a reworked clay with mobile ground water. As can be seen, there are four zones of increasingly severe attack, with a total depth of 25 mm, and the sulfate concentration in the surface zone was about twenty times that in the undamaged concrete. However, the TSA was not in itself the

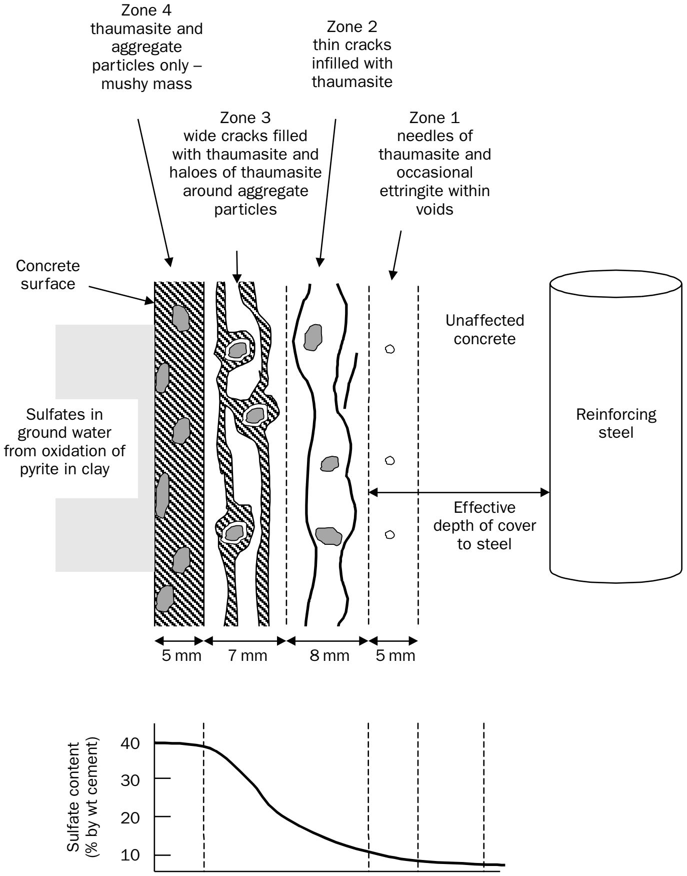

FIGURE 23.14 Typical effects of severe thaumasite attack in high-quality concrete after 29 years' exposure (Thaumasite Expert Group, 1999, HMSO. Crown copyright reproduced with the permission of the Controller of Her Majesty's Stationery Office).

greatest threat to the structural durability. Chlorides from the highway drainage system were able to penetrate the reduced cover to the reinforcing steel and initiate steel corrosion. This subject is discussed in detail later in this chapter.

Recommendations for minimising the risk of TSA are limited by the lack of complete information in some areas, as mentioned above. Those resulting from the UK investigation into TSA (Thaumasite Expert Group, 1999) are based on those for the other forms of sulfate attack discussed above, and include:

- classification of the soil and groundwater conditions in a similar way, but taking particular account of:
  - the whole ground profile to the full depth of the concrete penetration,
  - the amount of sulfides as well as sulfates,
  - the presence and mobility of groundwater;

- when carbonate-containing aggregates with a potential for contributing to TSA are used in sulfate classes 3 to 5 (see above), they are ranked according to their carbonate content, and enhanced concrete quality is required for the higher rankings. The ranking system takes account of the greater contribution of carbonates in the fine aggregate fractions.

23.3.3 Sea water attack

Concrete in sea water is exposed to a number of possible degradation processes simultaneously, including the chemical action of the sea salts, wetting and drying in the tidal zones and just above, abrasion from waves and water-borne sediment and, in some climates, freezing and thawing.

The total soluble salt content of sea water in the oceans is typically about 3.5 per cent by weight, the principal ionic contributors and their typical amounts being 2.0 per cent Cl^-, 1.1 per cent Na^+, 0.27 per cent SO_4^-, 0.12 per cent Mg^{++} and 0.05 per cent Ca^{++}. The action of the sulfates is similar to that of pure sulfate solutions described above, with the addition of some interactive effects. Importantly, the severity of the attack is not as great as for a similar concentration of sulfate acting alone and there is little accompanying expansion. This is due to the presence of chlorides; gypsum and ettringite are more soluble in a chloride solution than in pure water, and therefore tend to be leached out of the concrete by the sea water, and their formation does not, therefore, result in expansive disruption. The magnesium ions also participate in the reactions as in equation (23.8), and a feature of sea water damaged concrete is the presence of white deposits of $Mg(OH)_2$, often called *brucite*. In experiments on concrete permanently saturated with sea water, a form of calcium carbonate called *aragonite* has also been found, arising from the reaction of dissolved carbon dioxide with calcium hydroxide. The brucite and aragonite can have a pore-blocking effect, effectively reducing the permeability of the concrete near the surface (Buenfeld and Newman, 1984).

As illustrated in Figure 23.3, the transport of salts into concrete in a marine structure, or their leaching from it, may be a permeability, diffusion or absorption controlled process. In the areas subject to wetting and drying cycles, salts will crystallise as the water evaporates, which can lead to high salt concentrations and to disruption from the pressure exerted by the crystals as they rehydrate and grow during subsequent wetting/drying cycles – a process known as *salt weathering*. This can be compounded by damage from freeze–thaw cycles or wave action, depending on the environment. These areas therefore tend to be more vulnerable.

The key to elimination, or at least reduction, of all of these problems is, not surprisingly, the use of a low permeability concrete, perhaps combined with some limits on the C_3A content of the cement, or the use of cement replacement materials. However, for the reasons given above, the degradation processes in many climates do not cause rapid deterioration, which explains why concrete of even relatively modest quality has a long and distinguished history of use in marine structures, both coastal and offshore.

The salts in sea water can contribute to two other, potentially much more critical, degradation processes, namely alkali–aggregate reaction and corrosion of embedded steel. Both are discussed later.

23.3.4 Acid attack

We have seen that the hardened cement paste binder in concrete is alkaline, and therefore no Portland cement concrete can be considered acid resistant. However, it is possible to produce a concrete which is adequately durable for many common circumstances by giving attention to low permeability and good curing. In these circumstances, attack is only considered significant if the pH of the aggressive medium is less than about 6.

Examples of acids that commonly come into contact with concrete are dilute solutions of CO_2 and SO_2 in rain water in industrial regions, and CO_2 and H_2S-bearing groundwater from moorlands. The acids attack the calcium hydroxide within the cement paste, converting it, in the case of CO_2, into calcium carbonate and bicarbonate. The latter is relatively soluble, and leaches out of the concrete, destabilising it. The process is thus diffusion controlled, and progresses at a rate approximately proportional to the square root of time. The C–S–H may also be attacked, as can calcareous aggregates such as limestone. The rate of attack increases with reducing pH.

As mentioned above, the quality of the concrete is the most important factor in achieving acid resistance, but well-cured concretes containing cement replacement materials also have greater resistance due to the lower calcium hydroxide content as a result of the pozzolanic reaction. In cases where some extra acid resistance is required, such as in floors of chemical factories, the surface can be treated with diluted water glass (sodium silicate), which reacts with the calcium hydroxide forming calcium silicates, blocking the pores. In more aggressive conditions, the only option is to separate the acid and the concrete by, for example, applying a coating of epoxy resins or other suitable paint systems to the concrete.

23.3.5 Alkali–aggregate and alkali–silica reaction

We described the general nature and composition of natural aggregates in Chapter 16. Among many other constituents, they may contain silica, silicates and carbonates, which in certain mineral forms can react with the alkaline hydroxides in the pore water derived from the sodium and potassium oxides in the cement. The most common and important reaction involves active silica, and is known as *alkali–silica reaction* (ASR). The product is a gel which can destroy the bond between the aggregate and the hardened cement paste, and which absorbs water and swells to a sufficient extent to cause cracking and disruption of the concrete.

For the reaction to occur, both active silica and alkalis must be present. In its reactive form, silica occurs as the minerals opal, chalcedony, crystobalite and tridymite and as volcanic glasses. These can be found in some flints, limestones, cherts and tuffs. The sources of such aggregates include parts of the USA, Canada, South Africa, Scandinavia, Iceland, Australia, New Zealand and the midlands and south west of England. Only a small proportion of reactive material in the aggregate (as low as 0.5 per cent) may be necessary to cause disruption to the concrete.

In unhydrated cement, sodium and potassium oxides (Na_2O and K_2O) are present in small but significant quantities (see Table 13.1), either as soluble sulphates (Na_2SO_4 and K_2SO_4) or a mixed salt $(Na, K)_2SO_4$. There is also a small amount of free CaO, which is subsequently supplemented by $Ca(OH)_2$ from the hydration reactions of C_3S and C_2S. During hydration, these sulfates take part in a reaction with the aluminate phases in a similar way to gypsum (see Section 13.1.3), the product again being ettringite with sodium, potassium and hydroxyl ions going into solution:

$$\begin{gathered}(\mathrm{Na, K})_2\mathrm{SO_4} + 3\mathrm{CaO.Al_2O_3} + \mathrm{Ca(OH)_2} \rightarrow \\ (\mathrm{C_3A}) \\ 3\mathrm{CaO.Al_2O_3.3CaSO_4.32H_2O} + \\ (\text{ettringite}) \\ \mathrm{Na^+, K^+, OH^-} \qquad (23.9) \\ (\text{in solution})\end{gathered}$$

The resulting pH of the pore water is 13–14, higher than that of saturated calcium hydroxide solution alone. Alkalis may also be contributed by some admixtures, by pfa and ggbs and by external sources such as aggregate impurities, sea water or road de-icing salts.

The reactions between the reactive silica and the alkalis which forms the alkali–silicate gel occur first at the aggregate/cement paste interface. They require the presence of water, and, it is believed, Ca^{++} ions. The nature of the gel is complex, but it is clear that it is a mixture of sodium, potassium and calcium silicates. It is soft, but imbibes a large quantity of water by osmosis and swells considerably. The hydraulic pressure that is developed leads to overall expansion of the concrete and can be sufficient to cause cracking of the aggregate particles, the hcp and the transition zone between the two.

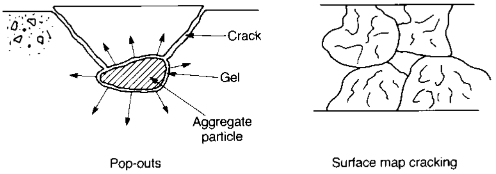

FIGURE 23.15 Typical cracking patterns resulting from alkali–silica reaction.

Continued availability of water causes enlargement and extension of the cracks which eventually reach the outer surface of the concrete, forming either pop-outs if the affected aggregate is close to the surface, or more extensive crazing, or map cracking, on the concrete surface, as illustrated in Figure 23.15. These surface cracks are often highlighted by staining from the soft gel oozing out of the cracks. In general, the cracking adversely affects the appearance and serviceability of structure before reducing its load-carrying capacity.

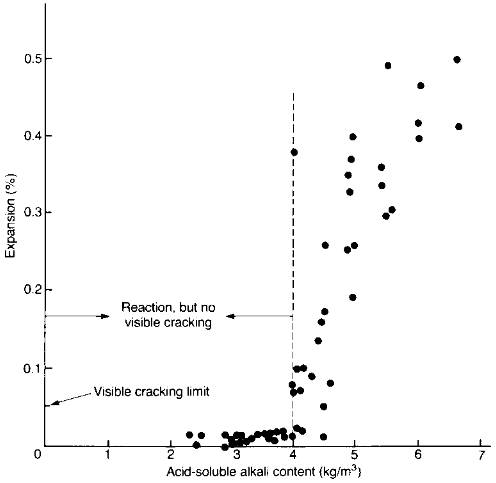

FIGURE 23.16 Effect of acid-soluble alkali content of concrete on expansion and cracking after 200 days from alkali–silica reactions (tests at critical silica/alkali ratio) (Hobbs, 1986 by permission, Thomas Telford Ltd).

The whole process is often very slow, and the cracking can take years to develop in structural concrete. A description was first published in the USA in 1940 (Stanton) since when numerous examples have been reported in many countries. Over 100 cases were identified in the UK between 1976 and 1987, triggering much research aimed at understanding and quantifying the mechanisms involved, determining its effect on structural performance and providing guidance for minimising the risk in new concrete. The latter can be considered successful as there have been no new confirmed cases of ASR in the UK since 1987.

Even though laboratory tests have sometimes not satisfactorily explained all field observations, the most important factors influencing the amount and rate of reaction can be summarised as follows:

- The amount of alkalis available, which is normally expressed as the total weight of sodium oxide equivalent = $Na_2O + 0.65\ K_2O$. The reaction rate and amount increase with increasing alkali level, but test data such as those shown in Figure 23.16 indicate that there is a threshold level below which no disruption will occur, due to the lowering of the pH of the pore water, even with reactive aggregates. This level is typically about 3.5–4 kg/m^3 of concrete, which corresponds to a lower limit of about 0.6 per cent by weight of cement. Cements with a sodium oxide equivalent of less than this are called low-alkali cements.
- The presence of cement replacement materials, which reduce the rate of reaction through two main mechanisms:
  - They remove $Ca(OH)_2$ (see Chapter 15), and hence reduce the amount of Ca^{++} ions in the pore water which are necessary for the reaction to take place.
  - They reduce the permeability of the concrete and therefore reduce the mobility of the aggressive agents, i.e. the same general effect as on other degradation processes.
- The amount of reactive silica. Typical effects from tests on mortars are shown in Figure

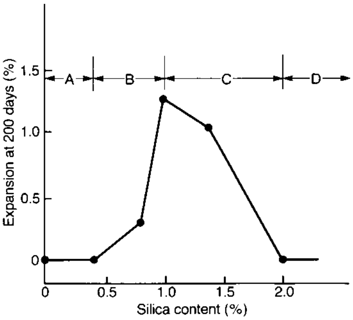

FIGURE 23.17 Effect of active silica content on expansion of mortars due to alkali–silica reaction (opaline silica, w/c = 0.53, A/c = 3.75, $Na_2O = 4.4 kg/m^3$) (Hobbs, 1988).

23.17. The expansion increases with active silica content, but only up to a certain content, beyond which the expansion reduces. There is thus a pessimum content of silica for maximum expansion, in this case about 1 per cent, but which is higher for lower water/cement ratios and higher cement contents. The following explanation for the behaviour in the four regions shown in Figure 23.17 has been proposed (Hobbs, 1988):

- Region A: the reactive silica content is low and gel growth after the concrete has hardened is insufficient to cause cracking.
- Region B: the reaction after the concrete has hardened is sufficient to cause cracking. There is an excess of alkalis, and the reaction continues until all the active silica has been used up.
- Region C: there is an excess of silica over alkalis, and the reaction continues until all the alkalis have been used up or their concentration falls below the threshold level. The uptake of water by the reaction product decreases with decreasing alkali/reactive silica ratio.
- Region D: the reactive silica content is so high and the reaction is so rapid that by the time the concrete has hardened the rate of gel growth is too slow to induce cracking.

At the pessimum point the amount of reactive silica is just sufficient to react with all the alkalis present; the reactive silica/alkali ratio usually lies in the range 3.5 to 5.5.

- The aggregate particle size, which affects the amount of reactive silica exposed to the alkali; fine particles (20 to 30 μm) can lead to expansion within a few weeks, larger ones only after many years.
- The availability of moisture. The gel swelling will cease if the relative humidity within the concrete, which depends on the environment and the concrete permeability, falls below about 85 per cent. Alternative wetting and drying may be the most harmful, possibly because it can lead to local high concentrations of the reacting materials.
- The ambient temperature. Higher temperatures accelerate the reaction, at least up to 40°C.

Once started, the only effective way of stopping ASR is by eliminating water, which is clearly impractical in many structural situations. It follows that it is important to reduce or eliminate the risk of ASR occurring by careful materials selection and concrete mix design. Consideration of the factors influencing the occurrence and rate of ASR described above leads to the following possibilities:

- Avoiding the use of reactive aggregates. This is more difficult than it sounds, particularly with mixed mineral aggregates. There is no universally agreed test for aggregate reactivity, and recent guidance notes (Concrete Society, 1999) suggest classifying the aggregate as either low, normal or high reactivity depending on its composition.
- Limiting the amount of alkalis in the cement, for example by using a low-alkali cement, i.e. with alkali content of less than 0.6 per cent by weight, as discussed above.
- Combining the Portland cement with a cement replacement material, which can be of benefit in three ways:
  - although pfa and ggbs themselves contain alkalis, the extent to which these contribute

to the total alkalinity of the pore water appears to be small when they are combined with a high alkalinity Portland cement, and only a proportion of their alkali content needs be taken into account (figures of 17% pfa and 50% for ggbs have been suggested) and therefore the alkali content of the binder may be reduced;
  - they reduce the permeability of the concrete, thus reducing the rates or reaction;
  - they contain divided reactive silica, and therefore, if added in adequate quantities will increase the total reactive content to well above the pessimum value, e.g. into region D of Figure 23.17, thereby reducing or eliminating expansion. However, sufficient quantities must be added to ensure that the pessimum level is exceeded by a wide margin, and minimum replacement levels of 30–40 per cent pfa, 20 per cent microsilica and 50–65 per cent ggbs have been suggested.

  However, the exact mechanisms and quantitative nature of the role of cement replacement materials are complex and unclear, and are the subject of continuing research.
- Limiting the total alkali content of the concrete. Alkalis from all sources – cement, CRMs (but taking account of the reduction factors discussed above), de-icing salts, etc. should total less than 3.0 kg/m^3 of concrete.
- Ensuring that the concrete remains dry throughout its life – obviously difficult or impossible in many structures.

Much more detailed guidance has recently been published (Concrete Society, 1999).

23.3.6 Frost attack – freeze–thaw damage

In cold climates, frost attack is a major cause of damage to concrete unless adequate precautions are taken. We discussed this briefly when considering air-entraining agents in Chapter 14. When free water in the larger pores freezes, it expands by about 9 per cent and, if there is insufficient space within the concrete to accommodate this, then potentially disruptive internal pressures will result. Successive cycles of freezing and thawing can cause progressive and cumulative damage, which takes the form of cracking and spalling, initially of the concrete surface.

It is the water in the larger capillary pores and entrapped air voids that has the critical effect; the water in the much smaller gel pores (see Chapter 13) is adsorbed on to the C–S–H surfaces, and does not freeze until the temperature falls to about −78°C. However, after the capillary water has frozen it has a lower thermodynamic energy than the still-liquid gel water, which therefore tends to migrate to supplement the capillary water, thus increasing the disruption. The disruptive pressure is also enhanced by osmotic pressure. The water in the pores is not pure, but is a solution of calcium hydroxide and other alkalis, and perhaps chlorides from road de-icing salts or sea water; pure water separates out on freezing, leading to salt concentration gradients and osmotic pressures which increase the diffusion of water to the freezing front.

The magnitude of the disruptive pressure depends on the capillary porosity, the degree of saturation of the concrete (dry concrete will clearly be unaffected) and the pressure relief provided by a nearby free surface or escape boundary. The extent of this pressure relief will depend on:

1. the permeability of the material;
2. the rate at which ice is formed; and
3. the distance from the point of ice formation to the escape boundary. In saturated cement paste, the disruptive pressures will only be relieved if the point of ice formation is within about 0.1 mm of an escape boundary. A convenient way of achieving this is by use of an air-entraining agent (see Chapter 14), which entrains air in the form of small discrete bubbles and an average spacing of about 0.2 mm is required.

As we saw in Chapter 13, the capillary porosity of a cement paste or concrete, and hence its susceptibility to frost attack, can be reduced by low-

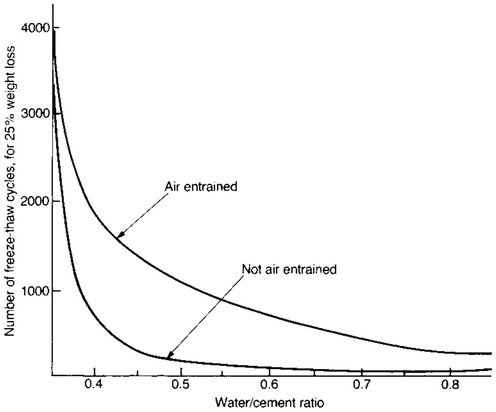

FIGURE 23.18 The effect of air entrainment and water/cement ratio on the frost resistance of concrete moist-cured for 28 days (US Bureau of Reclamation, 1955).

ering the water/cement ratio and ensuring that by proper curing the hydration is as complete as possible. Bleeding, which results in local high porosity zones, should also be minimised. The combined effects of air entrainment and water/cement ratio are illustrated in Figure 23.18.

Certain aggregates are themselves susceptible to frost action, and their use must be avoided if a durable concrete is to be achieved. The first sign of damage caused by aggregate disruption is normally pop-outs on the concrete surface. Vulnerable aggregates include some limestones and porous sandstones; these generally have high water absorption, but other rocks with high absorption are not vulnerable. Similar arguments of pore size and distribution for cement paste apply to the aggregates; for example, it has been found that pores of about 4 to 5 µm are critical, since these are large enough to permit water to enter but not large enough to allow dissipation of disruptive pressure. Aggregate size is also a factor, with smaller particles causing less disruption, presumably because the average distance to an escape boundary on the aggregate surface is less. The only satisfactory way of assessing an aggregate is by its performance when incorporated in concrete, using field experience or laboratory testing.

23.3.7 Fire resistance

Concrete is incombustible and does not emit any toxic fumes when exposed to high temperatures. It is thus a favoured material, both in its own right and as protection for steelwork, when structural safety is being considered. However, although it can retain some strength for a reasonable time at high temperatures, it will eventually degrade. The rate and amount of degradation depends on the maximum temperature, the period of exposure, the induced temperature gradients, the concrete constituents and moisture content and the size of the element, and will therefore vary considerably.

Figure 23.19 shows typical results of testing small elements by holding them at elevated temperatures for a reasonable period of time. For temperatures up to about 500°C the strength reduction is relatively gradual, but thereafter the decline is more rapid, giving almost total loss approaching 1000°C. There are three main contributions to the degradation:

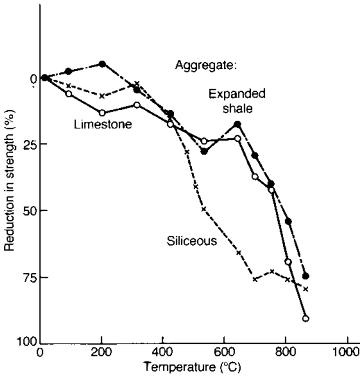

FIGURE 23.19 The effect of temperature and aggregate type on the compressive strength of concrete heated and tested hot (average initial strength = 28 MPa) (Abrams, 1971).

1. Evaporation of water within the concrete, which starts at 100°C, and continues with progressively more tightly held water being driven off. If the concrete is initially saturated and also of low permeability, then the steam cannot disperse quickly, and build-up of pressure can lead to cracking and spalling. This is therefore a particular problem with high-strength, low-porosity concrete. Even though the total volume of water in the concrete is low, the induced pressures are very high, and progressive explosive spalling of the surface layers can occur within a few minutes of exposure to the fire. The inclusion of polypropylene fibres in the mix is one way of overcoming this effect; these rapidly melt and provide pressure relief channels.
2. Differential expansion between the hcp and aggregate, resulting in thermal stresses and cracking, initiated in the transition zone. This is mainly responsible for the more rapid loss of strength above about 500°C, and also explains the superior performance of the limestone and lightweight aggregate concrete; the former has a coefficient of thermal expansion closer to that of the hcp (see Section 15.3) and the latter is less stiff and hence the thermal stresses are lower. Lightweight aggregates have the additional advantage of decreasing the thermal conductivity of the concrete, thus delaying the temperature rise in the interior of a structural member.
3. Breakdown of the hydrates in the hcp, which is not complete until the temperature approaches 1000°C, but results in a total loss of strength at this point.

23.4 Durability of steel in concrete

Nearly all structural concrete contains steel, either in the form of reinforcement to compensate primarily for the low tensile and shear strength of the concrete, or as stressed pretensioned tendons which induce stresses in the concrete to oppose those due to the subsequent loading. Sound concrete provides an excellent protective medium for the steel, but this protection can be broken down in some circumstances, leaving the steel vulnerable to corrosion. Crucially, the corrosion products – rust in various forms – occupy a considerably greater volume than the original steel. Rusting in the concrete can therefore cause cracking and spalling of the concrete covering the steel, leading to more rapid corrosion of the exposed steel and eventual loss of structural integrity.

Although the processes involved are less complex than those of the various degradation mechanisms of the concrete itself, described above, they are much more difficult to avoid and control. Corrosion of steel in concrete is the greatest threat to the durability and integrity of concrete structures in many countries. In the last few decades the concrete repair industry has benefited considerably and is thriving.

In this section we shall first describe the general nature of the phenomenon, and then consider the factors that control its onset and subsequent rate.

23.4.1 General principles of the corrosion of the steel in concrete

The electrochemical nature of the corrosion of steel was described in Chapter 11, but it is worth summarising the main reactions here:

at the anode: $$\mathrm{Fe} \rightarrow \mathrm{Fe}^{++} + 2\mathrm{e} \tag{23.10}$$

electron conductance:
$$2\mathrm{e}\ (\text{anode}) \rightarrow 2\mathrm{e}\ (\text{cathode}) \tag{23.11}$$

at the cathode:
$$4\mathrm{e} + \mathrm{O}_2 + 2\mathrm{H}_2\mathrm{O} \rightarrow 4\mathrm{OH}^- \tag{23.12}$$

near the surface:
$$\mathrm{Fe}^{++} + 2\mathrm{OH}^- \rightarrow \mathrm{Fe(OH)}_2 \quad \text{ferrous hydroxide, black rust} \tag{23.13}$$

followed by:
$$4\mathrm{Fe(OH)}_2 + \mathrm{O}_2 \rightarrow 2\mathrm{Fe}_2\mathrm{O}_3.\mathrm{H}_2\mathrm{O} + \mathrm{H}_2\mathrm{O} \quad \text{ferric hydroxide, red rust} \tag{23.14}$$

For iron or steel rusting in oxygenated water or moist air, the water on or near the metal surface acts as the electrolyte of the corrosion cell, and the anode and cathode are close together, e.g.

across a single crystal or grain. The oxide is formed and deposited near but not directly on the metal surface, as illustrated in Figure 23.20, allowing the corrosion to be continuous. In concrete, different conditions prevail. The electrolyte is the pore water in contact with the steel, and, as we have seen, this is normally highly alkaline (pH = 12.5–13) due to the $Ca(OH)_2$ from the cement hydration and the small amounts of Na_2O and K_2O in the cement. In such a solution, the primary anodic product is not Fe^{++} as in reaction (23.10) but is Fe_3O_4, which is deposited at the metal surface as a tightly adherent thin film, and stifles any further corrosion. The steel is said to be passive, and thus sound concrete provides an excellent protective medium. However, the passivity can be destroyed by either:

1. a loss of alkalinity by carbonation of the concrete, in which the calcium hydroxide is neutralised by carbon dioxide from the air, producing calcium carbonate; or
2. chloride ions, e.g. from road de-icing salts or sea water.

Either of these can therefore create conditions for the corrosion reactions (23.10) to (23.13) or (23.14) to occur. The corrosion can be localised, for example in load-induced cracks in the concrete, leading to pitting, or the corrosion cells can be quite large, for example if anodic areas have been created by penetration of chlorides into a locally poorly compacted area of concrete. However, it is important to remember that oxygen and water must still be available at the cathode to ensure reaction (23.12) continues.

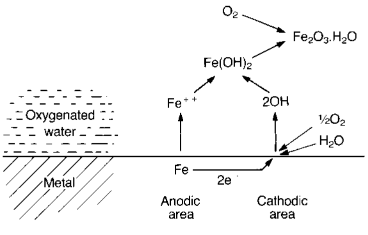

FIGURE 23.20 Spacial arrangement of corrosion reactions of iron in moist air or oxygenated water.

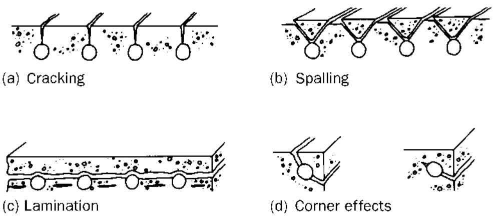
(a) Cracking (b) Spalling (c) Lamination (d) Corner effects

FIGURE 23.21 Different forms of damage from steel corrosion (Browne, 1985).

As mentioned above, the corrosion products (ferric and ferrous hydroxide) have a much larger volume than the original steel, by about two to three times, and hence lead to bursting pressures in the concrete and, eventually, cracking. This damage can take various forms, as illustrated in Figure 23.21. The steel is then completely exposed, and the corrosion can be very fast and destructive.

Since the carbon dioxide or chlorides will normally have to penetrate the concrete cover before the corrosion can be initiated, the total time to concrete cracking will consist of two stages, illustrated in Figure 23.22:

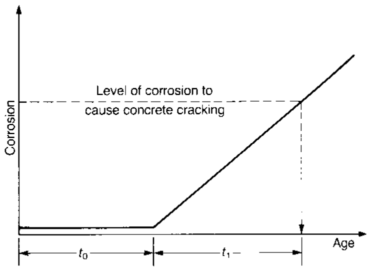

FIGURE 23.22 The two stages of corrosion damage: t_0 = time to initiation of corrosion, t_1 = time for sufficient corrosion to crack the concrete cover (Browne, 1983).

1. the time (t_0) for the depassivating agents (the carbon dioxide or chlorides) to reach the steel and initiate the corrosion;
2. the time (t_1) for the corrosion to then reach critical levels, i.e. sufficient to crack the concrete, which depends on the subsequent corrosion rate.

The processes of carbonation-induced corrosion and chloride-induced corrosion are now considered separately.

23.4.2 Carbonation-induced corrosion

We discussed carbonation and its associated shrinkage in Chapter 19. Atmospheric carbon dioxide, when dissolved in the pore water in concrete, reacts rapidly with the calcium hydroxide produced during the cement hydration, forming calcium carbonate, and reducing the pH from 12 or more to about 8. There are also some reactions between the carbon dioxide and the other hydrates, but these are not significant in this context.

The carbonation reaction occurs first at the surface of the concrete and then progresses inwards, further supplies of carbon dioxide diffusing through the carbonated layer. Extensive analysis by Richardson (1988) showed that the carbonation depth (x) and time (t) are related by the simple expression

$$x = k.t^{0.5} \tag{23.15}$$

where k is a constant closely related to the diffusion characteristics of the concrete. The form of this equation is the same as that of equation (23.4), which indicates that carbonation may be considered as a sorption process. The value of k depends on several factors, chiefly:

1. The degree of saturation of the concrete. It is necessary for the carbon dioxide to be dissolved in the pore water, and so concrete which has been dried by storing at low relative humidities will not carbonate. At the other extreme, the diffusion will be slow in concrete completely saturated with water, and so the fastest advance of the carbonation front occurs in partially saturated concrete at relative humidities of between 50 and 70 per cent. Thus concrete surfaces which are sheltered will carbonate faster than those exposed to direct rainfall.
2. The pore structure of the concrete. Parrott (1987) suggested that relating carbonation depth to concrete strength, as in Figure 23.23, is a useful way of combining the effects of water/cement ratio, cement content and incorporation of cement replacement materials. Adequate curing at early ages is also an important factor. Although cement replacement materials can result in lower overall porosity with full curing, the pozzolanic reaction can also reduce the calcium hydroxide content before carbonation, and so they do not necessarily have the same benefits as they do with other degradation processes.
3. The carbon dioxide content of the environment.

Observed rates of carbonation, such as those shown in Figure 23.23, are such that with high quality, well-cured concrete the carbonated region, even after many years' exposure to normal atmospheric conditions, is restricted to within 20 to 30 mm of the concrete surface. It is

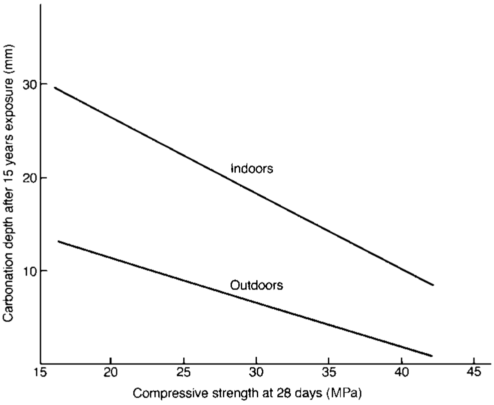

FIGURE 23.23 The relationship between carbonation depth and concrete strength (Nagataki *et al.*, 1986).

difficult to estimate or predict the rate of corrosion once the steel has been depassivated, and therefore design recommendations are aimed at ensuring that the depth and quality of concrete cover are sufficient to achieve a sufficiently long initiation period, t_0. It should also be noted that carbonation is not entirely detrimental. The calcium carbonate formed occupies a greater volume that the calcium hydroxide, and so the porosity of the carbonated zone is reduced, increasing the surface hardness and strength, and reducing the surface permeability.

23.4.3 Chloride-induced corrosion

There are four common sources of the chlorides:

1. calcium chloride, a cheap and effective accelerator (see Chapter 14);
2. contamination in aggregates;
3. sea water, for coastal or marine structures; and
4. road de-icing salts, a particular problem on bridge decks.

Calcium chloride, or any chloride-containing admixture, is normally no longer permitted in concrete containing steel, but it is generally accepted that small amounts of chlorides from any of the other sources can be tolerated and that a threshold level is required to depassivate the steel allowing the corrosion to start. There are, however, differences of opinion about the magnitudes involved, including the following (Glass and Buenfeld, 1997):

- some of the chlorides react with the aluminate phases in the cement forming chloroaluminates, and therefore are no longer free chloride ions. It was thought that these bound chlorides are not harmful, but this is no longer believed to be true;
- corrosion has occurred at a very wide range of total chloride contents, and it may be better to think of the chloride content as giving a risk of corrosion, rather than there being an absolute threshold value below which no corrosion can ever occur.

Despite this, many recommendations include a threshold limit, with a value of 0.4. per cent chloride ion by weight of cement being typical.

If the chlorides are included in the concrete on mixing, then the steel may never be passivated, and the initiation period, t_0, will be zero. Chlorides from the external sources, sea water or de-icing salts have to penetrate the concrete cover in sufficient quantities, however defined, to depassivate the steel before the corrosion is initiated: t_0 is finite in these circumstances. The transport mechanisms may be governed by the permeability in the case of, say, concrete permanently submerged in sea water; diffusivity, where salts are deposited onto saturated concrete; or sorptivity, where salts are deposited onto partially saturated concrete. The corrosion risk in situations in which the salts are water-borne and deposited onto the surface by evaporation, such as in the splash zone of marine structures or on run-off from bridge decks, is particularly high as the reservoir of salts is constantly replenished. An absorption mechanism may dominate in the early stages of such contamination, with diffusion being more important at later stages (Bamforth and Pocock, 1990).

These processes result in chloride profiles such as those shown in Figure 23.24(a). A large number of such profiles showing the effect of a large number of variables have been generated both experimentally and analytically, and these have been used to formulate design recommendations to ensure that the concrete properties and cover to the reinforcing is sufficient to keep the chloride content at the steel to acceptable levels for the required design life. Their form and magnitude depend on time of exposure, the exposure conditions and the concrete properties; clearly the properties in the cover zone are critical. Lower sorptivities and diffusivities, and hence increased values of t_0, are associated with lower water/cement ratios, higher cement contents and efficient curing. The use of CRMs can also reduce the chloride penetration significantly, as shown in Figure 23.24(b) for concrete containing pfa.

Although many recommendations for concrete cover and quality are aimed at extending the period t_0 as far as possible, there are circumstances in which it is impossible to prevent

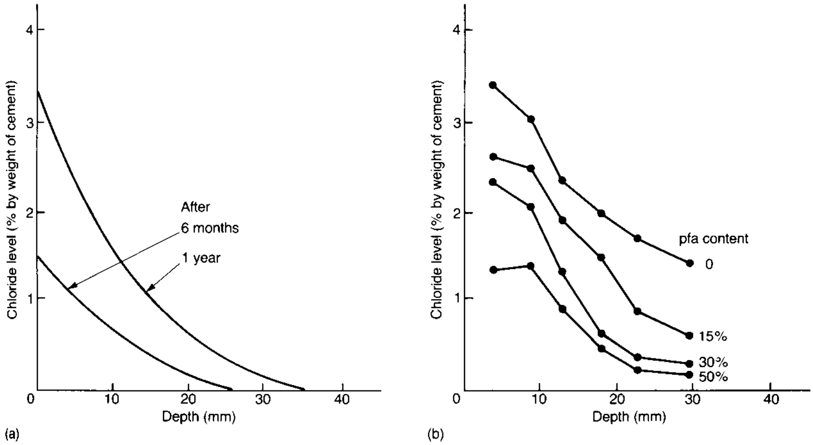

FIGURE 23.24 Chloride concentration profiles in concrete after marine exposure in tidal/splash zone: (a) the effect of exposure period (Portland cement concrete, moist-cured for 3 days, exposed from 28 days) (Bamforth and Pocock, 1990); (b) the effect of pfa (moist-cured for 1 day, exposed from 28 days for 2 years) (Thomas *et al.*, 1990).

corrosion being initiated. Much research has therefore been carried out to determine the factors which control the rate of corrosion. These have been found to include the following.

1. The spacing and relative size of the anode and cathode in the corrosion cell. Relatively porous areas of a concrete member, such as a poorly compacted underside of a beam, will allow rapid penetration of chlorides, depassivating a small area of steel to form the anode. The reinforcement throughout the structure is normally electrically continuous, and so the remainder forms a large area cathode, resulting in a concentration of corrosion current, and hence a high corrosion rate, at the anode.
2. The availability of oxygen and moisture, particularly to sustain the cathodic reaction. If the supply of either is reduced, then the corrosion rate is reduced. Hence little corrosion occurs in completely dry concrete, and only very low rates in completely and permanently saturated concrete, through which diffusion of oxygen is difficult.
3. The electrical resistivity of the electrolyte of the corrosion cell, i.e. the concrete. High resistivities reduce the corrosion current and hence the rate of corrosion, but increasing moisture content, chloride content and porosity all reduce the resistivity.

Much analysis of the extensive and increasing amount of data on this subject is aimed at producing guidelines to ensure adequate durability (see below). There are, however, circumstances in which protection against corrosion cannot be guaranteed by selection of the materials and proportions of the concrete, depth of cover and attention to sound construction practice. These include, for example, marine exposure in extreme climatic conditions, and regions in which aggregates containing excess chlorides must be used. One or more of the following extra protective measures may then be taken:

1. the addition of a corrosion inhibiting admixture such as calcium nitrite to the fresh concrete;
2. the use of corrosion-resistant stainless steel reinforcement bars, or epoxy-coated conventional bars;

3. applying a protective coating to the concrete, to reduce chloride and/or oxygen ingress;
4. cathodic protection of the reinforcement, i.e. applying a voltage from an external source sufficient to ensure that all of the steel remains permanently cathodic (see Section 11.4.3).

23.5 Recommendations for durable concrete construction

We have already discussed some of the measures that can be taken to avoid degradation from the specific problems of sulfates, acids, alkali–silica reaction and fire. A further example is the approach adopted in the UK for the action of other environmental conditions. This combines them into a single set of exposure conditions with corresponding requirements for concrete quality and cover to embedded steel, which is useful and convenient (BS 8110: 1997). The exposure conditions are given in Table 23.4, and the combination of concrete quality and cover in Figure 23.25. The engineer has some flexibility of choice of combination in each exposure condition. As

TABLE 23.4 Exposure conditions for concrete (BS 8110: 1997)

Exposure condition	*Environment of concrete surface*
Mild	Protected against weather or aggressive conditions
Moderate	Sheltered from severe rain or freezing whilst wet Subject to condensation Continuously under water In contact with non-aggressive soils
Severe	Exposed to severe rain, alternate wetting and drying or occasional freezing or severe condensation
Very severe	Occasionally exposed to sea-water spray, de-icing salts, corrosive fumes or severe freezing whilst wet
Most severe	Frequently exposed to sea-water spray or de-icing salts in sea-water tidal zone down to 1 m below lowest low water
Abrasive	Exposed to abrasive action, e.g. machinery, metal-tyred vehicles or water carrying solids

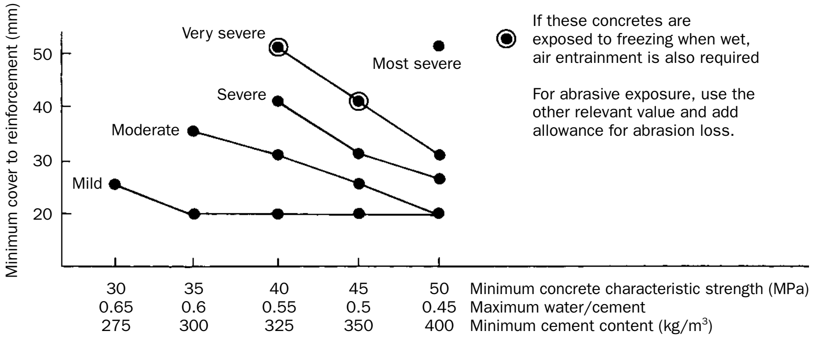

FIGURE 23.25 Requirements for concrete quality and cover to steel for the exposure conditions in Table 23.4 (BS 8110: 1997).

we mentioned in Chapter 21, the concrete quality requirements may form a limiting value for the concrete mix design.

As in other areas of construction technology and practice, there has been extensive recent work to produce combined European recommendations for durable concrete. These need interpretation for the requirements of individual countries, and a look at Hobbs (1998) will give an idea of the resulting extent and complexities of the subject.

23.6 References

Abrams, M.S. (1971) Temperature and concrete. *Amer. Conc. Inst. Special Publication* 25, pp. 33–58.

Bamforth, P.B. (1987) The relationship between permeability coefficients for concrete obtained using liquid and gas. *Magazine of Concrete Research*, 39, 138, March, 3–11.

Bamforth, P.B. and Pocock, D.C. (1990) *Proceedings of Third International Symposium on Corrosion of Reinforcement in Concrete Construction,* Elsevier Applied Science, pp. 119–31.

Browne, R.D. (1983) *Proceedings of the Symposium on Durable Concrete,* Institute of Concrete Technology, London.

Browne, R.D. (1985) *Proceedings of Seminar on Improvements in Concrete Durability,* Institute of Civil Engineers, London, pp. 97–130.

Buenfeld, N. and Okundi, E. (1998) Effect of cement content of transport in concrete. *Mag. of Conc. Res.* 50, 4, Dec. 339–51.

Buenfeld, N. and Newman, J.B. (1984) The permeability of concrete in a marine environment. *Magazine of Concrete Research* 36, 127, June, 67–80.

Building Research Establishment (1996) Sulfate and acid resistance of concrete in the ground. *Digest* 363, BRE, Garston, UK.

Concrete Society (1999) Alkali–silica reaction: minimising the risk of damage to concrete. *Technical Report* No. 30, 3rd edn, Slough, p. 72.

Concrete Society (1988) Permeability testing of site concrete. *Technical Report* No. 31, London.

Dhir, R.K., Hewlett, P.C. and Chan, Y.N. (1987) Near-surface characteristics of concrete: assessment and development of in-site test methods. *Magazine of Concrete Research* 39, No. 141, Dec., 183–95.

Glass, G.K. and Buenfeld, N.R. (1997) The presentation of the chloride threshold level for corrosion of steel in concrete. *Corrosion Science* 39, 5, May 1001–17

Hobbs, D.W. (1986) Deleterious expansion of concrete due to alkali–silica reaction: influence of PFA and slag. *Magazine of Concrete Research* 38, 137, Dec. 191–205.

Hobbs, D.W. (1988) *Alkali–Silica Reaction in Concrete,* Thomas Telford, London, p. 183.

Lawrence, C.D. (1985) Concrete Society Materials Research Seminar on Serviceability of Concrete Slough, July, published in *Concrete Society* (1988) above.

Nagataki, S., Ohga, H. and Kim, E.K. (1986) Proceedings of the 2nd International Conference on Fly Ash, Silica Fume, Slag and Natural Pozzolans in Concrete. *Amer. Conc. Inst. Special Publication* SP-91, 521–40.

Page, C.L., Short, N.R. and El Tarras, A. (1981) *Cement and Concrete Research* 11, 3, 395–406.

Parrott, L.J. (1987) *A Review of Carbonation in Reinforced Concrete,* Cement and Concrete Association, Slough.

Powers, T.C. (1958) Structure and physical properties of Portland cement paste. *Journ. Amer. Ceramic Soc.* 41, Jan., 1–6.

Powers, T.C., Copeland, L.E., Hayes, J.C. and Mann, H.M. (1954) Permeability of Portland cement paste. *Journ. Amer. Conc. Inst.* 51, November, 285–98.

Richardson, M.G. (1988) *Carbonation of Reinforced Concrete: Its Causes and Management,* CITIS Ltd, Dublin.

Rose, D.A. (1965) *RILEM Bulletin,* No. 29.

Stanton, T.E. (1940) The expansion of concrete through reaction between cement and aggregate. *Proc. Am. Soc. Civ. Engrs.* 66, 1781–811.

Thomas, M.D.A., Matthews, J.D. and Haynes, C.A. (1990) *Proceedings of Third International Symposium on Corrosion of Reinforcement in Concrete Construction,* Elsevier Applied Science, pp. 198–212.

Thaumasite Expert Group (1999) *The Thaumasite Form of Sulfate Attack: Risks, Diagnosis, Remedial Works and Guidance on New Construction*, Dept. of Environment, Transport and Regions, London, p. 180.

US Bureau of Reclamation (1955) *Concrete Laboratory Report* No. C-810, Denver, Colorado.

Verbeck, G.J. (1968) in *Performance of Concrete* (ed. E.G. Swenson), University of Toronto Press.

Chapter twenty-four

High performance concrete

'*High strength concrete*' became a familiar phrase in concrete technology in the late 1980s, and a few years later was widened to '*high performance concrete*'. It has been the subject of many papers, books and conferences, but it may have been preferable to use the term *higher* performance concrete, since it is essentially an extension and enhancement of existing conventional concrete practice.

High performance concrete is not a single type of concrete, but includes any concrete whose properties significantly exceed or extend the range of concrete currently being used. There is also another important condition – the concrete must be capable of being mixed, handled and placed with the same equipment and procedures as conventional concrete, albeit with higher standards of quality control and more careful selection of materials and mix design. The superior properties can thus be readily exploited in concrete practice. In nearly all cases the enhancement of properties is through the use of cement replacement materials and superplasticisers, both of which we have discussed in previous chapters.

We should add here that there are a number of specialist concretes that, although demonstrating the great versatility of the material, are not normally referred to as high performance concrete. Examples are underwater concrete, foamed concrete, autoclaved aerated concrete and roller compacted concrete; discussion of these is beyond the scope of this book.

There are three broad divisions of high performance concrete – high strength concrete, high durability concrete and self-compacting concrete. We will consider the first and last of these – in which the high performance involves the hardened and fresh properties respectively. As we discussed in the last chapter, the achievement of high durability often results in high strength, but this is not always the case, e.g. freeze–thaw resistance is obtained by air entrainment which reduces the strength.

24.1 High strength concrete

An accepted definition of a high strength concrete is a strength significantly higher than that used in normal practice. As practice is continually advancing, this means that the quantitative definition needs regular adjustment, and can vary from country to country. An accepted current value is a characteristic strength in excess of about 80 MPa.

It will be clear from Chapter 20 that the use of a low water/cement or water/binder ratio is a prime requirement, but this in itself is not sufficient. The main considerations arising from the many research studies and development programmes can be summarised as follows:

- Microsilica at levels of up to about 10 per cent of the binder is important, particularly for achieving very high strengths (Figure 24.1). The main benefit is improvement of the paste/aggregate transition zone.
- All materials must be very carefully selected for optimum properties:
  - high quality aggregates are required, with crushed rocks normally preferred, and some limestones giving particularly good performance. Limiting the maximum aggregate size to 10 mm is normally suggested.
  - Superplasticisers are essential for producing adequate workability, but the binder (particularly the cement) and superplasticiser must be compatible to avoid problems such as rapid loss of workability.
- Even at slumps in excess of 175 mm, the mixes can be cohesive and difficult to handle, i.e. they have a high plastic viscosity. Attention to aggregate gradings and particle size can reduce this problem; the lubrication provided by the very fine spherical microsilica particles is beneficial.
- Problems that are of minor significance for normal strength concrete, such as loss of workability and heat of hydration effects, will be exaggerated in high strength mixes, and therefore may become critical without due consideration. The use of ternary cement blends, i.e. Portland cement plus microsilica (csf) and either pfa or ggbs can be helpful in many cases
- Mix design is considerably more complex than for normal strength concrete because of the larger size of variables involved and their interactive effects. A more extensive set of trial mixes at both laboratory and full scale are required.
- All production and quality control issues need much greater attention than for normal strength concrete, since the consequences of variations and fluctuations will be much more serious.
- The elastic modulus continues to increase non-linearly with strength, with a typical relationship being (Kakizaki *et al.*, 1992):

$$E_c = 3.65(f_{\text{cyl}})^{0.5} \quad \text{for strengths between 80 and 140 MPa} \qquad (24.1)$$

where E_c = elastic modulus (in GPa) and f_{cyl} = cylinder compressive strength (in MPa).

However, the stress–strain behaviour becomes distinctly more brittle and the concrete fails at increasingly lower strains as

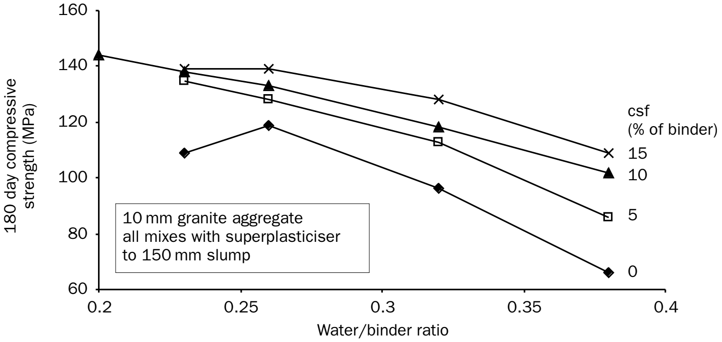

FIGURE 24.1 Strength versus water/binder ratio for high strength concrete (Domone and Soutsos, 1995).

strength increases. This has consequences for reinforcement design.

All of these factors mean that high strength concrete is relatively expensive, but its use may lead to overall structural economies, and there are growing numbers of successful examples of its use. Reduced section sizes mean much lower self-weights – a major factor in long-span bridges – and in high-rise buildings, another significant area of use, the reduced column cross-sections giving higher usable space, particularly in the lower storeys.

The upper limits of strength levels shown in Figure 24.1 are approaching those that can be achieved with 'conventional' concrete materials and practice, but do not represent an overall ceiling or a limit. There have been several developments of materials with water/binder ratios considerably less than 0.2. One example is the macro-defect free (MDF) cement already discussed in Chapter 13, p. 105. Another example is DSP cement (densified with small particles) which uses the action of a superplasticiser and microsilica to produce low porosity, which when combined with a strong aggregate of 4 mm maximum size produces compressive strengths of up to 260 MPa (Bache, 1994). RPC (reactive powder concrete) takes this a stage further by using a maximum aggregate size of, at most, 600 microns, increasing the density by optimising the proportions of all of the particles, and curing under pressure followed by heat treatment. Unconfined compressive strengths of more than 200 MPa are obtained, and ductility can be provided by including short steel fibres (Bonneau *et al.*, 1996).

Although such materials may only find use in specialist applications, they do demonstrate that, by understanding and applying the principles of materials science to cement composites, a wide and continuous spectrum of performance can be achieved.

24.2 Self-compacting concrete

Self-compacting concrete (SCC) can achieve full and uniform compaction without the need for any help from vibration. It is distinctly different from other types of high workability concrete in that it is able to flow through and around heavily congested reinforcement whilst retaining its integrity and homogeneity. It was developed in Japan in the late 1980s in response to a lack of skilled construction workers, and it was quickly adopted into Japanese construction practice, and its use is now rapidly spreading to other countries (RILEM, 2001). A major advantage is environmental – construction sites and precast works are much less noisy, and the health risks associated with hand-held vibrators are eliminated.

The high performance relates to the fresh properties only. It is possible to produce the complete range of strengths and other properties of concrete described hitherto in this book, apart from very low strengths. SCC requires a combination of:

- high fluidity and stability, achieved by a combination of low water/binder ratios and superplasticisers, often supplemented by viscosity-enhancing agents or 'thickeners'. These two properties are described as *filling ability* and *segregation resistance* respectively, and in rheological terms, require a very low yield stress and a moderate to high plastic viscosity (but not so high that flow times are excessive);
- the avoidance of aggregate particles bridging between reinforcing bars and blocking the flow, achieved by an increase in the volume of paste or mortar, and a consequent reduction in the coarse aggregate volumes (Figure 24.2). This property is called *passing ability*, and the volume of coarse aggregate in SCC is typically in the range 30–34 per cent of the concrete volume, compared to 40–55 per cent in normal concrete.

This combination of properties can only be achieved with a reasonably high binder content and low water/binder ratios, typically in the ranges 450–600 kg/m^3 and 0.3 to 0.5 respectively. Control of strength and heat of hydration effects is obtained through the use of significant quantities of CRMs and/or inert fillers such as limestone powder. Apart from the slump flow test, where a

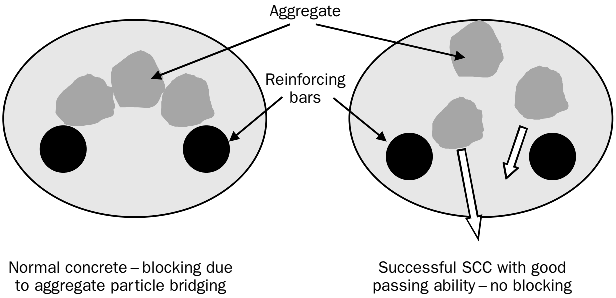

FIGURE 24.2 The passing ability of self-compacting concrete.

value of at least 600 mm is required, a consensus of appropriate tests and limiting values to measure and specify the properties of SCC has not yet emerged. However, it is clear that SCC will have an increasing impact on concrete practice in the next few years.

24.3 References

Bache, H.H. (1994) Design for ductility. In *Concrete Technology: New Trends, Industrial Applications* (ed. R. Gettu, A. Aguado and A. Shah), E & FN Spon, London, pp. 113–25.

Bonneau, O., Poulin, C., Dugat, J., Richard, P. and Aitcin, P.-C. (1996) Reactive powder concrete from theory to practice. *Concrete International* 18, 4, April, 47–9.

Domone, P.L. and Soutsos, M.N. (1995) Properties of high strength concrete mixes containing pfa and ggbs. *Mag. of Con. Res.* 437, 173, Dec. 355–67.

Kakizaki, M. (1992) Effect of mixing method on mechanical properties and pore structure of ultra-high strength, concrete. Proc. of 4th CANMET/ACI Int. Conf. on Fly Ash, Silica Fume, Slag and Natural Pozzalans in Concrete, Istanbul, Turkey, ACI SP-132, *American Concrete Institute*, Michigan, USA, 997–1015.

RILEM Technical Committee 174-SCC (2001) *Self-compacting Concrete: State-of-the-art Report* (ed. A. Skarendahl and O. Petersson), RILEM, Paris.

Further reading

General

Neville, A.M. (1995) *Properties of Concrete*, 4th edn, Pearson Education, Harlow, p. 844.

Since its first edition in 1963, this has been the definitive reference book of all aspects of concrete technology. This fourth edition encompasses the many recent developments, and it is the first source for all with an interest in concrete. It is not a teaching text, but a book to be consulted regularly.

Hewlett, P.C. (ed.) (1998) *Lea's Chemistry of Cement and Concrete*, Arnold, London, p. 1052.

An update of a book first published in 1935. The authoritative text on the subject, with much detail at an advanced level. Not for the faint-hearted, but worth consulting for project work, etc.

Murdock, L.J., Brook, K.M. and Dewar, J.D. (1992) *Concrete Materials and Practice,* 6th edn, Edward Arnold, London.

Aimed at professionals in the concrete industry, quite detailed, but useful when you want to know more about practice.

Clarke, J. (ed.) (1993) *Structural Lightweight Aggregate Concrete*, Blackie Academic and Professional, London.

A useful source for all aspects of this subject.

History of concrete

British Cement Association (1999) *Concrete Through the Ages*, BCA, Crowthorne, p. 37.

Fairly short, but interesting and well illustrated.

Cements/CRMs

Bye, G.C. (1999) *Portland Cement: Composition, Production and Properties*, 2nd edn, Thomas Telford, London, p. 225.

Detailed and comprehensive – a good reference source.

Concrete Society (1991) The use of ggbs and pfa in concrete. *Technical Report* No. 40, Wexham, p. 142, and

Concrete Society (1993) Microsilica in concrete. *Technical Report* No. 41, Wexham, p. 54.

Both summaries produced for professionals in the concrete industry, but also useful for students.

Admixtures

Ramachandran, V.S., Malhotra, V.M., Jolicoeur, C. and Spiratos, N. (1998) *Superplasticisers: Properties and Applications in Concrete*, CANMET, Ottawa, p. 404.

Specialised and not very easy reading, but comprehensive.

Rixom, R. and Mailvaganam, N. (1999) *Chemical Admixtures for Concrete,* 3rd edn, E & FN Spon, London, p. 456.

A welcome new edition – thorough.

Mix design

ACI 211.1–91 (2000) *Standard practice for selecting proportions for normal heavyweight and mass concrete: ACI Manual of Concrete Practice. Part 1: Materials and General Properties of Concrete*, American Concrete Institute, Farmington Mills, Michigan, USA.

The US procedure.

BRE (1997) *Design of Normal Concrete Mixes*, 2nd edn, Building Research Establishment, Watford.

A fairly straightforward UK method discussed in Chapter 21.

Day, K.W. (1995) *Concrete Mix Design, Quality Control and Specification*, E & FN Spon, London, p. 350.

deLarrard, F. (1999) *Concrete Mixture Proportioning: a Scientific Approach*, E & FN Spon, London, p. 350.

Dewar, J.D. (1999) *Computer Modelling of Concrete Mixtures*, E & FN Spon, London, p. 272.
All these three are for those with an interest in considering mix design in great detail. They contain a varying mixture of science, empiricism and practical advice.

Fresh concrete

Masterston, G.G.T. and Wilson, R.A. (1997) The planning and design of concrete mixes for transporting, placing and finishing. *CIRIA Report* 165, Construction Industry Research and Information Association, London.
Useful to those concerned with practical issues of concrete construction.

Tattersall, G.H. and Banfill, P.F.G. (1983) *The Rheology of Fresh Concrete*, Pitman, London.
Contains all the relevant theory, background and details of application of rheology to fresh cement and concrete, and summarises all the pioneering studies of the 1960s and 1970s. An excellent reference text.

Tattersall, G.H. (1991) *Workability and Quality Control of Concrete*, E & FN Spon, London.
Discusses the nature of workability and workability testing, summarises the background to rheological testing, and considers quality control issues in some detail. The source for much of the information in this chapter.

Non-destructive testing

Bungey, J. (1989) *The Testing of Concrete in Structures*, 2nd edn, Surrey University Press, London.
Fairly easy to read, and covers most aspects of NDT of concrete.

Malhotra, N.J. and Carino, V.M. (1991) *CRC Handbook on Non-destructive Testing of Concrete*, CRC Press, Boca Raton, Florida.
More detailed, a good reference source.

Durability

Mays, G.C. (1991) *Durability of Concrete Structures: Investigation, Repair, Protection,* E & FN Spon, London.
Considers the whole subject in detail, from fundamental mechanisms through to repair methods.

High performance concrete

Aitcin, P.-C. (1998) *High-performance Concrete*, E & FN Spon, London, p. 591.
A comprehensive text on this fast developing area of concrete technology; takes the subject from the background science to many case studies of applications.

Concrete Society (1997) *Technical Report TR47 Design with High-strength Concrete,* Concrete Society, Crowthorne, p. 150.
Provides design guidance for structural applications of high-strength concrete not covered by current codes of practice.

Nawy, E.G. (1996) *Fundamentals of High-strength Concrete Performance Concrete,* Longman, Harlow p. 340.
Considers the whole subject of high-strength concrete from selection of materials, properties, uses and applications, generally from an American perspective. Aimed at students and practising engineers.

Price, W.F. (2001) *The Use of High-performance Concrete*, E & FN Spon, London.
Considers the uses and practical applications of the various types of high performance concrete, including high strength, controlled density, high durability, high workability and self-compacting concrete.

Standards referred to in the text

UK Standards (published by the British Standards Institution)

BS 8110: 1997 *The structural use of concrete. Part 1: Code of practice for design and construction.*

Cements

BS 12: 1996 *Specification for Portland cement.*
BS 4027: 1991 *Specification for sulfate-resisting Portland cement.*
BS 6699: 1992 *Specification for ground granulated blast furnace slag for use with Portland cement.*
BS 3892: Part 1 1993 *Specification for pulverised fuel ash for use with Portland cement.*

Admixtures

BS 5075: *Concrete Admixtures.*
Part 1: 1982 *Specification for accelerating admixtures, retarding admixtures and water reducing admixtures.*

Part 2: 1982 *Specification for air-entraining admixtures.*
Part 3: 1985 *Specification for superplasticizing admixtures.*

Aggregates

BS 812 *Testing aggregates* (24 parts).
BS 882: 1992 *Specification for aggregates from natural sources for concrete.*

Test methods

BS 1881: Testing concrete.
Part 102: 1983 *Method for determination of slump.*
Part 102: 1983 *Method for determination of flow.*
Part 103: 1983 *Method for determination of compacting factor.*
Part 104: 1983 *Method for determination of Vebe time.*
Part 116: 1983 *Method for determination of compressive strength of concrete cubes.*
Part 201: 1986 *Guide to the use of non-destructive methods of test for hardened concrete.*
Part 202: 1986 *Recommendations for surface hardness testing by rebound hammer.*
Part 203: 1986 *Recommendations for measurement of velocity of ultrasonic pulses in concrete.*
Part 207: 1986 *Recommendations for the assessment of concrete strength by near-to-surface tests.*
Part 208: 1986 *Recommendations for the determination of the initial surface absorption of concrete.*
Part 209: 1986 *Recommendations for the measurement of dynamic modulus of elasticity.*
BS 5168: 1975 *Glossary of rheological terms.*

European Standards (published by the British Standards Institution)

EN 197–1: 2000 *Cement – Part 1: Composition, specifications and conformity criteria for common cements.*
EN 12350–2: 2000 *Testing fresh concrete. Slump test.*
EN 12350–3: 2000 *Testing of fresh concrete. Vebe test.*
EN 12350–4: 2000 *Testing of fresh concrete. Degree of compactability.*
EN 12350–5: 2000 *Testing of fresh concrete. Flow table test.*
DD ENV 1992–1–2: 1996 *Eurocode 2: Design of concrete structures.*
DD ENV 206: 1992 *Concrete: Performance, production placing and compliance criteria.*

US Standards (published by the American Society for Testing and Materials)

ASTM C150–94 *Specification for Portland cement.*
ASTM C494–92 *Specification for chemical admixtures for concrete.*
ASTM C618–94a *Specification for coal fly ash and raw or calcined natural pozzola for use as a mineral admixture in hydraulic-cement concrete.*
ASTM C989–93 *Specification for ground granulated blast furnace slag for use in concrete and mortars.*
ASTM C1240–93a *Specification for silica fume for use as a mineral admixture in hydraulic-cement concrete, mortar and grout.*
ASTM Specification C 143–90a *Test for slump of hydraulic cement concrete.*
ASTM Specification C 232–92 *Test for bleeding of concrete.*
ASTM Specification C 125–93 *Standard definitions and terms relating to concrete and concrete aggregates.*

Part Four

Bituminous materials

D.G. Bonner

Introduction

The term 'bituminous materials' is generally taken to include all materials consisting of aggregate bound with either bitumen or tar. Materials of this kind are used almost exclusively in road construction. However, bitumen and tar on their own have other uses in construction. For example bitumen is used in roofing materials and as a protective/waterproof coating. This part will concentrate on the use of bituminous materials in road construction.

The use of tar in road building materials began to grow significantly in the UK just after the turn of the century following the advent of the pneumatic tyre and the motor vehicle. Up to that time, roads were constructed following the principles developed by Macadam using waterbound, graded aggregate. Under the action of pneumatic tyres and the higher speeds of motor vehicles, a great deal of dust was generated on macadam roads which led to the use of tar as a dressing to bind the surface. Tar was eminently suitable for this purpose since it could be made sufficiently fluid by the use of heat to be sprayed, but stiffened on cooling. Furthermore, it protected the road from the detrimental effects of water. The benefits of using tar were quickly realized and a range of 'coated stone' materials, or 'tarmacadams', were developed.

References to natural sources of bitumen date back to biblical times. However, the first use of natural rock asphalt for paving roads was in the middle of the nineteenth century. The first refinery bitumens to be used in this country came from the Mexican oilfields around 1913. But it was the opening of the Shell Haven refinery in 1920 which gave rise to the rapid development of bitumen for road construction. Bitumen was found to be less temperature-susceptible than tar. Thus it is less soft than an equivalent grade of tar at high temperatures, making it more resistant to deformation, and less stiff than tar at low temperatures, making it less brittle and more resistant to cracking. As the performance required of bituminous materials increased, due to the increase in quantity and weight of traffic, bitumen became more widely used than tar. Although tar-bound materials predominated during the Second World War due to difficulties in importing crude oil, the introduction of North Sea gas in the late 1960s dramatically reduced the production of crude coal tar. Now the use of tar in road construction is limited to tar/bitumen blends for surface dressing and dense tar surfacing used in areas such as car parks where the greater resistance of tar to diesel and oil spillage is an advantage. Therefore the following chapters will deal only with bitumen.

A very wide range of bituminous mixtures have evolved to suit the wide variety of circumstances in which they are used. They vary according to their bitumen content and grade as well as their aggregate grading and size. However, they can all be classified into two groups, namely asphalts and macadams. (Here it should be noted that the term 'asphalt' is used with its European meaning, i.e. a particular type of mixture of bitumen and aggregate. In North America, 'asphalt' means bitumen.) Figure IV.1 illustrates the fundamentally different characteristics of asphalts and macadams. Asphalts rely on their dense, stiff mortar for strength and stiffness, whereas macadams rely on the stability of the aggregate through its grading. Thus the role of bitumen is quite different in each case, and the properties of asphalts are more strongly dependent on the nature of the bitumen than the properties of macadams. However, although Figure IV.1 portrays two very different types of material, there is, in fact, almost a continuous spectrum of materials between these two extremes. Thus there are asphalts which have a larger coarse aggregate content than suggested in Figure IV.1 so that the overall aggregate grading is more continuous and the materials resemble macadams in that respect. Similarly there are macadam mixes which are dense and contain more bitumen, and tend towards the model for asphalts. This will be discussed in more detail in Chapter 29.

Bituminous materials are used in so-called ‘flexible’ construction. The alternative is ‘rigid’ construction where the road consists essentially of a concrete slab. In flexible construction there are a number of layers to the road structure each having a specific function. Figure IV.2 illustrates those layers and where bituminous materials may be used. The nature of the materials will vary according to their position and function in the structure. Thus both the wearing course and basecourse may be asphalts but the properties required of the wearing course at the surface are different from those required just below the surface in the basecourse. Therefore a wearing course asphalt differs from a basecourse asphalt. Also, particular types of material are selected according to their suitability. Thus when traffic loads are very high, an asphalt roadbase may not provide sufficient resistance to deformation, but would give the necessary resistance to fatigue cracking. Therefore asphalt is used at the bottom of the roadbase where tensile stresses inducing cracks are greatest, and macadam is used for the upper part to provide improved resistance to deformation. This will be discussed more fully in Chapter 27.

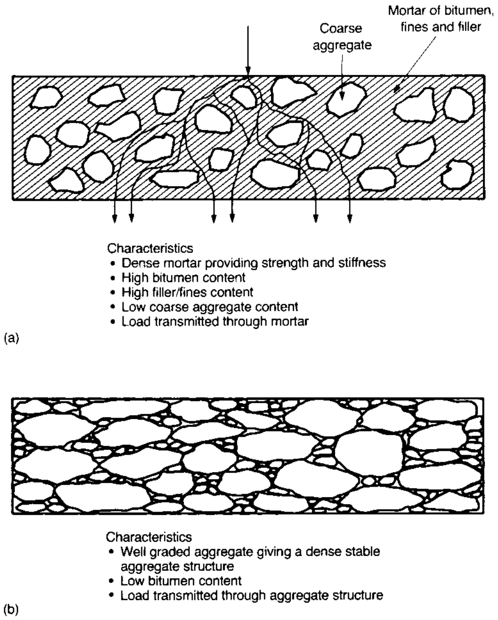

FIGURE IV.1 The essential features of asphalts and macadams: (a) asphalt; (b) macadam.

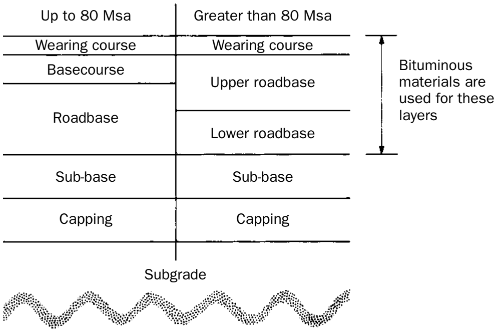

FIGURE IV.2 The structure of a flexible road according to the traffic loading in millions of standard axles (Msa).

Chapter twenty-five

Structure of bituminous materials

25.1 Constituents of bituminous materials

Bituminous materials consist of a graded aggregate bound together with bitumen. Thus they are two-phase materials and their properties depend upon the properties of the individual phases as well as the mix proportions. The two phases are quite different in nature. Whilst the aggregate is stiff and hard, the bitumen is flexible and soft and is particularly susceptible to temperature change. Therefore the proportion of bitumen in the mix has a great influence on the mix properties and is crucial in determining the performance of the material.

Bitumen may be supplied in a number of forms either to facilitate the mixing and laying process or to provide a particular performance. Aggregates may come from a wide range of rock types or from artificial sources such as slag. The grading of the aggregate is important and ranges from continuous grading for mix types known as macadams through to gap grading for mixes known as asphalts. The very fine component of the aggregate (passing 75 microns) is called filler. Although the graded aggregate will normally contain some material of this size, it is usually necessary to provide additional filler in the form of limestone dust, pulverized fuel ash or ordinary Portland cement.

25.2 Bitumen

25.2.1 Sources

There are two sources of bitumen: natural deposits and refinery bitumen.

Natural asphalts

Bitumen occurs naturally, formed from petroleum by geological forces, and always in intimate association with mineral aggregate. Types of deposit range from almost pure bitumen to bitumen-impregnated rocks and bituminous sands with only a few per cent bitumen.

Rock asphalt consists of porous limestone or sandstone impregnated with bitumen with a typical bitumen content of 10 per cent. Notable deposits are in the Val de Travers region of Switzerland and the ‘tar sands’ of North America.

Lake asphalt consists of a bitumen ‘lake’ with finely divided mineral matter dispersed throughout the bitumen. The most important deposit of this type, and the only one used as a source of road bitumen in the UK, is the Trinidad Lake.

The lake consists of an area of some 35 ha and extends to a depth of 100 m. Asphalt is dug from the lake, partially refined by heating to 160°C in open stills to drive off water, then filtered, barrelled and shipped. The material consists of 55 per cent bitumen, 35 per cent mineral matter and 10 per cent organic matter. It is too hard in this form to use directly on roads and is usually blended with refinery bitumen.

Refinery bitumen

This is the major source of bitumen in the UK. In essence, bitumen is the residual material left after the fractional distillation of crude oil. Crudes vary in their bitumen content. The lighter paraffinic crudes, such as those from the Middle East and North Sea, have a low bitumen content which must be obtained by further processes after distillation. Heavier crudes, known as asphaltic crudes, such as those from the United States, contain more bitumen which is more easily extracted.

25.2.2 Manufacture

The process of refining crude oil yields a range of products, as shown in Figure 25.1. These products are released at different temperatures with the volatility decreasing and viscosity increasing as the temperature rises. Bitumen is the residual material but its nature will depend on the distillation process and, in particular, on the extent to which the heavier oils have been removed. If the residual material contains significant amounts of heavy oils, it will be softer than if the heavy oils had been more thoroughly extracted. Modern refinery plant is capable of very precise control which enables bitumen to be produced consistently at a required viscosity.

25.2.3 Chemistry and molecular structure

Bitumen is a complex colloidal system of hydrocarbons and their derivatives which is soluble in trichloroethylene. The usual approach to determination of the constituents of a bitumen is through use of solvents. It may be subdivided into the following main fractions:

1. carbenes – fraction insoluble in carbon tetrachloride;
2. asphaltenes – fraction insoluble in light aliphatic hydrocarbon solvent, e.g. heptane;
3. maltenes – fraction soluble in heptane.

The last two fractions predominate and the maltenes may be further subdivided into resins (that part adsorbed on an active powder such as Fuller's earth) and oils. The asphaltenes have the higher molecular weight but their exact nature is dependent on the type of solvent and the volume ratio of solvent to bitumen. If small amounts of

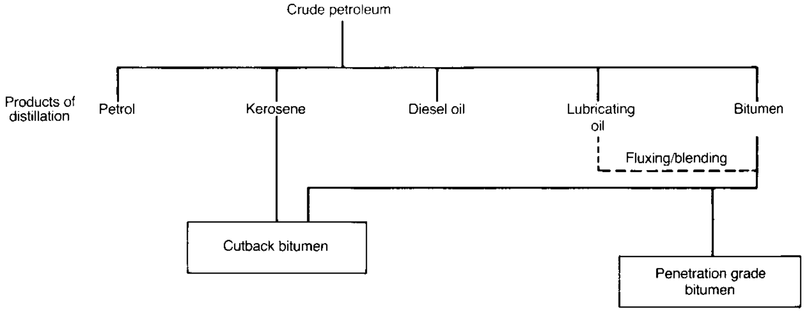

FIGURE 25.1 Preparation of refinery bitumens.

solvent are used, resins, which form part of the maltene fraction, may be adsorbed onto the asphaltene surfaces, yielding a higher percentage of asphaltene. Although they may vary according to method of extraction, the appearance of asphaltenes is always of a dark brown to black solid which is brittle at room temperature. They have a complex chemical composition but consist chiefly of condensed aromatic hydrocarbons and include complexes with nitrogen, oxygen, sulphur and metals such as nickel and vanadium. The structure of asphaltenes is not known with certainty. One suggestion is of two-dimensional condensed aromatic rings, short aliphatic chains and naphthenic rings combined in a three-dimensional network (Dickie and Yen, 1967). Another suggestion is that there are two different molecular types, one being a simple condensed aromatic unit and the other consisting of collections of these simple units (Speight and Moschopedis, 1979). It is likely that all of these may exist in bitumens from different sources since the nature of the molecules present in a crude oil will vary according to the organic material from which the crude was formed, and to the type of surrounding geology.

Maltenes contain lower molecular weight versions of asphaltenes called resins and a range of hydrocarbon groups known as ‘oils’ including olefins, naphthenes and paraffins. The aromatic oils are oily and dark brown in appearance and include naphtheno-aromatic type rings. The saturated oils are made up mainly of long, straight saturated chains and appear as highly viscous whitish oil.

Bitumen is normally described as a colloidal system where the asphaltenes are solid particles in the form of a cluster of molecules or micelles in a continuum of maltenes (Girdler, 1965). Depending on the degree of dispersion of the micelles in the continuous phase, the bitumen may be either a sol, where there is complete dispersal, or a gel, where the micelles are flocculated into flakes. Bitumens with more saturated oils of low molecular weight have a predominantly gel character. Those with more aromatic oils, which are more like asphaltenes, have a predominantly sol character.

In terms of their influence on the properties of bitumen, asphaltenes constitute the body of the material, the resins provide the adhesive and ductile properties, and the oils determine the viscosity and rheology.

Although bitumens are largely complex mixtures of hydrocarbons, there are other elements present. The high molecular weight fraction contains significant amounts of sulphur, the amount of which influences the stiffness of the material. Oxygen is also present, and some complexes with oxygen determine the acidity of the bitumen. This is important in determining the ability of the bitumen to adhere either to aggregate particles or to road surfaces.

25.3 Types of bitumen

25.3.1 Penetration grades

Refinery bitumens are produced with a range of viscosities and are known as penetration grade bitumens. The term derives from the test which is used to characterize them according to hardness. The range of penetration grades for road bitumens is from 15 to 450, although the most commonly used are in the range 50 to 200. The range is produced partly through careful control of the distillation process and partly by fluxing ‘residual’ bitumen with oils to the required degree of hardness. The specification for penetration grade bitumens is contained in BS 3690 Part 1(4).[1] Table 25.1 indicates a range of tests with which penetration grade bitumens for road purposes must comply. These bitumens are specified by their penetration value (BS 2000: Part 49: 1993) and softening point (BS 2000: Part 58: 1993) which indicate hardness and viscosity respectively. However, they are designated only by their penetration, e.g. 50 pen bitumen has a penetration of 50 ± 10. In addition there are limits for loss on heating (BS 2000: Part 45: 1993) which ensures that there are no volatile components present whose loss during preparation and laying

---

[1] A list of all standards referred to in the text is included in ‘Further reading’ on page 266.

would cause hardening of the bitumen, and solubility (BS 2000: Part 47: 1993), which ensures that there are only negligible amounts of impurity. The permittivity test (BS 2000: Part 357: 1983) measures the dielectric constant for the material which has been shown to be related to the weathering characteristics.

25.3.2 Oxidized bitumens

Refinery bitumen may be further processed by air blowing. This consists of introducing air under pressure into a soft bitumen under controlled temperature conditions. The oxygen in the air reacts with certain compounds in the bitumen resulting in the formation of compounds of higher molecular weight. Thus the asphaltene content increases at the expense of the maltene content, resulting in harder bitumens which are also less ductile and less temperature-susceptible. Although these bitumens are mostly used for industrial applications such as roofing and pipe coatings, there is a road bitumen produced by this process known as heavy duty bitumen. It is regarded as a penetration grade bitumen and is included in Table 25.1 (40 pen HD).

25.3.3 Cutbacks

Penetration grade bitumen is thermoplastic and thus its viscosity varies with temperature. At ambient temperature it can be more or less solid and to enable it to be used for road construction it must be temporarily changed into a fluid state. This may simply be achieved by raising the temperature. However, for surface dressing and some types of bituminous mixture it is necessary to have a fluid binder that can be applied and mixed at relatively low temperatures, but have an adequate hardness after laying. Cutback bitumens are penetration grade bitumens which have their viscosity temporarily reduced by dilution in a volatile oil. After application the volatile oil evaporates and the bitumen reverts to its former viscosity.

The curing time and viscosity of cutbacks can be varied according to the volatility of the diluting oil and the amount of dilutent used. In the UK, cutbacks are manufactured using 100 or 200 pen bitumen diluted with kerosene. Three grades are produced to comply with a viscosity specification based on the standard tar viscometer (STV). Table 25.2 from BS 3690 shows that cutbacks must also comply with solubility, distillation and recovered penetration requirements. The last two are to ensure that the dilutent will evaporate at the required rate and that the residual bitumen will have an appropriate hardness for the performance requirements.

TABLE 25.1 Specification for penetration grade bitumens (*The Shell Bitumen Handbook*, 1990)

Property		*Test method*	*Grade of bitumen*		
			40 pen HD	*50 pen*	*100 pen*
Penetration at 25°C dmm[1]		BS 2000: Part 49	40 ± 10	50 ± 10	100 ± 20
Softening point, °C	min	BS 2000: Part 58	58	47	41
	max		68	58	51
Loss on heating for 5 h at 163°C		BS 2000: Part 45			
(a) loss by mass, %	max		0.2	0.2	0.5
(b) drop in penetration, %	max		20	20	20
Solubility in trichloroethylene, % by mass	min	BS 2000: Part 47	99.5	99.5	99.5
Permittivity at 25°C and 1592 Hz	min	BS 2000: Part 357	2.630	2.630	2.630

Note:
1. 1 dmm = 0.1 mm.

TABLE 25.2 Specification for cutback bitumens (BS 3690: Part 1: 1989) Reproduced with the permission of the British Standards Institution under licence number 2001/SK0230.

Property		*Test method*	*Grade of cutback*		
			50 sec	*100 sec*	*200 sec*
Viscosity (STV) at 40°C, 10 mm cup, secs		BS 2000: Part 72	50 ± 10	100 ± 20	200 ± 40
Distillation		BS 2000: Part 27			
(a) distillate to 225°C, % by volume	max		1	1	1
360°C, % by volume			10 ± 3	9 ± 3	7 ± 3
(b) penetration at 25°C of residue from distillation to 360°C, dmm[1]		BS 2000: Part 49	100 to 350	100 to 350	100 to 350
Solubility in trichloroethylene, % by mass	min	BS 2000: Part 47	99.5	99.5	99.5

Note:
1. 1 dmm = 0.1 mm.

25.3.4 Emulsions

An emulsion is a two-phase system consisting of two immiscible liquids, one being dispersed as fine globules within the other. A bitumen emulsion consists of discrete globules of bitumen dispersed within a continuous phase of water, and is a means of enabling penetration grade bitumens to be mixed and laid.

Dispersal of the bitumen globules must be maintained electrochemically using an emulsifier which consists of a long hydrocarbon chain terminating with either a cationic or an anionic functional group. The hydrocarbon chain has an affinity for bitumen, whereas the ionic part has an affinity for water. Thus the emulsifier molecules are attracted to the bitumen globules with the hydrocarbon chain binding strongly to the bitumen leaving the ionic part on the surface of the globule as shown in Figure 25.2. Each droplet then carries a like-surface charge depending on the charge of the ionic part of the emulsifier. Cationic emulsions are positively charged and anionic emulsions are negatively charged. The globules therefore repel each other, making the emulsion stable. Cationic emulsions are preferred because they also aid adhesion, the positively charged bitumen globules being strongly attracted to the negatively charged aggregate surface.

Emulsions must satisfy two conflicting requirements in that they need stability for storage but

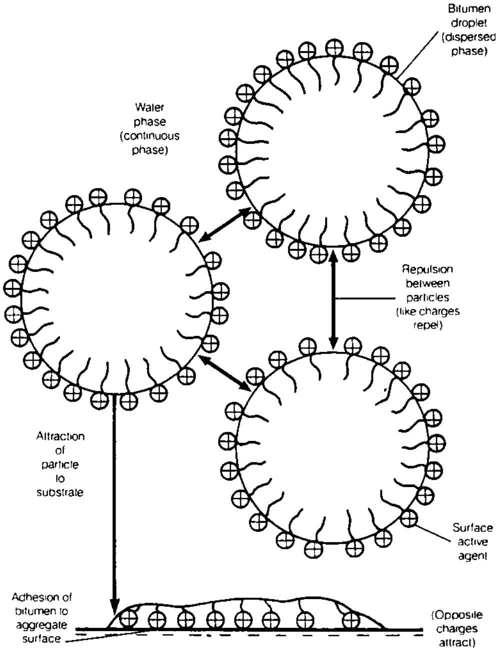

FIGURE 25.2 Schematic diagram of charges on bitumen droplets (*The Shell Bitumen Handbook*, 1990).

also may need to break quickly when put into use. The stability of an emulsion depends on a number of factors as follows:

1. The quantity and type of emulsifer present. Anionic emulsions require substantial water loss before they break, whereas cationic emulsions break by physicochemical action before much evaporation. The more free emulsifier ions there are in the continuous phase, the easier it is for the negatively charged aggregate surface to be satisfied without attracting the bitumen globules.
2. Rate of water loss by evaporation. This in turn depends on ambient temperature, humidity and wind speed as well as rate and method of application.
3. The quantity of bitumen. Increasing the bitumen content will increase the breaking rate.
4. Size of bitumen globules. The smaller their size, the slower will be the breaking rate.
5. Mechanical forces. The greater the mixing friction or, in the case of surface dressing, the rolling and traffic action, the quicker the emulsion will break.

The viscosity of emulsions is important because a large proportion of emulsions are applied by spray. The viscosity increases with bitumen content and is very sensitive for values greater than about 60 per cent. The chemistry of the aqueous phase is also important with viscosity being increased by decreasing the acid content or increasing the emulsifier content. The viscosity for road emulsions is specified in BS 434: Part 1.

25.4 Aggregates

Aggregates make up the bulk of bituminous materials; the percentage by weight ranges from about 92 per cent for a wearing course asphalt to about 96 per cent for an open-textured macadam. The aggregate has important effects on the strength and stiffness of bituminous mixtures. In more open-textured types of mix, the strength and resistance to deformation are largely determined by the aggregate grading with the bitumen acting principally as an adhesive. Here the grading is continuous and provides a dense packing of particles leading to a stable aggregate structure. In denser mixes, aggregate grading is again important, but the properties are largely determined by the matrix of fines and bitumen.

The majority of aggregates used in bituminous mixes are obtained from natural sources, either sands and gravels or crushed rock. The main non-natural aggregate source is slag, and blast furnace slag is the most commonly used. As with concrete, aggregates in bituminous mixes are regarded as inert fillers. However, whereas in concrete both the aggregate and the hardened cement paste are relatively stiff, in a bituminous mix, the bitumen is very soft compared to the aggregate. Therefore the role of the aggregate in determining mix stiffness and strength is more important in bituminous mixtures.

Three size ranges are recognized in aggregates for bituminous mixes. These are coarse, fine and filler. Coarse material is that retained on a 2.36 mm sieve, fine material passes 2.36 mm but is retained on the 75 μm sieve, and the filler is the material passing 75 μm.

25.4.1 Properties

The importance of grading has already been mentioned. In addition, aggregates suitable for use in bituminous mixes must have sufficient strength to resist the action of rolling during construction. For surfacing materials, they must also be resistant to abrasion and polishing in order to provide a skid-resistant surface. Here the shape and surface texture of aggregate particles are important.

Figure 25.3 gives typical grading curves for a dense macadam and an asphalt wearing course. The curve for the macadam clearly shows the continuous nature of the grading, whereas that for the asphalt shows a gap grading with a lack of material in the range 600 μm to 10 mm. This is typical of an asphalt where the 'mortar' of fines and filler bound with bitumen characterizes the material, the coarse aggregate providing the bulk.

The strength of aggregate is assessed in two

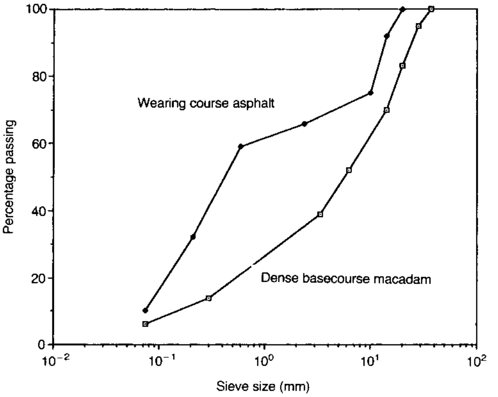

FIGURE 25.3 Aggregate grading curves.

ways. For resistance to crushing, the aggregate crushing value test is used. This test (BS 812: Part 110: 1990) determines the extent to which an aggregate crushes when subjected to a steadily increasing load up to 40 tonnes. The test sample consists of single-sized particles, 10–14 mm, and the amount of fines produced in the test is expressed as a percentage by weight of the original sample. A variation of this test for weaker aggregates is the 10 per cent fines test. Here the maximum crushing load which will produce 10 per cent fines from the original single-sized sample is determined. The importance of this test is to assess the extent of crushing which may occur during compaction.

Resistance to impact loads is also required for road aggregates. The impact value test (BS 812: Part 112: 1990) determines the response of aggregate to blows from a heavy hammer. Once again the outcome of the test is the percentage of fines produced from the original single-sized sample.

The skid resistance of a road surface is provided largely by the aggregate exposed at the surface. There are two components which are referred to as macrotexture and microtexture. The macrotexture is the overall road surface roughness which arises from the extent to which there are spaces between aggregate particles. This is a function of mix proportions. For example, an asphalt provides an extremely low macrotexture because the coarse aggregate content is low and coarse particles are immersed in the fines/filler/bitumen mortar. Consequently, a layer of single-sized aggregate particles is rolled into the surface to provide the required macrotexture. These are precoated with a film of bitumen to improve adhesion to the asphalt surface and are known as coated chippings. Macadams on the other hand have a lower proportion of fines and filler and provide a rough surface.

Macrotexture is measured in terms of texture depth using the sand patch test (BS 598: Part 105: 1990). The test involves spreading a known volume of sand in a circular patch over the road surface until it can be spread no further. The sand fills the spaces between aggregate particles as shown in Figure 25.4. The diameter of the patch is measured and, knowing the volume of sand, the average depth can be calculated.

Microtexture refers to the surface texture of individual particles and varies according to the type of aggregate. Here it is important not only to use an aggregate which has a rough surface texture, but also which will retain that texture

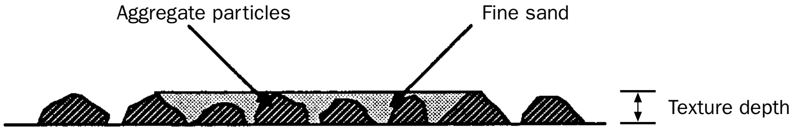

FIGURE 25.4 Measurement of macrotexture using the sand patch test.

under the action of traffic. This is assessed using the polished stone value test (BS 812: Part 114: 1989). Here samples of aggregate are subjected to a simulated wear test, where a pneumatic tyre runs continuously over the aggregate particles under the abrasive action of emery powder. The skidding resistance of the samples is determined after the test using the pendulum skid tester.

25.5 Reference

Dickie, T.P. and Yen, T.F. (1967) Macrostructure of asphaltic fractions by various instrumental methods. *Analytical Chemistry* 39, pp. 13–16.

Girdler, R.B. (1965) Constitution of asphaltenes and related studies. *Proceedings of the Association of Asphalt Paving Technologists* 34, p. 45.

Shell Bitumen UK (1990) *The Shell Bitumen Handbook*, Shell Bitumen UK.

Speight, J.G. and Moschopedis, S.E. (1979) Some observations on the molecular 'nature' of petroleum asphaltenes. *American Chemical Society*, Division of Petroleum Chemistry 24, pp. 22–5.

Chapter twenty-six

Viscosity and deformation of bituminous materials

26.1 Viscosity and rheology of binders

The viscosity of a liquid is the property that retards flow so that, when a force is applied to the liquid, the higher the viscosity, the slower will be the movement of the liquid. The viscosity of bitumen is dependent upon both its chemical make-up and its structure. In sol-type bitumens, the asphaltene micelles are well dispersed within the maltene continuum. The viscosity depends on the relative amounts of the asphaltenes and maltenes, decreasing as the asphaltene content reduces. In gel-type bitumens, where the asphaltene micelles have aggregated, the viscosity is higher and dependent upon the extent of the aggregation. The degree of dispersion of the asphaltenes is controlled by the relative amounts of resins, aromatics and saturated oils. If there are sufficient aromatics they form a stabilizing layer around the asphaltene micelles, promoting the dispersion. However, if they are not present in sufficient quantity the micelles will tend to join together. A schematic representation of the two states is shown in Figure 26.1 (*The Shell Bitumen Handbook*, 1990). In practice most bitumens are somewhere between these two states. The maltene continuum is influenced by the saturated oils which have low molecular weight and, consequently, a low viscosity. These saturates have little solvent power in relation to the asphaltenes, so that as the saturate fraction increases, there is a greater tendency for the asphaltenes to aggregate to form a gel structure. Thus a high proportion of saturates on the one hand tends to reduce viscosity because of their low molecular weight, but on the other hand encourages aggregation of the asphaltene micelles which increases viscosity. The relative importance of these two opposing effects depends on the stabilizing influence on the asphaltenes of the aromatics.

The asphaltenes exert a strong influence on viscosity in three ways. First, the viscosity increases as the asphaltene content increases. Second, the shape of the asphaltene particles governs the extent of the change in viscosity. The asphaltene particles are thought to be formed from stacks of plate-like sheets of aromatic/naphthenic ring structures. These sheets are held

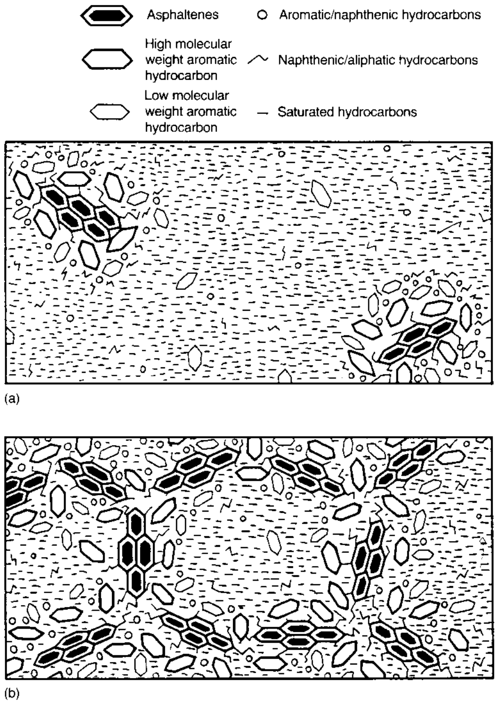

FIGURE 26.1 The structure of bitumen: (a) schematic diagram of a sol-type bitumen; (b) schematic diagram of a gel-type bitumen (*The Shell Bitumen Handbook*, 1990).

together by hydrogen bonds. However, the asphaltenes can also form into extended sheets and combine with aromatics and resins so that particle shape varies. Third, the asphaltenes may tend to aggregate, and the greater the degree of aggregation the higher is the viscosity.

26.2 Measurement of viscosity

An absolute measure of viscosity can be determined using the sliding plate viscometer. If a thin film of bitumen is held between two parallel plane surfaces, and one surface is moved parallel to the other, the movement is resisted by the bitumen, according to its viscosity. The force of resistance, *F*, depends on the area of the surfaces, *A*, the distance between them, *d*, and the speed of movement of one plate relative to the other, *V*, such that:

$$F = \eta \frac{AV}{d} \qquad (26.1)$$

The factor η is the coefficient of viscosity, and is given by:

$$\eta = \frac{F}{A} \div \frac{V}{d}$$

$$= \frac{\text{Shear stress}}{\text{Rate of strain}} \qquad (26.2)$$

This is known as the dynamic viscosity and has units of Pa sec. Viscosity may also be measured in units of mm^2/sec. This unit refers to kinematic viscosity and is related to dynamic viscosity by the expression:

$$\text{Kinematic viscosity} = \frac{\text{Dynamic viscosity}}{\text{Mass density}} \qquad (26.3)$$

However, it is not necessary to know absolute viscosity, and a number of tests have been developed which are empirical and provide arbitrary relative measures of viscosity. The two most common measures of viscosity are the softening point test and the standard tar viscometer.

The softening point (BS 2000: Part 58: 1983) is the temperature at which a bitumen reaches a specified level of viscosity. This viscosity is defined by the ring and ball test apparatus as the consistency at which a thin disc of bitumen flows under the weight of a 10 mm diameter steel ball by a distance of 25 mm. Figure 26.2 shows a diagrammatic representation of the test. The more viscous the bitumen, the higher the temperature at which this level of viscosity is reached.

The standard tar viscometer, as the name implies, is normally used to assess the viscosity of tars. Tars have a greater range of viscosity than bitumens, extending to lower values, and the test allows for this range by permitting a variation in test temperature. The test involves the measurement of the time taken for 50 ml of the tar to run out of a cup through a standard orifice (BS 2000:

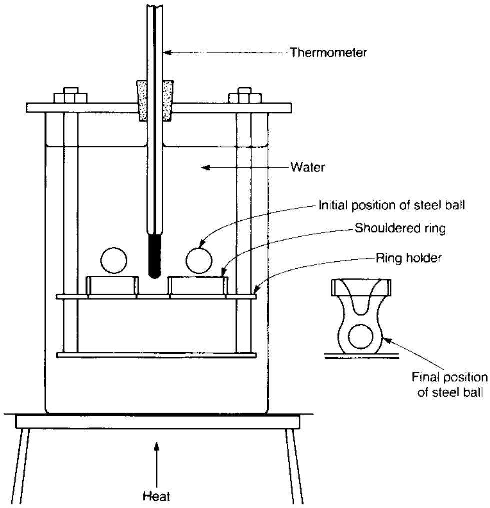

FIGURE 26.2 Apparatus for ring and ball test.

Part 72: 1993). Results obtained at different test temperatures selected to ensure that the efflux time lies between 10 and 140 sec are related to a common equiviscous temperature scale. The viscosity defined for this scale is that at which 50 ml flows out in 50 sec. The test is not used for penetration grade bitumens since these are too viscous to reach the defined viscosity except at very high temperatures which cannot confidently be converted to the empirical equiviscous temperature scale. However, the test is used for cutback bitumens. The efflux time depends on kinematic viscosity, and the test results may be converted to absolute viscosity in Pa sec according to:

$$\eta = \text{flow time} \times \text{density} \times \text{constant}. \tag{26.4}$$

For cutback bitumens, using a cup with a 10 mm orifice, the constant is 0.40.

Another test which is commonly applied to bitumens, and is the basis for their characterization, is the penetration test. The test measures hardness, but this is related to viscosity. The test consists of measuring the depth to which a needle penetrates a sample of bitumen under a load of 100 g over a period of 5 sec at a temperature of 25°C. Thus the test differs from the previous two in that, rather than determining an equiviscous temperature, the viscosity is determined at a particular temperature.

However, because bitumen is viscoelastic, the penetration will depend on the elastic deformation as well as the viscosity. Therefore, since viscosity changes with temperature, different bitumens may have the same hardness at 25°C but different hardnesses at other temperatures. It is the varying elasticity of bitumens which prevents correlation between these empirical tests.

26.3 Influence of temperature on viscosity

Bitumens are thermoplastic materials so that they soften as the temperature rises but become hard again when the temperature falls. The extent of the change in viscosity with temperature varies between different bitumens. It is clearly important, in terms of the performance of a bitumen in service, to know the extent of the change in viscosity with temperature. This is referred to as temperature susceptibility and, for bitumens, is determined from the penetration value, P, and softening point temperature, T. These are related empirically by the expression:

$$\log P = AT + k \tag{26.5}$$

where A is the temperature susceptibility of the logarithm of penetration and k is a constant. From this relationship, an expression has been developed (Pfeiffer and Van Doormaal, 1936) which relates A to an index, known as the penetration index (PI), such that for road bitumens the value of PI is about zero.

$$A = \frac{\mathrm{d}(\log P)}{\mathrm{d}T} = \frac{20 - \mathrm{PI}}{10 + \mathrm{PI}} \cdot \frac{1}{50} \tag{26.6}$$

It has been determined that, for most bitumens, the penetration at their softening point (SP) temperature is about 800. Thus if the penetration at 25°C and the softening point temperature are known, the PI can be evaluated from:

$$\frac{\mathrm{d}(\log P)}{\mathrm{d}T} = \frac{\log 800 - \log P}{\mathrm{SP} - 25} \tag{26.7}$$

$$= \frac{20 - \mathrm{PI}}{10 + \mathrm{PI}} \cdot \frac{1}{50}$$

For example, for a 50 pen bitumen with a softening point of 48°C:

$$\frac{\mathrm{d}(\log P)}{\mathrm{d}T} = \frac{\log 800 - \log 50}{48 - 25} \tag{26.8}$$

$$= \frac{1.204}{23} = 0.0523$$

Therefore:

$$0.0523 = \frac{20 - \mathrm{PI}}{10 + \mathrm{PI}} \cdot \frac{1}{50}$$

giving:

$$\mathrm{PI} = 1.7$$

Pfeiffer and Van Doormaal produced a nomograph (Figure 26.3) to evaluate the above expression, and it can be seen that for the above example a similar result is obtained.

Bitumens for road use normally have a PI in the range −2 to +2. If the PI is low, bitumens are more Newtonian in their behaviour and become very brittle at low temperatures. High PI bitumens have marked time-dependent elastic properties and give improved resistance to permanent deformation.

The influence of chemical composition on temperature susceptibility is illustrated in Figure 26.4. In general the PI increases as the asphaltenes increase at the expense of the aromatics. This change can be achieved by controlled air blowing. Heavy duty bitumen (40 pen) is produced by this technique and has a PI of about 2.5. As a consequence, mixes incorporating this bitumen have a better resistance to deformation.

26.4 Resistance of bitumens to deformation

Since bitumen is a viscoelastic material, the response to an applied load depends on the size of the load, the temperature, and the duration of

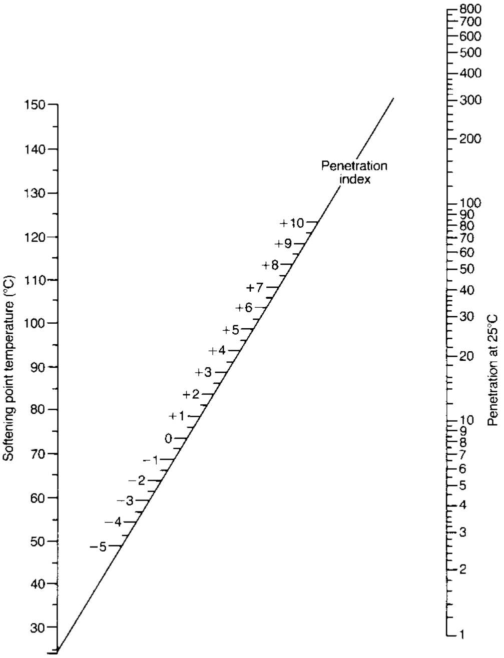

FIGURE 26.3 Nomograph to evaluate penetration index from softening point and penetration (Pfeiffer and Doormaal, 1936).

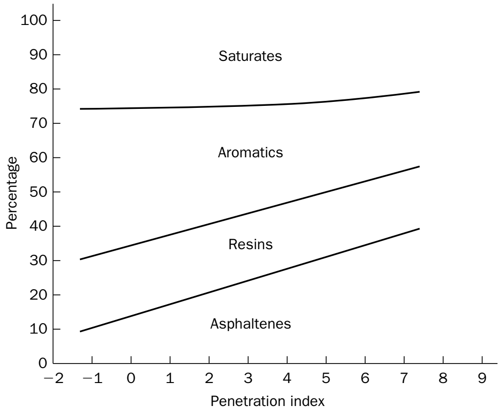

FIGURE 26.4 Relationship between chemical composition and penetration index (Lubbers, 1985).

its application. In other words there is no simple relationship between stress and strain. Therefore it is difficult to predict the elastic modulus of bitumen. However, this modulus is of crucial importance in determining the resistance of a bituminous mixture to permanent deformation. Therefore if the performance of a mix is to be assessed, it is necessary to obtain a value for elastic modulus. Van der Poel (1954) has introduced the concept of stiffness modulus to take account of the viscoelastic nature of bitumen. This modulus is dependent on both temperature and time of loading, and is given by:

$$S_{t,T} = \frac{\sigma}{\epsilon_{t,T}} \tag{26.9}$$

where σ is the tensile stress and $\epsilon_{t,T}$ is the resultant strain after loading time t at temperature T. Figures 26.5 and 26.6 illustrate the effect of loading time and temperature for bitumens of different PI. For low PI bitumens (Figure 26.5) the stiffness is constant for very short loading times and virtually independent of temperature. This represents elastic behaviour. For longer loading times the curves have a consistent slope of 45° and have a significant variation with temperature indicating viscous behaviour. The effect of increasing PI can be seen by comparing Figures 26.5 and 26.6. High PI bitumens are much stiffer at high temperatures and longer loading times. Thus under conditions which are more likely to give rise to deformation, namely slow-moving or stationary traffic and high temperatures, a high PI bitumen offers greater resistance to deformation by virtue of its higher stiffness.

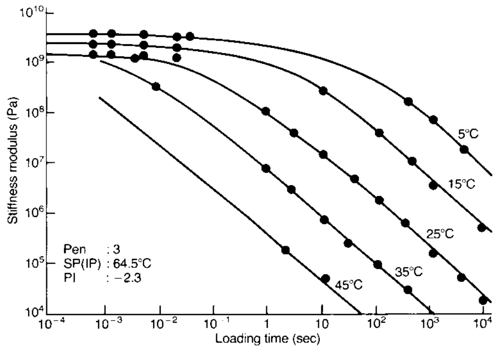

FIGURE 26.5 The effect of temperature and loading time on stiffness of a low PI bitumen (*The Shell Bitumen Handbook*, 1990).

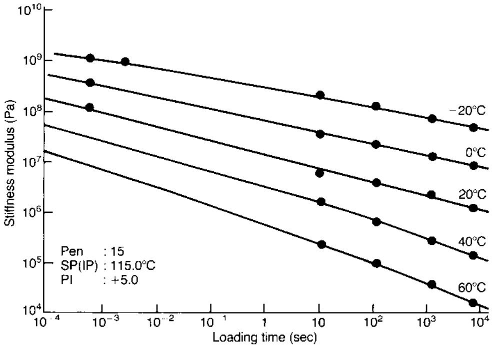

FIGURE 26.6 The effect of temperature and loading time on stiffness of a high PI bitumen (*The Shell Bitumen Handbook*, 1990).

When considering a bituminous mix, consisting of a graded aggregate bound with bitumen, the stiffness of the mix is dependent on the stiffness of the bitumen and the quantity and packing of aggregate in the mix. The quantity and packing of aggregate particles depends on grading, particle shape and texture, and method of compaction.

26.5 Determination of permanent deformation

Rutting of bituminous pavements is the most common type of failure in the UK. It is therefore important to be able to predict the deformation for a bituminous mix and this depends on the low stiffness response, that is the stiffness at long load times. Two tests which have been commonly used to determine fundamental values of stiffness are the creep test and the repeated load triaxial test.

In the creep test, a uniaxial load of 0.1 MPa is applied to a cylindrical specimen for 1 hour at

40°C. During the test, deformation is measured as a function of time. The stiffness, S_{mix}, of the mix may then be determined from:

$$S_{mix} = \frac{\text{Applied stress}}{\text{Axial strain}} \qquad (26.10)$$

Although simple, and giving good correlation with rutting measurements, the test does not employ a confining stress. In situ materials will clearly be confined and the effect of the confining stress on the vertical strain may be important.

The repeated load triaxial test overcomes this disadvantage and simulates more closely the actual conditions of stress in a bituminous pavement layer. This test is similar to that used in soil mechanics. A cylindrical specimen with a height/diameter ratio of at least 2.5:1 is subjected to a static confining pressure whilst a cyclic vertical stress is applied. The resulting vertical and horizontal strains can be measured and stiffness deduced. However, the good correlation between creep and rutting tests has led to the creep test being more commonly used.

A model has been developed (Hills *et al.,* 1974) linking creep results and rutting as follows:

$$R = \frac{C_m \times H \times \sigma_{av}}{S_{mix}} \qquad (26.11)$$

where R = rut depth, C_m = correlation factor varying between 1 and 2, H = layer thickness, σ_{av} = average stress in the pavement related to wheel load and stress distribution, and S_{mix} = stiffness of the mix as determined from the creep test.

26.6 Factors affecting permanent deformation

26.6.1 Bitumen viscosity

When a stress is applied to a bituminous material, both the aggregate particles and the bitumen will be subjected to the stress. But the aggregate particles, being hard and stiff, will undergo negligible strain, whereas the bitumen, being soft, will undergo considerable strain. Thus the deformation is associated with movement in the bitumen and the extent of the movement will depend on its viscosity. Figure 26.7 shows how the rate of deformation, as measured by the wheel-tracking test, varies with the softening point of the bitumen. It can be seen that a reduction in softening point of 5°C will approximately double the deformability.

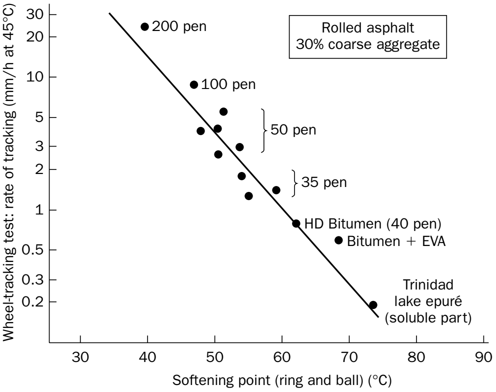

FIGURE 26.7 Effect of softening point of binder on resistance to deformation (Szatkowski, 1980).

26.6.2 Aggregate

Bituminous mixtures which utilize a continuously graded aggregate – macadams – rely mainly on aggregate particle interlock for their resistance to deformation. Thus the grading and particle shape of the aggregate are major factors governing deformation. The characteristics of the fine aggregate are particularly important in gap-graded materials which rely on a dense bitumen and fine mortar for their strength. These are the asphalt mixes. Sand particles can vary considerably from spherical glassy grains in dune sands, to angular and relatively rough grains from some pits. Mixes made with a range of sands all at the same bitumen content have been shown to give deformations, when tested in the laboratory wheel-tracking test, that varied by a factor of 4 from the best to the worst sand (Knight *et al.,* 1979).

26.6.3 Temperature

Figure 26.8 shows permanent strain against number of test cycles in a repeated load triaxial test. It can be seen that permanent strain increases with temperature. This is due to the reduction in viscosity of bitumen and consequent reduction in bitumen stiffness. The figure also indicates the effect of the aggregate grading. At low temperatures, the permanent strain in the asphalt and macadam are the same. Here the high degree of aggregate particle interlock in the macadam and the high viscosity bitumen in the asphalt provide a similar resistance to deformation. However, at higher temperatures, the asphalt deforms more because its stiffness is reduced by the reduced bitumen viscosity, which is not compensated by the aggregate interlock effect. In the macadam, although the bitumen will also be less stiff, the aggregate grading continues to provide a compensating resistance to deformation.

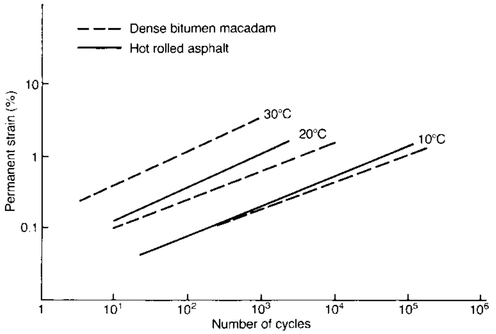

FIGURE 26.8 Comparison of permanent strain for dense macadam and hot rolled asphalt base mixes (Brown, 1978).

26.7 References

Brown, S.F. (1978) Material characteristics for analytical pavement design. In *Developments in Highway Pavement Engineering – I*, Applied Science Publishers, London.

Hills, J.F., Brien, D. and Van de Loo, P.J. (1974) *The Correlation of Rutting and Creep Tests on Asphalt Mixes*, Institute of Petroleum, IP-74–001.

Knight, V.A., Dowdeswell, D.A. and Brien, D. (1979) Designing rolled asphalt wearing courses to resist deformation. In *Rolled Asphalt Road Surfacings*, ICE, London.

Lubbers, H.E. (1985) *Bitumen in de weg – en waterbouw*. Nederlands Adviesbureau voor bitumentopassingen.

Pfeiffer, J.Ph. and Van Doormaal, P.M. (1936) The rheological properties of asphaltic bitumens. *Journal of Institute of Petroleum* 22.

Shell Bitumen UK (1990) *The Shell Bitumen Handbook*.

Szatkowski, W.S. (1980) Rolled asphalt wearing courses with high resistance to deformation. In *Rolled Asphalt Road Surfacings*, ICE, London.

Van der Poel, C. (1954) A general system describing the viscoelastic properties of bitumen and its relation to routine test data. *Journal of Applied Chemistry* 4, 224–36.

Chapter twenty-seven

Strength and failure of bituminous materials

27.1 The road structure

A flexible road structure consists of a number of layers of different materials, as illustrated in Figure IV.2 of the Introduction. In structural terms, the purpose of the road is to distribute the applied load from the traffic to a level which the underlying subgrade can bear. The stresses induced by the loads are high at the surface but reduce with depth. Thus, the surfacing material must be of high quality, but at greater depths below the surface, economies can be achieved by using materials of lower strength.

27.2 Modes of failure in a bituminous structure

Roads deteriorate in a number of ways, but broadly there are two forms of failure. First, the road surface may deteriorate. This may be through breakdown of the surface material either generally, for example through fretting or stone loss, or locally when a pot hole develops as a result of a local weakness. Alternatively, the surface texture of the wearing course may be reduced, through polish or abrasion, so that the skidding resistance drops below an acceptable level.

Second, the road structure deteriorates. It is this structural deterioration which will be discussed here. The key feature of such deterioration is that it is gradual, and develops with the continued application of wheel loads. In the early stages, the rate of deterioration is very small and the structural changes are not perceptible and are difficult to measure. But with continued service, signs of structural change become clearer and the rate of deterioration accelerates. There are two modes of breakdown which are illustrated in Figure 27.1. First, permanent deformation occurs in the wheel tracks. This ‘rutting’ is associated with deformation of all the pavement layers and is linked to a loss of support from the underlying subgrade. Deformation within the bituminous layers is an accumulation of the small irrecoverable part of the deformation caused by each wheel load. It is a function of the viscoelastic nature of the bitumen together with the mechanical support offered by the grading of the aggregate. The second mode of failure is cracking, which appears along the wheel tracks. The cracking is caused by the tensile strain developed in the bound layers as each wheel load passes. It is therefore a function of both the size of tensile strain, and the repetitive nature of the loading; that is a fatigue failure. It is important to note, as Figure 27.1 shows, that the cracking initiates at the base of the bound layer. This is where the tensile stresses are highest, as shown in Figure 27.2. It follows that, by the time the cracking is visible at the surface, the damage has been present for some time.

In both modes of failure, the breakdown is caused by (a) the repetitive nature of the loading, and (b) by the development of excessive strains in the structure. This leads to the notion that, if failure can be defined, the life of a road can be determined provided that the loading can be assessed and the performance of the materials evaluated. Alternatively, the structural design of the road together with the make-up of the materials to give required properties may be determined, in order to provide a given life. In either case, it is necessary to define failure. In most civil engineering structures, structural failure renders the structure unusable and is often associated with collapse. However, whilst roads may become less comfortable to drive on and less safe, they do not, except in very extreme cases, become unusable. Therefore failure for roads must be identified in terms of serviceability and/or repairability; that is,

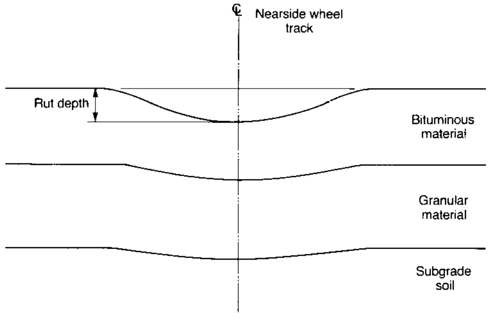

(a) Permanent deformation

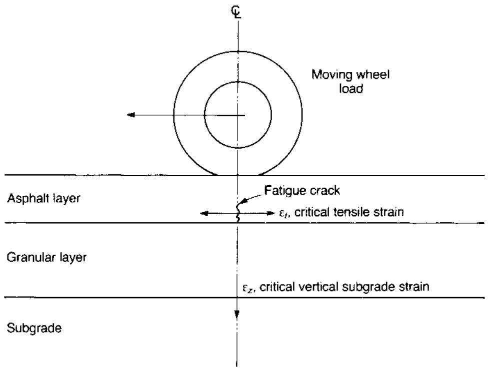

(b) Fatigue cracking and critical strains

FIGURE 27.1 Modes of failure and critical strains in a flexible pavement (Brown, 1980).

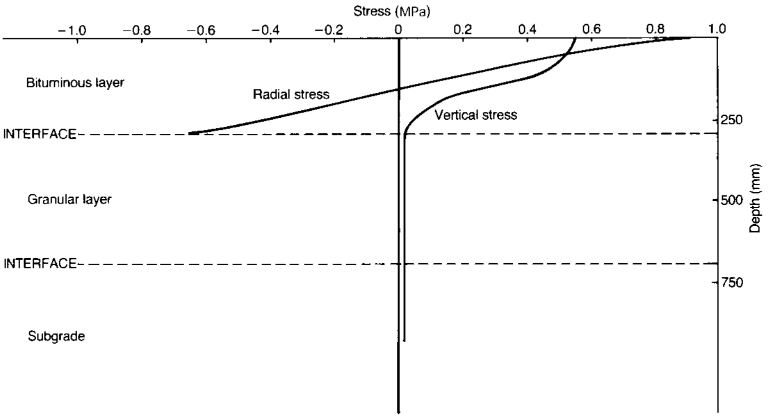

FIGURE 27.2 Variation of vertical and radial stresses below the centreline of a 40 kN wheel load acting over a circular area of radius 160 mm, with a contact pressure of 0.5 MN/m^2 (Peattie, 1978).

the extent of cracking and deformation must be defined which is just acceptable to drivers and/or which represents a condition which may be economically restored by repair. A definition is provided, in terms of both modes of failure, which identifies three conditions: sound, critical, and failed. Table 27.1 shows that if any cracking is visible at the surface, then the road is regarded as being at critical condition or as having failed. Here the term 'critical' means that failure is imminent but the road still has sufficient structural capability to support strengthening and to provide an extended life from the strengthened road. If there are no signs of cracking, then the condition is defined in terms of the extent of permanent deformation. Thus, if the rut depth reaches 20 mm, the road is regarded as having failed.

27.3 Fatigue characteristics

The development of permanent deformation has already been discussed. Here the fatigue characteristics of bituminous mixes, leading to cracking, will be examined. Fatigue cracking arises from the fact that, under repeated applications of tensile stress–strain, a bituminous material will eventually fracture. The higher the level of stress and strain applied, the smaller the number of load applications before cracking occurs. For a particular level of stress and strain, the mix proportions and nature of the bitumen dictate the number of cycles before cracking occurs.

A number of laboratory tests have been developed to assess the fatigue characteristics of bituminous materials. The tests, illustrated in Figure 27.3, are flexure tests and simulate the repeated bending action in the stiff bound layer of a pavement caused by the passage of each wheel load. The number of load cycles which a particular specimen can endure before failure depends on a number of factors discussed below.

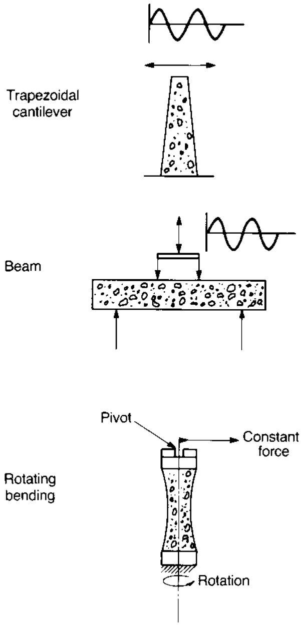

FIGURE 27.3 Methods for fatigue testing of bituminous materials (Brown, 1978).

TABLE 27.1 Criteria for determining pavement condition (Department of Transport, 1983, Advice Note HA/25/83. Reproduced with permission of the Controller of HMSO. © Crown copyright).

	Wheel-track rutting under a 2 m straight edge			
Wheel-track cracking	*Less than 5 mm*	*From 5 mm to <10 mm*	*From 10 mm to <20 mm*	*20 mm or greater*
None	Sound	Sound	Critical	Failed
< half width or single crack	Critical	Critical	Critical	Failed
> half width	Failed	Failed	Failed	Failed

27.3.1 Stress and strain conditions

Fatigue tests may be conducted in two ways. They may be constant stress tests, where each load application is to the same stress level regardless of the amount of strain developed. Alternatively they may be constant strain tests, where each load application is to the same strain level regardless of the amount of stress required.

These two alternatives produce quite different results. Figure 27.4(a) shows the general pattern of results from constant stress tests. Each line represents a different test temperature, i.e. a different stiffness, and it can be seen that mixes with higher stiffness have longer lives. Figure 27.4(c) shows the general pattern of results from constant strain tests. Again each line represents a different temperature or stiffness and it can be seen that the outcome is reversed, with the mixes of higher stiffness having the shortest lives. This contrast may be explained in terms of the failure mechanism. Cracks initiate at points of stress concentration and propagate through the material until fracture occurs. If the stress level is kept constant, the stress level at the tip of the crack continues to be high so that propagation is rapid. However, in a constant strain test, the development of a crack causes a steady reduction in the applied stress level because the cracks contribute more and more to the strain as they propagate. Thus the stress at the crack tips reduces and rate of propagation is slow. Thus it is important to establish which test condition is most relevant to actual pavement behaviour. It has been shown (Monismith and Deacon, 1969) that strain control is appropriate to thin layers (for example surfacing layers), whereas stress control is appropriate to thicker structural layers. This is because pavements are subject to a stress controlled loading system, so that the main (and normally thick) structural layers are stress controlled. However, the thin surface layer must move with the lower structural layers and so is effectively subject to strain control. Nevertheless, under low

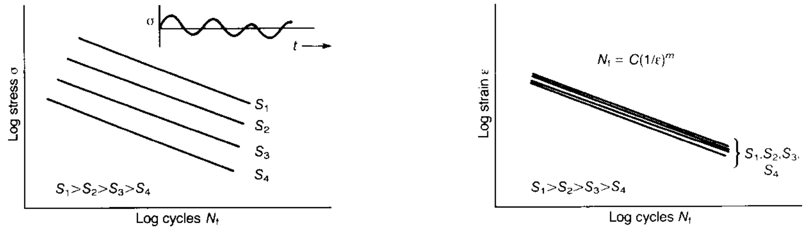

(a) Controlled stress tests
at different stiffnesses
S_1, S_2, etc.
Log σ v Log N_f

(b) Controlled stress tests
Log ε v Log N_f

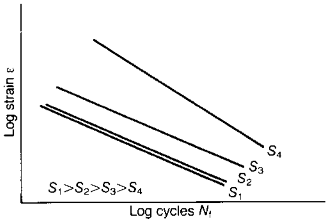

(c) Controlled strain tests
Log ε v Log N_f

FIGURE 27.4 Fatigue lines representing number of cycles to failure, N_f, under different test conditions (Brown, 1980).

temperature conditions giving high stiffness, crack propagation is relatively quick even under strain controlled loading so that the difference between the two loading conditions is small.

27.3.2 The strain criteria

If the results of a controlled stress test are expressed in terms of an equivalent strain then the log–log plot of strain against number of load cycles produces a single linear relationship for all test conditions for a particular mix, as shown in Figure 27.4 (b). In other words the relationship is independent of mix stiffness. This suggests that strain is the principal criterion governing fatigue failure, and it has been demonstrated (Cooper and Pell, 1974) that flexure tests on a wide range of mixes produce unique fatigue lines for each mix. The general relationship defining the fatigue line is:

$$N_f = C\left(\frac{1}{\epsilon}\right)^m \tag{27.1}$$

where N_f is the number of load cycles to initiate a fatigue crack, ϵ is the maximum applied tensile strain, and C and m are constants depending on the composition and properties of the mix.

The fatigue lines for a range of mixes are shown in Figure 27.5 together with details of the mix compositions in Table 27.2.

27.3.3 Effect of mix variables

A large number of variables associated with the mix affect the fatigue line. However, it has been shown (Cooper and Pell, 1974) that two variables are of prime importance. These are:

1. the volume of bitumen in the mix;
2. the viscosity of the bitumen as measured by the softening point.

As the volume of bitumen increases up to 15 per cent, the fatigue life increases, and as the bitumen becomes more viscous, with softening point increasing up to 60°C, the fatigue life also increases.

Other factors are important insofar as they affect the two main variables. The void content of the mix has an effect on the volume of bitumen. The total void content is, in turn, affected by the particle shape and grading of the aggregate, the compactive effort, and the temperature. In other words there is a link between workability, compactive effort and void content which is con-

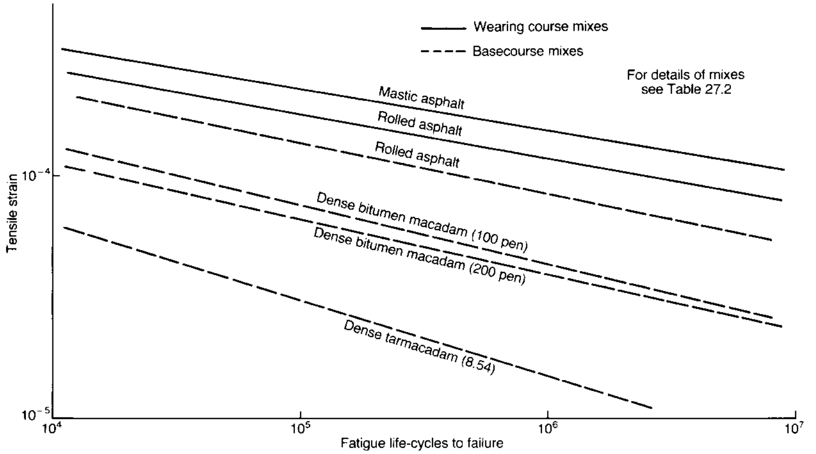

FIGURE 27.5 Fatigue lines under controlled stress conditions for a range of bituminous mixes (Brown, 1980).

TABLE 27.2 Details of mixes represented in Figure 27.5 (Brown, 1980)

Description of mix	*Coarse aggregate (% by mass)*	*Fine aggregate (% by mass)*	*Filler (% by mass)*	*Binder (% by mass)*	*Mean void content (%)*	*Fatigue line constants*	
						C	*m*
Mastic asphalt wearing course	42 crushed rock	23 limestone	20 limestone	15:70/30 TLA[1]/20 pen bit.	0	1.1×10^{-15}	5.5
Rolled asphalt wearing course	30 crushed rock	53.2 sand	8.9 limestone	7.9 45 pen	2.9	1.3×10^{-14}	5.1
Rolled asphalt basecourse	65 crushed rock	29.3 sand	–	5.7 45 pen	4.0	3.2×10^{-8}	3.2
Dense bitumen macadam basecourse	62 crushed rock	28.6 crushed rock	4.7 crushed rock	4.7 100 pen	6.8	2.0×10^{-11}	3.8
Dense bitumen macadam basecourse	62.3 crushed rock	28.7 crushed rock	4.7 crushed rock	4.3 200 pen	6.9	2.5×10^{-12}	4.0
Dense tar macadam basecourse	61.7 crushed rock	28.4 crushed rock	4.7 crushed rock	5.2 B54	7.5	1.0×10^{-7}	2.7

Notes:

1. Trinidad Lake asphalt.

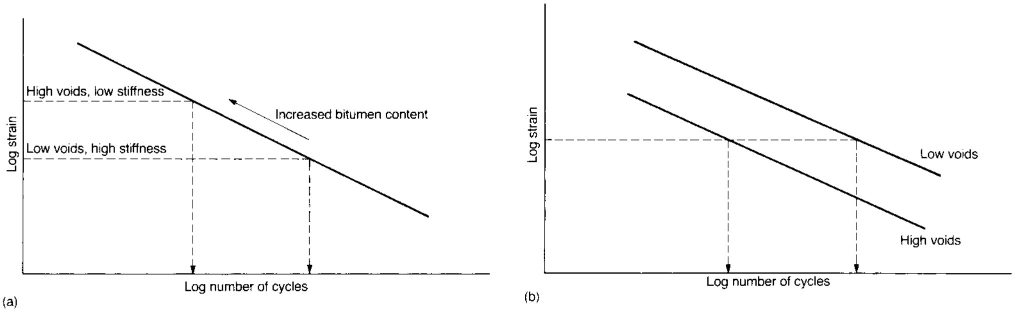

FIGURE 27.6 The influence of voids on fatigue life.

trolled by the bitumen content. However, whilst a higher bitumen content improves fatigue life, it also reduces stiffness which leads to increased strain. Figure 27.6 illustrates the double influence of void content. Figure 27.6 (a) shows the effect that an increased bitumen content has on stiffness. The stiffness is reduced which increases the strain under constant stress conditions causing a shift to the left along the fatigue line. Thus the fatigue life is reduced. Figure 27.6 (b) shows the influence that void content has on the fatigue line so that, for the same strain, the fatigue life is reduced as void content increases. The change in position of the fatigue line corresponds to a change in material type, as was seen in Figure 27.5, whereas the shift along a fatigue line due to a stiffness change corresponds to a change in degree of compaction. However, in practice, both effects occur if the change in void content is associated with a change in bitumen content.

27.4 References

Brown, S.F. (1978) Material characteristics for analytical pavement design. In *Developments in Highway Pavement Engineering – 1*, Applied Science Publishers, London.

Brown, S.F. (1980) *An Introduction to the Analytical Design of Bituminous Pavements*, Department of Civil Engineering, University of Nottingham.

Cooper, K.E. and Pell, P.S. (1974) The Effect of Mix Variables on the Fatigue Strength of Bituminous Materials. *Transport and Road Research Laboratory, Laboratory Report* 633, Department of Transport (1983) Departmental Advice Note *HA/25/83*.

Monismith, C.L. and Deacon, J.A. (1969) Fatigue of asphalt paving mixtures. *Journal of Transport Engineering Division, ASCE* 95, 154–61.

Peattie, K.R. (1978) Flexible pavement design. In *Developments in Highway Pavement Engineering,* Applied Science Publishers, London.

Chapter twenty-eight

Durability of bituminous mixtures

28.1 Introduction

Durability is the ability to survive and continue to give an acceptable performance. In the case of roads, it is necessary that the structure should survive for the specified design life, although it is accepted that not all aspects of performance can be sustained for this duration without some restorative maintenance. The design guide for UK roads suggests a design life of 40 years (Department of Transport, 1987), although this can only be achieved in stages, as shown in Figure 28.1. The durability of a flexible road structure depends on the durability of the materials from which it is constructed, in particular the bitumen-bound materials. Bituminous materials may deteriorate in a number of ways. The bitumen itself will harden with exposure to oxygen and temperature effects, the aggregate may not be of sufficient quality so that some individual particles may break down, or there may be loss of adhesion between the bitumen and aggregate particles. These forms of deterioration are caused by weathering and the action of traffic. These agents act at the road surface which is particularly vulnerable. However, deterioration can also occur in the body of the material and this is controlled by its permeability.

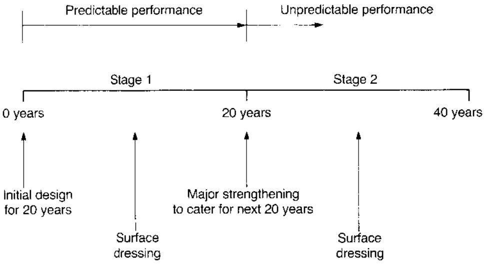

FIGURE 28.1 The life of a flexible road.

28.2 Ageing of bitumen

The ageing or hardening of bitumen is an inevitable result of exposure of bitumen to the atmosphere. The rate of hardening will depend on the conditions and the nature of the bitumen. There are two main processes which occur: oxidation and loss of volatiles.

28.2.1 Oxidation

In the oxidation process, oxygen molecules from the air combine with the resins to form asphaltenes. Thus there is an increase in the polar, high molecular weight fraction at the expense of the lower molecular weight resins. The result is an increase in viscosity of the bitumen. Also, the bitumen becomes unstable due to the discontinuity which develops between the saturates and the rest of the components. This instability causes a lack of cohesion within the bitumen which will lead to cracking. The rate of oxidation is highly dependent on temperature, and is rapid at the high temperatures used for mixing and laying bituminous materials.

28.2.2 Loss of volatiles

Loss of volatiles will occur if there is a substantial proportion of low molecular weight components in the bitumen, and if the bitumen is subjected to high temperatures. However, for penetration grade bitumens, the loss of volatiles once the material has been laid is relatively small.

28.2.3 Ageing index

The hardening of bitumen results in a lowering of penetration, an increase in softening point and an increase in penetration index. Therefore an excessive amount of hardening will cause the material to be brittle at low temperatures and vulnerable to cracking. A convenient means of evaluating the ability of a bitumen to resist hardening is to use the microfilm durability test (Griffin *et al.,* 1955). The test consists of ageing films of bitumen 5 microns thick on glass plates in an oven at 225°F for two hours. The hardening which occurs is determined by measuring the viscosity of the material before and after this exposure with the sliding plate microviscometer. The ratio of the viscosity of the aged asphalt to that of the original asphalt is the ageing index.

Ageing index is strongly influenced by the initial molecular weight of the asphalt. Figure 28.2 shows that ageing index can be large in asphalts with low molecular weight. A satisfactory durability (ageing index less than 10) can be obtained if components with a molecular weight less than 400 are eliminated.

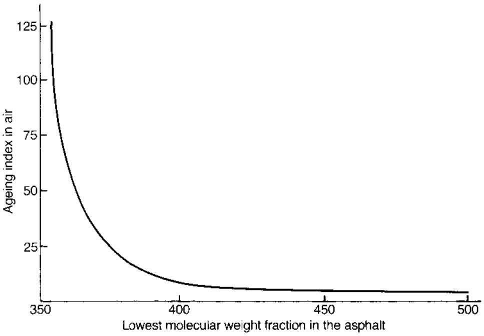

FIGURE 28.2 Influence of initial molecular weight on durability (Griffen *et al.*, 1959).

In practice, the ageing of bitumen is most marked during the mixing process because high temperatures are involved. For example, the penetration value of a 50 pen bitumen will fall to between 30 and 40 depending on the duration of the mixing and the temperature used; subsequent high temperature storage will cause further ageing. Thus the penetration value could be reduced by as much as half. Ageing of bitumen on the road is generally a much slower process. This is because the temperatures are much lower and the availability of oxygen is restricted by the permeability of the mix. In more open-textured mixes with a large volume of interconnected voids, air can readily permeate the material allowing oxidation to occur. Macadams generally fall into this category. However, in dense mixes such as asphalts, the permeability is low and there will be very little movement of air through the material. In both cases, ageing will be more rapid at the surface than in the bulk of the material because there is a continual availability of oxygen and the surface will reach higher temperatures.

28.3 Permeability

Permeability is an important parameter of a bituminous mixture because it controls the extent to which both air and water can migrate into the material. The significance of exposure to air was described in the previous section. Water may also bring about deterioration by causing the bitumen to strip from the aggregate particles, or causing breakdown of the aggregate particles themselves. Furthermore, permeability controls the extent of frost damage. Thus permeability may be regarded as a measure of durability.

28.3.1 Measurement and voids analysis

The measurement of permeability is, in essence, a simple task, achieved by applying a fluid under pressure to one side of a specimen of a bituminous mixture and measuring the resulting flow of fluid at the opposite side. Both air and water have been used as the permeating fluid. A permeability cell developed for the measurement of permeability of concrete, shown in Figure 28.3, has been used successfully to measure the permeability of hot rolled asphalt to oxygen (Robinson, 1991). Here a constant fluid pressure is maintained. By contrast, a falling head permeameter has been used (Khalid, 1990) with water as the permeating fluid. More recently an air permeability test (Cabrera and Hassan, 1994) has been described which can be used both in the laboratory and in the field.

28.3.2 Factors affecting permeability

The permeability of a bituminous mixture depends on a large number of factors. Of particular importance is the quantity of voids, the distribution of void size and the continuity of the voids. Figure 28.4 shows how permeability varies with total voids in the mix for an open-textured bituminous macadam. It can be seen that the permeability is more sensitive to void content at high binder contents. This is likely to be due to the size and continuity of pores. At low binder contents, the pores are large and although a reduction in the volume of voids will tend also to reduce the pore size, the size will remain sufficiently large to permit high permeability. At high binder contents, however, the pores are relatively small and a reduction in the volume of voids will cause a significant change in pore size with a much greater effect on permeability. A change in continuity of the voids is also more likely at higher binder contents when pores will be plugged with bitumen as the volume of voids reduces.

The voids are also affected by the nature of the aggregate. The shape, texture and grading of the particles will govern the packing and hence void content at a particular bitumen content. The amount of compactive effort employed is also important.

28.4 Adhesion

The quality of the adhesion of a bitumen to an aggregate is dependent on a complex assemblage of variables. Table 28.1 identifies a number of

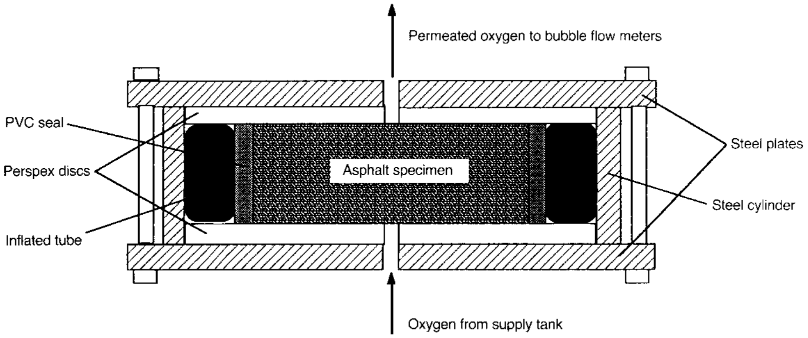

FIGURE 28.3 Schematic diagram of permeability test cell.

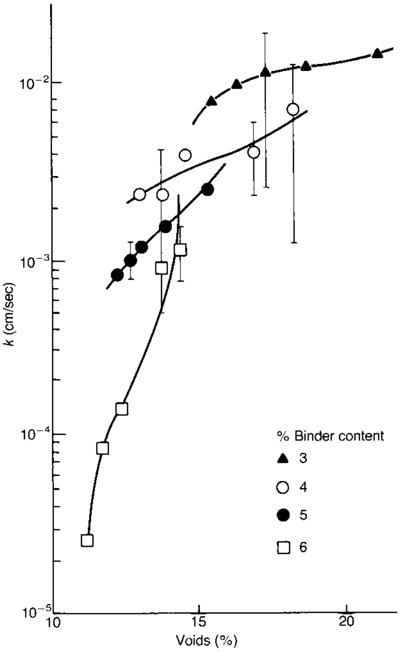

FIGURE 28.4 Relationship between the coefficient of permeability, *k*, and voids content of an open-textured bituminous macadam mix (Khalid, 1990).

factors which have an influence on the adhesion performance of bituminous mixes. Although some of these relate to the ambient conditions and aspects of the mix as a whole, the principal factors are the nature of the aggregate and, to a lesser extent, the bitumen.

28.4.1 The nature of the aggregate

The mineralogical and physical nature of the aggregate particles has an important bearing on adhesion, with the adhesive capacity being a function of chemical composition, shape and structure, residual valency, and the surface area presented to the bitumen.

Generalizations about the effect of mineralogy are difficult because the effects of grain size, shape and texture are also important. However, there seem to be a preponderance of reports of failures with the more siliceous aggregates such as granites, rhyolites, quartzites, siliceous gravel and cherts. The fact that good performance with these materials has also been reported, and that failures in supposedly good rock types such as limestones and basic igneous rocks have occurred, emphasizes the complexity of the various material interactions. Therefore caution should be exercised when attempting to make generalizations on the

TABLE 28.1 Material properties and external influences which can act singularly or together to affect the adhesion and stripping resistance of a bituminous mix

Aggregate properties	*Bitumen properties*	*Interactive mix properties*	*External influences*
Mineralogy	Composition and source	Compaction	Annual precipitation*
Surface texture	Durability and weathering	Grading	Relative humidity*
Porosity	Viscosity	Permeability	pH of water*
Surface coatings and dust	Curing time	Binder content	Presence of salts*
Mechanical durability	Oxidation	Cohesion	Temperature*
Surface area	Electrical polarity	Film thickness	Temperature cycling*
Absorption	Use of additives	Filler type	Light, heat and radiation*
Moisture content		Type of mix	Traffic
Abrasion pH		Method of production	Construction practice
Weathering grade		Use of additive	Design
Exposure history			Workmanship
Shape			Drainage
Additives			

* Factors considered uncontrollable.

adhesion performance of aggregates of different or even similar mineralogy.

The surface character of each individual aggregate type is important particularly in relation to the presence of a residual valency or surface charges. Aggregates with unbalanced surface charges possess a surface energy which can be attributed to a number of factors, including broken coordination bonds in the crystal lattice, the polar nature of minerals, and the presence of adsorbed ions. Such surface energy will enhance the adhesive bond if the aggregate surface is coated with a liquid of opposite polarity.

Absorption of bitumen into the aggregate depends on several factors, including the total volume of permeable pore space, and the size of the pore openings. The presence of a fine microstructure of pores, voids and microcracks can bring about an enormous increase in the absorptive surface available to the bitumen. This depends on the petrographic characteristics of the aggregate as well as its quality and state of weathering.

It is generally accepted that rougher surfaces exhibit a greater degree of adhesion. A balance is, however, required between the attainment of good wettability of the aggregate (smooth surfaces being more easily wetted), and a rougher surface which holds the binder more securely once wetting is achieved. The presence of a rough surface texture can mask the effects of mineralogy.

28.4.2 The nature of the bitumen

The important characteristics of the bitumen affecting adhesion to aggregate are its viscosity and surface tension, and its polarity.

The viscosity and surface tension will govern the extent to which bitumen is absorbed into the pores at the surface of the aggregate particles. Both these properties are altered with temperature, and mixing of aggregate and bitumen is always done at high temperature – up to 180°C for 50 pen bitumen – in order that the bitumen coats the aggregate surface readily.

Bitumen will also chemically adsorb onto aggregate surfaces. Strongly adsorbed bitumen fractions have been identified at the bitumen aggregate interface, forming a band of the order of 180 Å thick. Ketones, dicarboxylic anhydrides, carboxylic acids, sulphoxides and nitrogen-bearing components have been found in this layer (Ensley, 1975). The strongly adsorbed components have been found to have sites capable of hydrogen bonding to the aggregate, though in the presence of water the available bonds prefer the more active water. A migration of some bitumen components to the interface is inferred and therefore a dependence on binder composition, mixing temperature and viscosity. Figure 28.5 illustrates the process, with molecules of bitumen at the surface aligned in the direction of polarity of the substrate (aggregate), usually a negative surface. The zone of orientation of bitumen molecules extends for a thickness of several thousand molecules.

28.4.3 Mechanisms for loss of adhesion

Breakdown of the bond between bitumen and aggregate, known as stripping, may occur for a

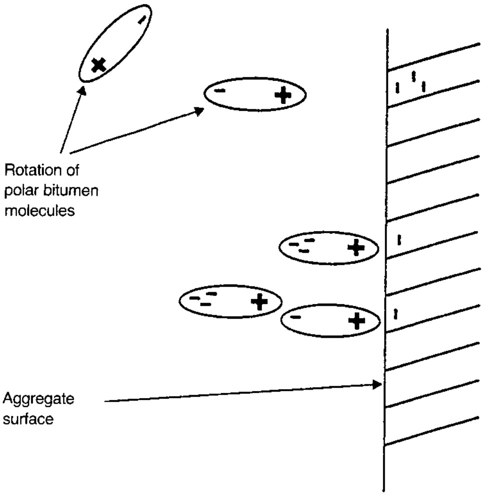

FIGURE 28.5 Adsorption of bitumen molecules to the aggregate surface (Ensley, 1975).

number of reasons. However, the principal agencies are the action of traffic, weathering and moisture, and these often act in combination.

Weathering may affect the aggregate itself but is a strong influence on the bitumen causing ageing through exposure to ultra-violet light. The consequent loss of ductility of the bitumen will render it more vulnerable to brittle fracture and the coating of aggregate particles may be broken.

The effect of moisture is more significant since it causes loss of adhesion in a number of ways (Hargreaves, 1987). A number of mechanisms have been postulated for adhesion loss and most involve the action of water. These are described below and each may occur depending on the circumstances.

Displacement

This occurs when the bitumen retracts from its initial equilibrium position as a result of contact with moisture. Figure 28.6 illustrates the process in terms of an aggregate particle embedded in a bituminous film (Majidzadeh and Brovold, 1968). Point *A* represents the equilibrium contact position when the system is dry. The presence of moisture will cause the equilibrium point to shift to *B* leaving the aggregate particle effectively displaced to the surface of the bitumen. The positions of points *A* and *B* will depend on the type and viscosity of bitumen.

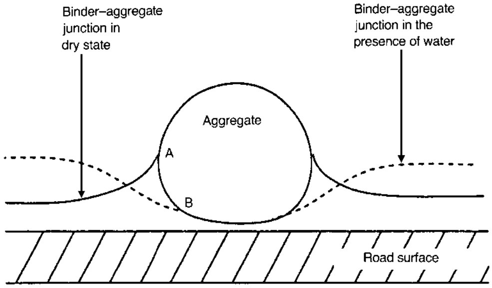

FIGURE 28.6 Retraction of the binder–water interface over the aggregate surface in the presence of water (Majidzadeh and Brovold, 1968).

Detachment

This occurs when the bitumen and aggregate are separated by a thin film of water or dust though no obvious break in the bitumen film may be apparent. Although the bituminous film coats the aggregate particle, no adhesive bond exists and the bitumen can be clearly peeled from the surface.

Film rupture

This occurs when the bitumen fully coats the aggregate but where the bitumen film thins, usually at the sharp edges of the aggregate particle (Figure 28.7).

Blistering and pitting

If the temperature of bitumen at the surface of a road rises, its viscosity reduces. This reduced viscosity allows the bitumen to creep up the surface of any water droplets which fall on the surface, and may eventually form a blister (Figure 28.8). With further heating, the blister can expand and cause the bitumen film to rupture, leaving a pit.

Spontaneous emulsification

Water and bitumen have the capacity to form an emulsion with water at the continuous phase. The

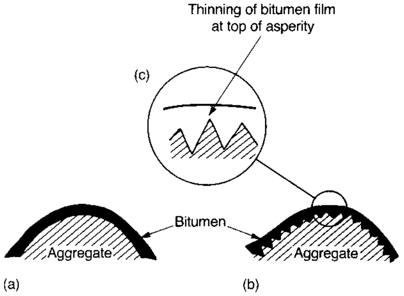

FIGURE 28.7 Thinning of the bitumen film on an aggregate with rough surface texture (b, c). Smooth aggregates (a) retain an unstressed and even film.

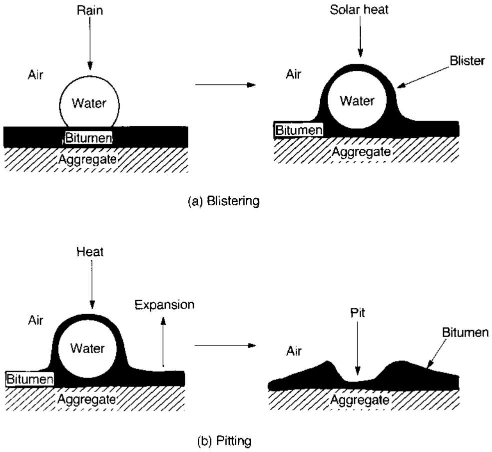

FIGURE 28.8 Formation of blisters and pits in a bituminous coating (Thelan, 1983).

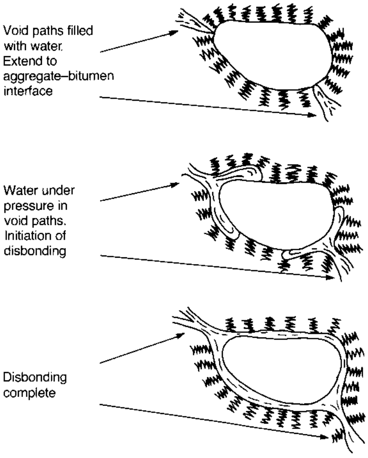

FIGURE 28.9 Pore pressure disbonding mechanism (McGennis *et al.*, 1984).

emulsion formed has the same negative charge as the aggregate surface and is thus repelled. The formation of the emulsion depends on the type of bitumen, and is assisted by the presence of finely divided particulate material such as clay materials, and the action of traffic.

Hydraulic scouring

This is due principally to the action of vehicle tyres on a wet road surface. Water can be pressed into small cavities in the bitumen film in front of the tyre and, on passing, the action of the tyre sucks up this water. Thus a compression–tension cycle is invoked which can cause disbonding.

Pore pressure

This mechanism is most important in open or poorly compacted mixes. Water can become trapped in these mixes as densification takes place by trafficking. Subsequent trafficking acts on this trapped water and high pore pressures can result. This generates channels at the interface between bitumen and aggregate (Figure 28.9) and eventually leads to disbonding.

Chemical disbonding

Diffusion of moisture through the bituminous coatings can lead to the layers of water building up in the interfacial region.

28.5 References

Cabrera, J.G. and Hassan, T.Q.M. (1994) Quality control during construction of bituminous mixtures using a simple air permeability test. In: *Performance and Durability of Bituminous Materials*, E & FN Spon, London.

Ensley, E.K. (1975) Multilayer absorption with molecular orientation of asphalt on mineral aggregate and other substrates. *Journal of Applied Chemistry and Biotechnology* 25, 671–82.

Griffin, R.L., Miles, T.K. and Penther, C.J. (1955) Microfilm durability test for asphalt. *Proceedings of the Association of Asphalt Paving Technologists* 24, 31.

Griffin, R.L., Simpson, W.C. and Miles, T.K. (1959) Influence of composition of paving asphalt on viscosity, viscosity–temperature susceptibility, and durability. *Journal of Chemical and Engineering Data* 4, 89–93.

Hargreaves, A. (1987) An investigation of the premature failure of bituminous macadam wearing courses with particular reference to the effects of moisture and aggregate quality. PhD thesis, Hatfield Polytechnic.

Khalid, H. (1990) Permeability: implications in asphalt mix design. Highways Asphalt 90 Supplement, *Highways,* Faversham House Group.

Majidzadeh, K. and Brovold, F.N. (1968) *State of the Art: Effect of Water on Bitumen–Aggregate Mixtures*, Highway Research Board, Publication 1456, Special Report 98, 77.

McGennis, R.B., Kennedy, T.W. and Machemehl, R.B. (1984) *Stripping and Moisture Damage in Asphalt Mixtures*, Research Report 253.1, Project 39–79–253, Centre for Transportation Research, University of Texas, USA.

Robinson, D. (1991) An Investigation into Wearing Course Failure on the A414 Breakespeare Way, Hemel Hempstead. Unpublished project report, Hatfield Polytechnic.

Thelan, E. (1958) Surface energy and adhesion properties in asphalt–aggregate systems. *Highway Research Board Bulletin* 192, 63–74.

Chapter twenty-nine

Practice and processing of bituminous materials

29.1 Bituminous mixtures

There are a very large number of bituminous mixtures which vary according to density, bitumen content, bitumen grade, and aggregate size and grading. However, most can be classified into two groups, namely asphalts and macadams.

29.1.1 Asphalts

Asphalts are dense materials and are characterized by their high bitumen content and high filler/fines content. They derive their strength and stiffness from a dense, stiff mortar of bitumen, filler and fines. The coarse aggregate content is relatively low so that the overall particle size distribution is gap-graded. Figure IV.1 (a) of the Introduction illustrates these features and it can be seen that the material transmits load through the mortar continuum. This mortar, being rich in bitumen, is expensive and the coarse aggregate serves to increase the volume of the mortar with a relatively cheap material, thereby reducing the overall cost. The binder used for asphalt will normally be 50 or 70 pen and may either be penetration grade bitumen or a blend of bitumen with pitch or lake asphalt. Because of the hardness of the binder and the higher filler/fines content, the workability is low, and high temperatures have to be used to mix, lay and compact the material, which adds to the cost. Freshly laid wearing course asphalt (known as hot rolled asphalt) presents a smooth surface with coarse aggregate particles submerged with the mortar. In order to provide a skid-resistant surface, coated chippings are rolled into the surface. This also adds to the cost. Asphalts have a very low permeability, and are capable of transmitting high stresses whilst providing some ductility. They are therefore very durable, and normally used where traffic loads are high or durability is important.

There are three groups of asphalt mixtures (BS 594: 1992): Group 1 mixtures are for roadbases, base courses and regulating courses; Group 2 mixtures are designed wearing course mixtures; Group 3 mixtures are recipe wearing course mixtures. Wearing course mixtures may be either type F incorporating fine sand, or type C incorporating crushed rock or slag fines which are more coarsely graded. The coarse aggregate is either 14 mm or 20 mm nominal size and varies in content from

30–55 per cent. Higher proportions are associated with larger size. In the designed wearing course mixtures, the binder content is determined from a design process which will be described in the following section. Table 29.1 shows the specification for Group 1 mixtures as an example. It can be seen that each mixture is designated according to the coarse aggregate content and its nominal size. Thus a 50/20 mixture has 50 per cent coarse aggregate with a nominal size of 20 mm.

29.1.2 Macadams

Macadams range from dense mixtures to open-textured mixtures. They are characterized by a relatively low binder content and a continuously graded aggregate.

Macadams rely on the packing and interlock of the aggregate particles for their strength and stiffness. The binder coats the aggregate, and acts as a lubricant when hot and an adhesive and waterproofer when cold. The grade of binder used is softer than for asphalts being 100 or 200 pen. Figure IV.1 (b) of the Introduction illustrates these features and it can be seen that the material transmits load through the aggregate structure. Because of their lower binder content, macadams are cheaper than asphalts. In general macadams have a higher void content than asphalts so they are more permeable and less durable. They lack ductility and are generally used on less heavily trafficked roads.

Macadams are classified according to the nominal size of the aggregate, the grading of the

TABLE 29.1 Composition of roadbase, basecourse and regulating course hot rolled asphalt mixtures (BS 594: 1992) Reproduced with the permission of the British Standards Institution under licence number 2001/SK0230.

Column number	*1*	*2*	*3*
Designation*	50/14†	50/20†	60/20
Nominal thickness of layer (mm)	35 to 65	45 to 80	45 to 80
Percentage by mass of total aggregrate passing BS test sieve			
50 mm	–	–	–
37.5 mm	–	–	–
28 mm	–	100	100
20 mm	100	90 to 100	90 to 100
14 mm	90 to 100	65 to 100	30 to 65
10 mm	65 to 100	35 to 100	–
6.3 mm	–	–	–
2.63 mm	35 to 55	35 to 55	30 to 44
600 μm	15 to 55	15 to 55	10 to 44
212 μm	5 to 30	5 to 30	3 to 25
75 μm	2 to 9	2 to 9	2 to 8
Binder content, % by mass of total mixture for:			
Crushed rock or steel slag	6.5	6.5	5.7
Gravel	6.3	6.3	5.5
Blast furnace slag: bulk density (kg/m^3)			
1440	6.6	6.6	5.7
1360	6.7	6.7	5.9
1280	6.8	6.8	6.0
1200	6.9	6.9	6.1
1120	7.1	7.1	6.3

* The mixture designation numbers (e.g. 50/14 in column 1) refer to the nominal coarse aggregate content of the mixture/nominal size of the aggregate in the mixture respectively.

† Suitable for regulating course.

aggregate and the intended use of the material (BS 4987: 1993). The main mixtures available are:

1. roadbase – 40 mm dense roadbase
2. basecourse – 40 and 20 mm open-textured basecourse
   - 40 mm single course
   - 40, 28 and 20 mm dense basecourse
3. wearing course – 14 and 10 mm open-textured wearing course
   - 14 and 10 mm dense wearing course
   - 10 mm medium-texture wearing course
   - 6 mm fine-textured wearing course.

(The last two mixes are referred to as coarse cold asphalt and fine cold asphalt respectively even though they are macadams.)

For the open-textured mixes, the fines content is low (less than 15 per cent), whereas for the medium- and fine-textured materials, the fines content is higher (40–60 per cent and more than 75 per cent respectively). The dense materials have a closely specified aggregate grading and a low voids content (about 4 per cent). Their density and consequent strength are more in line with some types of asphalt.

Although asphalts and macadams have distinctive features, they in fact represent opposite ends of a spectrum of materials. This range covers a variation in the proportions of the constituents and the void content, and is illustrated in Figure 29.1. It can be seen that in the middle of the range the roadbase asphalts and dense macadams are not so different from one another.

29.1.3 Other mixtures

There are other bituminous mixtures which do not fit the general description of asphalts or macadams described in the previous sections. Two that are beginning to be used widely are porous asphalt and stone mastic asphalt.

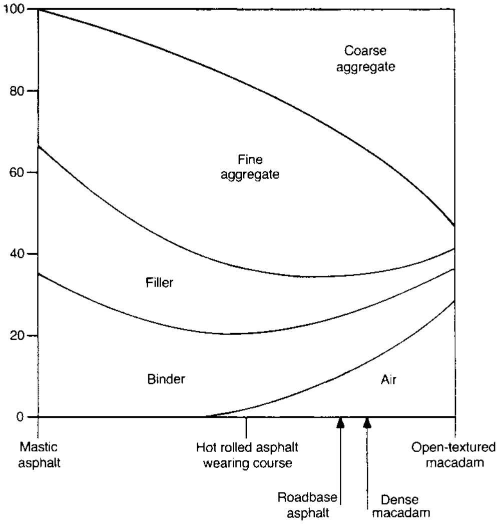

FIGURE 29.1 Constituent proportions of various bituminous materials.

Porous asphalt

In spite of its name, porous asphalt is essentially a graded aggregate bound with bitumen, and is included in the British Standard for macadam mixtures (BS 4987: 1993). It is designed to provide a large volume (at least 20 per cent) of interconnected air voids so that water can drain through the material and run off within the thickness of the layer. This requires the underlying basecourse to be impermeable. The aggregate grading consists predominantly of coarse aggregate: about 75 per cent passing 2.36 mm. The fine aggregate fractions are added to enhance the cohesion and stiffness of the mixture but in sufficiently small quantity so as not to interfere with the interlock of the coarse particles, and to leave enough voids to provide a pervious structure. Because of its porous nature, the material is vulnerable to ageing through oxidation of the bitumen. To counteract this, the bitumen content must be sufficient to provide a thick coating on the coarse aggregate particles. Typically 5 per cent of 100 pen bitumen is used. The advantages of porous asphalt are that it minimizes spray in wet weather, reduces surface noise, improves skidding resistance, and offers lower rolling resistance than dense mixtures. However, it is less strong than denser mixtures and UK pavement design practice assumes that a 60 mm layer of porous asphalt is structurally equivalent to 20 mm of hot rolled asphalt wearing course.

Stone mastic asphalt

Stone mastic asphalt (SMA) has a coarse aggregate skeleton but the voids are filled with a mortar of fines, filler and bitumen. It thus resembles hot rolled asphalt, particularly the high stone content mixtures, but it may best be considered as having a coarse aggregate structure similar to porous asphalt but with the voids filled. SMA differs from hot rolled asphalt in that the quantity of mortar is just sufficient to fill the voids in the coarse aggregate structure. It therefore provides high stiffness due to the interlock of the coarse aggregate particles, and good durability because of a low void content. Since SMAs do not have a mortar continuum, they are less well able to withstand tensile strain than hot rolled asphalt. In order to improve their resistance to tensile strain, it is usual to include cellulose fibres in the mixture.

29.2 Recipe and designed mixes

The majority of bituminous mixtures are recipe mixes. In other words, the mixtures are put together according to prescribed proportions laid down in the appropriate British Standard. These mix proportions have been derived through experience in use and, provided the separate ingredients meet their specifications, the mix will provide the required performance in most situations. This approach is consistent with the empirical method for the structural design of roads which has predominated until relatively recently. Thus an empirical chart to determine the thickness of roadbase was used which depended on the roadbase material having the same mix proportions as the materials in the roads from which the design chart was originally established.

It is important to note that tests for compliance of recipe mixes can only be compositional tests and tests of the nature of individual ingredients. Typically, these materials are broken down to determine binder content and the aggregate grading. It is axiomatic that there are no tests of the properties of the material produced or of its performance.

Recipe mixes provide a satisfactory performance in many cases and there is some advantage in the simplified approach which recipe mixes offer. However, there are limitations to the use of recipe mixes which match the limitations of empirical structural design of roads. These are as follows:

1. Non-specified materials cannot be used. For example, a locally available sand may not meet the grading requirements of the specification but may produce a satisfactory mix. Recipe mixes preclude any assessment of the properties of a mix containing that sand.
2. Modified binders cannot be used. The use of chemical additives in binders can give useful enhancements to their properties. The absence of any end-test of recipe mixes prevents the evaluation of these changes.
3. No procedure is available to assess causes of failure.
4. No procedure is available to optimize the mix proportions. This is particularly important as far as the bitumen is concerned because this is the most expensive ingredient and has a strong bearing on the performance of mixes, especially those which are more dense.

These drawbacks have led to the development of a procedure for the design of bituminous mixes, which has occurred in parallel with the development of analytical procedures for the structural design of roads. An analytical approach to road design enables the determination of the thickness of the road structure through an analysis of its behaviour under the applied load. This clearly requires a knowledge of certain properties of the materials and it follows that materials will have to be produced with particular characteristics. However, the design system, with material properties feeding into the analysis, has not yet been fully developed and what are now called designed mixes are, in fact, only partially designed.

The procedure for mix design (BS 598: Part 107: 1990) is based upon the Marshall test which was originally developed in the USA for designing mixes for use on airfield runways. The objective of the procedure is to determine an optimum binder content from a consideration of:

1. mix strength (stability);
2. mix density;
3. mix deformability (flow).

Test samples of binder/aggregate mixtures are prepared using the materials to be used in the field. The aggregate grading is kept constant and samples with a range of binder contents are produced. The samples are prepared and compacted in a standard way into moulds 101.6 mm in diameter and 70 mm high. The state of compaction achieved is determined by measuring the bulk density and calculating the compacted aggregate density. At low binder contents the mix will lack workability and the densities will be correspondingly low. At high binder contents, aggregate will effectively be displaced by bitumen, and again the densities will be low. Each of these measures of density will thus produce an optimum binder content as shown in Figures 29.2 (a) and (b).

To test the strength and resistance to deformation of the material, the specimens are heated to 60°C and subjected to a compression test using special curved jaws which match the curved sides of the specimens as shown in Figure 29.3. Thus the load is applied radially. The jaws of the machine are driven together at a constant rate of 50 mm per minute until the maximum load is obtained which is termed the ‘stability’. The deformation of the sample at this maximum load is also recorded and termed the ‘flow’. Typical plots of stability and flow against binder content are shown in Figures 29.2 (c) and (d). The stability plot gives a third optimum binder content, and the design binder content is obtained from the average of this and the optima from the two density plots. The flow at this design binder content can then be read off. Minimum values of stability and flow are specified according to the amount of traffic which the road will carry.

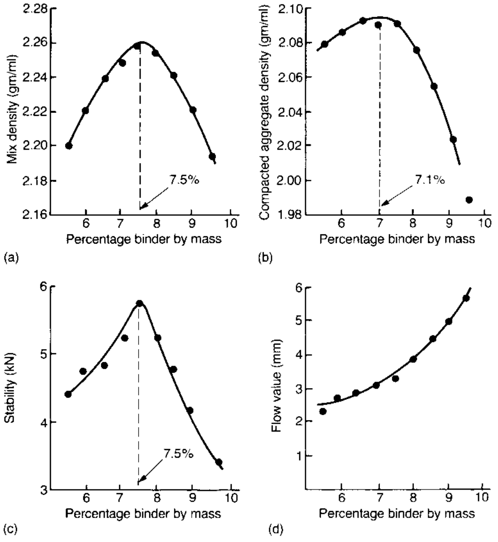

FIGURE 29.2 Analysis of mix design data from the Marshall test.

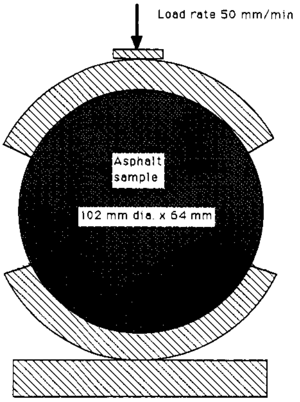

FIGURE 29.3 Testing arrangement for a Marshall asphalt design.

In evaluating mixes it is helpful to consider the Marshall quotient, Q_m. This is derived from the stability and flow:

$$Q_m = \text{stability/flow} \qquad (29.1)$$

Thus Q_m bears some resemblance to a modulus (ratio of stress to strain) and may be taken as a measure of mix stiffness. It has been found to correlate well with wheel-tracking tests to assess deformation resistance. Since stability is used to determine the optimum binder content, the design procedure may be regarded as determining stiffness at optimum binder content, and the larger the value of Q_m, the more resistant the mix will be to deformation.

More recently new approaches to bituminous mix design have been proposed. A complete design process has been suggested (Cabrera, 1994) which is applicable to all hot bituminous mixtures, i.e. both hot rolled asphalts and macadams. The procedure, known as the Leeds Design Method, aims to design mixtures to meet both structural requirements and in-service performance requirements. It involves measurement of a range of parameters: workability, air permeability, Marshall stability and flow, static stiffness and vapour diffusion.

Another development is the use of a repeated load compression test for assessing resistance to deformation as part of a design process (Gibb and Brown, 1994). The test employs the Nottingham Asphalt Tester which enables a specimen to be subjected to repeated load in a controlled environment. In order to represent vehicle loading effects, stress pulses of 100 kPa are applied for a duration of one second with an interval of one second between pulses. Results correlate well with wheel tracking tests.

29.3 Methods of production

The process of manufacture of bituminous materials involves three stages. First, the aggregates must be proportioned to give the required grading, second the aggregates must be dried and heated, and third, the correct amount of binder must be added to the aggregate and mixed to thoroughly coat the aggregate particles and produce a homogeneous material.

The most common type of plant in the UK is the indirectly heated batch mixing plant. A schematic diagram of this type of plant is shown in Figure 29.4. The aggregate is blended from cold bins and passed through a rotary

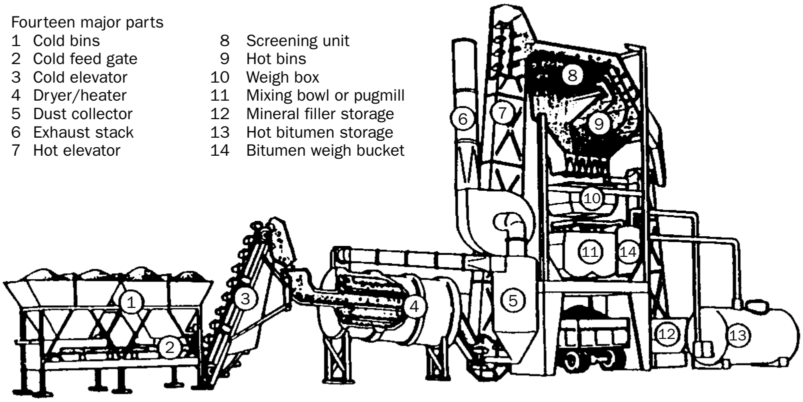

FIGURE 29.4 Schematic diagram of an indirectly heated batch mixing plant (*The Shell Bitumen Handbook*, 1990).

drier/heater. Here the moisture is driven off and the aggregate temperature raised to the prescribed mixing temperature for the type of material being produced. The aggregate is then transported by hot elevator to hot storage bins where it is separated into fractions of specified size. Aggregates are released into the weigh box in the desired proportions and then released into the mixer. Bitumen heated to the prescribed temperature is also introduced to the mixer, the quantity being determined using a weigh bucket or volumetrically using a flow meter. The mixing time varies up to 60 seconds but should be as short as possible in order to limit oxidation of the binder. After mixing, the material is discharged directly into a wagon.

This type of plant is very versatile, being capable of producing both asphalt and macadam mixes, and being able to easily adjust to a wide range of mix specifications.

A variation on this type of plant is to dry and heat the aggregate in batches before being charged into the mixer. This eliminates the need for hot aggregate storage but the proportioning of the cold aggregate needs to be very carefully controlled.

An alternative type of mixer is the drum mixer which gives continuous production rather than batches. Here the cold aggregates are proportioned and conveyed directly into a drum mixer. The drum has two zones. The first zone is where drying and heating occur, and in the second zone the bitumen is introduced and the mixing takes place. The advantages of this type of plant are that the amount of dust emission is reduced, the process is simpler and, above all, the rate of production can be very high – up to 500 tonnes per hour. This is advantageous where large quantities of the same type of material are required, but it is difficult to change production to a different mix.

29.4 References

Cabrera, J.G. (1994) Hot bituminous mixtures – design for performance. In *Performance and Durability of Bituminous Materials*, E & FN Spon, London.

Gibb, J.M. and Brown, S.F. (1994) A repeated load compression test for assessing the resistance of bituminous mixes to permanent deformation. In *Performance and Durability of Bituminous Materials*, E & FN Spon, London.

Shell Bitumen UK (1990) *The Shell Bitumen Handbook*.

Further reading

Hunter, R. (2000) (ed.) *Asphalts in Road Construction*, Thomas Telford, August.

This book gives an excellent coverage of asphalts including recent developments in asphalt technology such as stone mastic asphalt, thin surfacings, and high modulus bases. As well as covering the materials themselves, it deals with the design and maintenance of pavements, laying and compaction, surface dressing and other surface treatments, and failure of surfacings. The book is an updated version of *Bituminous Materials in Road Construction*. This too is worth reading since it deals with all types of bituminous material.

O'Flaherty, C.A. (2000) *Highways: The Location, Design, Construction and Maintenance of Road Pavements*, Butterworth-Heinemann, June.

A comprehensive textbook on all aspects of road engineering from the planning stages through to the design, construction and maintenance of road pavements.

Whiteoak, D. (1990) *The Shell Bitumen Handbook*, Shell.

Essential reading if you want to get to grips with the fundamentals of bitumen. It deals with the structure and constitution of bitumen and goes on to link this to the engineering properties. The book also covers the design and testing of bituminous mixes as well as pavement design.

Standards

British Standard 434: Part 1: 1984: *Bitumen road emulsions (anionic and cationic). Part 1. Specification for bitumen road emulsions.*

British Standard 594: 1992: *Hot rolled asphalt for roads and other paved areas. Part 1: Specification for constituent materials and asphalt mixtures.*

British Standard 598: Part 105: 1990: *Methods of test for the determination of texture depth.*

British Standard 598: Part 107: 1990: *Method of test for the determination of the composition of design wearing course asphalt.*

British Standard 812: Part 110: 1990: *Methods for determination of aggregate crushing value.*

British Standard 812: Part 112: 1990: *Methods for determination of aggregate impact value.*

British Standard 812: Part 114: 1989: *Method for determination of polished stone value.*

British Standard 2000: Part 27: 1993: *Distillation of cutback asphaltic (bituminous) products.*

British Standard 2000: Part 45: 1993: *Loss on heating of bitumen and flux oil.*

British Standard 2000: Part 47: 1983: *Solubility of bituminous binders.*

British Standard 2000: Part 49: 1983: *Penetration of bituminous materials.*

British Standard 2000: Part 58: 1983: *Softening point of bitumen (ring and ball).*

British Standard 2000: Part 72: 1993: *Viscosity of cutback bitumen and road oil.*

British Standard 2000: Part 357: 1983: *Permittivity of bitumen.*

British Standard 3690: Part 1: 1989: *Bitumens for building and civil engineering. Part 1: Specification for bitumens for road purposes.*

British Standard 4987: 1993: *Coated macadam for roads and other paved areas. Part 1: Specification for constituent materials and for mixtures.*

Department of Transport (1987) *Departmental Standard HD 14/87.*

Part Five

Brickwork and Blockwork

R.C. de Vekey

Introduction

This introduction outlines the history of masonry and explains the terminology used. The subsequent chapters cover: materials, composition and manufacturing processes for the components of masonry; structural forms, architecture and detailing; structural behaviour and response to actions such as wind and movement; and durability and other important properties in relation to heat, noise, fire and rain, and weather.

The title 'Brickwork and blockwork' has been chosen to emphasize that these materials are the most common of this type used in construction at the present time. The term 'masonry'

- has recently been widened from its traditional meaning of structures built of natural stone to encompass all structures produced by stacking, piling or bonding together discrete chunks of rock, fired clay, concrete, etc., to form the whole
- 'masonry', in this wider sense, is what these chapters are about.

Second to wood, masonry is probably the oldest building material used by man, and it certainly dates from the ancient civilizations of the Middle East and was used widely by the Greeks and Romans. Early cultures used mud building bricks and very little of their work has survived, but stone structures such as the Egyptian pyramids, Greek temples and many structures made from fired clay bricks have survived for thousands of years. The Romans used both fired clay bricks and hydraulic (lime/pozzolana) mortar and spread this technology over most of Europe.

The basic principle of masonry is of building stable bonded (interlocked) stacks of handleable pieces. The pieces are usually chosen or manufactured to be of a size and weight that one person can place by hand but, where additional power is available, larger pieces may be used which give potentially more stable and durable structures.

This greater stability and durability is conferred by the larger weight and inertia which increases the energy required to remove one piece and makes it more resistant to natural forces such as winds and water as well as human agency. There are four main techniques for achieving stable masonry:

1. Irregularly shaped and sized but generally laminar pieces are chosen and placed by hand in an interlocking mass (e.g. dry stone walls).
2. Medium to large blocks are made very precisely to a few sizes and assembled to a basic grid pattern either without mortar or with very thin joints (e.g. ashlar).
3. Small to medium units are made to normal precision in a few sizes and assembled to a basic grid pattern and the inaccuracies are taken up by use of a packing material such as mortar (e.g. normal brickwork).
4. Irregularly shaped and sized pieces are both packed apart and bonded together with adherent mortar (e.g. random rubble walls).

Only type (4) structures depend largely on the mortar for their stability; all the other types rely largely on the mechanical interlocking of the pieces. Figure V.1 shows typical examples.

These descriptions are given to emphasize that most traditional masonry owes much of its strength and stability to interlocking action, weight and inertia while the mortar, when present, is not acting as a glue but as something to fill in the gaps resulting from the imperfect

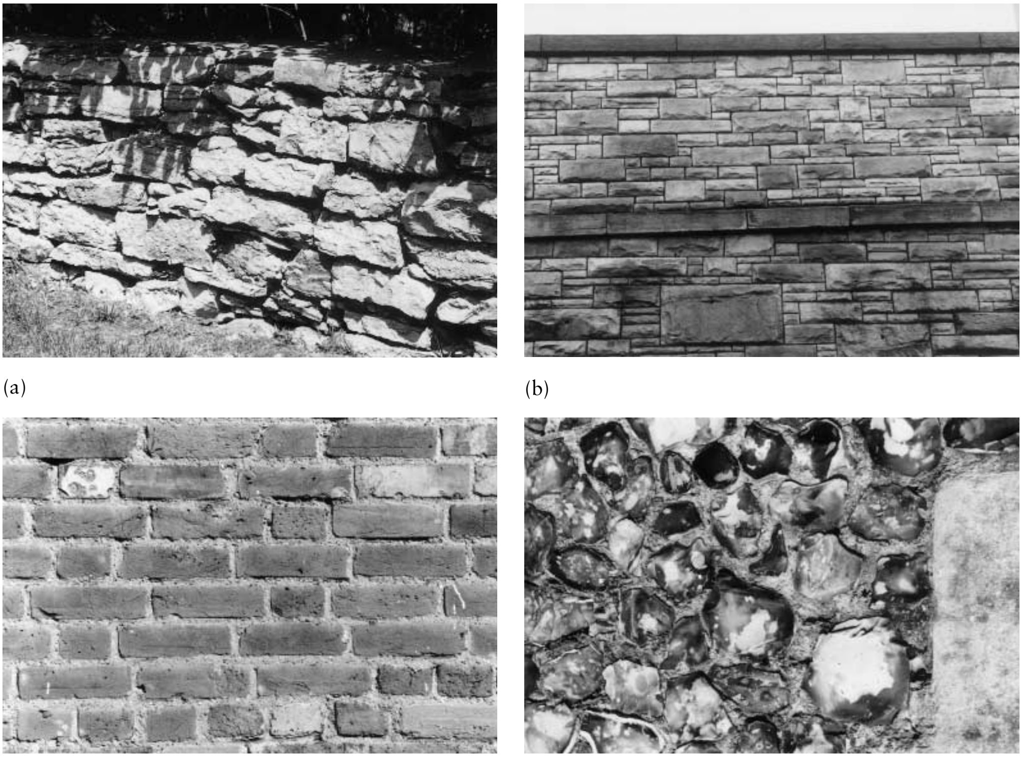

(a)

(b)

(c)

(d)

FIGURE V.1 The main types of masonry: (a) dry stone walls, (b) ashlar, (c) jointed brick and blockwork and (d) rubble masonry.

fitting together of the pieces. Most contemporary masonry is type (3) and modern mortars do have an adhesive role but much of the strength still derives from the mass and interlocking of shapes and it is important to remember this in design.

It is also important to remember that, although the wall is the most useful and effective masonry structure, many other structural forms are used such as columns, piers, arches, tunnels, floors and roads. Normal plain masonry must be designed such that the predominant forces put it into compression since it cannot be relied on to resist tensile forces. If, however, tension structures such as cantilevers, earth-retaining walls and beams are required, masonry may be reinforced or post-tensioned in the same way as concrete.

Terminology

Components

Units – pieces of stone, brick, concrete or calcium silicate which may be assembled to make masonry. Usually, but not invariably, they are in the form of rectangular parallelepipeds.

Mortar – a material that is plastic (flows) when fresh but sets hard over a period of hours to days. Its purpose is to fill the gaps caused by variations in the size and shape of units such that the masonry is stable and resists the flow of air and water. Mortar is compounded from a binder (e.g. cement) and a filler/aggregate (usually sand). The binder is a finely ground material which, when mixed with water, reacts chemically and then sets hard and binds aggregates into solid masses.

Size and dimensions (Figure V.2)

Work size – the size of a masonry unit specified for its manufacture, to which its actual size should conform within specified permissible deviations. As a rough guide for the following sections, bricks are considered to be units with face dimensions of up to 337.5 mm long by 112.5 mm high and with a maximum width of 225 mm, while blocks are larger units up to face dimensions of 1500 mm by 500 mm. UK units are smaller than these limits. A standard UK brick is 215 mm long by 65 mm high and with a depth of 102.5 mm. There is no standard block size but the commonest size is 440 mm long by 215 mm high and with a width of 100 mm, with a limiting size of 650 mm for any dimension for standard concrete units.

Co-ordinating size – the size of a co-ordinating space allocated to a masonry unit, including allowances for joints and tolerances. This coordination grid into which they fit is generally 10 mm larger for each dimension.

Units

Units may be produced in a number of forms, illustrated in Figures 30.6 and 31.7.

- Solid – having no designed voids (holes, depressions or perforations) other than those inherent in the material.
- Frogged – with a depression (or frog) in one or both of the bed faces where the total volume of the frog(s) does not exceed 20 per cent of the gross volume.
- Cellular – having one or more deep holes or depressions in one bed face with an aggregate volume exceeding 20 per cent of the gross

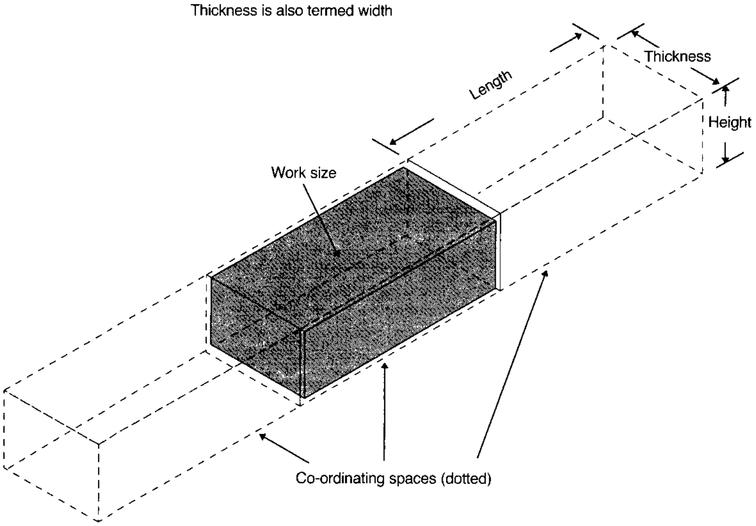

FIGURE V.2 Masonry dimensions.

volume and which do not penetrate through to the other side.

- Perforated – having one or more holes passing from one face to the opposite face. UK products have vertical perforations, i.e. the holes pass from one bed face to the other and will be vertical when laid normally in a stretcher bonded wall. Horizontally perforated clay blocks are, however, not uncommon in continental Europe.
- Hollow – having one or more formed holes or cavities which pass through the units.
- Specials (special shapes) – a range of standard bricks for curves, non-right-angled corners, plinths, cappings, etc., are available. They are described in BS 4729: 1990.

General

Fair-faced – masonry, within the variability of individual units, precisely flat on the visible face. This is normally only possible on one side of solid walls.

Other relevant definitions are contained in BS 6100: Part 3: 1984.

Chapter thirty

Materials and components for brickwork and blockwork

30.1 Materials used for manufacture of units and mortars

30.1.1 Sands and fillers

Sand

Sand is used widely as a constituent of masonry in mortar, in concrete units and sandlime units, in grouts and renders. It is a mixture of rock particles of different sizes from about 10 mm diameter down to 75 μm diameter.

Sand is usually extracted from recent naturally occurring alluvial deposits such as river beds and sea beaches, or from older deposits from alluvial or glacial action. In some areas it may be derived from dunes or by crushing quarried rocks. The chemical and geological composition will reflect the area from which it is derived. The commonest sands are those based on silica (SiO_2), partly because of its wide distribution in rocks such as sandstones and the flint in limestones, and partly because silica is hard and chemically resistant. Other likely constituents are clay, derived from the decomposition of feldspars, calcium carbonate ($CaCO_3$), in the form of chalk or limestone from shells in some marine sands, and micas in sands from weathered granites. Crushed rocks such as crushed basalts and granites will reflect their origins.

Sands should be mostly free of particles of clay (with a size of between 75–30 μm) which cause unsatisfactory shrinkage characteristics and chemical interactions with binders. Most of the constituents of sand are relatively chemically inert to environmental agents but chalk or limestone particles will be dissolved slowly by mild acids and clays may react in time with acids, or alkalis. Most sand constituents are also fairly hard and are resistant, in themselves, to mechanical abrasion and erosion by dust in wind and water.

Mortar and rendering sands

Mortar sand must contain no particles with a diameter greater than about half the thinnest joint thickness, i.e. around 5 mm. It should also

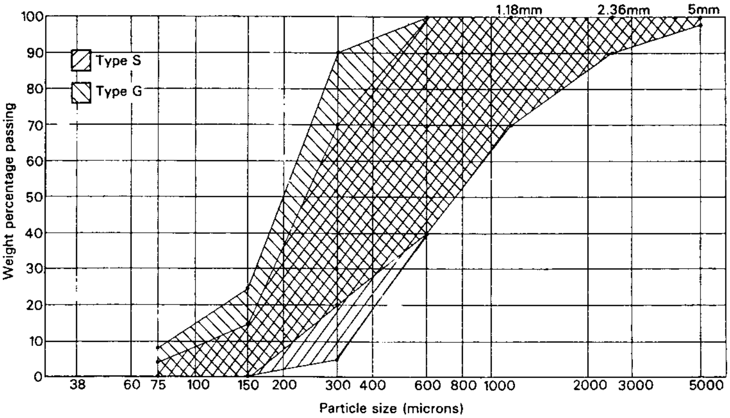

FIGURE 30.1 Grading curves for S and G sands.

have a good range of particle sizes from the largest to the smallest (a good grading) since this leads to good packing of the particles to give a dense, strong mass resistant to erosion, permeation and chemical attack. Many naturally occurring alluvial deposits fall naturally into the required grading and may be used as dug or just with a few coarser particles screened off. These are usually termed pit sands. Sands that are outside the normal range must be sieved to remove coarse fractions and washed to remove excess clay particles.

The shape of the particles is also important for mortar sands. Very flaky materials such as slates and micas are not very suitable as it is difficult to make them workable. Very absorbent materials are also unsatisfactory for dry-mixed mortars since they cause rapid falls in workability by absorbing the mixing water. They may be suitable for mixes based on wet premixed lime-sand 'coarse stuff'. Sand may be sieved into fractions and regraded but this is rarely done for a mortar sand. Figure 30.1 shows the grading curves for the sands allowed under BS 1200: 1976.[1] This gives two allowed grades, S for structural use and G, with slightly wider limits, for general purposes. Rendering mixes require sands with broadly similar characteristics to mortars but a good grading is even more important to avoid shrinkage, cracking and spalling and to give good bond to the substrate.

Concreting sands

These have been discussed in Chapter 16.

Ground sand

Finely ground silica sand is used particularly in the manufacture of autoclaved aerated cement (AAC) materials.

Pulverized fuel ash (pfa)

Pfa is the main by-product of modern coal-fired electricity generating stations which burn finely ground coal. Typical composition ranges are given in Table 30.1 and fuller information is available in Central Electricity Generating Board (1972). It has also been discussed in Chapter 15.

---

[1] A list of all standards referred to in the text is included in 'Further reading' on page 329.

TABLE 30.1 Typical chemical composition ranges of pulverized fuel ash (weight %)

Range	*SiO_2*	*Al_2O_3*	*Fe_3O_4*	*CaO*	*MgO*	*K_2O*	*Na_2O*	*TiO_2*	*SO_3*	*Cl*
Minimum	45	24	7	1.1	1.5	2.8	0.9	0.8	0.3	0.05
Maximum	51	32	11	5.4	4.4	4.5	1.7	1.1	1.3	0.15

Chalk (calcium carbonate, $CaCO_3$)

In a finely ground state, chalk is used as a filler and plasticity aid in masonry cement and some grouts.

30.1.2 Clays

Clay is a very widely distributed material which is produced by weathering and decomposition of acid alumino-silicate rocks such as the feldspars, granites and gneisses. Typical broad types are the kaolin group of which kaolinite has a composition $Al_2O_3.2SiO_2.2H_2O$, the montmorillonite group of which montmorillonite itself has the composition $Al_2O_3.4SiO_2.nH_2O$, and the clay micas which typically have a composition $K_2O.MgO.4Al_2O_3.7SiO_2.2H_2O$.

They will frequently contain iron, which can substitute for the aluminium, and other transition metals. The clays used for clay brick manufacture are normally only partly actual clay minerals, which impart the plasticity when wetted, the balance being made up of other minerals. Brick earths, shales, marls, etc., mostly contain finely divided silica, lime and other materials associated with the particular deposit, e.g. carbon in coal measure shales. Most brick clays contain iron compounds which give the red, yellow and blue colours to fired bricks. Table 30.2 gives the compositions of some typical clays in terms of their content of oxides and organic matter (coal, oil, etc.).

The properties of clays are a result of their layer structure which comprises SiO_4 tetrahedra bonded via oxygen to aluminium atoms which are also bonded to hydroxyl groups to balance the charge. The layers form loosely bound flat sheet-like structures which are easily parted and can adsorb and bond lightly to varying amounts of water between the sheets. As more water is absorbed the clay swells and the intersheet bond becomes weaker, i.e. the clay becomes more plastic and allows various shaping techniques to be used.

30.1.3 Aggregates

Natural aggregates, sintered pfa nodules, expanded clay and foamed slag have been described in

TABLE 30.2 Chemical compositions of some representative clays (weight % of oxides) (X = alkali metal ion)

Broad type	*SiO_2*	*Al_2O_3*	*Fe_3O_4*	*CaO*	*MgO*	*X_2O*	*CO_2*	*H_2O*	*Organic matter*
London brick	49.5	34.3	7.7	1.4	5.2	_	_	_	1.9
Blue clay	46.5	38	1	1.2	_	_	_	_	13.3
Loam	66.2	27	1.3	0.5	_	_	_	_	5
Fletton clay	50	16	7	10	1	3	_	6	6
Marl	33	10	3	26	3.5	_	20.5	4	_
Burnham clay	42.9	20.9	5	10.8	0.1	0.3	8.1	6.9	5
Red brick clay	49	24	8	7	_	1	11	_	_
Gault clay	44	15	6	17	_	_	_	18	_
Washed china clay	46	40	_	1	_	_	_	13	_
Stourbridge fireclay	65	22	2	1	_	_	_	10	_

Chapter 16. Other aggregates used particularly for unit manufacture are the following:

1. Furnace clinker, a partially fused ash from the bottom of solid-fuelled industrial furnaces.
2. Furnace bottom ash. Most large, modern furnaces, especially those used to raise steam in power stations, burn finely ground coal dust as a dust/air mixture. A proportion of the ash sinters together in the gas stream, then falls to the base of the furnace as particles too large to stay suspended in the gas stream. This clinker-like material is termed 'furnace bottom ash'.
3. Perlite. Volcanic ash is deposited as a fine glassy dust and can be converted to a lightweight aggregate by hot sintering.
4. Pumice, a light foamed rock formed when volcanic lava cools. It is normally imported from volcanic regions such as Italy.

30.1.4 Binders

The binder is the component which binds together mixtures of sands, aggregates, fillers, plasticizers, pigments, etc., used to make mortars, concrete units, sandlime units and grouts. All those used widely are based on: hydraulic cements which react chemically with water at normal factory/site temperatures; lime–silica mixtures which react only in the presence of high-pressure steam; or lime which sets slowly in air by carbonation. Because they must be finely divided to be able to penetrate the spaces between sand grains and to react in some way to give the change from a formable plastic material to a hard adhesive, they must inherently be more chemically reactive than the other components. Their chemical reactivity is their weakness in that they often react with chemicals in the environment with resultant deterioration.

Portland cement

Currently, the most popular binder for general purposes is Portland cement, often still known as opc (ordinary Portland cement). Related products are rapid hardening Portland cement and sulfate resisting Portland cement. The chemistry and manufacturing methods of hydraulic cements have been discussed in Chapter 13.

Masonry cement

A factory prepared mixture of opc with a fine inert filler/plasticizer (around 20 per cent) and an air-entraining agent to give additional plasticity is supplied as masonry cement. It is intended solely for mixing with sand and water to make bedding mortars. The fine powder is normally ground chalk but a wide range of inert and semi-inert materials can be substituted. In the future, Portland cements blended with pulverized fuel ash (pfa) may well be used for mortars either as masonry cements or as blended cements.

Lime and hydraulic lime

Lime (CaO) is widely used as an ingredient in mortars, plasters and masonry units. The pure oxide form, called quicklime, was used widely in the past for mortars for stonework. It is prepared by heating pure limestone to a high temperature and then 'slaking' with water to produce hydrated lime, $Ca(OH)_2$. Since it does not have any setting action in the short term, it may be kept wet for days or weeks provided it is covered and prevented from drying out. The wet mix with sand is termed 'coarse stuff'. Contemporary lime mortar may be made from pre-hydrated lime but is otherwise similar. The initial setting action of this mortar depends only on dewatering by contact with the units so it is not suitable for construction of slender structures which require rapid development of flexural strength. Over periods of months or years the lime in this mortar carbonates and hardens to form calcium carbonate as in equation (30.1), but it is never as hard or durable as properly specified hydraulic cement mortars.

Impure lime was widely used in the past and is gaining popularity for repairing historic buildings to match the existing mortar. It is basically a quicklime – calcium oxide – produced by heating impure limestone to a high temperature. The impurities, usually siliceous or clay, lead to the formation of a proportion of hydraulically active compounds such as calcium silicates or aluminates. The mortar is made as normal by gauging (mixing in prescribed proportions) with sand and water, but there will be some emission of heat while the lime is slaking. The classic systematization work was done by Vicat (1837) and later Cowper (1927) and more recent background is given by Ashurst (1983).

$$Ca(OH)_2 + CO_2 \rightarrow CaCO_3 + H_2O \quad (30.1)$$

Most of the hydraulic cements may be blended with pure hydrated lime in various proportions to make hybrid binders which give mortars with a lower strength and rigidity but still maintain the plasticity of the 1:3 binder:sand ratio. This leads to mortars which are more tolerant of movement and more economical.

Sandlime

The binder used for sandlime bricks and autoclaved aerated concrete (AAC) blocks is lime (calcium hydroxide, $Ca(OH)_2$) which reacts with silica during autoclaving to produce calcium silicate hydrates. The reaction, in a simplified form, is:

$$Ca(OH)_2 + SiO_2 \rightarrow CaSiO_3 + H_2O \quad (30.2)$$

The lime is usually added directly as hydrated calcined limestone or may be derived in part from opc which is also incorporated in small quantities to give a green strength to the unit.

30.2 Other constituents and additives

30.2.1 Organic plasticizers

Many organic compounds improve plasticity, or workability, of mortars, rendering mortars, infilling grouts and concrete used for manufacture of units. All the classic mortar plasticizers operate by causing air to be entrained as small bubbles. These bubbles fill the spaces between the sand grains and induce plasticity. Typical materials are based on Vinsol resin, a by-product of cellulose pulp manufacture, or other naturally available or synthetic detergents. They are surfactants and alter surface tension and other properties. Super plasticizers, used only for concrete and grout mixes, plasticize by a different mechanism which does not cause air entrainment. Admixtures are discussed in more detail in Chapter 14.

30.2.2 Latex additives

A number of synthetic copolymer plastics may be produced in the form of a 'latex', a finely divided dispersion of the plastic in water usually stabilized by a surfactant such as a synthetic detergent. Generally the solids content is around 50 per cent of the dispersion. At a temperature known as the film-forming temperature, they dehydrate to form a continuous polymer solid. When combined with hydraulic cement mixes these materials have a number of beneficial effects: they increase adhesion of mortar to all substrates; increase the tensile strength and durability; reduce the stiffness and the permeability. Because of these effects they are widely used in flooring screeds and renders but are also used to formulate high-bond mortars and waterproof mortars. The better polymers are based on copolymerized mixtures of butadiene, styrene and acrylics. Polyvinylidene dichloride (PVDC) has also been marketed for this application but it can lose chlorine which can attack buried metals. Polyvinyl acetate (PVA) is not suitable as it is unstable in moist conditions. Polyvinyl propionate has been found to give less satisfactory flow properties than the acrylic copolymers. These materials should never be used with sands containing more than 2 per cent of clay or silt particles. Dosage is usually in the range of 5–20 per cent of the cement weight. Table 30.3 gives some properties of common types from data in de Vekey (1975) and de Vekey and Majumdar (1977).

30.2.3 Pigments

Through-coloured units and mortars of particular colours may be manufactured either by selecting

TABLE 30.3 Latex polymer additives

Chemical name: Polymer-of or copolymer-of	*Reaction product with cement slurry*	*Properties of polymer/cement[1] as proportion of neat cement paste*			
		Elastic Modulus		*Flexural strength*	
		Air[2]	*Water[2]*	*Air[2]*	*Water[2]*
Vinyl acetate	Acetate ions	0.62[3]	0.59[3]	1.60[3]	0.66[3]
Vinyl proprionate	None	0.62[3]	0.74	1.24[3]	1.22[3]
Butadiene and styrene	None	0.51	0.71	1.00[3]	1.63[3]
Vinylidene dichloride	Chloride ions	0.66[4]	0.84[4]	1.52[4]	1.36[4]
Acrylic acid and styrene	None	0.59	0.69	1.56	1.95
Acrylic acid	None	0.4	0.65	1.29	1.91
Acrylic acid and methacrylic acid	None	0.32	0.73	1.44	1.68

Notes:

1. Properties are for an opc cement paste with a w/c of 0.3 and a polymer solids/cement ratio of 0.1 after storage for two years.
2. Storage conditions are air at 65 per cent relative humidity or water at 20°C.
3. These figures are the mean of two products.
4. These figures are the mean of four products.

suitably coloured natural sands and binders or by adding pigments. Units may also be coloured by applying surface layers but this is more common for fired clay than for concrete or calcium silicate units. Pigments are in the form of inert coloured powders of a similar fineness to the binder, so they thus tend to dilute the mix and reduce strength. Most pigments should be limited to a maximum of 10 per cent by weight of the binder in mortars and carbon black to 3 per cent. Some typical pigments, from information in ASTM task group C09.03.08.05 (1980) are synthetic red iron oxide, Fe_2O_3; yellow iron oxide; black iron oxide, FeO (or Fe_3O_4) and brown iron oxide, Fe_2O_3, xH_2O; natural brown iron oxide, Fe_2O_3, xH_2O; chromium oxide green, Cr_2O_3; carbon black (concrete grade); cobalt blue; ultramarine blue; copper phthalocyanine; and dalamar (hansa) yellow. Only pigments resistant to alkali attack and wettable under test mix conditions are included. All but the last two are not faded by light.

30.2.4 Retarders

Retarders are used to delay the initial set of hydraulic cement mortars. They are generally polyhydroxycarbon compounds. Typical examples are sugar, lignosulphonates and hydroxycarboxylic acids. These have been more fully discussed in Chapter 14.

30.2.5 Accelerators

Accelerators have been marketed, usually based on calcium chloride ($CaCl_2$), which is used in small amounts in concrete block manufacture. Alternatives such as calcium formate ($Ca(CHO_2)_2$) may be satisfactory. Accelerators are not effective when building with mortar in frosty weather and are no substitute for proper protection of the work.

Again, they have been discussed in Chapter 14.

30.3 Mortar

Mortar has to cope with a wide range of, sometimes conflicting, requirements. To obtain optimum performance the composition must be tailored to the application. The broad principles are as follows:

1. Mortars with a high content of hydraulic cements are stronger, denser, more impervious

and more durable, bond better to units under normal circumstances and harden rapidly at normal temperatures. They also lead to a high drying shrinkage and rigidity of the masonry. They are likely to cause shrinkage cracks if used with shrinkable, low-strength units, particularly for long, lightly loaded walls such as parapets and spandrels.

2. Mortars with decreased or no content of hydraulic cements are weaker and more ductile and thus more tolerant of movement. They are matched better to low-strength units but at the cost of a reduction in strength, durability. and bond. There is a corresponding reduction in shrinkage and hardening rate.
3. Mortars made with sharp, well-graded sands can have very high compressive strength, low permeability and generally good bond but poor workability, while fine loamy sands give high workability but generally with reduced compressive strength and sometimes reduced bond.
4. Lime addition confers plasticity and, particularly for the wet stored mixes, water retentivity – the ability of the mortar to retain its water in contact with highly absorbent bricks – which facilitates the laying process and makes sure that the cement can hydrate. Lime mortars perform poorly if subjected to freezing while in the green (unhardened) state but, when hardened, are very durable. Lime is white and thus tends to lighten the colour of the mortar. In some circumstances it can be leached out and may cause staining.
5. Air entrainment improves the frost resistance of green mortar and allows lower water/cement ratios to be used, but such plasticized mixes may be less durable and water-retentive than equivalent lime mixes. Air-entrained mixes also need careful manufacture and control of use since over-mixing gives very high air contents, and retempering (adding more water and reworking the mix) can lead to very poor performance due to the high porosity of the set dry mortar.
6. Pigment addition weakens mortar and the content should never exceed 10 per cent of the weight of the cement in the mortar. Carbon black is a special case and should be limited to 3 per cent.
7. Polymer latex additives can markedly improve some properties, such as bond, flexural strength and resistance to permeation by water and air but, they are costly and should only be used where there is a particular requirement.
8. Retarders are widely used in the manufacture of ready-mixed mortars, delivered to site in the same way as ready-mixed concrete. The retarder is dosed as required by the supplier to give a ‘pot life’ of between 1 and 3 days. Care is needed in the use of retarded mortars, especially in hot weather, because if they dry out too rapidly, the curing process never takes place and the mortar never hardens.
9. Mortar has a relatively high thermal conductivity and thus causes heat loss in walls of low-density units. To achieve better thermal insulation, insulating mortars are now available which use a low-density replacement for the coarse sand particles. Another option is to just use a thinner layer. Special high-bond ‘Thin-bed mortars’ (see BRE Digest (1998)[2]) designed for use in thicknesses from 1–5 mm are now available but require units with close tolerances on their size.

30.3.1 Properties of unset mortar

Test methods for fresh mortar are given in BS 4551 (1980), RILEM (1978), ISO (1991) and the EN 1015 series (1998–9). The important properties of unset mortar are the workability, i.e. how easy it is to handle and place on to the masonry; the pot life, i.e. how long it may be used for after mixing (see EN 1015–9 (1999)); the water retentivity, i.e. how good it is at retaining water against the suction of the units; the setting time; and the hardening rate. Associated parameters are the cement content, water content (often

[2] A list of BRE Digests on brickwork and blockwork is included in ‘Further reading’ on page 330.

expressed as the water/cement ratio w/c) and the air content (see EN 1015–7 (1999)).

The workability is measured in terms of the slump, consistence or the flow. The slump test is seldom now used for mortar. Flow is measured on a standard 254 mm diameter (ASTM) flow table in EN 1015–3 (1999). Consistence is measured by the dropping ball test or by the plunger penetration test in EN 1015–4 (1999).

Water retentivity is measured by weighing the amount of water extracted from a dropping ball mould full of mortar by weighted layers of filter paper through two layers of cotton gauze (see EN 1015–8 (1999)). The consistence retentivity is measured by repeating the consistence test on the dewatered mortar.

Air content may be measured by weighing a known volume (0.5 litres) of mortar and then calculating, using data on the relative densities and proportions of the constituents, from the following formula:

$$A = 100(1 - K\rho) \qquad (30.3)$$

where A is the air content, ρ is the relative density of the mortar and K is derived from:

$$K = \frac{\left[\dfrac{M_1}{d_1} + \dfrac{M_2}{d_2} + \ldots + M_w\right]}{M_1 + M_2 + \ldots + M_w}$$

where M_1, $M_2, \ldots$, etc., are the relative masses of the constituents of the mortar of relative densities (specific gravities) d_1, d_2, etc., and M_w is the relative mass of water. The sum of all the values of M_1, M_2, … and M_w will be equal to 1. For precise measurements it is necessary to measure the specific gravity of all the constituents separately by use of the density bottle method. If this cannot be done, the following default values are suggested: opc 3.12, masonry cement 3.05, silica sand 2.65, white hydrated building lime 2.26, grey hydrated lime 2.45. Alternatively the pressure method can be used. All the methods are detailed in BS 4551 (1980), which will be replaced by the BS EN 1015-series (1999). The water content can be determined independently on fresh mortar by rapid oven drying of a weighed quantity. A simple site test to independently measure cement content of fresh and unhardened mortars has been described (Southern, 1989). A quantity of mortar is weighed and dissolved in a prediluted and measured volume of acid held in an insulated container. The cement content can be calculated from the temperature rise measured with an electronic thermometer.

30.3.2 Properties of hardened mortar

The important properties of hardened mortar are the density, permeability, Young's modulus, compressive strength, flexural strength, bond strength to units and drying shrinkage. Most of these properties may be measured by tests given in standards BS 4551 (1980), RILEM (1978), ISO (1991) and the BS EN 1015 series (1998–9). The durability is influenced by the combination of other properties and may be determined using the methods proposed by Harrison *et al.* (1981, 1986, 1990) and Bowler *et al.* (1995) now standardized by RILEM (1998) and the draft European method – prEN 1015–14 (1999).

The compressive strength is measured by a cube-crushing test and the flexural strength is measured by the three-point bend (or modulus of rupture) test (see BS 4551 (1980)) the draft of EN 1015–11 (1999). The modulus of rupture (MOR) is based on the formula:

$$\mathrm{MOR} = 3PL/2bd^2 \qquad (30.4)$$

where P is the maximum load applied, L is the span of the support rollers, b is the width of the prism and d is the depth of the prism.

The bond strength to typical units is conventionally measured by the parallel wallette test. In this test, a small wall is built and tested in the vertical attitude by a four-point bend test using articulated loading arms and supports, to prevent the application of any twisting moments, and resilient bolsters to prevent uneven loading.

The bond wrench has been introduced and specified in some codes and standards such as ASTM C1072–86 (1986) and Standards Association of Australia (1988) as a simpler way to measure bond, although it may give slightly

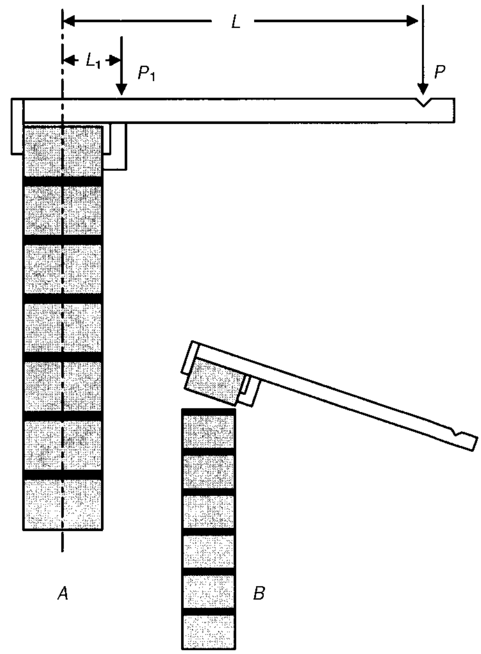

FIGURE 30.2 Bond wrench *A* before and *B* after test.

higher values than the wallette test. This device measures the moment required to detach a single unit from the top of a wall or stack-bonded prism using a lever clamped to the unit as in Figure 30.2. The load may be applied in a variety of ways, most simply by filling a container with lead shot. An electronically gauged version is described in BRE Digest 360 (1991) where the load is applied manually via a load cell transducer. Its main advantage is that it can be used on site for quality control and diagnosis of problems and failures as well as a laboratory tool.

Table 30.5 gives the common formulations of mortars used today and also lime mortars for restoration works. The table gives some ranges for the performance of the mortars in terms of the range of compressive, flexural and bond strength. A 'designation' is a term used for a group of prescribed mortars giving approximately similar performance.

It is clear from the table that a very wide range of strengths is possible for any nominal mix ratio and that parameters other than just the binder type and content influence the strength, including water/cement ratio, sand grading and air content. A further factor which only affects the properties of the mortar in the bed (and not, of course, mortar specimens cast in impervious moulds) is the amount of dewatering and compaction by the units. Where dewatering occurs, it generally increases the intrinsic strength and density of the mortar but may reduce the bond by also causing shrinkage and local microcracking.

Other key parameters are: density, porosity (indicative of permeability), Young's modulus and drying shrinkage (see Chapter 19). Density (ρ) is measured by dividing the weight of a prism or cube by its volume. The volume may be obtained by measuring all the dimensions or by weighing the prism/cube submerged in water and calculating:

$$\rho = m/bdL \quad \text{or} \quad \rho = m/(m - m_s) \qquad (30.5)$$

where m = mass derived from a weighing, b is the width of the prism/cube, d is the depth of the prism/cube, L is the length of the prism/cube and m_s is the submerged mass. The density will vary with moisture content and W is measured as saturated or oven dry. Typical densities for mortars are usually in the range 1500–2000 kg/m^3. The water porosity is obtained by measuring the water absorption by evacuating the weighed dry specimen then immersing it in water at atmospheric pressure and weighing. The gain in weight of water can be converted to volume and then divided by the volume of the specimen to give the percentage of porosity. The Young's modulus may be derived from the flexural strength test provided deflection is measured. Drying shrinkage is measured by attaching precision reference points to the ends of a damp or saturated prism and then measuring the length with a micrometer screw gauge or other precision length measuring device. After a drying regime the length is again measured and the change is expressed as a percentage of the overall length. Various drying regimes have been used (BRE Digest 35 (1963), RILEM (1975) and CEN (1991)). Some data on these properties are given in Table 32.4.

30.3.3 Thin bed and lightweight mortars

Thin bed mortars (see BRE Digest 432 (1998), Fudge and Barnard (1998) and Phillipson *et al.* (1998)) are proprietary formulas but normally contain some fine sand and cement plus bond-improving additives. They are normally supplied as a dry premix which just needs thorough mixing with water before use. The application technique is similar to that used for bedding tiles by use of serrated spreaders to produce thin ribbed layers of the order of 2–5 mm thick. Accurate levelling is crucial for good quality work. Lightweight mortars (see Stupart *et al.* (1998)) are thermally more efficient replacements for normal mortars and contain cement, optionally lime and low-density fine aggregates such as pumice, pfa and perlite.

30.4 Fired clay bricks and blocks

Fired clay units are made by forming the unit from moist clay by pressing, extrusion or casting, followed by drying and firing (burning) to a temperature usually in the range 850–1300°C. During the firing process there are complex chemical changes and the clay and other particles that go to make up the brick are bonded together by sintering (transfer of ions between particles at points where they touch) or by partial melting to a glass. During the drying and the firing process the units generally shrink by several per cent from their first-made size and this has to be allowed for in the process. Some clays contain organic compounds, particularly the coal measure shales and the Oxford clay used to make Fletton bricks. Some clays are deliberately compounded with waste or by-product organic compounds since their oxidation during firing contributes to the heating process and thus saves fuel. The burning out of the organic material leaves a more open, lower density structure. The ultimate example of this is ‘Poroton’ which is made by incorporating

TABLE 30.4 Strength ranges for mortar

Mortar designation	*Proportions by volume of ingredients*			*Strength properties (ranges)*		
	Cement: lime:sand	*Masonry: cement:sand*	*Cement: sand +plasticizer*	*Observed strength ranges at 28 days for cement mortars and 90 days for lime mortars*		
				Compressive (MPa)	*Flexural (MPa)*	*Bond (MPa)*
(i)	1:0–$\frac{1}{4}$:3	–	–	8–30	2.8–6.6	0.6–1.6
(ii)	1:$\frac{1}{2}$:4$\frac{1}{2}$	1:2.5–3.5	1:3–4	5–18	1.8–4.5	0.3–1.0
(iii)	1:1:5–6	1:4–5	1:5–6	2–12	0.7–3.7	0.2–1.1
(iv)	1:2:8–9	1:5.5–6.5	1:7–8	0.8–5.5	(0.7–1.7)	(.36–.5)
(v)	1:3:10–12	1:6.5–7	1:8	0.5–1.0	(0.7–0.9)	no data
(vi)[1]	0:1:2–3	–	–	0.5–1.0	no data	no data
(vii)[2]	0:1:2–3	–	–	0.5–1.0	no data	no data
Thin bed	–	–	[3]	5–10	–	0.14–0.66
Lightweight	1:1:5[3]	-	1:5[3]	1.7–3.6	0.7–1.4	0.05

Notes:
1. Hydraulic lime mortars.
2. Pure lime mortars (referred to as ‘air lime motars’ in Europe).
3. The exact composition of thin bed and lightweight mortars is a commercial secret.

fine polystyrene beads in the clay. Wood and coal dust can be used to achieve a similar effect in some products.

30.4.1 Forming and firing

Soft mud process

The clay is dug, crushed and ground then blended with water using mixers to make a relatively sloppy mud. A water content of 25–30 per cent is required for this process. In some plants other additives may be incorporated such as a proportion of already fired clay from crushed reject bricks (grog), lime, pfa, crushed furnace clinker and organic matter to act as fuel. In the well-known yellow or London Stock brick, ground chalk and ground refuse are added. The mud is formed into lumps of the size of one brick and the lump is dipped in sand to reduce the stickiness of the surface. In the traditional technique the lump is thrown by hand into a mould and the excess is cut off with a wire. This gives rise to the characteristic 'folded' appearance of the faces of the brick caused by the dragging of the clay against the mould sides as it flows. Nowadays most production is by machine which mimics the handmaking process. These bricks usually have a small frog (depression) formed by a raised central area on the bottom face of the mould. Because of the high drying shrinkage of such wet mixes and the plasticity of the unfired (green) brick, the size and shape of such units are fairly variable. This variability adds to their 'character' but means that precision brickwork with thin mortar beds is not feasible. The finished brick is also fairly porous which improves its insulation properties, and, paradoxically, its effectiveness as a rain screen, but limits the strength.

Stiff plastic process

The clay is dug, crushed and ground then blended with water using mixers to make a very stiff but plastic compound with a water content of 10–15 per cent. This is then extruded from the mixer and cut into roughly brick-shaped pieces and allowed to dry for a short period before being pressed in a die. The clay is very stiff so, when ejected straight from the mould, it retains very precisely the shape of the die. The low moisture content means that the shrinkage is low and therefore the size is easier to control and the drying time is relatively short. Another advantage is that the unfired brick is strong enough to be stacked in the kiln or on kiln cars without further drying. This type of unit will usually have at least one shallow frog and may have frogs in both bed faces. The process is used to produce engineering bricks, facing bricks, bricks with very accurate dimensions and pavers.

Wire cut process

Clay of softer consistency than the stiff plastic process is used with a moisture content of 20–25 per cent and the clay is extruded from a rectangular die with the dimensions of the length and width of the finished unit. The ribbon of clay, the 'column', is then cut into bricks by wires set apart by the height of the unit plus the allowance for process shrinkage. The cutting machines are usually arranged such that the group of cutting wires can travel along at the same speed as the column while the cut is made. This means that the process is fully continuous and the cut is perpendicular to the face and ends of the unit. A plain die produces a solid column with just the characteristic wire cut finish, and these bricks will have no depressions in their bed faces. In this process it is easy, however, to include holes or perforations along the length of the column by placing hole-shaped blockages in the die face. This has the following advantages:

1. Reduction in the weight of clay required per unit, so transport costs at every stage of the production and use of the units and all clay preparation costs, i.e. for shredding, grinding, mixing, etc., are also reduced.
2. A reduction in the environmental impact by reducing the rate of use of clay deposits and therefore the frequency of opening up new deposits.

3. Reduction in the mass and opening up of the structure of the units, thus speeding up drying and firing, cutting the fuel cost for these processes and reducing the capital cost of the plant per unit produced.
4. The oxidation of organic matter in the clay is facilitated by increasing the surface area to volume ratio and reducing the chance of blackhearting.
5. The thermal insulation is improved. This has a modest effect for UK-Standard size bricks but the improvement can be substantial for large clay blocks.
6. The units are less tiring to lay because of the lower weight.

Because of these factors and the very large proportion of the production cost spent on fuel, most clay units are perforated at least to the extent of 10–25 per cent by volume. It should be stressed that there is a penalty in that the clay must be very well ground and uniform in consistence for successful production of perforated units. Any lumps or extraneous air pockets can ruin the column. To improve consistence, the mixers are commonly heated and the front of the extruder is de-aired (evacuated) to prevent air bubbles. Figure 30.3 illustrates the production of a typical three-hole perforated brick by stiff plastic extrusion and wirecutting.

Semi-dry pressing

This is one of the simplest processes of forming bricks. In the UK only Lower Oxford clay (or shale) is used, which comes from the Vale of Aylesbury and runs in a band towards the east coast. This clay contains about 7 per cent natural shale oil which reduces the cost of firing but gives rise to some pollution problems. It is dug and then milled and ground to go through a 2.4 mm or 1.2 mm sieve without altering the water content markedly from that as-dug (8 to 15 per cent). The coarser size is used for common bricks and the finer for facings. The powdered clay is then fed into very powerful automated presses which form a deep frogged, standard size brick

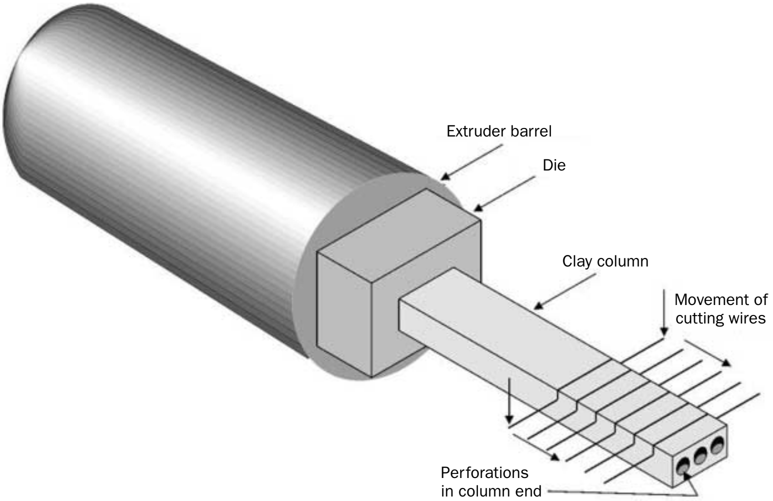

FIGURE 30.3 Stiff plastic extrusion of perforated clay bricks.

known as a Fletton (named after one of the early manufacturers). Unmodified Flettons are limited to a single barred pink/cream colour. All facing Flettons are either mechanically deformed to give a patterned surface (rusticated) or an applied surface layer, such as coloured sand, is fired on.

Drying and firing in Hoffman kilns

The Hoffman kiln is a multichamber kiln in which the bricks remain stationary and the fire moves. It is mainly used for manufacture of Flettons. In the classic form it consists of a row of chambers built of firebricks in the form of short tunnels or arches. In the most efficient form the tunnels form a circle or oval shape and are connected together and to a large central chimney by a complex arrangement of ducts. A single 'fire' runs round the circle and at any one time one chamber will be being loaded or 'set' ahead of the fire and one will be being unloaded behind the fire. The bricks are stacked in the kiln in groups of pillars termed 'blades', which leaves lots of space between units to enable the gases to circulate freely. Chambers immediately in front of the fire will be heating up using the exhaust gases from the hottest chamber and those further ahead will be being dried or warmed by gases from chambers behind the fire which are cooling down.

Figure 30.4 illustrates the broad principles of the system showing only the ducts actually in use for the fire in one position. In practice the ducts are positioned to ensure a flow through from the inlets to the outlets. The whole process is very efficient, particularly as a large proportion of the fuel is provided by the oil in the bricks themselves. Because of the organic content of the bricks, the firing has to be done under oxidizing conditions during the last phases in order to burn out the oil. If this is not done the bricks have a dark, unreduced central volume, known as a blackheart, which can give rise to deleterious soluble salts. During this phase some fuel is added to keep the temperature up. This is essentially a batch process and the average properties of the contents will vary a little from chamber to

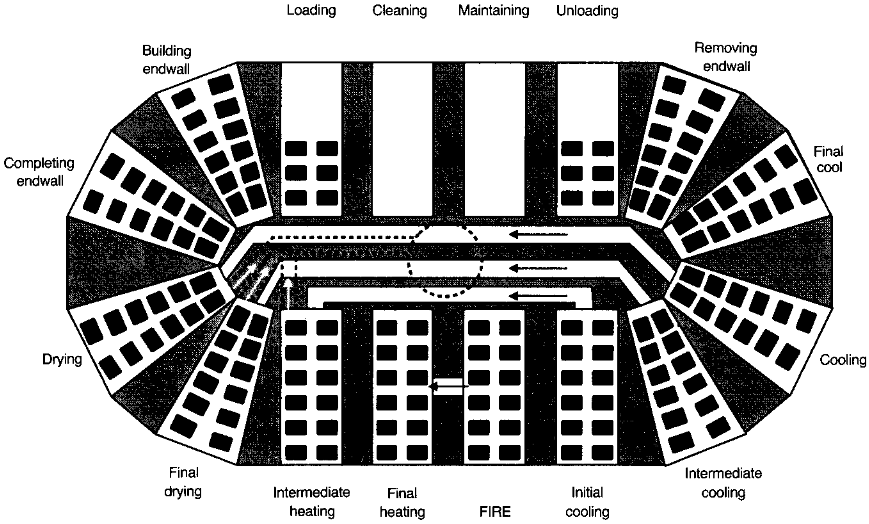

FIGURE 30.4 Principles of the Hoffman kiln.

chamber. Additionally, the temperature and oxidizing condition will vary with position in the chamber and thus some selection is necessary to maintain the consistency of the product.

Drying and firing in tunnel kilns

Tunnel kilns, as in Figure 30.5, are the complement of Hoffman kilns in that the fire is stationary and the bricks move through the kiln as stacks on a continuous train of cars. In practice a long insulated tunnel is heated in such a way that temperature rises along its length, reaches a maximum in the centre and falls off again on the other side. To maximize efficiency, only the firing zone is fuelled and hot gases are recycled from the cooling bricks and used to heat the drying and heating-up zones of the kiln. Most extruded wirecuts and stiff plastic bricks are now fired in such kilns which are continuous in operation. Stocks and other mud bricks may also be fired this way after a predrying phase to make them strong enough to withstand the stacking forces.

Clamps

Clamps are the traditional batch kilns comprising a simple insulated refractory beehive-shaped space with air inlets at the base and a chimney from the top.

Intermittent kilns

These are the modern version of the clamp where the units are fired in batch settings using oil or gas as a fuel. They are now only used for production of small runs of specially shaped brick 'specials'.

30.4.2 Properties

Clay bricks probably have the widest range of strengths of any of the manufactured masonry materials with the compressive strength ranging from 10 MPa for an underfired soft mud brick to as much as 200 MPa for a solid engineering brick. The common shapes and terminology are shown in Figure 30.6. The compressive strength is meas-

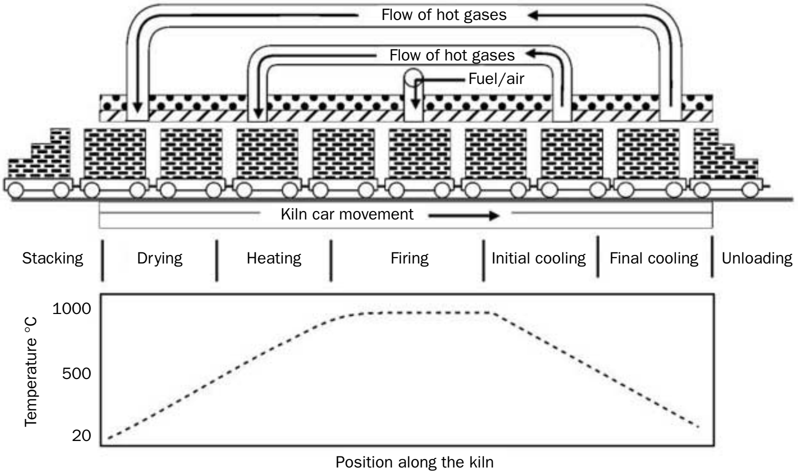

FIGURE 30.5 Tunnel kiln – principles.

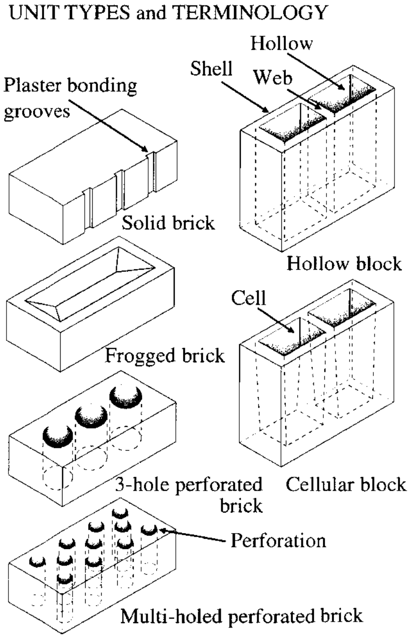

FIGURE 30.6 Shape types and terminology of masonry units. Based on Figure 1 in *BRE Digest–441* published by CRC Ltd.

ured by a crushing test on whole units with the stress applied in the same direction as the unit would be loaded in a wall. Solid and perforated units are tested as supplied, but frogs are normally filled with mortar as they would be in a wall. In BS 3921 (1985), thin plywood sheet packing is used to try to reduce the effect of high spots and unevenness of the faces. The new European test method EN 772–1 (2000) uses either mortar capping or face grinding to achieve even loading. The quoted strength is the average of six to ten determinations of stress based on the load divided by the area of the bed face. The flexural strength and modulus of elasticity is not normally a designated test parameter in unit standards but is important to obtain data for Finite element models. A standard three-point bending method is available in RILEM LUM A.2 (1994). Units having a span to depth ratio in the test geometry exceeding 4 may be tested without any further preparation provided they are sufficiently flat and true to allow even loading. Units which are not flat or true may need to be made true by applying a layer of rapid-setting mortar or plaster to the bearing area. Units having a span/depth ratio of less than 4 have too low an aspect ratio to give true bending. The span/depth ratio may be increased by gluing three units together in a line and testing the central unit.

The flexural strength (S) is given by:

$$S = M/Z \qquad (30.6)$$

where

M = the bending moment at failure, in Newton millimetres = $Pl/4$,
Z = section modulus of test specimen in cubic millimetres = $bd^2/6$,
P = maximum load applied to the prism, in Newtons,
l = distance between the axes of the support rollers, mm,
b = the mean width of prism at the line of fracture, mm = $(b_1 + b_2)/2$,
d = the mean height of prism at the line of fracture, mm = $(d_1 + d_2)/2$.

Units having a span/depth ratio of less than 4 have too low an aspect ratio to give true bending. The span/depth ratio may be increased by gluing three units together in a line and testing the central unit.

Other important properties are the dimensions, water absorption (and porosity), suction rate, density and soluble salts content. In BS 3921 the dimensions are measured by laying twenty-four units in a line and dividing the overall length by twenty-four, i.e. it is an averaging process and gives no data on individual variability. The process is repeated for each dimension with the units in the appropriate attitude. The equivalent CEN standard has individual tolerances for each unit. Water absorption and density are measured in the same way as for mortar (see Section 30.3.2), except that the preferred saturation technique is to boil the units in water for 5 hours.

TABLE 30.5 Properties (typical ranges) for UK brick types

Brick type	*Compressive strength (MPa)*	*Water absorption (Weight %)*	*Water porosity (Volume %)*	*Suction rate (IRA) (kg/m²/min)*	*Bulk density (kg/m³)*	*Flexural strength (MPa)*
Handmade facing	10–60	9–28	19–42	–	–	–
London Stock	5–20	22–37	36–50	–	1390	1.6
Gault wirecut	15–20	22–28	38–44	–	1720	–
Keuper marl wirecut	30–45	12–21	24–37	–	2030	–
Coalmeasure shale	35–100	1–16	2–30	–	2070	–
Fletton	15–30	17–25	30–40	1.0–2.0	1630	2.8
Perforated wirecut	35–100	4,5–17	–	0.2–1.9	1470–2060	7
Solid wirecut	20–110	4–21	10–35	0.25–2.00	1700–2400	6.5

The initial rate of absorption (IRA, suction rate) is measured to give some idea of the effect of the unit on the mortar. Units with high suction rates need very plastic, high water/cement ratio mortars, while units with low suction rates need stiff mortars. The parameter is measured by standing the unit in 3 mm depth of water and measuring the uptake of water in 60 seconds.

The IRA is calculated using:

$$w_i = (m_2 - m_1)/Lb \qquad (30.7)$$

where

w_i = initial rate of absorption,
m_1 = initial mass of the unit/specimen,
m_2 = mass after 60 seconds of water absorption,
L = length of the bed (mortar) face in service to an accuracy of 0.5 per cent,
b = width of the bed (mortar) face in service to an accuracy of 0.5 per cent.

The result is normally given in units of kg/m²/min.

The content of soluble salts is measured by standard wet chemical analysis techniques or by modern instrumental techniques such as flame photometry. The elements and compounds of concern are sulfates, sodium, potassium, calcium and magnesium. Table 30.5 gives typical values/ranges for some of the key properties of clay bricks.

In most brickwork, bricks are loaded upon their normal bed face but often they are loaded on edge or on end. Typical examples are headers and soldiers (see Figure 31.3) in normal walls, stretchers in arches and reinforced beams and headers in reinforced beams. While solid bricks show a small variation in strength for loading in different directions, due to the change in aspect ratio (height/thickness), perforated, hollow or frogged units may show marked differences as illustrated in Table 30.6 from data in Lenczner (1977), Davies and Hodgkinson (1988) and Sinha and de Vekey (1990).

Taking the simplest geometry as an example, it can be seen from Figure 30.7 that the minimum cross-sectional area of the 5-slot unit resisting the load will be 80 per cent on bed but 71 per cent on edge and 25 per cent on end. The ratios of the strengths in Table 30.6 follow approximately the ratios of the areas. Other factors such as the slenderness of the load-bearing sections and the effect of high local stresses at rectangular slot ends complicate the behaviour and may explain the variations between different types. It can also be shown that porosity, in the form of vertical perforations result in a smaller reduction of the strength of a material than does generally distributed porosity and is the more efficient way of reducing the weight. This is illustrated in Figure 30.8. More detailed information on clay brick properties is contained in BRE Digests 441 Part 1 and 2 (1999).

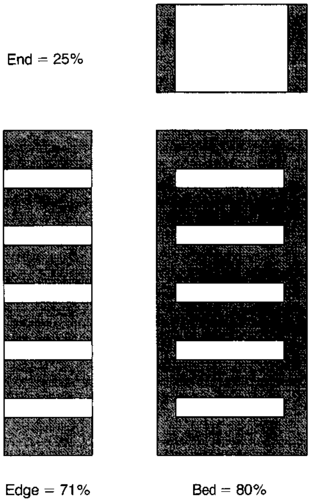

FIGURE 30.7 Area of 5-slot brick resisting load in the three orientations.

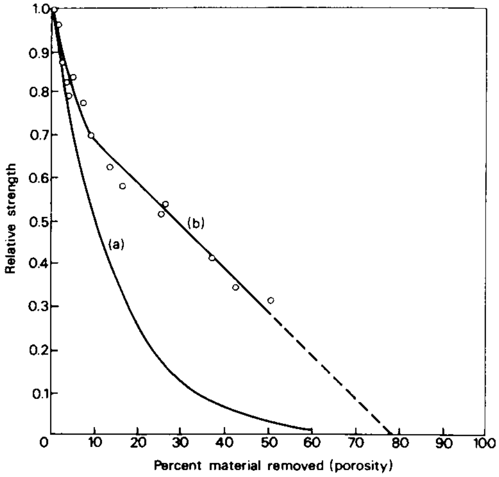

FIGURE 30.8 Compressive strength of ceramic bodies as a function of: (a) general porosity; (b) vertically aligned perforations of constant diameter.

TABLE 30.6 Properties of some UK brick types in various orientations

Type	*Ref.*	*Perforation (Vol. %)*	*Compressive strength on bed (MPa)*	*Proportion of the on-bed strength as a percentage*			*Water absorption (Weight %)*	*Suction rate (IRA) (kg/m²/min)*
				On bed	*On edge*	*On end*		
23 hole	(a)	?	65.5	100	29	11	6.9	0.6
14-hole	(b)	21.3	74.3	100	35	14	3.9	–
14 hole	(c)	?	44.8	100	29	11	4.7	1.8
10 hole	(d)	23.1	70.2	100	42	31	5.4	–
3 hole	(e)	12.2	82	100	65	49	4.2	–
3 hole	(f)	?	57.8	100	36	25	8.5	1.5
5 cross slots	(g)	20	64.1	100	81	22	3.4	–
16 hole	(A)	20.1	64.7	100	31	13	5.5	0.35
Frogged	(B)	15.1	25.4	100	41	36	21.7	2.86
Frogged	(C)	6.2	33.7	100	49	51	14.4	1.06
Frogged	(D)	8.6	31.7	100	92	50	11.9	0.54
Solid	(E)	0	43.5	100	67	65	22.8	3.31

Note: The reference given links the strength data in this table to strength data for masonry specimens in Table 32.1.

TABLE 30.7 Property ranges of calcium silicate bricks (West *et al.*, 1979)

Brick type	*Compressive strength (MPa)*	*Water absorption (weight %)*	*Initial rate of suction (kg/m²/min)*	*Bulk density (kg/m³)*	*Frog volume (%)*
Solid	20–50	8–22	0.25–2.0	1750–2000	0
Frogged	20–55	13–20	0.5–1.2	1650–1950	4–7

30.5 Calcium silicate units

These are manufactured from mixtures of lime, silica sand and water. Aggregates such as crushed rocks or flints may be incorporated to alter the performance and appearance, and pigments may be used to vary the colour. Common colours are whites, blacks, buffs and grey-blues. Reds are produced but they seldom have the richness of fired clay units. There is only one basic process, in which the mixture is pressed to high pressures in a die in a static press, ejected, set on cars and then placed in autoclaves and cured in high pressure steam for several hours. The mix is invariably fully compacted and makes a very precisely shaped, low tolerance unit with sharp, well-defined corners (arrises) and a fairly smooth finish. The properties commonly measured are given in Table 30.7. Additionally a drying shrinkage test may be carried out.

30.6 Concrete units

Concrete units have been made since the 1920s and were widely used, in the form of the 'breeze' block, to build partitions in houses in the building boom of the 1930s. In the past 40 years, however, the range of products has expanded enormously to cover facing bricks and blocks, high-strength units, simulated stone units, thermally insulating blocks and pavers. Chapters 13 to 24 describe the performance and behaviour of concrete. Most aggregate concrete units are produced by pressing specially designed mixes. Some of the processes used and the resulting products,

TABLE 30.8 Properties of some typical aggregate concrete blocks

Unit type	*Size L × H × T (mm)*	*Void (%)*	*Bulk density (kg/m³)*	*Concrete density (kg/m³)*	*Compressive strength[1] (MPa)*	*Flexural strength[2] (MPa)*	*Young's modulus (GPa)*	*Water[3] absorption (weight %)*
Brick	215 × 65 × 103	0	2160	2160	32.5	–	–	6.3
DA Block	438 × 213 × 98	0	2140	2140	15.5	2.59	–	10.9
DA Block	390 × 190 × 140	41.6	1350	2320	31.6	–	42.3	–
LWA Block	390 × 190 × 140	22.1	1630	2090	21.5	–	32.8	–
LWA Block	390 × 190 × 140	0	2170	2170	29.9	–	23.6	–
LWA Block	390 × 190 × 90	0	2060	2060	21.6	–	17.5	–
LWA Block	390 × 190 × 90	19.9	1100	1380	8.1	–	9	–
LWA Block	439 × 215 × 98	0	2190	2190	6.6	0.5	–	35

Notes:

1. Compressive strength tested wet and mortar capped in accordance with BS 6073 Appendix B. Similar values are obtained by testing between fibreboard at ex-factory water content.
2. Flexural strength (MOR) measured in accordance with BS 6073 Appendix C.
3. Measured by vacuum absorption.

e.g. autoclaved aerated concrete (AAC), are wholly different from normal concrete; thus a full description is given.

30.6.1 Production processes

Casting concrete

Concrete blocks can be manufactured by pouring or vibrating a concrete mix into a mould and demoulding when set. While this method is used, particularly for some types of reconstituted stone or faced blocks, it is not favoured because of its slowness and labour demands.

Pressing of concrete

This is a widely used method for producing solid and hollow bricks and blocks either in dense concrete or as a porous open structure by using gap-graded aggregates and not compacting fully. The machine is basically a static mould (or die), which is filled automatically from a mixer and hopper system, and a dynamic presshead which compacts the concrete into the die. After each production cycle the green block is ejected onto a conveyor system and taken away to cure either in air or often in steam. The presshead may have multiple dies. A variation of the method is the ‘egg layer’. This performs the same basic function as a static press but ejects the product straight onto the surface on which it is standing and then moves itself to a new position for the next production cycle.

Curing

All aggregate concrete products may either be cured at ambient or elevated temperature. The elevated temperatures are usually achieved by the use of steam chambers and allow the manufacturer to decrease the curing period or increase the strength or both. Products cured externally should not be made when the temperature is near or below 0°C since they will be damaged by freezing while in the green state.

Autoclaved aerated concrete (AAC)

AAC is made by a process, developed originally in Scandinavia, to produce solid microcellular units which are light and have good insulating properties. The method involves mixing a slurry containing a fine siliceous base material, a binder, some lime and the raising agent, aluminium powder, which reacts with the alkalis (mainly calcium hydroxide) to produce fine bubbles of hydrogen gas as per equation (30.8). This mixture is poured into a mould maintained in warm surroundings and the hydrogen gas makes the slurry rise like baker’s dough and set to a weak ‘cake’. The cake is then cured for several hours at elevated temperature, demoulded, trimmed to a set height and cut with two orthogonal sets of oscillating parallel wires to the unit size required using automatic machinery. The cut units are then usually set, as cut, onto cars which are run on rails into large autoclaves. The calcium silicate binder forms by reaction under the influence of high-pressure steam. Additional curing after autoclaving is not necessary as all the units can be incorporated in work as soon as they have cooled down.

The binder reaction is conventional, as given in Section 30.1. The cellular structure gives the product good thermal properties and a high strength/density ratio. The light weight allows larger units to be handled comfortably so some double-size units are now produced for use with thin-bed mortar.

$$\mathrm{Ca(OH)_2 + 2Al + 2H_2O \rightarrow CaAl_2O_4 + 3H_2} \quad (30.8)$$

This produces a structure of small, closed cells surrounded by cell walls composed of a fine siliceous aggregate bound together by calcium silicate hydrates. The nature of the principal siliceous material is identifiable from the colour: ground sand produces a white material and pulverized fuel ash a grey material.

Because of the light weight (low density), the product can be made into large-sized blocks while remaining handleable. The largest units currently available are 447 mm by 447 mm face size which are designed for building thin-joint masonry (see

BRE Digest 432 (1998)). Still the most common size for normal work is 440 × 215 × 100 (or thicker).

30.6.3 Products and their properties

Dense aggregate concrete blocks and concrete bricks

These are generally made from well-graded natural aggregates, sands, pigments and ordinary or white Portland cement by static pressing to a well-compacted state. Figure 30.9 (a) illustrates the principle of such materials where the voids between large particles are filled with smaller particles. They are strong, dense products and are often made with a good surface finish suitable for external facing masonry. They are also suitable for engineering applications. Bricks are produced mainly as the standard size (215 × 102 × 65 mm) in the UK but in a wide range of sizes in continental Europe. Blocks are produced either solid or hollow by varying the quantity of mix and the shape of the press platen. In order to facilitate demoulding the hollows will always have a slight taper. The hollows in UK products are all designed to run vertically in the finished masonry as this gives the optimum strength to weight ratio. The face size of UK units is generally 440 mm long by 215 mm high but the thickness may vary from 50 mm to 300 mm. Some of the important properties are summarized in Table 30.9.

Reconstructed stone masonry units

These have essentially the same specification as dense-aggregate concrete blocks except that the main aggregate will be a crushed natural rock such as limestone or basalt and the other materials will be chosen such that the finished unit mimics the colour and texture of the natural stone.

Lightweight aggregate concrete blocks

These are generally produced as load-bearing building blocks for housing, small industrial buildings, in-fill for frames and partition walling. High strength and attractive appearance are rarely the prime consideration but handling weight, thermal properties and economy are important. Inherently low-density aggregates are used and are often deliberately gap-graded, as illustrated by Figure 30.9 (b), and only partly compacted to keep the density down. They will frequently be made hollow as well to reduce the weight still further. The aggregates used are sintered pfa nodules, expanded clay, furnace clinker, furnace bottom ash, pumice or foamed slag together with sand and binder. Breeze is a traditional term for a lightweight block made from furnace clinker. Often low-density fillers or aggregates such as sawdust, ground bark or polystyrene beads are incorporated to further reduce the density. They are produced either by static pressing or in egglayer plants. Some of the important properties are summarized in Table 30.8. The properties commonly measured include the compressive strength by the method used for clay bricks for brick-sized units but capped with mortar to achieve flat parallel test faces for blocks. The flexural strength has also been used to evaluate partition blocks which bear lateral loads but only self-weight compressive loads. It is a simple, three-point bend test of the type described in Section 30.4.3 for clay units with an aspect ratio greater than 4. Other properties measured include dimensions, water absorption by the method of vacuum absorption, density and drying shrinkage.

Autoclaved aerated concrete (AAC)

Fine sand or pulverized fuel ash or mixtures thereof is used as the main ingredient. The binder is a mixture of ordinary Portland cement (opc), to give the initial set to allow cutting, and lime which reacts with the silica during the autoclaving to produce calcium silicate hydrates and gives the block sufficient strength for normal

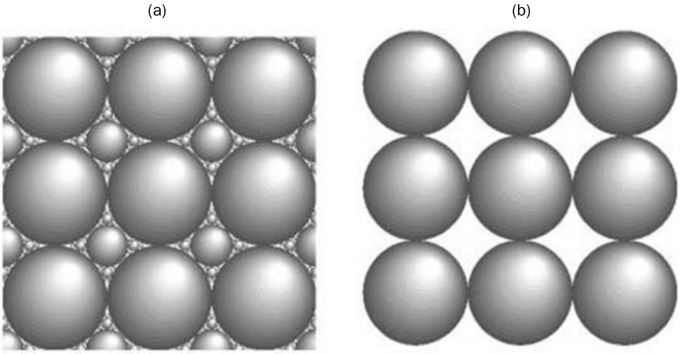

FIGURE 30.9 Types of aggregate (a) well graded; (b) gap graded (schematic).

building purposes. Some of the key properties are summarized in Table 30.9.

30.7 Natural stone

The UK possesses a great variety of geological types of natural stone and has a long tradition of building masonry using locally available stones. Used locally, it is environmentally friendly since the only energy input is for cutting and transportation. The main types used in the UK are 'sedimentary rocks' formed from compressed sediments from the bottom of ancient seas – the limestones and sandstones; 'metamorphic rocks' formed by the action of pressure and high temperature on sedimentary deposits – the marbles and slates; and 'igneous rocks' formed by melting of rock during volcanic activity – the granites and basalts. Both strength and durability are very variable and will depend on the porosity and the distribution of pores. Generally, strength increases and porosity decreases from sedimentary through metamorphic to igneous. Igneous rocks are fairly homogeneous, i.e. have similar

TABLE 30.9 Properties of AAC

Type	*Dry density (Typical kg/m³)*	*Compressive strength tested to BS 6073: 1981*		*Flexural strength (Typical MPa)*	*Tensile strength (Typical MPa)*	*Young's modulus[2] (GPa)*	*Thermal conductance @ 3% moisture (W/m°K)*
		(Nominal MPa)	*(Typical[1] MPa)*				
Low density	450	2.8	3.2	0.65	0.41	1.6	0.12
	525	3.5	4	0.75[3]	0.52	2.00[3]	0.14
Standard	600	4	4.5	0.85	0.64	2.4	0.16
	675	5.8	6.3	1.00[3]	0.76	2.55	0.18
High density	750	7	7.5	1.25	0.88	2.7	0.2

Notes:

1. Nominal values are manufacturer's declared values while the alternatives are values typical of modern production plants.
2. Linear extrapolation of a limited range of splitting tests (Grimer and Brewer, 1965).
3. Interpolated value.

TABLE 30.10 Properties of some types and examples of stone

Type of stone	*Density* (*kg/m³*)	*Water absorption* (*% w/w*)	*Porosity* (*% v/v*)	*Compressive strength* (*MPa*)	*Young's modulus* (*GPa*)
Typical ranges					
Limestone	1800 to 2700	0.1 to 17	0.3 to 30	20 to 240	1 to 8
Sandstone	2000 to 2600	0.4 to 15	1 to 30	20 to 250	0.3 to 8
Marble	2400 to 2800	0.4 to 2	0.4 to 5	40 to 190	–
Slate	2600 to 2900	0.04 to 2	0.1 to 5	50 to 310	–
Granite	2500 to 2700	0.04 to 2	0.1 to 4	80 to 330	2 to 6
Basalt	2700 to 3100	0.03 to 2	0.1 to 5	50 to 290	6 to 10
Individual examples					
York sandstone	2560	2.62	7.6	72.6	–
Portland limestone	2209	5.33	11.8	32	–

properties in all directions, but the other types have a layer structure and will be significantly stronger normal to the bed plane than in the other two directions (inhomogeneous). To ensure the optimum performance the layered rocks are usually cut to maintain the bed plane perpendicular to the compressive stress field in the building, e.g. horizontal in normal load-bearing masonry. This also gives the optimum durability. BRE Digest 420 (1997) is a good introduction and gives a useful set of references, and the Geological Society SP16 (1999) has up-to-date and comprehensive coverage. Some performance characteristics of well-known types are given in Table 30.10 and movement data is given in Table 32.4.

30.8 Ancillary devices – ties and other fixings/connectors

In order to ensure their stability, masonry elements need to be connected to either other masonry elements to form stable box structures or to other elements such as frames, floors, roofs, beams and partitions. A huge range of devices exists, summarized in Table 30.10 together with information on the current and future European Standards and guidance literature. Most of these devices are made from metal, predominantly galvanized mild steel, austenitic stainless steel and bronzes. A few light-duty tie products are made from plastic.

30.9 References

Ashurst, J. (1983) Mortars, plasters and renders. In *Conservation*, Ecclesiastical Architects and Surveyors Association, London.

BRE Digest–441, Clay bricks and clay brickwork (parts 1 and 2) (1999) CRC Ltd, Watford.

BS EN 772–1 (2000) Methods of test for masonry units. Part 1. Determination of compressive strength (Note other BS EN standards are listed in the further reading section).

Central Electricity Generating Board (1972) *PFA Utilization.*

Cowper, A.D. (1927) *Lime and Lime Mortars* (reprinted 1998, BRE Ltd).

Davies, S. and Hodgkinson, H.R. (1988) *The Stress–Strain Relationships of Brickwork When Stressed in Directions Other Than Normal to the Bed Face: Part 2, RP755,* British Ceramic Research Establishment, Stoke on Trent.

Fudge, C.A. and Barnard, M. (1998) Development of AAC masonry units with thin joint mortar for housebuilding in the UK, Proc. 5th International Mas. Conf. London 1998 (BMS Proc. 8), 384–7.

Grimer, F.J. and Brewer, R.S. (1965) The within cake variation of autoclaved aerated concrete. *Proceedings of Symposium on Autoclaved Calcium Silicate Building Products,* Society of Chemical Industry, May, 163–70.

Harrison, W.H. (1981) Conditions for sulphate attack on brickwork. *Chemistry and Industry.*

TABLE 30.11 Ancillary devices

Connecting device	*Purpose*	*Specification document*[1]	*Guidance documents*[1]
Cavity wall ties	To link the two leaves of cavity walls and share tension, compression and shear loads	BS 1243, BS DD140, EN 845–1[2]	BRE IP16/(1988), BS 5628 (1993),[3] BRE IP11 (2000)
Support ties	To link walls to frames	BS DD140, EN 845–1[2]	BRE IP17/(1988), BS 5628:p1 (1993) BRE IP11 (2000)
Shear ties	To give shear connections between elements	EN 845–1[2]	BS 5628:p1 (1993)[4] BRE IP11 (2000)
Slip ties	To give shear connections between elements while allowing in-plane movement	EN 845–1[2]	BS 5628:p3 (1985) BRE IP11 (2000)
Straps	To tie walls to roofs and floors	BS 8103, EN 845–1[2]	BS 8103 (1995), BRE GBG 29 (1997)
Joist hangers	To support floors on unperforated walls via the joists	BS 6178: Part 1, EN 845–1[2]	BS 8103 (1995), BS 5628:p1 (1993)
Brackets	To support the load of walls on frames	EN 845–1[2]	[1]
Angles	To support walls on frames	[1]	[1]
Anchors and fixings	Fixing devices such as screws, nails, screw-plug systems, resin-anchors, expanding anchors, for attaching fittings to walls	[1]	BRE Digest 329, (2000 edition) CIRIA TN 137: 1991 W.S. Paterson

Notes:

1. Most manufacturers can supply data on specification and installation instructions.
2. The CEN standard EN 845–1 covers most of these devices but is unlikely to be issued in its final BS EN form till 2001.
3. Illustrated in Figure 31.4.
4. Illustrated in Figure 31.5.

Harrison, W.H. (1986) Durability tests on building mortars – effect of sand grading. *Magazine of Concrete Research* 38, 135, 95–107.

Harrison, W.H. and Bowler, G.K. (1990) Aspects of mortar durability. Br. Ceram. Trans. J. 89, 3, 93–101.

Lenczner, D. (1977) *Strength of Bricks and Brickwork Prisms in Three Directions,* Report No. 1, University of Wales Institute of Science and Technology, Cardiff.

Phillipson, M.C., Fudge, C.A., Garvin, S.L. and Stupert, A.W. (1998) Construction with thin joint mortar systems and AAC blockwork, Proc. 5th International Mas. Conf. London (BMS Proc. 8), 388–90.

RILEM (1975) Recommendations for testing methods of aerated concrete. *Materials and Structures* 8, 4S, 211.

RILEM (1978) Recommendations for the testing of mortars and renderings. *Materials and Structures* 11, 63, 207.

RILEM *Technical recommendations for the testing and use of construction materials* (1994), E & FN Spon, London, LUM A.2 Flexural strength of masonry units, 459–61.

Sinha, B.P. and de Vekey, R.C. (1990) A study of the compressive strength in three orthogonal directions of brickwork prisms built with perforated bricks. *Masonry International* 3, 3, 105–10.

Smith, M.R. (ed.) (1999) *Building Stone, Rock Fill and Armourstone in Construction*, Special Publication No. 16, Geological Society, London.

Southern, J.R. (1989) *BREMORTEST: A Rapid Method of Testing Fresh Mortars for Cement Content,* BRE Information Paper IP8/89, Building Research Establishment, Watford.

Stupert, A., Skandamoorthy, J.S. and Emerson, F. (1998) Thermal and strength performance of two lightweight mortar products, Proc. 5th International Mas. Conf. London (BMS Proc. 8), 103–6.

Task group of ASTM Subcommittee section C09.03.08.05 (1980) Pigments for integrally coloured concrete. *Cement, Concrete and Aggregates*, CCAGDP, 2, 2, Winter 1980, 74–7.

de Vekey, R.C. (1975) The properties of polymer modified cement pastes. *Proceedings of the First International Polymer Congress*, Congress on Polymer Concrete, London, VI, 94–104.

de Vekey, R.C. and Majumdar, A.J. (1977) Durability of cement pastes modified by polymer dispersions. *Materials and Structures* 8, 46, 315–21.

Vicat, L.J. (1837) *Treatise on Calcareous Mortars and Cements*, translated by Smith, J.T., reprinted Donhead Publishing, Shaftesbury, 1997.

West, H.W.H., Hodgkinson, H.R., Goodwin, J.F. and Haseltine, B.A. (1979) *The Resistance to Lateral Loads of Walls Built of Calcium Silicate Bricks,* BCRL, Technical Note 288.

WRC Information and Guidance Note IGN 4–10–01 (1986) *Bricks and Mortar,* Water Research Council, Oct.

Chapter thirty-one

Masonry construction and forms

31.1 Introduction

This chapter is concerned with how masonry is built and the architectural forms used. Appearance is a very important aspect; the basic structural form of many types of masonry is expressed on the surface of the buildings and other structures and can be a very attractive and reassuring aspect of these structures. Appearance is a synthesis of the size, shape and colour of the units, the bond pattern, the mortar colour and finish, the masonry elements – walls, piers, columns, corbels, arches, etc. – and the scale and proportion of the whole structure. Other key aspects are the workmanship, the accuracy, the detailing in relation to other features and the use of specially shaped units.

The basic method of construction has hardly changed for several thousand years: units are laid one on top of another in such a way that they form an interlocking mass in at least the two horizontal dimensions. It is not practical to achieve interlocking in a third dimension with normal rectangular prismatic units but a degree of such interlocking is sometimes used in ashlar stonework. Most practical masonry employs a mortar interlayer to allow for small inaccuracies of size between units and to make walls watertight, airtight and soundproof.

31.2 Mortar

Mortar must be mixed thoroughly and its proportions kept constant. It should not be overmixed as this will introduce too much air and reduce the durability. Portland cement mortars have a pot life of about one hour and they should be discarded after the time limit or if they become unworkable. Traditional lime mortars and retarded opc mortars have a much longer pot life which makes them easier to use. For optimum bond and ease of laying, the mortar should always be matched to the units being laid. As a general rule dense low absorption units need a fairly firm, dry mortar (e.g. with a dropping ball consistence of around 10 or less), while high absorption units need a sloppy wet mortar with a dropping ball consistence of 13–15. Alternative techniques for improving usability are the use of agents in the mortar which hold water in (water retentivity aids) or wetting the units to reduce their suction.

31.3 Walls and other masonry forms

Walls are built by laying out a plan at foundation level and bringing the masonry up layer by layer. To maximize the strength and attractiveness it is important to make sure that all the foundation levels are horizontal, are accurate to the plan and allow multiples of whole units to fit most runs between returns, openings, etc. It is also essential to maintain the verticality (plumb), the level of bed joints and the straightness of the masonry within reasonable limits. The thickness of the mortar joints must be kept constant within a small range, otherwise the masonry will look untidy. The standard technique used is to generate reference points by building the corners (quoins) accurately using a plumb bob and line, a builder's level, a straight edge and a rule. Any openings are then filled with either a temporary or permanent frame placed accurately in the plan position. Lines are stretched between the reference points and the intervening runs of masonry are built up to the same levels.

Columns, piers and chimneys are built in the same way but need plumbing in two dimensions and more care because of their small dimensions.

Arches and tunnels must follow a curved shape defined by the architect or engineer and are traditionally built on timber formwork. Adjustable reusable metal formwork systems are also available. Some arches use special tapered units called voussoirs but large radius or shallow arches may be built with standard units and tapered joints. Figure 31.1 illustrates the main

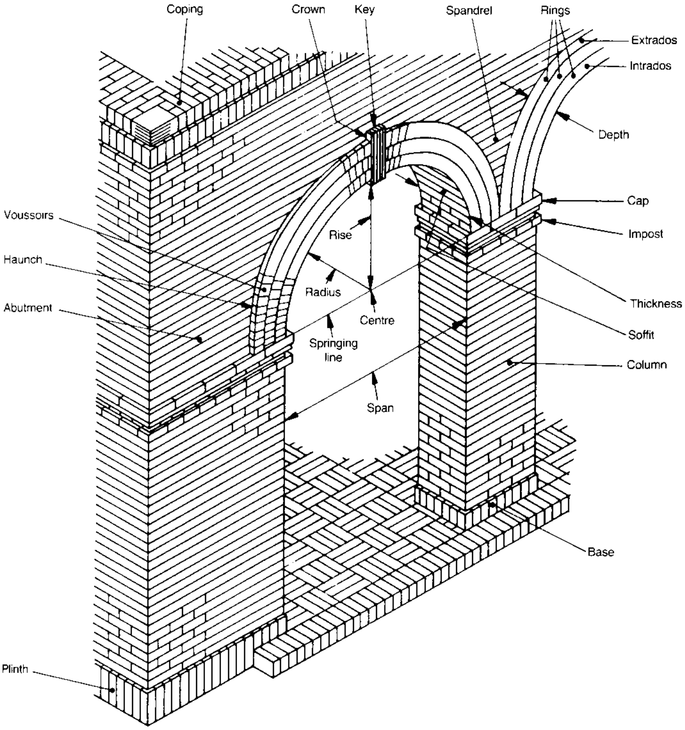

FIGURE 31.1 Structural elements and terminology of arches.

elements of arches and the special vocabulary for them.

Reinforced and post-tensioned masonry are used to a limited extent in the UK mainly for civil engineering structures, high single-storey halls, retaining walls and lintels within walls. Masonry lintels may sometimes be constructed by laying special bed joint reinforcement in the mortar. This acts as a tension reinforcement for a masonry beam. Most other reinforced masonry is formed by building masonry boxes in the form of hollow piers, walls with cavities or walls with slots in them, and then locking the reinforcing elements into the voids using a concrete grout. Post-tensioned masonry may be built in the same way but the reinforcement is then passed through the cavities and stressed against end plates which removes any necessity to fill with grout. Figure 31.2 shows some typical reinforced masonry forms.

31.4 Bond patterns

Most modern masonry is the thickness of a single unit breadth and is built by overlapping half the length with the next unit. This is known as stretcher bond or half bond and is shown in Figure 31.3. Variations of stretcher bond may be

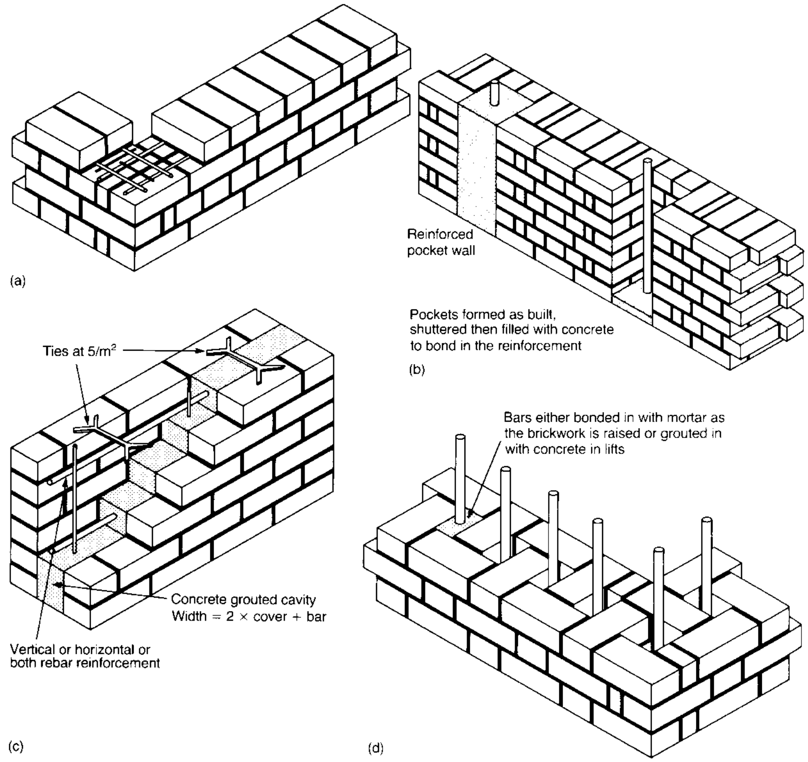

FIGURE 31.2 Reinforced and post-stressed masonry forms: (a) bed joint reinforced; (b) reinforced pocket walls; (c) grouted cavity; (d) quetta bond.

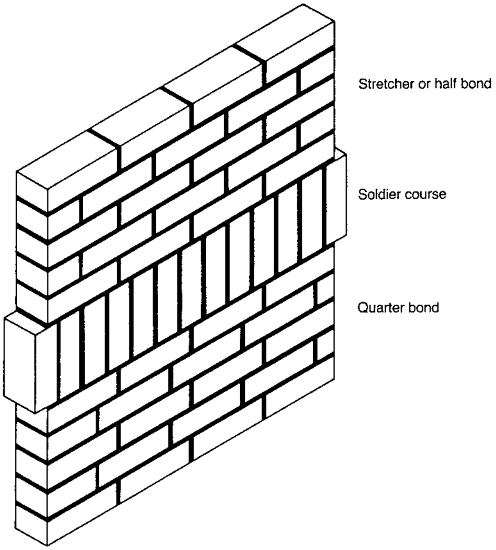

FIGURE 31.3 Half-brick bonds.

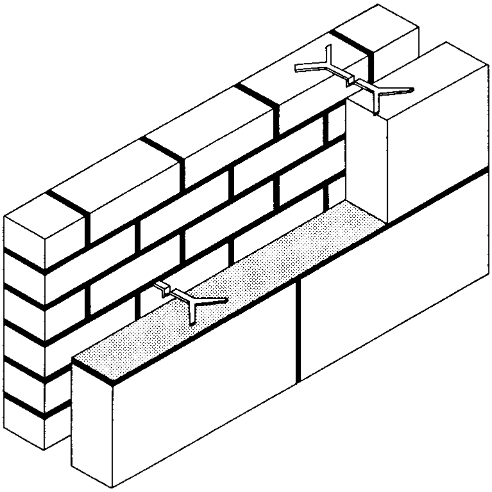

FIGURE 31.4 Typical block/brick cavity wall.

achieved by using third or quarter bond (also shown). Soldier courses, where all the units stand on their ends, may be incorporated as a decorative feature but reduce the strength and robustness of the masonry. Much of this stretcher bonded work is used as cladding to frame structures where the strength is less important because of the presence of the supporting structure. In occupied structures it is widely used in the form of the cavity wall, as illustrated in Figure 31.4, which comprises two such walls joined with flexible metal ties across a space which serves principally to keep out rain and keep the inner wall dry. Blockwork is almost universally built with this bond and broader units are used to achieve thicker walls. Stretcher bonded walls may be built thicker by linking two or more layers with strong metal ties and filling the vertical 'collar' joint with mortar. The collar jointed wall, Figure 31.5, may be built with a smooth true face ('fair face') on both visible sides by taking up any thickness variations by varying the thickness of the collar joint.

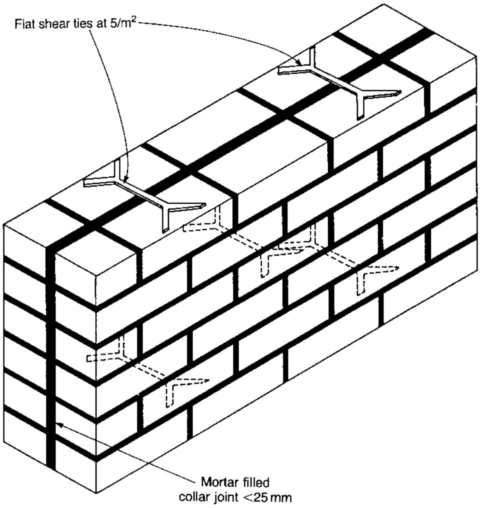

FIGURE 31.5 Collar-jointed brick wall.

In thicker walls, built in multiples of a single unit breadth, there are a large number of possible two-dimensional bonding patterns available known by the traditional names. A few of the widely practised bonds are shown in Figure 31.6 and more are given in BS 5628: Part 3 and Handisyde and Haseltine (1980).

31.5 Specials

It has always been possible to make structures more interesting by using specially shaped units to vary angles from 90°, to generate tapers, plinths, curves, etc. In recent years such features have, if anything, become more popular. A very large range of shapes is available on a regular basis and are known as 'standard specials'. Additionally, it is possible to get almost any shape manufactured to order although it is inevitably quite expensive for small quantities. As an alternative, some specials can be made by gluing cut pieces of standard bricks with high performance adhesives. Some of the typical varieties are illustrated in Figure 31.7.

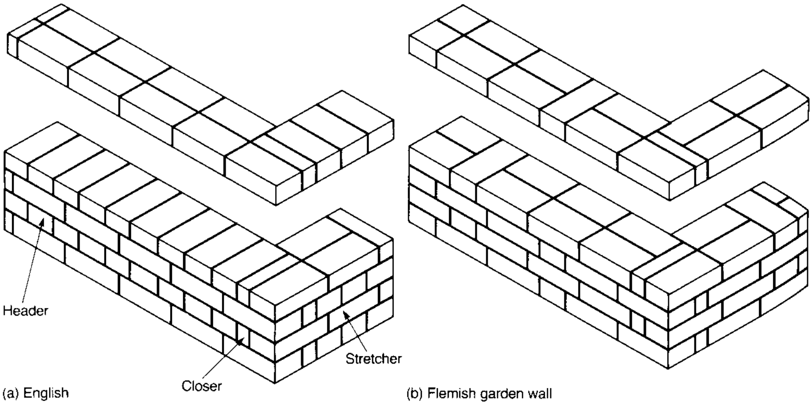

(a) English

(b) Flemish garden wall

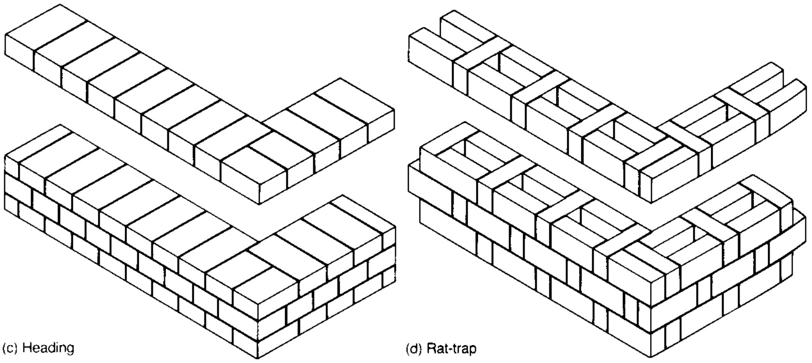

(c) Heading

(d) Rat-trap

FIGURE 31.6 Bonded wall types: (a) English bonded wall; (b) Flemish garden wall; (c) Heading bond; (d) Rat-trap bond.

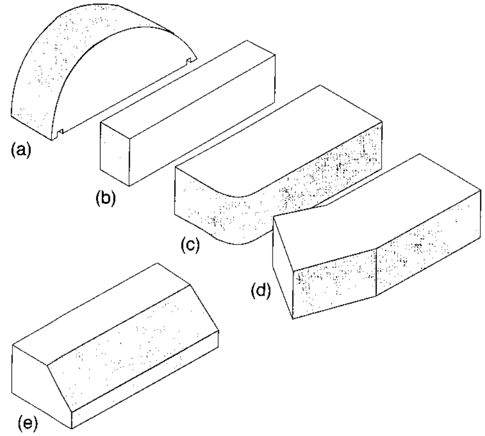

FIGURE 31.7 Standard special bricks (a) Coping (b) Queen-closer (c) Single bull-nose (d) External angle (e) Plinth.

31.6 Joint-style

It is often not realized how much the joint colour and shape influence the appearance and performance of masonry. Obviously the colour contrast between the mortar and the units must have a profound effect on the appearance but so does the shape of the finished joint. The common joint styles are shown in Figure 31.8. Recessed and weathered joints cast shadows and increase the contrast between mortars and light-coloured bricks in most lighting conditions.

31.7 Workmanship and accuracy

Standards of good workmanship in terms of how to lay out work and avoid weather problems by protection of new work against rain, wind and frost are covered in BS 5628 (1985). Realistic tolerances for position on plan, straightness, level, height and plumb are given in BS 8000: Part 3 (1985) based on BS 5606 (1999); principles and tighter tolerances are specified in SP56 (1980) for structural quality masonry. The draft of EN 1996–2 contains similar information.

31.8 Buildability, site efficiency and productivity

The process of constructing masonry has traditionally been regarded as difficult to mechanize and 'bring fully up to date'. This is partly because it is a skilled craft and often has to be adapted to compensate for inaccuracies in other components. There is also a tendency to a high wastage rate, because of the use of mortar which has a finite life and because of poor handling and storage conditions on site and losses between stores and the workpoint. Many of these problems have been improved by innovations such as shrink wrapping of materials, crane delivery of packs direct to the work points and the use of retarded ready-to-use mortar with a long shelf life.

Despite many attempts it has not yet been possible to economically automate the site construction of masonry. Bricklaying machines have been

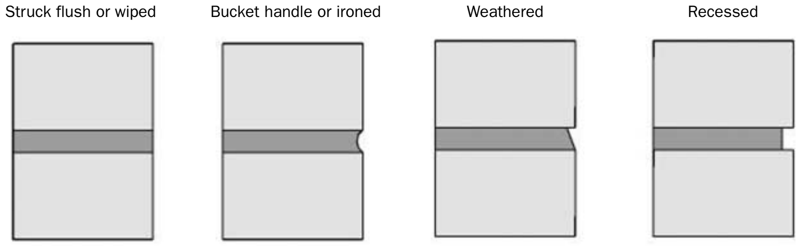

FIGURE 31.8 Joint styles.

developed but only suitable for building the simplest of walls. For a brief period in the 1960/70s prefabricated brickwork cladding panels became popular in the USA and some degree of mechanized construction was feasible for relatively simple factory-built panels. Recent continental innovations are the use of very large masonry units, with cranes to lift them if necessary, and the use of thin joint mortar to bond them. The larger size and simple technique necessary can improve productivity and speed to similar levels to that of timber frame for building the structural core of small–medium buildings. They can then be clad with conventional brickwork or other finishes. Since the cladding is off the critical path, it is possible to simultaneously finish the outside and the inside in the same way as framed buildings.

31.9 Appearance

This is very much a matter of taste and expectation but there are some general rules to follow. Precisely shaped bricks with sharp arrises demand accurate layout with perpends lined up vertically and evenly sized mortar joints throughout, otherwise they tend to look untidy. Less accurate, uneven bricks will tolerate some variation in joint size and position without looking ugly. Except with very accurate bricks, walls can only be made fair faced on one side while the other side has to suffer from any variability in thickness of the units. If a solid, 220 mm thick wall is required to have two fair faces it should be built as a collar jointed wall. If an internal half-brick wall is exposed on both faces it is probably best to use a joint which is tolerant of some inaccuracy, such as a recessed joint.

Exposed external walls should be protected as much as possible from run-off of rain. Any detail which causes large amounts of rain water to course down the wall in one spot or leach out through mortar joints at damp-proof membranes will eventually lead to discoloration due to staining by lichen, lime or efflorescence.

31.10 References

BS 5628: Part 3: (1985) British Standard Code of Practice for use of masonry: Part 3: Materials, components design and workmanship. BSI, London. (New issue due in 2001).

BS 8000: Part 3: (1989) British Standard Code of Practice for Workmanship on Building Sites: Part 3: Masonry. BSI, London (New issue due in 2001).

BS 4729: (1990) Specification for dimensions of bricks of special shapes and sizes. BSI, London (New version due 2001).

BS 5606: (1990) British Standard Guide to accuracy in building. BSI, London.

Draft EN 1996–2 Eurocode 6 Design of Masonry Structures: Part 2 Design, selection of materials and execution.

Handisyde, C.C. and Haseltine, B.A. (1980) *Bricks and Brickwork,* Brick Development Association. Windsor.

SP 56 (1980) *Model Specification for Clay and Calcium Silicate Structural Brickwork*, British Ceramic Research Establishment, Stoke on Trent.

Chapter thirty-two

Structural behaviour and movement of masonry

32.1 Introduction

Like any structural material, masonry must resist loads or forces due to a variety of external influences (actions) and in various planes. Figure 32.1 from BRE Digest 246 (1981) illustrates the various forces that can arise and the likely actions. Like plain concrete, unreinforced masonry is good at resisting compression forces, moderate to bad at resisting shear but very poor when subjected to direct tension. Masonry structures which are required to resist significant tensile forces should be reinforced by adding steel or other tension components. Unlike concrete, however, masonry is highly anisotropic because of its layer structure and this must always be borne in mind in design.

Masonry is quite effective at resisting bending forces when spanning horizontally between vertical supports, but it is somewhat less effective at resisting bending forces when spanning vertically or cantilevering from a support (Figure 32.2) because the resistance of a lightly loaded wall in that direction is dependent solely on the mass and the adhesion of the units to the mortar. Much of the resistance to bending and collapse, especially of simple cantilever masonry structures, is simply due to self-weight. Masonry is a heavy material,

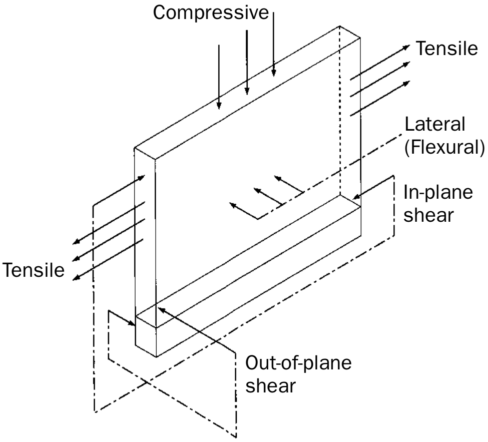

FIGURE 32.1 Forces on walls.

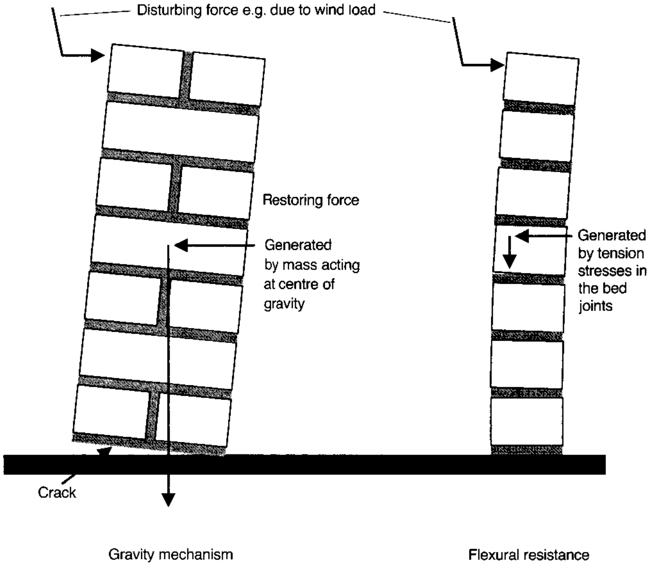

FIGURE 32.2 Mechanisms for resisting bending forces in masonry cantilevers.

usually with a density in the range 500–2500 kg/m^3, i.e. between 0.5 and 2.5 tonnes per cubic metre. In relatively squat structures such as some chimneys, parapets or low or thick boundary walls, the force needed to rotate the wall to a point of instability is sufficient to resist normal wind forces and minor impacts. Any masonry under compressive stress also resists bending since the compressive prestress in the wall must be overcome before any tensile strain can occur.

There is much empirical knowledge about how masonry works and many small structures are still designed using experience-based rules. The Limit State Code of Practice in the UK (BS 5628: Part 1: 1992) gives a calculated design procedure but much of this code is based on empirical data such as given by Davey (1952), Simms (1965), West *et al.* (1977, 1986), de Vekey *et al.* (1986, 1990). Broadly, it predicts the characteristic strength of masonry elements, such as walls, from data on the characteristic strength or other characteristics of the materials using various engineering models for the different loading conditions. A check is then made that the predicted strength is greater than the expected worse loading derived from data about wind, dead loads, snow loads and occupancy loads. To allow for statistical uncertainty in loading data, a safety factor γ_f is applied, and to allow for uncertainty about the strength of the masonry a further factor γ_m is used. The combination of these partial factors of safety (FOS) gives an overall safety factor against failure of the structure which is usually in the range 3.5–5. This relatively high FOS is used because of the high variability of masonry properties and the brittle failure mode which gives very little warning of failure.

32.2 Compressive loading

Masonry is most effective when resisting axial compressive loads normal to the bedding plane (Figure 32.1). This is, clearly, the way in which most load-bearing walls function but also the way that arches and tunnels resist load since an inward force on the outside surface of a curved plate structure or tube will tend to put the material into compression, as in Figure 32.3. If a load or force is put on a wall at a point, it would logically spread outward from the point of application in a stretcher bonded wall since each unit is supported by the two units below it. This mechanism, shown diagrammatically in Figure 32.4 by representing the magnitude of the force by the width of the arrows, leads to some stress being spread at 45° in a half-bond wall but the stress still remains higher near the axis of the load for 2 m or more. Such a compressive force causes elastic shortening (strain) of the masonry. As a result of Poisson's ratio effects, a tension strain and hence a stress is generated normal to the applied stress. In bonded masonry the overlapping of the units restrains the propagation of cracks which are generated in the vertical joints by the tension until the stress exceeds the tensile resistance of the units.

The compressive strength of masonry is measured by subjecting small walls or prisms or larger walls of storey height (2–3 m) to a force in a compression test machine. Loading is usually axial but may be made eccentric by offsetting the wall and loading only part of the thickness.

Masonry is not so good at resisting compression forces parallel to the bedding plane because there is no overlapping and the bed joints fail easily under the resultant tensile forces. Additionally, most bricks with either frogs, perforations or slots are weaker when loaded on end than on bed because the area of material resisting the load is reduced and the stress distribution is distorted by the perforations. Data on bricks are given in Table 30.6. The equivalent data in Table 32.1 for prisms show that the strength does vary with loading direction, although not to the same extent as for units because the aspect ratios of the masonry specimens are all similar.

The axial strength of masonry might be expected to depend on the strength of the units and of the mortar and, to a first approximation, the contribution of each to the overall strength should be related in some way to the volume proportion of each. This gives a reasonable model for behaviour of squat structures. A complication is that most masonry comprises units that are much stronger than the mortar, and the three-

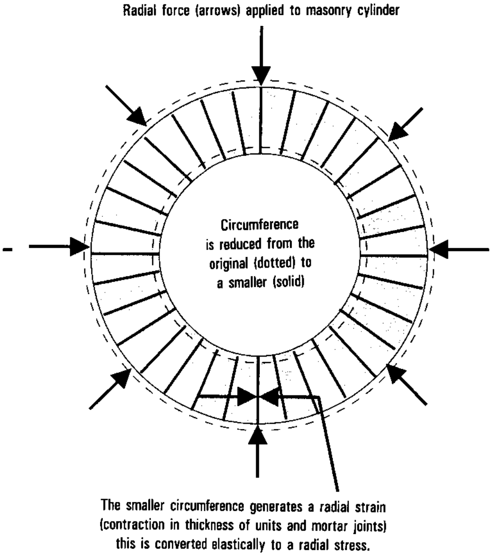

FIGURE 32.3 Forces on masonry cylinders, e.g. arches, tunnels and sewers.

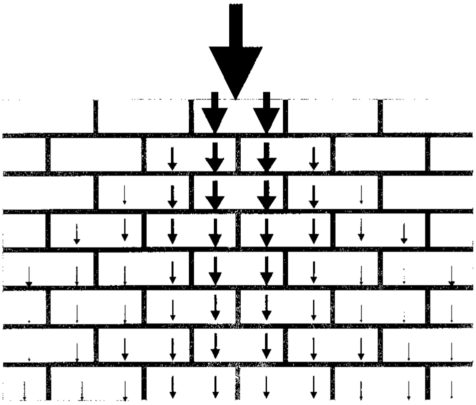

FIGURE 32.4 Load spreading in stretcher bonded walls.

TABLE 32.1 Masonry prism strengths with bricks loaded in various directions

Type	*Ref.*	*Mortar mix*		*Prism compressive strength on bed*	*Proportion of the on-bed strength (%)*		
		(C:L:S)	*(MPa)*	*(MPa)*	*On bed*	*On edge*	*On end*
23 hole	(a)	1:$\frac{1}{4}$:3	23.1	22.4	100	71	48
14 hole	(b)	1:$\frac{1}{4}$:3	26.6	28.9	100	29	51
14 hole	(c)	1:$\frac{1}{4}$:3	23.1	19.9	100	58	57
10 hole	(d)	1:$\frac{1}{2}$:4$\frac{1}{2}$	8.3	15.2	100	104	111
10 hole	(d)	1:$\frac{1}{4}$:3	26.6	22	100	68	91
3 hole	(e)	1:$\frac{1}{4}$:3	26.6	37.6	100	81	58
3 hole	(e)	1:$\frac{1}{2}$:4$\frac{1}{2}$	7.8	20.3	100	96	83
3 hole	(f)	1:$\frac{1}{4}$:3	23.1	23.2	100	61	29
5 cross slots	(g)	1:$\frac{1}{4}$:3	26.6	34.1	100	85	41
5 cross slots	(g)	1:$\frac{1}{2}$:4$\frac{1}{2}$	7.7	18	100	132	54
16 hole	(A)	1:$\frac{1}{4}$:3	–	26	100	20	29
Frog	(B)	1:$\frac{1}{4}$:3	–	9.7	100	55	55
Frog	(C)	1:$\frac{1}{4}$:3	–	10.8	100	133	122
Frog	(D)	1:$\frac{1}{4}$:3	–	19.2	100	93	86
Solid	(E)	1:$\frac{1}{4}$:3	–	16	100	73	64

Note: The reference relates the data in this table to those in Table 30.6.

dimensional confining restraint increases the effective strength of the thin mortar beds. Figure 32.5, based on data for wallettes tested in compression in de Vekey *et al.* (1990) and Edgell *et al.* (1990), shows the minor effect of mortar strength (i) and (iii) on the compressive strength of masonry made with a range of strengths of bricks but the considerable influence of the brick strength. The diagram shows a linear relationship between brick strength and brickwork strength for two strengths of mortar, one 4× the strength of the other. The third line shows the different behaviour of blocks tested to BS 6073. Platen restraint in the standard test method, which inhibits tension failure in the zones shown shaded in Figure 32.6, enhances the measured strength of

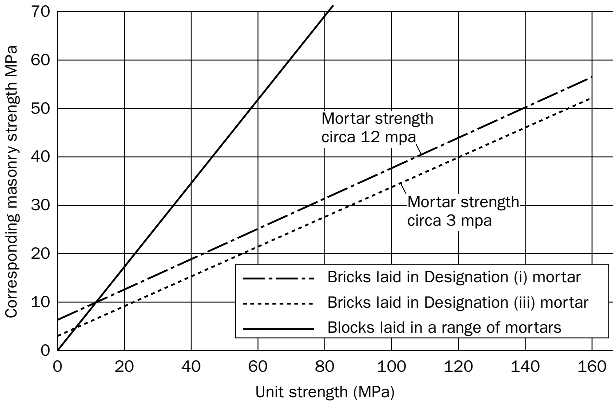

FIGURE 32.5 Influence of mortar and units on masonry strength.

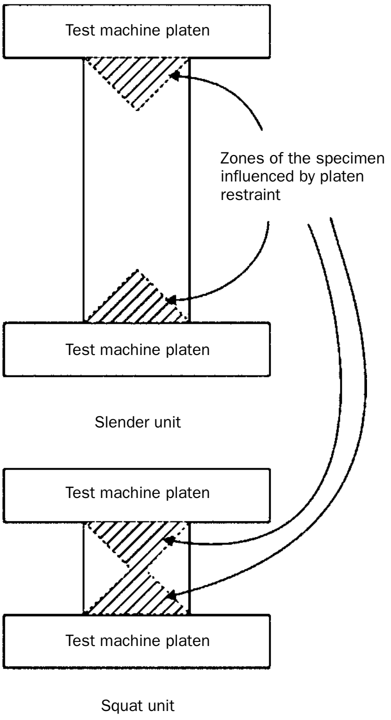

FIGURE 32.6 Platen restraint (shown as shaded areas) which enhances the measured strength of squat units more than slender units.

squat units (units wider than they are high) as opposed to slender units. This anomaly is taken account of in BS 5628 by using different tables for differently shaped units. In BS DD ENV 1996–1–1 the measured strength of units is corrected to a common value for a unit with a square cross-section using a conversion table. The process, called normalization, also corrects to a standard air-dry state whatever the test condition is.

To calculate masonry strength, BS DD ENV 1996–1–1 uses an equation of the form:

$$f_k = K.f_b^a.f_m^b \qquad (32.1)$$

Where f_k, f_b and f_m are the strength of the masonry, the normalized strength of the units and the strength of the mortar respectively, K is a factor which may vary to take into account the shape or type of the units, a is a fractional power of the order of 0.7–0.8, and b is a fractional power of the order 0.2–0.3.

32.2.1 Stability: slender structures and eccentricity

If a structure in the form of a wall or column is squat, so that the ratio of height to thickness (slenderness ratio) is small, then the strength will depend largely on the strength of the constituent materials. In real structures the material will be stiffer on one side than the other, the load will not be central and other out-of-plane forces may occur. This means that if the slenderness ratio is increased, at some point the failure mechanism will become one of instability and the structure will buckle and not crush.

Loads on walls, typically from floors and roofs, are commonly from one side and thus stress the wall eccentrically. Figure 32.7 illustrates, in an exaggerated form, the effect of an eccentric load in reducing the effective cross-section bearing the load and putting part of the wall into tension.

This is recognized in practice and usually a formula is used to reduce the design load capacity of structures in which the reduction is a function of the slenderness ratio and the net eccentricity of all the applied loads. BS 5628: 1992 gives a standard formula, where β is the reduction factor, e_m is the design eccentricity and t is the thickness of the element as follows:

$$\beta = 1.1(1 - (2e_m/t)) \qquad (32.2)$$

32.2.2 Concentrated load

Many loads are fairly uniform in nature, being derived from the weight of the structure above or more locally to floors. There will always be, however, some point loads, termed ‘concentrated loads’, in structures at the ends of beams, lintels, arches, etc. In general the masonry must be capable of withstanding the local stresses resulting from the concentrated loads but the designer

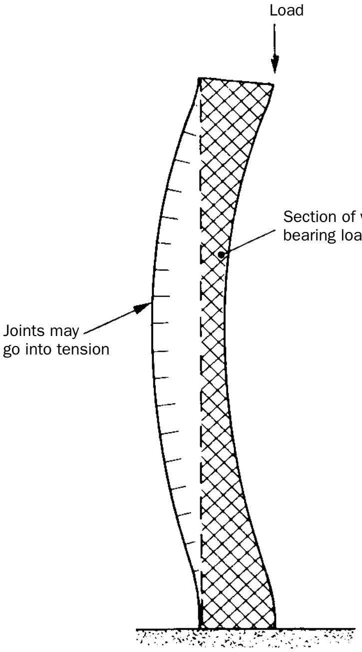

FIGURE 32.7 Effect of eccentric load on masonry (exaggerated).

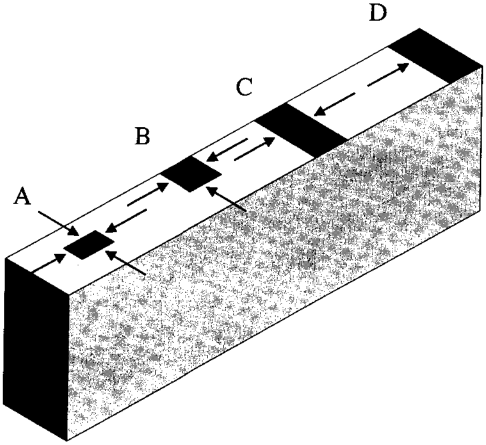

FIGURE 32.8 Concentrated loads on masonry (restraint indicated by arrows).

may assume that the load will spread out in the manner of Figure 32.4 so that it is only critical in the first metre or so below the load. Additionally, because the area loaded is restrained by adjacent unloaded areas, some local enhancement can be assumed.

Figure 32.8 (a) shows the condition for a small isolated load applied via a pad where there is restraint from four sides, and Figures 32.8 (b), (c) and (d) show further conditions with reducing restraint. The local load capacity of the masonry in the patches compared to the average load capacity (the enhancement factor) can vary from 0.8 for case (d) to as much as 4 for case (a) (Ali and Page (1986), Arora (1988) and Malek and Hendry (1988)). The enhancement factor decreases as the ratio of the area of the load to the area of the wall increases, as the load moves nearer the end of a wall and as the load becomes more eccentric. Formulae describing this behaviour are proposed in many of the references in Section 32.8.

32.2.3 Cavity walls in compression

If a compression load is shared equally by the two leaves of a cavity wall then the combined resistance is the sum of the two resistances, provided their elastic moduli are approximately the same. If one leaf is very much less stiff than the other, the stress is all likely to predominate in the stiffer wall and be applied eccentrically, and then the combined wall may have less capacity than the single stiff wall loaded axially. It is common practice to put all the load on the inner leaf and use the outer leaf as a rain screen. In this load condition more stress is allowed on the loaded wall because it is propped by the outer leaf. This is achieved mathematically by increasing the effective thickness of the loaded wall used for slenderness calculations.

32.3 Shear load in the bed plane

If a wall is loaded by out-of-plane forces, e.g. by wind, impact, or seismic (earthquake) actions, the force will act to try to slide the wall sideways (like a piston in a tube). In practice the action can be at any angle in the 360° plane although it is most common parallel or normal to the wall face. This is a very complex loading condition and the result is rarely a pure shearing failure. For small test pieces measured in an idealized test, the shear strength *tv* can be shown to follow a friction law with a static threshold 'adhesion' f_{v0} and a dynamic friction term K dependent on the force normal to the shearing plane s_a. The formula is simply:

$$f_v = \mathrm{f}_{v0} + s_a.K \tag{32.3}$$

Measurement of pure shear is very difficult because of the tendency to induce rotation in virtually any physical test arrangement. The simple double shear test of the type shown in Figure 32.9 is suitable for measuring shear resistance of damp-proof course (dpc) materials as per EN 1052–4 (1999) but is unsatisfactory for mortar joints where a much shorter specimen is preferred of the type described in EN 1052–3 (1999). Table 32.2 gives some typical shear data derived from Hodgkinson and West (1981).

In the example sketched in Figure 32.10 the ends are supported so the wall tends to adopt a curved shape. In this case it is shown as failing by shear at the line of the dpc. If a wall is loaded by lateral forces acting on the end, as in Figure 32.11 (which can arise from wind load on a flank wall at right angles), the force will initially tend to distort the wall to a parallelogram shape as in Figure 32.11 (a). If the wall fails it may be by crushing at the load point or at the 'toe' of the wall as in Figure 32.11 (a), by sliding shear failure along the dpc, by 'shear' failure, i.e. actual diagonal tensile failure, or by rotation as in Figure 32.11 (b).

A further important shear condition occurs between masonry elements bonded together, i.e. where piers or buttressing walls join other walls, as in Figure 32.11 (a), or in box structures at the corners. If the composite is loaded to generate flexure there is a vertical shear force at the interface which is resisted by the punching shear resis-

TABLE 32.2 Shear data for two mortars and some damp proof course (dpc) materials (Hodgkinson and West, 1981)

Brick	*dpc*	*1:$\frac{1}{4}$:3 Mortar*		*1:1:6 Mortar*	
		s_a	K	s_a	K
16 hole w/c	Blue brick[1]	0.72	0.82	0.44	1.14
	Bituminous	0.4	0.8	0.31	0.91
	Permagrip[2]	0.8	0.58	0.43	0.61
	Hyload[3]	0.21	0.8	0.17	0.58
	Vulcathene[4]	0.06	0.47	0.04	0.54
Frogged semi-dry pressed	Blue brick[1]	0.73	0.95	0.36	1.57
	Bituminous	0.45	0.84	0.36	0.72
	Permagrip[2]	0.55	0.93	0.41	0.72
	Hyload[3]	0.17	0.82	0.18	0.79
	Vulcathene[4]	0.09	0.52	0.06	0.49

Notes:
1. Where blue engineering bricks are used for the dpc the shear strength is limited effectively by the mortar.
2. Permagrip is a trade name for a reinforced bitumen product with a coarse sand surface.
3. Hyload is probably a pitch/polymer system.
4. Vulcathene is a trade name for a polyethylene-based dpc.

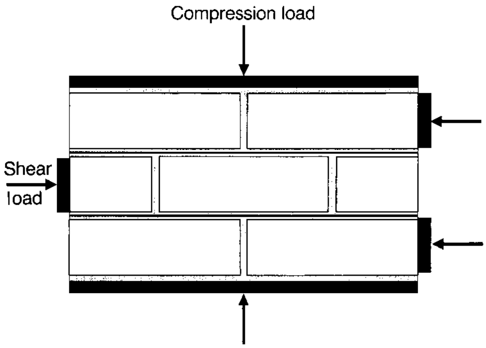

FIGURE 32.9 Specimen for measuring shear resistance of dpc materials, etc.

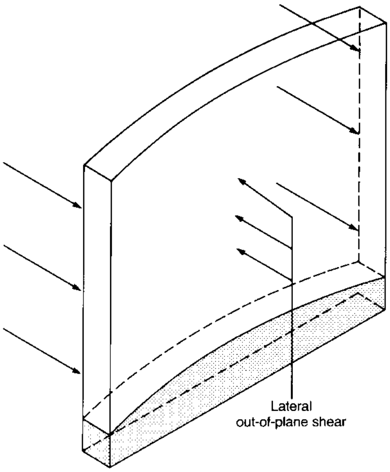

FIGURE 32.10 Shear failure on dpc line of laterally loaded wall.

tance of the units crossing the junction. In standard bond, units cross the shear plane for 50 per cent of the height of the structure and the shear strength will be, at best, the sum of these resistances plus a small contribution from the mortar.

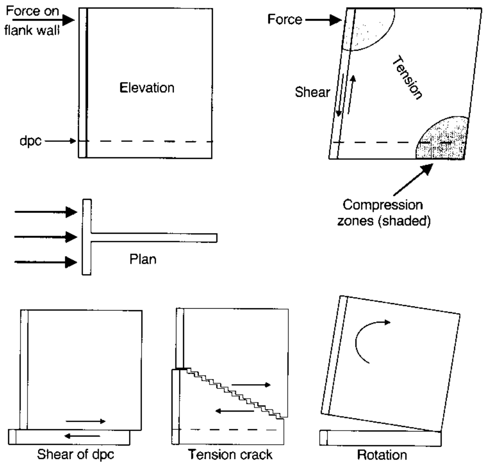

FIGURE 32.11 Stresses and strains resulting from an in-plane shear load. The wall may fail by crushing in the zones of higher compressive stress or by shear at the junction of the two walls at right angles, by horizontal shear at the dpc line, by tension splitting or by rotation.

32.4 Flexure (bending)

Traditionally, masonry was made massive or made into shapes which resisted compression forces. Such structures do not depend to any great extent on the bond of mortar to units. Much of the masonry built in the last few decades has, however, been in the form of thin walls for which the critical load condition can result from lateral forces, e.g. wind loads. This phenomenon was largely made possible by the use of opc mortars which give a positive bond to most units and allow the masonry to behave as an elastic plate. There are two distinct principal modes of flexure about the two main orthogonal planes: (1) the vertically spanning direction shown in Figure 32.2 which is commonly termed the parallel (or *p*) direction because the stress is applied about the plane parallel to the bed joints; and (2) the horizontally spanning direction, shown in Figure 32.12, which is commonly termed the normal (or

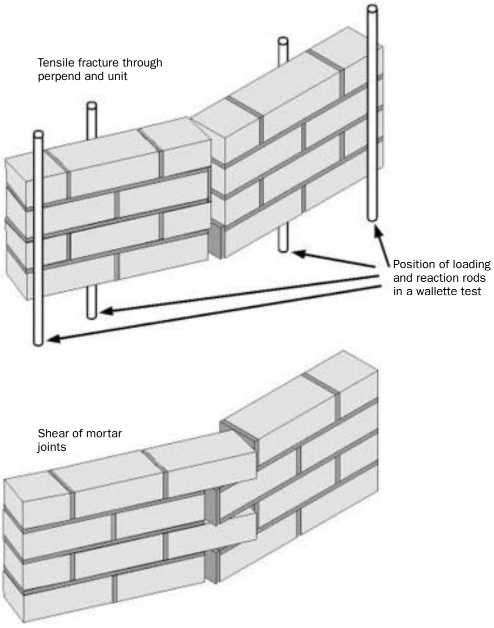

FIGURE 32.12 Modes of failure for laterally loaded masonry in the strong (*n*) direction.

n) direction because the stress is applied about the plane normal to the bed joints. Clearly the strength is likely to be highly anisotropic since the stress in the parallel direction is only resisted by the adhesion of the units to the mortar while the stress in the normal direction is resisted (a) by the shear resistance of the mortar beds, (b) by the elastic resistance of the head joints to the rotation of the units, (c) by the adhesion of the head joints and (d) by the flexural resistance of the units themselves. Generally the limiting flexural resistance will be the lesser of (a) + (b) or (c) + (d) giving two main modes of horizontal spanning failure – shearing, shown in the lower part of Figure 32.12 and snapping, shown in the upper part of Figure 32.12.

Using small walls (wallettes), either as shown in Figure 32.12 for measuring horizontal bending, or ten courses high by two bricks wide for vertical bending, and tested in four-point bending mode, the flexural strength of a large range of combinations of UK units and mortars has been measured for the two orthogonal directions and a typical range is given in Table 32.3; further data are given in West *et al.* (1986), de Vekey *et al.* (1986) and de Vekey *et al.* (1990).

The ratio of the strength in the two directions, expressed as *p*-direction divided by *n*-direction, is termed the orthogonal ratio and given the symbol μ. In cases where only the bond strength (*p*-direction) is required, a simpler and cheaper test is the bond wrench discussed in Section 23.3.2.

The flexural strengths given in Table 32.3 are for simply supported pieces of masonry spanning in one direction. If the fixity of the masonry at the

TABLE 32.3 Flexural strength ranges (MPa) for common masonry units bedded in designation (iii) mortar

Material	*Normal (strong) direction*	*Parallel (weak) direction*
Clay brick (0–7% water absorption)	1.8 to 4.7	0.35 to 1.1
Clay brick (7–12% water absorption)	1.9 to 3.2	0.3 to 1.3
Clay brick (>12% water absorption)	1.0 to 2.1	0.3 to 0.8
Concrete brick (25–40 MPa strength)	1.9 to 2.4	0.5 to 0.9
Calcil brick (25–40 MPa strength)	0.7 to 1.5	0.05 to 0.4
AAC block (100 mm thick)	0.3 to 0.7	0.3 to 0.6
LWAC block (100 mm thick)	0.7 to 1.3	0.3 to 0.5
DAC block (100 mm thick)	0.7 to 1.7	0.2 to 0.7

Note: The ranges given are for designation (iii) mortars (1:1:6 or equivalent). There is some dependence of flexural strength on mortar strength and thicker blocks lead to reduced strengths.
LWAC = lightweight aggregate concrete and DAC = dense aggregate concrete.

supports (the resistance to rotation) is increased, the load resistance will increase in accordance with normal structural principles (Figure 32.13). Again, if one area of masonry spans in two directions the resistances in the two directions are additive. Haseltine *et al.* (1977), Sinha *et al.* (1978, 1997), Seward (1982) and Lovegrove (1988) cover some aspects of the resistance of panels.

32.5 Tension

Masonry made with conventional mortars has a very limited resistance to pure tension forces and, for the purposes of design, the tensile strength is usually taken to be zero. In practice it does have some resistance in the horizontal direction and somewhat less in the vertical direction. In an attempt to make a viable prefabricated masonry panel product for use as a cladding material, polymer latex additives can be used to improve the tensile strength. Panels of storey height and a metre or more wide have been manufactured and could be lifted and transported without failure.

Horizontal tensile strength of masonry was measured but little other data exists, and no standard test or any significant data are available.

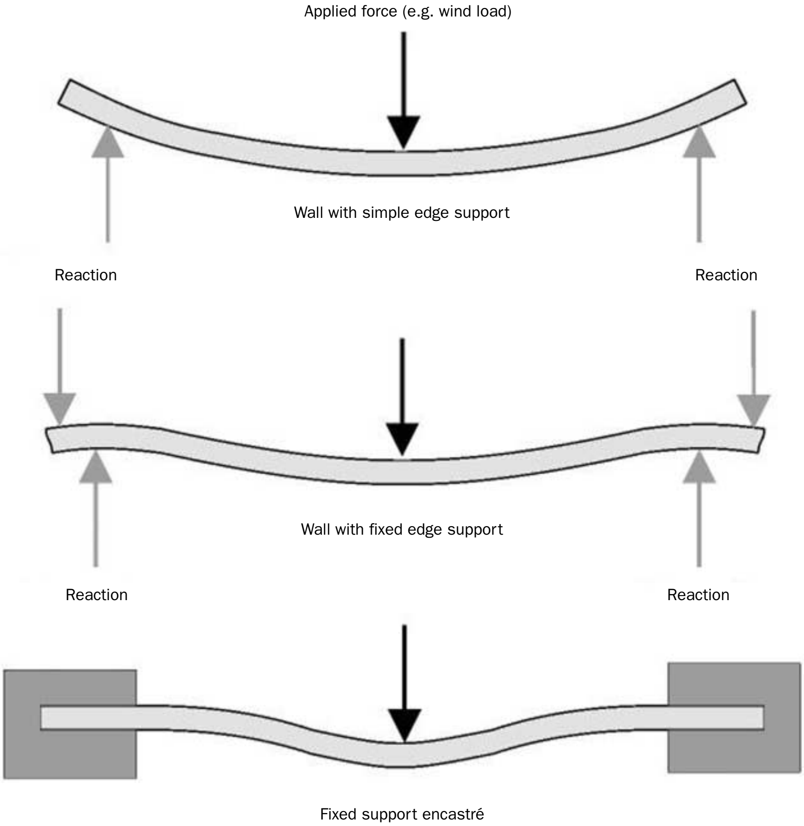

FIGURE 32.13 Effect of edge support conditions on the flexural behaviour of masonry.

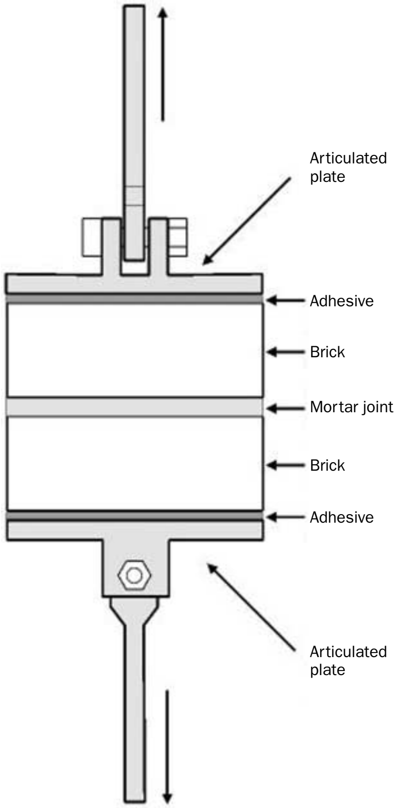

FIGURE 32.14 Stack-bond couplet tensile test.

Tensile bond strength is often measured, the most commonly reported test being the ASTM cross brick test (ASTM C952–76), but this has now been discontinued and simple two-brick prisms illustrated in Figure 32.14 are now favoured. Data from such tests indicate that the direct tensile strength across the bond is between one-third and two-thirds of the parallel flexural strength (see Table 32.3). Other tests have been developed along similar lines including one in which one unit is held in a centrifuge and the bond to another unit is stressed by centrifuging. A useful review is given by Jukes and Riddington (1998).

32.6 Elastic modulus

The stiffness or elastic modulus of masonry is an important parameter required for calculations of stresses resulting from strains arising from loads, concentrated loads, constrained movement and also for calculating the required area of reinforcing and post-stressing bars.

The most commonly measured value is the Young's modulus (E) but the Poisson's ratio (v) is also required for theoretical calculations using techniques such as finite element analysis. If required the bulk (K) and shear (G) moduli may be derived from the other parameters. Young's modulus is normally measured in a compression test by simultaneously measuring strain (ϵ_p) parallel to the applied stress (σ) whereupon:

$$E = \sigma/\epsilon_p \qquad (32.4)$$

If the strain (ϵ_N) perpendicular to the applied stress is also measured, Poisson's ratio (υ) may be derived:

$$\upsilon = \epsilon_N/\epsilon_p \qquad (32.5)$$

Masonry is not an ideally elastic material because it is full of minor imperfections such as microcracks in the bond layers and because the differences between the unit and mortar stiffnesses and Poisson's ratios produce high local strains at the interface which result in non-linear behaviour. This means that the stress–strain curve is typically of a broadly parabolic form with an early elastic region. The instantaneous Young's modulus is derived from the tangent to the curve at any point but for some calculations, such as creep loss of post-stressed masonry, the effective Young's modulus required is derived from the secant value. Figure 32.15 illustrates this behaviour. Data on elastic properties in compression are given in Davies and Hodgkinson (1988). Elastic modulus is also important in estimating the deflections of walls out of plane due to lateral loads such as wind. In this case the modulus can be measured by using load deflection data for small walls tested in four-point bending. In this case E is derived from:

$$E = 8Wa(3L^2 - 4a^2)/384I\delta \qquad (32.6)$$

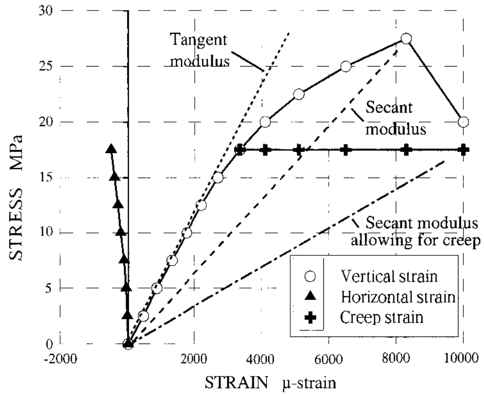

FIGURE 32.15 Stress–strain behaviour of masonry.

where *W* is the applied force, *L* is the span of the supports, *a* is the distance from the supports to the loading points, *I* is the moment of inertia and δ is the deflection.

In compression tests the value of *E* has generally been found to be in the range 500–1000 times the compressive strength. For typical materials this is likely to be around 2 to 30 GPa

In flexure the early tangent modulus has been found to be in the range 2–4 GPa for tests in the strong (normal) direction and 1–2 GPa for equivalent tests in the weak (parallel) direction. Some more data are given in Table 32.4.

32.7 Movement and creep of masonry materials

Unrestrained masonry is subject to cyclic movement due to moisture and temperature changes, permanent creep due to dead loads or post stress loads, permanent shrinkage due to drying/carbonation of mortar, concrete and calcium silicate materials and expansion due to adsorption of moisture by fired clay materials. Table 32.4 contains some typical ranges for common masonry components derived mainly from Digest 228 (1979).

In simple load-bearing masonry elements, vertical movements are accommodated by the structure going up and down as required and are no problem. Problems can arise, however, where materials with different movement characteristics are joined or where thick elements have differential temperature/moisture gradients through them. Elements with a vertical prestress much larger than the differential stresses will tolerate the movement, but lightly stressed and unrestrained elements will need a slip plane or soft joint between the elements to avoid problems. A classic case is (expanding) clay masonry on

TABLE 32.4 Movements and elastic modulus of masonry materials

Masonry component material	*Thermal expansion coefficient* a *(per °C × 10^{-6})*	*Reversible moisture movement (± %)*	*Irreversible moisture movement (%)*	*Modulus of elasticity* E *(GPa)*
Granite	8 to 10	–	–	20 to 60
Limestone	3 to 4	0.01	–	10 to 80
Marble	4 to 6	–	–	35
Sandstone	7 to 12	0.07	–	3 to 80
Slate	9 to 11	–	–	10 to 35
Mortar	10 to 13	0.02 to 0.06	−0.04 to −0.1	20 to 35
Dense concrete brick/blockwork	6 to 12	0.02 to 0.04	−0.02 to −0.06	10 to 25
LWAC blockwork	8 to 12	0.03 to 0.06	−0.02 to −0.06	4 to 16
AAC blockwork	8	0.02 to 0.03	−0.05 to −0.09	3 to 8
Calcil brickwork	8 to 14	0.01 to 0.05	−0.01 to −0.04	14 to 18
Clay brickwork	5 to 8	0.02	+0.02 to −0.10	4 to 26

(shrinking) concrete frames where soft joints are used to stop stress transfer to the masonry.

Where restraint is present, horizontal shrinkages will be converted into tensile forces and expansions into compressive forces. Since walls are probably two orders of magnitude weaker in tension than in compression the result is that restrained walls in tension usually crack while those in compression usually just build up stress. Where walls are unrestrained the reverse is usually the case: the shrinking wall simply contracts but the expanding wall interacts with flank walls (those at right angles) and causes cracking by generating rotation at the corner.

Because there is nearly always differential restraint the pure tensile or compressive forces will usually give rise to some associated shear forces.

32.8 References

Ali, S. and Page, A.W. (1986) An elastic analysis of concentrated loads on brickwork. *International Journal of Masonry Construction,* 6, Edinburgh, 9–21.

Arora, S.K. (1988) Review of BRE research into performance of masonry walls under concentrated load. *Proceedings of the 8th International Brick/Block Masonry Conference,* Dublin, 446.

Davey, N. (1952) Modern research on loadbearing brickwork. *The Brick Bulletin* 1–16.

Davies, S. and Hodgkinson, H.R. (1988) *The Stress–Strain Relationships of Brickwork, Part 2,* BCRL research paper *7S5.*

Haseltine, B.A., West, H.W.H. and Tutt, J.N. (1977) Design of walls to resist lateral loads. *The Structural Engineer 55,* 10, 422–30.

Hodgkinson, H.R. and West, H.W.H. (1981) *The Shear Resistance of Some Damp-proof Course Materials,* Technical Note 326, British Ceramic Research Ltd, Stoke on Trent.

Jukes, P. and Riddington, J.R. (1998) A review of masonry tensile bond strength test methods. *Masonry International* 12, 2, 51–7.

Lovegrove, R. (1988) The effect of thickness and bond pattern upon the lateral strength of brickwork. *Proc. Brit. Masonry Soc.* 2, 95–7.

Malek, M.H. and Hendry, A.W. (1988) Compressive strength of brickwork masonry under concentrated loading. *Proc. Brit. Masonry Soc.,* 2, 56–60.

Seward, D.W. (1982) A developed elastic analysis of lightly loaded brickwork walls with lateral loading. *International Journal of Masonry Construction* 2, 2, 129–34.

Simms, L.G. (1965) The strength of walls built in the laboratory with some types of clay bricks and blocks. *Proc. Brit. Ceram. Soc.* July, 81–92.

Sinha, B.P. (1978) A simplified ultimate load analysis of laterally loaded model orthotropic brickwork panels of low tensile strength. *The Structural Engineer* 56B, 4, 81–4.

Sinha, B.P., Ng, C.L. and Pedreschi, R.F. (1997) Failure criteria and behaviour of brickwork in biaxial bending. *J. of Materials in Civil Engg,* 9, 2, 61–6.

de Vekey, R.C., Bright, N.J., Luckin, K.R. and Arora, S.K. (1986) Research results on autoclaved aerated concrete blockwork. *The Structural Engineer* 64A, 11, 332–41.

de Vekey, R.C., Edgell, G.J. and Dukes, R. (1990) The effect of sand grading on the performance and properties of masonry. *Proc. Brit. Masonry Soc.* 4, 152–9.

West, H.W.H., Hodgkinson, H.R. and Davenport, S.T.E. (1968) *The Performance of Walls Built of Wirecut Bricks With and Without Perforations,* Special Publication No. 60, British Ceramic Research Ltd, Stoke on Trent.

West, H.W.H., Hodgkinson, H.R. and Haseltine, B.A. (1977) The resistance of brickwork to lateral loading. *The Structural Engineer* 55, 10, 411–21.

West, H.W.H., Hodgkinson, H.R., Haseltine, B.A. and de Vekey, R.C. (1986) Research results on brickwork and aggregate blockwork since 1977. *The Structural Engineer* 64A, 11, 320–31.

Chapter thirty-three

Durability and non-structural properties of masonry

33.1 Introduction

The main non-structural function of masonry elements is as a cladding to buildings and the key function of such elements is to maintain habitable conditions within the building. It is thus paramount that the masonry be durable with respect to the external actions it is subjected to. It is also important to know how effective masonry is in controlling the temperature, preventing ingress of wind and rain, reducing noise transmission and limiting the spread of fire should it break out. Another key concern that is becoming increasingly important is the effect of a product on the environment – the sustainability or 'green' credentials of a product. Increasingly, materials will be chosen not just for their inherent performance, appearance or economy but their energy cost and other effects on the global environment such as emission of greenhouse gases will be taken into account.

33.2 Durability

There are a large number of mechanisms by which masonry structures can deteriorate which can be categorized into:

1. chemical/biological attack on either the mortar or the units or both, due to water and waterborne acids, sulfates, pollution and chemicals released by growing plants;
2. corrosion of embedded metal (usually steel) components, particularly ties, straps, reinforcing rods, hangers, etc., which is a special case of chemical attack;
3. erosion of units or mortar by particles in flowing water and wind, by frost attack and by salt crystallization;
4. stress-related effects due to movement of foundations, movement/consolidation/washout of in-fill, vibration, overloading, moisture movement of bricks and blocks, thermal movement, growth of plants;
5. staining due to efflorescence, lime, iron, vanadium and biological growth.

Mortar is generally a less durable material than fired clay or dense concrete, because it contains reactive and finely divided binders such as opc and it usually has a relatively high porosity and, comparatively, a lower hardness and abrasion resistance. The durability of natural stone is very variable, ranging from the highest given by dense impermeable granites and marbles to quite poor performance of porous limestones and sandstones. Erosion processes such as wind and water scour attack both units and mortar but erode the softer of the two at a faster rate. Frost and salt crystallization are complex processes where the susceptibility is dependent as much on pore distribution as hardness and overall porosity. Stress effects normally cause cracking of varying types but the effect is on the masonry composite and not on the individual components. There are some problems related to faults in manufacture of the units, particularly under- or over-firing of clay bricks and the inclusion of foreign particles in bricks or other types of unit. A good range of coloured illustrations of problems is given in BRE Digest 361 (1991) and in BRE Digest 441 (1999).

33.3 Chemical attack

33.3.1 Water and acid rain

Water percolating into masonry is always a potential source of damage and, where possible, the structure should be designed to channel water away or at least to allow it to escape via weepholes. Absolutely pure water will have no direct chemical effect but some of the constituents of mortar are very slightly soluble and will leach away very slowly. Rain water contains dissolved carbon dioxide which forms a very mild acid that dissolves calcium carbonate by formation of the soluble bicarbonate via the reaction:

$$CO_2 + H_2O \rightarrow H_2CO_3 + CaCO_3 \rightarrow Ca(HCO_3)_2 \quad (33.1)$$

This means that lime mortars, weak opc : lime mortars, porous limestones, porous limebonded sandstones and porous concrete blocks made with limestone aggregate will eventually be destroyed by percolating rain water because calcium carbonate is a key constituent. Strong opc mortars with well-graded sand and most concrete and sandlime units are less susceptible, partly because the calcium silicate binder is less soluble but mainly because they are less permeable and so prevent free percolation. Typical visible effects of water leaching on mortar are loose sandy or friable joints, loss of mortar in the outside of the joints giving a raked joint appearance, and in serious cases the loss of bricks from the outer layer of masonry particularly from tunnel/arch heads. The process will sometimes be accompanied by staining due to reprecipitation of the dissolved materials. Stones lose their surface finish and may develop pits or rounded arrises.

Sulphur dioxide reacts with water to form initially sulphurous acid but can oxidize further in air to sulphuric acid:

$$2SO_2 + 2H_2O \rightarrow 2H_2SO_3 + O_2 \rightarrow 2H_2SO_4 \quad (33.2)$$

There is no systematic evidence that rain acidified by sulphur dioxide from flue gases at the normal levels has a significant effect on mortar, but in special cases such as where there is a high level of gaseous pollution near industrial sites there may be a very significant increase in the deterioration rate of all forms of structure including mortar and limestones. Unlined chimneys are a particular case and can suffer severe sulfate attack in the exposed parts where rain saturation or condensation of fumes containing sulphur occurs. One mechanism of failure is the conversion of calcium carbonate to gypsum:

$$CaCO_3 + H_2SO_4 \rightarrow CaSO_4 + H_2CO_3 \quad (33.3)$$

33.3.2 Carbonation

Gaseous carbon dioxide (CO_2) at humidities between about 30 per cent and 70 per cent neutralizes any alkalis present. This process occurs for all lime and opc binders with the conversion of compounds such as sodium hydroxide (NaOH) and, most commonly, calcium hydroxide ($Ca(OH)_2$) to their respective carbonates. In lime mortars this process probably increases the strength and durability. In opc-based materials the key effect of the process is to reduce the pH from around 12–13 down to below 7, i.e. converting the material from highly alkaline to slightly acid. This can have a profound effect on the durability of buried steel components (see Section 17.4.2). There is also some evidence that there is a slight associated shrinkage which may reduce the strength of very lightweight concrete units. Very dense concrete and calcium silicate units will carbonate slowly and may take 50–100 years or more to carbonate through.

33.3.3 Sulfate attack

Sulfate attack is the next most common problem which is due to the reaction between sulfate ions in water solution and the components of set Portland cement to form Ettringite. A detailed coverage of the physical and chemical mechanisms was given in Chapter 23.

The resulting expansion, which can be of the order of several per cent, causes both local disruption of mortar beds and stresses in the brickwork but only in wet or saturated conditions and where there is a source of water-soluble sulfate compound. It will never occur in dry or slightly damp masonry. The common sulfates found in masonry are the freely soluble sodium, potassium and magnesium salts and calcium sulfate which is less soluble but will leach in persistently wet conditions. The sulfates may be present in groundwaters and can affect masonry below the dpc, and masonry in contact with the ground such as retaining walls, bridges and tunnels. In this situation porous concrete units are also affected – see BRE Digest 363 (1996). Sulfates are also present in some types of clay brick and will be transported to the mortar in wet conditions. Old types of solid brick with unoxidized centres ('blackhearts') often have large amounts of soluble sulfates, as do some Scottish composition bricks, while semi-dry pressed bricks made from Oxford clay (Flettons) have high levels of calcium sulfate. Sulfates may attack lime mortars by conversion of the lime to gypsum in a similar reaction to equation (33.3). Sulfate-resisting Portland cement is deliberately formulated to have a low C_3A content but may be attacked in very extreme conditions. Sulfate attack is more likely in porous mortars while rich, dense, impervious mortars are affected less despite their higher cement content. Recent research reported by the Thaumasite experts group (1999) has indicated that thaumasite may also form in brickwork mortar as the product of the reaction between dicalcium and tricalcium silicate, sulfate, carbonate and water. This process can turn mortar to a mush. Although no known failures have occurred where sulfate-resisting cement has been used, this cement may not protect mortar against thaumasite formation.

Visible effects of such attack on mortar are expansion of the masonry where it is unrestrained and stress increases where it is restrained. Typically the mortar is affected more within the body of the wall than on the surface, so small horizontal cracks are sometimes visible in the centre of each bed joint as in Figure 33.1. In thick masonry, vertical cracks may appear on the external elevations due to the greater expansion in the centre of the wall which remains wetter for longer than the outside which can dry out by evaporation. Horizontal cracking may also occur, but it is likely to be less obvious where there is a high vertical deadload stress. Rendered masonry exhibits a network of cracks termed 'map-cracking'. If walls also have a face to an internal space which is kept dry, then efflorescence (growth of crystals) may occur due to transport of the sulfates to the surface. These faults are most common where the water is leaking into the structure from faulty details, leaking roofs or from ground contact, especially with sulfate-bearing groundwaters. The susceptibility of mortar to sulfate attack (and frost attack or a combination of the two) can be tested using the Harrison technique (see references in Section 30.3.2) which has been standardized as RILEM (1999) and CEN 1015–14 (2000).

Sulfates do not usually have a significant chemical effect on properly fired clay units, although they are commonly the source of such compounds. Sulfate attack on concrete blocks and bricks can occur but is not a common problem.

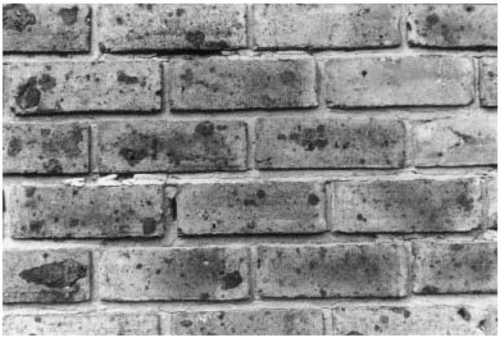

FIGURE 33.1 Sulfate attack.

Certain precautions are advisable when building in ground containing sulfates (see BRE Digest 363 (1996)) or constructing flumes and tunnels to carry contaminated water (WRC, 1986).

A special type of 'engineering quality' concrete brick is now available which is designed to be stable in effluents containing sulfates and other harmful compounds. These units are manufactured to a high strength and low permeability with srpc as the binder. A limited test has been carried out on samples of three different 'engineering quality' concrete bricks using simulated industrial and commercial effluent solutions (*Concrete*, 1986).

Mundic concrete blocks made using tin-mine tailings as aggregate in south-west England have suffered attack from indigenous sulfates (see Section 17.3.1, Bomley and Pettifer (1997) and RICS (1997)).

33.3.4 Acids

The effects of acids, e.g. rain run-off from peat moors, or industrial or agricultural pollution, on cement-based products is covered in Section 17.3.1. Clay products are normally resistant.

33.3.5 Chlorides

Chlorides can have a weakening effect on calcium silicate units but have little effect on mortars, clay units or concrete masonry units.

33.3.6 Corrosion of buried metals

Iron and steel expand on rusting, and a typical crack pattern from wall tie corrosion is shown in Figure 33.2. A detailed discussion of the corrosion of steel in cement and concrete was given in Chapter 24, and specific coverage of wall tie corrosion is given in de Vekey (1990a, 1990b and 2000).

FIGURE 33.2 Corroded timber frame masonry wall tie showing both white rust (ZnO) and red rust (FE_2O_3 H_2O).

33.4 Erosion

33.4.1 Frost

Frost is the principal eroding agent of masonry exposed to normal exterior conditions. Quite clearly it will not affect masonry buried more than a few feet and so will not affect foundations, the insides of tunnels or buried culverts. It may affect any masonry exposed on the exterior of structures but is more likely to affect exposed components that become saturated. Typical problem areas are civil engineering structures such as bridges, earth-retaining walls and exposed culverts and parts of buildings such as parapets, chimneys, freestanding walls and masonry between the ground and the damp-proof course.

Frost attack is due to the stresses created by the expansion of water on freezing to ice in the pore systems of units and mortars and thus only occurs in water-saturated or near-saturated masonry. Some clay bricks and natural stones are particularly susceptible, whereas most good quality clay engineering bricks, stock bricks and concrete and calcium silicate units are very resistant. Mortar is also subject to frost damage, particularly in combination with any of the other forms of chemical deterioration.

Typical effects are the spalling of small pieces of either the unit or the mortar or both forming a layer of detritus at the foot of the wall. Figure 33.3 is a case where the brick has a lower resistance than the mortar. Clay bricks, particularly lightly fired examples of types made from some shales and marls, are especially susceptible and tend to delaminate. Semi-dry pressed bricks made from the Oxford clay tend to break down into grains the same size as they were made from (e.g. around 7–14 mesh). Old types of solid clay brick with unoxidized centres tend to spall from the boundary between the heart and the outside of the brick. Some natural stones with a large proportion of fine pores are also susceptible. Modern perforated clay bricks are generally more frost-resistant because the more open structure allows more even drying and firing with less chance of shrinkage/firing cracks forming.

FIGURE 33.3 Erosion due to frost attack.

The susceptibility of building materials to frost attack can be very difficult to understand. Clearly materials such as glass, plastic and metals which are totally non-porous to water are not affected. Materials such as well-fired 'glassy' clay bricks, well-compacted concretes, low-porosity granites, marbles and slates are also affected very little by frost, since the tiny amount of water that can penetrate will cause only a trivial level of stress on freezing. Materials with water absorptions ranging from about 4 per cent to 50 per cent tend to suffer frost damage but not invariably. As a general rule, materials with a wide range of pore sizes from very large to fine tend to be resistant, while those having a limited range of pore sizes, usually of the finer sizes, tend to fail. This is probably because it is difficult to saturate fully the mixed pore system, the water filling the fine but not the larger pores. Providing around 10 per cent of the pore system is still air filled, there is sufficient space for the ice crystals to expand into without damaging the structure.

This has given rise to tests of pore distribution being used to predict frost durability. For stone a test is used in which the stone is saturated with water then pressurized to a level at which the larger pores will be emptied. This gives a measure of the ratio between the volume of pores above and below a chosen critical size and some idea of durability.

Most of the older data on susceptibility to frost attack are based on experience but this is a very slow and inefficient way of evaluating new products. To try to speed up the process, accelerated freezing tests have been developed. A typical example is the panel test (West *et al.*, 1984) which has latterly been published both by RILEM (1998) and as a draft CEN standard (1999). Work has also been done by Beardmore *et al.* (1987 and 1990) and Stupart (1996) to evaluate the number of days of frost cycling combined with driving rain which is what causes the damage.

The method is designed to test small panels of brickwork. The panel is first totally immersed in water for seven days, then one face is exposed to repeated cycles of freezing and thawing usually up to a limit of 100 cycles. The other face and the top and the sides of the panel are enclosed in a close-fitting jacket of 25 mm thick expanded polystyrene. Bricks showing no signs of failure after 100 cycles should be frost-resistant, those failing between 10 and 100 cycles would be expected to be durable under most conditions of exposure, but some failure could occur if they were used in a situation where repeated freeze–thaw cycling occurred when the bricks were saturated with water. Bricks which fail in less than 10 cycles are considered to be suitable for internal use only.

33.4.2 Crypto-efflorescence damage

This is basically the same process as efflorescence (see below) but at certain temperature/humidity conditions it occurs just below the surface of the masonry unit. The hydrated crystals of species such as calcium and sodium sulfates growing in the pore structure result in a tensile force on the surface layers in a way which is analogous to frost attack. In UK conditions it is more likely to affect natural stones than other units. It normally occurs in warm conditions where there is rapid drying of water from the face causing the salts to crystallize out. Additionally there needs to be a source of water or water containing salts.

Typical appearance is similar to that of frost damage but it will usually be associated with efflorescence crystals.

33.4.3 Abrasion

Abrasion by particles in wind and water probably acts more in concert with other processes than in isolation. Likely areas for such erosion are bridge columns founded in river beds and buildings near road surfaces where splash-up can occur from vehicles. All types of marine/hydraulic structures such as dams, culverts, lock walls, flumes, etc., where high-velocity flows can occur may suffer from localized abrasion damage known as ‘scour’.

33.5 Staining

33.5.1 Efflorescence

This is simply a staining process caused by dissolution of soluble salts such as sodium, potassium, magnesium and calcium sulfates by rain or construction water from within brickwork which then crystallize on the surface as a white powder or encrustation. The surface may be any surface from which drying occurs. It is commonly the external façade but may be the interior of solid walls particularly those in contact with earth, e.g. cellar walls and ground-floor walls in older structures without damp courses. The salts commonly derive from clay bricks, but may also come from groundwaters.

Lime staining, shown in Figure 33.4, is caused by calcium hydroxide leaching from mortar and being carbonated at the surface to form a white deposit of calcium carbonate crystals. It may also result from the dissolution of calcium carbonate in carbonated rainwater to form calcium bicarbonate which reverts to the carbonate at the surface (stalagtites grow by this mechanism). It is most commonly seen as white ‘runs’ from mortar joints on earth-retaining walls but can occur on walls of buildings.

33.5.2 Iron staining

Iron compounds can be present in either bricks or mortars or both. They give little problem if well distributed as in many red-brown sands but will give ugly brown run-off stains if present as larger discreet particles. Iron may be present in the clay

FIGURE 33.4 Lime staining.

deposit in the form of pyrites and is sometimes a constituent of additives to clay.

33.5.3 Biological staining

Coloured deposits, usually white/green to brown/black, can build up due to the growth of algae fungi, lichens, mosses, etc. Such deposits only form if the masonry is wet for significant periods and is frequently the result of blocked downpipes or leaking gutters. Differential deposition can result from water streaming unequally off features such as windows and mullions and this can become noticeable due to the colour change.

33.6 Thermal conductivity

The thermal conductivity determines the rate of heat flow through a given material. Generally metals have the higher and very porous materials (containing a lot of air or other gas) at the lower conductivities. Masonry materials fall in a band between the two extremes. The property is important in that it affects the amount of heat loss from a building through the walls and thus the energy efficiency of the structure. Surprisingly, although it is often of lower density and quite porous, normal bedding mortar is frequently a poorer insulator than many bricks and blocks, as illustrated by Figure 33.5. This has led to the development of insulating mortars containing low-density aggregate particles and thin-joint mortar. The latter type reduces heat loss because of its much smaller area proportion of the wall face. Because porosity is a key parameter, the thermal conductivity is bound to be partially related to material density and general equations for dry solid porous building materials tend to be a function of density and give a regression expression of the form:

$$k = 0.0536 + 0.000213\rho - 0.0000002\rho^2 \qquad (33.4)$$

The presence of moisture increases the conductivity of porous materials because evaporation/condensation heat transfer mechanisms become possible.

Hollow and perforated products give some improvement over plain, solid products, although the potential gain from the trapped air pockets is compromised by the convection of the air within them. If the air is prevented from convecting by filling the hollows with foamed plastic materials such as urea–formaldehyde or polyurethane there is a further substantial improvement. Clay bricks or blocks with many small perforations also perform better than solid units because the smaller size of the holes reduces convection and the smaller solid cross-section reduces conduction. There is also an improvement if the holes are staggered such that the direct conduction path through the solid material is as long as possible. Figure 33.6 illustrates the effects of different perforation patterns on thermal resistance.

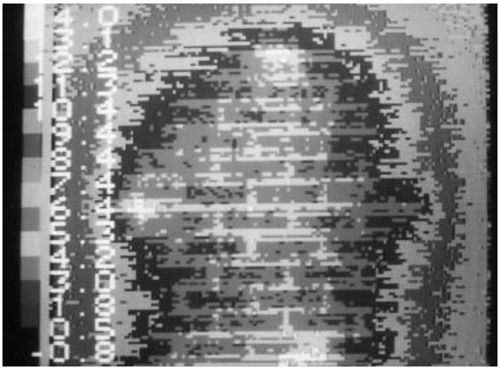

FIGURE 33.5 Infra-red photograph showing heat loss through joints.

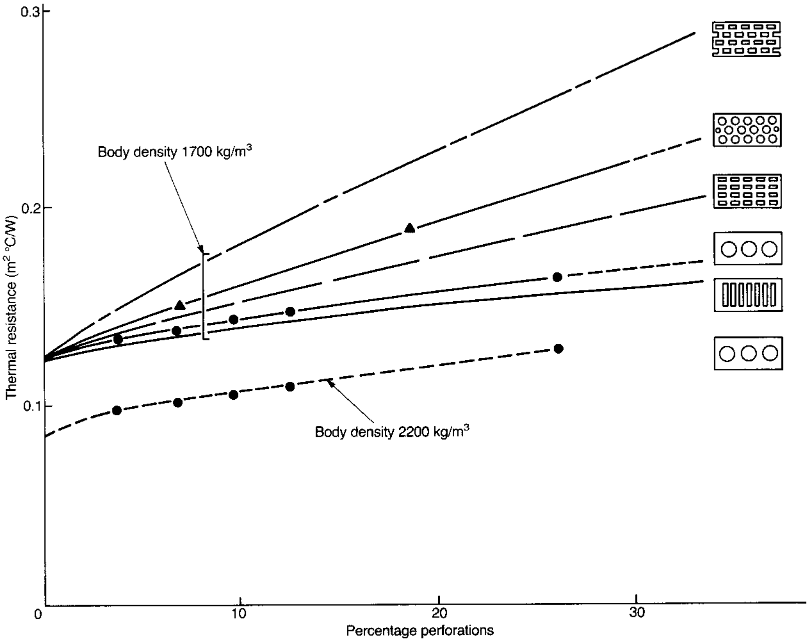

FIGURE 33.6 Effect of perforations on thermal resistance.

The properties of walls used as thermal barriers are normally expressed in the form of the 'U value', the overall heat transfer coefficient which is a synthesis of the *k* value of the actual materials and the heat transfer coefficients at the hot and cold sides. More detail on thermal insulation is given in Diamant (1986), BRE Digest 108 (1975) and BRE Digest 273 (1983).

33.7 Rain resistance

From the earliest use of built housing it has been one of the primary requirements that the walls will keep the occupants dry, and thus most masonry forming the perimeter walls of houses and other buildings is called upon to resist the ingress of rain. All masonry component materials are porous, however, and there are always some imperfections in the bond and seal of the mortar joints (de Vekey *et al.*, 1998) and the workmanship (Newman *et al.*, 1981 and 1982) which will admit some water, so no solid masonry wall is likely to be absolutely watertight.

Paradoxically, it is normally easier under UK conditions to make a rain-resistant wall from porous bricks. This is because some leakage always occurs at the joints which is mopped up by high absorption units but allowed free passage by low absorption units. Provided the rain does not persist until the units are saturated, they can dry out in the intervening dry spell and do not actually leak significant amounts of moisture to the inner face. Under similar conditions, some modern, low-absorption facings may leak quite seriously during a moderate storm. As would be expected, resistance is greater for thicker walls or if a coating is applied to the wall which reduces the surface rate of absorption. Typical coatings are renders and paints or overcladding systems such as vertical tiling.

The commonest technique for avoiding rain penetration in the UK is the cavity wall. This is a twin layer wall with an enclosed air space between the two leaves. Some leakage through the outer layer (leaf) is anticipated and any such water is directed back out through weepholes before it reaches the inner leaf by use of damp-proof membranes and cavity trays. This is sometimes thought of as a very recent wall form but it was probably used in ancient Greece and has been in use in the damper parts of the UK for nearly 200 years. It has given remarkably good service and is quite tolerant of workmanship variations and the main problems have been leakage of rainwater, which affects a small percentage of cases, and the corrosion of the steel ties used to ensure shared structural action of the two leaves. Figure 33.7 illustrates some routes for moisture and dampness to penetrate firstly the outer leaf (or a solid masonry wall) and then to reach the inner leaf usually because of bad design or workmanship in the construction of the cavity.

33.8 Sound transmission

Sound transmission is another parameter which is very dependent on density because it is the mass of the wall which is critical. Generally, the greater the mass, m, of a wall the more effective it is at attenuating (absorbing) the sound passing through it. A typical equation for the resistance, R, in decibels, dB, is given by BRE Digest 273 (1983).

$$R = 14.3 \log \mathrm{m} + 1.4\,\mathrm{dB} \qquad (33.5)$$

Any holes will short circuit the wall so that wet plastered walls where any minor perforations or imperfections are repaired by the plaster layer are more effective than dry-lined walls (walls covered with plasterboard). There are additional techniques to try to cut out sound such as air gaps and cavities with fireproof blankets hung in them which will damp out some frequencies.

More details on principles and basic values are given in Diamant (1986), BRE Digest 337 (1988), BRE Digest 338 (1988) and BRE Digest 333 (1988).

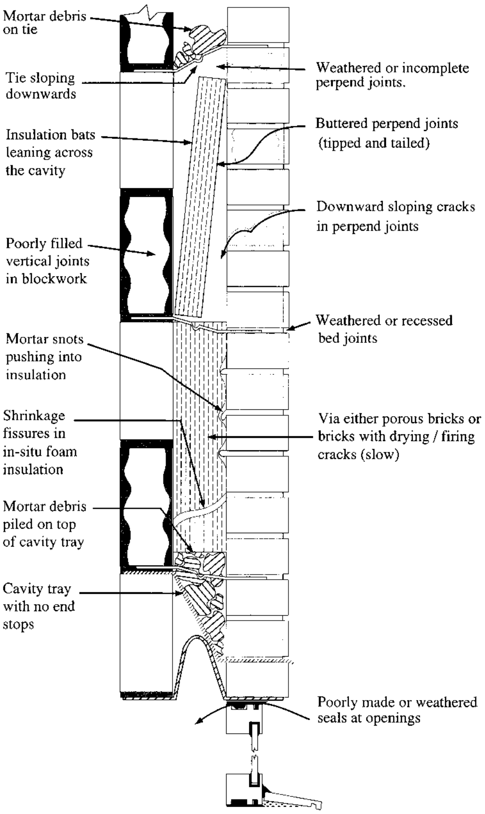

FIGURE 33.7 Mechanisms for rain water leakage through the external leaf and for tracking across cavities.

33.9 Fire resistance

Fire resistance of masonry is an important characteristic since it has long been recognized that masonry is a very effective material for resisting and preventing the spread of fire. This is now enshrined in various building regulations dating from the Great Fire of London. Its effectiveness in this role is due to the following characteristics:

1. a relatively low thermal conductivity which prevents the fire spreading by inhibiting the rise in temperature of the side of a wall away from the fire;
2. a relatively high heat capacity which also inhibits the rise in temperature of the side of a wall away from the fire (this is especially true of concrete-based products which contain a lot of loosely bound water which absorbs heat while being boiled away);
3. zero flammability and surface spread of flame;
4. refractory properties which mean that it retains its strength and integrity up to very high temperatures, approaching 1000°C in some cases.

These properties mean that it does not catch fire itself, it inhibits spread of fire by conduction and radiation and it is not easily breached by the fire. Insulating finishes such as vermiculite plaster improve performance still further. It has been shown to resist fire for between half-an-hour and six hours, depending on material, thickness and finishes. The classic data on masonry walls are contained in Davey and Ashton (1953). Relevant Codes of Practice are BS 5628: Part 3: 1985 and BS DD EN 1996–1–2 (1998).

33.10 Sustainability issues

There is a social trend in existence to make buildings and structures more ‘sustainable’ which is interpreted as both minimizing the inputs of resources and the impact on the environment at all stages of use from original construction to eventual removal and replacement. This broad intention is interpreted as the minimization of energy and raw materials input and output of pollutants at the manufacturing stage, over the life of the building or component and ultimately its recycling at the end of life of the building. Materials are ideally fully sustainable, i.e. they come from renewable sources like timber from trees (which also absorb CO_2 as they grow) whereas materials which are mined or quarried and/or require fossil fuel energy to manufacture are not fully sustainable and cause a net gain of CO_2 and other pollutants. It should be remembered, however, that most materials have to be transported and that will consume some fossil fuels. The BRE have published a broad green guide to building materials, Howard *et al.* (1998), which tries to assess them on a broad spectrum of green issues and give a combined rating on a scale of three. In this chapter the simpler principle has been adopted that, excepting unusual toxic/carcinogenic materials, most of the harmful effects of materials can be linked to the energy cost to produce and deliver them (their embodied energy).

For example, clay bricks are inherently fairly high-energy input materials and therefore there is a considerable emission of greenhouse gases during manufacture and transport, together with other pollutants such as sulphur dioxide and particulates. Additionally the quarrying operations to win the clay and mining operations to obtain the energy input (i.e. coal, oil or gas) will create aesthetic problems. Thus clay bricks cannot be treated as fully renewable; however, they have a long life, on average, and can be recycled in many situations where the building they form has come to the end of its useful life. The industry has sought to minimize the environmental impact by making plant more efficient and optimizing the recycling of heat during the process and by moving to more highly perforated bricks which minimize resource usage. Data from the BCRL surveys of energy usage (Beardmore, 1988, 1993, 1998) in Figure 33.8, indicates that the overall energy input to clay brick manufacture and transport has fallen by about 20 per cent over the period 1974 to 1999.

The other common materials, concrete and calcium silicate, have lower embodied energy than clay bricks and also have a long life.

Masonry, if correctly specified and constructed, has the advantage of a very long-life with very low maintenance costs, and this can reasonably be set against its high initial environmental cost provided it is used for long-life structures such as housing and public buildings. For shorter life structures it would be reasonable to use it if it were readily recyclable. There is a difficulty here

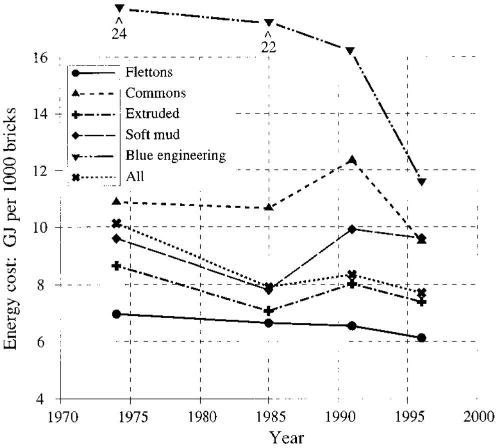

FIGURE 33.8 Gross manufacturing energy input per clay brick unit (including fuel embodied in the clay and transport). Reproduction of Figure 9 from *BRE Digest-441*, CRC Ltd (1999) Watford.

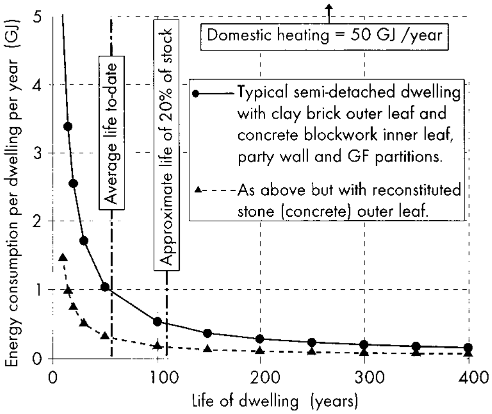

FIGURE 33.9 Lifetime embodied energy cost of masonry component of dwellings as a function of the life of the building compared to current heating cost. Based on Figure 10 from *BRE Digest-441*, CRC Ltd. Watford.

because modern opc-based mortars are too adherent and make recycling of whole bricks uneconomic. The current UK code of practice does not provide a basis for design of slender walls constructed with air lime mortar which would facilitate recycling. However, this is not a significant problem because the replacement rate of housing in the UK is only of the order 0.25 per cent per annum and the overall construction rate is only just over 1 per cent. The current replacement rate implies that the UK expects its dwellings to last several hundred years which is perhaps the reason why long-lived materials are popular.

The average life, to date, for all the standing stock of masonry dwellings, is around 58 years but a significant proportion is over 125 years old. Figure 33.9 illustrates the annual cost per dwelling of the process energy for contemporary brick or block manufacture as a function of the life of the dwelling (or walls). The upper curve is based on a typical clay brick outer leaf with concrete block inner walls, while the lower line is based on an all-concrete unit wall system.

If the reasonable assumption is made of a minimum average of 100-year life for all the existing stock, the energy consumption per annum of the clay brick option is around $\frac{1}{2}$GJ/year and under half this if only concrete units are used, assuming that no energy-consumptive maintenance is necessary. To put this into context, the annual average energy cost for heating in the UK, according to Shorrock *et al.* (1993) is about 50 GJ per dwelling, thus the long-term energy cost of the brick masonry is between $\frac{1}{2}$ per cent and 1 per cent of the heating cost or less.

Thus the typical contemporary masonry wall system usually gives a long, low maintenance, low overall energy cost lifetime with a future option to recycle. Improvements in the sustainability can be effected by use of more timber components, by incorporating recycled materials, e.g. aggregates PFA, etc., in the materials, by improving process efficiency and by engineering to expedite eventual recycling, e.g. by using mortars which separate easily from bricks.

33.11 References

Beardmore, C. (1988) Fuel usage in the manufacture of clay building bricks (6). *Ceram. Research* RP761,.

Beardmore, C. (1990) Winter weather records relating to potential frost failure of brickwork (2). *Research Paper* 781, British Ceramic Research Ltd.

Beardmore, C. (1993) Fuel usage in the manufacture of clay building bricks (11). *Ceram. Building Technology* Research Paper 804, BCRL, Stoke on Trent.

Beardmore, C. (1998) Fuel usage in the manufacture of clay building bricks (16). *Ceram. Research* Research Paper 812, BCRL, Stoke on Trent.

Beardmore, C. and Ford, R.W. (1987) Winter weather records relating to potential frost failure of brickwork (1). *Trans. Brit. Ceram. Soc. J.* 86, 7.

Bomley, A.V. and Pettifer, K. (1997) *Sulfide-related degradation of concrete in Southwest England.*

Concrete (1986) The concrete engineering quality brick. *Concrete* April.

Davey, N. and Ashton, L.A. (1953) *Investigation of Building Fires. Part V. Fire Tests on Structural Elements*, National Building Studies No. 12, HMSO, London.

Diamant, R.M.E. (1986) *Thermal and Acoustic Insulation*, Butterworth, London.

Howard, N., Shiers, D. and Sinclair, M. (1998) *The Green Guide to Specification and Environmental Profiling System for Building Materials and Components*, BRE, Watford.

Newman, A.J. (1988) *Rain Penetration Through Masonry Walls: Diagnosis and Remedial Measures.* Building Research Occasional Paper 117. Garston, Construction Research Communications Ltd.

Newman, A.J. and Whiteside, D. (1981) Water and air penetration through brick walls – a theoretical and experimental study. *Trans. Brit. Ceram. Soc.* 80, 27.

Newman, A.J., Whiteside, D. and Kloss, P.B. (1982) Full-scale water penetration tests on twelve cavity fills – Part II. Three built-in fills. *Building and Environment* 17, 3, 193–207.

Newman, A.J., Whiteside, D., Kloss, P.B. and Willis, W. (1982) Full-scale water penetration tests on twelve cavity fills – Part I. Nine retrofit fills. *Building and Environment* 17, 3, 175–91.

Royal Institute of Chartered Surveyors (1997) *The 'Mundic' Problem – A Guidance Note*. 2nd edn. RICS, London.

Shorrock, L.D., Henderson, G. and Bown, J.H.F. (1992 and 1993) *Domestic Energy Fact File*. BR 220 and BR 251 (update report). Garston, Construction Research Communications Ltd.

Stupart, A.W. (1996) Possible extensions to developing a frost index. *Masonry International* 7, 1, 4–9.

Thaumasite Experts Group, Department of the Environment, Transport and the Regions (1999) *The Thaumasite Form of Sulfate Attack: Risks, Diagnosis, Remedial Works and Guidance on New Construction*, DETR, London.

de Vekey, R.C. (1990a) *Corrosion of Steel Wall Ties: Background, History of Occurrence and Treatment*, BRE Information Paper IP12/90, Building Research Establishment, Watford.

de Vekey, R.C. (1990b) *Corrosion of Steel Wall Ties: Recognition and Assessment*, BRE Information Paper IP13/90, Building Research Establishment, Watford.

de Vekey, R.C. (1993) Cavity walls – Still a good solution. *BMS Proc.* M(5), 35.

de Vekey, R.C. (1999) *BRE Digest 441: Clay Bricks and Clay Brick Masonry, Part 1 and Part 2*. CRC Ltd. Watford.

de Vekey, R.C., Russell, A.D., Skandamoorthy, J. and Ferguson, A. (1997) Bond and water resistance of masonry walls. *Proceedings of 11th International Brick/Block Masonry Conference,* Shanghai 2, 836–44.

West, H.W.H., Ford, R.W. and Peake, F.A. (1984) A panel freezing test for brickwork. *Proc. Brit. Ceram. Soc.* 83, 112.

Further reading

British Standards

BS 187: 1978 *Calcium silicate bricks.*

BS 1200: 1976 (amended in 1984) *Sands from natural sources: sands for mortar for plain and reinforced brickwork, blockwork and stone masonry.*

BS 3921: 1985 *Specification for clay bricks.*

BS 4551: 1980 *Methods of testing mortars, screeds and plasters.*

BS 4729: 1990 *Specifications for dimensions of bricks of special shapes and sizes.*

BS 5606: 1999 *Code of practice for accuracy in building.*

BS 5628: Part 1: 1993 *Code of practice for the use of masonry. Part 1: Structural use of unreinforced masonry.*

BS 5628: Part 2: 1985 *Structural use of reinforced and prestressed masonry.*

BS 5628: Part 3: 1985 *Materials and components, design and workmanship.*

BS 6073: Part 1: 1981 *Precast concrete masonry units. Part 1: Specification for precast concrete masonry unit; Part 2: Method for specifying precast concrete masonry units.*

BS 6100: Part 5.3: 1984 *Glossary of building and civil engineering terms. Part 5: Masonry.*

BS 6677: Part 1: 1985 *Specification for clay and calcium silicate pavers.*

BS 6717: Part 1: 1986 *Specification for precast concrete paving blocks.*

BS 8000: Part 3: 1985 *Workmanship in building. Part 3: Masonry.*

Codes of Practice and guides

BS S606: 1978 *Code of practice for accuracy in building.*

BS 5628: Part 1: 1978 covers normal unreinforced structural masonry such as walls, arches, tunnels, columns, etc., subject to compressive, lateral and shear loads.

BS 5628: Part 2: 1985 is the section for design of reinforced or prestressed brickwork, e.g. for earth-retaining walls, chamber covers, etc., and has a useful treatment of the use of corrosion-resistant reinforcement for service in harsh conditions such as foul drains.

BS 5628: Part 3: 1985 covers all non-structural aspects of brickwork design, particularly the specification of units and mortars for durability over a wide range of applications and also workmanship, detailing, bonding patterns, fire resistance and resistance to weather conditions.

BS 6100: Part 5.3: 1986 defines terms relevant to bricks and brickwork.

British Masonry Society. Eurocode for masonry, ENV 1996–1–1: Guidance and worked examples. Special Publication No. 1, 1997. Stoke-on-Trent, British Masonry Society, 1997.

Materials standards

DRAFT EN 771–1 Clay units.

DRAFT EN 771–2 Calcium silicate units.

DRAFT EN 771–3 Aggregate concrete units.

DRAFT EN 771–4 Autoclaved aerated concrete units.

DRAFT EN 771–5 Reconstituted stone units.

DRAFT EN 771–6 Natural stone units.

DRAFT EN 845–1 Specification for ancillary components for masonary: Part 1: Ties, straps, hangers and brackets.

DRAFT EN 845–2 Specification for ancillary components for masonry: Part 2: Lintels.

DRAFT EN 845–3 Specification for ancillary components for masonry: Part 3: Bed joint reinforcement.

DRAFT EN 998–1 Specification for mortar for masonry: Part 1: Rendering and plastering mortar.

DRAFT EN 998–2 Specification for mortar for masonry: Part 2: Masonry mortar.

Methods of test for masonry units

BS EN 772–1: 2000 Determination of compressive strength.

BS EN 772–2: 1998 Determination of percentage area of voids in aggregate concrete masonry units (by paper indentation).

BS EN 772–3: 1998 Determination of net volume and percentage area of voids of clay masonry units by hydrostatic weighing.

BS EN 772–4: 1998 Determination of real and bulk density and of total and open porosity for natural stone masonry units.

prEN 772–5: Determination of active soluble salts content of clay masonry units.

prEN 772–6: Methods of test for masonry units – Determination of bending tensile strength of conrete masonry units.

BS EN 772–7: 1998 Determination of water absorption of clay masonry damp course units by boiling in water.

BS EN 772–9: 1998 Determination of volume and percentage area of voids and net volume of calcium silicate masonry units by sand filling.

BS EN 772–10: 1999 Determination of moisture content of calcium silicate and autoclaved aerated concrete units.

BS EN 772–11: 2000 Methods of test for masonry units – Determination of water absorption of clay, aggregate concrete, autoclaved aerated concrete, manufactured stone and natural stone masonry units due to capillary action.

prEN 772–12: Determination of length change during moisture movement in autoclaved aerated concrete units.

BS EN 772–13: 2000 Determination of net and gross dry density of masonry units (except for natural stone).

prEN 772–14: Methods of test for masonry units – Determination of moisture movement of aggregate concrete masonry units.

BS EN 772–15: 2000 Determination of water vapour permeability of autoclaved aerated concrete masonry units.

BS EN 772–16: 2000 Determination of dimensions.

BS EN 772–18: 2000 Determination of freeze–thaw resistance of calcium silicate masonry units.

BS EN 772–19: 2000 Determination of moisture expansion of large horizontally-perforated clay masonry units.

BS EN 772–20: 2000 Methods of test for masonry units – Determination of flatness of faces aggregate concrete manufactured stone and natural stone masonry units.

prEN 772–22: Determination of freeze–thaw resistance of clay masonry units.

Methods of test for mortar for masonry

EN 1015–1999: Determination of particle size distribution (by sieve analysis).

BS EN 1015–2: 1999 Bulk sampling of mortars and preparation of test mortars.

BS EN 1015–3: 1999 Determinatoin of consistence of fresh mortar (by flow table).

BS EN 1015–4: 1999 Determination of consistence of fresh mortar (by plunger penetration).

BS EN 1015–6: 1999 Determination of bulk density of fresh mortar.

BS EN 1015–7: 1999 Determination of air content of fresh mortar.

prEN 1015–8: Determination of water retentivity of fresh mortar.

BS EN 1015–9: 1999 Determination of workable life and correction time of fresh mortar.

BS EN 1015–10: 1999 Determination of dry bulk density of hardened mortar.

BS EN 1015–11: 1999 Determination of flexural and compressive strength of hardened mortar.

BS EN 1015–12: 1999 Determination of adhesive strength of rendering and plastering mortars on substrates.

BS EN 1015–14: 1999 Determination of durability of hardened mortar.

BS EN 1015–17: 2000 Determination of water-soluble chloride content of fresh mortars.

prEN 1015–18 Determination of water absorption coefficient due to capillary action of hardened rendering mortar.

BS EN 1015–19: 1999 Determination of water vapour permeability of hardened rendering and plastering mortars.

prEN 1015–21 Determination of the compatibility of one-coat rendering mortars with backgrounds through assessment of adhesive strength and water permeability after conditioning.

Methods of test for masonry

BS EN 1052–1: 1999 Determination of compressive strength.

BS EN 1052–2: 1999 Methods of test for masonry – Determination of flexural strength.

prEN 1052–3: Methods of test for masonry – Determination of initial shear strength.

BS EN 1052–4: 2000 Methods of test for masonry – Determination of shear strength including damp proof course.

prEN 1052–5 Methods of test for masonry – Determination of bond strength.

Eurocodes

BS ENV 1996–1–1: Eurocode 6 Design of masonry structures – Part 1–1: Structural design of masonry.

BS ENV 1996–1–2: Eurocode 6 Design of masonry structures – Part 1–2: General rules – Structural Fire design.

ENV 1996–1–3: Eurocode 6 Design of masonry structures – Part 1–3: General rules for Buildings – Detailed rules on lateral loading.

ENV 1996–2: Eurocode 6 Design of masonry structures – Design, selection of materials and execution of masonry (Together with UK National Application Document – NAD).

ENV 1996–3: Eurocode 6 Design of masonry structures – Part 3: Simplified calculation methods and simple rules for masonry structures.

EN 1745: Masonry and masonry products – Methods for determining design thermal values.

Methods of test for ancillary components for masonry

BS EN 846–2: 2000 Determination of bond strength of prefabricated bed joint reinforcement in mortar joints.

BS EN 846–3: 2000 Determination of shear strength of welds in bed joint reinforcement.

PR EN 846–4 Determination of tensile and compressive load capacity and stiffness of wall ties (wall test).

EN 846–5: 2000 Determination of tensile and compressive load capacity and stiffness of wall ties (couplet test).

EN 846–6: 2000 Determination of tensile and compressive load capacity and stiffness of wall ties (single end test).

BS EN 846–7: 2000 Determination of shear load capacity and load-displacement characteristics of shear ties and slip ties (couplet test for mortar joint connections).

EN 846–8: 2000 Determination of strength and stiffness of joist hangers.

EN 846–9: 2000 Determination of flexural resistance, shear load resistance and stiffness of lintels.

EN 846–10: 2000 Determination of flexural resistance and stiffness of shelf angles.

EN 846–11: 2000 Determination of dimensions and straightness or bow of lintels.

PR EN 846–12 Determination of strength and stiffness of straps.

PR EN 846–13 Determination of resistance to impact, abrasion and corrosion of organic coatings.

Other standards

ASTM C9S2–76 (1976) *Standard test method for bond strength of mortar to masonry units.*

ASTM C1072–86 *Standard method for measurement of masonry flexural bond.*

Building Research Establishment publications

The BRE, Watford, have an extensive series of publications, particularly Digests, relating to brickwork and blockwork. The following are those of the most relevance to the content of this book.

Digest 35 (1963) *Shrinkage of natural aggregates in concrete* (revised 1968).

Digest 108 (1975) *Standard U-values.*

Digest 157, *Calcium silicate (sandlime, flintlime) brickwork.*

Digest 164, *Clay brickwork: 1.*

Digest 165, *Clay brickwork: 2.*

Digest 228 (1979) *Estimation of thermal and moisture movements and stresses.*

Digest 240, *Low rise buildings on shrinkable clay soils: Part 1.*

Digest 246 (1981) *Strength of brickwork and blockwork walls: design for vertical load.*

Digest 250, *Concrete in sulphate bearing soils and groundwaters.*

Digest 273 (1983) *Perforated clay bricks.*

Digest 298, *The influence of trees on house foundations in clay soils.*

Digest 329, *Installing wall ties in existing construction.*

Digest 333 (1988) *Sound insulation of separating walls and floors. Part 1: Walls.*

Digest 337 (1988) *Sound insulation: basic principles.*

Digest 338 (1988) *Insulation against external noise.*

Digest 359, *Repairing brickwork.*

Digest 360 (1991) *Testing bond strength of masonry.*

Digest 361 (1991) *Why do buildings crack?.*

Digest 362, *Building mortar.*

Digest 363 (1991) *Sulfate and acid resistance of concrete in the ground.*

Digest 420 (1997) *Selecting natural building stones.*

Digest 432 (1998) *Aircrete: thin joint mortar systems.*

Performance specifications for wall ties – BRE report.

BRE CP24/70, (ATO) *Some results of exposure tests on durability of calcium silicate bricks.*

BRE CP23/77 (1977) Chemical resistance of concrete. *Concrete*, 11, 5, 35–7.

Harrison, W.H. (1987) Durability of concrete in acidic soils and groundwaters. *Concrete*, 21, 2.

Harrison, H.W. and de Vekey, R.C. (1998) *Walls, Windows and Doors.* In BRE Building Elements series, CRC, Watford.

Brick Development Association publications

Brick diaphragm walls in tall single storey buildings (and earth retaining walls).

BDA Design note 3, *Brickwork Dimensions Tables*.
BDA Design note 7, *Brickwork Durability*.

British Ceramic Research Limited publications

Technical Note 368, *The performance of calcium silicate brickwork in high sulphate environments*.
SP56: 1980: *Model specification for clay and calcium silicate structural brickwork* (in process of updating).
Supplement No. 1 to SP56, *Glossary of terms relating to the interaction of bricks and brickwork with water*.
SP108, *Design guide for reinforced clay brickwork pocket-type retaining walls*.
SP109, *Achieving the functional requirements of mortar*.

British Cement Association

Miscellaneous publications

Technical report TRA/145, *The effects of sulphates on Portland cement concretes and other products*.

Concrete Brick Manufacturers Association publications

CBMA Information Sheet 2, *Concrete bricks – product information*.

Miscellaneous publications

Hendry, A.W., Sinha, B.B. and Davies, S.R. *An lntroduction to Load Bearing Brickwork Design*, Ellis Horwood, Chichester.

Part Six

Polymers

L. Hollaway

Introduction

Pioneers in the development of plastics include Alexander Parkes in the UK in the 1860s and the US chemist Leo Baekeland, who developed 'Parkesine' and 'Bakelite' respectively. Much of the development and exploitation of polymers over the past 100 years has stemmed from the growth of the oil industry. Since the 1930s oil has been our main source of organic chemicals, from which synthetic plastics, fibres, rubbers and adhesives are made. The by-products of the distillation of petroleum are called basic chemicals and they provide the building blocks from which many chemicals and products, including plastics, can be made.

A large variety of polymers, with a wide range of properties, have been developed commercially since 1955. For example, phenol formaldehyde (PF) is a hard thermosetting material, polystyrene is a hard, brittle thermoplastic; polythene and plasticised polyvinyl chloride (PVC) are soft, tough thermoplastic materials. Plastics can also exist in various physical forms: bulk solids, rigid or flexible foams, sheet or film.

Many of these have found use in the construction industry, and this section describes the processing, properties and applications of those that have been used as sealants, adhesives, elastomers and geosynthetics.

Although many of the materials are relatively strong, their stiffness is too low for most structural applications. As we will see in the next section they can be combined with fibres of high stiffness and strength to form composites with improved structural properties.

Chapter thirty-four

Polymers

Types, properties and applications

34.1 Polymeric materials

Polymers are produced by combining a large number of small molecular units (monomers) by the chemical process known as polymerisation to form long-chain molecules. There are two main types. Thermoplastics consist of a series of long-chain polymerised molecules. All the chains of the molecules are separate and can slide over one another. In thermosetting polymers the chains become cross-linked so that a solid material is produced which cannot be softened and which will not flow.

Polymers are usually made in one of two polymerisation processes. In condensation-polymerisation the linking of molecules creates by-products, usually water, nitrogen or hydrogen gas. In addition-polymerisation no by-products are created. Both thermosetting and thermoplastic polymers can be manufactured by these processes.

34.1.1 Thermoplastic polymers

In a thermoplastic polymer the long-chain molecules are held together by relatively weak Van der Waals forces, but the chemical bond along the chain is extremely strong (Figure 34.1 (a)). When the material is heated, the intermolecular forces are weakened and the polymer becomes soft and flexible; at high temperatures it becomes a viscous melt. When it is allowed to cool again it solidifies. The cycle of softening by heating and hardening by cooling can be repeated almost indefinitely, but with each cycle the material tends to become more brittle.

Thermoplastic materials can have either a semi-crystalline ordered structure or an amorphous random structure. Polypropylene, Nylon 66 and polycarbonate are examples of amorphous thermoplastic polymers. Recent developments in the field of engineering polymers include the introduction of high-performance polymers, such as

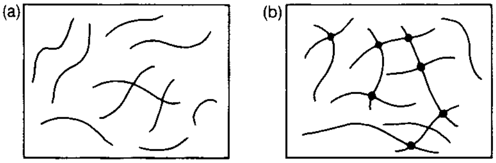

FIGURE 34.1 (a) Schematic representation of long-chain molecules of a thermoplastic polymer; (b) schematic representation of long-chain molecules of a thermosetting polymer illustrating the cross-linking.

polyethersulphone (PES), which is amorphous, and polyetheretherketone (PEEK), which is semi-crystalline. These offer properties far superior to those of the normal thermoplastic polymers.

34.1.2 Thermosetting polymers

The principal thermosetting polymers which are used in composites in construction are polyesters, epoxies and phenolics. Thermosetting polymers are formed in a two-stage chemical reaction. First, a substance consisting of a series of long-chain polymerised molecules, similar to those in thermoplastics, is produced; then the chains become cross-linked. This reaction can take place either at room temperature or under the application of heat and pressure. As the cross-linking is by strong chemical bonds, thermosetting polymers are rigid materials and their mechanical properties are affected by heat. Figure 34.1 (b) shows a schematic representation.

34.1.3 Foamed polymers

A rigid foam is a two-phase system of gas dispersed in solid polymer, and is produced by adding a blowing agent to molten resin. In the exothermic polymerisation reaction the gas is released and causes the polymer to expand, increasing its original volume many times by the formation of small gas cells. Like solid polymers, rigid foam polymers can be either thermoplastic or thermosetting and generally any polymer can be foamed.

34.2 Processing of thermoplastic polymers

Thermoplastic polymers may readily be processed into sheets or rods or complex shapes in one operation, which is often automated. Stages such as heating, shaping and cooling will ideally be a single event or a repeated cycle. The principal processing methods are extrusion, injection moulding, thermoforming and calendering.

The first is the most important method from the civil engineering viewpoint, and this is therefore outlined below. Powder or granules of thermoplastic polymer are fed from a hopper to a rotating screw inside a heated barrel; the screw depth is reduced along the barrel so that the material is compacted. At the end of the barrel the melt passes through a die to produce the desired finished article. Changing the die allows a wide range of products to be made, such as:

1. profile products;
2. film-blown plastic sheet;
3. blow-moulded hollow plastic articles;
4. co-extruded items;
5. highly orientated grid sheets.

34.2.1 Profile products

With different extrusion dies, many profiles can be manufactured, such as edging strips, pipes, window-frames, etc. However, success depends upon the correct design of the die.

34.2.2 Film-blown plastic sheet

Molten plastic from the extruder passes through an annular die to form a thin tube; a supply of air inside the tube prevents collapse and when the film is cooled it passes through collapsing guides and nip rolls and is stored on drums. Biaxial orientation of the molecules of the polymer can be achieved by varying the air pressure in the polymer tube, which in turn controls the circumferential orientation. Longitudinal orientation can be achieved by varying the relative speeds of the nip roll and the linear velocity of the bubble; this is known as draw-down.

34.2.3 Blow-moulded hollow plastic articles

A molten polymer tube, the Parison, is extruded through an annular die. A mould closes round the Parison and internal pressure forces the polymer against the sides of the mould. This method is used to form such articles as bottles and cold water storage tanks. The materials commonly used are polypropylene, polyethylene and PET.

34.2.4 Co-extruded items

A multilayered plastic composite is sometimes needed to withstand the end use requirements. Two or more polymers are combined in a single process by film blowing with an adhesive film between them. Reactive bonding processes to chemically cross-link the polymers are under development.

34.2.5 Highly orientated grid sheets

Polymer grids are used in civil engineering as the reinforcement to soil in reinforced earth. Continuous sheets of thermoplastic polymers, generally polypropylene or polyethylene, are extruded to very fine tolerances and with a controlled structure. A pattern of holes is stamped out in the sheet and the stampings are saved for re-use. The perforated sheet is stretched in the longitudinal and then in the transverse direction to give a highly orientated polymer in the two directions with a tensile strength similar to that of mild steel. The low original stiffness of the material can be increased ten-fold. The stiffness of unorientated high-density polyethylene (HDPE), for instance, is initially only 1 GPa and after forming into an orientated molecular structure it increases to 10 GPa. The use of these sheets is discussed later in the chapter.

In injection moulding, softened thermoplastic polymer is forced through a nozzle into a clamped cold mould. When the plastic becomes cold, the mould is opened and the article is ejected; the operation is then repeated.

34.3 Polymer properties

34.3.1 Mechanical properties

The physical and mechanical properties of thermosetting resins, specifically polyesters and epoxies, can vary greatly. As mentioned above, thermosetting polymers are cross-linked and form a tightly bound three-dimensional network of polymer chains; the mechanical properties are highly dependent upon the network of molecular units and upon the lengths of cross-link chains. The characteristics of the network units are a function of the chemicals used and the length of the cross-linked chains is determined by the curing process. It is usual to cure composites by heating to achieve optimum cross-linking and hence to enable the mechanical properties to realise their potential. Shrinkage during curing does occur, particularly with polyesters, and contraction on cooling to ambient temperature can lead to stress build-up. This latter problem is due to the differences between the thermal expansion coefficients of the matrix and fibre, and it can have a major effect on the internal micro-stresses which are sometimes sufficient to produce micropacking, even in the absence of external loads.

Thermoplastic polymers which are not cross-linked derive their strength and stiffness from the properties of the monomer units and the high molecular weight. Consequently, in crystalline thermoplastic polymers there is a high degree of molecular order and alignment, and during any heating the crystalline phase will tend to melt and form an amorphous viscous liquid. In amorphous thermoplastic polymers, there is a high degree of molecular entanglement so that they act like a cross-linked material. On heating, the molecules become disentangled and the polymer changes from a rigid solid to a viscous liquid.

Table 34.1 gives the most important mechanical properties of thermosetting and thermoplastic polymers.

34.3.2 Time-dependent characteristics

Polymer materials exhibit a time-dependent strain response to a constant applied stress; this behaviour is called creep. Conversely, if the stress on a polymer is removed it exhibits a strain recovery. Figure 34.2 illustrates the total creep curve for a polymer under a given uni-axial tensile stress at constant temperature, which is divided into five regions. When a polymer is subjected to a constant tensile stress, its strain increases until the material fails at the end of tertiary creep region. This process is called creep rupture, and the failure point depends on the level of stress. The

TABLE 34.1 Mechanical properties of common thermosetting and thermoplastic polymers

Material properties	*Specific weight*	*Ultimate tensile strength (MPa)*	*Modulus of elasticity in tension (GPa)*	*Coefficient of linear expansion (10^{-6}/°C)*
Thermosetting				
Polyester	1.28	45–90	2.5–4.0	100–110
Epoxy	1.30	90–110	3.0–7.0	45–65
Phenolic (with filler)	1.35–1.75	45–59	5.5–8.3	30–45
Thermoplastics				
Polyvinyl chloride (PVC)	1.37	58.0	2.4–2.8	50
Acrylonitrile butadiene styrene (ABS)	1.05	17–62	0.69–2.82	60–130
Nylon	1.13–1.15	48–83	1.03–2.76	80–150
Polyethylene (high-density)	0.96	30–35	1.10–1.30	120

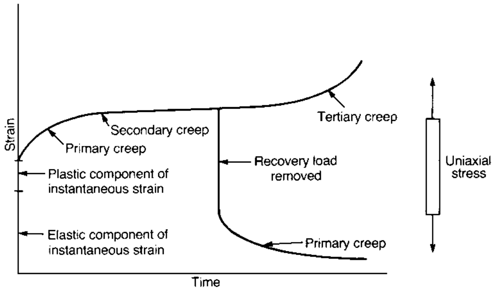

FIGURE 34.2 Total creep curve for a polymer under a given uniaxial stress state.

designer must be aware of this failure mode and realise that polymers, which are tough under short static loads, may become embrittled under long-term loading.

A further important consequence of the time-dependent behaviour of polymers is that when they are subjected to a particular strain, the stress necessary to maintain this strain decreases with time.

Polymer materials have mechanical properties which lie somewhere between the ideal Hookean material, where stress is proportional to strain, and the Newtonian material, where stress is proportional to rate of strain. They are termed 'visco-elastic' materials and their stress is a function of strain and time, and can be described by an equation of the form:

$$\sigma = f(\epsilon, t) \tag{34.1}$$

This non-linear visco-elastic behaviour can be simplified for design purposes into the form:

$$\sigma = \epsilon f(t) \tag{34.2}$$

This linear visco-elastic response indicates that, under sustained tensile stress, after a particular time interval the stress is directly proportional to strain. Figure 34.3 describes the various types of response discussed above.

Short-term tensile tests are commonly used to characterise metals. However, they must be treated with caution when testing polymers. It is possible to obtain quite different results by changing, for instance, the rate of extension of the specimen under a tensile force. At high rates of strain an un-plasticised PVC will show brittle characteristics and relatively high modulus and strength, whereas at low rates of strain the material will be ductile and have a lower modulus and strength. Consequently, the test conditions must be consistent with the service condition for which the material is being designed.

Creep tests are often used to measure the deformational behaviour of polymeric materials. The variation of strain with time, when the specimen is under constant load, is usually recorded on a

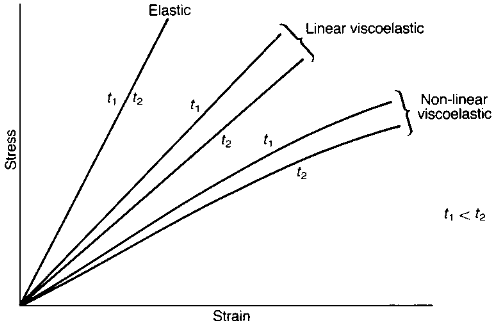

FIGURE 34.3 Stress–strain behaviour of elastic and viscoelastic materials at two values of time.

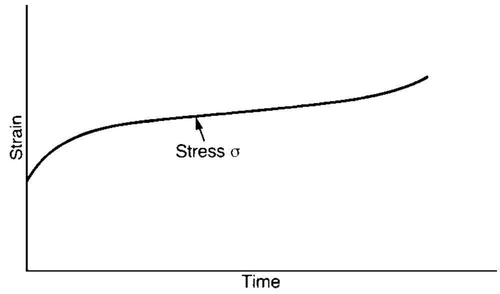

FIGURE 34.4 Typical relationship for a linear viscoelastic material.

logarithmic time-scale so that the time dependence for long periods can be extrapolated if necessary. Figure 34.4 represents a typical relationship between strain and time; a family of curves may be obtained for different stress levels. Figure 34.5 shows the relationship drawn on a logarithmic time-scale.

Figure 34.6 (a) shows a family of strain–time graphs for a typical non-linear polymer. From this, it is clear that the higher the stress applied to the polymer, the higher is the creep rate. Replotted as a stress–time relationship, Figure 34.6 (b) represents the relaxation of stress in the polymer at constant strain; this is termed an isometric graph. If the stresses at a particular time *t* on the creep curve are divided by the respective strain values, then the modulus of elasticity–time curve is shown in Figure 34.6 (c). Finally, if at time *t* the stress values are plotted against the respective strain values, an isochronous graph, Figure 34.6 (d), results. Isochronous data are often represented on log–log scales; the graph will generally be a straight line and its slope will indicate the degree of non-linearity of the polymer material; a slope of 45° represents a linear material, whereas a non-linear material will have a slope less than 45°.

34.4 Applications and uses of polymers

34.4.1 Sealants

Sealants are elastomeric materials which can be used for sealing joints against wind and water in construction. Thin curtain wall construction employs highly effective materials to provide the heat installation, but generally there is no cavity for the dispersion of water that may leak through the joints on the outside. In addition, in the event of air blowing directly to the inside of a joint there must be an effective material to provide heat insulation; consequently, a baffling system to provide this must be installed. Therefore, adhesive and elastic sealants are required to enable this type of construction to be used efficiently.

The largest variety of sealants fall into the classification of solvent release and are composed of three component parts:

1. the basic non-volatile vehicle (the liquid portion of the compound);
2. the pigment component;
3. a solvent or thinner to make application easier.

The non-volatile vehicle can vary from a vegetable oil (e.g. linseed) to a synthetic elastomer. Opacity or colour will be introduced into the material by the pigment component. To enable the sealant to be applied easily and to ensure the

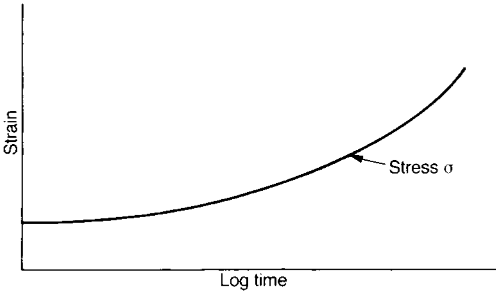

FIGURE 34.5 Typical relationship for a linear viscoelastic material drawn on a logarithmic time-scale.

correct thickness is achieved a solvent is introduced. The sealant is cured and its required viscosity is reached by the evaporation of the solvent. The butyl rubber solution and the acrylic copolymer solution fall into this category.

Another group of sealants are those which are chemically cured. The polysulphide compounds and the silicone-based compounds are the main sealants under this heading. The latter, which is a two-part sealant, is highly dependent upon the environmental conditions for its rate of cure; thus, if the temperature and humidity are low, the curing period could be very long. The chemically cured compounds require adhesion additives in order to develop a bond to a surface as they do not generally contain much solvent.

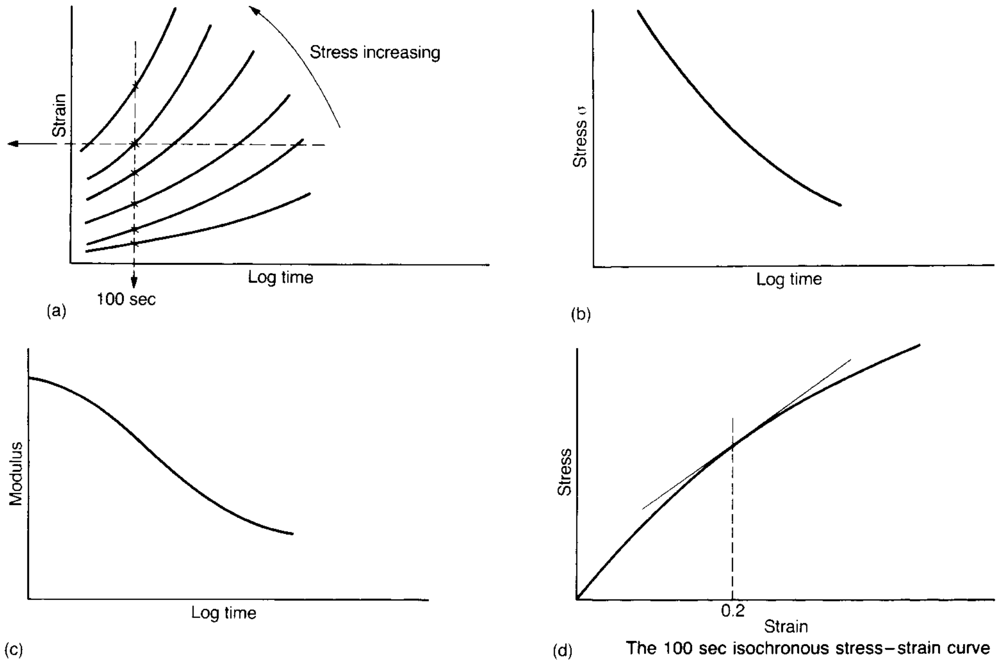

FIGURE 34.6 Typical creep curves for a non-linear viscoelastic material for varying stress values. Isometric and isochronous stress–strain curves.

The desired properties of a sealant are:

- a good adhesion with the joint;
- low rate of hardening;
- low rate of shrinkage;
- permanent elasticity.

The choice of sealants is a compromise as no one product has all the above-mentioned attributes.

34.4.2 Adhesives

Within the context of the construction industry the term adhesive embraces not only those materials which are used to bond together two components of a structure, but also those materials which provide a specific function in themselves (e.g. protection, decoration) and are at the same time self-adhesive to the substrate whose surface they modify. Thus, a mortar which may be used to bond bricks together, may also be applied as a self-adhesive protection and often decorative rendering over the finished blockwork.

Adhesive bonded connections are the primary concern. The physical nature of the fibre/matrix composites does introduce problems that are not encountered in metals. The fibre type and arrangement, as well as the resin type and fibre volume fraction will influence the behaviour of the joint. In addition, composites are not generally homogeneous throughout their thickness as many thermosetting polymers have gel coats; resin-rich surface layers are brittle and when overloaded are liable to display a brittle fracture. An appropriate resin should therefore be chosen, such as a compliant one, which will distribute the applied load over a large area, thus reducing the stress taken by the friable surface of the composite. There are two particular problems associated with adhesive bonding of FRP materials:

- the attachment to the surface of a layered material;
- the surface may be contaminated with mould release agents remaining on it from the manufacturing procedures.

As the matrix material in a polymer composite is also an organic adhesive, the polymers which are then used to join composite materials together are likely to be similar in terms of chemical composition and mechanical properties. Currently the epoxy and the acrylic based toughened adhesives are used for general application and have proved over the years to be very versatile and easy to use. Durable, robust and relatively free from toxic hazards, the toughened adhesives exhibit high pull strengths.

The basic requirements for the production of a satisfactory joint are:

- selection of a suitable adhesive (the common generic type of adhesive used in civil engineering is an epoxy, which can be formulated in a wide range of forms to provide a broad range of application characteristics);
- adequate preparation of the adherend surfaces;
- appropriate design of the joint;
- controlled fabrication of the joint itself.

Adhesive formulations are, in general, complex. To the base resin is added one of a range of different types of hardener and additives, such as fillers, toughening agents, plasticisers surfactants, anti-oxidants and any other required materials. The hardeners are chosen depending upon whether the cure of the resin is to be at ambient or at elevated temperatures; the rate of chemical reaction is approximately doubled for every 8°C rise in temperature. It will be clear that the properties of the adhesive will be altered with the large variety of additives that can be incorporated into the base resin.

If the adhesive is required to join two dissimilar materials, such as polymer composite and concrete or steel, the mechanical and thermal properties should be considered in relation to these two materials. The effects of environmental and other service conditions on the adhesive material and on the behaviour of bonded joints must be considered carefully.

With some bonding surfaces, such as steel, it will generally be necessary to apply an adhesive-compatible primer coat to generate a reliable and reproducible surface. With concrete surfaces it might be advisable to use a primer to enable suitable conditions on which to apply a relatively viscous adhesive. It will not generally be necessary to prime a composite surface.

As with all resins it is necessary to keep a close check on the following items to ensure that the adhesive, when used in the field, is in pristine condition:

- the shelf life is within the manufacturer's recommended time limit;
- the viscosity and wetting ability is satisfactory;
- the curing rate is correct;
- the ambient temperature does not fall below the specification value;
- post cure is complete before load is applied to the joint.

34.4.3 Elastomers

The elastomer is another member of the polymer family. The material consists of long chain molecules which are coiled and twisted in a random manner and the molecular flexibility is such that the material is able to undergo very large deformations. The material is cross-linked by a process known as vulcanisation, which prevents the molecules of the elastomer under load, moving irreversibly relative to each other. After a curing process, the molecules are cross-linked like a thermosetting polymer. As the vulcanisation process does not change the form of the coiled molecules, but merely prevents them from sliding, the elastomeric material will completely recover its original shape after the removal of an external force.

34.4.4 Geosynthetics

One area of the major advances made by polymers in the last 25 years has been the burgeoning use of these materials in the geotechnical engineering industry. The most commonly known material is the geotextile; a simple definition of this is a *textile material used in a soil environment*.

In the early 1970s, these materials were referred to as civil engineering fabric or filter fabric where their primary use was for filter applications. In the latter part of the 1970s, they were referred to as geotechnical fabrics as they were primarily used in the geotechnical soil engineering applications. It was in the early 1980s that the term geotextile was suggested as suitable. At the same time impermeable polymeric membranes were also being increasingly used, and these became known as geomembranes. Thus in the mid 1980s many types of polymeric-based materials were being used in the geotechnical engineering industry and many of these could not be classed as either a geotextile or a geomembrane. To encompass all these polymeric materials the new name 'geosynthetic' was derived, which is defined as a *synthetic (polymeric) material used in a soil environment.*

Geosynthetics, which are all thermoplastic polymers, can be divided into five broadly based categories:

- *Geotextiles*: polymeric textile materials used in geotechnical engineering applications. These materials are essentially permeable to the passage of water.
- *Geogrids*: open, mesh-like polymeric structures.
- *Geomembranes*: polymeric materials in sheet form which are essentially impermeable to the passage of water.
- *Geo-linear elements*: long, slender, polymeric materials normally used as reinforcing tendons in soils and rocks.
- *Geocomposites*: covers all polymeric materials used in a soil environment not covered by the above four categories.

Each of these is now discussed.

Geotextiles

Geotextiles are usually classified by their method of manufacture and are made in two stages: the manufacture of the linear elements, such as fibres, tapes, etc., and the fabrication of those linear elements into geotextiles. The fibres are the basic load-bearing elements in the material and the forming technique determines the structure and hence the physical and mechanical characteristics of the system. The main fibres used in geotextiles are the synthetic ones such as polyethylene, polypropylene, polyester and polyamide; these will be described in more detail in the next section.

Geomembranes

Geomembranes are synthetic materials manufactured in impermeable sheet form from thermoplastic polymers or bituminous materials. Both materials can be reinforced or unreinforced; the former is manufactured on a production line and the latter can be produced on a production line or in situ. The matrix can be reinforced by textiles.

Geo-linear elements

Geo-linear elements are long, slender strips or bars consisting of a unidirectional filament fibre core which is made from a polyester, aramid or glass fibre in a polymer sheath of a low-density polyethylene or a resin. The components of the system form a composite, in that the fibre provides the strength and extension characteristics and the matrix protects the fibre from internal influences and provides the bonding characteristics with the soil.

Geogrids

Geogrids are often grid-like structures of thermoplastic polymer material, and in conjunction with the soil form a quasi-composite system, where the grid structure is the fibre and the soil is assumed to be the 'matrix' and forms an efficient bond with the fibre. Geogrids are of two forms:

1. cross-laid strips; and
2. punched thermoplastic polymer sheets.

The manufacturing techniques will be discussed in Chapter 35.

Geocomposites

Geocomposites consist of two or more different types of thermoplastic polymer systems combined into a hybrid material. Their main function is to form a drainage passage along the side of the water course, with a polymer core as the drainage channel and the geotextile skin as the filter.

As is apparent, many of the materials in each of the above groups are fibre composites of a parent polymer reinforced with polymer fibres, and so will be discussed in more detail in the next section.

34.5 References

Brandon, D. and Kaplan, W.D. (1997) *Joining Processes*, John Wiley and Sons, Chichester.

Hollaway, L. (1993) *Polymer Composites for Civil and Structural Engineering*, Blackie Academic and Professional, London.

Rodriguez, F. (1996) *Principles of Polymer Systems*, E & FN Spon, London.

Part Seven

Fibre Composites

Section One: Polymer composites

L. Hollaway

Section Two: Fibre-reinforced cements and concrete

D.J. Hannant

Introduction

This part is divided into two sections to reflect the difference in the mechanics of the reinforcing process between fibre-reinforced polymers and cementitious materials. The first, on fibre-reinforced polymers, is mostly concerned with pre-cracking behaviour, and the second, on fibre-reinforced cement and concrete, is mainly concerned with post-cracking performance.

The history of fibre-reinforced composites as construction materials is more than 3000 years old. Well-known examples are the use of straw in clay bricks, mentioned in Exodus, and horsehair in plaster. Other natural fibres have been used over the ages to reinforce mud walls and give added toughness to rather brittle building materials.

In the last section we commented that polymers, although relatively strong, have low stiffness. They can, however, be combined with fibres of high stiffness and strength to form a range of composites with improved structural performance which have an increasing number of applications. These include 'hi-tech' uses of carbon fibres in resin systems for aircraft components and sports equipment and glass fibre reinforced systems (GFRP) for car bodies and ships' hulls. In civil engineering there has been a steadily increasing use of the latter group for in-fill panels supported by main structural elements of steel or reinforced concrete, and for modest span lightweight bridges consisting entirely of the fibre composite. An increasing use of both types of system is for panels fitted to existing structures for strengthening after damage or for upgrading. The composition, manufacture, analysis, properties and uses of these systems are described in Section 1.

Fibre-reinforced composites can also be based on inorganic cements and binders. These are described in Section 2. Most fibre-reinforced, cement-based composites differ from fibre-reinforced polymers in that most of the reinforcing effects of the fibres occur after the brittle matrix has cracked either at the microscopic level or with visible cracks through the composite. This is the result of the relatively low strain to failure of the cement matrix (~0.01–0.05 per cent) compared with the high elongation of the fibres (~1–5 per cent). The fibres in cement-based systems often have a lower modulus of elasticity than the cement matrix and hence little or no increase in cracking stress is expected from the fibre reinforcement.

The most notable exception to this division is asbestos cement which has been the most commercially successful fibre-reinforced composite this century, in terms of both tonnage and turnover, the latter having been in excess of £1 billion per annum world-wide for many years. Asbestos cement was invented in about 1900 by Hatschek and its high tensile cracking stress and failure strain (in excess of 0.1 per cent) results in part from the suppression of cracks propagating from flaws. Usage of asbestos fibres has been reduced since about 1980 due to their carcinogenic effects and this has stimulated the search for alternative fibre systems, chiefly glass and polypropylene, which have enabled the traditional products to be safely marketed even if with considerably changed properties.

Starting in the 1960s, there has been growing interest in modifying the properties of fresh and hardened concrete by the addition of fibres. These include both steel and polypropylene, and, to a limited extent, glass fibres. Their use is now widespread in the construction industry, and the range of materials, their properties and most common applications are described.

Section 1

Polymer composites

Introduction

Composites which are used to form engineering materials and which consist of strong, stiff fibres in a polymer resin require scientific understanding from which design procedures may be developed. The mechanical and physical properties of the composite are clearly controlled by their constituent properties and by the micro-structural configurations. It is, therefore, necessary to be able to predict properties when parameter variations take place.

The next important aspect of composite material design is the property of anisotropy; it is necessary to give special attention to the methods of controlling this property and its effect on analytical and design procedures.

Research work has demonstrated that with the correct process control and a soundly based material design approach, it is possible to produce composites that can satisfy stringent structural requirements. However, in the construction industry, because it is difficult to establish the durability of the composite over a period of, say, 50 years, great care has to be exercised in predicting stress and deformations over this time span. It will, however, be apparent from this section that there are many examples of successful structural applications of polymer composites. Some of the examples discussed below are outside the construction field, but they have been included because they are particularly noteworthy, demonstrating how fibre-reinforced polymer composites have offered unique solutions to a range of product demands

Chapter thirty-five

Fibres for polymer composites

35.1 Fibre manufacture
35.2 Fibre properties

When a load is applied to a fibre-reinforced composite consisting of a low-modulus matrix reinforced with high-strength, high-modulus fibres, the visco-elastic flow of the matrix under stress transfers the load to the fibre; this results in a high-strength, high-modulus material which determines the stiffness and strength of the composite and is in the form of particles of high aspect ratio (i.e. fibres), is well dispersed and bonded by a weak secondary phase (i.e. matrix).

Many amorphous and crystalline fibres can be used, including glass, carbon and boron and fibres produced from synthetic polymers. Making a fibre involves aligning the molecules of the material, and the high tensile strength is associated with improved intermolecular attraction resulting from this alignment. Polymeric fibres are made from those polymers whose chemical composition and geometry are basically crystalline and whose intermolecular forces are strong. As the extensibility of the material has already been utilised in the process of manufacture, fibres have a low elongation.

The following sections will discuss the manufacture and make-up of fibres which can be used to upgrade polymers, cements, mortars and concretes. The last three will be covered in greater detail in Chapters 42 and 43. Glass, carbon and Kevlar fibres are used in conjunction with thermosetting polymers such as polyesters and epoxies.

35.1 Fibre manufacture

35.1.1 Glass fibres

Glass fibres are manufactured by drawing molten glass from an electric furnace through platinum bushings at high speed; see Figure 35.1. The filaments cool from the liquid state at about 1200°C to room temperature in 10^{-5} seconds. On emerging from the bushings the filaments are treated with a lubricant or size and 204 filaments are bundled together to form a strand. The lubricant

1. facilitates the manufacturing of the strands and moulding of the composite;
2. reduces damage to the fibres during mechanical handling;
3. reduces the abrasive effect of the filaments against one another.

The following four types of glass are used for fibres.

1. E-glass of low alkali content is the commonest glass on the market and is the major one used in composites in the construction industry. It was first used in 1942 with polyester resin and is now widely used with polyester and epoxy resin.

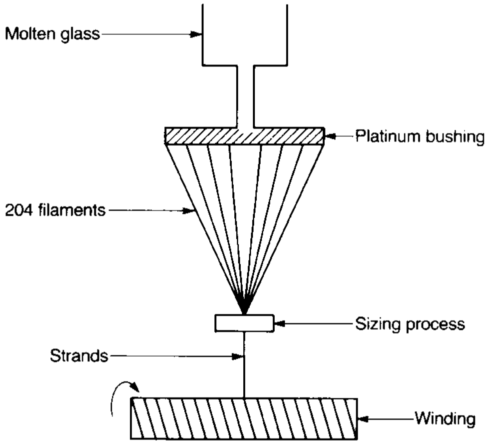

FIGURE 35.1 Schematic representation of the manufacture of glass fibre.

2. A-glass fibre of high alkali content was formerly used in the aircraft industry, but it is now little used.
3. Z-glass (zirconia glass) was developed for reinforcing cements, mortars and concretes because of its high resistance to alkali attack (see Chapter 42).
4. S2-glass fibre is used in extra-high-strength and high-modulus applications in aerospace.

Strands of glass fibre are combined to form thicker parallel bundles called rovings which, when twisted, can form several different types of yarn; rovings or yarns can be used individually or in the form of woven fabric.

Glass strands for reinforcing thermosetting polymers may be used in a number of different forms:

1. woven rovings, to provide high strength and stiffness characteristics in the direction of the fibres;
2. chopped fibres, to provide a randomly orientated dispersion of fibres in the composite;
3. chopped strand mat, to provide a quasi-isotropic reinforcement to the composite;
4. surface tissues, to provide a thin glass-fibre mat when a resin-rich surface of composite is required.

35.1.2 Carbon fibres

Carbon fibres are produced commercially as synthetic fibres similar to those used for making textiles and from pitch, which is obtained by the destructive distillation of coal.

There are three different precursor materials used at present to produce carbon fibres.

Rayon precursors – the earliest precursors used to make carbon fibres were derived from cellulosic materials. The significant disadvantage of this precursor is that only a small part (typically 25 per cent) of the initial fibre mass remains after carbonisation which makes it an expensive fibre.

Polyacrylonitrile (PAN) precursors – the majority of carbon fibres commercially available are derived from this precursor. The carbon fibre conversion yield is 50–55 per cent. Carbon fibres based upon the PAN precursor have a higher tensile strength than fibres based upon other precursors. This is due to their having less surface imperfections than other manufactured carbon fibres.

Pitch precursors – pitch is a relatively low-cost and a high-yield material. However, non-uniformity from batch to batch is a serious problem.

The conversion process for carbon fibre includes stabilisation at temperatures up to 400°C, carbonisation at temperatures from 800°C to 1200°C and graphitisation in excess of 2000°C. Surface treatments of the fibres are then undertaken which includes sizing and spooling.

With the increased use of carbon fibres in the engineering field and particularly civil engineering, new processes are being developed. All commercial production of PAN precursor carbon fibres is by spinning and the cross-section is round. New manufactured carbon fibres are now commercially available to produce different precursor shapes including 'I' and 'cross' types. The advantage of non-round shapes is that closer fibre packing in composites is possible, permitting higher load-carrying capacity than that for round-section fibres.

There are three grades of carbon fibres:

- Type I is the stiffest and has the highest modulus of elasticity of the three. The heat treatment temperature is in excess of 2000°C.
- Type II is the strongest and is heat treated at about 1500°C.
- Type III is the least stiff of the three and has a heat treatment at about 1350°C.

35.1.3 Aramid fibres

The aramid fibre (aromatic polyamide) was introduced in 1972 by Du Pont under the trade name of Kevlar. Recently several other manufacturers have produced related aramid fibres. The structure of the fibre is anisotropic, resulting in higher strength and stiffness in the fibre longitudinal direction.

Aramid fibres are resistant to fatigue, both static and dynamic. They are elastic in tension but exhibit non-linear characteristics under compression and care must be taken when high strain compressive or flexural loads are involved. Aramid fibres exhibit good toughness and general damage tolerance characteristics.

There are two forms of Kevlar fibre, the Kevlar 29 with a high strength and intermediate stiffness and Kevlar 49 with a high modulus and equivalent strength to that of the Kevlar 29. Table 35.2 gives the mechanical properties of the two fibres. The Kevlar 49 is used for high-performance composite materials.

The fibre is produced by an extrusion and spinning process. A solution of the polymer in a suitable solvent at a temperature between −50°C and −80°C is extruded into a hot-walled cylinder at 200°C; this causes the solvent to evaporate and the resulting fibre is wound onto a bobbin. The fibre then undergoes a stretching and drawing process to increase its strength and stiffness.

35.1.4 Linear organic fibres

By arranging the molecular structure of simple polymers during their manufacture, to be orientated into one direction, a high-strength and high-modulus organic fibre can be produced. This fibre, in future, could be one of the major reinforcements for civil engineering structures. With a specific weight of 0.97, high modulus polyethylene fibres, produced in the USA and The Netherlands, have mechanical properties of the same order as those of aramid fibres with modulus of elasticity and strength values of 117 GPa and 2.9 GPa respectively. These values were determined at ambient temperature but will decrease rapidly with increasing temperature. Furthermore, with non-cross-linked thermoplastic polymer fibres, creep will be significant. However, recently it has been claimed that these problems can be overcome by cross-linking using radiation.

35.1.5 Other synthetic fibres

The most important fibres for upgrading cements and mortars or for use in reinforced earth situations are polypropylene, polyethylene, polyester and polyamide. The first two are utilised in the manufacture of cement/mortar composites and are discussed further in Chapter 42, but all four are used in geosynthetics, especially to form geotextiles and geogrids as described in Chapter 39. Synthetic fibres are the only ones which can be engineered chemically, physically and mechanically to suit particular geotechnical engineering applications. Natural fibres (e.g. cotton, jute) and the majority of regenerated fibres (e.g. cellulose, rayon) are seldom used to make geotextiles because they are biodegradable; however, geotextiles made from natural fibres and even paper (another fibrous product) may serve temporary functions where biodegradation is desirable (e.g. temporary erosion control).

Manufacture begins with the transformation of the raw polymer from solid to liquid either by dissolving or melting. Synthetic polymers such as acrylic, modacrylic, aramid and vinyladpolymers are dissolved into solution, whereas the polyolefin and polyester polymers are transformed into molten liquid; chlorofibre polymers can be transformed into a liquid by either means. A spinneret consisting of many holes is used to extend the liquid polymer which is then solidified into continuous filaments.

The filaments undergo further extension in their longitudinal axes, thus further increasing the orientation of the molecular chain within the filament structure, with a consequent improvement in the stress–strain characteristics. Different types of synthetic fibre or yarn may be produced, including monofilament fibres, heterofilament fibres, multifilament yarns, staple fibres, staple yarns, split-film tapes and fibrillated yarns.

35.2 Fibre properties

The advantage of composite materials over conventional ones is that they have high specific strength and high specific stiffness, achieved by the use of low-density fibres with high strength and modulus values. The strength and stiffness values of carbon, glass and Kevlar fibres are given in Table 35.1.

It has been stated that there are three types of carbon fibre: the high-modulus, the high strength and the intermediate-modulus fibre. The degree of alignment of the small crystalline units in the fibres varies considerably with the manufacturing technique, which thus affects the stiffness of the fibre. The arrangement of the layer planes in the cross-section of the fibre is also important, because it affects the transverse and shear properties. Table 35.1 gives the principal mechanical properties of these fibres and illustrates this point.

The strength and modulus of elasticity of glass fibres are determined by the three-dimensional structure of the constituent oxides which can be of calcium, boron, sodium, iron or aluminium. The structure of the network and the strength of the individual bonds can be varied by the addition of other metal oxides and so it is possible to produce glass fibres with different chemical and physical properties. Unlike carbon fibres the properties of glass fibres are isotropic and the modulus of elasticity is the same along and across the fibre.

The main factors which determine the ultimate strength of glass fibres are the processing condition and the damage sustained during handling and processing. The mechanical properties of two types of glass fibre are given in Table 35.1.

The manufacturing processes for Kevlar fibres align the stiff polymer molecules parallel to the fibre axes, and the high modulus achieved indicates that a high degree of alignment is possible. Typical properties of Kevlar fibres are given in Table 35.1. When the fibres have been incorporated into a matrix material, composite action takes place and as discussed in the next chapter, a knowledge of the fibre alignment, fibre volume fraction and method of manufacture is necessary to obtain the mechanical characteristic of the material. To illustrate this, Table 35.2 gives the tensile characteristics of the different systems of GFRP composites; the various methods of manufacture of the composites are given in Chapter 37.

TABLE 35.1 Typical mechanical properties for the three fibres used in construction

Material properties	*Relative density*	*Ultimate tensile strength (GPa)*	*Modulus of elasticity in tension (GPa)*
Carbon fibre			
Type I	1.92	2.00	345
Type II	1.75	2.41	241
Type III	1.70	2.21	200
E-glass fibre	2.55	2.4	72.4
S2-glass fibre	2.47	4.6	88.0
Kevlar fibres			
29	1.44	2.65	64
49	1.45	2.65	127

TABLE 35.2 Typical mechanical properties for glass-reinforced polymer composites

Material	*Glass content (weight %)*	*Relative density*	*Tensile modulus (GPa)*	*Tensile strength (MPa)*
Unidirectional rovings (filament winding or pultrusion)	50–80	1.6–2.0	20–50	400–1250
Hand lay-up with chopped strand mat	25–45	1.4–1.6	6–11	60–180
Matched dye moulding with preform	25–50	1.4–1.6	6–12	60–200
Hand lay-up with woven rovings	45–62	1.5–1.8	12–24	200–350
DMC polyester (filled)	15–20	1.7–2.0	6–8	40–60
SMC	20–25	1.75–1.95	9–13	60–100

35.3 References

Hull, D. (1992) *An Introduction to Composite Materials*, Cambridge University Press, Cambridge.

Holloway, L. (1993) *Polymer Composites for Civil and Structural Engineering*, Blackie Academic and Professional, Glasgow.

Kim, D.-H. (1995) *Composite Structures for Civil and Architectural Engineering*, E & F Spon, London.

Chapter thirty-six

Analysis of the behaviour of polymer composites

36.1 Characterisation and definition of composite materials

The mechanical properties of polymers can be greatly enhanced by incorporating fillers and/or fibres into the resin formulations. Therefore, for structural application, such composite materials should:

1. consist of two or more phases, each with their own physical and mechanical characteristics;
2. be manufactured by combining the separate phases such that the dispersion of one material in the other achieves optimum properties of the resulting material;
3. have enhanced properties compared with those of the individual components.

In fibre-reinforced polymer materials, the primary phase (the fibre) uses the plastic flow of the secondary phase (the polymer) to transfer the load to the fibre; this results in a high-strength, high-modulus composite. Fibres generally have both high strength and high modulus but these properties are only associated with very fine fibres with diameters of the order of 7–15 mm; they tend to be brittle. Polymers, however, may be either ductile or brittle and will generally have low strength and stiffness. By combining the two components a bulk material is produced with a strength and stiffness dependent upon the fibre volume fraction and the fibre orientation.

The properties of fibre/matrix composite materials are highly dependent upon the micro structural parameters such as:

1. fibre diameter;
2. fibre length;
3. fibre volume fraction of the composite;
4. fibre orientation and packing arrangement.

It is important to characterise these parameters when considering the processing of the composite material and the efficient design and manufacture of the composite made from these materials.

The interface between the fibre and the matrix plays a major role in the physical and mechanical properties of the composite material. The transfer of stresses between fibre and fibre takes place through the interface and the matrix, and in the analysis of composite materials a certain number of assumptions are made to enable solutions to mathematical models to be obtained:

1. the matrix and the fibre behave as elastic materials;
2. the bond between the fibre and the matrix is perfect and consequently there will be no strain discontinuity across the interface;
3. the material adjacent to the fibre has the same properties as the material in bulk form;
4. the fibres are arranged in a regular or repeating array.

The properties of the interface region are very important in understanding the stressed composite. The region is a dominant factor in the fracture toughness of the material and in its resistance to aqueous and corrosive environments. Composite materials which have weak interfaces have low strength and stiffness but high resistance to fracture, and those with strong interfaces have high strength and stiffness but are very brittle. This effect is a function of the ease of debonding and pull-out of the fibres from the matrix material during crack propagation.

Using the above assumptions, it is possible to calculate the distribution of stress and strain in a composite material in terms of the geometry of the component materials.

36.2 Elastic properties of continuous unidirectional laminae

36.2.1 Longitudinal stiffness

A basic laminate is shown in Figure 36.1 and it is assumed that the orthotropic layer has three mutually perpendicular planes of property symmetry; it is characterised elastically by four independent elastic constants (refer to Section 36.6 and to Section 36.8, Figure 36.5). They are:

E_{11} = modulus of elasticity along fibre direction
E_{22} = modulus of elasticity in the transverse direction
υ_{12} = Poisson's ratio, i.e. strains produced in direction 2 when specimen is loaded in direction 1
G_{12} = longitudinal shear modulus
υ_{21} = Poisson's ratio, i.e. obtained from the equation $E_{11}\upsilon_{21} = E_{22}\upsilon_{12}$

If the line of action of a tensile or compressive force is applied parallel to the fibres of a unidirectional lamina, the strain ϵ_m in the matrix will be equal to the strain ϵ_f in the fibre, provided the bond between the two components is perfect. As both fibre and matrix behave elastically then:

$$\sigma_f = E_f \epsilon_t \text{ and } \sigma_m = E_m \epsilon_m \text{ where } \epsilon_t = \epsilon_m$$

As $E_f > E_m$ the stress in the fibre must be greater than the stress in the matrix and will therefore bear the major part of the applied load.

The composite load $P_c = P_m + P_f$ or

$$\begin{aligned} \sigma_c A_c &= \sigma_m A_m + \sigma_f A_f \\ \sigma_c &= \sigma_m V_m + \sigma_f V_f \qquad (36.1) \end{aligned}$$

where A = the area of the phase, V = volume fraction of the phase with $V_c = 1$, V_c = the volume of composite.

As the bond is perfect

$$\epsilon_c = \epsilon_m = \epsilon_f$$

from equation (36.1)

$$\begin{aligned} E_c \epsilon_c &= E_m \epsilon_c V_m + E_f \epsilon_c V_f \qquad (36.2) \\ E_c &= E_m V_m + E_f V_f \\ E_c &= E_{11} = E_m(1 - V_f) + E_f V_f. \qquad (36.3) \end{aligned}$$

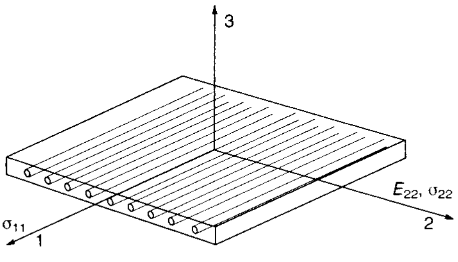

FIGURE 36.1 Basic laminate.

This equation is often referred to as a law of mixtures equation.

36.2.2 Transverse stiffness

The same approach can be used to obtain the transverse modulus of a unidirectional lamina E_{22}.

The applied load transverse to the fibres acts equally on the fibre and matrix and therefore

$$\sigma_f = \sigma_m$$

$$\epsilon_f = \sigma_{22}/E_f \text{ and } \epsilon_m = \sigma_{22}/E_m \qquad (36.4)$$

$$\epsilon_{22} = V_f\epsilon_f + V_m\epsilon_m \qquad (36.5)$$

Substituting equation (36.4) into equation (36.5)

$$\epsilon_{22} = V_f\sigma_{22}/E_f + V_m\sigma_{22}/E_m \qquad (36.6)$$

Substituting

$$\sigma_{22} = E_{22}\epsilon_{22} \text{ into equation (36.6)}$$

$$E_{22} = E_fE_m/[E_f(1 - V_f) + E_mV_f] \qquad (36.7)$$

Equation (36.7) predicts E_{22} with reasonable agreement when compared with experimental results. The equation (36.8) has been proposed and takes account of Poisson contraction effects.

$$E_{22} = E'_mE_f/[E_f(1 - V_f) + V_fE'_m] \qquad (36.8)$$

where

$$E'_m = E_m/(1 - v_m^2).$$

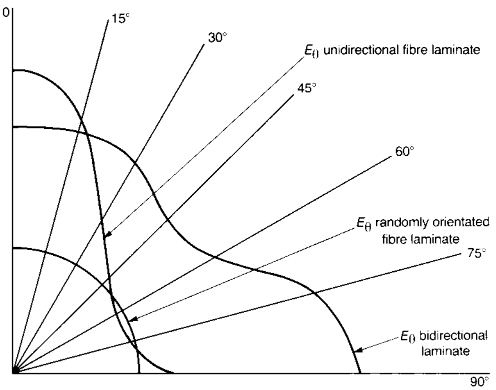

FIGURE 36.2 Orientation dependence of the modulus of elasticity of a fibre/matrix composite.

36.3 Elastic properties of in-plane random long-fibre laminate

Laminae manufactured from long randomly orientated fibres in a polymer matrix are, on a microscopic scale, isotropic in the plane of the lamina. The general expression (the proof is given in Hollaway (1989)) for the elastic modulus of laminae consisting of long fibres is:

$$\begin{aligned}1/E_\theta = {} & (1/E_{11})(\cos^4\theta) + (1/E_{22})(\sin^4\theta) \\ & + [(1/G_{12}) \\ & - (2v_{12}/E_{11})]\cos^2\theta\sin^2\theta \qquad (36.9)\end{aligned}$$

where θ = angle defining the direction of required stiffness. Figure 36.2 shows the relationship of E_o when angle θ varies between 0° and 90°.

It can be seen then that laminae can be made with predetermined fibre orientation distribution so that elastic and other mechanical properties can be designed to meet specific needs.

36.4 Macro-analysis of stress distribution in a fibre/matrix composite

The behaviour of composites reinforced with fibres of finite length l cannot be described by the above equations. As the aspect ratio, which is defined by the fibre length divided by the fibre diameter *(l/d)*, decreases, the effect of fibre length becomes more significant.

When a composite containing uniaxially aligned discontinuous fibres is stressed in tension parallel to the fibre direction there is a portion at the end of each finite fibre length, and in the surrounding matrix, where the stress and strain fields are modified by the discontinuity. The efficiency of the fibre to stiffen and to reinforce the matrix decreases as the fibre length decreases. The critical transfer length over which the fibre stress is decreased from the maximum value, under a given lamina load, to zero at the end of the fibre is referred to as half the critical length of the fibre. To achieve the maximum fibre stress, the fibre length must be equal to or greater than the critical value l_c.

Figure 36.3 shows diagrammatically the deformation field around a discontinuous fibre embedded in a matrix and subjected to a tensile force where the line of action of the force is parallel to the fibre. Figure 36.4 shows a schematic representation of a discontinuous fibre/matrix lamina subjected to an axial stress; the stress distributions of the tensile and shear components are shown.

36.5 Elastic properties of short-fibre composite materials

As discussed above the reinforcing efficiency of short fibres is less than that for long fibres. In addition the orientation of short fibres in a lamina is random and therefore the lamina can be assumed to be isotropic on a macro scale.

The rule of mixtures as given in equation (36.3) can be modified by the inclusion of a fibre orientation distribution factor η, thus the composite modulus of elasticity is given by

$$E_c = E_{11} = \eta E_f V_f + E_m V_m. \qquad (36.10)$$

Values of η have been calculated by Krenchel (1964) for different fibre orientations:

η = 0.375 for a randomly orientated fibre array
= 1.0 for unidirectional laminae when tested parallel to the fibre
= 0 for unidirectional laminae when tested perpendicularly to the fibre
= 0.5 for a bidirectional fibre array.

The following sections are important for a complete understanding of composite theory and you may find that you have to go back to study them in more detail after the first reading.

36.6 Laminate theory

Sections 36.2, 36.3, 36.4 and 36.5 discussed the individual lamina properties; this section concentrates upon laminates which are formed when two or more laminae are combined to produce a composite. It describes the methods used to calculate the elastic properties of the laminates, and briefly introduces the elasticity theory.

The stresses at a point in a body are generally represented by stress components acting on the surface of a cube; Figure 36.5 shows the three normal and the three shear stresses. The notation

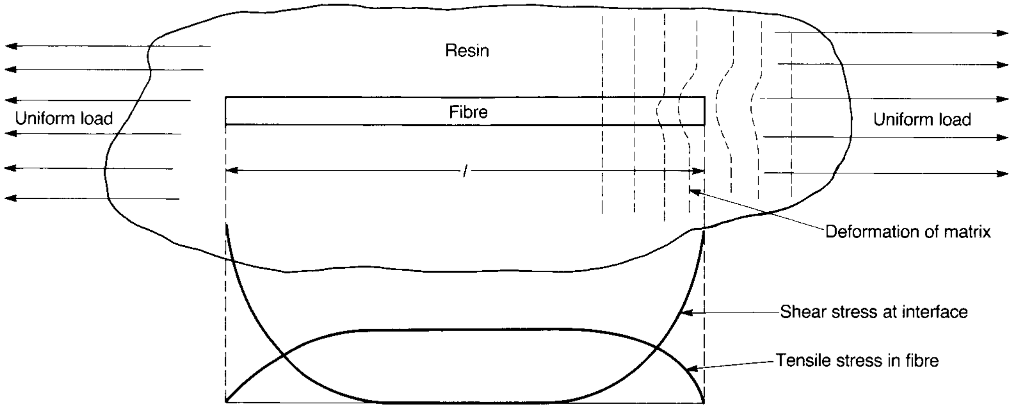

FIGURE 36.3 Diagrammatic representation of the deformation field around a discontinuous fibre embedded in a matrix.

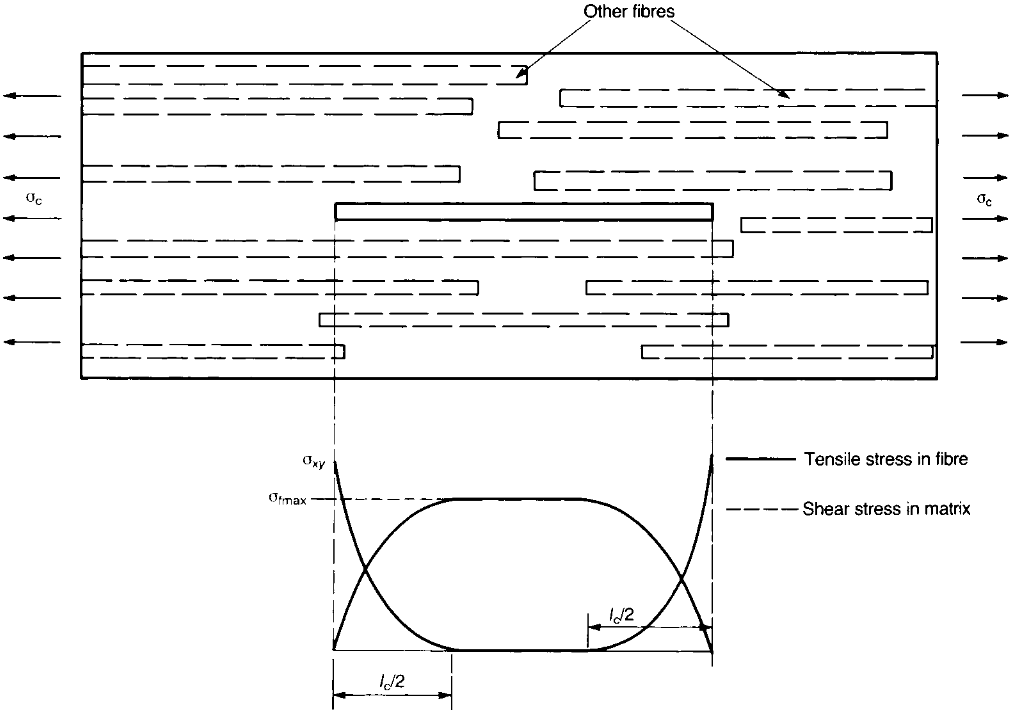

FIGURE 36.4 Schematic representation of an aligned, discontinuous fibre composite subjected to an axial stress; stress distribution at failure is shown.

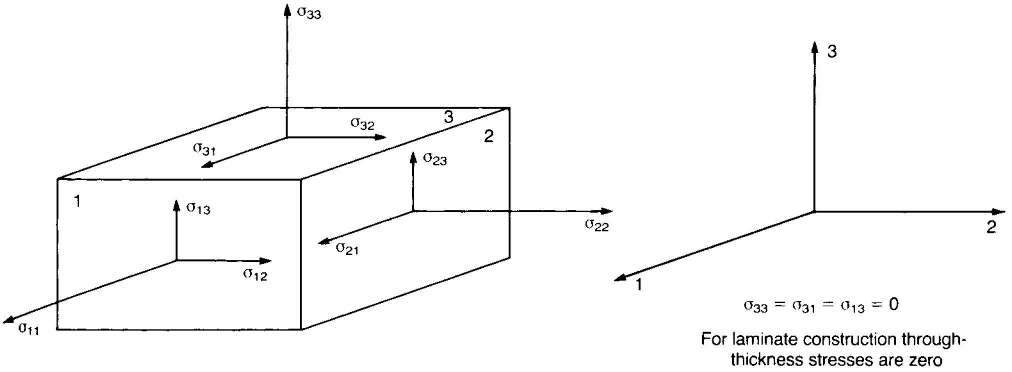

FIGURE 36.5 Components of stress acting on an elemental unit cube.

employed here is such that the first subscript refers to the plane upon which the stress acts and the second subscript is the coordinate direction in which the stress acts; the equivalent strains have the same notation. As laminae are assumed to be sufficiently thin the through thickness stresses are zero. Thus $\sigma_{33} = \sigma_{31} = \sigma_{13} = 0$ and plane stress conditions hold.

36.7 Isotropic lamina

For homogeneous isotropic lamina the stress–strain relationship for a lamina and laminates is:

$$\begin{aligned}\sigma_{11} &= (E/(1-v^2))(\epsilon_{11} + v\epsilon_{22})\\ \sigma_{22} &= (E/(1-v^2))(\epsilon_{22} + v\epsilon_{11})\\ \sigma_{12} &= (E/2(1+v))(\epsilon_{12}) \qquad (36.11\text{a})\end{aligned}$$

or in matrix form

$$\begin{bmatrix}\sigma_{11}\\ \sigma_{22}\\ \sigma_{12}\end{bmatrix} = \begin{bmatrix}Q_{11} & Q_{12} & 0\\ Q_{21} & Q_{22} & 0\\ 0 & 0 & Q_{33}\end{bmatrix}\begin{bmatrix}\epsilon_{11}\\ \epsilon_{22}\\ \epsilon_{12}\end{bmatrix}$$

$$[\sigma] = [Q][\epsilon] \qquad (36.11\text{b})$$

where

$$\begin{aligned}Q_{11} &= E/(1-v^2) = Q_{22}\\ Q_{12} &= vE/(1-v^2) = Q_{21}\\ Q_{33} &= E/2(1+v) = G.\end{aligned}$$

There are two independent constants in these equations; these are E and υ and this indicates isotropic material properties.

The corresponding set of equations to those in equation (36.11b), which relate strains to stresses, are:

$$\begin{bmatrix}\epsilon_{11}\\ \epsilon_{22}\\ \epsilon_{12}\end{bmatrix} = \begin{bmatrix}S_{11} & S_{12} & 0\\ S_{21} & S_{22} & 0\\ 0 & 0 & S_{33}\end{bmatrix}\begin{bmatrix}\sigma_{11}\\ \sigma_{22}\\ \sigma_{12}\end{bmatrix} \qquad (36.12\text{a})$$

$$[\epsilon] = [S][\sigma] \qquad (36.12\text{b})$$

where

$$\begin{aligned}S_{11} &= 1/E = S_{22}\\ S_{33} &= 1/G\\ S_{12} &= -v/E.\end{aligned}$$

36.8 Orthotropic lamina

The orthotropic lamina can be assumed to be isotropic in plane 1, as shown in Figure 36.5 (i.e. the plane normal to the axis direction 1), as the properties are independent of direction in that plane. The stress–strain relationship for an orthotropic lamina is

$$\begin{aligned}\sigma_{11} &= [E_{11}/(1-v_{12}v_{21})][\epsilon_{11} + v_{21}\epsilon_{22}]\\ \sigma_{22} &= [E_{22}/(1-v_{12}v_{21})][\epsilon_{22} + v_{12}\epsilon_{11}]\\ \sigma_{12} &= G_{12}\epsilon_{12} \qquad (36.13\text{a})\end{aligned}$$

or in matrix form

$$\begin{bmatrix}\sigma_{11}\\ \sigma_{22}\\ \sigma_{12}\end{bmatrix} = \begin{bmatrix}Q_{11} & Q_{12} & 0\\ Q_{21} & Q_{22} & 0\\ 0 & 0 & Q_{33}\end{bmatrix}\begin{bmatrix}\epsilon_{11}\\ \epsilon_{22}\\ \epsilon_{12}\end{bmatrix}$$

$$[\sigma] = [Q][\epsilon] \qquad (36.13\text{b})$$

where

$$\begin{aligned}&Q_{11} = E_{11}/(1-v_{12}v_{21}); \quad Q_{22} = E_{22}/(1-v_{12}v_{21})\\ &Q_{12} = v_{21}E_{11}/(1-v_{12}v_{21}); \; Q_{21} = v_{12}E_{22}/(1-v_{12}v_{21})\\ &Q_{33} = G_{12}.\end{aligned}$$

As the Q matrix is symmetric we have $v_{21}E_{11} = v_{12}E_{22}$. The Poisson's ratio v_{12} refers to the strains produced in direction 2 when the lamina is loaded in direction 1.

There are four independent constants in these equations; these are E_{11}, E_{22}, υ_{12} and υ_{21} and this indicates orthotropic material properties.

From the above equation it can be seen that the shear stress $\sigma 12$ is independent of the elastic properties E_{11}, E_{22}, υ_{12} and υ_{21}, and therefore no coupling between tensile and shear strains takes place.

The corresponding set of equations to those in equation (36.13b) which relate strains to stresses are:

$$\begin{bmatrix}\epsilon_{11}\\ \epsilon_{22}\\ \epsilon_{12}\end{bmatrix} = \begin{bmatrix}S_{11} & S_{12} & 0\\ S_{21} & S_{22} & 0\\ 0 & 0 & S_{33}\end{bmatrix}\begin{bmatrix}\sigma_{11}\\ \sigma_{22}\\ \sigma_{12}\end{bmatrix} \qquad (36.14\text{a})$$

$$[\epsilon] = [S][\sigma] \qquad (36.14\text{b})$$

where

$$S_{11} = 1/E_{11}; \quad S_{33} = 1/G_{12}$$

$S_{22} = 1/E_{22}; \quad S_{12} = -v_{21}/E_{22} = -v_{12}/E_{11}.$

If the line of application of the load is along some axis other than the principal one, then the lamina principal axes do not coincide with the reference axes x, y of the load and the former axes must be transformed to the reference axes. Figure 36.6 illustrates the orientation of the orthotropic lamina about the reference axis.

Hollaway (1989) shows that the stress–strain relationship in the (x, y) coordinate system at an angle θ to the principal material direction becomes

$$\begin{bmatrix} \sigma_{xx} \\ \sigma_{yy} \\ \sigma_{xy} \end{bmatrix} = \begin{bmatrix} \bar{Q}_{11} & \bar{Q}_{12} & \bar{Q}_{13} \\ \bar{Q}_{21} & \bar{Q}_{22} & \bar{Q}_{23} \\ \bar{Q}_{31} & \bar{Q}_{32} & \bar{Q}_{33} \end{bmatrix} \begin{bmatrix} \epsilon_{xx} \\ \epsilon_{yy} \\ \epsilon_{xy} \end{bmatrix} \qquad (36.15a)$$

or

$$\begin{bmatrix} \sigma_{xx} \\ \sigma_{yy} \\ \sigma_{xy} \end{bmatrix} = [\bar{Q}] \begin{bmatrix} \epsilon_{xx} \\ \epsilon_{yy} \\ \epsilon_{xy} \end{bmatrix} \qquad (36.15b)$$

where

$$\begin{aligned}
\bar{Q}_{11} &= Q_{11}m^4 + Q_{22}n^4 + 2(Q_{12} + 2Q_{33})n^2m^2 \\
\bar{Q}_{12} = \bar{Q}_{21} &= (Q_{11} + Q_{22} - 4Q_{33})n^2m^2 + Q_{12}(n^4 + m^4) \\
\bar{Q}_{13} = \bar{Q}_{31} &= (Q_{11} - Q_{12} - 2Q_{33})nm^3 + (Q_{12} - Q_{22} + 2Q_{33})n^3m \\
\bar{Q}_{22} &= Q_{11}n^4 + Q_{22}m^4 + 2(Q_{12} + 2Q_{33})n^2m^2 \\
\bar{Q}_{23} = \bar{Q}_{32} &= (Q_{11} - Q_{12} - 2Q_{33})n^3m + (Q_{12} - Q_{22} + 2Q_{33})nm^3 \\
\bar{Q}_{33} &= (Q_{11} + Q_{22} - 2Q_{12} - 2Q_{33})n^2m^2 + Q_{33}(n^4 + m^4)
\end{aligned}$$

where Q_{11}, Q_{22}, Q_{12}, Q_{21} and Q_{33} have been defined in equation (36.13b) and $m = \cos\theta$, $n = \sin\theta$ and the equivalent expression for strain components in the reference axis x, y in terms of the stress components in that axis become:

$$\begin{bmatrix} \epsilon_{xx} \\ \epsilon_{yy} \\ \epsilon_{xy} \end{bmatrix} = [\bar{S}] \begin{bmatrix} \sigma_{xx} \\ \sigma_{yy} \\ \sigma_{xy} \end{bmatrix} \qquad (36.16)$$

where $[\bar{S}]$ is a 3×3 compliance matrix where the components are:

$$\begin{aligned}
\bar{S}_{11} &= S_{11}m^4 + S_{22}n^4 + (2S_{12} + S_{33})n^2m^2 \\
\bar{S}_{12} &= \bar{S}_{21} = S_{12}(n^4 + m^4) + (S_{11} + S_{22} - S_{33})n^2m^2 \\
\bar{S}_{13} &= \bar{S}_{31} = 2(S_{11} - 2S_{12} - S_{33})nm^3 - (2S_{22} - S_{12} - S_{33})n^3m \\
\bar{S}_{23} &= S_{32} = (2S_{11} - 2S_{12} - S_{33})n^3m - (2S_{22} - 2S_{12} - S_{33})nm^3
\end{aligned}$$

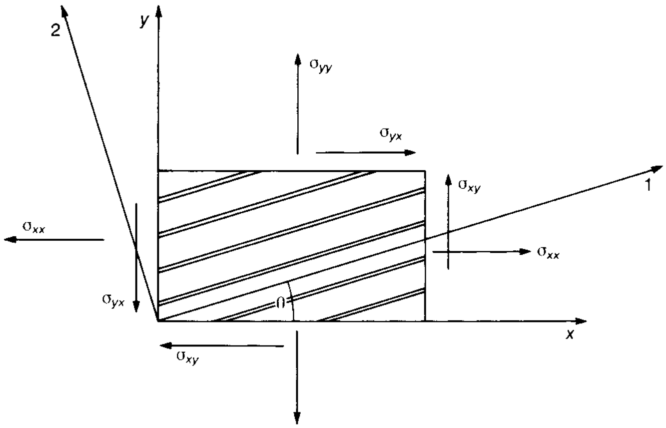

FIGURE 36.6 Orientation of orthotropic lamina about reference axis.

$$\begin{aligned}\bar{S}_{22} &= S_{11}n^4 + S_{22}m^4 + (2S_{12} + S_{33})n^2m^2 \\ \bar{S}_{33} &= 2(2S_{11} + 2S_{22} - 4S_{12} - S_{33})n^2m^2 \\ &\quad + S_{33}(n^4 + m^4)\end{aligned}$$

where S_{11}, S_{22}, S_{12}, S_{21} and S_{33} have been defined in equation (36.14b).

36.9 The strength characteristics and failure criteria of composite laminae

In the two preceding sections, the stiffness relationships in terms of stress and strain were presented for isotropic and orthotropic materials. It is now necessary to have an understanding of the ultimate strengths of the laminae to enable a complete characterisation of the composite material to be made. The stress–strain relationship stated in the previous sections described the actual stresses occurring at any point in a lamina, and the strength characteristics may be considered as describing the allowable stress at any point.

When the formulation of the stiffness characteristics of the lamina was developed, properties in both tension and compression were assumed. However, the ultimate strength behaviour of composite systems may be different in tension and compression and the characteristics of the failure mode will be highly dependent upon the component materials. Therefore, a systematic development of the strengths of these materials is not possible; consequently a series of failure criteria for composite materials will be given.

36.9.1 Strength theories for isotropic laminae

In isotropic materials both normal and shear failure can occur, but it is usual to equate the combined stress situation to the experimentally determined uniaxial tension or compression value. When a tensile load is applied to a specimen in a uniaxial test it is possible for failure in the specimen to be initiated by either an ultimate tensile stress or a shear stress, because a tensile stress of s (the maximum principal stress in this type of test) on the specimen produces a maximum shear value of s/2. Consequently the failure theories are related to the applied tensile or compressive stress that causes failure, irrespective of whether it was a normal or a shear stress failure.

Many theories and hypotheses have been developed to predict the failure surface for composite materials under tensile loads and probably the best known theories which have been used to predict failure and which are discussed in Holmes and Just (1983) are:

Maximum principal stress theory

$$\sigma_{xx} = \sigma_t^* \qquad (36.17)$$

where

σ_{xx} = maximum principal stress
σ_t^* = failure stress in a uniaxial tensile test

or $\sigma_{zz} = \sigma_c^*$

σ_{zz} = minimum principal stress
σ_c^* = failure stress in a uniaxial compressive test.

Figure 36.7 shows the principal stresses acting on an element of material.

Maximum principal strain theory

$$\epsilon_{xx} = \epsilon_t^* \qquad (36.18)$$

where

ϵ_{xx} = maximum principal tensile strain
ϵ_t^* = tensile strain at failure

in terms of stress

$$(\sigma_{xx} - v\sigma_{yy} - v\sigma_{zz})/E = \sigma_t^*/E$$

or

$$(\sigma_{xx} - v\sigma_{yy} - v\sigma_{zz}) = \sigma_t^*$$

v = Poisson's ratio.

Similarly

$$\epsilon_{zz} = \epsilon_c^*$$

ϵ_{zz} = minimum principal strain
ϵ_c^* = compression strain at failure

or $\sigma_{zz} - v(\sigma_{xx} + \sigma_{yy}) = \sigma_c^*$.

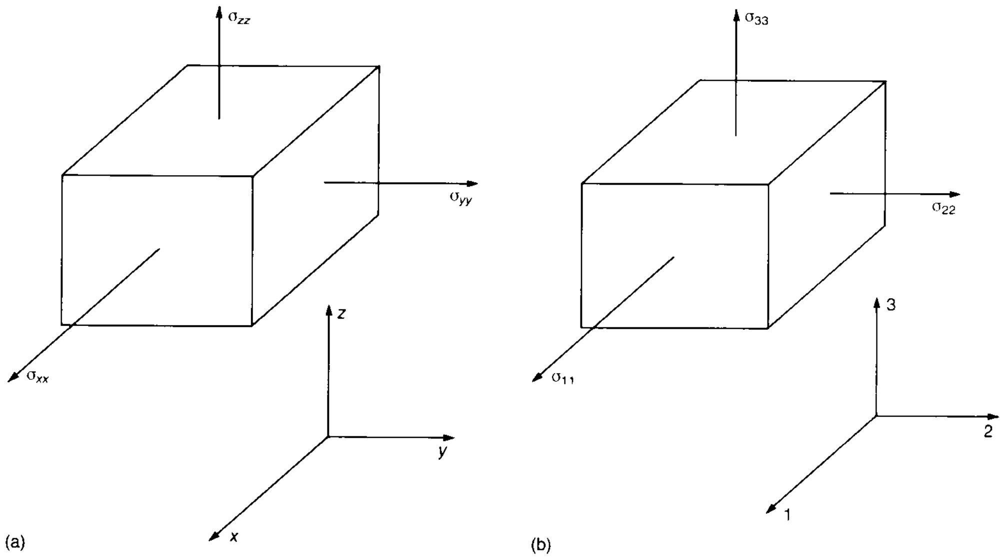

FIGURE 36.7 Isotropic and orthotropic materials under normal stress: (a) element under three principal stresses $\sigma_{xx} > \sigma_{yy} > \sigma_{zz}$; (b) orthotropic material under normal stress.

Both the above theories assume failure to be due to normal stresses and ignore any shear stress present. Consequently the theories are relevant to the failure of brittle materials under tension.

The total strain energy theory

The above theories express the failure criterion as either limiting stress or limiting strain; the total strain energy theory attempts to combine these two theories. The development of the theory, which is based upon strain energy principles, has been discussed in Hollaway (1989) and only the final solution will be given here.

The lamina theory gives the solution as:

$$\sigma^{*2} = \sigma_{xx}^2 + \sigma_{yy}^2 - 2\sigma_{xx}\sigma_{yy}\nu. \qquad (36.19)$$

The theory applies particularly to brittle materials where the ultimate tensile stress is less than the ultimate shear stress.

Deviation strain energy theory

This theory is known as the von Mises criterion and in it the principal stresses σ_{xx}, σ_{yy} and σ_{zz} can be expressed as the sum of two components, namely the hydrostatic stresses σ_{xx}, σ_{yy} and σ_{zz} which causes only a change in volume and the deviation stress which causes distortion of the body. The system is shown in Figure 36.8.

The hydrostatic stress components produce equal strains in magnitude and are consistent in the three directions and therefore produce equal strain in these directions. The system, therefore, undergoes change in volume but not change in shape. The stress deviation system will cause the body to undergo changes in shape but not in volume.

Again the theory has been developed in Hollaway (1989) and will not be repeated here; the lamina theory gives the solution as:

$$\sigma_{xx}^2 + \sigma_{yy}^2 - \sigma_{xx}\sigma_{yy} = \sigma^{*2} \qquad (36.20)$$

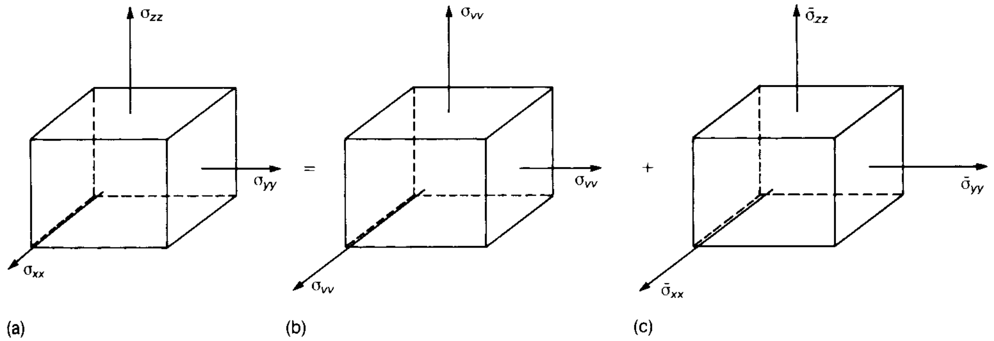

FIGURE 36.8 Volume and deviation stress system: (a) principal stress; (b) volume stress system; (c) stress deviation (or distortion) system.

The above failure criterion is most relevant to ductile materials. It is not obvious which of the above failure criteria is most relevant to composites as the fibre volume fraction and orientation of the fibres in the polymer will influence their strength and ductility properties. However, the last theory has been applied to quasi-isotropic composites with some success.

Strength theories of orthotropic laminae

The theories based upon the strength characteristics of orthotropic materials are considerably more complicated than those for the isotropic ones. As with these latter materials the strength hypothesis is based upon simple fundamental tests, but because orthotropic materials have different strengths in different directions a more intensive set of data is required than for isotropic materials. Three uniaxial tests are required, one in each of the principal axis directions to determine the three moduli of elasticity, Poisson's ratio and the strength characteristics; tests in these directions will eliminate any coupling effects of shearing and normal strains which would occur if the laminate were tested in any other direction. The shearing strengths with respect to the principal directions must be determined from independent experiments.

Figure 36.9 shows schematically the critical stress values in the principal material axes. For orthotropic materials the stress condition at a point is resolved into its normal and shearing components relative to the principal material axis at the point. Consequently the failure criteria in these materials become functions of the basic normal and shearing strengths described for isotropic materials.

Maximum stress theory

The maximum stress theory of failure assumes that failure occurs when the stresses in the principal material axes reach a critical value. The three possible modes of failure are:

$\sigma_{11} = \sigma_{11}^*$ the ultimate tensile or compressive stress in direction 1.
$\sigma_{22} = \sigma_{22}^*$ the ultimate tensile or compressive stress in direction 2. (36.21)
$\sigma_{12} = \sigma_{12}^*$ the ultimate shear stress acting in plane 1 in direction 2.

If the load were applied to the lamina at an angle θ to the principal axis direction shown in Figure 36.6 then by transformation

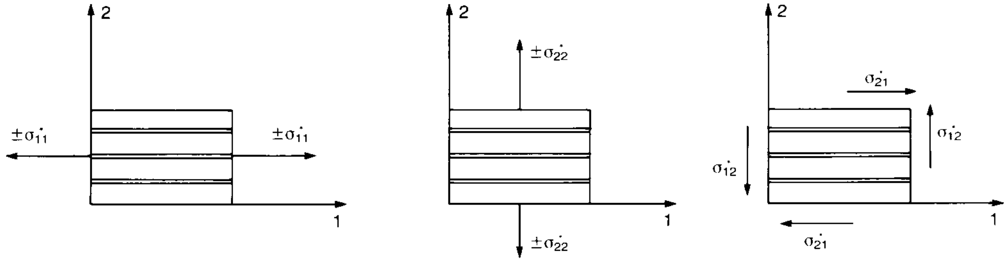

FIGURE 36.9 Critical stress values in the principal material axes.

$$\begin{aligned}\sigma_{11} &= \sigma_{xx}\cos^2\theta = \sigma_\theta\cos^2\theta\\ \sigma_{22} &= \sigma_{xx}\sin^2\theta = \sigma_\theta\sin^2\theta\\ \sigma_{12} &= -\sigma_{xx}\sin\theta\cos\theta = -\sigma_\theta\sin\theta\cos\theta\end{aligned} \tag{36.22}$$

The failure strength produced by the maximum stress theory would depend upon the relative values of s_{11}, s_{22} and s_{12} and would therefore be the smallest value of the following:

$$\begin{aligned}\sigma_\theta &= \sigma^*_{11}/\cos^2\theta\\ \sigma_\theta &= \sigma^*_{22}/\sin^2\theta\\ \sigma_\theta &= \sigma^*_{12}/\sin\theta\cos\theta\end{aligned} \tag{36.23}$$

Maximum strain theory

The maximum strain theory of failure assumes that failure occurs when the strains in the principal material axes reach a critical value. Here again there are three possible modes of failure:

$$\begin{aligned}\epsilon_{11} &= \epsilon^*_{11}\\ \epsilon_{22} &= \epsilon^*_{22}\\ \epsilon_{12} &= \epsilon^*_{12}\end{aligned} \tag{36.24}$$

Where ϵ^*_{11} is the maximum tensile or compressive strain in direction 1, ϵ^*_{22} is the maximum tensile or compressive strain in direction 2 and ϵ^*_{12} is the maximum shear strain on plane 1 in direction 2.

Tsai-Hill energy theory

The Tsai-Hill criterion is based upon the von Mises failure criterion which was originally applied to homogeneous isotropic bodies. It was then modified by Hill to suit anisotropic bodies, and finally applied to composite materials by Tsai.

Hollaway (1989) has discussed the derivation of the equation which describes the failure envelope and this may be expressed as:

$$\frac{\sigma^2_{11}}{\sigma^{*2}_{11}} - \frac{\sigma_{11}\sigma_{22}}{\sigma^{*2}_{11}} + \frac{\sigma^2_{22}}{\sigma^{*2}_{22}} + \frac{\sigma^2_{12}}{\sigma^{*2}_{12}} = 1. \tag{36.25}$$

For most composite materials $\sigma^*_{11} \gg \sigma_{22}$; consequently, the second term of equation (36.25) is negligible and this equation becomes:

$$\frac{\sigma^2_{11}}{\sigma^{*2}_{11}} + \frac{\sigma^2_{22}}{\sigma^{*2}_{22}} + \frac{\sigma^2_{12}}{\sigma^{*2}_{12}} = 1. \tag{36.26}$$

Equations (36.25) and (36.26) only apply to orthotropic laminae under in-plane stress conditions.

To enable a prediction to be made of the failure strength in direction θ to the principal axes (Figure 36.6) on unidirectional laminae, equations (36.25) and (36.23) can be combined to give:

$$\sigma_{xx} = \sigma_\theta = \left[\frac{\cos^4\theta}{\sigma^{*2}_{11}} + \left(\frac{1}{\sigma^{*2}_{12}} - \frac{1}{\sigma^{*2}_{11}}\right)\sin^2\theta\cos^2\theta + \frac{\sin^4\theta}{\sigma^{*2}_{22}}\right]^{-1/2} \tag{36.27}$$

Hull (1992) has stated that when equation (36.27) has been fitted to the results of experimental tests on carbon fibre-epoxy resin laminates the predicted values are much better than for the maximum stress theory, equation (36.21).

Finally, Figure 36.10 shows a laminate made from three lamina. Providing lamina 1 and 3 have the same thickness, the laminate would be described as symmetric; lamina 2 could have any value of thickness. If, however, the thickness of lamina 1 and 3 were different, the laminate would be described as non-symmetric. Under a thermal and mechanical load, coupling forces are introduced into a non-symmetric laminate because of the different mechanical properties of the individual lamina. For this reason it is common practice in many applications to use symmetric laminates which are not subjected to this type of coupling.

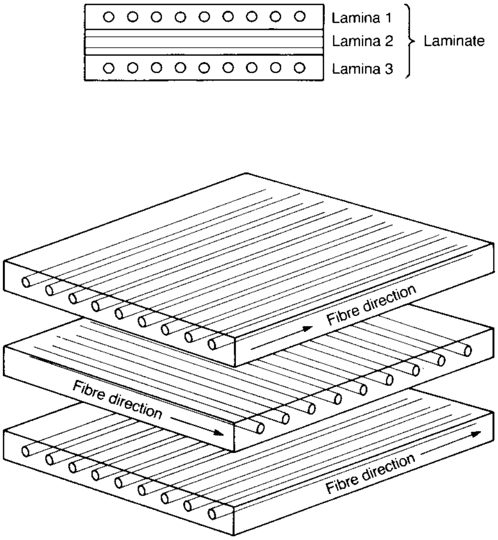

FIGURE 36.10 Laminate arrangements.

36.10 References

Hollaway, L. (1989) Design of composites. In *Design with Advanced Composite Materials* (ed. L. Phillips), The Design Council, London.

Holmes, M. and Just, D.J. (1983) *GRP in Structural Engineering,* Applied Science Publishers, London and New York.

Hull, D. (1992) *An Introduction to Composite Materials,* Cambridge University Press, Cambridge.

Krenchel, H. (1964) *Fibre Reinforcement,* Akademisk Forlag, Copenhagen.

Chapter thirty-seven

Manufacturing techniques for polymer composites

The two parts of this chapter concentrate upon the manufacturing techniques for fibre-reinforced thermosetting and thermoplastic polymer composites respectively.

37.1 Manufacture of fibre-reinforced thermosetting composites

Fibre-reinforced thermosets are manufactured in three ways and examples of each are given here:

1. manually – hand lay-up, spray-up, pressure bag and autoclave moulding;
2. semi-automatically – cold pressing, compression moulding and resin injection;
3. automatically – pultrusion, filament winding and injection moulding.

Processes which use only one mould are known as open-mould techniques; the surface of the product in contact with the mould is able to reproduce the surface of the mould completely. Processes in which the product is formed within a closed space by two moulds are known as closed-mould techniques. Figure 37.1 shows a schematic diagram of the various fabrication processes.

37.1.1 Manual processes

Manual processes are all open-mould processes, involving contact moulding, resin transfer moulding and resin infusion processes.

The hand lay-up technique

This is the simplest and most common technique for producing fibre-reinforced polymer components (Figure 37.2 (a)). It is ideally suited to the

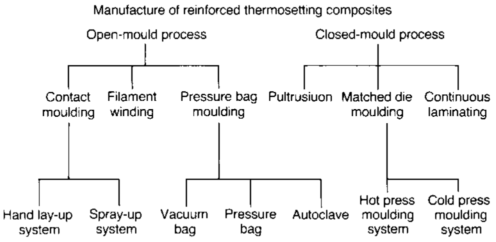

FIGURE 37.1 Schematic diagram of the fabrication processes for thermosetting polymer composites.

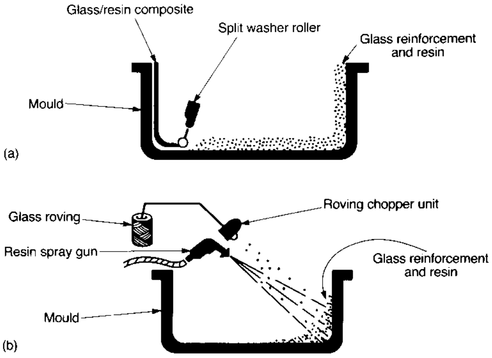

FIGURE 37.2 (a) Hand lay-up moulding method; (b) spray-up moulding technique.

production of a small number of similar components such as fibre-reinforced polymer infill panels which could be used in civil engineering. Most materials are suitable for mould making, but the most common are glass fibre reinforced polymers (GFRP). A master pattern is prepared from which GFRP moulds may be made. A release agent is used to prevent bonding to the moulds during manufacture. It is necessary to protect fibres from exposure to the atmosphere to prevent fracture and this protection is achieved by applying a resin-rich area, known as a gel coat, on the exposed surface of the composite.

The function of the gel coat is:

1. to protect fibres from external influences, especially moisture penetration to the interface of the fibre and matrix with consequent breakdown of the interface bond;
2. to provide a smooth finish and to reproduce precisely the surface texture of the mould.

The thickness of the gel coat is generally about 0.35 mm. Sometimes a surface tissue mat is used to reinforce the gel coat.

After the gel coat has become tacky but firm, a liberal coat of resin is brushed over it and the first layer of glass reinforcement is placed in position and consolidated with brush and roller. The glass fibre may be in the form of chopped strand mat or woven fabric, precut to the correct size. Layers of resin and reinforcement are then applied until the required thickness of composite is reached.

Spray-up technique

The spray-up technique, shown in Figure 37.2 (b), is less labour intensive than the hand lay-up method. It involves the simultaneous deposition of chopped glass fibre roving and polymer onto the mould with a spray gun. The roving is fed through a chopping unit and projected into the resin stream. The glass resin mixture is then rolled by a split washer roller to remove any air.

The technique requires considerable operator skill to control the thickness of the composite and to maintain a consistent glass/polymer ratio. After the initial polymerisation of the composite, and when it has been demoulded, the unit must be cured usually by heating for eight hours at 60°C.

As the tooling costs for the above two processes are low, the designer has considerable versatility from the point of view of shape and form.

Pressure bag techniques

Pressure is exerted on the open face of the moulding to enable:

1. a greater compaction of the composite (the voids are reduced to zero);
2. a higher fibre volume ratio;
3. a higher quality of surface finish on this face.

These techniques are ideal for the manufacture of low-cost open-mould products such as structural panels without sophisticated mechanisation.

Vacuum bag

A contact moulding is produced by the hand lay-up method, but before curing commences a rubber membrane is placed over the composite component and all joints between the membrane and mould are sealed and a vacuum is applied between the bag and composite (Figure 37.3 (a)). The pressure of about one atmosphere applied to the surface of the moulding forces out air and excess polymer; glass/polymer weight ratios of up to 55 per cent are possible. A protective sheet of cellophane is used between the rubber and composite.

Pressure bag

This technique is similar to the vacuum bag except that a pressure is applied to the open surface (Figure 37.3(b)). The contact moulding is produced and before curing commences a rubber bag with the cellophane sheet is sealed to the mould with a plate and pressurised up to about three atmospheres. Because of the higher pressure compared with that for the vacuum bag, a greater fibre/matrix weight ratio is obtained. This value can be increased to about 65 per cent. Superior composites can be manufactured by this technique but more equipment is required than for the vacuum bag, with a consequent increase in cost.

Autoclave

The autoclave is a modification of the pressure bag method; pressures of up to 6 atmospheres are developed within the autoclave and the system produces a high-quality composite with a fibre/matrix weight ratio of up to 70 per cent. The cost of production also increases.

In addition to manufacturing structures, made completely from polymer composites, by the hand lay-up or spray-up techniques, commercially available procedures to retrofit composite materials to existing structures, to improve their tensile and shear strengths, do exist.

Hand lay-up process for retrofitting

A commercially available method of retrofitting is the REPLARK process (REPLARK is a trade name used by Sumotomo Corporation, Europe Plc) which is utilised, in industry, to strengthen structures in flexure and shear by retrofitting the material to their tensile and shear faces. (In these cases the surface of the structure forms the mould for the composite; the technique is more fully described in Chapter 39.) The fabrication technique to form this material is basically a hand lay-up method in which the mould is usually the structural unit onto which is retrofitted the polymer composite. In addition, planar and non-planar composites can be manufactured independently and used as structural units.

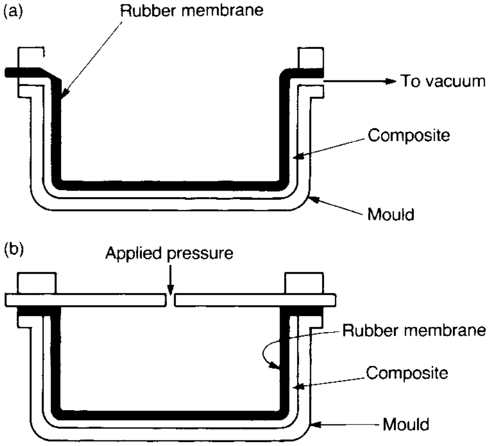

FIGURE 37.3 Pressure bag techniques.

A second method for retrofitting procedures is known as the Dupont method which uses Kevlar fibres; it is marketed as a repair system for concrete structures.

37.1.2 Semi-automated process for retrofitting

These methods are used for the manufacture of the composite material and to retrofit them, in situ, onto concrete, steel and cast-iron structures. The semi-automated resin infusion under flexible tooling (RIFT) process has been developed by DML, Devonport, Plymouth, to allow quality composites to be formed. In this process dry fibres are preformed in a mould in the fabrication shop and the required materials are attached to the preform before packaging. The preform is taken to site and is attached to the structure; a resin supply is then channelled to the prepreg. The prepreg and resin supply is then enveloped in a vacuum bagging system. As the resin flows into the dry fibre preform it develops both the composite material and the adhesive bond between the CFRP and the structure. The process provides high fibre volume fraction composites of the order of 55 per cent; these have high strength and stiffness values.

XXsys Technologies, Inc., San Diego, California has developed a wrapping system for seismic retrofitting to columns. The technology associated with the technique is based upon the filament winding of prepreg carbon fibre toes around the structural unit thus forming a carbon fibre jacket; currently, the structural unit to be upgraded would be a column. The polymer is then cured by a controlled temperature oven and can, if desired, be coated to match the existing structure.

37.1.3 Automated processes

Filament winding

Filament winding is a highly mechanised and sophisticated technique for the manufacture of pressure vessels, pipes and rocket casings when exceptionally high strengths are required. It is an open mould-process in which continuous reinforcement, usually rovings, is fed through a traversing bath of activated resin and is then wound onto a rotating mandrel. If resin preimpregnated reinforcement is used, it is passed over a hot roller until tacky and is then wound onto the rotating mandrel. Figure 37.4 illustrates the process and it is evident that the angle of the helix is determined by the relative speeds of the traversing bath and the mandrel. After completion of the initial polymerisation, the composite is removed from the mandrel and cured; the composite unit is then placed into an enclosure at 60°C for eight hours.

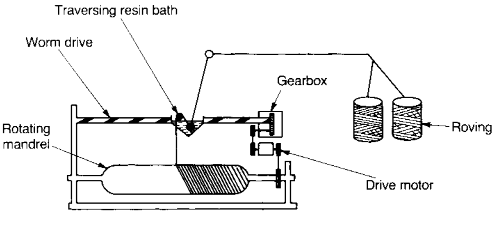

FIGURE 37.4 Filament winding technique.

In the construction industry, filament winding has been used to form high-pressure pipes and pressure vessels. Sewerage pipes have also been manufactured in this way.

The rest of the automated processes that are described below are closed-mould processes, in which the product is formed within a closed-mould system, utilising pressure and sometimes heat rapidly to produce high-quality units. Because of the high capital equipment outlay, particularly for the manufacture of the metal moulds, it is essential that large production runs are performed. Because of the mechanisation of the system only a small, skilled workforce is required. There are two types of process – matched die and pultrusion and modified pull-winding.

Matched die

In *cold press moulding*, pressure is applied to two unheated matched metal moulds to disperse resin throughout a prepared fibre fabric stack placed in the mould; a release agent and a gel coat would be applied to the mould surface before the fibre stack is placed in position. The activated polymer is poured onto the top of the mat and the mould is then closed; the polymer spreads throughout the fabric under the mould pressure. Pressures applied may be as low as 100 kPa and the heat generated during the exothermic polymerisation process warms the tools; this helps in the curing process but additional curing after demoulding is essential.

In *hot press moulding*, glass fibre reinforcement and a controlled quantity of hot curing catalysed resin are confined between heated, matched, polished metal dies brought together under pressure (Figure 37.5). The pressures vary depending upon the process but will normally be between 0.5 and 15 MPa and the mould temperatures will be between 120°C and 150°C. The heat ensures rapid curing and so no subsequent curing is required. Both preform moulding and premix moulding of the fibre and the polymer can be used in this process.

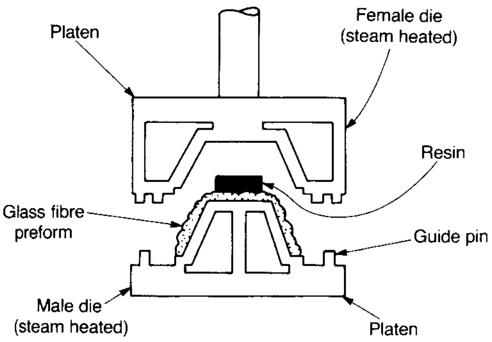

FIGURE 37.5 Hot press moulding technique.

In *preform moulding* chopped rovings are projected onto a rotating fine metal mesh screen shaped to the required dimensions; the fibres are held on the screen by suction. The strands are bonded together by spraying the preform with a resinous binder in the form of a powder or an emulsion and the whole is transferred to an oven at 150°C for two to three minutes, after which time the preform is ready for the press.

Sheet moulding compound (or prepreg) is a polyester-resin-based moulding material which consists of a mixture of chopped strand mat or chopped fibre resin, fillers, catalyst and pigment. It is produced and supplied in the form of a continuous sheet wound into a roll and protected on both sides by sheets of polythene film which are removed before loading into the press. An advantage of this method is that no liquid resin is involved and the prepreg sheets can be prepared to the design size by cutting.

Dough moulding compound (or bulk moulding compound) contains a mixture of chopped strands (20 per cent by weight) with resin, catalyst and pigment. As the compound flows readily it may be formed into shape by compression transfer or injection and the pressure required to produce a component is relatively low so that large mouldings can readily be produced. Curing takes about 2 minutes for moulding temperatures in the region of 120–160°C although this will depend upon the section thickness.

Resin injection

Resin injection is a cold mould process using low pressures of about 450 kPa. The surfaces of the mould are prepared with release agents and gel coat before the glass fibre reinforcement is placed in position in the bottom mould and allowed to extend beyond the sides of the moulds. The upper mould is clamped in position to stops and the activated resin is injected under pressure into the mould cavity. Figure 37.6 shows the arrangement. It is possible to obtain a fibre/matrix ratio by weight of 65 per cent.

Pultrusion and modified pull-winding

The pultrusion technique consists of impregnating continuous strands of a reinforcing material with a polymer and drawing them through a die as shown in Figure 37.7. Thermosetting polymers are used in this process although research is being undertaken currently to pultrude thermoplastic materials. Curing of the composite component is undertaken when the die is heated to about 135°C. A glass content of between 60 and 80 per cent by weight can be achieved. Composites manufactured by this method tend to be reinforced mainly in the longitudinal direction with only a relatively small percentage of fibres in the transverse direction. A technique has been developed (Shaw-Stewart, 1988) to 'wind' fibres in the transverse direction simultaneously with the pultrusion operation. The process is known as pull-winding and gives the designer greater flexi-

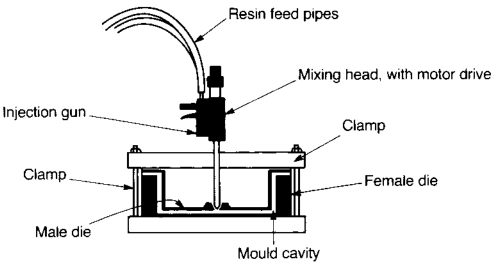

FIGURE 37.6 The resin injection process.

bility in the production of composites, particularly those of circular cross-section.

The pultrusion technique is the process used extensively in the reinforced plastics industry and is becoming an important technique in civil engineering to form structural units. The finished pultrusion sections are generally straight and dies can be manufactured to give most geometrical shapes; the most common of these are I, L, Tee, and circular sections

37.2 Manufacture of fibre-reinforced thermoplastic composites

Reinforced thermoplastic composites can be manufactured by most of the thermoplastic processing techniques such as extrusion, blow moulding and thermoforming of short-fibre reinforced thermoplastics. However, the most important technique for industrial use is injection moulding. It is a similar technique to the manufacture of unreinforced thermoplastics but the melt viscosity is higher in the reinforced polymer process and consequently the injection pressures are higher. With all the techniques, production difficulties can occur because the reinforced composite is stiffer than the unreinforced one. The cycle time is less but the increased stiffness can affect the ejection from the mould so the mould design has to be modified from that of the unreinforced polymer mould.

One of the problems of thermoplastic composites is that they use short fibres (typically 0.2–0.4 mm long) and consequently their full strength is not developed. Continuous fibre tapes and mats in the form of prepregs can help to overcome this. The best known examples of these systems are the aromatic polymer composites (APC) and the glass-mat-reinforced thermoplastic composites (GMT). The systems use unidirectional carbon fibre in a matrix of polyethersulphone (PES) or polyetheretherketone (PEEK). The material for the APC comes in prepreg form of unidirectional or 0°/90° fibre and for GMT in a tape prepreg form. The composite is manufactured by the film stacking process with the prepregs arranged in the desired directions.

37.2.1 The film stacking process

This is a relatively new method in which the prepreg is made from cloth reinforcement and has a polyethersulphone polymer content of about 15 per cent by weight. The final volume fractions of fibre and resin are obtained by adding matrix in the form of film. The film stacking process, therefore, consists of alternating layers of fibre impregnated with insufficient matrix, with polymer films of complementary mass to bring the overall laminate to the correct fibre volume ratios. The required stacked sequence is placed into one part of a split mould; the two half moulds are brought together and heat and pressure are applied.

This technique is used mainly for high technology composites in the aerospace and space industries.

37.3 References

Hollaway, L.C. and Head, P.R. (2001) *Advanced Polymer Composites and Polymers in the Civil Infrastructure*, Elsevier Science, Oxford.

Shaw-Stewart, D. (1988) Pullwinding. *Proceedings of the Second International Conference on Automobile Composites* 88, Noordwijkerhout, The Netherlands.

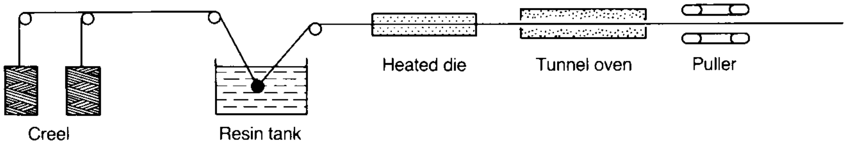

FIGURE 37.7 The pultrusion technique.

Chapter thirty-eight

Durability and design of polymer composites

Polymer composites change with time and the most significant influencing factors are:

1. elevated temperatures;
2. fire;
3. moisture, particularly when immersed for long periods;
4. adverse chemical environments;
5. natural weathering particularly when exposed to the sun's ultra-violet radiation.

38.1 Temperature

As we have seen in the preceding chapter, temperature plays an important part in the manufacture of GFRP composites which are normally cured (and post-cured) with heat to a state of chemical and physical stability. A certain amount of shrinkage takes place during the curing process, due to the polymer chains being drawn together. On occasions post-curing of composites at elevated temperatures presents practical difficulties for large structural composites and a gradual change in physical and dimensional properties may be expected for a period if a laminate is imperfectly cured. However, this effect is not normally significant unless there is excessive undercure. This situation could occur if, for instance, immediately after manufacture the units were placed in the fabricator's yard because there was no room in the fabrication shop. In this situation only partial curing would have occurred before the unit was exposed to environmental conditions.

Constantly fluctuating temperatures have a greater deleterious effect on GFRP. At a micro scale, the difference in the coefficients of thermal expansion of the glass and the resin may contribute to progressive debonding and weakening of the materials, although the extensibility of the resin system will usually accommodate differential movement.

When GFRP composites are exposed to high temperatures a discoloration of the resin may occur; this is noticed by the composite becoming yellow. Both polyester and epoxy show this effect and the problem will be aggravated if flame retardants are added to the resin during manufacture of the composite. In addition, as a result of the exposure to high temperatures, the composite will become brittle.

38.2 Fire

A composite material must meet the appropriate standards of fire performance. It is usually possible to select a resin system which will achieve the standard laid down in British Standard Specification BS 476. The Building Regulations require that, depending upon their use, building components or structures should conform to given standards of fire safety. The fire tests by which these are measured fall into two categories:

1. reaction to fire – tests on materials;
2. fire resistance – tests on structures.

The tests under these two headings are laid down in BS 476: Parts 4–7, and in BS 476: Parts 3–8 respectively.

Resins will probably contain fillers and colourants which may affect fire properties. Some mineral fillers, such as specially treated calcium carbonate, can improve the mechanical properties of composites made from polyester and epoxies. No more than 25 per cent of the filler should be used, although as an exposed aggregate in a decorative surface a greater proportion of the coarse particles may be used. To enable flame-retardant properties of the plastic to be improved, aluminium trihydrate and antimony trioxide may be used as fillers for both lamination and gel-coated resins, but the use of flame retardants can affect the colour retention of the polymer; the pigment would have been added to produce a particular colour in a structural component. Het-acid-based resins can be used where flame-retardant characteristics are required.

38.3 Moisture

Polymers which are cross-linked are not easily hydrolysed but they are sufficiently hydrophilic for water to be absorbed. The effect of this uptake of water is to reduce the modulus of elasticity and strength. Wet strength can be 25 per cent lower than that of the dry specimen. The wet strength values are sometimes used in design to reflect the possible effects of water and weather. The long-term effects on these two properties seem to be greater for epoxy resins than for polyesters. The absorption of water by both the polyesters and epoxies leads to swelling of the laminate with an increase in thickness; the wet laminates can also warp if the structure is unbalanced.

Water can have a deleterious effect on glass fibre. The high strength of fibres is largely due to surface imperfections but a small amount of solution on the surface of the fibres can produce surface flaws which will reduce the overall strength of the laminate. The alkali-resistant glass fibre has a better resistance to water than the E-glass fibre which is generally used for the manufacture of GFRP.

On a short-term basis water absorption is a surface effect and, if the composite has a gel coat (see later in the section), this effect is of little consequence. On a long-term basis, however, immersion of the composite in water will allow penetration through the thickness of the coating and water-filled voids will occur at the fibre/polymer interface and may weaken the bond. High-quality materials and good control of the composite fabricating process can reduce the above effects to a minimum. The glass fibres, as mentioned earlier, are treated with a size to protect them after manufacture and when the in-service requirements demand it, a water-resistant size should be used to minimise blistering.

The ends of fibres will be exposed if GFRP is cut during shaping of the component, and the fibres may suffer from a wicking action, but experience shows that only a narrow strip at the cut edge will be affected by water penetration. If, however, the composite fibre volume fraction is high the effect of water may be significant and should be investigated.

Work by the Building Research Establishment (1963) showed that wetting and drying of GFRP composites, from natural exposure to environmental conditions, is much less severe than continuous exposure to water in producing changes at the glass/resin interface.

38.4 Solution and solvent action

A fully cured polyester resin exhibits good resistance to acidic and alkaline attack if selected and designed properly; resin manufacturers should be consulted when choosing a resin to be utilised for a specific corrosive environment.

38.5 Weather

Natural weathering does cause some deterioration of GFRP composites; sunlight degrades both polyester and epoxy resins. The first sign of degradation is a discoloration of the material which develops into a breakdown of the surface of the composite. In addition there is a loss of light transmission in translucent sheeting. The ultraviolet component of sunlight is largely responsible for this degradation; the short wavelength band at 330 nm has most effect on polyesters but longer wavelengths are also significant. To reduce this weathering problem with polyester resin, ultraviolet absorbers and stabilisers are added to the resin formulations during fabrication of the composite. There is, however, little improvement in the stability of epoxy resins when ultraviolet stabilisers are added.

When pigments are placed in polyester resin infra-red and visible radiation can accelerate the rate of degradation of the polymer by raising its temperature; a rise of 10°C approximately doubles chemical reaction and hence degradation. Consequently, resin degradation proceeds more rapidly in hot than in more temperate climates. The rate of degradation of epoxy resins is similar to that of polyesters.

Weathering can affect the mechanical properties of GFRP composites; surface debonding of fibres as a result of degradation of the resin will reduce the load-bearing capacity. The deterioration could be caused by solar effects or by water on the surface of the composite. Because weathering is largely a surface effect, the thickness of the composite has a significant influence upon the mechanical properties. It has been shown (Scholz, 1978) that a 3 mm thick GFRP laminate has a reduction in flexural strength of between 12 per cent and 20 per cent after 15 years' exposure to natural weathering, whereas it has been estimated that for a 10 mm laminate a reduction of no more than 3 per cent would take place after 50 years' exposure.

The above discussion has assumed a general purpose resin without any surface protection. If a polyester resin has been specifically designed by the manufacturer to resist weathering, degradation would not be so severe.

The three principal types of polyester used as a laminating resin are orthophthalic, isophthalic and het acid resins. The orthophthalic type is a general-purpose resin, the isophthalic one has superior weathering and chemical resistance properties and the het acid resin is used for flame-retardant purposes. Fillers and pigments may be used in resins, the former principally to improve mechanical properties and the latter for appearance and protective action. Fillers such as aluminium trihydrate may be used to improve flame-retardant characteristics, but it is important that the correct amount of the fillers should be incorporated; if too high a proportion is employed, adverse effects on weathering properties may result. This is only applicable for composites exposed to the weather and internal applications; where water or chemicals are not in contact with the polymer, the composites are not affected. Ultraviolet stabilisers can be incorporated into the resin at the time of fabrication and a gel coat surface coating can be applied to the composite for increased weather protection.

It is clear that the durability of a GFRP laminate depends upon the quality of the exposed surface and a good in-service performance is most commonly achieved by the use of a surface coat or gel coat of pigmented resin. This protects the glass fibre reinforcement from the action of moisture and the laminating resin from harmful radiation and from moisture. The polymer that is used for this purpose has been formulated to provide good weathering and chemical resistance properties. The gel coat is generally applied in a uniform thickness of 0.5 mm to the mould surface and can be pigmented to give the required colour. A surface tissue of glass fibre is often incorporated into the gel coat to reinforce it and to enhance its appearance, whilst maintaining the resin-rich surface.

It is important that, for the satisfactory design of composites, the resin system, the reinforcement and the structure of the laminate should be assessed properly. This may involve an evaluation programme to assess the design and manufacture of the system to ensure that the product gives and maintains satisfactory performance throughout its service life. As an aid, the British Plastics Federation has produced guidance notes on the construction of glass-reinforced plastics cladding panels, dealing mainly with the in-service requirements.

38.6 Design with composites

Designing with composites is an interactive process between the designer and the production engineer responsible for the manufacturing technique. It is essential that a design methodology is selected and rigorously used, because many different materials are on the market and they can be affected by quality, the environment and the manufacturing process. It is also important that the designer recognises the product cost, because the constituents of composite materials (the fibre and the matrix) can vary significantly in price and the manufacturing process can range from simple compact moulded units cured at room temperature to sophisticated high-temperature and pressure-cured composites.

The design process can be divided into five main phases:

1. the design brief and an estimation of cost;
2. the structural, mechanical and in-service details;
3. the manufacturing processes and cost details;
4. the material testing and specification information;
5. the quality control and structural testing information.

The selection of design factors of safety is an important aspect of the work; these factors are likely to be covered in the relevant code of practice. However, if the design is unique, it may be necessary for the designer/analyst to select them, bearing in mind the exactness of the calculations, the manufacturing processes, the in-service environment, the life of the product and the loading. The selection follows the pattern for other materials but, with the variation in properties, due to the anisotropic nature and the different manufacturing techniques of the composites, a more involved calculation and a greater reliance upon the design factors will result.

Polymer composite structures can be manufactured from thin plate and shell laminated plies to form continuum systems or from pultruded or filament wound tubes to form skeletal structures. The properties of these thin laminated plate or tube elements may be calculated in terms of laminate structures and ply thicknesses and properties by using laminate theory or by commercially available microcomputer programs such as Engineering Science Data Unit (1987a, b) and Think Composites Software (1987).

38.7 References

BS 476: British Standards Institution, London.

Building Research Establishment (1963) Internal records, Building Research Establishment, Garston, UK.

Engineering Science Data Unit (1987a) *Stiffnesses and Properties of Laminated Plates,* ESDU 20–22, ESDU International, London.

Engineering Science Data Unit (1987b) *Failure of Composite Laminates,* ESDU 20–33, ESDU International, London.

Hollaway, L. (1993) *Polymer Composites for Civil and Structural Engineering*, Blackie Academic and Professional, London.

Hollaway, L.C. and Head, P.R. (2001) *Advanced Polymer Composites and Polymers in the Civil Infrastructure*, Elsevier Science, Oxford.

Kim, D.-H. (1995) *Composite Structures for Civil and Architectural Engineering*, E & FN Spon, London.

Scholz, D. (1978) *Kunststoffe,* 68, 556.

Think Composites Software (1987) MIC-MAC, Think Composites Software, Dayton.

Chapter thirty-nine

Uses of polymer composites

The use of polymers and polymer composites for 'all composite' construction in the civil engineering industry falls into three categories. These are:

1. non-load-bearing;
2. semi-load-bearing;
3. load-bearing.

As we have seen in Chapter 34, unreinforced polymers are used in non-load-bearing and semi-load-bearing applications, whilst fibre-reinforced polymers are used in load-bearing applications. Thermoplastic materials can be drawn into fibres which are then used in geotextiles.

Polymers and fibre-reinforced polymers offer many advantages over other materials, but the most appropriate resin must be selected for the particular end use since every material does not possess all the following characteristics:

1. high light transmission for glazing and lighting fixtures;
2. infinite texture possibilities;
3. minimum maintenance requirements;
4. infinite design possibilities;
5. resistance to water and corrosion;
6. high specific strength;
7. high impact resistance.

The disadvantages that have impeded the utilisation of polymers in construction are:

1. The cost of the materials is relatively high, although when their low density is considered and the structure as a whole has been designed as a composite system (e.g. the reduced foundation size compared with what would be required for conventional material), then polymers are competitive.
2. The stiffness and strength of the polymer or the composite is less than that of competitor materials and therefore they must be used in conjunction with the latter.
3. The scratch resistance is poor.
4. Ultraviolet light can attack the material unless stabilisers are incorporated into the resin formulations.
5. Organic materials will burn, but fire-retardant additives can be used with the polymers to retard or eliminate burning.

In this chapter we will discuss some typical examples of successful structural applications of polymer composites; some other applications outside construction are first briefly discussed because they are particularly noteworthy in demonstrating how such composites have offered unique solutions to a range of product demands.

39.1 Marine applications

Polymer composites are now the dominant materials for pleasure craft. These materials have been particularly effective in replacing wood because of the following factors:

1. Design: the moulds to obtain the hydrodynamic and aesthetic forms of the craft can be readily manufactured.
2. Manufacture: the operations of cutting, fitting, assembly and finishing are reduced or eliminated in composite constructions compared with those required for a wood construction.
3. Structure: continuous stiff and strong shell forms can be produced in a composite construction.

The Sandown Class Single Role Minehunter has been built for the Royal Navy by Vosper Thorneycroft and features an advanced glass-reinforced plastic hull structure.

39.2 Applications in truck and automobile systems

Polymer composites are used in the manufacture of certain sports car bodies and truck cabs. Strength, stiffness, toughness, corrosion resistance and the high-quality finishes are the physical and mechanical properties that must be satisfied, but economics is the crucial consideration governing the choice of composites over conventional materials.

39.3 Aircraft, space and civil applications

The high technology composites are increasingly being used for components in the aircraft industry. The fin of the European Airbus is a component made from a sandwich construction with carbon fibre/epoxy resin face material. The Westland helicopter rotor blades are made from carbon fibre composite material. In space, the solid-fuel rocket-motor cases house the propellant for many missiles. These cases are fabricated in the form of a cylinder, having dome ends made by the filament winding process.

39.4 Pipes and tanks for chemicals

The chemical industry uses polymer composite pipes and tanks for storage. Whilst the critical consideration is the corrosive resistance under extreme environmental conditions, the ease of fabrication of complex tank shapes and the simplicity of connections makes the composite material cost-effective.

39.5 Development of uses in civil engineering structures

Two sophisticated GFRP structures have played a major role in the development of polymer composite materials for construction; these are the dome structure erected in 1968 in Benghazi, Libya, and the roof structure at Dubai Airport, built in 1972. The composite units for the latter were designed and manufactured in the United Kingdom and shipped to Dubai.

During the 1970s and early 1980s, prestigious buildings were erected in this country, notably Morpeth School, Mondial House (the GPO Headquarters in London), Covent Garden Flower Market and the American Express Building in Brighton. Figure 39.1 shows a photograph of Mondial House situated on the bank of the Thames. Because of the relatively low modulus of elasticity of the material, these buildings were erected as a composite system, with either steel or reinforced concrete units as the main structural elements and the GFRP composite as the load-bearing infill panels.

In the mid 1970s, Lancashire County Council manufactured a classroom system, using only GFRP, by folding flat plates into a folded plate system so that the structural shape provided the stiffness to the building. In the late 1980s, more ambitious structural elements were produced. Two examples are the Manchester City Football Club grandstand, in which the construction is a barrel vault system using glass-reinforced polyester composite, and the dome at Sharjah Airport,

FIGURE 39.1 Mondial House International telephone exchange on the River Thames.

where the dome is manufactured in the form of curved panels which in the erected position drain to composite channels concealed under the panels.

Hollaway (1993) has given further examples of the use of polymers and polymer composites in construction.

39.6 Composite bridges

The development of bridges constructed entirely out of polymer/fibre composites commenced with the prototype footbridges in Europe and North America in the late 1970s. The first GFRP highway bridge is believed to be the 10 metres span bridge constructed in Bulgaria in 1982/1983 using the hand lay-up technique. The bridge was built rather like Ironbridge 200 years earlier, to show what could be achieved with the material. The second all GFRP bridge to be built is the Miyun Bridge in Beijing, China.

There have been some polymer composite bridges built in this country just recently; the best known one is the Aberfeldy cable stayed footbridge over the river Tay in Scotland. The deck of the bridge was manufactured using a modular system known as the Advanced Composite Construction System (ACCS) manufactured by the pultrusion technique (described in Chapter 37). The ACCS module consists of a number of interlocking fibre-reinforced polymer composite units which can be assembled into a large range of high performance structures for use in construction. The tower of the bridge, which has a main span of 63 metres and an overall length of 113 metres, was also fabricated from the ACCS plank. The cable stays are made from aramid fibres. Figure 39.2(a) shows a section of the Maunsell plank from which the deck was constructed; the whole system was designed by Maunsell Structural Plastics. Figure 39.2(b) shows a cross-section of ten ACCS planks fabricated into a box beam from which the single bascule lift bridge at Bonds Mill in Gloucester was manufactured and is shown in Figure 39.3. There have been other all-composite bridges built in Europe and North America during the latter part of the 1990s.

39.7 Retrofitting bonded composite plates to concrete beams

In recent years various research groups throughout the world have focused, not only upon the utilisation of polymer composites as civil engineering structural units or complete composite structures, but also upon retrofitting the material to concrete and steel structures to improve their strength. The rehabilitation topics considered have included the confinement of concrete columns with composite sheets or plates bonded to them, the use of polymer composite plates for the flexural and shear strengthening of beams and slabs, wrapping of reinforced concrete structural elements for corrosion protection and the durability of concrete repairs. Figure 39.4 shows the retrofitting of a pultruded plate to a concrete bridge to upgrade it to take greater load capacity.

39.7.1 Flexural and shear upgrading

Reinforced concrete structures may for a variety of reasons (e.g. marginal design/design errors caused by inadequate factors of safety, use of inferior materials, etc.) be found to be unsatisfactory. In service, increased safety requirements, a change in use or modification causing redistribu-

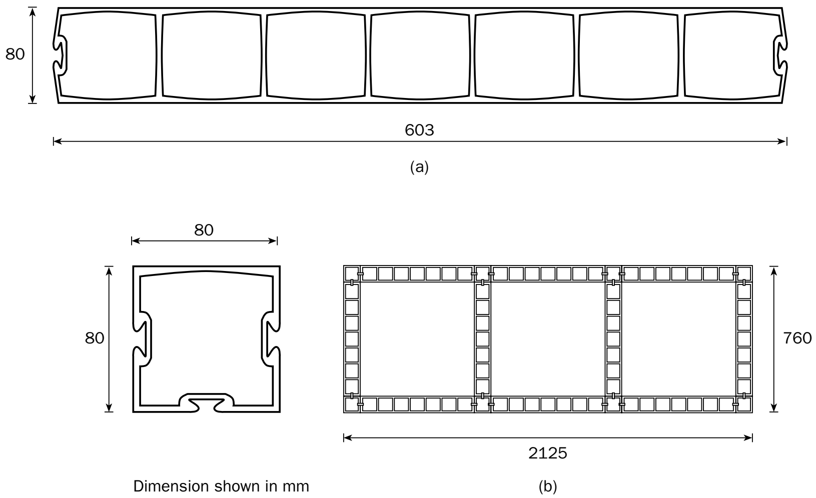

FIGURE 39.2 Cross section of the ACCS Structural Unit (The Maunsell Plank).

FIGURE 39.3 Bonds Mill Lift Bridge, Gloucestershire (photograph by kind permission of Maunsell Structural Plastics, Beckenham, Kent).

tion of stresses, an increase in magnitude or intensity of the applied loads required to be supported, or an upgrade of design standards may render all or part of a structure inadequate. On all highway structures, corrosion of the internal reinforcement is exacerbated by the application of de-icing salts.

These inadequacies may manifest themselves by poor performance under service loading in the form of excessive deflections and material failure. When maintenance or local repair can restore the structure to the required standard, there are two alternatives, complete or partial demolition and rebuild or a programme of strengthening.

Strengthening can be carried out by several techniques to achieve the desired improvement. These include increasing the size of the defective member, replacing non-structural toppings, external post tensioning, etc. The development of structural adhesive has lead to the evolution of a further method of structural repair in which initially steel plates were externally bonded to the structure but latterly carbon fibre composite plates are being used due to several disadvantages inherent in the use of steel plates.

The directional reinforcing fibres are positioned longitudinally relative to the beam and the composite would have a high fibre volume fraction to

FIGURE 39.4 Plate bonding on the soffit of a bridge (photograph by kind permission of Sika Ltd, Welwyn Garden City, Herts, UK).

obtain maximum efficiency, thus allowing the composite to be tailor made to suit the required shape and specification. The resulting materials are easy to handle and to transport, require little falsework on site and can be used in areas of limited access and do not add significant dead loads to the structure after installation. The method of manufacture of the composite plates would be either pultrusion, hand-lay REPLARK or semi-automated RIFT methods (described in Chapter 37)

As with all bonding operations the adherends must be free of all dust, dirt and surface grease. Consequently, the concrete, or steel surface onto which the composite is to be bonded, would be grit blasted to roughen and clean the surface. It would then be air blasted to remove any loose particles and wiped with acetone or equivalent to remove any grease before the bonding operation. The thickness of the carbon fibre composite plate would generally not be greater than about 1.2 mm. The total length, as delivered to site, would be of the order of 18 metres. It is possible to roll the material into a cylinder of about 1.5 metre diameter for transportation and for bonding the plate onto the beam in one operation. Both flexural and shear upgrading can be undertaken using carbon fibre composites.

39.7.2 Wrapping technique to upgrade structural columns

It is already known that confinement of concrete enhances its durability and strength. Currently, to enhance reinforced concrete columns, additional longitudinal steel bars and concrete are added around existing columns. Another method consists of placing a steel jacket around a column. The two methods are difficult to apply.

Confinement of concrete columns with polymer composite strands or sheets of composite prepreg shows many advantages in compression over other confinement methods. These include the advantageous properties of the composite methods such as high specific strength and stiffness and the relative ease of applying the composite materials to construction site situations.

Composite wrapping systems have been used throughout the world on a number of bridges, mainly in seismic loading, predominately in Japan and the USA. The available composite systems include epoxy with glass fibre, aramid fibre or carbon fibre fabric materials. A column consisting of a hybrid of fibre/polymer composite and concrete can deform much more under an extreme stress state than a conventional material system before failure. Confinement of the concrete laterally provides an order of magnitude in the improvement of the ultimate compressive strain. The REPLARK and the XXsys (described in Chapter 37) are the two main systems available

FIGURE 39.5 The use of REPLARK to wrap a column with carbon fibre polymer composite (photograph by kind permission of Sumitomo Corporation (UK) London).

for site work. Figure 39.5 illustrates the REPLARK system applied to a column

39.8 Composite rebars

Concrete structures have traditionally been reinforced with steel rebars which are durable in the alkaline environment of the concrete. However, concrete beams crack in the tensile region under load, thus allowing aggressive environments to come into contact with the steel. The corrosion of the steel reinforcement in concrete is a major concern in some civil engineering construction environments such as coastal, marine and chemical plants. In order to overcome this problem, polymer composite rebars may be used in place of the steel rebars.

The most suitable fibres currently used for the reinforcement of concrete are glass, carbon and aramid. The reinforced polymer matrix rebars would be manufactured by the pultrusion process using thermosetting polymers such as epoxy, vinylester and polyester. The final choice will depend upon their durability and cost. There are no limits on the size and shapes of pultruded bars which could be manufactured. The bars and rods would be manufactured in straight lengths but unlike steel they cannot be bent (thermoplastics/fibre composites can be bent by heating but these composites have not been developed sufficiently yet to be used as rebars). Other methods of developing the bond length of composite rebars have to be developed, such as lap splicing onto it; a 90° hook of the same cross-section as the main reinforcement could be used.

The most suitable fibres for use as prestressed tendons for concrete are the glass, aramid and carbon fibres. These materials are possible replacements for the high tensile strength steels. The first two fibre types have been utilised as prestressing tendons; the latter fibre is available but no actual applications are known. The three commercial systems which are currently available, all utilise parallel filaments but they differ in construction techniques. ‘Polystal’ is a pultrusion of glass fibre in a resin matrix; ‘Parafil’ is a rope that derives its strength from aramid yarns; ‘Arapree’ is a pultrusion of aramid fibres.

39.9 References

Hollaway, L. (1993) *Polymer and Polymer Composites for Civil and Structural Engineering,* Blackie Academic and Professional, Glasgow.

Hollaway, L.C. and Head, P.R. (2001) *Advanced Polymer Composites and Polymers in the Civil Infrastructure*, Elsevier Science, Oxford.

Section 2

Fibre-reinforced cements and concrete

Chapter forty

Properties of fibres and matrices

40.1 Physical properties

The performance of the composite is controlled mainly by the volume of the fibres, the physical properties of the fibres and the matrix, and the bond between the two. Values for bond strength rarely exceed 4 MPa and may be much less for some polymer fibres. The bond strengths will also change with time and with storage conditions which may permit densification of the interface region due to continuing hydration. Typical ranges for other physical properties of fibres and matrices are shown in Table 40.1.

It is apparent from this table that the elongations at break of all the fibres are two or three orders of magnitude greater than the strain at failure of the matrix and hence the matrix will usually crack long before the fibre strength is approached. This fact is the reason for the emphasis on post-cracking performance in the theoretical treatment. On the other hand, the modulus of elasticity of the fibre is generally less than five times that of the matrix and this, combined with the low fibre volume fraction, means that the modulus of the composite is not greatly different from that of the matrix.

The low modulus organic fibres are generally subject to relatively high creep which means that if they are used to support permanent high stresses in a cracked composite, considerable elongations or deflections may occur over a period of time. They are therefore more likely to be used in situations where the matrix is expected to be uncracked, but where transitory overloads such as handling stresses, impacts or wind loads are significant.

Another problem with the low modulus fibres of circular cross-section is that they generally have large values of Poisson's ratio and this, combined with their low moduli, means that if stretched along their axis, they contract sideways much more than the other fibres. This leads to a high lateral tensile stress at the fibre–matrix interface which for smooth circular section fibres is likely to cause a short aligned fibre to debond and pull out. Devices such as woven meshes, fibrillated fibres with loose hairs on the surface or fibrillated networks may therefore be necessary to give efficient composites.

Even the high modulus short fibres may require mechanical bonding to avoid pull out unless the specific surface area is very large. Thus steel fibres are commonly produced with varying cross-sections or bent ends to provide anchorage and glass fibre bundles may be penetrated with cement hydration products to give a more effective mechanical bond after a period of time.

The mortar and concrete matrices in Table

TABLE 40.1 Typical properties of cement-based matrices and fibres

Material or fibre	*Relative density*	*Diameter or thickness (microns)*	*Length (mm)*	*Elastic modulus (GPa)*	*Tensile strength (MPa)*	*Failure strain (%)*	*Volume in composite (%)*
Mortar matrix	1.8–2.0	300–5000	–	10–30	1–10	0.01–0.05	85–97
Concrete matrix	1.8–2.4	10 000–20 000	–	20–40	1–4	0.01–0.02	97–99.9
Aromatic polyamides (aramids)	1.45	10–15	5-continuous	70–130	2900	2–4	1–5
Asbestos	2.55	0.02–30	5–40	164	200–1800	2–3	5–15
Carbon	1.16–1.95	7–18	3-continuous	30–390	600–2700	0.5–2.4	3–5
Cellulose	1.5	20–120	0.5–5.0	10–50	300–1000	20	5–15
Glass	2.7	12.5	10–50	70	600–2500	3.6	3–7
Polyacrylonitride (PAN)	1.16	13–104	6	17–20	900–1000	8–11	2–10
Polyethylene pulp	0.91	1–20	1	–	–	–	3–7
HDPE filament	0.96	900	3–5	5	200	–	2–4
High modulus	0.96	20–50	continuous	10–30	>400	>4	5–10
Polypropylene monofilament	0.91	20–100	5–20	4	–	–	0.1–0.2
Chopped film	0.91	20–100	5–50	5	300–500	10	0.1–1.0
Continuous nets	0.91–0.93	20–100	continuous	5–15	300–500	10	5–10
Polyvinyl alcohol (PVA, PVOH)	1–3	3–8	2–6	12–40	700–1500	–	2–3
Steel	7.86	100–600	10–60	200	700–2000	3–5	0.3–2.0

40.1 are differentiated mainly by particle size and strain to failure. The maximum particle size of the matrix is important because it affects the fibre distribution and the quantity of fibres which can be included in the composite. The average particle size of cement paste before hydration is between 10 and 30 microns whereas mortar is considered to contain aggregate particles up to 5 mm maximum size. Concrete which is intended to be used in conjunction with fibres should not have particles greater than 20 mm and preferably not greater than 10 mm otherwise uniform fibre distribution becomes difficult to achieve.

In order to avoid shrinkage and surface crazing problems in finished products it is advisable to use at least 50 per cent by volume of inert mineral filler, which may be aggregate or could include pulverised fuel ash, or limestone dust. However, if the inert filler consists of a large volume of coarse aggregate the volume of fibres which can be included will be limited which will, in turn, limit the tensile strength and ductility of the composite.

Strength of the matrix is mainly affected by the free water/cement ratio and this parameter also has a lesser effect on the modulus so that the properties of the matrices can vary widely.

40.2 Structure of the fibre–matrix interface

The strength, deformation and failure characteristics of the whole range of fibre-reinforced cementitious materials is critically dependent on the bond between fibre and cement, which itself depends on the microstructure of the interface. The interface consists of an initially water-filled transition zone which does not develop the dense microstructure typical of the bulk matrix and contains a large volume of calcium hydroxide crystals which deposit in large cavities. Three layers are commonly observed in this zone, a thin (less than one micron) calcium hydroxide-rich rather discontinuous layer directly in contact with the fibre, a massive calcium hydroxide layer and a porous zone up to 40 microns from the surface consisting of calcium silicate hydrate and some ettringite. The porosity of these layers is affected by W/C ratio, age and whether or not microsilica, metakaolin or other additives are used in the mixture.

When a force is applied to the composite, particularly local to a crack, high shear stresses exist at the fibre cement interface, but failure may be initiated in the porous layer rather than at the interface itself. It is partly the changing nature with continuing hydration of this rather weak interfacial zone which is used to explain the embrittlement of some fibre cements with time.

When considering the microstructure in the interfacial zone, a distinction should be made between discrete monofilaments such as steel and elements of polypropylene nets and bundled filaments such as glass or asbestos. With monofilaments the entire surface of the fibre can be in direct contact with the matrix and the perimeter (P_f) carrying the shear forces is known. With bundled filaments only the external fibres initially have direct contact with the matrix and the perimeter transferring shear stress can only be estimated. As time goes on the vacant spaces between filaments in a strand may slowly become filled with hydration products. An intermediate stage is when some central fibres in a bundle are free to slide while the outside fibres are rigidly locked into the matrix. The final stage is complete penetration of the bundle which may then show brittle fracture.

Thus the accurate calculation of bond stress (τ), which relies on a knowledge of the perimeter in contact with cement, is not possible with fibre bundles because this area is unknown and changes with time.

Chapter forty-one

Structure and post-cracking composite theory

As mentioned in the introduction to fibre composites, the main benefits of the inclusion of fibres in hardened cement-based products relate to the post-cracking state, where the fibres bridging the cracks contribute to the increase in strength, failure strain and toughness of the composite. This type of reinforcing mechanism requires a different theoretical approach from that described in Chapter 36 although the principles covered in that chapter adequately describe the pre-cracking behaviour.

Another significant difference from fibre-reinforced polymers is that the fibre volume in fine-grained cement-based products rarely exceeds 15 per cent and is more commonly less than 10 per cent. In concrete the fibre volume is usually less than 2 per cent, often with low modulus fibres being included, and it is for these reasons, together with the relatively stiff matrix, that little emphasis is placed on increasing the elastic modulus of the composite by the inclusion of fibres.

41.1 Theoretical stress–strain curves in uniaxial tension

41.1.1 Characteristic shapes of stress–strain curves

Fibre-reinforced cements and concretes are generally considered to be most useful when carrying bending or impact loads but unfortunately a theoretical analysis of the mechanics of reinforcement in these systems is very complex. A more fundamental and a more easily understood stress system is that of direct tension and a sound knowledge of the behaviour of fibres in such a system provides a good background by which an engineer can judge the potential merits of a fibre cement composite for a given end use.

The three basic types of tensile stress–strain curve available to the engineer are shown in Figure 41.1. Curves *B* and *C* are based on the assumption that the stress in the composite is increased at a constant rate.

For all three curves, the portion *OX* defines the elastic modulus of the uncracked composite (E_c). Curves *A* and *C* are for composites in which there are insufficient fibres to carry the load in the composite after continuous cracks in the matrix propagate completely across the component. In curve *A*, after the cracks have formed at *X* the fibres

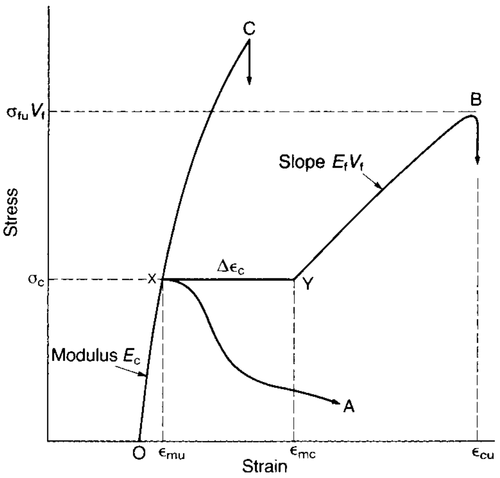

FIGURE 41.1 Theoretical tensile stress–strain curves for different fibre composites.

slowly pull out and absorb energy leading to a tough but rather weak composite typified by steel fibre concrete or short random fibre polypropylene concrete. In curve *C*, which is representative of asbestos-cement and of some cellulose fibre-based composites when dry, the relatively high crack propagation stress leads to a sudden large release of energy and to an almost instantaneous fibre fracture or fibre pull-out at *C*. However, stable micro-cracks may exist well before point *C* is reached. The mechanism of the reinforcement of cement by asbestos fibre is very complex and leads to a special case of a high tensile strength, rather brittle, composite. A full understanding of the fracture process has not yet been achieved but it appears to require a combination of the reinforcing theory described for curve *B* with a knowledge of fracture mechanics as outlined in Section 41.2.

Curve *B* is typical of a composite in which there are sufficient fibres to maintain the load on the composite when the matrix cracks. The horizontal portion *X–Y* is a result of multiple cracking at approximately constant stress and *Y–B* represents extension or pull-out of fibres up to separation of the component into two parts at point *B*. Curve *OXYB* is typified by fine-grained materials such as glass-reinforced cement or some continuous fibre composites such as polypropylene network reinforced cement.

As will be seen from the equations in this chapter, the specific value of the bond strength (τ) does not affect the shape of the stress–strain curve *OXYB* in Figure 41.1, the length of the multiple crack region ($\Delta\epsilon_c$), nor the failure strain (ϵ_{cu}). Bond strength does, however, affect crack spacing and crack width which are significant parameters affecting the performance of the composites in practical situations and, thus, time and weathering will affect crack spacing and crack width.

Apart from the special case of curve *OXC* it is unusual for fibres to significantly increase the cracking stress (σ_c) of the cement-based composite and therefore it is of value to consider the load-carrying ability of the fibres after matrix cracking has occurred. An important concept which it is necessary to understand in this respect is the critical volume fraction of fibres.

41.1.2 Critical volume fraction (V_{fcrit}) in uniaxial tension

The critical fibre volume is the volume of fibres which after matrix cracking will carry the load which the composite maintained before cracking.

This definition needs to be used with a little care because material which has less than the critical volume of fibre in tension (curve *OXA*) may have considerably greater than the critical fibre volume required for flexural strengthening. However, it is common practice to assume that the above definition of critical fibre volume refers only to uniaxial tensile stresses.

For the simplest case of aligned fibres with fractional bond, let:

ϵ_{mu} = matrix cracking strain
σ_c = composite cracking stress
V_{fcrit} = critical volume of fibres
σ_{fu} = fibre strength or average pull-out stress of fibre depending on whether fibres break or pull out at a crack.

Just before cracking

$$\sigma_c = E_c\epsilon_{mu} \qquad (41.1)$$

After cracking, the whole stress is carried by the fibres. Assume that there are just sufficient fibres to support this stress, i.e. fibre volume = V_{fcrit}

$$\sigma_c = \sigma_{fu} V_{fcrit} \qquad (41.2)$$

From (41.1) and (41.2)

$$V_{fcrit} = \frac{E_c\epsilon_{mu}}{\sigma_{fu}} \qquad (41.3)$$

From (41.2)

$$V_{fcrit} = \frac{\sigma_c}{\sigma_{fu}} \qquad (41.4)$$

There are important points to note about equations (41.3) and (41.4).

1. E_c, ϵ_{mu} and hence σ_c may vary with time and E_c and σ_c will generally increase if the cement continues to hydrate. This implies that a composite which has just sufficient fibre volume to exceed V_{fcrit} at early ages may, after some years, have less fibre than V_{fcrit} at that age and hence may suffer brittle fracture.
2. V_{fcrit} can be decreased by decreasing σ_c.
3. Poor bond may reduce σ_{fu} by allowing fibre pull-out at a fraction of the fibre strength. Additionally the orientation of the fibres will have a large effect on V_{fcrit} because random fibre orientation will reduce the number of fibres across a crack surface compared with the aligned case.

In the common practical case of short, randomly orientated fibres where the fibres pull out at a crack rather than break, the stress in the fibre causing pull-out may be substantially less than σ_{fu} and hence V_{fcrit} for such composites may be up to ten times that required for continuous aligned fibres. In the equations in Section 41.1.3 it is assumed that the orientation and stress efficiency factors are 1.0 and hence V_f and σ_{fu} for the wide variety of composites in current use must be modified by the use of efficiency factors to allow for the effective volume of fibres in the direction of stress. The effect of short random fibres on V_{fcrit} may be calculated using the equations in Section 41.1.6.

41.1.3 Stress–strain curve, multiple cracking and ultimate strength

If the critical fibre volume for strengthening has been reached then it is possible to achieve multiple cracking of the matrix. This is a desirable situation because it changes a basically brittle material with a single fracture surface and low energy requirement to fracture, into a pseudo-ductile material which can absorb transient minor overloads and shocks with little visible damage. The aim of the materials engineer is often therefore to produce a large number of cracks at as close a spacing as possible so that the crack widths are very small (say <0.1 mm). These cracks are almost invisible to the naked eye in a rough concrete surface and the small width reduces the rate at which aggressive materials can penetrate the matrix when compared with commonly allowable widths in reinforced concrete of up to 0.3 mm.

High bond strength helps to give a close crack spacing but it is also essential that the fibres debond sufficiently local to the crack to give ductility which will absorb impacts.

The principles behind the calculation of the complete stress–strain curve, the crack spacing and the crack width for long aligned fibres for the simplified case where the bond between the fibres and matrix is purely frictional and the matrix has a well-defined single value breaking stress has been given by Aveston *et al.* (1971) and Aveston *et al.* (1974). The following has been simplified from these publications.

Long fibres with frictional bond

The idealised stress–strain curve for a fibre-reinforced brittle matrix composite is *OXYB* in Figure 41.1.

If the fibre diameter is not too small, the matrix will fail at its normal failure strain (ϵ_{mu}) and the subsequent behaviour will depend on whether the fibres can withstand the additional load without breaking, i.e. whether $\sigma_{fu}V_f > \sigma_c$.

If they can take this additional load, it will be transferred back into the matrix over a transfer length χ' (Figure 41.2) and the matrix will eventually be broken down into a series of blocks of length between χ' and $2\chi'$ with an average spacing (C) of $1.364\chi'$.

We can calculate χ' from a simple balance of the load $\sigma_{mu}V_m$ need to break a unit area of the matrix and the load carried by N fibres of individual cross-sectional area A_f and perimeter P_f across the same area after cracking. This load is transferred over a distance χ' by the limiting maximum shear stress τ. i.e.

$$N = V_f/Af \tag{41.5}$$

$$P_f N \tau \chi' = \sigma_{mu}V_m \tag{41.6}$$

or

$$\chi' = \frac{V_m}{V_f} \cdot \frac{\sigma_{mu}}{\tau} \frac{A_f}{P_f} \tag{41.7}$$

This stress distribution in the fibres and matrix (crack spacing $2\chi'$) will then be as shown in Figure 41.2.

The additional stress ($\Delta\sigma_f$) on the fibres due to cracking of the matrix varies between $\sigma_{mu}V_m/V_f$ at the crack and zero at distance χ' from the crack so that the average additional strain in the fibres, which is equal to the extension per unit length of composite at constant stress σ_c, is given by:

$$\Delta\epsilon_c = \frac{1}{2}\sigma_{mu} \cdot \frac{V_m}{V_f} \cdot \frac{1}{E_f} \tag{41.8}$$

i.e.

$$\Delta\epsilon_c = \frac{\epsilon_{mu}E_m V_m}{2E_f V_f} = \frac{\alpha\epsilon_{mu}}{2} \tag{41.9}$$

where

$$\alpha = E_m V_m / E_f V_f \tag{41.10}$$

and the crack width (ω), bearing in mind that the matrix strain relaxes from ϵ_{mu} to $\epsilon_{mu}/2$ will be given by

$$\omega = 2\chi'\left(\frac{\alpha\epsilon_{mu}}{2} + \frac{\epsilon_{mu}}{2}\right) \tag{41.11}$$

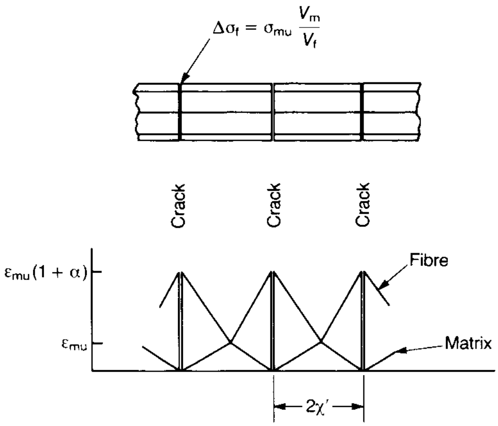

FIGURE 41.2 Strain distribution after cracking of an aligned brittle matrix composite (Aveston *et al.*, 1971). (Crown copyright reserved.)

or

$$\omega = \epsilon_{mu}(1 + \alpha)\chi' \tag{41.12}$$

For practical composites, the factor α may range from about 2 for asbestos-cement to over 100 for some polymer-fibre composites, thus making a very wide range of properties available to the engineer.

At the completion of cracking the blocks of matrix will all be less than the length ($2\chi'$) required to transfer their breaking load ($\sigma_{mu}V_m$) and so further increase in load on the composite results in the fibres sliding relative to the matrix, and the tangent modulus becomes ($E_f V_f$) (see Figure 41.1).

In this condition, the load is supported entirely by the fibres and the ultimate strength (σ_{cu}) is given by

$$\sigma_{cu} = \sigma_{fu}V_f \tag{41.13}$$

If the average crack spacing $C = 1.364\ \chi'$ is used in the calculations instead of the $2\chi'$ crack spacing then parameters associated with curve *OXYB* in Figure 41.1 are:

Average crack spacing,

$$C = 1.364\frac{V_m}{V_f}\frac{\sigma_{mu}}{\tau}\frac{A_f}{P_f} \tag{41.14}$$

Length *X*–*Y*,

$$\Delta\epsilon_c = 0.659\alpha\epsilon_{mu} \qquad (41.15)$$

Average crack width between *X* and *Y* = *W*

$$W = \epsilon_{mu} \cdot 0.9\,(1+\alpha)\chi' \qquad (41.16)$$

Composite failure strain

$$\epsilon_{cu} = \epsilon_{fu} - 0.341\alpha\epsilon_{mu} \qquad (41.17)$$

The relationship between the average crack width *W* at the end of multiple cracking and fibre volume is shown in Figure 41.3 for the case in which α is much greater than unity. It is apparent that, even using the most optimistic assumption, large variations in crack width are likely to occur for small variations in fibre volumes at less than 2 per cent by volume of fibre and volumes above 5 per cent are desirable if a uniformly and invisibly cracked composite is to be achieved. Hence the fabrication techniques must be adjusted to produce a uniformly dispersed fibre and preferably a high (5–10 per cent) fibre volume if invisible cracking is required in the product.

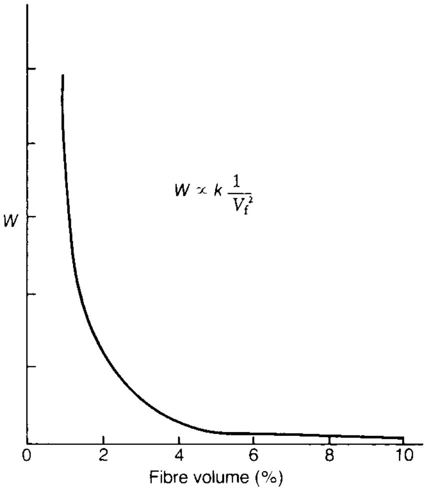

FIGURE 41.3 Relationship between crack width (*W*) at the end of multiple cracking and fibre volume (V_f) for the case in which α is much greater than unity.

41.1.4 Efficiency of fibre reinforcement

The efficiency of fibre reinforcement depends on fibre length and orientation. Different efficiency factors are required for pre-cracking performance, as described in the chapter on polymer composites, and post-cracking performance. Allowance has also to be made for static frictional resistance prior to sliding and dynamic frictional resistance during sliding. A detailed treatment of efficiency factors is beyond the scope of this section but may be found in Laws (1971), Aveston (1974), Hannant (1978) and Bentur and Mindess (1990). A simplified approach for specific cases is given in paragraph 41.1.6.

41.1.5 Application of theory to real composites

Typical stress–strain curves for real composites may be obtained using the theory in the previous sections and four such curves for different fibre types are shown in Figure 41.4, in which V_f' is the effective volume of fibre in the direction of stress calculated from the total V_f using the appropriate efficiency factors.

The values for α shown in Figure 41.4 have been calculated from equation (41.10), and, when substituted in equation (41.15), they give an indication of the possible range for real composites of the horizontal part $\Delta\epsilon_c$ of Figure 41.1.

Figure 41.4(b) shows that it is possible for glass-reinforced cement to have a typical extension due to multiple cracking alone of about twelve times the matrix cracking strain, whereas asbestos cement (Figure 41.4(a)) can only extend by about one times the matrix cracking strain before the fibres take over completely. Likewise, a similar effective volume of continuous polypropylene to that of asbestos (Figure 41.4(c)) could increase the strain due to multiple cracking alone by fifty-one times the matrix cracking strain even under fairly rapid loading. This would probably be exceeded for extended loading periods because the modulus of polypropylene is time dependent.

The lack of a horizontal portion in Figure

41.4(a) is a serious deficiency in that it results in the material having limited capability to absorb shock and accidental over-strains. It is possible that the asbestos fibres have such a small diameter (0.02–20 μm) that matrix cracking is suppressed until successively higher strains are reached as described in Section 41.2 and final failure is by single fracture with some pull-out.

The strain to failure for the polypropylene continuous fibre composite in Figure 41.4(c) is an order of magnitude greater than for the other composites and hence the energy-absorbing capability under overload conditions, which depends on the area under the stress–strain curve, is likely to be higher. However, the ultimate strain may not be reached in practice due to excessive deformation.

Figure 41.4(d) is typical of concretes containing less than the critical volume of short chopped fibres, generally steel or polypropylene in random three-dimensional orientation. The fibres in these circumstances are generally sufficiently short to pull-out, rather than break, when cracks occur in the matrix and the ultimate load on the composite is then controlled by the numbers of fibres across a crack, the length/diameter ratio of the fibres and the bond strength.

The stress in the fibre at pull-out is often less than half the strength of the fibre and hence higher bond strength, rather than high fibre strength may be the most important requirement for this type of composite.

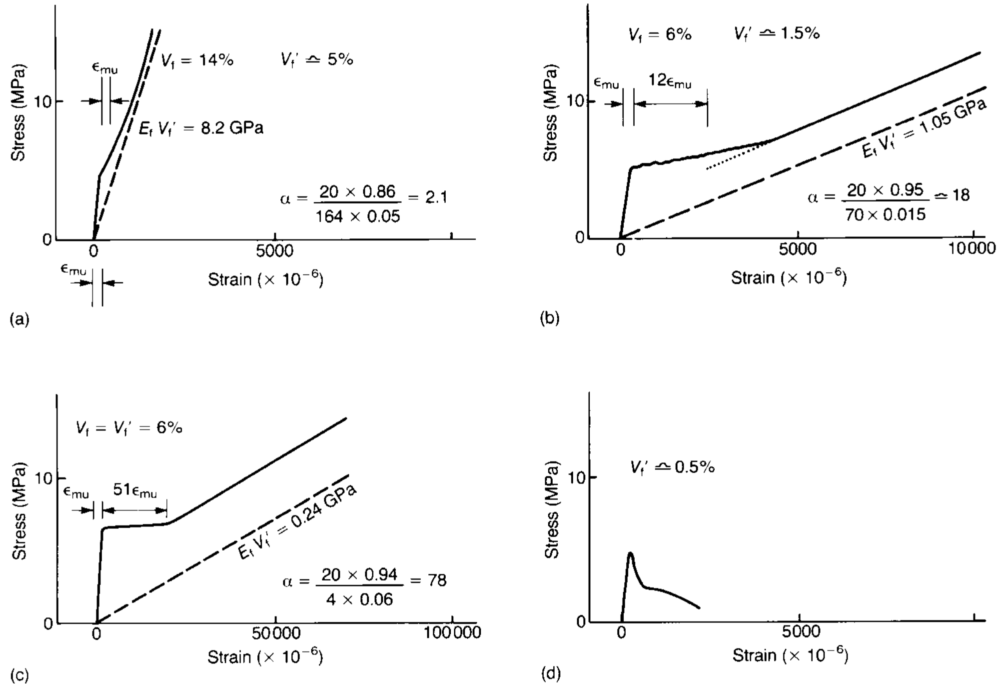

FIGURE 41.4 Typical stress–strain curves for real composites: (a) asbestos fibres in cement paste; (b) two-dimensional random glass fibres in cement paste; (c) continuous aligned polypropylene fibres in cement paste; (d) short, random, chopped steel or polypropylene fibres in concrete.

41.1.6 Short random fibres which pull out rather than break

Factors affecting a realistic estimate of $V_{f(crit)}$ and post cracking strength are:

1. number of fibres across a crack;
2. bond strength and fibre pull out load.

Number of fibres across a crack

The situation in a cracked composite may be represented by Figure 41.5. For short random fibres, such as steel or chopped fibrillated polypropylene, which are generally shorter than the critical length for fibre breakage, the fibres mostly pull-out across a crack. A realistic estimate of the load carried after cracking can therefore be obtained by multiplying the number of fibres crossing a unit area of crack by the average pull-out force per fibre. For fibres which break before pulling out, the situation is more complicated.

The appropriate number of fibres, N per unit area, can be calculated as follows:

A_f = cross-sectional area of a single fibre.

For fibres aligned in one direction:

$$N = \frac{V_f}{A_f} \tag{41.18}$$

For fibres random in two dimensions:

$$N = \frac{2}{\pi}\frac{V_f}{A_f} \tag{41.19}$$

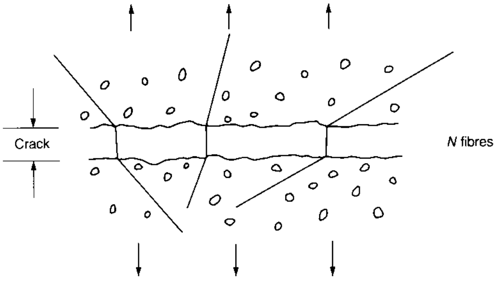

FIGURE 41.5 Change in fibre orientation at a crack. (Reprinted by permission of John Wiley & Sons Ltd, from D.J. Hannant (1978).)

For fibres random in three dimensions:

$$N = \frac{1}{2}\frac{V_f}{A_f} \tag{41.20}$$

Bond strength and fibre pull-out force

If the composite failure is by fibre pull-out, it has been shown that the mean fibre pull-out length is ($l/4$) (see Figure 41.6).

Provided that the average sliding friction bond strength (τ) is known and assuming that this does not vary with the angle of the fibre to the crack then the average pull-out force per fibre (F) is given by:

$$F = \tau P_f l/4 \tag{41.21}$$

where P_f = the individual fibre perimeter in contact with the cement.

The ultimate stress (σ_{cu}) sustained by a unit area of composite after cracking is therefore given by $N \times F$, i.e.

$$\sigma_{cu} = \frac{N\tau P_f l}{4} \tag{41.22}$$

and the average fibre stress at pull-out (σ_f) is

$$\sigma_f = \frac{\tau P_f}{A_f}\frac{l}{4} \tag{41.23}$$

which for round fibres reduces to

$$\sigma_f = \tau \cdot \frac{l}{\mathrm{d}}$$

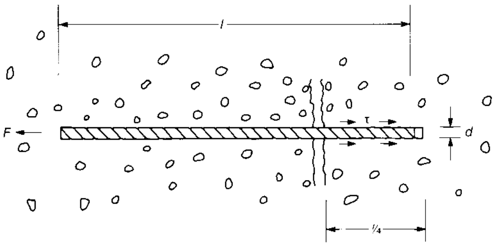

FIGURE 41.6 Average pull-out force per fibre. (Reprinted by permission of John Wiley & Sons Ltd, from D.J. Hannant (1978).)

Substituting for N from equations (41.18), (41.19) and (41.20) in equation (41.22) gives the following:

Aligned fibres in one direction

$$\sigma_{\mathrm{cu}} = V_{\mathrm{f}}\tau\frac{l}{4}\cdot\frac{P_{\mathrm{f}}}{A_{\mathrm{f}}} \tag{41.24}$$

Random two-dimensional

$$\sigma_{\mathrm{cu}} = \frac{2}{\pi}V_{\mathrm{f}}\tau\frac{l}{4}\cdot\frac{P_{\mathrm{f}}}{A_{\mathrm{f}}} \tag{41.25}$$

Random three-dimensional

$$\sigma_{\mathrm{cu}} = \frac{1}{2}V_{\mathrm{f}}\tau\frac{l}{4}\,\frac{P_{\mathrm{f}}}{A_{\mathrm{f}}} \tag{41.26}$$

Thus, the 3-D random fibre concrete should have about half the post crack strength of the aligned composite.

The critical fibre volume for short random fibres can be obtained by re-arranging equations (41.24), (41.25) and (41.26) to give V_{f} on the left-hand side of the equation.

In contrast to the use of the above equations for short chopped polypropylene fibre or steel fibre concrete, the glass-reinforced cement industry has sometimes used empirical efficiency factors. Thus, for a commonly used, two-dimensional random chopped glass fibre–cement composite the effectiveness of the fibre at the end of the multiple cracking zone has been shown to be between 0.16 and 0.27 depending on the direction of stress to the spray-up direction.

41.1.7 Toughness in uniaxial tension

One of the major attributes of fibre–cement composites is their increased toughness in comparison with plain concrete. However, the theoretical prediction of the increased toughness and its measurement in practice are both fraught with problems. Commercial tests tend to rely on empirical comparisons between composites with and without fibres, tested with drop weights to 'no rebound' or with beams deflected to specific values. These tests do not determine basic material parameters and are often highly dependent on support conditions or on specimen and machine dimensions and stiffnesses.

A more fundamental approach is to calculate the very large increase in area of the tensile stress–strain curve resulting from the presence of the fibres. This increase, which may be several orders of magnitude, is indicative of greatly enhanced toughness and ductility, properties often loosely associated with impact strength or impact resistance. The theory outlined in Section 41.1.3 can therefore be used as the basis of toughness predictions.

In fibre cements and concretes there are essentially two modes of failure, one mainly involving fibre pull-out after single fracture and the other involving multiple fracture of the matrix followed by fibre pull-out or fracture. In the former case, which is typical of steel fibre concrete, the energy *U* to pull-out *N* fibres per unit area of composite cross-section is proportional to the frictional fibre matrix bond strength, τ, and to the square of the fibre length (*l*) as in equation (41.27) (see Hibbert and Hannant, 1982).

$$U = \frac{\mathrm{N}\cdot\mathrm{P}_{\mathrm{f}}\cdot\tau l^2}{24} \tag{41.27}$$

In the case where failure occurs by multiple cracking followed by fibre fracture rather than fibre pull-out, the energy is absorbed throughout the volume of material and may be calculated from the area under the tensile stress–strain curve *OXYB* in Figure 41.1. The resulting energy is that absorbed per unit volume of composite:

i.e. $$U = 0.5\sigma_{\mathrm{fu}}\epsilon_{\mathrm{fu}}V_{\mathrm{f}} + 0.159\alpha E_{\mathrm{c}}\epsilon_{\mathrm{mu}}^2 \tag{41.28}$$

where the first term represents the fibre strain energy and the second term the contribution from multiple cracking of the matrix.

For practical situations, we really require to know the energy which can be absorbed by the product before it breaks into two pieces or before it is rendered unserviceable. The amount of energy which can be absorbed before reaching an acceptable amount of damage in terms of visible cracking depends very much on whether fracture occurs mainly by a single crack opening or by multiple cracking. Thus a careful decision has to be made as to whether the energy should be predicted from a material parameter related to unit *area* of fracture surface (J/m^2) for the case of a single crack or from a parameter for energy absorbed per unit *volume* of material (J/m^3) for multiple cracks.

An additional complexity is that because the composite modulus (E_c) and the matrix failure strain (ϵ_{mu}) may increase with time in external environments, then $V_{f(crit)}$ calculated from equation (41.3) may increase above the original value required to ensure multiple cracking. Thus a composite which is tough and ductile at early ages may suffer single fracture after some years with an energy to failure defined by the area under the curve OX in Figure 41.1 (equation 41.29).

$$U = 0.5 E_c \epsilon_{mu}^2 \tag{41.29}$$

Although E_c and ϵ_{mu} may have increased with ageing, the energy calculated from equation (41.29) is very much less than the energy given by equation (41.28).

Some typical toughness values for real composites calculated from the area under the tensile stress–strain curves are shown in Table 41.1.

41.2 Uniaxial tension – fracture mechanics approach

It has been observed that asbestos cement has a strain to failure or to first visible crack often in excess of 1000×10^{-6} and sometimes up to 2000×10^{-6}. This implies that the cracking strain of the matrix has been increased by the presence of fibres since the cracking strain of the cement paste from which the composite is made is usually less than 400×10^{-6}. The composite materials approach outlined in Section 41.1 is not adequate to explain this observation.

TABLE 41.1 Typical toughness values for real composites

Material	*Energy to failure (kJ/m^3)*
Asbestos cement	5.5
Glass-reinforced cement	
dry	120
wet	3
Continuous polypropylene networks in cement	1000
Kevlar in cement	150

The implication is that microcrack propagation from pre-existing flaws in the matrix has been suppressed by the very high volume (~12 per cent) of very small diameter, high modulus of elasticity fibres and the concepts of fracture mechanics are required to quantify the possible improvements in performance. It has been shown that typical pre-existing flaws in the matrix may be 3 mm long with a critical opening of about 1 micron. For asbestos cement and some other fibre composites the flaws will be crossed by many fibres but to demonstrate the principle of the argument, Figure 41.7 shows a flaw traversed by a single fibre (Hannant *et al.*, 1983)

If the strain in the specimen is increased from zero with the crack initially closed, the fibre will be stressed by the crack opening to width B and this stress will be transferred back into the matrix as shown in the strain diagram in Figure 41.7. The matrix will slide back over the fibres by a distance l, producing a difference in strain between fibre and matrix at the crack face of ϵ_f.

$$\therefore\ E_f \epsilon_f = \frac{P_f \tau l}{A_f} \tag{41.30}$$

Also, the crack opening B is obtained from the integrated difference in strain between reinforcing fibres and matrix, i.e.

$$l = \frac{B}{\epsilon_f} \tag{41.31}$$

So, by eliminating l, the stress in the fibre σ_f is given by

$$\sigma_f = \left(\frac{P_f}{A_f} \tau E_f B \right)^{1/2} \tag{41.32}$$

The fibres therefore exert a closing force on the crack and reduce its opening. If there are N fibres crossing a crack, the total closing force F reducing the crack opening is

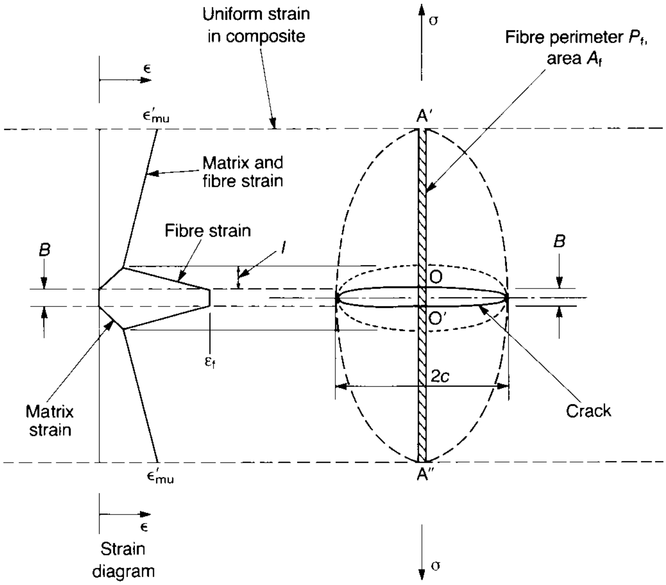

FIGURE 41.7 Possible zone of relaxation of strain around a crack under stress that is traversed by a single fibre. The left side of the figure illustrates the variation in strain within the fibre and matrix along the line *A′A″* (Hannant *et al.*, 1983).

$$F \sim N\sigma_{\text{fmax}}A_{\text{f}} \qquad (41.33)$$

Using typical values for bond, modulus and specific surface area for glass fibres indicates stresses in the fibres of ~300 MPa before the pre-existing cracks reach sufficient width to propagate. The flaws will propagate catastrophically as soon as the rate of energy release becomes infinitesimally greater than the rate of energy absorption. The calculation is made using a computer-iterative process which shows, in accord with experiment, that the ultimate failure strain of asbestos fibres in asbestos cement at $V_f = 5\%$ and 10% is reached before the crack becomes unstable. We therefore could expect breaking of the specimen and first cracking of the matrix to occur simultaneously at a strain of 860×10^{-6} for $V_f = 5\%$ and at 1200×10^{-6} for $V_f = 10\%$.

Although similar effects should exist in all fibre cements where the fibre spacing is less than the flaw size, it is only where composites contain very high volumes, of high-modulus small-diameter fibres with high surface area and good bonding characteristics, that the effects of increased matrix cracking strain become sufficiently significant to be observable in practice.

41.3 Principles of fibre reinforcement in flexure

41.3.1 Necessity for theory

In many of their major applications, cement-bound fibre composites are likely to be subjected to flexural stresses in addition to direct stresses, and hence an understanding of the mechanism of strengthening in flexure may be of equal importance to the analysis of the direct stress.

The need for a special theoretical treatment for flexure arises because of the large differences which are observed experimentally between the flexural strength and the direct tensile strengths, both in glass-reinforced cement and in steel-fibre concrete. In both of these materials the so-called flexural strength can be up to three times the direct tensile strength even though, according to elastic theory, they are nominally a measure of the same value. The same situation occurs to a lesser degree with plain concrete.

The main reason for the discrepancy in fibre–cement composites is that the post-cracking stress–strain curve *X–A* and *XYB* in Figure 41.1 on the tensile side of a fibre cement or fibre concrete beam are very different from those in compression and, as a result, conventional beam theory is inadequate. The flexural strengthening mechanism is mainly due to this quasi-plastic behaviour of fibre composites in tension as a result of fibre pull-out or elastic extension of the fibres after matrix cracking.

Figures 41.8 (a) and (b) show a cracked fibre reinforced beam with a linear strain distribution and the neutral axis moved towards the compression surface. At a crack the fibres effectively provide point forces holding the section together (Figure 41.8 (c)). However, the exact stresses in the fibres are generally ignored in flexural calculations and an equivalent composite stress block such as in Figure 41.8 (d) is assumed. The shape of this stress block depends on fibre volume, bond strength, orientation and length efficiency factors. An accurate analysis of such a system presents formidable problems but a simplified treatment which is satisfactory for many practical situations is given below.

41.3.2 Analysis using a rectangular stress block in the tensile zone of a beam

The analysis which follows is based on a simplified assumption regarding the shape of the stress block in the tensile zone after cracking.

The stress block for an elastic material in bending is shown in Figure 41.9 (a) and this is usually used to calculate the flexural strength (σ_{fl}) even though it is known to be grossly inaccurate for quasi-ductile fibre composites.

Figure 41.9 (b) shows a simplified stress block in bending for the type of tensile stress–strain curve *OXY* in Figure 41.1. This is typical of a fibre–concrete composite after cracking, where the fibres are extending or are pulling out at constant load across a crack throughout the tensile section. The ultimate post-cracking tensile strength of the composite is σ_{cu} and σ_{comp} is the compressive stress on the outer face of the beam. Figure 41.9 (b) approximates to the stresses in steel-fibre concrete where the crack widths are small (<0.3 mm) compared with the fibre length and possibly to glass-reinforced cement at early ages when the fibres are poorly bonded and extend before fracture or pull-out after fracture at roughly constant load. It also simulates composites with $>V_{\mathrm{fcrit}}$ of continuous polypropylene nets.

A conservative estimate for the distance of the neutral axis from the compressive surface is $D/4$ and using this assumption the moments of resistance of the two stress blocks can be compared:

$$\text{moment of resistance} = \frac{1}{6}\sigma_{\mathrm{fl}}D^2 \text{ for Figure 41.9 (a)} \quad (41.34)$$

$$\text{moment of resistance} = \frac{13}{32}\sigma_{\mathrm{cu}}D^2 \text{ for Figure 41.9 (b)} \quad (41.35)$$

In order that the two beams represented in Figure 41.9 can carry the same load, their moments of resistance should be equal, i.e.

$$\frac{1}{6}\sigma_{\mathrm{fl}}D^2 = \frac{13}{32}\sigma_{\mathrm{cu}}D^2 \quad (41.36)$$

Therefore

$$\sigma_{\mathrm{fl}} = 2.44\sigma_{\mathrm{cu}} \quad (41.37)$$

Equation 41.37 implies that if the critical fibre volume in uniaxial tension has just been achieved as shown in Figure 41.10 (b) then the flexural tensile strength will appear to be about 2.44 times the composite cracking stress. Conversely, a material with less than half the critical fibre volume in tension which has the uniaxial tensile stress–strain curve shown in Figure 41.10 (a) will not exhibit a decrease in flexural load capacity

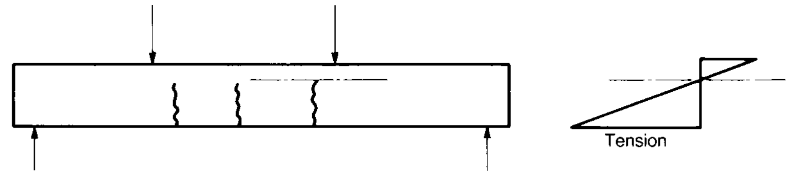

(a)

(b) Strain distribution at a crack

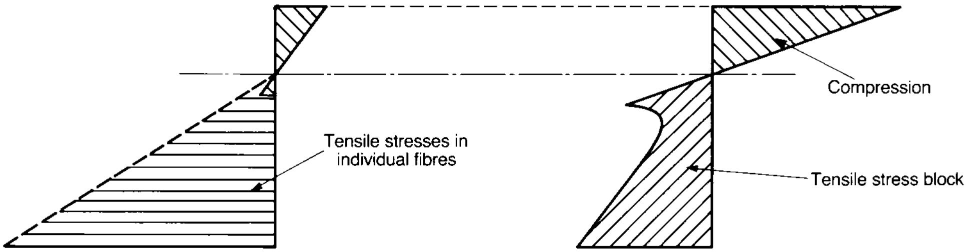

(c) Stress distribution at a crack

(d) Equivalent stress block in the composite

FIGURE 41.8 Strain and stress distributions in a cracked fibre-reinforced concrete beam. (Note: scales of (c) and (d) are different.)

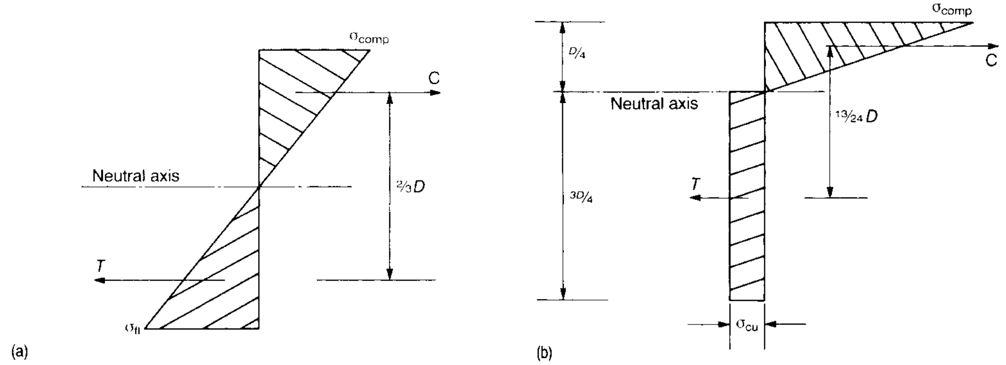

FIGURE 41.9 Stress blocks in flexure. (a) Elastic material; moment of resistance = $(1/6)\sigma_{fl}D^2$. (b) Elastic in compression, plastic in tension; moment of resistance = $13/32\sigma_{cu}D^2$.

after cracking, implying that the critical fibre volume in flexure has been achieved.

The limiting condition in Figure 41.9 (b) is when the neutral axis reaches the compressive surface of the beam while maintaining the maximum tensile strength (σ_{cu}) throughout the section. In this case:

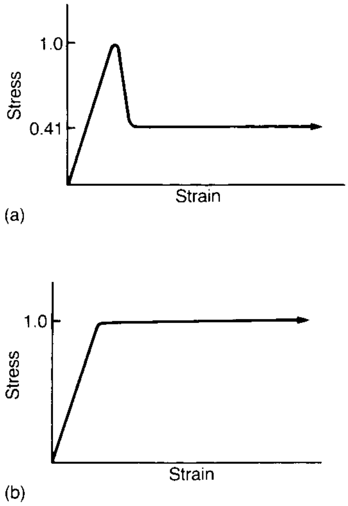

FIGURE 41.10 Stress–strain curves in uniaxial tension: (a) no decrease in flexural load capacity after cracking; (b) load capacity after cracking = 2.44 times the cracking load for compressive strength/tensile strength ⩾6.

$$\frac{1}{2}\sigma_{\mathrm{cu}}D^2=\frac{1}{6}\sigma_{\mathrm{fl}}D^2, \quad \text{i.e. } \sigma_{\mathrm{fl}}=3\sigma_{\mathrm{cu}} \qquad (41.39)$$

This type of simplified analysis explains why the flexural strength for fibre cements and fibre concretes is often quoted to be between 2 and 3 times the tensile strength. Because the flexural strengths calculated using the normal 'elastic theory' approach often imply unrealistically high tensile strengths, it is unwise to use such strengths in the design of fibre-reinforced cement or concrete components. For the same reason it is preferable to avoid flexural tests wherever possible when the tensile strengths of fibre-reinforced cement-based composites are required.

41.3.3 Effect of loss in ductility in tension on the flexural strength

The importance of the post-cracking tensile strain capacity in relation to the area of the tensile stress block in bending has already been demonstrated. A further result of this major factor is that changes in strain to failure in the composite can result in changes in the flexural strength even when the tensile strength remains constant. This is particularly relevant to glass-reinforced cement where the tensile strain capacity can reduce by an order of magnitude (1 to 0.1 per cent) over a period of years of natural weathering or water curing. The movement of the neutral axis towards the compressive surface depends on a high post-cracking strain in tension and if this tensile strain decreases sufficiently, the composite will have a reduced moment of resistance (Laws and Ali, 1977). This effect is shown in Figure 41.11. For instance, *OAC* is a tensile strain curve

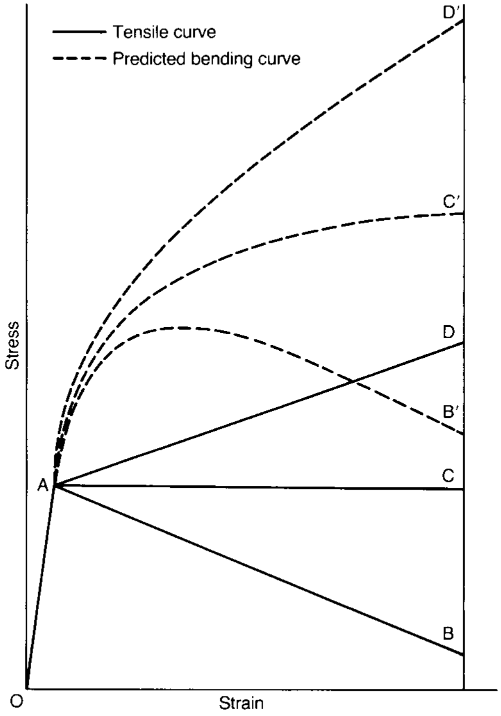

FIGURE 41.11 Apparent bending flexural strength curves predicted for assumed direct tensile curves (Laws and Ali, 1977). (By permission of the Institution of Civil Engineers.)

and OAC' is the associated bending curve. If the tensile strain reduces from C to A at constant stress, the bending strength will reduce from C' to A with an increasing rate of reduction as A is approached and the material becomes essentially elastic.

41.4 References

Aveston, J., Cooper, G.A. and Kelly, A. (1971) Single and multiple fracture. Paper 2 in *The Properties of Fibre Composites, Conference Proceedings of the National Physical Laboratory,* IPC Science and Technology Press, Guildford, UK

Aveston, J., Mercer, T.A. and Sillwood, J.M. (1974) Fibre-reinforced cement – scientific foundations for specifications. *Composites Standards Testing and Design,* National Physical Laboratory Conference Proceedings, Guildford, UK

Bentur, A. and Mindess, S. (1990) *Fibre Reinforced Cementitious Composites,* Elsevier Applied Science, Guildford, UK

Hannant, D.J. (1978) *Fibre Cements and Fibre Concretes*, Wiley, Chichester, UK

Hannant, D.J., Hughes, D.C. and Kelly, A. (1983) Toughening of cements and other brittle solids with fibres. *Phil. Trans. R. Soc. Lond.* A, 310, 175–90.

Hibbert, A.P. and Hannant, D.J. (1982) Toughness of fibre–cement composites. *Composites,* 105–11.

Laws, V. (1971) The efficiency of fibrous reinforcement of brittle matrices. *J. Physics D: Applied Physics,* **4**, 1737–46.

Laws, V. and Ali, M.A. (1977) The tensile stress–strain curve of brittle matrices reinforced with glass fibre. *Fibre Reinforced Materials Design and Engineering Applications Conference*, Institution of Civil Engineers, London, pp. 101–9.

Chapter forty-two

Fibre-reinforced cements

42.1 Asbestos cement

Asbestos cement is familiar to all engineers as the ubiquitous roofing and cladding material which has had a very low cost and excellent durability during the past 100 years. A reason for its success has been the great durability of asbestos fibres which are shown in Figure 42.1. The fibres shown in this micrograph have been exposed to weathering for more than 10 years but the submicron fibres within the fibre bundle show no sign of deterioration. Other studies have shown that the strengths of the fibre bundles vary between 400 MPa and 1400 MPa irrespective of exposure up to seven years.

However, due to the well-publicised health hazards associated with asbestos fibres, which are known to be carcinogens, there has been a rapid decrease since 1980 in the UK in sales of asbestos cement sheeting products. Stringent safety precautions are essential not only during the manufacturing process but also to prevent inhalation of dust during cutting and drilling such sheets on site.

Another significant problem is that the material is brittle and the impact strength is notoriously low so that there are a number of deaths in the UK every year as a result of people falling through roofs when not using the required crawling boards.

The net result of these adverse factors has been to virtually eliminate sales of asbestos cement products in Europe and the USA but nevertheless there is still more asbestos cement on structures throughout the world than all other types of fibre cement combined and therefore a detailed description of its properties is warranted herein.

42.1.1 Mix design and manufacture

The proportion by weight of asbestos fibre is normally between 9 to 12 per cent for flat or corrugated sheet, 11 to 14 per cent for pressure pipes and 20 to 30 per cent for fire-resistant boards, and the binder is normally a Portland cement. Fillers such as finely ground silica at about 40 per cent by weight may also be included in autoclaved processes where the temperature may reach 180°C. Fibre volume, stress direction and product density all have an effect on properties and hence the properties depend to a certain extent on the manufacturer.

The most widely used method of manufacture of asbestos cement was developed from papermaking principles in about 1900 and is known as the Hatschek process. A slurry or suspension of asbestos fibre and cement in water at about 6 per cent by weight of solids is continuously agitated and allowed to filter out on a fine screen cylinder. The filtration rate is critical and coarser cement than normal (typically with a specific surface area of 280 m^2/kg compared with the normal value of

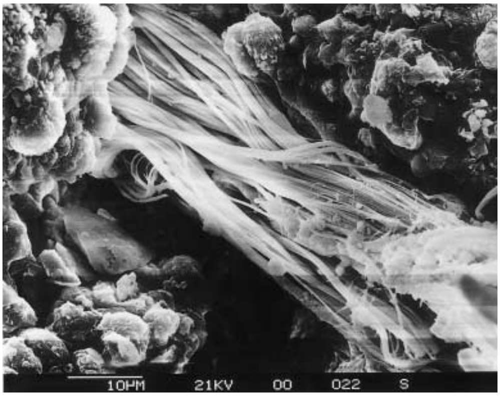

FIGURE 42.1 Asbestos fibre bundle in cement paste after natural weathering for more than 10 years.

320 m^2/kg) is used to minimise filtration losses. Referring to Figure 42.2, in very much simplified terms, the Hatschek machine operates as follows. A dilute slurry pours into the vat and drains through a porous sieve cylinder depositing the solid contents as a layer on the surface of the sieve. The water passes through the sieve surface and returns to the vat via the backwater circuit. The sieve cylinder rotates and the layer rises out of the vat. A continuous felt runs in a loop from the sieve cylinder to an accumulation roll. Surface tension forces the layer to transfer from the top of the sieve cylinder to the underside of the felt. The movement of the felt transfers the layer from the sieve to the accumulation roll and on the way it is vacuum dewatered.

Typical outputs are 1 tonne per hour per metre width of vat. Felt speeds range from 40 to 70 metres per minute. A typical three-vat machine will make a 6 mm thick sheet in six to nine revolutions and will make one sheet every 20 seconds.

Manufacturing costs are therefore very low. Due to the process, the fibres are essentially dispersed in two directions with the predominant alignment of the fibres in the direction of rotation of the sieve drum. The stacks of products may reach 60°C and autoclaving is sometimes used to reduce the shrinkage of the products.

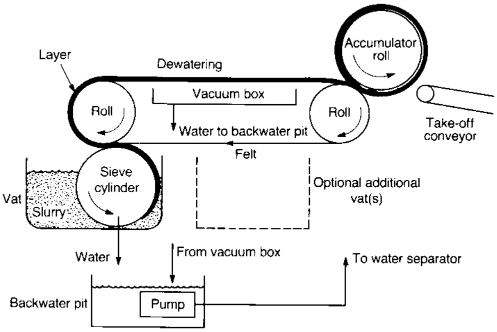

FIGURE 42.2 Hatschek manufacturing process for asbestos cement sheeting.

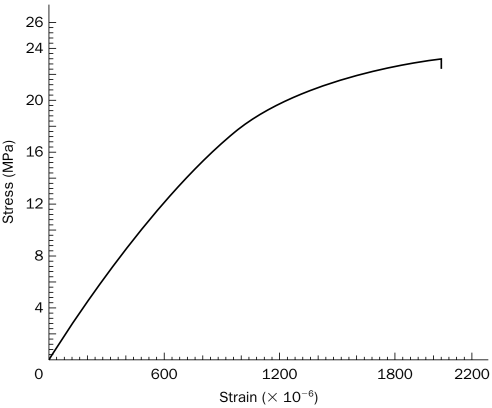

FIGURE 42.3 Tensile stress–strain curve for asbestos cement.

42.1.2 Properties

Asbestos cement is the only fibre composite for which there are International Standards requirements for certain properties. These are generally expressed in terms of minimum bending strength, density, impermeability and frost resistance. For instance, the minimum bending strength generally varies between 15 MPa and 23 MPa when tested under defined conditions and depending on whether the sheet is semi- or fully compressed.

Also, various loading requirements are defined for corrugated sheets such as snow loads up to 1.5 kPa, and point loads to simulate men working on a roof. Water absorption should not exceed 20 to 30 per cent of the dry weight depending on the type of product.

A typical tensile stress–strain curve for a commercial product is shown in Figure 42.3 where the failure strain is about 2000×10^{-6}. No cracks were visible before failure which may be controlled by crack suppression as described in Section 41.2. A modulus of elasticity of about 20 GPa in tension and compression and a modulus of rupture well in excess of 30 MPa have combined to provide probably the most successful example of all time of a fibre-reinforced composite both in terms of tonnage and profitability.

42.1.3 Durability

Asbestos cement is known to be very durable under natural weathering conditions and little deterioration in flexural properties takes place due to weathering, although the material becomes progressively more brittle.

However, it has been shown that asbestos fibres in cement sheets at ages of 2, 16 and 58 years do suffer a certain amount of corrosion which is compensated for, in terms of composite strength, by an increase in bond between the fibre and the cement. The corrosion of the fibre is promoted by the penetration of airborne carbon dioxide which causes carbonation at the surface of the fibre. Also, certain magnesium hydroxides and carbonates may be formed as reaction products. The natural variability in fibre strength tends to mask any measured changes in fibre strength due solely to weathering.

42.1.4 Uses

Corrugated roofing and cladding for agricultural and industrial buildings has formed by far the largest application, and the ability to be moulded into complex shapes has enabled a wide range of accessories to be produced for roofing applications. Flat sheet has been used for diagonal tiles to replace natural slate. Asbestos cement pressure pipes have been used for many years for conveying mains water, sewage, sea water, slurries and industrial liquors. Diameters range from 50 mm to 900 mm with working pressures from 0.75 MPa to 1.25 MPa. It is the extraordinary ability of the asbestos fibres to suppress cracking in the matrix which has made these watertight applications possible and no other fibre cement has been able to emulate its performance. Also, non-pressure fluid containers such as rainwater goods, conduits, troughs, tanks and flue pipes have accounted for a large proportion of the minor applications of asbestos cement.

42.2 Glass-reinforced cement (GRC)

Glass-reinforced cement is normally made with alkali-resistant glass fibre bundles combined with a matrix consisting of Ordinary Portland cement plus inorganic fillers. E-Glass fibres have been used with a polymer modified cement matrix to protect the glass against attack by the alkalis in the cement. The material described in this section relates to zirconia-based alkali-resistant fibres which are normally produced in the form of strands consisting of 204 filaments each of between 14 and 20 microns in diameter. Up to 64 strands may be wound together as a roving which is cut during the making of GRC into strands 12 mm to 38 mm long. Pre-chopped strands may be supplied in lengths as short as 3 mm. The individual filaments are bonded together in the strand by an organic 'size' which determines the physical nature of the end product. A photograph of a strand embedded in cement is shown in Figure 42.4.

The presence of zirconia (ZrO_2) in the glass imparts resistance to the alkalis in the cement because the Zr—O bonds, in contrast to the Si—O bonds, are only slightly attacked by the OH^- ions thus improving the stability of the glass network.

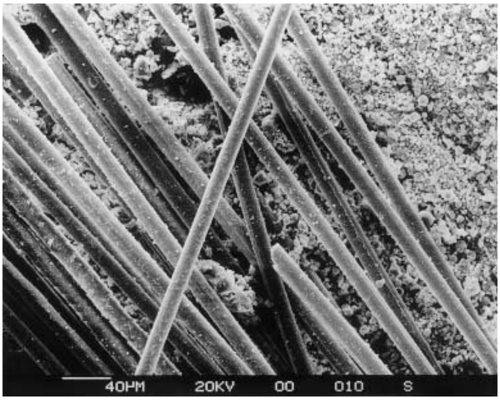

FIGURE 42.4 Glass fibre strand in cement paste.

42.2.1 Manufacture

Spraying and premixing are the main production processes for glass-reinforced cement.

In *spray processes* the cement/sand mortar slurry is fed to the spray gun and is broken into droplets by compressed air. Glass fibre roving is fed to a chopper on the spray head which chops the fibre into 25 mm to 40 mm lengths and injects them into the mortar spray to be deposited on the mould. The slurry mortar is typically 1:1 sand:cement ratio with a W/C ratio of 0.33. Admixtures are used to increase the workability and the resulting composite contains typically 5 per cent by weight of glass fibre.

The composite may be sprayed manually or by machine and some processes use dewatering by vacuum to result in an end product with a free W/C ratio of about 0.28 which has greater density and strength that the non-dewatered product.

Premixing processes, as the name implies, involve the blending together of cement, sand, water, admixtures and chopped strands in a mixer before placing in the mould. The fibres are added at the end of the mixing process at a lower speed to avoid damage. Typical mixes contain a sand:cement ratio of 2:3, a water:cement ratio of about 0.35, workability aids and, typically, 3 per cent by weight of 12 mm long fibres. Having been mixed, the composite may be cast by pumping with or without vibration and also by spraying. Pressing combined with dewatering may also be used with premixes.

Prebagged formulations containing between 0.5 per cent and 2.5 per cent by weight of glass fibre have also been developed for rendering brickwork or blockwork.

As with all cement-based products, it is important to moist cure glass-reinforced cement products for as long as possible to ensure that a maximum amount of hydration and hence strength gain has occurred before loading.

42.2.2 Properties

The tensile stress–strain curves for glass-reinforced cement will typically follow either of curves of type *A* or *B* in Figure 41.1. Curve type *A* is representative of the lower fibre volumes used in the premix composite where a single crack and no increase in the post-cracking stress is expected. Curve *B* is representative of the early age sprayed composite with more than the critical fibre volume at that age. This results in multiple cracking and a high failure strain as shown in Figure 42.5.

Fibre length, volume and orientation also affect the performance of the composite at 28 days in uniaxial tension (Ali *et al.*, 1975). The shape of the curves is approximated by the theoretical approach described in Section 41.1 and it can be seen that strength and strain to failure are both increased by increases in fibre length and volume. Nominal flexural tensile strengths may vary between 15 MPa and 50 MPa and follow the relationship between tension and flexure shown in Figure 41.11.

However, although the mechanical properties are good at early ages, the strength and toughness of some GRC formulations may change with time and hence design stresses are conservative. Typical design stresses quoted from trade literature are shown in Table 42.1. In this table, the difference in performance between sprayed and

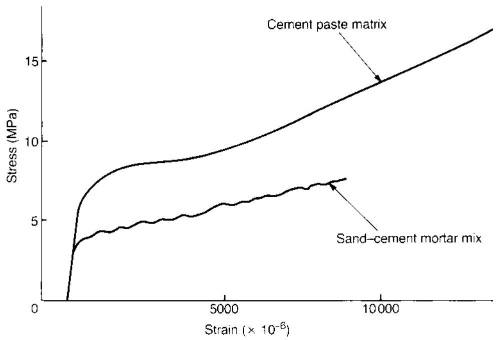

FIGURE 42.5 Tensile stress–strain curves of spray dewatered glass-reinforced cement (Oakley and Proctor, 1975).

premixed material due to fibre volume and orientation is demonstrated.

42.2.3 Durability

In the 1970s, the durability of GRC was found to be strongly influenced by the environment to which it was exposed (Majumdar *et al.*, 1991) For instance, in dry air, there was little change in flexural or tensile strength during a 10-year period, whereas under water or in natural weathering there was a decrease in tensile strength of the composite by more than 50 per cent. The decrease in impact strength was even more severe, reducing by an order of magnitude. The changes were due to a combination of factors including a loss in fibre strength and failure strain due to alkali attack, and an increase in matrix cracking stress due to continuing cement hydration which increases the critical fibre volume above the included fibre volume. Another contributing factor was the filling of the voids in the fibre bundles with lime crystals and calcium silicate hydrates which increased the bond with individual glass filaments so that matrix cracks easily propagated through the fibre bundle. The net result of these changes was to reduce the composite strain to failure, in some cases to matrix failure strain, thus reducing the once ductile material to a brittle material.

An example of the way in which the increase in matrix strength and reduction in composite strain to failure can affect the critical fibre volume and toughness of the composite is shown below using Figure 42.6.

For glass-reinforced cement, the following values have been published (Building Research Establishment, 1979):

28 days, $E_c = 22.5\,\text{GPa}$ with a bend-over point at 9.5 MPa, which gives $\epsilon_{mu} = 422{*}10^{-6}$, $\sigma_{fu} = 1000\,\text{MPa}$;

10 years, $E_c = 28.5\,\text{GPa}$, no accurate value for the bend-over point is given. If we assume no change in ϵ_{mu} and take σ_{fu} equal to 600 MPa after 10 years, equation (41.3) gives an increase in V_{fcrit} from 1 per cent at 28 days to 2 per cent at 10 years for aligned fibres.

Most glass-reinforced cement is sprayed with short fibres in a random (2-D) orientation. To

TABLE 42.1 Typical Cem-FIL GRC design stresses for different manufacturing methods (from trade literature)

Design value	*Loading example*	*Hand or premix*	*Machine spray*
Compression	compressive	12 MPa	12 MPa
Tension	cylinder hoop stress	3 MPa	2 MPa
	bending of sandwich panels		
Tension/bending	bending of box sections or channels	4 MPa	2.5 MPa
Bending	bending of solid beams or plates	6 MPa	4 MPa
Shear	shear loading	1 MPa	1 MPa

Note: These design values may be varied in certain product areas, e.g. formwork. Limit state methods are also used.

take account of the non-alignment, we multiply the value of σ_{fu} by 0.27 (the efficiency factor for stress) and find that a total fibre volume fraction of more than 3.5 per cent at 28 days, and more than 7.4 per cent at 10 years is required to maintain ductility. Typical total fibre volumes are about 4 per cent and it is known that the energy absorbed to failure, found from the area under the measured stress–strain curve, reduces from about 120 kJ/m^3 at 28 days to less than 5 kJ/m^3 at 5 years. This change may therefore be explained by the increase in critical fibre volume with time.

An understanding of these potential problems resulted in research to eliminate calcium hydroxide growth by including a metakaolin synthetic pozzolana (described in Chapter 15) to react with the free lime in a controlled way to prevent lime build up within the fibre bundle. The metakaolin particles also appear not to migrate into the fibre bundle. Results from these modified matrices using accelerated tests have indicated that greatly improved durability and long-term toughness of GRC composites should now be possible using about 25 per cent cement replacement by metakaolin. Thus, long-term stable properties for metakaolin-based matrices approximate to curve *A* in Figure 42.6 rather than the embrittled curve type *B*. In contrast, silica fume with a particle size of less than 0.1 micron, although reacting with the lime, may penetrate to individual filaments and result in the formation of hard calcium silicate hydrates which are as damaging to the fibres as lime deposition.

However, a note of caution should be made regarding the long-term predictive ability of high-temperature accelerated tests because, as with many durability problems with cement-based materials, total confidence can only be gained by 'real time' trials in natural weathering conditions over many years.

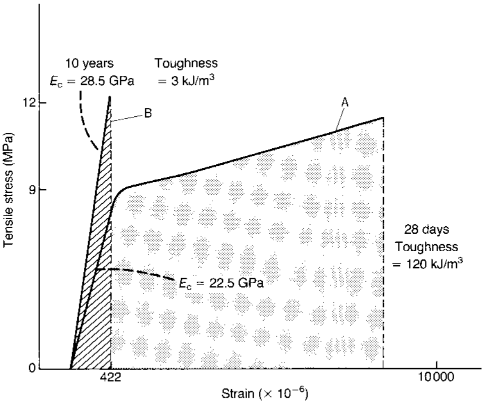

FIGURE 42.6 Effect of natural weathering on the toughness of glass-reinforced cement.

42.2.4 Uses

Cladding panels are a major field of application for glass-reinforced cement. Due to cracking caused by restrained warping in early applications particular attention should be paid to thermal and moisture movements and to fixing details in large, double-skinned sandwich panels of this type of construction. Light colouring of the panels is preferred because this helps to reduce thermal stresses particularly where there is an insulating core. There is increasing emphasis on the use of single-skin cladding panels attached to prefabricated steel frames by flexible anchors. This is known as a GRC Stud Frame system. The fixings are designed to allow unrestrained thermal or moisture movements of the glass-reinforced cement skin which may be 6 m long by storey height.

An important use where the early age strength and toughness are beneficial is in permanent formwork for bridge decks, the advantage being that no temporary support works are required and a dense, high-quality cover is provided to the reinforcement.

The greater efficiency ensured by using continuous glass fibre rovings in the main stress direction has been utilised in a process for producing corrugated sheeting. The corrugated sheets start as a continuous flat sheet made from two layers, each 3.25 mm thick. Short strands as cross reinforcement are immersed in the matrix on the upper/underside and this leads to an ideal sandwich structure. The lengthwise reinforcement is mostly made up of one-directional inlaid glass fibre rovings, which are sandwiched between the two layers that make up the sheet. The flat sheets are then corrugated on formers before curing.

There are many other uses such as cable ducts, agricultural products, sewer linings, culverts, sound barriers, drainage channels, fire-resistant boards, septic tanks, roofing slates and mortar renders for dry block wall construction. Some trials have been made using glass fibre tendons protected with polyester resin as prestressing tendons in prestressed concrete structures.

42.3 Natural fibres in cement

The use of natural cellulose or vegetable fibres in cement or mortar products is common in both ‘developed’ and ‘developing’ countries and the subject has been reviewed in detail by Swamy (1988) and Bentur (1990).

42.3.1 Wood fibre products

Manufacture

In developed countries the bulk usage is for wood cellulose fibres from trees. The wood is mechanically and chemically pulped to separate the individual fibres which may be between 1 mm and 3 mm long and up to 45 microns in width. Hardwoods and softwoods are used and the elastic modulus of individual fibres may vary between 18 GPa and 80 GPa with strengths between 350 MPa and 1000 MPa depending on the angle of cellulose chains in the cell wall. Cellulose fibres produced from timber have several advantages when used in thin cement or autoclaved calcium silicate sheets. The fibres are low cost compared with most man-made fibres, they are a renewable resource, there is considerable experience in the use of such fibres in existing plant for asbestos cement, and they have an adequate tensile strength for cement reinforcement. However, cellulose is sensitive to humidity changes and the elastic modulus of the fibres reduces when wet so that the properties of the composite may vary considerably from dry to wet. The fibres are used in volumes up to 10 per cent in conjunction with polymer fibres in asbestos-free products in which manufacturing procedures are very similar to the Hatschek process already described for asbestos cement.

Properties

When suitably pre-treated by refining, wood fibres used in conjunction with polyvinyl alcohol fibres in a matrix of Portland cement and fillers can provide a tough and durable fibre cement. This composite is suitable for the commercial production of corrugated sheeting and pressed tiles on traditional slurry dewatered systems such as the Hatschek machine (Figure 42.2). The variation in composite properties wet to dry and pressed to unpressed is shown in typical tensile stress–strain curves for commercial composites in Figure 42.7.

Uses

In Australia, cellulose fibres have completely replaced asbestos fibres in flat sheeting products made from an autoclaved calcium silicate. Autoclaved systems are said to have the advantage over air-cured hydrated cement binders in that there is greater dimensional stability in relation to moisture and temperature movements. Also because of the absence of free alkalinity the boards can be more easily decorated. In the UK, flat sheet for internal and external applications has been available for a number of years, produced from cellulose fibres in an autoclaved calcium silicate matrix. A wide range of properties is available in cellulose fibre boards, typical values being an elastic modulus of 12 GPa with the tensile strength varying between 6 MPa and 20 MPa and the modulus of rupture between 15 MPa and 30 MPa depending on whether the composite is wet or dry and on the fibre volume. Typical tensile stress–strain curves in the dry and wet states for these materials are shown in Figure 42.8.

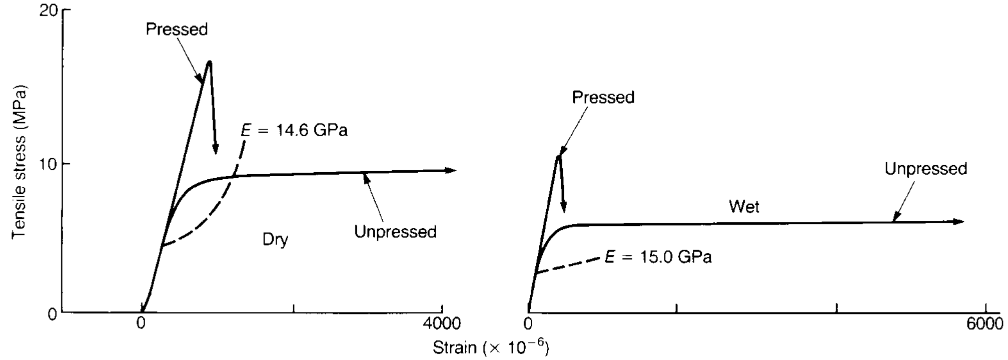

FIGURE 42.7 Effect of moisture condition on the tensile properties of a cement composite containing cellulose fibres and artificial fibres – pressed, unpressed.

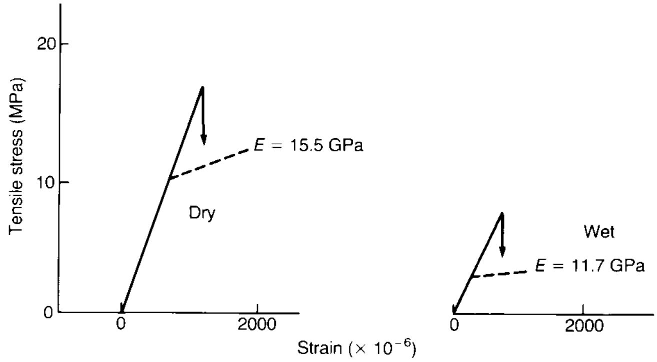

FIGURE 42.8 Effect of moisture condition on tensile properties of autoclaved calcium silicate containing cellulose fibres.

Wood cellulose fibres in concrete

Wood cellulose fibres are not suitable for use in bulk concrete applications because of difficulties in mixing and compaction and their use is therefore limited to automated factory processes. In some of these processes wood chips or flakes at up to 20 per cent are mixed with cement and fine sand to make a variety of compressed wood chip boards or particle boards. These are generally used internally and have low flexural tensile strength, often below 1 MPa. They are not strictly fibre-reinforced cements.

42.3.2 Vegetable fibre products

The use of vegetable stem fibres in developing countries is generally aimed at producing cheap but labour-intensive, locally constructed cement-based roof sheeting often of corrugated or folded plate design. Long fibres which are indigenous to the locality are used, such as akwara, banana, bamboo, coir, elephant grass, flax, henequen, jute, malva, musamba, palm, plantan, pineapple leaf, sisal, sugar cane and water reed. Lengths of fibres may be up to 1 m or more and are hand placed in a matrix of sand and cement. Corrugated sheets of up to 2 m by 1 m in size of 6–10 mm thickness and tiles may be produced with fibres in preferential directions.

Manufacture and applications

Composites made from vegetable stem fibres are manufactured by simple hand lay-up processes which are potentially suitable for low-cost housing applications.

In these applications the fibre content is usually less than 5 per cent when applying mixing technologies, but it may be greater when using the technologies of hand lay-up of long fibre rovings. Hand laying involves the application of a thin mortar layer on a mould, followed by alternate layers of fibres and mortar matrix. The fibres can be rolled into the matrix or worked into it manually, and the process may involve some vibration. In the mixing technique, there is a limit to the content and length of fibres that can be incorporated, since as with any other fibres workability is reduced. However, many of the natural fibre composites are intended for the production of thin components such as corrugated sheets and shingles, and for these applications there is a requirement for both plasticity and fresh strength that will permit the shaping of the product. For such purposes, reduced flow properties are not as detrimental as in the case of conventional concrete. In these components, which have a typical thickness of about 10 mm, the matrix is a cement mortar, and the mix with fibres, or with hand-laid fibres, is spread on a mould surface and then shaped. Corrugation can be achieved by pressing between two corrugated sheets.

Properties

The cracking stress and strength of the composites are not greatly increased compared with the unreinforced matrix (i.e. about 1 MPa to 3 MPa) but the fibres enable the sheets to be formed in the fresh state and handled and transported in the hardened state. Considerable toughness is achieved in the short term.

Bamboo, when split into strips and woven into meshes, has been used as reinforcement for a variety of applications from roads and structures to water tanks. Tensile strengths of the fibre are commonly in excess of 100 MPa with elastic moduli between 10 and 25 GPa. Toughening and post-cracking performance are the most important characteristics and optimum fibre volumes between 1.5 per cent and 3 per cent have been quoted.

Durability

The high alkalinity of the pore water prevents microbiological decay in the fibres but, to set against this, the calcium hydroxide penetrates the fibre to mineralise or petrify it. The high alkalinity can cause severe reduction in fibre strength but where carbonation has penetrated, this rate of reduction of strength is reduced. However, natural stem fibres are not expected to give the composite a long lifetime, although short cellulose fibres as used in alternatives to asbestos cement products have been shown to be more durable than natural stem fibres.

42.4 Polymer fibre-reinforced cement

The inclusion of polymer fibres into cement-based products is potentially a very large world-wide market. For instance, about 90 countries have produced asbestos cement for cladding, roofing or pipes and about 3.5 million tonnes of asbestos fibre have been used annually in the asbestos cement and building products industries, giving about 28 million tonnes of products. This market will either be lost to other products or man-made fibres will be substituted for the asbestos fibres. It is clear therefore that there is a potential market and considerable inroads have been made since the early 1980s by polymer fibres into this industry.

Although a wide variety of polymers has been used on a trial basis in cement-based materials, only a few have been commercially successful. Polypropylene and polyvinyl alcohol have been the most used although polyethylene pulp is also used in some thin sheet products.

42.4.1 Chopped polypropylene films

Chopped polypropylene films have been used at fibre volumes of 3 per cent to 5 per cent to produce alternative products to asbestos cement with some modifications being required to the traditional machinery.

The polypropylene in this case was specially stretched and heat treated to give elastic moduli of 9 to 18 GPa with tensile strengths from 500 to 700 MPa and ultimate strain of 5 to 8 per cent. Various surface treatments to improve wetting of the films and increase their bond were carried out before splitting the tape and chopping into lengths between 6 and 24 mm to give fibres with a basically rectangular cross-section but with frayed edges.

42.4.2 Continuous opened polypropylene networks

Layers of networks of continuous polypropylene films, as shown in Figure 42.9, in combination with continuous glass fibre rovings have been used commercially in fine grained cement-based materials to produce alternative products to asbestos cement. The advantage of this system is that the full fibre strength of both fibres is used because there is no pull-out and excellent mechanical bonding in the polypropylene is achieved by virtue of the uneven micro- and macro-slits in the films and the many fine hairs produced in the production process. Also it has been found that there is a synergistic interaction between the fibre types so the performance of each fibre is enhanced by the presence of the other fibre.

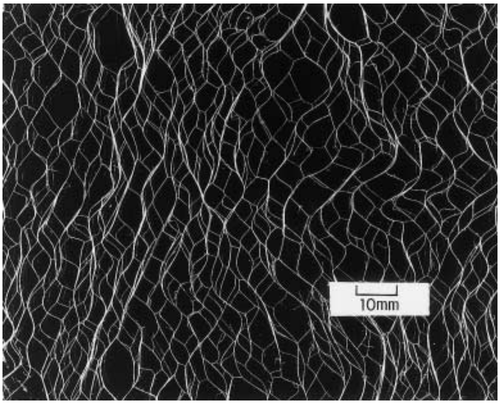

FIGURE 42.9 Polypropylene networks.

Manufacture

The continuous networks are laid up in two directions in twelve-layer packs. Three or four packs are fed simultaneously to a machine which impregnates them with cement slurry in sequence, producing a wet, flat sheet with good two-dimensional strength. This is then corrugated in a vacuum corrugator. Both chopped and continuous glass fibres can be included in the process.

Properties

All the requirements for roofing sheet can be met and additionally, toughness values of 1000 kJ/m^3 are possible. The failure strain remains in excess of 5 per cent after weathering, provided that the critical fibre volume is exceeded at the appropriate age.

Durability

Polypropylene fibres show excellent resistance to alkalis and in a cement matrix have been shown to have good resistance to a variety of weathering

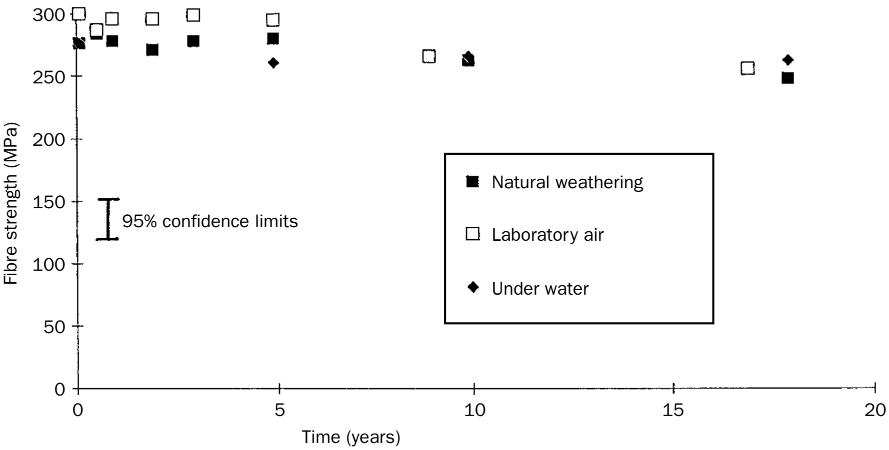

FIGURE 42.10 Durability of polypropylene networks in cement.

conditions up to 18 years of real time exposure (Figure 42.10). Equally important is that the bond strength has been shown to be time stable up to 18 years (Hannant, 1999), giving confidence in the long-term toughness of polypropylene fibre composites.

42.4.3 Polyvinyl alcohol fibres (PVA)

High-strength and stiffness PVA fibres are used widely as an asbestos replacement in asbestos cement products. However, taken by themselves in a cement slurry, they offer little retention of the cement grains and hence must be used in conjunction with cellulose pulp to keep the cement in the system as water is sucked out by vacuum. The fibres are treated on the surface to enhance their compatibility with the matrix, the quantity of fibres being typically 3 per cent by volume. Flexural strengths of the sheeting are adequate to meet the requirements of the appropriate European standards. Alkali resistance has been stated to be excellent and the fibres can survive exposure to temperatures of 150°C without loss in strength.

42.4.4 Polyethylene pulp

Polyethylene pulp made from short fibres has mainly been used as a cement retention and drainage aid as a substitute for asbestos fibres in Hatschek type process for the manufacture of thin sheet products. Up to 12 per cent by volume has been used and at this level improvements in flexural strength and ductility have also been observed. Because the fibres do not swell in the presence of water, the durability of the products is said to be improved in comparison with similar systems using cellulose fibres.

42.4.5 Continuous networks of high-modulus polyethylene fibres

Highly orientated polyethylene fibres may be produced by gel spinning or high draw ratios and fibres have been produced with the elastic modulus of glass and the strength of steel. Commercial fibrillated tapes with initial elastic moduli of about 30 GPa have been used in thin cement sheets in a similar fashion to polypropylene nets.

Durability in alkalis is expected to be good but the films which have been available have suffered from high creep strain in comparison with polypropylene.

42.5 References

Ali, M.A., Majumdar, A.J. and Singh, B. (1975) Properties of glass fibre cement – the effect of fibre length and content. *J. Materials Science*, 10, 1732–40.

Bentur, A. and Mindess, S. (1990) *Fibre Reinforced Cementitious Composites*, Elsevier Applied Science, London and New York.

Hannant, D.J. (1999) The effects of age up to 18 years under various exposure conditions on the tensile properties of polypropylene fibre reinforced cement composites. *Materials and Structures, RILEM*, 32, March, 83–8.

Oakley, D.R. and Proctor, B.A. (1975) Tensile stress–strain behaviour of glass fibre reinforced cement composites. In *Fibre Reinforced Cement and Concrete*, Construction Press Ltd, Lancaster, UK, pp. 347–59.

Swamy, R.N. (ed.) (1988) *Natural Fibre Reinforced Cement and Concrete*, Vol. 5, Concrete Technology and Design, Blackie, Glasgow.

Chapter forty-three

Fibre-reinforced concrete

43.1 Steel fibre concrete

Concrete reinforced with chopped steel fibres in volumes generally less than 1 per cent has a tensile stress–strain curve of the type shown as *OXA* in Figure 41.1. The reason for this is that it is physically very difficult to include sufficient fibres in the mix to exceed the critical fibre volume which, for short random 3-D oriented fibres, is twice the value given by equation (41.4).

This critical fibre volume for short steel fibres generally exceeds 2 per cent. Apart from the economics, it is physically difficult to include these fibre volumes because concrete contains about 70 per cent by volume of aggregate particles which obviously cannot be penetrated by fibres. Also, the fibres tend to end up in a three-dimensional random distribution when mixed in a rotary mixer which, together with their short length, makes them very inefficient at reinforcement in any given direction of tensile stress. Nevertheless, useful properties in the composite have been achieved by many practical, if rather specialist, systems.

A great variety of fibre shapes and lengths are available depending on the manufacturing process, a few of the more common types being shown in Figure 43.1. Cross-sectional shapes include: circular (from drawn fibres); rectangular (from slit sheet or milled from ingots); sickle shaped (from the melt extract process); and mechanically deformed in various ways to improve the bond strength. Fibre lengths range from 10 to 60 mm with equivalent diameters between 0.1 and 1.0 mm. Mild steel, high-tensile steel and stainless steel fibres are available.

It should be realised that the average fibre pull-out length is 1/4 which, for the longest 60 mm fibres, is only 15 mm. This length is insufficient to allow efficient use to be made of the high tensile strength of drawn wire unless devices such as bends or crimps are used to improve anchorage efficiency.

43.1.1 Mix design and composite manufacture

In the early development of steel fibre concrete, mixing problems often occurred with balling up of fibres in unsuitable mixes. These problems have now largely been resolved by an appropriate choice of fibre type and volume although inappropriate mix designs and poor introduction of the fibres to the mix can still cause balling problems. Advice on mix proportions for specific fibre types and volumes is readily available from fibre manufacturers.

Mix designs for rotary mixers generally recommend the use of fibres with an equivalent length/diameter ratio of 70 or less, and typical weights of fibre are between 25 kg/m^3 and 60 kg/m^3. These weights are equivalent to fibre volumes between 0.3 per cent and 0.8 per cent.

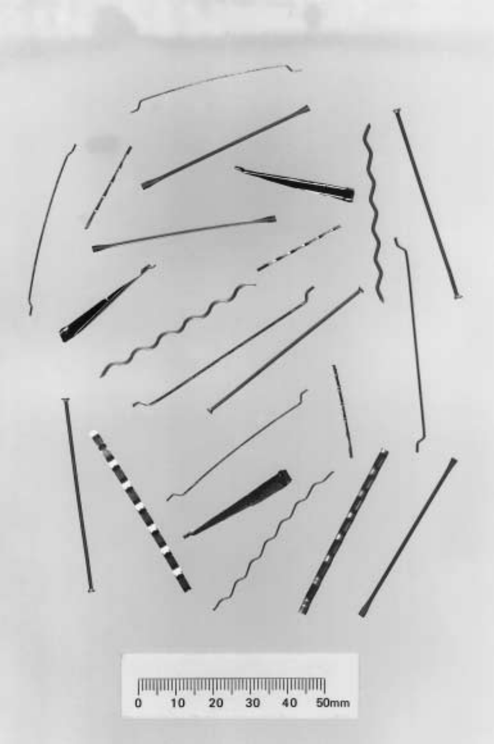

FIGURE 43.1 Steel fibres showing a variety of types of mechanical deformation.

It is important to use a relatively high proportion of fines, for example a typical mix may contain 800 kg/m^3 of river sand and 300 to 350 kg/m^3 of cement, often with the further addition of pulverised fuel ash. Aggregates larger than 20 mm should be avoided, and it is preferable to limit the aggregate fraction larger than 14 mm to 15 per cent to 20 per cent. Free water cement ratios of less than 0.55 are preferable and workability is commonly improved by the addition of plasticisers or superplasticisers to give slumps of more than 100 mm.

It is unfortunate that workability is reduced by an increase in fibre volume and equivalent length/diameter ratio (l/d ratio) because the post-cracking tensile strength of the composite (equations (41.24), (41.25), (41.26)) is improved by an increase in both these parameters.

Therefore the requirements of reinforcement and workability act against each other and a compromise must be reached usually at l/d ratios between 40 and 70 with fibre lengths between 20 mm and 60 mm.

Generally the fibres are added last to the fresh concrete, care being taken to ensure that no clumps are added and the fibres are rapidly removed from the entry point to the mixer. Alternatively they may be added onto the aggregate on the conveyor belt. Proprietary systems exist for introducing fibres into a ready-mix truck by blowing the individual fibres at high velocity into the back of the truck. Collated fibres with a water soluble glue also considerably assist the batching and mixing actions with bags of fibres being added to the mixer drum, the paper bags themselves also being water soluble.

Guniting or sprayed steel fibre concrete is another manufacturing process which is widely used for tunnel linings and rock slope stabilisation. Fibre lengths typically range from 25 mm to 40 mm. As with normal concrete, the greater the fibre aspect ratio and fibre volume, the better is the performance of the sprayed concrete but the more difficult it is to mix, convey and spray. Mixes generally have less than 10 mm maximum sized aggregate with cementitious contents in excess of 400 kg/m^3 and fibre contents between 30 kg/m^3 and 80 kg/m^3. Cement replacements and admixtures are widely used.

In a third manufacturing process known as SIFCON fibre volumes up to 20 per cent are preplaced into a mould before mixing and are then infiltrated with a fine-grained cement-based slurry. This gives very high strength and toughness in localised regions such as beam/column intersections. Flexural strengths up to 60 MPa and tensile strengths up to 16 MPa are said to be possible with this system.

43.1.2 Properties

Steel fibres provide virtually no increase in the compressive or uniaxial tensile strength of concrete. The main benefits in uniaxial tension result from the control of crack widths due to shrinkage or thermal effects in slabs and tunnel linings and this is not an easily quantifiable parameter but relates to post-cracking fibre pull-out forces. Post-cracking uniaxial tensile strengths of 0.4 to 1.0 MPa are possible at commonly used fibre volumes, at crack openings up to about 2 mm.

The relationship between tensile strength and flexural strength for various fibre volumes is shown in Figure 43.2 from which it can be seen that at the fibre volumes commonly used in practice of less than 0.8 per cent, the increase in post-cracking flexural strength is rather limited. Nevertheless, this post-cracking flexural strength, which results from the increased area of the tensile part of the stress block, as shown in Figures 41.8 and 41.9, is a most important part of the commercial uses of steel fibre concrete, enabling reductions of thickness to be made in sections subject to flexure or point loads. Typical stress/deflection curves for beams are shown in Figure 43.3 and demonstrate the post-cracking characteristics in bending which result from the ductile characteristics of the tensile stress block even though the fibre volume is less than the critical fibre volume in tension. Impact strength and toughness are greatly increased, the increased toughness resulting from the increased area under the load deflection curve in tension and flexure. A variety of toughness indices have been proposed in the literature depending on the flexural deflection which is chosen to represent a typical serviceability limit. Improved fatigue resistance is often claimed but this is a complex parameter which depends so heavily on fibre type and volume that no generalised improvements can be stated.

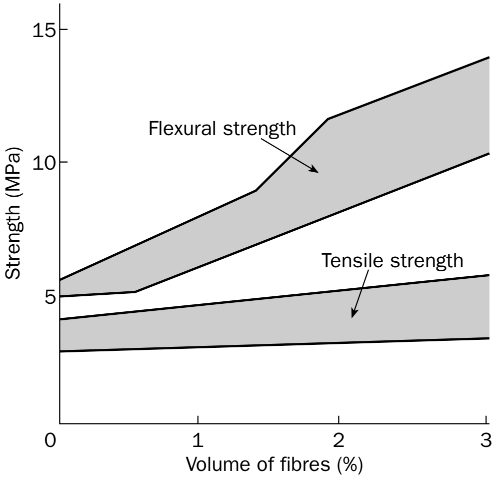

FIGURE 43.2 Typical direct tensile and flexural strengths of steel fibre-reinforced concrete and mortar (Edgington, 1973).

43.1.3 Durability

Steel fibres are generally well protected in uncracked concrete where the high alkalinity provides a passive layer on the fibre surface. Even when the fibres are near the surface in a carbonated zone, serious corrosion takes many years to occur and surface spalling is rare. It may be that the short fibre length results in a more or less uniform potential adjacent to the fibre which

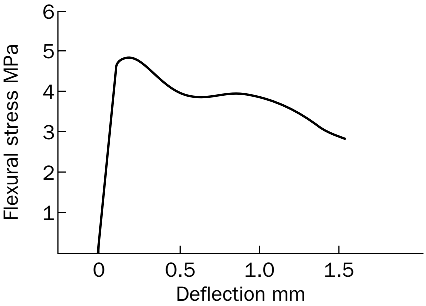

FIGURE 43.3 Typical stress–deflection curve for 40 kg/m^3 of steel fibres in a 100 mm square beam at 400 mm span.

limits the setting up of corrosion cells. Any fibres protruding from a concrete surface will readily corrode or wear away and have not been found to give significant problems.

The main durability problem is likely to occur where load-bearing carbon steel fibres are exposed across cracked sections in the presence of chlorides, where they will readily corrode and it would be wise in such conditions to use stainless steel fibres. If these precautions are not taken, the mode of failure in cracked concrete subject to water and chlorides will eventually change from ductile with fibre pull-out, to brittle with fibre fracture and this sudden change will not be predictable by the extrapolation of real time data from durability experiments.

43.1.4 Applications

A major use of steel fibres in the developed countries is to use them as a replacement for conventional steel mesh in industrial ground floor slabs. Fibre weights of between 15 kg/m^3 and 60 kg/m^3 are commonly used in floor thicknesses between 120 mm and 200 mm. The fibres are particularly beneficial in the laser screed process (Figure 43.4) for large area pours (>1000 m^2/day) because they avoid interruptions to the construction process caused by placing formed joints and mesh reinforcement. Joints are normally still necessary and induced joints should be cut to about 1/4 of the slab depth with a diamond saw within the first 24 hours after casting at between 5 m and 10 m centres. Alternatively, where joints have to be formed, steel-edged permanent shutters with lateral movement capability are beneficial in preventing edge breakdown. When sawn joints have formed due to restrained contraction, the fibres restrict joint opening and maintain aggregate interlock at the joint surface. Also when subjected to flexural stresses, the load at which cracks become visible on the top surface can be increased compared to plain concrete slabs.

The main advantages claimed by specialist users of the laser screed process are: elimination of mesh which makes faster, more simplified construction, reduction of manpower costs, saving of dowel bars, tie wire, etc., better performance of joint arises induced by diamond blade cutting, and more uniform joint opening than when no mesh or fibres are used.

FIGURE 43.4 Laser-screed machine placing a steel fibre-reinforced concrete floor (by permission of Bekaert Building Products).

The typical stress maintained across a joint after cracking may be calculated from equation (41.26), i.e. for 30 kg/m^3 of steel fibres, 60 mm long by 1 mm in diameter with a bond strength $\tau = 4$ MPa, the post-cracking tensile strength σ_{cu} will be:

$$\sigma_{cu} = \tfrac{1}{2} V_f . \tau . \frac{l}{4} . \frac{P_f}{A_f} \qquad (41.26)$$

$$V_f = 30/7860 = 0.0038$$

$$\therefore \sigma_{cu} = 0.5 \times 0.0038 \times 4 \times \frac{60}{4} \times \frac{\pi \times 1}{\pi \times 1^2}$$
$$= 0.46\,\text{MPa}$$

This theoretical post-cracking strength is supported by experimental studies of stresses sustained across induced cracks. This apparent composite post-cracking strength is equivalent to a force of about 75 kN/m (7.5 T/m) width of a 200 mm thick ground floor slab sawn to a depth of 50 mm to induce cracks. This force can be compared with a force of 65 kN/m (6.5 T/m) width supplied by a typical mesh reinforcement consisting of one layer of fabric. Hence the replacement of fabric with steel fibres for the control of induced crack widths appears to be a practical proposition.

There are a few specialist systems in which the need for saw cut joints is eliminated completely and this prevents any problems with curling or spalling of the slabs.

Other uses of mild steel fibres with conventional mixing and compaction techniques have included hydraulic structures such as spillways and sluices, airfield pavements and precast components such as segments for tunnel linings. When overlaying concrete roads, an isolating layer of 30 mm of asphalt has been found to be important and bonding the new and old work together is a critical part of the operation. Joints between 10 m and 15 m are essential and reflected cracks must be expected. However, performance has been shown to be very good when properly designed and constructed.

Another major application of steel fibre concrete is in situ tunnel lining and rock slope stabilisation using the gunite technique and the use of steel mesh in these situations is being steadily replaced.

One of the most successful uses of stainless steel fibres has been in castable refractory concretes for use at temperatures up to 1500°C. In these products, aluminous cement is used and initial cost is not the prime consideration provided that product life can be increased, typically by 100 per cent.

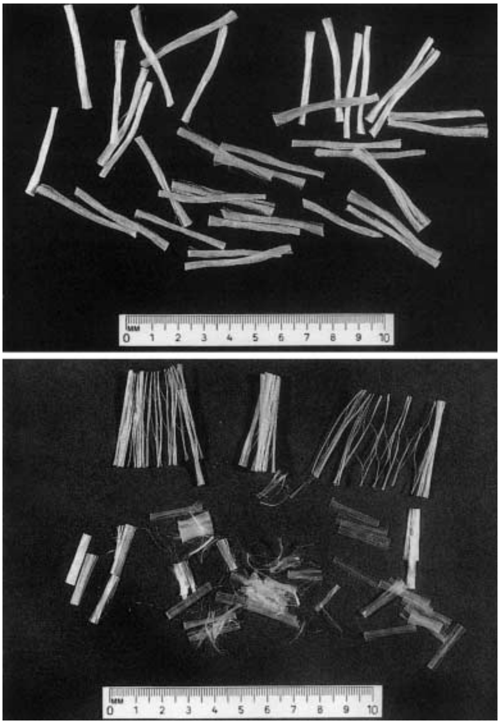

FIGURE 43.5 Types of chopped polypropylene fibres: (a) twisted twine; (b) untwisted.

43.2 Polypropylene fibre-reinforced concrete

Extensive use has been made in the construction industry of small quantities (0.1 per cent by volume) of short (<25 mm long) fibrillated or monofilament polypropylene fibres as shown in Figure 42.15 (b) to alter the properties of the fresh concrete. Fresh concrete means in the first four or five hours after mixing, either before or just after the concrete has stiffened but could not be described as hardened. 'Reinforcement' is probably not a correct term to use to describe the effects of the fibres and there is no theoretical treatment which adequately predicts their effects. Also, the type of polymer from which the fibre is formed is probably not very important because little use is made of the fibre stiffness or strength during this critical initial period and alkalis have had no time to cause damage. The description of their mode of action is therefore mainly qualitative.

Claims made for the benefits endowed by these small volumes of fibres include:

- reduction in sedimentation and plastic shrinkage;
- elimination of the need for crack control steel mesh;
- increases in strength, durability, impact and abrasion resistance.

The other type of polypropylene used for many years is chopped twisted fibrillated twine (Figure 43.5 (a)) typically in volumes of 0.44 per cent in

40 mm lengths. This fibre has only been used for precast products subject to impact loading such as pile shells.

43.2.1 Mix design and manufacture

In the most used mixes the fibre volume is so low (typically 0.1 per cent) that mixing techniques require little or no modification from normal practice. Usually, the fibre comes prepackaged in 0.9 kg water-soluble bags which are placed in the mixer for each cubic metre of concrete mixed. The fibres are released and dispersed during the normal mixing cycle. For the higher fibre volumes containing chopped twine, about 30 seconds of mixing time is recommended to prevent the fibre bundles from breaking down into individual elements.

Water-soluble bags containing a combination of steel and polypropylene fibres are also marketed; these give some of the benefits of each fibre type.

43.2.2 Properties of fresh concrete

As discussed in Chapter 18, badly made and cured concrete may suffer from sedimentation of the aggregate particles with consequential bleeding of water to the surface of the cast layer. With excessive sun or wind, this water may rapidly evaporate with an increase in suction and shrinkage on a horizontal surface which can cause substantial cracks to form, known as plastic shrinkage cracks. Some tests have shown that small quantities of fibres in the mix increase the cohesion and prevent sedimentation due to their interlocking network characteristics. The result may be that in some, but not all cases, the quantity of bleed water may be reduced. This will not necessarily have a beneficial effect on plastic shrinkage cracking but may help to limit plastic settlement cracking. The small reduction in bleeding where this is validated is unlikely to be due to the additional specific surface area of the fibres because a similar surface area increase could also be gained by an additional 1 kg/m^3 of cement.

43.2.3 Plastic shrinkage cracking

This is a topic which is so complex that there is no agreed mechanism for plain concrete let alone an understanding of the effects of fibres. However, it is an area where the earlier theory can indicate some possibilities.

For plastic shrinkage cracks to occur, it is presumed that the tensile stress exceeds the concrete tensile strength, which is very low during the first 4 hours. It has been found that typical concretes may have a tensile strength of about 0.02 N/mm^2 at 4 hours. In order that the cracking stress of 0.02 N/mm^2 should be sustained by 0.1 per cent of random fibres, the fibre stress can be calculated from:

$$\sigma_f = 2 \cdot \sigma_c / V_f = 2 \times 0.02/0.001 = 40\,\text{MPa} \quad (43.1)$$

Sufficient bond stress with the polypropylene can be developed during the first 4 to 5 hours after placing for fibre stresses of this order to be developed so that the width of plastic shrinkage cracks can be limited by fibres. The fibres also endow the concrete with some post-cracking ductility and increased strain capacity at these very early ages which could influence plastic shrinkage cracking.

43.2.4 Properties of hardened concrete

For a system containing 0.1 per cent by volume of polypropylene fibres it can easily be shown theoretically that the fibres will have little measurable affect on the tensile or flexural strength of hardened concrete and that they cannot be considered as a primary reinforcement. This is because the most optimistic estimate of critical fibre volume from a rearranged equation (43.1) is for the unlikely case of all fibres breaking (rather than pulling out) at a stress of 400 MPa. Thus for a typical concrete tensile strength of 3 MPa

$$V_{fcrit} = 2 \times 3/400 = 1.5\%$$

More realistically σ_f ~200 MPa and hence V_{fcrit} ~3%.

The actual post-cracking stress for 0.1% V_f will depend on the fibre–cement bond strength.

Assuming that an average fibre stress of 200 MPa can be sustained then

$$\sigma_{cu} = \frac{V_f}{2} \cdot \sigma_f \sim \frac{0.001}{2} \cdot 200 \sim 0.1\,\text{MPa}$$

thus giving minimal post-cracking strength in the hardened state.

This estimate is supported by experimental evidence where the maximum pull-out force across a pre-formed crack is about 0.15 MPa. In a ground floor slab of the same dimensions as described for steel fibres this would result in a restraining force of only 22.5 kN/m (2.25 T/m) width, which is much less than for the steel fibre case.

Systems using 0.44 per cent by volume of polypropylene twine, as in shell piles and marine defence units, contain sufficient volume of fibre to increase the impact strength of the concrete by holding cracked sections together to enable them to withstand further impacts. The tensile and bending strengths are virtually unchanged but greater ductility and toughness in the post-cracking zone compared with plain concrete can be achieved.

43.2.5 Durability

Polypropylene is extremely resistant to the alkalis in concrete and the concrete matrix protects the fibres from ultra-violet light which otherwise would cause chain scission and degradation. Little change in fibre strength has been observed up to 18 years in a variety of exposure environments (Figure 42.10) and accelerated tests have predicted a lifetime considerably in excess of 30 years. However, for the early age properties, the durability of the fibres is not critical and it is only second order effects on hardened properties which are affected by fibre durability. An important consideration for the long-term toughness of fibre concrete in general is the potential increase in bond strength with time which could lead to fibre fracture rather than fibre pull-out, thus reducing the toughness. However, for fibrillated films, the bond strength has been shown to be time stable, thus giving increased confidence in long-term composite performance.

43.2.6 Applications

Regardless of the theoretical technical merits of using 0.1 per cent by volume of polypropylene fibres, there is an increasing use in the industrial ground floor industry for similar reasons as for steel fibre concrete. Also, an indication of its growing use in general construction is that nearly 10 per cent of ready-mixed concrete in the USA contains polypropylene fibres.

Concrete containing 0.44 per cent by volume of chopped twine has been extensively used since 1970 in piling shells, and in two tonne blocks as sea defences. This type of application where impact loads form a substantial proportion of the applied stress is likely to remain a useful and continuing specific use for chopped polypropylene twine.

43.3 Glass fibre-reinforced concrete

There are few uses for glass fibre reinforcement in bulk concrete because the cost of including a sufficient quantity of random glass fibre would rarely be cost effective. Also, significant mixing difficulties would occur for the normal range of concretes at fibre volumes in excess of 1 per cent.

However, fibre quantities as low as 0.03 per cent by volume (0.8 kg/m^3) of 12 mm long fibres can offer improved resistance to plastic shrinkage cracking for normal concretes in a similar way to polypropylene fibres. These mixes will inhibit bleeding and plastic shrinkage cracking and will have between 2 million and 200 million fibres per m^3 of concrete depending on whether the filaments are allowed to disperse from the strands.

43.4 Reference

Edgington, J. (1973) Steel fibre reinforced concrete. Ph.D. Thesis, University of Surrey.

Further reading

Ashbee, K. (1989) *Fibre Reinforced Composites*, Technomic Publishing Co. Ltd, Lancaster, Pennsylvania: Basel.

Balaguru, P.N. and Shah, S.P. (1992) *Fibre Reinforced Cement Composites*, Mcgraw-Hill, New York.

Bentur, A. and Mindess, A. (1990) *Fibre Reinforced Cementitious Composites*, Elsevier Applied Science, London.

Clarke, J.L. (1993) *Alternative Materials for the Reinforcement and Prestressing of Concrete*, E & FN Spon, London.

Fordyce, M.W. and Wodehouse, R.G. (1983) *GRC and Buildings*, Butterworth, London.

Hannant, D.J. (1978) *Fibre Cements and Fibre Concretes*, Wiley, Chichester, UK.

Hollaway, L. (1986) Pultrusion, Chapter 1 of *Developments in Plastic Technology – 3* (eds A. Whelan and J.L. Craft), Elsevier Applied Science, London.

Hollaway, L. (ed.) (1990) *Polymers and Polymer Composites in Construction*, Thomas Telford, London.

Hollaway, L. (1993) *Polymer Composites for Civil and Structural Engineering*, Blackie Academic and Professional, London.

Hollaway, L. (ed.) (1994) *BPF Handbook of Polymer Composites for Engineers,* Woodhead Publishing Ltd, Cambridge.

Hollaway, L.C. and Head, P.R. (2001) *Advanced Polymer Composites and Polymers in the Civil Infrastructure*, Elsevier Science, Oxford.

Hollaway, L.C. and Leeming, M.B. (eds) (1999) *Strengthening of Reinforced Concrete Structures – Using Externally Bonded FRP Composites in Structural and Civil Engineering*, Woodhead Publishing Ltd, Cambridge.

Hull, D. (1992) *An Introduction to Composite Materials*, Cambridge University Press, Cambridge.

Majumdar, A.J. and Laws, V. (1991) *Glass Fibre Reinforced Cement*, Blackwell Scientific Publications, London.

Meier, U. and Kaiser, H.P. (1991) Strengthening of structures with CFRP laminates. *Proc. Advanced Composite Materials in Civil Engineering Structures,* Mats Div ASCE, Las Vegas, Jan. 1991, 224–32.

Phillips, L.N. (1989) Introduction. In *Design with Advanced Composite Materials* (ed. L.N. Phillips), The Design Council, London.

Priestley, M.J.N., Seible, F. and Calvi, M. (1996), *Seismic Design and Retrofit of Bridges*, John Wiley & Sons, Inc., New York.

Richmond, B.R. and Head, P.R. (1988) Alternative materials in long span bridge structures. Kerensky Memorial Conference, London, June.

Swamy, R.N. (ed.) (1988) *Natural Fibre Reinforced Cement and Concrete*, Blackie, London.

Triantafillou, T.C. and Plevris, N. (1995) Reliability analysis of reinforced concrete beams strengthened with CFRP laminates. In *Non-metallic (FRP) Reinforcement for Concrete Structures* (ed. L. Taerwe), E & FN Spon, London, pp. 576–83.

Weatherhead, R.C. (1980) *FRP Technology: Fibre Reinforced Resin Systems*, Applied Science Publishers, London.

Part Eight

Timber

J.M. Dinwoodie

Introduction

In the industrial era of the nineteenth century timber was used widely for the construction not only of roofs but also of furniture, water-wheels, gearwheels, rails of early pit railways, sleepers, signal poles, bobbins and boats. The twentieth century saw an extension of its use in certain areas and a decline in others, due to its replacement by newer materials. Despite competition from the lightweight metals and plastics, whether foamed or reinforced, timber continues to be used on a massive scale.

World production of timber in 1993 (the last year for which complete data is available) was $3400 \times 10^6\,m^3$. As much as 55 per cent of this volume ($1880 \times 10^6\,m^3$) is used as fuelwood, but there is still $1520 \times 10^6\,m^3$ used for industrial and constructional purposes.

In 1997, the UK consumed $48.3 \times 10^6\,m^3$ of timber, panels, paper and pulp based on an underbark wood raw material equivalent basis (Anon, 1998); this was equivalent to a per capita annual consumption of $0.82\,m^3$. Consumption of timber and wood-based panels on a wood raw material basis was $27.07 \times 10^6\,m^3$ comprising $17.48 \times 10^6\,m^3$ of softwood, $1.86 \times 10^6\,m^3$ of hardwood, and $7.73 \times 10^6\,m^3$ of wood-based panels.

About 80 per cent of consumption is met by imports; the cost of these for timber and wood-based panels (after deduction of a small volume of re-exports) was £4843×10^6, a far from insignificant import bill and one that is more than 15 per cent of the total UK annual trade deficit.

The remaining 20 per cent of consumption is met from home production, equivalent to $5.51 \times 10^6\,m^3$ with a value of about £900×10^6. Although this contribution will increase steadily over the next two decades, it is then expected to peak at a value corresponding to only 25 per cent of expected consumption.

In the UK, timber and timber products are consumed by a large range of industries, but the bulk of the material continues to be used in construction, either structurally, such as roof trusses or floor joists (about 43 per cent of total consumption), or non-structurally, e.g. doors, window frames, skirting boards and external cladding (about 9 per cent of total consumption). The construction industry, therefore, consumed in 1997 timber and wood-based panels to a value of about £3000×10^6. On a volume basis, annual consumption continues to increase slightly and there is no reason to doubt that this trend will be maintained in the future, especially with the demand for more houses, the increasing price of plastics, the favourable strength–weight and strength–cost factors of timber and panel products, and the increased emphasis on environmental performance and sustainability in which timber is the only renewable construction material.

Timber is cut and machined from trees, themselves the product of nature and time. The structure of the timber of trees has evolved through millions of years to provide a most efficient system which will support the crown, conduct mineral solutions and store food material. Since there are approximately 30 000 different species of tree, it is not surprising to find that timber is an extremely variable material. A quick mental comparison of the colour, texture and density of a piece of balsa and a piece of lignum vitae, formerly used to make playing bowls, will illustrate the wide range that occurs. Nevertheless, modern society has found timber to be a cheap and effective material and, as we have seen, continues to use it in vast quantities. However, we must never forget that the methods by which we utilise this product are quite different from the purpose that nature intended and many of the criticisms levelled at timber as a material are a consequence of our use or misuse of nature's product. Unlike so many other materials, especially those used in the construction industry, timber cannot be manufactured to a particular specification. Instead the best use has to be made of the material already produced, though it is possible from the wide range available to select timbers with the most desirable range of properties. Timber as a material can be defined as a low-density, cellular, polymeric composite, and as such does not conveniently fall into any one class of material, rather tending to overlap a number of classes. In terms of its high strength performance and low cost, timber remains the world's most successful fibre composite.

Four orders of structural variation can be recognised – macroscopic, microscopic, ultrastructural and molecular – and in subsequent chapters the various physical and mechanical properties of timber will be related to these four levels of structure. In seeking correlations between performance and structure, it is tempting to describe the latter in terms of smaller and smaller structural units. Whilst this desire for refinement is to be encouraged, a cautionary note must be recorded, for it is all too easy to overlook the significance of the gross features. This is particularly so where large sections of timber are being used under practical conditions; in these situations gross features such as knots and grain angle are highly significant factors in reducing performance.

Reference

Anon (1998) A reference for the forestry industry. *1997 Yearbook of the Forestry Industry Council of Great Britain*, Stirling, 72 pp.

Chapter forty-four

Structure of timber and the presence of moisture

44.1 Structure at the macroscopic level

The trunk of a tree has three physical functions to perform; first, it must support the crown, a region responsible for the production not only of food, but also of seed; second, it must conduct the mineral solutions absorbed by the roots upwards to the crown; and third, it must store manufactured food (carbohydrates) until required. As will be described in detail later, these tasks are performed by different types of cell.

Whereas the entire cross-section of the trunk fulfils the function of support, and increasing crown diameter is matched with increasing diameter of the trunk, conduction and storage are restricted to the outer region of the trunk. This zone is known as *sapwood,* while the region in which the cells no longer fulfil these tasks is termed the *heartwood.* The width of sapwood varies widely with species, rate of growth and age of the tree. Thus, with the exception of very young trees, the sapwood can represent from 10 to 60 per cent of the total radius, though values from 20 to 50 per cent are more common (Figures 44.1 and 44.2); in very young trees, the sapwood will extend across the whole radius. The advancement of the heartwood to include former sapwood cells results in a number of changes, primarily chemical in nature. The acidity of the wood increases slightly, though certain timbers have heartwood of very high acidity. Substances, collectively called *extractives,* are formed in small quantities and these impart not only coloration to the heartwood, but also resistance to both fungal and insect attack. Different substances are found in different species of wood and some timbers are devoid of them altogether: this explains the very wide range in the natural durability of wood about which more will be said in Section 47.3.1. Many timbers develop gums and resins in the heartwood while the moisture content of the heartwood of most timbers is appreciably lower than that of the sapwood in the freshly felled state. However, in exceptional cases high moisture contents can occur in certain parts of the heartwood. Known as *wetwood*, these zones are frequently of a darker

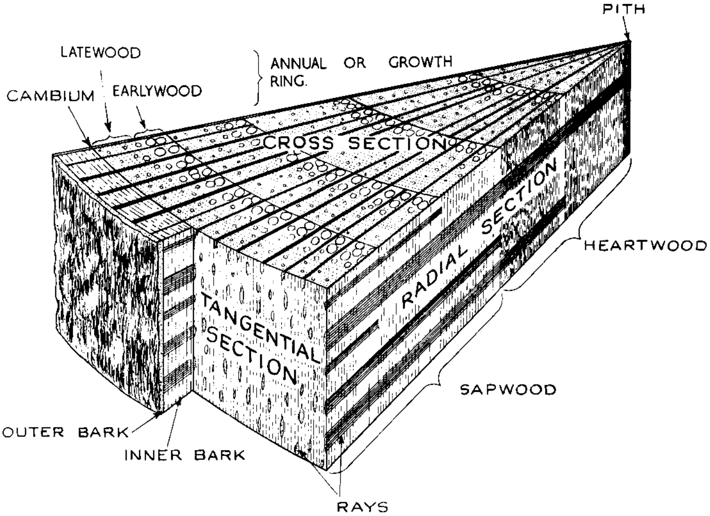

FIGURE 44.1 Diagrammatic illustration of a wedge-shaped segment cut from a five-year-old hardwood tree, showing the principal structural features (© Building Research Establishment).

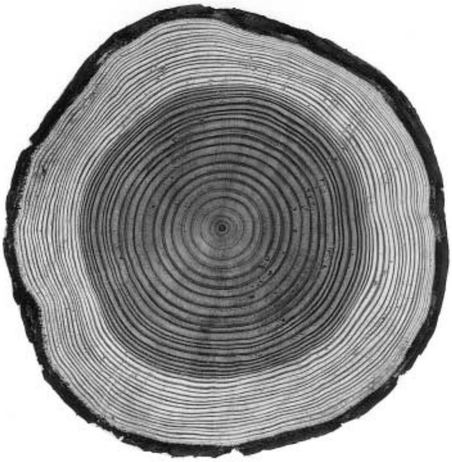

FIGURE 44.2 Cross-section through the trunk of a Douglas fir tree showing the annual growth rings, the darker heartwood, the lighter sapwood and the bark (© Building Research Establishment).

colour than the remainder of the heartwood and are thought to be due to the presence of micro-organisms which produce aliphatic acids and gases (Ward and Zeikus, 1980: Hillis, 1987).

With increasing radial growth of the trunk by division of the cambial cells, commensurate increases in crown size occur, resulting in the enlargement of existing branches and the production of new ones; crown development is not only outwards but upwards. Radial growth of the trunk must accommodate the existing branches and this is achieved by the structure that we know as the *knot*. If the cambium of the branch is still alive at the point where it fuses with the cambium of the trunk, continuity in growth will arise even though there will be a change in orientation of the cells. The structure so formed is termed a *green* or *live* knot (Figure 44.3). If, however, the cambium of the branch is dead, and this frequently happens to the lower branches, there will be an absence of continuity, and the

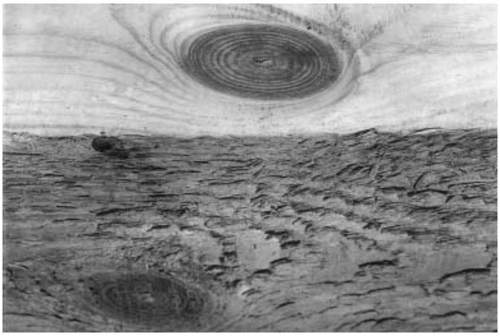

FIGURE 44.3 Green or live knot showing continuity in structure between the branch and tree trunk (© Building Research Establishment).

trunk will grow round the dead branch, often complete with its bark. Such a knot is termed a *black* or *dead* knot (Figure 44.4), and will frequently drop out of planks on sawing. The grain direction in the vicinity of knots is frequently distorted and in a later section the loss of strength due to different types of knots will be discussed.

FIGURE 44.4 Black or dead knot surrounded by the bark of the branch and hence showing discontinuity between branch and tree trunk (© Building Research Establishment).

44.2 Structure at the microscopic level

The cellular structure of wood is illustrated in Figures 44.5 and 44.6. These three-dimensional blocks are produced from micrographs of samples of wood 0.8 × 0.5 × 0.5 mm in size removed from a coniferous tree, known technically as a *softwood* (Figure 44.5), and a broad-leaved tree, known as a

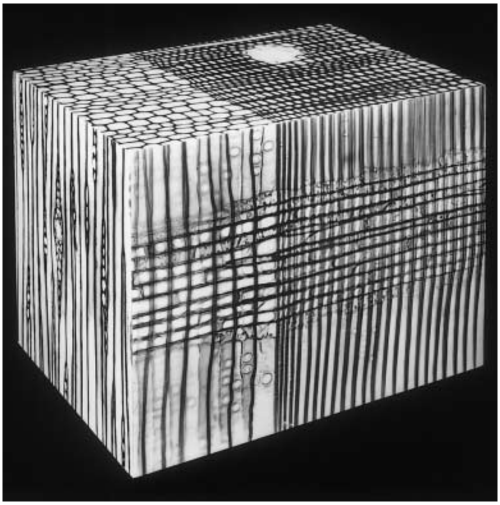

FIGURE 44.5 Cellular arrangement in a softwood *(Pinus sylvestris* – Scots pine, redwood) (© Building Research Establishment).

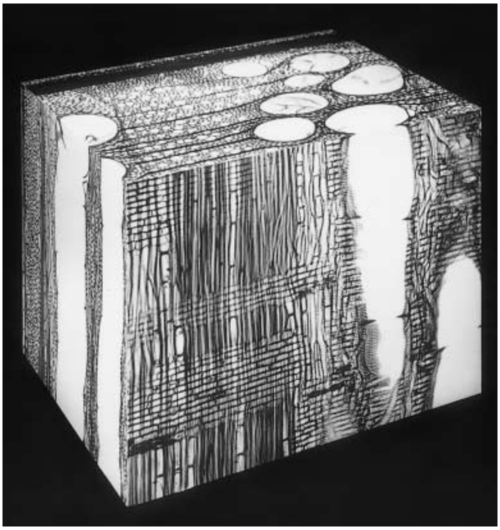

FIGURE 44.6 Cellular arrangement in a ring-porous hardwood (*Quercus robur* – European oak) (© Building Research Establishment).

hardwood (Figure 44.6). In the softwoods about 90 per cent of the cells are aligned in the vertical axis, while in the hardwoods there is a much wider range in the percentage of cells that are vertical (80–95 per cent); the remaining percentage is present in bands, known as *rays*, aligned in one of the two horizontal planes known as the radial plane or quarter-sawn plane (Figure 44.1). This means that there is a different distribution of cells on the three principal axes and this is one of the two principal reasons for the high degree of anisotropy present in timber.

It is popularly believed that the cells of wood are living cells: this is certainly not the case. Wood cells are produced by division of the *cambium*, a zone of living cells which lies between the bark and the woody part of the trunk and branches (Figure 44.1). In the winter the cambial cells are dormant and generally consist of a single circumferential layer. With the onset of growth in the spring, the cells in this single layer subdivide radially to form a cambial zone some ten cells in width. This is achieved by the formation within each dividing cell of a new vertical wall called the primary wall. During the growing season these cells undergo further radial subdivision to produce what are known as daughter cells and some of these will remain as cambial cells while others, to the outside of the zone, will develop into bark or, if on the inside, will change into wood. There is thus a constant state of flux within the cambial zone with the production of new cells and the relegation of existing cambial cells to bark or wood. Towards the end of the growing season the emphasis is on relegation and a single layer of cambial cells is left for the winter period.

To accommodate the increasing diameter of the tree, the cambial zone must increase circumferentially and this is achieved by the periodic tangential division of the cambial cells. In this case, the new wall is sloping and subsequent elongation of each half of the cell results in cell overlap, often frequently at shallow angles to the vertical axis, giving rise to the formation of spiral grain in the timber. The rate at which the cambium divides tangentially has a significant effect on the average cell length of the timber produced.

The daughter cells produced radially from the cambium undergo a series of changes extending over a period of about three weeks; this process is known as *differentiation*. Changes in cell shape are paralleled with the formation of the secondary wall, the final stages of which are associated with the death of the cell; the degenerated cell contents are frequently to be found lining the cell cavity. It is during the process of differentiation that the standard daughter cell is transformed into one of four basic cell types (Table 44.1).

Chemical dissolution of the lignin–pectin complex cementing the cells together will result in their separation and this is a useful technique for separating and examining individual cells. In the softwood (Figure 44.7) two types of cell can be observed. Those present in greater number are known as *tracheids,* some 2–4 mm in length with an aspect ratio (*L/D*) of about 100:1. These cells, which lie vertically in the tree trunk, are responsible for both the supporting and conducting roles. The small block-like cells, some $200 \times 30\,\mu\text{m}$ in size, known as *parenchyma,* are mostly located in the *rays* and are responsible for the storage of food material.

In contrast, in the hardwoods (Figure 44.8), four types of cell are present, albeit that one, the tracheid, is present in small amounts. The role of storage is again primarily taken by the parenchyma, which can be present horizontally in the form of a ray, or vertically, either scattered or in distinct zones. Support is effected by long, thin cells with very tapered ends, known as *fibres;* these are usually about 1–2 mm in length with an aspect ratio of about 100:1. Conduction is carried out in cells whose end walls have been dissolved away either completely or in part. These cells, known as *vessels* or *pores,* are usually short (0.2–1.2 mm) and relatively wide (up to 0.5 mm) and, when situated above one another, form an efficient conducting tube. It can be seen, therefore, that while in the softwoods the three functions are performed by two types of cell, in the hardwoods each function is performed by a single cell type (Table 44.1).

Although all cell types develop a secondary wall, this varies in thickness, being related to the function that the cell will perform. Thus, the wall thickness of fibres is several times that of the

TABLE 44.1 The functions and wall thicknesses of the various types of cell found in softwoods and hardwoods

Cells	*Softwood*	*Hardwood*	*Function*	*Wall thickness*
Parenchyma	✓	✓	Storage	
Tracheids	✓	✓	Support conduction	
Fibres		✓	Support	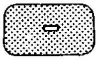
Vessels (pores)		✓	Conduction	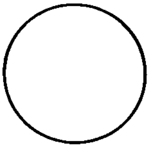

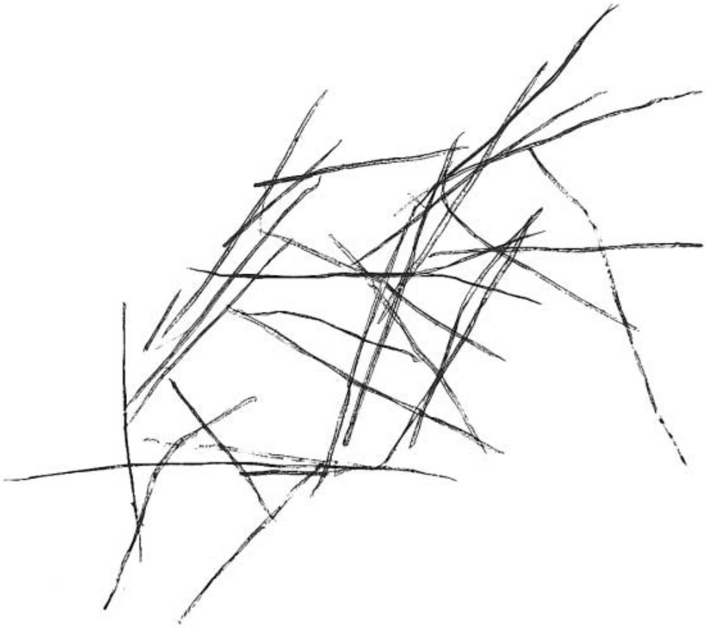

FIGURE 44.7 Individual softwood cells (×20) (© Building Research Establishment).

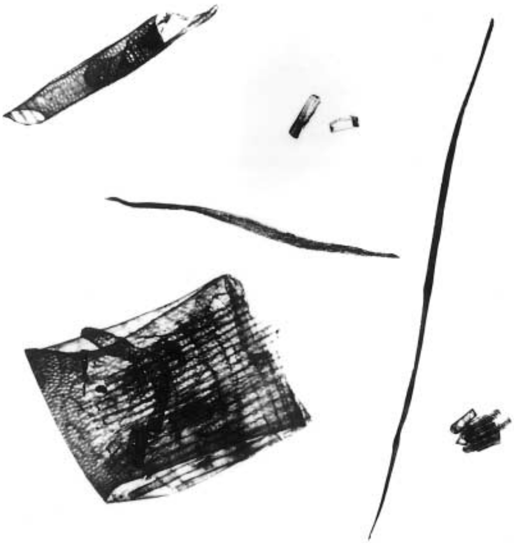

FIGURE 44.8 Individual cells from a ring-porous hardwood (×50) (© Building Research Establishment).

vessel (Table 44.1). Consequently, the density of the wood, and hence many of the strength properties, will be related to the relative proportions of the various types of cell. Density, of course, will also be related to the absolute wall thickness of any one type of cell, for it is possible to obtain fibres of one species of wood with a cell wall several times thicker than those of another. The range in density of timber is from about 120 to 1200 kg/m^3 corresponding to pore volumes from 92 per cent to 18 per cent (see Section 44.6.1).

Growth may be continuous throughout the year in certain parts of the world and the wood formed tends to be uniform in structure. In the temperate and subarctic regions and in parts of the tropics growth is seasonal, resulting in the formation of *growth rings*; where there is a single growth period each year these rings are referred to as *annual rings (*Figure 44.1).

When seasonal growth commences, the dominant function appears to be conduction, while in the latter part of the year the dominant factor is support. This change in emphasis manifests itself in the softwoods with the presence of thin-walled tracheids (about 2 μm) in the early part of the season (the wood being known as *earlywood*) and thick-walled (up to 10 μm) and slightly longer (10 per cent) in the latter part of the season (the *latewood*) (Figure 44.5).

In some of the hardwoods, but certainly not all of them, the early-wood is characterised by the presence of large-diameter vessels surrounded primarily by parenchyma and tracheids; only a few fibres are present. In the latewood, the vessel diameter is considerably smaller (about 20 per cent) and the bulk of the tissue comprises fibres. It is not surprising to find, therefore, that the technical properties of the earlywood and latewood are quite different from one another. Timbers with this characteristic two-phase system are referred to as having a *ring-porous* structure (Figure 44.6).

The majority of hardwoods, whether of temperate or tropical origin, show little differentiation into earlywood and latewood. Uniformity across the growth ring occurs not only in cell size, but also in the distribution of the different types of cells (Figure 44.9): these timbers are said to be *diffuse-porous.*

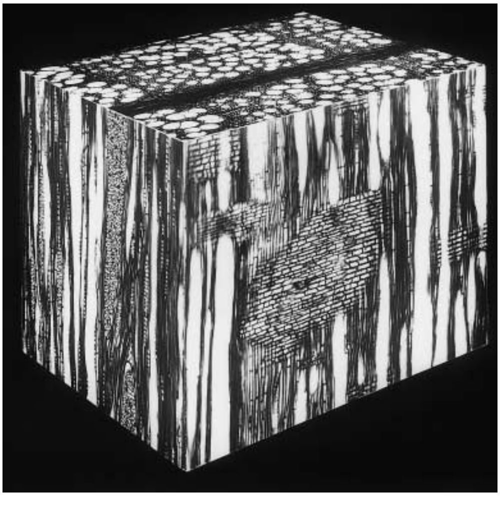

FIGURE 44.9 Cellular arrangement in a diffuse-porous hardwood *(Fagus sylvatica* – beech) (© Building Research Establishment).

In addition to determining many of the technical properties of wood, the distribution of cell types and their sizes is used as a means of timber identification.

Interconnection by means of pits occurs between cells to permit the passage of mineral solutions and food in both longitudinal and horizontal planes. Three basic types of pit occur. *Simple pits*, generally small in diameter and taking the form of straight-sided holes with a transverse membrane, occur between parenchyma and parenchyma, and also between fibre and fibre. Between tracheids, a complex structure known as the *bordered pit* occurs (Figure 44.10; see also Figure 44.27(a) for sectional view). The entrance to the pit is domed and the internal chamber is characterised by the presence of a diaphragm (the *torus*) which is suspended by thin strands (the *margo strands*). Differential pressure between adjacent tracheids will cause the torus to move against the pit aperture, effectively stopping flow. As will be discussed later, these pits have a profound influence on the degree of artificial preservation of the timber. Similar structures are to be found interconnecting vessels in a horizontal plane. Between parenchyma cells and tracheids or vessels, *semi-bordered pits* occur and are often referred to as ray pits. These are characterised by the presence of a dome on the tracheid or vessel wall and the absence of such on the parenchyma wall: a pit membrane is present, but the torus is absent. Differences in the shape and size of these pits is an important diagnostic feature in the softwoods.

The general arrangement of the vertically aligned cells is referred to as *grain*. While it is often convenient when describing timber at a general level to regard these cells as lying truly vertical, this is not really true in the majority of cases; these cells generally deviate from the vertical axis in a number of different patterns.

In many timbers, and certainly in most of the softwoods, the direction of the deviation from the vertical axis is consistent and the cells assume a distinct *spiral* mode which may be either left- or right-handed. In young trees the helix is usually left-handed and the maximum angle which is near to the core is frequently of the order of 4°, though considerable variability occurs both within a

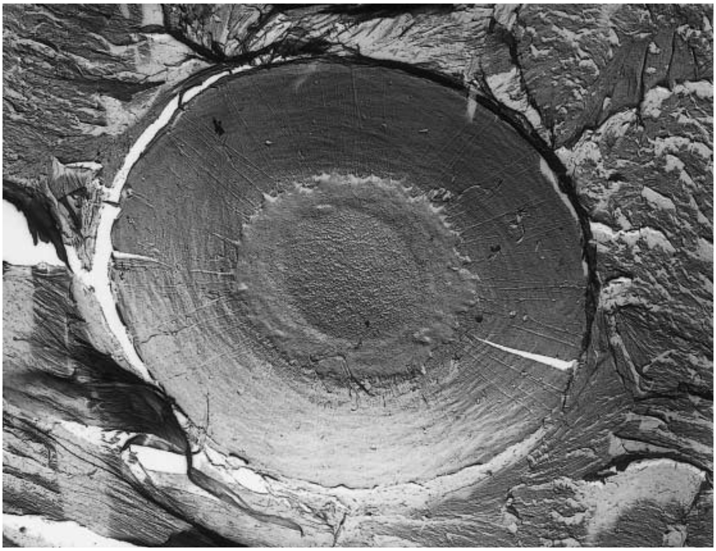

FIGURE 44.10 Electron micrograph of the softwood bordered pit showing the margo strands supporting the diaphragm (torus), which overlaps the aperture (×3600) (© Building Research Establishment).

species and also between different species of timber. As the trees grow, so the helix angle in the outer rings decreases to zero and quite frequently in very large trees the angle in the outer rings subsequently increases, but the spiral has changed hand. Spiral grain has very significant technical implications; strength is lowered, while the degree of twisting on drying and the amount of pick-up on machining increase as the degree of spirality of the grain increases (Brazier, 1965).

In other timbers the grain can deviate from the vertical axis in a number of more complex ways, of which *interlocked* and *wavy* are perhaps the two most common and best known. Since each of these types of grain deviation give rise to a characteristic decorative figure, further discussion on grain is reserved until Section 44.5.

44.3 Molecular structure and ultrastructure

44.3.1 Chemical constituents

Chemical analysis reveals the existence of four constituents and provides data on their relative proportions. This information may be summarised as in Table 44.2: proportions are for timber in general and slight variations in these can occur between timber of different species, or in different parts of a single tree.

Cellulose

Cellulose $(C_6H_{10}O_5)_n$ occurs in the form of long, slender filaments or chains, these having been built up within the cell wall from the glucose monomer $(C_6H_{12}O_6)$. Whilst the number of units per cellulose molecule (the degree of polymerisation) can vary considerably even within one cell wall, it is thought that a value of 8000–10 000 is a realistic average for the secondary cell wall while the primary cell wall has a degree of polymerisation of only 2000–4000 (Simson and Timell, 1978). The anhydroglucose unit $C_6H_{10}O_5$ which is not quite flat, is in the form of a six-sided ring consisting of five carbon atoms and one oxygen atom (Figure 44.11); the side groups play an important part in intra- and intermolecular bonding as will be noted later. Successive glucose units are covalently linked in the 1,4 positions giving rise to a potentially straight and extended chain; i.e. moving in a clockwise direction around the ring, it is the first and fourth carbon atoms after the oxygen atom that combine with adjacent glucose units to form the long-chain molecule. The anhydroglucose units comprising the molecule are not flat, as noted above; rather they assume a chair configuration with the hydroxyl groups (one primary and two secondary) in the equatorial positions and the hydrogen atoms in the axial positions (Figure 44.11).

TABLE 44.2 Chemical composition of timber

Component	*Per cent mass*		*Polymeric state*	*Molecular derivatives*	*Function*
	Softwood	*Hardwood*			
Cellulose	42 ± 2	45 ± 2	Crystalline highly oriented large linear molecule	Glucose	'fibre'
Hemicelluloses	27 ± 2	30 ± 5	Semi-crystalline smaller molecule	Galactose Mannose Xylose	'matrix'
Lignin	28 ± 3	20 ± 4	Amorphous large 3-D molecule	Phenyl-propane	
Extractives	3 ± 2	5 ± 4	Generally compounds soluble in organic solvents	Terpenes Polyphenols Stilbenoids	extraneous

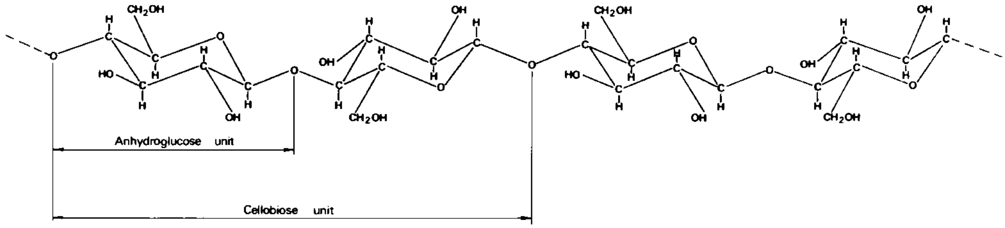

FIGURE 44.11 Structural formula for the cellulose molecule in its chair configuration (© Building Research Establishment).

Glucose, however, can be present in one of two forms dependent on the position of the —OH group attached to carbon 1. When this group lies above the ring, i.e. on the same side as that on carbon 4, the unit is called α-glucose, and when this combines with an adjacent unit with the removal of H—O—H (known as a condensation reaction) the resulting molecule is called starch, a product which is manufactured in the crown and stored in the parenchyma cells.

When the —OH group lies below the ring, the unit is known as β-glucose and on combining with adjacent units, again by a condensation reaction, a molecule of cellulose is produced in which alternate anhydroglucose units are rotated through 180°: it is this product which is the principal wall-building constituent of timber.

Cellulose chains may crystallise in many ways, but one form, namely cellulose I, is characteristic of natural cellulosic materials. Over the years there have been various attempts to model the structure of cellulose I. One of the more recent, and one which has gained wide acceptance, is that proposed by Gardner and Blackwell (1974). Using X-ray diffraction methods on the cellulose of *Valonia*, these authors proposed an eight-chain unit cell with all the chains running in the same direction. Forty-one reflections were observed in their X-ray diffractions and these were indexed using a monoclinic unit cell having dimensions $a = 1.634$ nm, $b = 1.572$ nm and $c = 1.038$ nm (the cell axis) with $\beta = 97°$; the unit cell therefore comprises a number of whole chains or parts of chains totalling eight in number.

All but three of the reflections can be indexed by a two-chain unit cell almost identical to the earlier model by Meyer and Misch (1937), though this model had adjacent chains aligned in opposite directions. These three reflections are reported as being very weak, which means that the differences between the four Meyer and Misch unit cells making up the eight-chain cell must be small. Gardner and Blackwell therefore take a two-chain unit cell ($a = 0.817$ nm, $b = 0.786$ nm and $c = 1.038$ nm) as an adequate approximation to the real structure. Their proposed model for cellulose I is shown in Figure 44.12, which shows the chains lying in a parallel configuration, the centre chain staggered by $0.266 \times c$ ($= 0.276$ nm).

Cellulose which has regenerated from a solution displays a different crystalline structure and is known as cellulose II: in this case there is complete agreement that the unit cell possesses an antiparallel arrangement of the cellulose molecule.

Within the structure of cellulose I, both primary and secondary bonding are represented and many of the technical properties of wood can be related to the variety of bonding present. Covalent bonding both within the glucose rings and linking together the rings to form the molecular chain contributes to the high axial tensile strength of timber. There is no evidence of primary bonding laterally between the chains: rather this seems to be a complex mixture of the fairly strong hydrogen bonds and the weak van der Waals forces. The same OH groups that give rise to this hydrogen bonding are highly attractive to water molecules and explain the affinity of cellulose for water. Whereas some earlier workers, though placing the intermolecular hydrogen bonds in the *ac* plane, recorded that the intramolecular hydrogen bonds were on a diagonal plane thereby linking different layers, Gardner and Blackwell (1974) identify the existence of both intermolecular and intramolecular hydrogen bonds, all of which, however, are interpreted as lying only on the *ac* plane (Figure 44.12); they consider the structure of cellulose as an array of hydrogen-bonded sheets held together by van der Waals forces across the *cb* plane.

The degree of crystallinity of the cellulose is usually assessed by X-ray and electron diffraction techniques, though other methods have been employed. Generally, a value of about 60 per cent is obtained, though values as high as 90 per cent are recorded in the literature. This wide range in values is due in part to the different techniques employed in the determination of crystallinity and in part to the fact that wood is comprised not just of the crystalline and non-crystalline constituents, but rather a series of substances of varying crystallinity. Regions of complete crystallinity and regions with a total absence of crystalline structure (amorphous zones) can be recognised, but the transition from one state to the other is gradual.

The length of the cellulose molecule is about 5000 nm (0.005 mm) whereas the average size of each crystalline region determined by X-ray analysis is only 60 nm in length, 5 nm in width and 3 nm in thickness. This means that any cellulose molecule will pass through several regions of high crystallinity – known as *crystallites* or *micelles* – with intermediate non-crystalline or low-crystalline zones in which the cellulose chains are in only loose association with each other (Figure 44.12). Thus, the majority of chains emerging from one crystallite will pass to the next, creating a high degree of longitudinal coordination; this collective unit is termed a *microfibril* and has infinite length. It is clothed with chains of cellulose mixed with chains of sugar units other than glucose (see below) which lie parallel, but are not regularly spaced. This brings the microfibril in timber to about 10 nm in breadth, and in some algae, such as *Valonia*, to 30 nm. The degree of crystallinity will therefore vary along its length and it has been proposed that this could be periodic.

Readers desirous of a more comprehensive account of the structure of cellulose are referred to Chapter 1 of Dinwoodie (2000).

Hemicelluloses and lignin

In Table 44.2 reference was made to the other constituents of wood additional to cellulose. Two of these, the hemicelluloses and lignin, are regarded as cementing materials contributing to the structural integrity of wood and also to its high stiffness. The hemicelluloses, like cellulose itself, are carbohydrates built up of sugar units, but unlike cellulose in the type of units they comprise; these units differ between softwoods and hardwoods and generally, the total percentage of the hemicelluloses present in timber is greater in hardwoods compared with softwoods (Table 44.2). Both the degree of crystallisation and the degree of polymerisation of the hemicelluloses are generally low, the molecule containing less than 200 units; in these respects, and also in their lack of resistance to alkali solutions, the hemicelluloses are quite different from true cellulose (Siau, 1984).

Lignin, present in about equal proportions to the hemicelluloses, is chemically dissimilar to these and to cellulose. Lignin is a complex, three-dimensional, aromatic molecule composed of phenyl groups with a molecular weight of about 11 000. It is non-crystalline and the structure varies between wood from a conifer and from a broad-leaved tree. About 25 per cent of the total lignin in timber is to be found in the middle lamella, an intercellular layer composed of lignin and pectin together with the primary cell wall. Since this compound middle lamella is very thin, the concentration of lignin is correspondingly high (about 70 per cent). Deposition of the lignin in this layer is rapid.

The bulk of the lignin (about 75 per cent) is present within the secondary cell wall, having

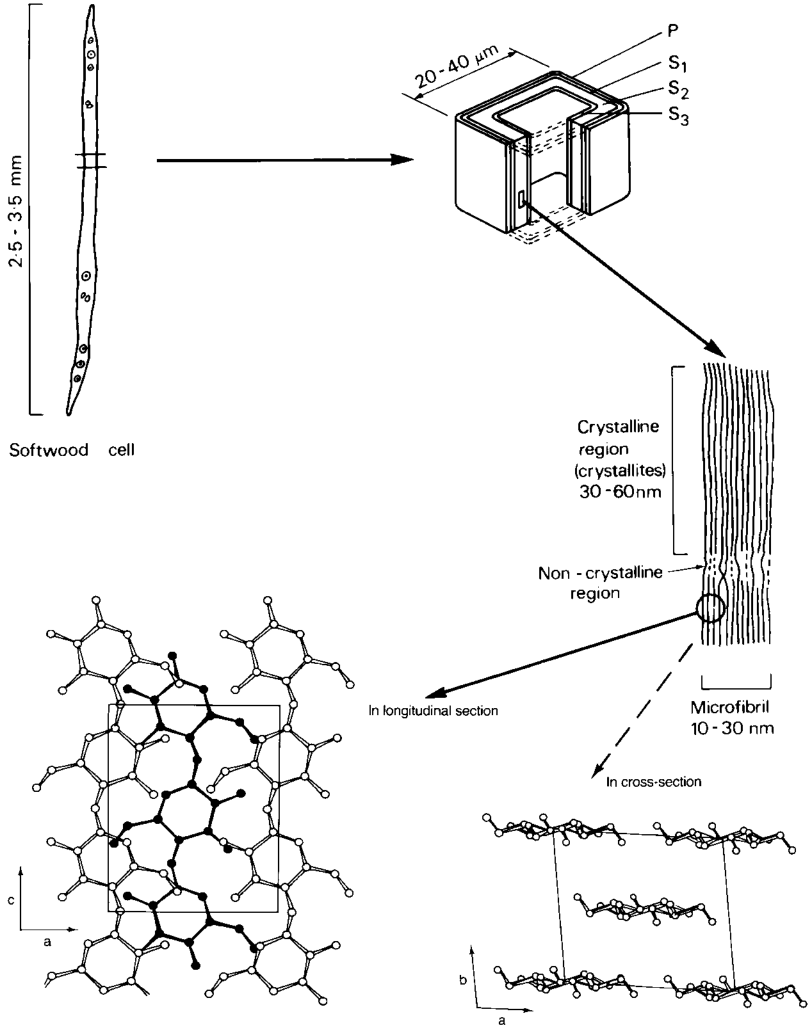

FIGURE 44.12 Relationship between the structure of timber at different levels of magnitude. The lower two diagrams are projections of the Gardner and Blackwell two-chain cell used as an approximation to the eight-chain unit cell of the real structure. On the left is the projection viewed perpendicular to the *ac* plane; on the right, the projection viewed perpendicular to the *ab* plane (i.e. along the cell axis). Planes are characterised according to North American rather than European terminology. Note that the central chain (in black) has the same orientation as the other chains and is staggered vertically with respect to them by an amount equal to *c*/4. (The lower two diagrams from K.H. Gardner and J. Blackwell (1974), by permission of John Wiley and Sons, Inc; the upper diagrams adapted from J.F. Siau (1971), reproduced by permission of Syracuse University Press.)

been deposited following completion of the cellulosic framework. Initiation of lignification of the secondary wall commences when the compound middle lamella is about half completed and extends gradually inwards across the secondary wall (Saka and Thomas, 1982). Termination of the lignification process towards the end of the period of differentiation coincides with the death of the cell. Most cellulosic plants do not contain lignin and it is the inclusion of this substance within the framework of timber that is largely responsible for the stiffness of timber, especially in the dried condition.

Extractives

Before leaving the chemical composition of wood, mention must be made of the presence of extractives (Table 44.2). This is a collective name for a series of highly complex organic compounds which are present in certain timbers in relatively small amounts. Some, like waxes, fats and sugars, have little economic significance, but others, for example rubber and resin (from which turpentine is distilled), are of considerable economic importance. The heartwood of timber, as described previously, generally contains extractives which, in addition to imparting coloration to the wood, bestow on it its natural durability, since most of these compounds are toxic to both fungi and insects. Readers desirous of more information on extractives are referred to the comprehensive text by Hillis (1987).

Minerals

Elements such as calcium, sodium, potassium, phosphorous and magnesium are all components of new growth tissue, but the actual mass of these inorganic materials is small and constitutes on the basis of the oven-dry mass of the timber less than 1 per cent for temperate woods and less than 5 per cent for tropical timbers.

Certain timbers show a propensity to conduct suspensions of minerals which are subsequently deposited within the timber. The presence of silica in the rays of certain tropical timbers, and calcium carbonate in the cell cavities of iroko are two examples where large concentrations of minerals cause severe problems in log conversion and subsequent machining.

Acidity

Wood is generally acidic in nature, the level of acidity being considerably higher in the heartwood compared to the sapwood of the same tree. The pH of the heartwood varies in different species of timber, but is generally about 4.5 to 5.5; however, in some timbers such as eucalypt, oak and western red cedar, the pH of the heartwood can be as low as 3.0. Sapwood generally has a pH at least 1.0 higher than the corresponding heartwood; i.e. the acidity is at least ten times lower than the corresponding heartwood.

Acidity in wood is due primarily to the generation of acetic acid by hydrolysis of the acetyl groups of the hemicelluloses in the presence of moisture; this acidity in wood can cause severe corrosion of certain metals and care has to be exercised in the selection of metallic fixings especially at higher relative humidities.

44.3.2 The cell wall as a fibre composite

In the introductory remarks, wood was defined as a natural composite and the most successful model used to interpret the ultrastructure of wood from the various chemical and X-ray analyses ascribes the role of 'fibre' to the cellulosic microfibrils while the lignin and hemicelluloses are considered as separate components of the 'matrix'. The cellulosic microfibril, therefore, is interpreted as conferring high tensile strength to the composite owing to the presence of covalent bonding both within and between the anhydroglucose units. Experimentally it has been shown that reduction in chain length following gamma irradiation markedly reduces the tensile strength of timber; the significance of chain length in determining strength has been confirmed in studies of wood with inherently low degrees of polymerisation. While slippage between the cellulose chains was previously considered to be an important contributor to the development of ultimate tensile strength, this is now thought to be unlikely due to the forces involved in fracturing large numbers of hydrogen bonds.

Preston (1964) has shown that the hemicelluloses are usually intimately associated with the cellulose, effectively binding the microfibrils together. Bundles of cellulose chains are therefore seen as having a polycrystalline sheath of hemicellulose material and consequently the resulting high degree of hydrogen bonding would make chain slippage unlikely: rather it would appear that stressing results in fracture of the C—O—C linkage.

The deposition of lignin is variable in different parts of the cell wall, but it is obvious that its prime function is to protect the hydrophilic (water-seeking) non-crystalline cellulose and the hemicelluloses which are mechanically weak when wet. Experimentally, it has been demonstrated that removal of the lignin markedly reduces the strength of wood in the wet state, though its reduction results in an increase in its strength in the dry state calculated on a net cell wall area basis. Consequently, the lignin is regarded as lying to the outside of the microfibril forming a protective sheath.

Since the lignin is located only on the exterior it must be responsible for cementing together the fibrils and in imparting shear resistance in the transference of stress throughout the composite. The role of lignin in contributing towards stiffness of timber has already been mentioned.

There has been great debate over the years as to juxtaposition of the cellulose, hemicellulose and lignin in the composition of a microfibril, and to the size of the basic unit. Two of the many models proposed are illustrated in Figure 44.13. The model on the left (a) depicts cellulosic subunits some 3 nm in diameter. These units, comprising some 40 cellulose chains, are known as *elementary fibrils* or *protofibrils*. Gaps (1 nm)

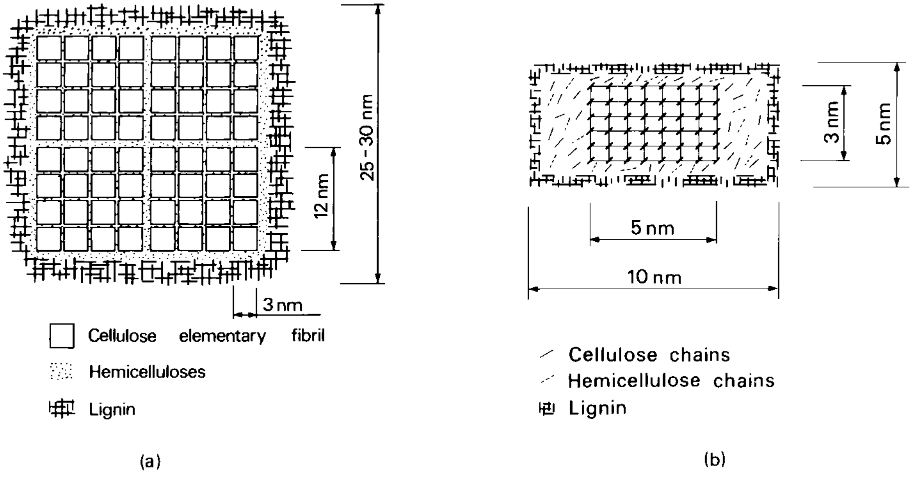

FIGURE 44.13 Models of the cross-section of a microfibril. In (a) the crystalline core has been subdivided into elementary fibrils, while in (b) the core is regarded as being homogeneous ((a) adapted from D. Fengel (1970) reproduced by permission of TAPPI; (b) adapted from R.D. Preston (1974) reproduced by permission of Chapman and Hall).

between these units are filled with hemicellulose while more hemicellulose and lignin form the sheath. In passing, it is interesting to note that sub-units as small as 1 nm (sub-elementary fibril) have been claimed by some researchers.

In the second model (Figure 44.13 (b)), the crystalline core is considered to be about 5 nm × 3 nm containing about 48 chains in either 4- or 8-chain unit cells; this latter configuration has received wider acceptance. Both these models, however, are in some agreement in that passing outwards from the core of the microfibril the highly crystalline cellulose gives way first to the partly crystalline layer containing mainly hemicellulose and non-crystalline cellulose, and then to the amorphous lignin: this gradual transition of crystallinity from fibre to matrix results in high interlaminar shear strength which contributes considerably to the high tensile strength and toughness of wood.

44.3.3 Cell wall layers

When a cambial cell divides to form two daughter cells a new wall is formed comprising the middle lamella and two primary cell walls, one to each daughter cell. These new cells undergo changes within about three days of their formation and one of these developments will be the formation of a secondary wall. The thickness of this wall will depend on the function the cell will perform, as described earlier, but its basic construction will be similar in all cells.

Early studies on the anatomy of the cell wall used polarisation microscopy, which revealed the direction of orientation of the crystalline regions. These studies indicated that the secondary wall could be subdivided into three layers and measurements of the extinction position was indicative of the angle at which the microfibrils were orientated. Subsequent studies with transmission electron microscopy confirmed these findings and provided some additional information with particular reference to wall texture and variability of angle. However, much of our knowledge on microfibrillar orientation has been derived using X-ray diffraction analysis. Most of these techniques yield only mean angles for any one layer of the cell wall, but recent analysis has indicated that it may be possible to determine the complete microfibrillar angle distribution of the cell wall (Cave, 1997).

The relative thickness and mean microfibrillar angle of the layers in a sample of spruce timber are illustrated in Table 44.3.

The middle lamella, a lignin–pectin complex, is devoid of cellulosic microfibrils while in the primary wall (*P*) the microfibrils are loose packed and interweave at random (Figure 44.14); no lamellation is present. In the secondary wall layers the microfibrils are closely packed and parallel to each other. The outer layer of the secondary wall, the S_1, is again thin and is characterised by having from four to six concentric lamellae, the microfibrils of each alternating between a left- and right-hand spiral (*S* and *Z* helix) both with a pitch to the longitudinal axis of from 50° to 70° depending on the species of timber.

The middle layer of the secondary wall (S_2) is thick and is composed of 30–150 lamellae, the closely packed microfibrils of which all exhibit a similar orientation in a right-hand spiral (*Z* helix) with a pitch of 10–30° to the longitudinal axis as illustrated in Figures 44.14 and 44.15. Since over three-quarters of the cell wall is composed of the S_2 layer, it follows that the ultrastructure of this layer will have a very marked influence on the behaviour of the timber. In later sections, anisotropic behaviour, shrinkage, tensile strength and failure morphology will all be related to the microfibrillar angle in the S_2 layer.

Kerr and Goring (1975) were among the first workers to question the extent of these concentric

TABLE 44.3 Microfibrillar orientation and percentage thickness of the cell wall layers in spruce timber (*Picea abies*)

Wall layer	*Approximate thickness (%)*	*Angle to longitudinal axis*
P	3	Random
S_1	10	50–70°
S_2	85	10–30°
S_3	2	60–90°

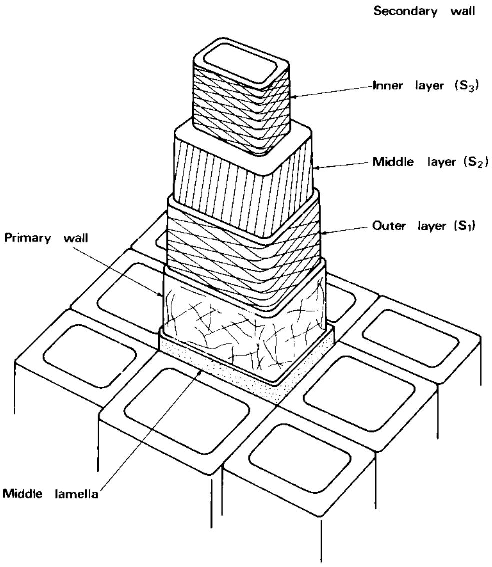

FIGURE 44.14 Simplified structure of the cell wall showing mean orientation of microfibrils in each of the major wall layers (© Building Research Establishment).

FIGURE 44.15 Electron micrograph of the cell wall in Norway spruce timber (*Picea abies*) showing the parallel and almost vertical microfibrils of an exposed portion of the S_2 layer (© Building Research Establishment).

lamellae in the S_2 layer; these workers found that though there was a preferred orientation of lignin and carbohydrates in the S_2 layer, the lamellae were certainly not continuous. Thus, the interrupted lamellae model proposed by them embraced lignin and carbohydrate entities which were greater in the tangential than in the radial direction. Cellulose microfibrils were envisaged as being embedded in a matrix of hemicelluloses and lignin.

The existence within the S_2 layer of concentric lamellae has been questioned again in the last few years. Evidence has been presented (Sell and Zinnermann, 1993) from both electron and light microscopy which indicates radial, or near radial, orientations of the transverse structure of the S_2 layer. The transverse thickness of these agglomerations of microfibrils is 0.1–1.0 nm and they frequently extend the entire width of the S_2 layer. A modified model of the cell wall of softwoods has been proposed (Sell and Zinnermann, 1993).

The S_3 layer, which may be absent in certain timbers, is very thin with only a few concentric lamellae; it is characterised, as in the S_1 layer, by alternate lamellae possessing microfibrils orientated in opposite spirals with a pitch of 60–90° though the presence of the right-handed spiral (*Z* helix) is disputed by some workers. Generally, the S_3 has a looser texture than the S_1 and S_2 layers and is frequently encrusted with extraneous material. The S_3, like the S_1, has a higher concentration of lignin than in the S_2 (Saka and Thomas, 1982). Electron microscopy has also revealed the presence of a thin, warty layer overlaying the S_3 layer in certain timbers.

Investigations have indicated that the values of microfibrillar angle quoted in Table 44.3 are only average for the layers and that systematic variation in angle occurs within each layer. Thus, Abe *et al.* (1991) have shown in *Abies sachalinensis* that the microfibrillar angle of the secondary wall, as seen from the lumen, changed in a clockwise direction from the outermost S_1 to the middle of the S_2 and then in a counter-clockwise direction to the innermost S_3. This resulted in the boundaries between the three principal layers being very indistinct confirming reports by previous workers on other species and suggesting that the wall structure can be viewed as a systematically varying continuum.

Microfibrillar angle appears to vary systematically along the length of the cell as well as across the wall thickness. Thus, the angle of the S_2 layer has been shown to decrease towards the ends of the cells, while the average S_2 angle appears to be related to the length of the cell, itself a function of rate of growth of the tree. Systematical differences in microfibrillar angle have been found between radial and tangential walls and this has been related to differences in degree of lignification between these walls. Openings occur in the walls of cells and many of these pit openings are characterised by localised deformations of the microfibrillar structure.

Further information on the variability of microfibrillar angle is to be found in Dinwoodie (2000).

44.4 Variability in structure

Variability in performance of wood is one of its inherent deficiencies as a material. It will be discussed later how differences in mechanical properties occur between timbers of different species and how these are manifestations of differences in wall thickness and distribution of cell types. However, superimposed on this genetical source of variation is both a systematic and an environmental one.

There are distinct patterns of variation in many features within a single tree. Length of the cells, thickness of the cell wall and hence density, angle at which the cells are lying with respect to the vertical axis (spiral grain), angle at which the microfibrils of the S_2 layer of the cell wall are located with respect to the vertical axis, all show systematic trends outwards from the centre of the tree to the bark and upwards from the base to the top of the tree. This pattern results in the formation of a core of wood in the tree with many undesirable properties including low strength and high shrinkage. This zone, usually regarded as some ten to twenty growth rings in width, is known as *core wood* or *juvenile wood* as opposed to the *mature wood* occurring outside this area. The boundary between juvenile and mature wood is usually defined in terms of the change in slope of the variation in magnitude of one anatomical feature (e.g. cell length, density) when plotted against ring number from the pith.

Environmental factors have considerable influence on the structure of the wood and any environmental influence, including forest management, which changes the rate of growth of the tree will affect the technical properties of the wood. However, the relationship is a complex one; in softwoods, increasing growth rate generally results in an increase in the width of earlywood with a resulting decrease in density and mechanical properties. In diffuse-porous hardwoods increasing growth rate, provided it is not excessive, has little effect on density, while in ring-porous hardwoods, increasing rate of growth, again provided it is not excessive, results in an increase in the width of latewood and consequently in density and strength.

There is a whole series of factors which may cause defects in the structure of wood and consequent lowering of its strength. Perhaps the most important defect with regard to its utilisation is the formation of *reaction wood*. When trees are inclined to the vertical axis, usually as a result of wind action or of growing on sloping ground, the distribution of growth-promoting hormones is disturbed, resulting in the formation of an abnormal type of tissue. In the softwoods, this reaction tissue grows on the compression side of the trunk and is characterised by having a higher than normal lignin content, a higher microfibrillar angle in the S_2 layer resulting in increased longitudinal shrinkage, and a generally darker appearance (Figure 44.16): this abnormal timber, known as *compression wood*, is also considerably more brittle than normal wood. In the hardwoods, reaction wood forms on the tension side of trunks and large branches and is therefore called *tension wood*. It is characterised by the presence of a gelatinous cellulosic layer (the *G layer*) to the inside of the cell wall; this results in a higher than normal cellulose content to the total cell wall which imparts a rubbery characteristic to the fibres resulting in difficulties in sawing and machining.

One other defect of considerable technical significance is *brittleheart*, which is found in many low-density tropical hardwoods and is one manifestation of the presence of longitudinal growth stresses in large diameter trees. Yield of the cell wall occurs under longitudinal compression with the formation of shear lines through the cell wall and throughout the core wood; compression failure will be discussed in greater detail in Section 46.7.1.

More information on the variability in structure and its influence on the technical performance of timber is to be found in Chapters 5 and 12 of Desch and Dinwoodie (1996).

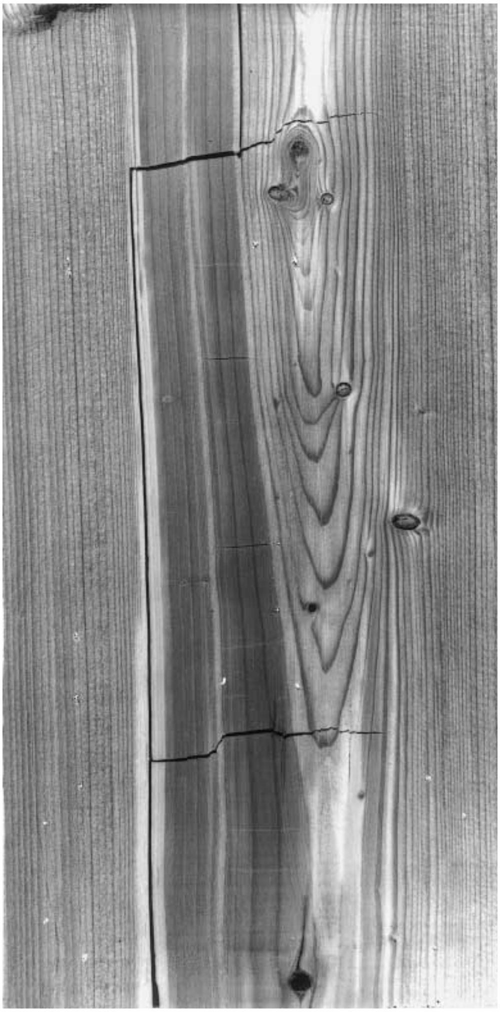

FIGURE 44.16 A band of compression wood (centre left) in a Norway spruce plank, illustrating the darker appearance and higher longitudinal shrinkage of the reaction wood compared with the adjacent normal wood (© Building Research Establishment).

44.5 Appearance of timber in relation to its structure

Most readers will agree that many timbers are aesthetically pleasing and the various and continuing attempts to simulate the appearance of timber in the surface of synthetic materials bears testament to the very attractive appearance of many timbers. Although a very large proportion of the timber consumed in the UK is used within the construction industry, where the natural appearance of timber is of little consequence, excepting the use of hardwoods for flush doors, internal panelling and wood-block floors, a considerable quantity of timber is still utilised purely on account of its attractive appearance particularly for furniture and various sports goods. The decorative appearance of many timbers is due to the *texture*, or to the *figure,* or to the *colour* of the material and, in many instances, to combinations of these.

44.5.1 Texture

The texture of timber depends on the size of the cells and on their arrangement. A timber such as boxwood in which the cells have a very small diameter is said to be *fine-textured*, while a *coarse-textured* timber such as keruing has a considerable percentage of large-diameter cells. Where the distribution of the cell-types or sizes across the growth ring is uniform, as in beech, or where the thickness of the cell wall remains fairly constant across the ring, as in some of the softwoods, e.g. yellow pine, the timber is described as being *even-textured*: conversely, where variation occurs across the growth ring, either in distribution of cells as in teak or in thickness of the cell walls as in larch or Douglas fir, the timber is said to have an *uneven texture*.

44.5.2 Figure

Figure is defined as the 'ornamental markings seen on the cut surface of timber, formed by the structural features of the wood', but the term is also frequently applied to the effect of marked variations in colour. The four most important structural features inducing figure are *grain*, *growth rings*, *rays* and *knots*.

Grain

Mention was made in Section 44.2 that the cells of wood, though often described as vertically orientated, frequently deviate from this convenient concept. In the majority of cases this deviation takes the form of a spiral, the magnitude of the angle varying with distance from the pith. Although of considerable technical importance because of loss in strength and induced machining problems, the common form of spiral grain has no effect on the figure presented on the finished timber. However, two other forms of grain deviation do have a very marked influence on the resulting figure of the wood. Thus, in certain hardwood timbers, and the mahoganies are perhaps the best example, the direction of the spiral in the longitudinal–tangential plane alternates from left to right hand at very frequent intervals along the radial direction; grain of this type is said to be *interlocked*. Tangential faces of machined timber will be normal, but the radial face will be characterised by the presence of alternating light and dark longitudinal bands produced by the reflection of light from the tapered cuts of fibres inclined in different directions (Figure 44.17). This type of figure is referred to as *ribbon* or *stripe* and is desirous in timber for furniture manufacture.

If instead of the grain direction alternating from left to right within successive layers along the radial direction as above, the grain direction alternates at right angles to this pattern, i.e. in the longitudinal–radial plane, a *wavy* type of grain is produced. This is very conspicuous in machined tangential faces where it shows up clearly as alternating light and dark horizontal bands (Figure 44.18); this type of figure is described as *fiddleback*, since timber with this distinctive type of figure has been used traditionally for the manufacture of the backs of violins: it is to be found also on the panels and sides of expensive wardrobes and bookcases.

Growth rings

Where variability occurs across the growth ring, either in the distribution of the various cell types or in the thickness of the cell walls, distinct patterns will appear on the machined faces of the timber. Such patterns, however, will not be regular like many of the man-made imitations, but will vary according to changes in width of the growth ring and in the relative proportions of early and latewood.

On the radial face the growth rings will be vertical and parallel to one another, but on the tangential face a most pleasing series of concentric

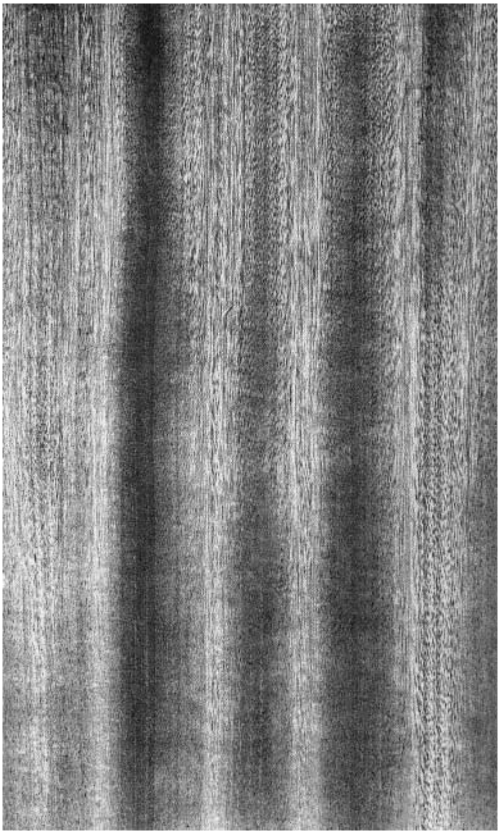

FIGURE 44.17 Illustration of ribbon or stripe figure on the cut longitudinal–radial plane. The fibres in successive radial zones are inclined in opposite directions (© Building Research Establishment).

arcs is produced as successive growth layers are intersected. In the centre part of the plank of timber illustrated in Figure 44.19, the growth rings are cut tangentially forming these attractive arcs, while the edge of the board with parallel and vertical growth rings reflects timber cut radially. In the case of ring-porous timbers, it is the presence of the large earlywood vessels which makes the growth ring so conspicuous, while in

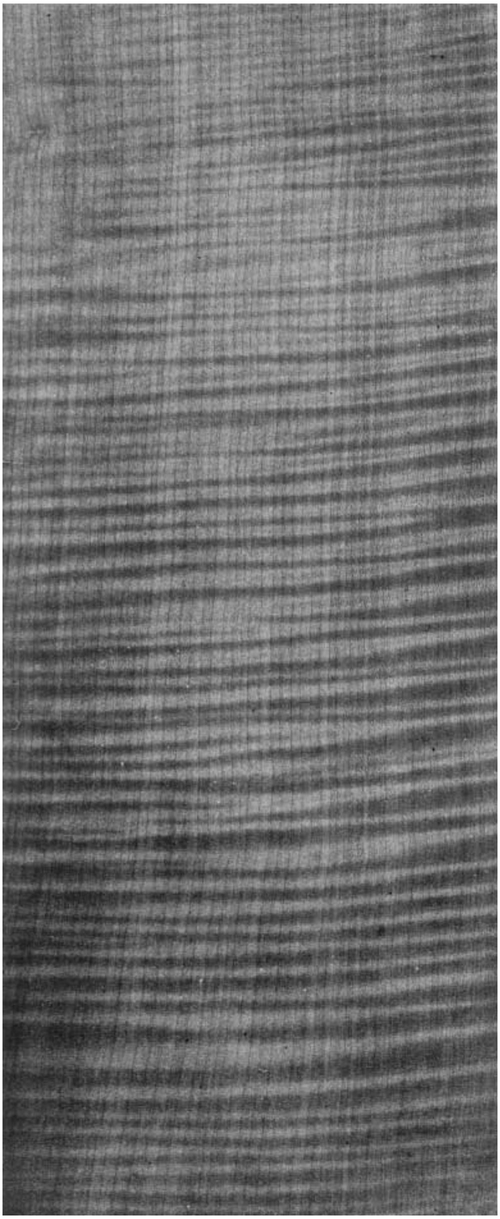

FIGURE 44.18 'Fiddleback' figure due to wavy grain (© Building Research Establishment).

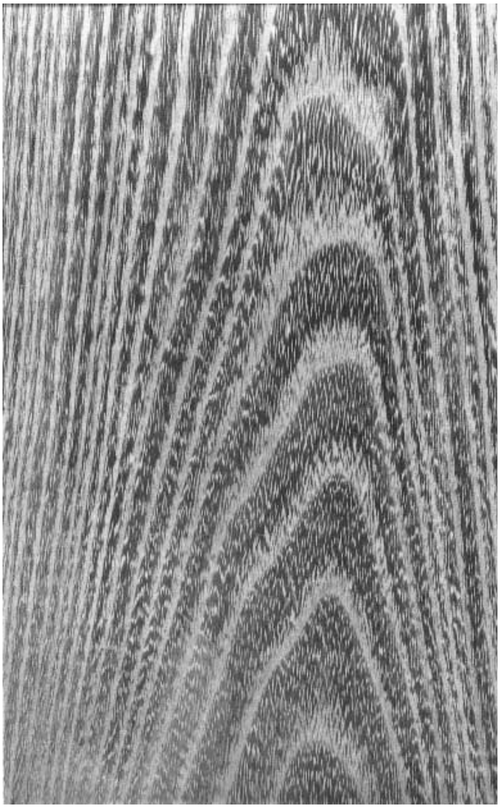

FIGURE 44.19 The effect of growth rings on figure (© Building Research Establishment).

timbers like Douglas fir or pitch pine, the striking effect of the growth ring can be ascribed to the very thick walls of the latewood cells.

Rays

Another structural feature which may add to the attractive appearance of timber is the ray, especially where, as in the case of oak, the rays are both deep and wide. When the surface of the plank coincides with the longitudinal–radial plane, these rays can be seen as sinuous light-coloured ribbons running across the grain.

Knots

Knots, though troublesome from the mechanical aspects of timber utilisation, can be regarded as a decorative feature; the fashion of knotty-pine furniture and wall panelling in the early 1970s is a very good example of how knots can be a decorative feature. However, as a decorative feature, knots do not possess the subtlety of variation in grain and colour that arises from the other structural features described above.

Exceptionally, trees produce a cluster of small shoots at some point on the trunk and the timber subsequently formed in this region contains a multitude of small knots. Timber from these *burrs* is highly prized for decorative work, especially if walnut or yew.

44.5.3 Colour

In the absence of extractives, timber tends to be a rather pale straw colour which is characteristic of the sapwood of almost all timbers. The onset of heartwood formation in many timbers is associated with the deposition of extractives, most of which are coloured, thereby imparting coloration to the heartwood zone. In passing, it should be recalled that although a physiological heartwood is always formed in older trees, extractives are not always produced; thus, the heartwood of timbers such as ash and spruce is colourless.

Where coloration of the heartwood occurs, a whole spectrum of colour exists among the different species. The heartwood may be yellow, e.g. boxwood; orange, e.g. opepe; red, e.g. mahogany; purple, e.g. purpleheart; brown, e.g. African walnut; green, e.g. greenheart; or black, e.g. ebony. In some timbers the colour is fairly evenly distributed throughout the heartwood, while in other species considerable variation in the intensity of the colour occurs. In zebrano, distinct dark brown and white stripes occur, while in olive wood patches of yellow merge into zones of brown. Dark gum-veins, as present in African walnut, contribute to the pleasing alternations in colour. Variations in colour such as these are regarded as contributing to the ‘figure’ of the timber.

It is interesting to note in passing that the non-coloured sapwood is frequently coloured artificially to match the heartwood, thereby adding to the amount of timber converted from the log. In a few rare cases, the presence of certain fungi in timber in the growing tree can result in the formation of very dark coloured heartwood: the activity of the fungus is terminated when the timber is dried. Both *brown oak* and *green oak*, produced by different fungi, have always been prized for decorative work.

44.6 Mass–volume relationships

44.6.1 Density

The *density* of a piece of timber is a function not only of the amount of wood substance present, but also the presence of both extractives and moisture. In a few timbers extractives are completely absent, while in many they are present, but only in small amounts and usually less than 3 per cent of the dry mass of the timber. In some exceptional cases, the extractive content may be as high as 10 per cent and in these cases it is necessary to remove the extractives prior to the determination of density.

The presence of moisture in timber not only increases the mass of the timber, but also results in the swelling of the timber, and hence both mass and volume are affected. Thus, in the determination of density where

$$\rho = \frac{m}{v} \tag{44.1}$$

both the mass (m) and volume (v) must be determined at the same moisture content. Generally, these two parameters are determined at zero moisture content. However, as density is frequently quoted at a moisture content of 12 per cent since this level is frequently experienced in timber in use, the value of density at zero moisture content is corrected for 12 per cent if volumetric expansion figures are known, or else the density determination is carried out on timber at 12 per cent moisture content.

Thus, if

$$m_x = m_0(1 + 0.01\,\mu) \tag{44.2}$$

where m_x is the mass of timber at moisture content x, m_0 is the mass of timber at zero moisture content, and μ is the moisture content percentage, and

$$v_x = v_0\,(1 + 0.01\,s_v) \tag{44.3}$$

where v_x is the volume of timber at moisture content x, v_0 is the volume of timber at zero moisture content, and s_v is the volumetric shrinkage/expansion percentage, it is possible to obtain the density of timber at any moisture content in terms of the density at zero moisture content thus:

$$\rho_x = \frac{m_x}{v_x} = \frac{m_0(1 + 0.01\,\mu)}{v_0(1 + 0.01\,s_v)} = \rho_0\left(\frac{1 + 0.01\,\mu}{1 + 0.01\,s_v}\right) \tag{44.4}$$

As a very approximate rule of thumb, the density of timber increases by approximately 0.5 per cent for each 1.0 per cent increase in moisture content up to 30 per cent. Density therefore will increase, slightly and curvilinearly, up to moisture contents of about 30 per cent as both total mass and volume increase; however, at moisture contents above 30 per cent, density will increase rapidly and curvilinearly with increasing moisture content, since, as will be explained later in this chapter, the volume remains constant above this value, whilst the mass increases.

The determination of density by measurement of mass and volume takes a considerable period of time and over the years a number of quicker techniques have been developed for use where large numbers of density determinations are required. These methods range from the assessment of the opacity of a photographic image which has been produced by either light or β-irradiation passing through a thin section of wood, to the use of a mechanical device (the Pilodyn) which fires a spring-loaded bolt into the timber, after which the depth of penetration is measured. In all these techniques, however, the method or instrument has to be calibrated against density values obtained by the standard mass/volume technique.

In Section 44.2, timber was shown to possess different types of cell which could be characterised by different values of the ratio of cell-wall thickness to total cell diameter. Since this ratio can be regarded as an index of density, it follows that density of the timber will be related to the relative proportions of the various types of cells. Density, however, will also reflect the absolute wall thickness of any one type of cell, since it is possible to obtain fibres of one species of timber, the cell wall thickness of which can be several times greater than that of fibres of another species.

Density, like many other properties of timber, is extremely variable; it can vary by a factor of ten, ranging from an average value at 12 per cent m.c. of 176 kg/m^3 for balsa, to about 1230 kg/m^3 for lignum vitae (Figure 44.20). Balsa, therefore, has a density similar to that of cork, while lignum vitae has a density slightly less than half that of concrete or aluminium. The values of density quoted for different timbers, however, are merely average values: each timber will have a range of densities reflecting differences between early and latewood, between the pith and outer rings, and between trees on the same site. Thus, for example, the density of balsa can vary from 40 to 320 kg/m^3.

In certain publications, reference is made to the *weight* of timber, a term widely used in commerce; it should be appreciated that the quoted values are really densities.

44.6.2 Specific gravity

The traditional definition of *specific gravity* (G) (also known as relative density) can be expressed as:

$$G = \frac{\rho_t}{\rho_w} \tag{44.5}$$

where ρ_t is the density of timber, and ρ_w is the density of water at 4°C = 1.0000 g/ml. G will therefore vary with moisture content and consequently the specific gravity of timber is usually based on the oven-dry mass, and volume at some specified moisture content. This is frequently taken as zero though, for convenience, green or other moisture conditions are sometimes used when the terms *basic specific gravity* and *nominal specific gravity* are applied respectively. Hence:

$$G_\mu = \frac{m_0}{V_\mu \rho_w} \tag{44.6}$$

where m_0 is the oven-dry mass of timber, V_μ is the volume of timber at moisture content μ, ρ_w is the density of water, and G_μ is the specific gravity at moisture content μ.

At low moisture contents, specific gravity decreases slightly with increasing moisture content up to 30 per cent, thereafter remaining constant. In research activities specific gravity is defined usually in terms of oven-dry mass and volume. However, for engineering applications specific gravity is frequently presented as the ratio of oven-dry mass to volume of timber at 12 per cent moisture content; this can be derived from the oven-dry specific gravity, thus:

$$G_{12} = \frac{G_0}{1 + 0.01\,\mu G_0/G_{s12}} \tag{44.7}$$

where G_{12} is the specific gravity of timber at 12 per cent moisture content, G_0 is the specific gravity of timber at zero moisture content, μ is the moisture content percentage, and G_{s12} is the specific gravity of bound water at 12 per cent moisture content.

The relationship between density and specific gravity can be expressed as

$$\rho = G(1 + 0.01\,\mu)\rho_w \tag{44.8}$$

where ρ is the density at moisture content μ, G is the specific gravity at moisture content μ, and ρ_w is the density of water. Equation (44.8) is valid for all moisture contents. When $\mu = 0$ the equation reduces to

$$\rho = G_0 \tag{44.9}$$

i.e. density and specific gravity are numerically equal.

44.6.3 Density of the dry cell wall

Although the density of timber may vary considerably among different timbers, the density of the actual cell wall material remains constant for

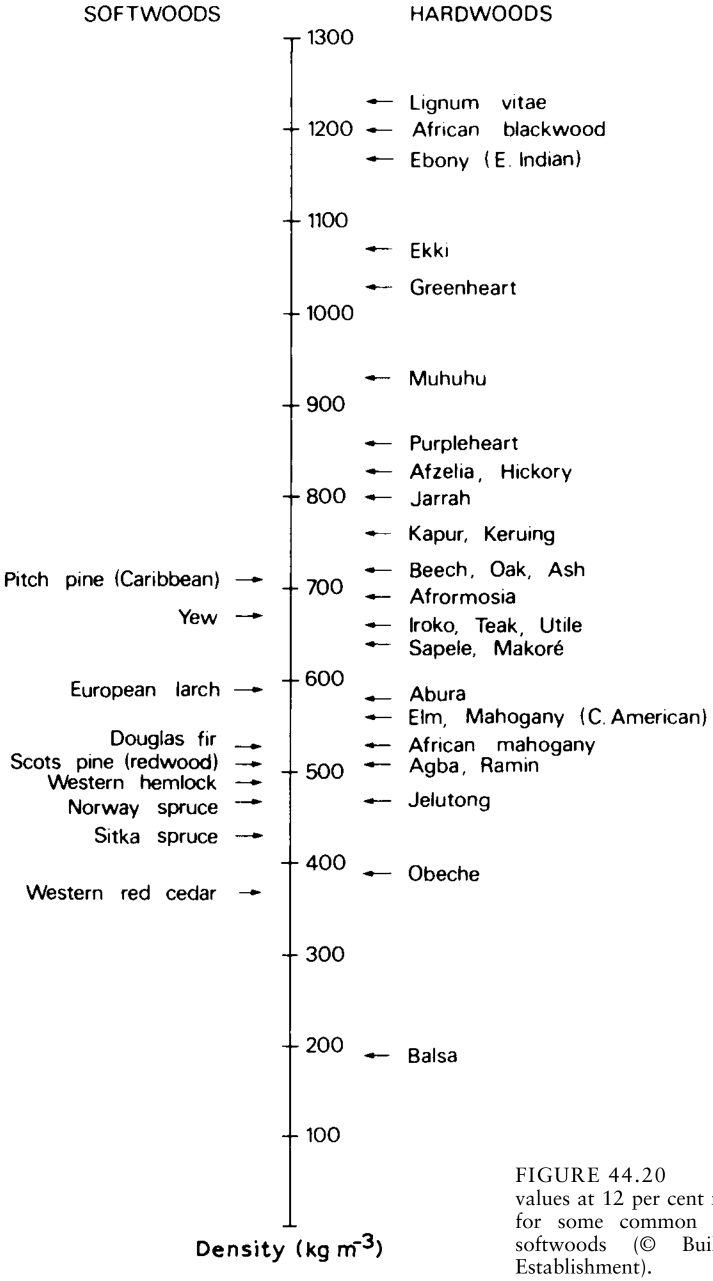

FIGURE 44.20 Mean density values at 12 per cent moisture content for some common hardwoods and softwoods (© Building Research Establishment).

all timbers with a value of approximately 1500 kg/m^3 (1.5 g/ml) when measured by volume-displacement methods.

The exact value for cell-wall density depends on the liquid used for measuring the volume: thus, densities of 1.525 and 1.451 g/ml have been recorded for the same material using water and toluene respectively.

44.6.4 Porosity

In Section 44. 2 the cellular nature of timber was described in terms of a parallel arrangement of hollow tubes. The *porosity (p)* of timber is defined as the fractional void volume and is expressed mathematically as

$$p = 1 - V_f \qquad (44.10)$$

where V_f is the volume fraction of cell wall substance.

The calculation of porosity is set out in Chapter 3 of Dinwoodie (2000).

44.7 Moisture in timber

44.7.1 Equilibrium moisture content

Timber is hygroscopic, that is it will absorb moisture from the atmosphere if it is dry and, correspondingly, yield moisture to the atmosphere when wet, thereby attaining a moisture content which is in equilibrium with the water vapour pressure of the surrounding atmosphere. Thus, for any combination of vapour pressure and temperature of the atmosphere there is a corresponding moisture content of the timber such that there will be no inward or outward diffusion of water vapour: this moisture content is referred to as the *equilibrium moisture content* (emc). Generally, it is more convenient to use relative humidity rather than vapour pressure. Relative humidity is defined as the ratio of the partial vapour pressure in the air to the saturated vapour pressure, expressed as a percentage.

The fundamental relationships between moisture content of timber and atmospheric conditions have been determined experimentally and the average equilibrium moisture content values are shown graphically in Figure 44.21. A timber in an atmosphere of 20°C and 22 per cent relative humidity will have a moisture content of 6 per cent (see below), while the same timber if moved to an atmosphere of 40°C and 64 per cent relative humidity will double its moisture content. It should be emphasised that the curves in Figure 44.21 are average values for moisture in relation to relative humidity and temperature, and that slight variations in the equilibrium moisture content will occur due to differences between timbers and to the previous history of the timber with respect to moisture.

44.7.2 Determination of moisture content

It is customary to express the moisture content of timber in terms of its oven-dry mass using the equation

$$\mu = \frac{m_{\text{init}} - m_{\text{od}}}{m_{\text{od}}} \times 100 \qquad (44.11)$$

where m_{init} = initial mass of timber sample (g), m_{od} = mass of timber sample after oven-drying at 105°C (g) and μ = moisture content of timber sample (per cent).

The expression of moisture content of timber on a dry mass basis is in contrast to the procedure adopted for other materials where moisture content is expressed in terms of the wet mass of the material.

Determination of moisture content in timber is usually carried out using the basic gravimetric technique above, though it should be noted that at least a dozen different methods have been recorded in the literature. Suffice it here to mention only two of these alternatives. First, where the timber contains volatile extractives which would normally be lost during oven drying, thereby resulting in erroneous moisture content values, it is customary to use a distillation process, heating the timber in the presence of a water-immiscible liquid such as toluene, and collecting the condensed water vapour in a

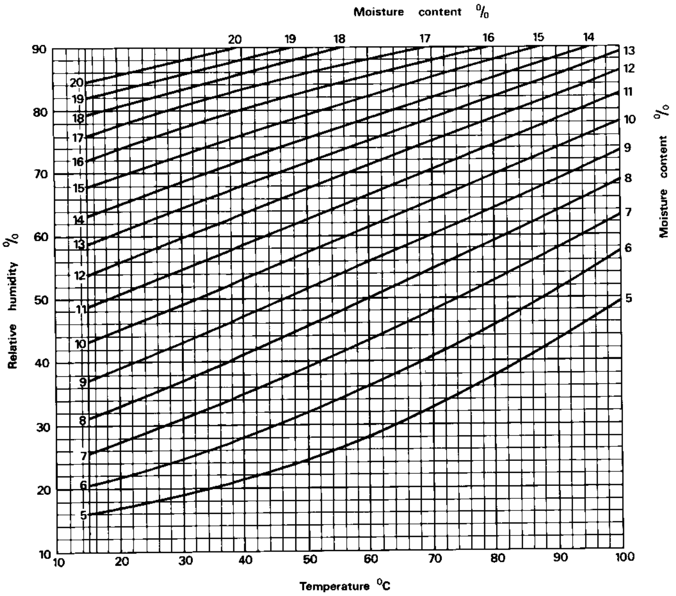

FIGURE 44.21 Chart showing the relationship between the moisture content of timber and the temperature and relative humidity of the surrounding air; approximate curves based on values obtained during drying from green condition (Building Research Establishment).

calibrated trap. Second, where ease and speed of operation are preferred to extreme accuracy, moisture contents are assessed using electric moisture meters. The type most commonly used is known as the *resistance meter*, though this battery-powered hand-held instrument actually measures the conductance or flow (the reciprocal of resistance) of an electric current between two probes. Below the fibre saturation point (about 27 per cent moisture content, see later) an approximately linear relationship exists between the logarithm of conductance and the logarithm of moisture content. However, this relationship, which forms the basis for this type of meter, changes with species of timber, temperature and grain angle. Thus, a resistance-type meter is equipped with a number of alternative scales, each of which relates to a different group of timber species; it should be used at temperatures close to 20°C with the pair of probes inserted parallel to the grain direction.

Although the measurement of moisture content is quick with such a meter, there are, however, two drawbacks to its use. First, moisture content is measured only to the depth of penetration of the two probes, a measurement which may not be representative of the moisture content of the entire depth of the timber member; the use of longer probes can be beneficial, though these are difficult to insert and withdraw. Second, the working range of the instrument is only from 7 to 27 per cent moisture content.

44.7.3 The moisture content of green timber

In the living tree, water is to be found not only in the cell cavity, but also within the cell wall.

Consequently the moisture content of green wood (newly felled) is high, usually varying from about 60 per cent to nearly 200 per cent depending on the location of the timber in the tree and the season of the year. However, seasonal variation is slight compared to the differences that occur within a tree between the sapwood and heartwood regions. The degree of variation is illustrated for a number of softwoods and hardwoods in Table 44.4: within the former group the sapwood may contain twice the percentage of moisture to be found in the corresponding heartwood, while in the hardwoods this difference is appreciably smaller or even absent. However, pockets of 'wet' wood can be found in the heartwood as described in Section 44.1.

Green timber will yield moisture to the atmosphere with consequent changes in its dimensions: at moisture contents above 20 per cent many timbers, especially their sapwood, are susceptible to attack by fungi: the strength and stiffness of green wood is considerably lower than for the same timber when dry. For all these reasons it is necessary to dry or *season* timber following felling of the tree and prior to its use in service.

44.7.4 Removal of moisture from timber

Drying or seasoning of timber can be carried out in the open, preferably with a top cover. However, it will be appreciated from the previous discussion on equilibrium moisture contents that the minimum moisture content that can be achieved is determined by the lowest relative humidity of the summer period. In this country it is seldom possible to achieve moisture contents less than 16 per cent by air seasoning. The planks of timber are separated in rows by stickers (usually 25–30 mm across) which permit air currents to pass through the pile; nevertheless it may take from two to ten years to air-season timber depending on the species of timber and the thickness of the timber members.

The process of seasoning may be accelerated artificially by placing the stacked timber in a drying kiln, basically a large chamber in which the temperature and humidity can be controlled and altered throughout the drying process: the control may be carried out manually or programmed automatically. Humidification is sometimes required in order to keep the humidity of the surrounding air at a desired level when insufficient moisture is coming out of the timber; it is frequently required towards the end of the drying run and is achieved either by the admission of small quantities of live steam or by the use of water atomisers or low-pressure steam evaporators. Various designs of kilns are used and these are reviewed in detail by Pratt (1974).

Drying of softwood timber in a kiln can be accomplished in from four to seven days, the optimum rate of drying varying widely from one timber to the next; hardwood timber usually takes about three times longer than softwood of the same dimension. Following many years of experimenta-

TABLE 44.4 Average green moisture contents of the sapwood and heartwood

		Moisture content (%)	
Botanical name	*Commercial name*	*Heartwood*	*Sapwood*
Hardwoods			
Betula lutea	Yellow birch	64	68
Fagus grandifolia	American beech	58	79
Ulmus americana	American elm	92	84
Softwoods			
Pseudotsuga menziesii	Douglas fir	40	116
Tsuga heterophylla	Western hemlock	93	167
Picea sitchensis	Sitka spruce	50	131

tion, kiln schedules have been published for different groups of timbers; these schedules provide wet- and dry-bulb temperatures (maximum of 70°C) for different stages in the drying process and their use should result in the minimum amount of degrade in terms of twist, bow, spring, collapse and checks (Pratt, 1974). Most timber is now seasoned by kilning: little air drying is carried out. Dry stress-graded timber in the UK must be kiln-dried to a mean value of 20 per cent moisture content with no single piece greater than 24 per cent. However, UK and some Swedish mills are now targeting 12 per cent ('superdried'), as this level is much closer to the moisture content in service.

Recently, *solar kilns* have become commercially available and are particularly suitable for use in the developing countries to season many of the difficult slow-drying tropical timbers. These small kilns are very much cheaper to construct than conventional kilns and are also much cheaper to run. They are capable of drying green timber to about 7 per cent moisture content in the dry season and about 11 per cent in the rainy season.

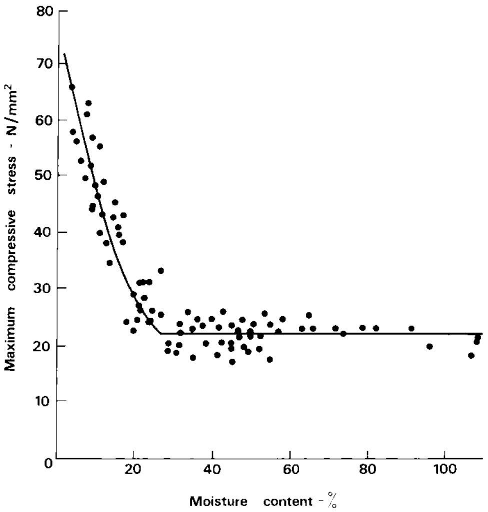

FIGURE 44.22 Relationship between longitudinal compressive strength and moisture content (© Building Research Establishment).

44.7.5 Influence of structure

As previously mentioned in Section 44.7.3, water in green or freshly felled timber is present both in the cell cavity and within the cell wall. During the seasoning process, irrespective of whether this is by air or within a kiln, water is first removed from within the cell cavity: this holds true down to moisture contents of about 27–30 per cent. Since the water in the cell cavities is *free*, not being chemically bonded to any part of the timber, it can readily be appreciated that its removal will have no effect on the strength or dimensions of the timber. The lack of variation of the former parameter when moisture content is reduced from 110 to 27 per cent is illustrated in Figure 44.22.

However, at moisture contents below 27 per cent water is no longer present in the cell cavity, but is restricted to the cell wall where it is chemically bonded (hydrogen bonding) to the matrix constituents, to the hydroxyl groups of the cellulose molecules in the non-crystalline regions and to the surface of the crystallites; as such, this water is referred to as *bound water*. The uptake of water by the lignin component is considerably lower than that by either the hemicellulose or the amorphous cellulose; water may be present as a monomolecular layer though frequently up to six layers can be present. Water cannot penetrate the crystalline cellulose since the hygroscopic hydroxyl groups are mutually satisfied by the formation of both intra- and intermolecular bonds within the crystalline region as described in Section 44.3.1. This view is confirmed from X-ray analyses which indicate no change of state of the crystalline core as the timber gains or loses moisture.

However, the percentage of non-crystalline material in the cell wall varies between 8 and 33 per cent and the influence of this fraction of cell wall material as it changes moisture content on the behaviour of the total cell wall is very significant. The removal of water from these areas within the cell wall results first in increased strength and second in marked shrinkage. Both changes can be accounted for in terms of drying out of the water-reactive matrix, thereby causing the microfibrils to come into closer proximity, with a commensurate increase in interfibrillar bonding and decrease in overall dimensions. Such changes are reversible, or almost completely reversible.

44.7.6 Fibre saturation point

The increase in strength on drying is clearly indicated in Figure 44.22, from which it will be noted that there is a threefold increase in strength as the moisture content of the timber is reduced from about 27 per cent to zero. The moisture content corresponding to the inflexion in the graph is termed the *fibre saturation point* (fsp), where in theory there is no free water in the cell cavities while the walls are holding the maximum amount of bound water. In practice this rarely exists; a little free water may still exist while some bound water is removed from the cell wall. Consequently, the fibre saturation 'point', while a convenient concept, should really be regarded as a 'range' in moisture contents over which the transition occurs.

The fibre saturation point therefore corresponds in theory to the moisture content of the timber when placed in a relative humidity of 100 per cent; in practice, however, this is not so since such an equilibrium would result in total saturation of the timber (Stamm, 1964). Values of emc above 98 per cent are unreliable. It is generally found that the moisture content of hardwoods at this level are from 1 to 2 per cent higher than for softwoods. At least nine different methods of determining the fibre saturation point are recorded in the literature; the value of the fibre saturation point is dependent on the method used.

44.7.7 Sorption

Timber, as already noted in Section 44.7.1, assumes with the passage of time a moisture content which is in equilibrium with the relative vapour pressure of the atmosphere. This process of water sorption is typical of solids with a complex capillary structure and this phenomenon has also been observed in concrete. The similarity in behaviour between timber and concrete with regard to moisture relationships is further illustrated by the presence of S-shaped isotherms when moisture content is plotted against relative vapour pressure. Both materials have isotherms which differ according to whether the moisture content is reducing (desorption) or increasing (adsorption), thereby producing a *hysteresis loop* (Figure 44.23).

Readers desirous of more information on sorption and diffusion, especially on the different theories of sorption, are referred to the comprehensive text by Skaar (1988).

44.8 Flow in timber

The term *flow* is synonymous with the passage of liquids through a porous medium such as timber, but the term is also applicable to the passage of gases, thermal energy and electrical energy; it is this wider interpretation of the term that is applied in this chapter, albeit that the bulk of the chapter is devoted to the passage of both liquids and gases (i.e. fluids).

The passage of *fluids* through timber can occur in one of two ways, either as *bulk flow* through the interconnected cell lumens or other voids, or by *diffusion*. The latter embraces both the transfer of water vapour through air in the lumens and the movement of bound water within the cell wall (Figure 44.24). The magnitude of the bulk flow of a fluid through timber is determined by its *permeability*.

Looking at the phenomenon of flow of moisture in wood from the point of view of the type of moisture, rather than the physical processes involved as described above, it is possible to identify the involvement of three types of moisture:

(a) *free water* in the cell cavities giving rise to bulk flow above the fibre saturation point (see Section 44.7.5);
(b) *bound water* within the cell walls which moves by diffusion below the fibre saturation point (see Section 44.7.5);
(c) *water vapour* which moves by diffusion in the lumens both above and below the fibre saturation point.

It is convenient when discussing flow of any type to think of it in terms of being either constant or

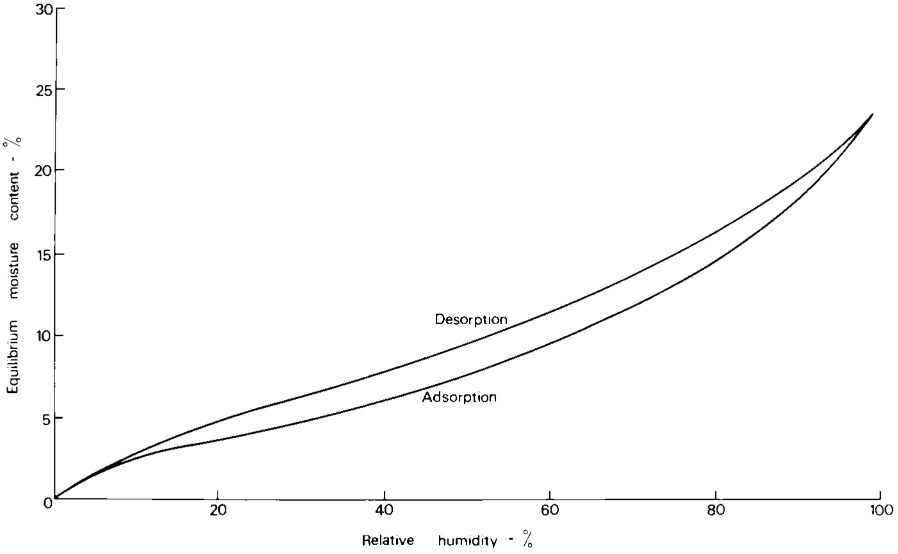

FIGURE 44.23 Hysteresis loop resulting from the average adsorption and desorption isotherms for six species of timber at 40°C (© Building Research Establishment).

variable with respect to either time or location within the specimen; flow under the former conditions is referred to as *steady-state flow*, whereas when flow is time and space dependent it is referred to as *unsteady-state flow*. Because of the complexity of the latter, only the former is covered in this text; readers desirous of information on unsteady-state flow are referred to Siau (1984).

One of the most interesting features of steady-state flow in timber in common with many other materials is that the same basic relationship holds, irrespective of whether one is concerned with liquid or gas flow, diffusion of moisture, or thermal and electrical conductivity. The basic relationship is that the flux or rate of flow is proportional to the pressure gradient:

$$\frac{\text{flux}}{\text{gradient}} = k \qquad (44.12)$$

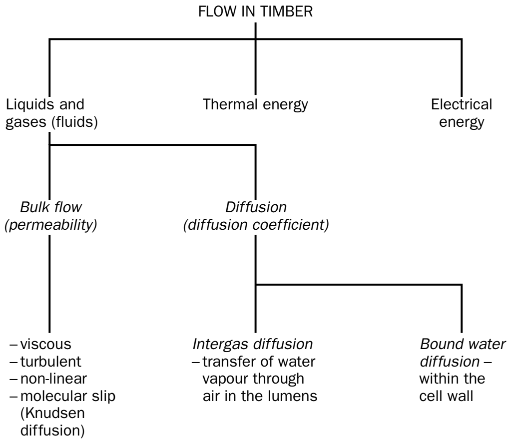

FIGURE 44.24 The different aspects of flow in timber which are covered in this chapter.

where flux is the rate of flow per unit cross-sectional area, gradient is the pressure difference per unit length causing flow, and k is a constant, dependent on form of flow, e.g. permeability, diffusion or conductivity.

44.8.1 Bulk flow and permeability

Permeability is simply the quantitative expression of the bulk flow of fluids through a porous material. Flow in the steady-state condition is best described in terms of Darcy's law. Thus,

$$\text{permeability} = \frac{\text{flux}}{\text{gradient}} \tag{44.13}$$

and for the flow of liquids, this becomes

$$k = \frac{QL}{A\Delta P} \tag{44.14}$$

where k is the permeability (cm^2/atm s), Q is the volume rate of flow (cm^3/s), ΔP is the pressure differential (atm), A is the cross-sectional area of the specimen (cm^2), and L is the length of the specimen in the direction of flow (cm).

Because of the change of pressure of a gas and hence its volumetric flow rate as it moves through a porous medium, Darcy's law for the flow of gases has to be modified as follows:

$$k_g = \frac{QLP}{A\Delta P\overline{P}} \tag{44.15}$$

where k_g is the superficial gas permeability and Q, L, A and ΔP are as in equation (44.14), P is the pressure at which Q is measured, and $\overline{P}$ is the mean gas pressure in the sample (Siau, 1984).

Of all the numerous physical and mechanical properties of timber, permeability is by far the most variable; when differences between timbers and differences between the principal directions within a timber are taken into consideration, the range is of the order of 10^7. Not only is permeability important in the impregnation of timber with artificial preservatives, fire retardants and stabilising chemicals, but it is also significant in the chemical removal of lignin in the manufacture of wood pulp and in the removal of *free* water during drying.

Flow of fluids

The bulk of flow occurs as *viscous (or laminar) flow* in capillaries where the rate of flow is relatively low and when the viscous forces of the fluid are overcome in shear, thereby producing an even and smooth flow pattern. In viscous flow Darcy's law is directly applicable, but a more specific relationship for flow in capillaries is given by the Poiseuille equation, which for liquids is:

$$Q = \frac{N\pi r^4 \Delta P}{8\eta L} \tag{44.16}$$

where N is the number of uniform circular capillaries in parallel, Q is the volume rate of flow, r is the capillary radius, ΔP is the pressure drop across the capillary, L is the capillary length and η is the viscosity. For gas flow, the above equation has to be modified slightly to take into account the expansion of the gas along the pressure gradient. The amended equation is:

$$Q = \frac{N\pi r^4 \Delta P\overline{P}}{8\eta LP} \tag{44.17}$$

where $\overline{P}$ is the mean gas pressure within the capillary and P is the pressure of gas where Q was measured. In both cases

$$Q \propto \frac{\Delta P}{L} \tag{44.18}$$

or flow is proportional to the pressure gradient, which conforms with the basic relationship for flow.

Other types of flow can occur, e.g. turbulent, non-linear and molecular diffusion, the last mentioned being of relevance only to gases. Information on all these types is to be found in Siau (1984).

Flow paths in timber

Softwoods

Because of their simpler structure and their greater economic significance, much more attention has been paid to flow in softwood timbers than in hardwood timbers. It will be recalled from Section 44.2 that both tracheids and parenchyma cells have closed ends and that movement of liquids and gases must be by way of the pits in the cell wall. Three types of pit are present. The first is the bordered pit (Figure 44.10) which is almost entirely restricted to the radial walls of the tracheids, tending to be located towards the ends of the cells. The second type of pit is the ray or semi-bordered pit which interconnects the vertical tracheid with the horizontal ray parenchyma cell, while the third type is the simple pit between adjacent parenchyma cells.

For very many years it was firmly believed that since the diameter of the pit opening or of the openings between the margo strands was very much less than the diameter of the cell cavity, and since permeability is proportional to a power function of the capillary radius, the bordered pits would be the limiting factor controlling longitudinal flow. However, it has been demonstrated that this concept is fallacious and that at least 40 per cent of the total resistance to longitudinal flow in *Abies grandis* sapwood that had been specially dried to ensure that the torus remained in its natural position could be accounted for by the resistance of the cell cavity (Petty and Puritch, 1970).

Both longitudinal and tangential flowpaths in softwoods are predominantly by way of the bordered pits as illustrated in Figure 44.25, while the horizontally aligned ray cells constitute the principal pathway for radial flow, though it has been suggested that very fine capillaries within the cell wall may contribute slightly to radial flow. The rates of radial flow are found to vary very widely between species.

It is not surprising to find that the different pathways to flow in the three principal axes result in anisotropy in permeability. Permeability values quoted in the literature illustrate that for most timbers longitudinal permeability is about 10^4 times the transverse permeability; mathematical modelling of longitudinal and tangential flow supports a degree of anisotropy of this order. Since both longitudinal and tangential flow in softwoods are associated with bordered pits, a good correlation is to be expected between them; radial permeability is only poorly correlated with that in either of the other two directions and is frequently found to be greater than tangential permeability.

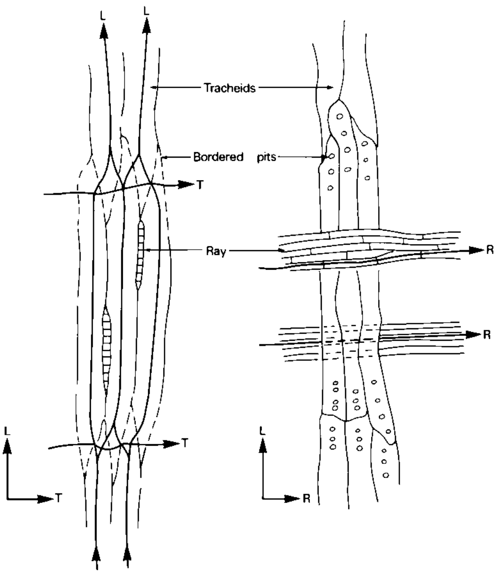

FIGURE 44.25 On the left, a representation of the cellular structure of a softwood in a longitudinal–tangential plane illustrating the significance of the bordered pits in both longitudinal and tangential flow; on the right, softwood timber in the longitudinal radial plane, indicating the role of the ray cells in defining the principal pathway for radial flow (© Building Research Establishment).

Permeability is not only directionally dependent, but is also found to vary with moisture content, between earlywood and latewood, between sapwood and heartwood (Figure 44.26) and between species. In the sapwood of *green* timber the torus of the bordered pit is usually located in a central position and flow can be at a maximum (Figure 44.27(a)). Since the earlywood cells possess larger and more frequent bordered pits, the flow through the earlywood is considerably greater than that through the latewood. However, on drying, the torus of the earlywood cells becomes aspirated (Figures 44.10 and

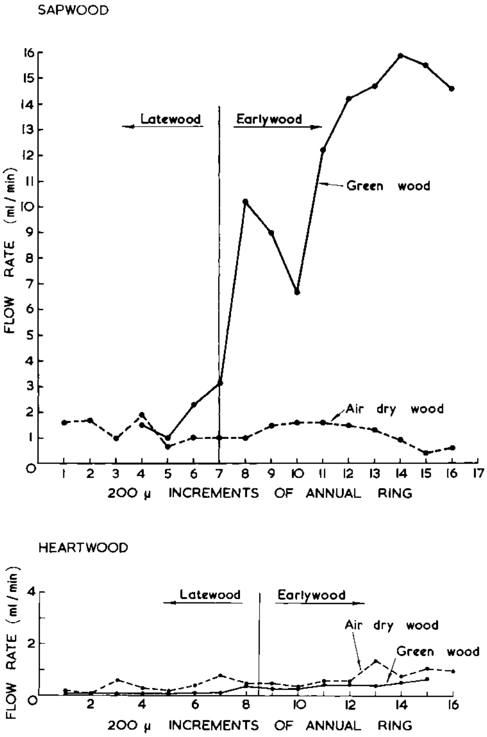

FIGURE 44.26 The variation in rate of longitudinal flow through samples of green and dry earlywood and latewood of Scots pine sapwood and heartwood (from Banks (1968), © Building Research Establishment).

44.27(b)), owing, it is thought, to the tension stresses set up by the retreating water meniscus (Hart and Thomas, 1967). In this process the margo strands obviously undergo very considerable extension and the torus is rigidly held in a displaced position by strong hydrogen bonding

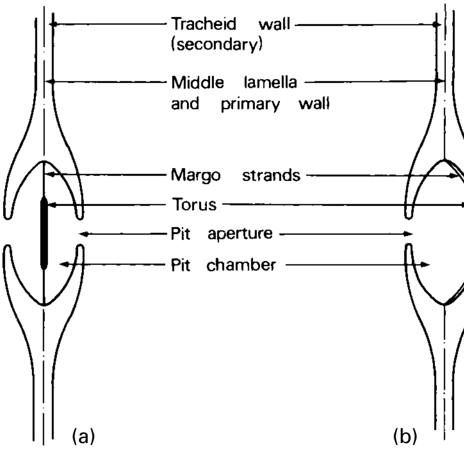

FIGURE 44.27 Cross-section of a bordered pit in the sapwood of a softwood timber: (a) in timber in the green condition with the torus in the 'normal' position; and (b) in timber in the dried state with the torus in an aspirated position (© Building Research Establishment).

This displacement of the torus effectively seals the pit and markedly reduces the level of permeability of dry earlywood. In the latewood, the degree of pit aspiration is very much lower on drying than in the earlywood, a phenomenon that is related to the smaller diameter and thicker cell wall of the latewood pit. Thus, in dry timber in marked contrast to green timber, the permeability of the latewood is at least as good as that of the earlywood and may even exceed it (Figure 44.26). Rewetting of the timber causes only a partial reduction in the number of aspirated pits and it appears that aspiration is mainly irreversible.

Quite apart from the fact that many earlywood pits are aspirated in the heartwood of softwoods, the permeability of the heartwood is usually appreciably lower than that of the sapwood due to the deposition of encrusting materials over the torus and margo strands and also within the ray cells (Figure 44.26).

Permeability varies widely among different species of softwoods. Thus, Comstock (1970) found that the ratio of longitudinal-to-tangential permeability varied between 500:1 to 80 000:1. Generally, the pines are much more permeable than the spruces, firs or Douglas fir. This can be attributed primarily, though not exclusively, to the markedly different type of semi-bordered pit present between the vertical tracheids and the ray parenchyma in the pines (fenestrate or pinoid type) compared with the spruces, firs or Douglas fir (piceoid type).

Hardwoods

The longitudinal permeability is usually high in the sapwood of hardwoods. This is because these timbers possess vessel elements, the ends of which have been either completely or partially dissolved away. Radial flow is again by way of the rays, while tangential flow is more complicated, relying on the presence of pits interconnecting adjacent vessels, fibres and vertical parenchyma; however, intervascular pits in sycamore have been shown to provide considerable resistance to flow (Petty, 1981). Transverse flow rates are usually much lower than in the softwoods, but somewhat surprisingly, a good correlation exists between tangential and radial permeability; this is due in part to the very low permeability of the rays in hardwoods.

Since the effects of bordered pit aspiration, so dominant in controlling the permeability of softwoods, are absent in hardwoods, the influence of drying on the level of permeability in hardwoods is very much less than is the case with softwoods.

Permeability is highest in the outer sapwood, decreasing inwards and reducing markedly with the onset of heartwood formation as the cells become blocked either by the deposition of gums or resins or, as happens in certain timbers, by the ingrowth into the vessels of cell wall material of neighbouring cells, a process known as the formation of *tyloses*.

Permeability varies widely among different species of hardwoods. This variability is due in large measure to the wide variation in vessel diameter that occurs among the hardwood species. Thus, the ring-porous hardwoods which are characterised with having earlywood vessels that are of large diameter, generally have much higher permeabilities than the diffuse-porous timbers which have vessels of considerably lower diameter; however, in those ring-porous timbers that develop tyloses (e.g. the white oaks) their heartwood permeability may be lower than that in the heartwood of diffuse-porous timbers. Interspecific variability in permeability also reflects the different types of pitting on the end walls of the vessel elements.

Timber and the laws of flow

The application of Darcy's law to the permeability of timber is based on a number of assumptions, not all of which are upheld in practice. Among the more important are that timber is a homogeneous porous material and that flow is always viscous and linear; neither of these assumptions is strictly valid, but the Darcy law remains a useful tool with which to describe flow in timber.

By de-aeration and filtration of their liquid, many workers have been able to achieve steady-state flow, the rate of which is inversely related to the viscosity of the liquid, and to find that, in very general terms, Darcy's law was upheld in timber (see e.g. Comstock, 1967).

Gas, because of its lower viscosity and the ease with which steady flow rates can be obtained, is a most attractive fluid for permeability studies. However, at low mean gas pressures, due to the presence of slip flow, deviations from Darcy's law have been observed by a number of investigators. At higher mean gas pressures, however, an approximately linear relationship between conductivity and mean pressure is expected and this, too, has been observed experimentally. However, at even higher mean gas pressures, flow rate is sometimes less than proportional to the applied pressure differential due, it is thought, to the onset of non-linear flow. Darcy's law may thus appear to be valid only in the middle range of mean gas pressures.

44.8.2 Moisture diffusion

Flow of water below the fibre saturation point embraces both the diffusion of water vapour through the void structure comprising the cell cavities and pit membrane pores and the diffusion of bound water through the cell walls (Figure 44.24). In passing, it should be noted that because of the capillary structure of timber, vapour pressures are set up and vapour can pass through the timber both above and below the fibre saturation point; however, the flow of vapour is usually regarded as being of secondary importance to that of both bound and free water.

Moisture diffusion is another manifestation of flow, conforming with the general relationship between flux and pressure. Thus, it is possible to express diffusion of moisture in timber at a fixed temperature in terms of Fick's first law, which states that the flux of moisture diffusion is directly proportional to the gradient of moisture concentration; as such, it is analogous to the Darcy law on flow of fluids through porous media.

The total flux F of moisture diffusion through a plane surface under isothermal conditions is given by

$$F = \frac{dm}{dt} = -D.\frac{dc}{dx} \qquad (44.19)$$

where dm/dt is the flux (rate of mass transfer per unit area), dc/dx is the gradient of moisture concentration (mass per unit volume) in the x direction, and D is the moisture diffusion coefficient which is expressed in m^2/s (Siau, 1984; Skaar, 1988).

Under steady-state conditions the diffusion coefficient is given by

$$D = \frac{100mL}{tA\rho\Delta M} \qquad (44.20)$$

where m is the mass of water transported in time t, A is the cross-sectional area, L is the length of the wood sample, and ΔM is the moisture content difference driving the diffusion.

The vapour component of the total flux is usually much less than that for the bound water. The rate of diffusion of water vapour through timber at moisture contents below the fibre saturation point has been shown to yield coefficients similar to those for the diffusion of carbon dioxide, provided corrections are made for differences in molecular weight between the gases. This means that water vapour must follow the same pathway through timber as does carbon dioxide and implies that diffusion of water vapour through the cell walls is negligible in comparison to that through the cell cavities and pits (Tarkow and Stamm, 1960).

Bound water diffusion occurs when water molecules bound to their sorption sites by hydrogen bonding receive energy in excess of the bonding energy, thereby allowing them to move to new sites. At any one time the number of molecules with excess energy is proportional to the vapour pressure of the water in the timber at that moisture content and temperature. The rate of diffusion is proportional to the concentration gradient of the migrating molecules, which in turn is proportional to the vapour pressure gradient.

The most important factors affecting the diffusion coefficient of water in timber are temperature, moisture content and density of the timber. Thus, Stamm (1959) has shown that the bound water diffusion coefficient of the cell wall substance increases with temperature approximately in proportion to the increase in the saturated vapour pressure of water, and increases exponentially with increasing moisture content at constant temperature. The diffusion coefficient has also been shown to decrease with increasing density and to differ according to the method of determination at high moisture contents. It is also dependent on grain direction; the ratio of longitudinal to transverse coefficients is approximately 2.5.

Various alternative ways of expressing the potential which drives moisture through wood have been proposed. These include percentage moisture content, relative vapour pressure, osmotic pressure, chemical potential, capillary pressure and spreading pressure, the last mentioned being a surface phenomenon derivable from the surface sorption theory of Dent which in turn is a modification of the Brunauer-Emmet-Teller (BET) sorption theory (Skaar and Babiak, 1982). Although all this work has led to much debate on the correct flow potential, it has no effect in the calculation of flow; moisture flow is the same irrespective of the potential used, provided the mathematical conversions between transport coefficients, potentials and capacity factors are carried out correctly (Skaar, 1988).

As with the use of the Darcy equation for permeability, so with the application of Fick's law for diffusion, there appears to be a number of cases in which the law is not upheld and the model fails to describe the experimental data. Claesson (1997) in describing some of the failures of Fickian models claims that this is due to a complicated, but transient sorption in the cell wall; it certainly cannot be explained by high resistance to flow of surface moisture.

The diffusion of moisture through wood has considerable practical significance since it relates to the drying of wood below the fibre saturation point, the day-to-day movement of wood through diurnal and seasonal changes in climate, and in the quantification of the rate of vapour transfer through a thin sheet such as the sheathing used in timber frame construction.

What is popularly called 'vapour permeability' of a thin sheet, but is really vapour diffusion, is determined using the *wet-cup* test and its reciprocal is now quantified in terms of the *water vapour resistance factor* (μ). Values of μ for timber range from 30–50, while for wood-based panels, μ ranges from 15 for particleboard to 130 for OSB (see also Dinwoodie, 2000).

44.8.3 Thermal conductivity

The basic law for flow of thermal energy is ascribed to Fourier and when described mathematically is:

$$K_h = \frac{HL}{tA\Delta T} \qquad (44.21)$$

where K_h is the thermal conductivity for steady-state flow of heat through a slab of material, H is the quantity of heat, t is time, A is the cross-sectional area, L is the length, and ΔT is the temperature differential. This equation is analogous to that of Darcy for fluid flow.

Compared with permeability, where the Darcy equation was shown to be only partially valid for timber, thermal flow is explained adequately by the Fourier equation, provided the boundary conditions are defined clearly.

Thermal conductivity will increase slightly with increased moisture content, especially when calculated on a volume-fraction-of-cell-wall basis; however, it appears that conductivity of the cell wall substance is independent of moisture content (Siau, 1984); at 12 per cent mc, the average thermal conductivity of softwood timber parallel to the grain is of the order of 0.38 W/mK. Conductivity is influenced considerably by the density of the timber, i.e. by the volume-fraction-of-cell-wall substance, and various empirical and linear relations between conductivity and density have been established. Conductivity will also vary with timber orientation due to its anisotropic structure: the longitudinal thermal conductivity is about 2.5 times the transverse conductivity. Values of thermal conductivity are given in Siau (1984) and Dinwoodie (2000).

Compared with metals, the thermal conductivity of timber is extremely low, though it is generally up to eight times higher than that of insulating materials. The average transverse value for softwood timber (0.15 W/mK) is about one-seventh that for brick, thereby explaining the lower heating requirements of timber houses compared with the traditional brick house.

Thermal insulation materials in the UK are usually rated by their U-value, where U is the conductance or the reciprocal of the thermal resistance. Thus

$$U\text{-value} = K_h/L \qquad (44.22)$$

where K_h is the thermal conductivity and L is the thickness of the material.

44.9 References

Abe, H., Ohtani, J. and Fukazawa, K. (1991) FE-SEM observations on the microfibrillar orientation in the secondary wall of tracheids. *IAWA Bull. new series* 12, 4, 431–8.

Banks, W.B. (1968) A technique for measuring the lateral permeability of wood. *J. Inst. Wood Sci.* 4, 2, 35–41.

Brazier, J. (1965) An assessment of the incidence and significance of spiral grain in young conifer trees. *For. Prod. J.* 15, 8, 308–12.

Cave, I.D. (1997) Theory of x-ray measurement of microfibril angle in wood. Part 2 The diffraction diagram, x-ray diffraction by materials with fibre type symmetry. *Wood Sci. Technol.* 31, 225–34

Claesson, J. (1997) Mathematical modelling of moisture transport. *Proc. International conference on wood-water relations* (ed. P. Hoffmeyer), Copenhagen, and published by the management committee of EC COST Action E8, 61–8.

Comstock, G.L. (1967) Longitudinal permeability of wood to gases and nonswelling liquids. *For. Prod. J.* 17, 10, 41–6.

Desch, H.E. and Dinwoodie, J.M. (1996) *Timber – Structure, Properties, Conversion and Use*, 7th edn, Macmillan, Basingstoke, 306 pp.

Dinwoodie, J.M. (2000) *Timber – Its Nature and Behaviour*, 2nd edn, E & FN Spon, London, 257 pp.

Fengel, D. (1970) The ultrastructural behaviour of cell wall polysaccharides. In *The Physics and Chemistry of Wood Pulp Fibres*, TAPPI STAP 8, 74–96.

Gardner, K.H. and Blackwell, J. (1974) The structure of native cellulose. *Biopolymers* 13, 1975–2001.

Hart, C.A. and Thomas, R.J. (1967) Mechanism of bordered pit aspiration as caused by capillarity. *For. Prod. J.* 17, 11, 61–8.

Hillis, W.E. (1987) *Heartwood and Tree Exudates,* Springer-Verlag, Berlin, 268 pp.

Kerr, A.J. and Goring, D.A.I. (1975) Ultrastructural arrangement of the wood cell wall. *Cellulose Chem. and Technol.* 9, 6, 563–73.

Meyer, K.H. and Misch, L. (1937) Position des atomes dans le nouveau modele spatial de la cellulose. *Helvetica Chimica Acta* 20, 232–44.

Petty, J.A. (1981) Fluid flow through the vessels and intervascular pits of sycamore woods. *Holzforschung* 35, 213–16.

Petty, J.A. and Puritch, G.S. (1970) The effects of drying on the structure and permeability of the wood of *Abies grandis*. *Wood Sci. and Techol.* 4, 2, 140–54.

Pratt, G.H. (1974) *Timber Drying Manual*, HMSO, London, 152 pp.

Preston, R.D. (1964) Structural and mechanical aspects of plant cell walls. In *The Formation of Wood in Forest Trees* (ed. H.M. Zimmermann), Academic Press, New York, 169–88.

Preston, R.D. (1974) *The Physical Biology of Plant Cell Walls*, Chapman & Hall, London, 491 pp.

Saka, S. and Thomas, R.J. (1982) A study of lignification in Loblolly pine tracheids by the SEM-EDXA technique. *Wood Sci. Technol.* 12, 51–62.

Sell, J. and Zinnermann, T. (1993) Radial fibril agglomeration of the S_2 on transverse fracture surfaces of tracheids of tension-loaded spruce and white fir. *Holz, Roh-Werkstoff* 51, 384.

Siau, J.F. (1971) *Flow in Wood*, Syracuse University Press, Syracuse, New York, 99 pp.

Siau, J. (1984) *Transport Processes in Wood*, Springer-Verlag, Berlin, 245 pp.

Simson, B.W. and Timell, T.E. (1978) Polysaccharides in cambial tissues of *Populus tremuloides* and *Tilia americana*. V. Cellulose. *Cellul. Chem. Technol.* 12, 51–62.

Skaar, C. (1988) *Wood–Water Relations,* Springer-Verlag, Berlin, 283 pp.

Skaar, C. and Babiak, M. (1982) A model for bound-water transport in wood. *Wood Sci. Technol.* 16, 123–38

Stamm, A.J. (1959) Bound water diffusion into wood in the fiber direction. *For. Prod. J.* 9, 1, 27–32.

Stamm, A.J. (1964) *Wood and Cellulose Science*, Ronald, New York, 549 pp.

Tarkow, H. and Stamm, A.J. (1960) Diffusion through the air filled capillaries of softwoods: I, Carbon dioxide; II, Water vapour. *For. Prod. J.* 10, 247–50 and 323–4.

Ward, J.C. and Zeikus, J.G. (1980) Bacteriological, chemical and physical properties of wetwood in living trees. In *Natural Variations of Wood Properties* (ed. J. Bauch). Mitt Bundesforschungsanst Forst-Holzwirtsch, 131: 133–66.

Chapter forty-five

Deformation in timber

45.1 Introduction

Timber may undergo dimensional changes solely on account of variations in climatic factors; on the other hand, deformation may be due solely to the effects of applied stress. Frequently stress and climate interact to produce enhanced levels of deformation.

This chapter commences by examining the dimensional changes that occur in timber following variations in its moisture content and/or temperature. The magnitude and, consequently, the significance of such changes in the dimensions of timber are much greater in the case of alterations in moisture content compared with temperature. Consequently, the greater emphasis in this first section is placed on the influence of changing moisture content. Later in the chapter the effect of stress on deformation will be examined in detail.

45.2 Dimensional change due to moisture

In timber it is customary to distinguish between those changes that occur when green timber is dried to very low moisture contents (e.g. 12 per cent), and those that arise in timber of low moisture content due to seasonal or daily changes in the relative humidity of the surrounding atmosphere. The former changes are called *shrinkage* while the latter are known as *movement*.

45.2.1 Shrinkage

As explained in Chapter 44, removal of water from below the fibre saturation point occurs within the amorphous region of the cell wall and manifests itself by reductions in strength and stiffness, as well as inducing dimensional shrinkage of the material.

Anisotropy in shrinkage

The reduction in dimensions of the timber, technically known as shrinkage, can be considerable but, owing to the complex structure of the material, the degree of shrinkage is different on the three principal axes; in other words, timber is anisotropic in its water relationships. The variation in degree of shrinkage that occurs between different timbers, and, more important, the variation among the three different axes within any one timber is illustrated in Table 45.1. It should be noted that the values quoted in the table represent shrinkage on drying from the green state (i.e. >27 per cent) to 12 per cent moisture content, a level which is of considerable practical significance. At 12 per cent moisture content, timber is in equilibrium with an atmosphere having a relative humidity of 60 per cent and a temperature of 20°C; these conditions would be found in buildings having regular, but intermittent heating.

TABLE 45.1 Shrinkage (%) on drying from green to 12 per cent moisture content

		Transverse		
Botanical name	*Commercial name*	*Tangential*	*Radial*	*Longitudinal*
Chlorophora excelsa	Iroko	2.0	1.5	<0.1
Tectona grandis	Teak	2.5	1.5	<0.1
Pinus strobus	Yellow pine	3.5	1.5	<0.1
Picea abies	Whitewood	4.0	2.0	<0.1
Pinus sylvestris	Redwood	4.5	3.0	<0.1
Tsuga heterophylla	Western hemlock	5.0	3.0	<0.1
Quercus robur	European oak	7.5	4.0	<0.1
Fagus sylvatica	European beech	9.5	4.5	<0.1

From Table 45.1 it will be observed that shrinkage ranges from 0.1 per cent to 10 per cent, i.e. a 100-fold range. Longitudinal shrinkage, it will be noted, is always an order of magnitude less than transverse, while in the transverse plane radial shrinkage is usually some 60–70 per cent of the corresponding tangential figure.

The anisotropy between longitudinal and transverse shrinkage amounting to approximately 40:1 is due in part to the vertical arrangement of cells in timber and in part to the particular orientation of the microfibrils in the middle layer of the secondary cell wall (S_2). Thus, since the microfibrils of the S_2 layer of the cell wall are inclined at an angle of about 15° to the vertical, the removal of water from the matrix and the consequent movement closer together of the microfibrils will result in a horizontal component of the movement considerably greater than the corresponding longitudinal component (see Table 45.1).

Various theories have been developed over the years to account for shrinkage in terms of microfibrillar angle. The early theories were based on models which generally consider the cell wall to consist of an amorphous hygroscopic matrix in which are embedded parallel crystalline microfibrils which restrain swelling or shrinking of the matrix. One of the first models considered part of the wall as a flat sheet consisting only of an S_2 layer in which microfibrillar angle had a constant value (Barber and Meylan, 1964). This model treated the cells as square in cross-section and there was no tendency for the cells to twist as they began to swell. An improved model (Barber, 1968) was to treat the cells as circular in cross-section and embraced a thin constraining sheath outside the main cylinder which acted to reduce transverse swelling; experimental confirmation of this model was carried out by Meylan (1968). Later models have treated the cell wall as two layers of equal thickness having microfibrillar angles of equal and opposite sense, and these two-ply models have been developed extensively over the years to take into account the layered structure of the cell wall, differences in structure between radial and tangential walls, and variations in wall thickness. The principal researcher using this later type of model was Cave whose models are based on an array of parallel cellulose microfibrils embedded in a hemicellulose matrix, with different arrays for each wall layer; these arrays of basic wall elements were bonded together by lignin microlayers. Earlier versions of the model included consideration of the variation in the stiffness of the matrix with changing moisture content (1972, 1975). The model was later modified to take account of the amount of high energy water absorbed rather than the total amount of water (1978a,b). Comparison with previously obtained experimental data was excellent at low moisture contents, but poorer at moisture contents between 15 and 25 per cent. All these theories are extensively presented and discussed by Skaar (1988).

The influence of microfibrillar angle on degree of longitudinal and transverse shrinkage described for normal wood is supported by evidence derived from experimental work on compression wood, one of the forms of reaction wood described in Section 44.4. Compression wood is characterised by possessing a middle layer to the cell wall, the microfibrillar angle of which can be as high as 45° though 20–30° is more usual. The longitudinal shrinkage is much higher and the transverse shrinkage correspondingly lower than in normal wood, and it has been demonstrated that the values for compression wood can be accommodated on the shrinkage–microfibrillar angle curve for normal wood.

Differences in the degree of transverse shrinkage between tangential and radial planes (Table 45.1), are usually explained in terms of, first, the restricting effect of the rays on the radial plane; second, the increased thickness of the middle lamella on the tangential plane compared with the radial; third, the difference in degree of lignification between the radial and tangential cell walls; fourth, the small difference in microfibrillar angle between the two walls; and fifth, the alternation of earlywood and latewood in the radial plane, which, because of the greater shrinkage of latewood, induces the weaker earlywood to shrink more tangentially than it would if isolated. Considerable controversy reigns as to whether all five factors are actually involved and their relative significance. Comprehensive reviews of the evidence supporting these five possible explanations of differential shrinkage in the radial and tangential planes is to be found in Boyd (1974) and Skaar (1988).

Recently Kifetew (1997) has demonstrated that the gross transverse shrinkage anisotropy of Scots pine timber, with a value approximately equal to two, can be explained primarily in terms of the earlywood–latewood interaction theory by using a set of mathematical equations proposed by him; the gross radial and transverse shrinkage values were determined from the isolated early and latewood shrinkage values taken from the literature.

Volumetric shrinkage, s_v, is slightly less than the sums of the three directional components.

Practical significance.

In order to avoid shrinkage of timber after fabrication, it is essential that it is dried down to a moisture content which is in equilibrium with the relative humidity of the atmosphere in which the article is to be located. A certain latitude can be tolerated in the case of timber frames and roof trusses, but in the production of furniture, window frames, flooring and sports goods it is essential that the timber is seasoned to the expected equilibrium conditions, namely 12 per cent for regular intermittent heating and 10 per cent in buildings with central heating, otherwise shrinkage in service will occur with loosening of joints, crazing of paint films, and buckling and delamination of laminates. An indication of the moisture content of timber used in different environments is presented in Figure 45.1.

45.2.2 Movement

So far only those dimensional changes associated with the initial reduction in moisture content have been considered. However, dimensional changes, albeit smaller in extent, can also occur in seasoned or dried wood due to changes in the relative humidity of the atmosphere. Such changes certainly occur on a seasonal basis and frequently also on a daily basis. Since these changes in humidity are usually fairly small, inducing only slight changes in the moisture content of the timber, and since a considerable delay occurs in the diffusion of water vapour into or out of the centre of a piece of timber, it follows that these dimensional changes in seasoned timber are small, considerably smaller than those for shrinkage.

To quantify such movements for different timbers, dimensional changes are recorded over an arbitrary range of relative humidities. In the UK, the standard procedure is to condition the timber in a chamber at 90 per cent relative humidity and 25°C, then to measure its dimensions and to transfer it to a chamber at 60 per cent relative humidity, allowing it to come to equilibrium before remeasuring it; the

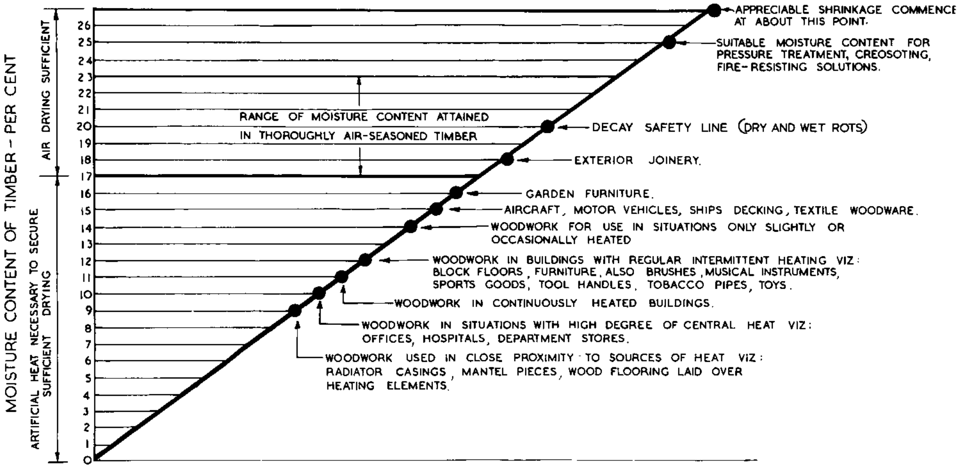

FIGURE 45.1 Equilibrium moisture content of timber in various environments. The figures for different species vary, and the chart shows only average values (© Building Research Establishment).

corresponding average change in moisture content is from 21 per cent to 12 per cent. Movement values in the tangential and radial planes for those timbers listed in Table 45.1 are presented in Table 45.2. The timbers are recorded in the same order, thus illustrating that although a broad relationship holds between values of shrinkage and movement, individual timbers can behave differently over the reduced range of moisture contents associated with movement. Since movement in the longitudinal plane is so very small, it is generally ignored. Anisotropy within the transverse plane can be accounted for by the same set of variables that influence shrinkage.

Where timber is subjected to wide fluctuations in relative humidity, care must be exercised to select a species that has low movement values.

Moisture in timber has a very pronounced effect not only on its strength (Figure 44.22), but also on its stiffness, toughness and fracture morphology; stiffness is discussed later in this chapter, while the other two parameters are discussed in Chapter 46.

Aware of the technological significance of the instability of wood under changing moisture content, many attempts have been made over the years to find a solution to the problem; these are summarised in Section 48.3.1 on dimensional stabilisation.

45.3 Thermal movement

Timber, like other materials, undergoes dimensional changes commensurate with increasing temperature. This is attributed to the increasing distances between the molecules as they increase the magnitude of their oscillations with increasing temperature. Such movement is usually quantified for practical purposes as the *coefficient of linear thermal expansion* and values for certain timbers are listed in Table 45.3. Although differences occur between species these appear to be smaller than those occurring for shrinkage and movement. The coefficient for transverse expansion is an order of magnitude greater than that in the longitudinal direction. This degree of anisotropy (10:1) can be related to the ratio of length to

TABLE 45.2 Movement (%) on transferring timber from 90 per cent relative humidity to 60 per cent at 25°C

		Transverse	
Botanical name	*Commercial name*	*Tangential*	*Radial*
Chlorophora excelsa	Iroko	1.0	0.5
Tectona grandis	Teak	1.2	0.7
Pinus strobus	Yellow pine	1.8	0.9
Picea abies	Whitewood	1.5	0.7
Pinus sylvestris	Redwood	2.2	1.0
Tsuga heterophylla	Western hemlock	1.9	0.9
Quercus robur	European oak	2.5	1.5
Fagus sylvatica	European beech	3.2	1.7

TABLE 45.3 Coefficient of linear thermal expansion of various woods and other materials per degree centigrade

<table>
<tr><th><i>Timber</i></th><th></th><th colspan="2"><i>Coefficient of thermal expansion</i> $\times 10^{-6}$</th></tr>
<tr><th></th><th></th><th><i>Longitudinal</i></th><th><i>Transverse</i></th></tr>
<tr><td><i>Picea abies</i></td><td>Whitewood</td><td>5.41</td><td>34.1</td></tr>
<tr><td><i>Pinus strobus</i></td><td>Yellow pine</td><td>4.00</td><td>72.7</td></tr>
<tr><td><i>Quercus robur</i></td><td>European oak</td><td>4.92</td><td>54.4</td></tr>
<tr><td>GRP, 60/40, unidirectional</td><td></td><td>10.0</td><td>10.0</td></tr>
<tr><td>CFRP, 60/40, unidirectional</td><td></td><td>10.0</td><td>−1.00</td></tr>
<tr><td>Mild steel</td><td></td><td colspan="2">12.6</td></tr>
<tr><td>Duralumin (aluminium alloy)</td><td></td><td colspan="2">22.5</td></tr>
<tr><td>Nylon 66</td><td></td><td colspan="2">125.0</td></tr>
<tr><td>Polypropylene</td><td></td><td colspan="2">110.0</td></tr>
</table>

breadth dimensions of the crystalline regions within the cell wall. Transverse thermal expansion appears to be correlated with specific gravity, but somewhat surprisingly this relationship is not sustained in the case of longitudinal thermal expansion where the values for different timbers are roughly constant (Weatherwax and Stamm, 1946).

The expansion of timber with increasing temperature appears to be linear over a wide temperature range: the slight differences in expansion which occur between the radial and tangential planes are usually ignored and the coefficients are averaged to give a transverse value as recorded in Table 45.3. For comparative purposes, the coefficients of linear thermal expansion for glass- and carbon-reinforced plastic, two metals and two plastics are also listed. Even the transverse expansion of timber is considerably less than that for the plastics.

The dimensional changes of timber caused by differences in temperature are small when compared to changes in dimensions resulting from the uptake or loss of moisture. Thus for timber with a moisture content greater than about 3 per cent, the shrinkage due to moisture loss on heating will be greater than the thermal expansion, with the effect that the net dimensional change on heating will be negative. For most practical purposes thermal expansion or contraction can be safely ignored over the range of temperatures in which timber is generally employed.

45.4 Deformation under load

This section is concerned with the type and magnitude of the deformation that results from the application of external load. As in the case of both concrete and polymers, the load–deformation relationship in timber is exceedingly complex, resulting from the fact that:

1. timber does not behave in a truly elastic mode, rather its behaviour is time-dependent; and,
2. the magnitude of the strain is influenced by a wide range of factors; some of these are property dependent, such as density of the timber, angle of the grain relative to direction of load application, and angle of the microfibrils within the cell wall; others are environmentally dependent, such as temperature and relative humidity.

Under service conditions timber often has to withstand an imposed load for many years, perhaps even centuries; this is particularly relevant in construction applications. When loaded, timber will deform and a generalised interpretation of the variation of deformation with time together with the various components of this deformation is illustrated in Figure 45.2. On the application of a load at time zero an instantaneous (and reversible) deformation occurs which represents true elastic behaviour. On maintaining the load to time t_1 the deformation increases, though the rate of increase is continually decreasing; this increase in deformation with time is termed *creep*. On removal of the load at time t_1 an instantaneous reduction in deformation occurs which is approximately equal in magnitude to the initial elastic deformation. With time, the remain-

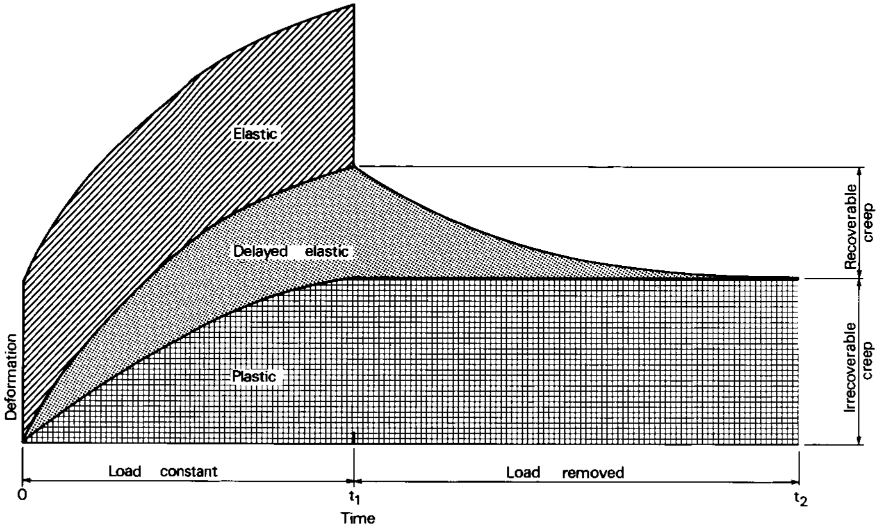

FIGURE 45.2 The various elastic and plastic components of the deformation of timber under constant load (© Building Research Establishment).

ing deformation will decrease at an ever-decreasing rate until at time t_2 no further reduction occurs. The creep that has occurred during loading can be conveniently subdivided into a *reversible* component, which disappears with time and which can be regarded as *delayed elastic* behaviour, and an *irreversible* component which results from *plastic* or *viscous* flow. Therefore, timber on loading possesses three forms of deformation behaviour – elastic, delayed elastic and viscous. Like so many other materials, timber can be treated neither as a truly elastic material where, by Hooke's law, stress (see Section 45.4.1) is proportional to strain but independent of the rate of strain, nor as a truly viscous liquid where, according to Newton's law, stress is proportional to rate of strain, but independent of strain itself (see Section 45.4.2). Where combinations of behaviour are encountered the material is said to be viscoelastic and timber, like many high polymers, is a viscoelastic material.

Having defined timber as such, the reader will no doubt be surprised to find that half of this chapter is devoted to the elastic behaviour of timber. It has already been discussed how part of the deformation can be described as elastic and the section below will indicate how, at low levels of stressing and short periods of time, there is considerable justification for treating the material as such. Perhaps the greatest incentive for this viewpoint is the fact that classical elasticity theory is well established and, when applied to timber, has been shown to work very well. The question of time in any stress analysis can be accommodated by the use of safety factors in design calculations.

Consequently, this section will deal first with elastic deformation as representing a very good approximation of what happens in practice, while the following section will deal with viscoelastic deformation, which embraces both delayed elastic and irreversible deformation. Although technically more applicable to timber, viscoelasticity is certainly less well understood and developed in its application than is the case with elasticity theory.

45.4.1 Elastic deformation

When a sample of timber is loaded in tension, compression or bending, the instantaneous deformations obtained with increasing load are approximately proportional to the values of the applied load. Figure 45.3 illustrates that this approximation is certainly truer of the experimental evidence in longitudinal tensile loading than in the case of longitudinal compression. In both modes of loading, the approximation appears to become a reality at the lower levels of loading. Thus, it has become convenient to recognise a point of inflection on the load-deflection

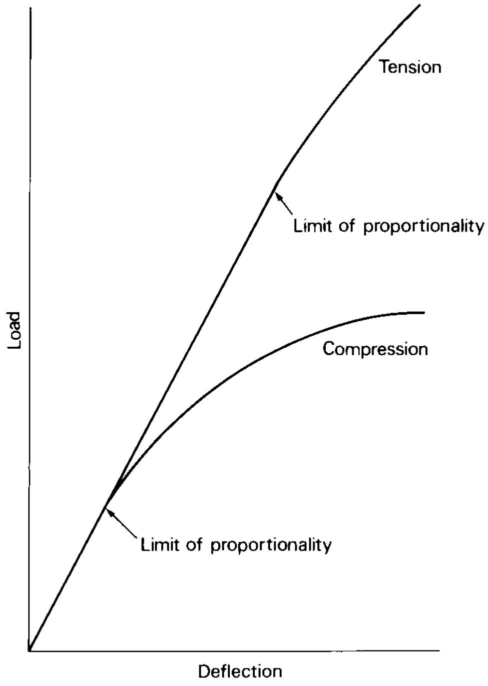

FIGURE 45.3 Load-deflection graphs for timber stressed in tension and compression parallel to the grain. The assumed limit of proportionality for each graph is indicated (© Building Research Establishment).

curve known as the *limit of proportionality*, below which the relationship between load and deformation is linear, and above which non-linearity occurs. Generally, the limit of proportionality in longitudinal tension is found to occur at about 60 per cent of the ultimate load to failure while in longitudinal compression the limit is considerably lower, varying from 30 per cent to 50 per cent of the failure value.

At the lower levels of loading, therefore, where the straight-line relationship appears to be valid, the material is said to be linearly elastic. Hence:

$$\text{deformation} \propto \text{applied load}$$

$$\text{i.e.} \qquad \frac{\text{applied load}}{\text{deformation}} = \text{a constant}$$

The applied load must be quantified in terms of the cross-sectional area carrying that load, while the deflection or extension must be related to the original dimension of the test piece prior to load application. Hence:

$$\frac{\text{load (N)}}{\text{csa (mm}^2\text{)}} = \text{stress (N/mm}^2\text{), denoted by } \sigma$$

$$\text{and} \quad \frac{\text{deformation (mm)}}{\text{original length (mm)}} = \text{strain (unitless), denoted by } \epsilon$$

$$\text{Therefore,} \qquad \frac{\text{stress } (\sigma)}{\text{strain } (\epsilon)} = \text{a constant} = E \text{ (N/mm}^2\text{)} \qquad (45.1)$$

where ϵ is the strain (change in dimension/original dimension), σ is the stress (load/cross-sectional area), and E is a constant, known as the modulus of elasticity. The modulus of elasticity (MOE), is also referred to in the literature as the elastic modulus, Young's modulus, or simply and frequently, though incorrectly, as stiffness.

The apparent linearity at the lower levels of loading is really an artefact introduced by the rate of testing. At fast rates of loading, a very good approximation to a straight line occurs, but as the rate of loading decreases, the load-deflection line assumes a curvilinear shape (Figure 45.4). Such curves can be treated as linear by introducing a straight line approximation, which can take the form of either a tangent or secant. Traditionally for timber and wood fibre composites, tangent lines have been used as linear approximations of load-deflection curves.

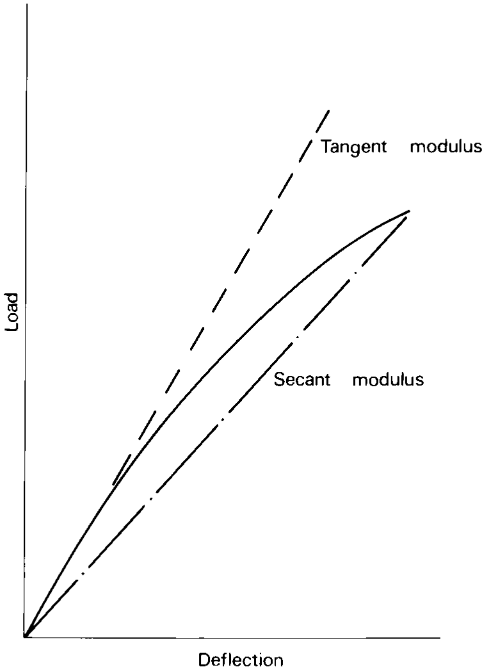

FIGURE 45.4 The approximation of a curvilinear load-deflection curve for timber stressed at low loading rates, by linear tangents or secants (© Building Research Establishment).

Thus, while in theory it should be possible to obtain a true elastic response, in practice this is rarely the case, though the degree of divergence is frequently very low. It should be appreciated in passing that a curvilinear load-deflection curve must not be interpreted as an absence of true elastic behaviour. The material may still behave elastically, though not linearly elastically: the prime criterion for elastic behaviour is that the load-deflection curve is truly reversible, i.e. no permanent deformation has occurred on release of the load.

The modulus of elasticity or elastic modulus in the longitudinal direction is one of the principal elastic constants of our material. Readers desirous of information on the different methods used to determine the value of the modulus under both static and dynamic loading are referred to Dinwoodie (2000).

The elastic behaviour of a material can be characterised by three elastic constants, the first of which, the modulus of elasticity, E, has been described above. The second constant is the *modulus of rigidity*, G. Within the elastic range of the material, shearing stress is proportional to shearing strain. Thus

$$G = \frac{\tau}{\gamma} \tag{45.2}$$

where τ is the shearing stress and γ is the shearing strain.

The third constant is *Poisson's ratio*, υ. Generally, when a body is subjected to a stress in one direction, the body will undergo a change in dimensions at right angles to the direction of stressing. The ratio of the contraction or extension to the applied strain is known as Poisson's ratio and for isotropic bodies is given as:

$$\upsilon = -\frac{\epsilon_y}{\epsilon_x} \tag{45.3}$$

where ϵ_x, ϵ_y are strains in the x, y directions resulting from an applied stress in the x direction. (The minus sign indicates that, when ϵ_x is a tensile positive strain, ϵ_y is a compressive negative strain.) In timber, because of its anisotropic behaviour and its treatment as a rhombic system, six Poisson's ratios occur.

Orthotropic elasticity and timber

In applying the elements of orthotropic elasticity to timber, the assumption is made that the three principal elasticity directions coincide with the longitudinal, radial and tangential directions in the tree. The assumption implies that the tangential faces are straight and not curved, and that the radial faces are parallel and not diverging. However, by dealing with small pieces of timber removed at some distance from the centre of the tree, the approximation of rhombic symmetry for a system possessing circular symmetry becomes more and more acceptable.

The nine independent constants required to specify the elastic behaviour of timber are the three moduli of elasticity, one in each of the longitudinal (L), radial (R) and tangential (T) directions; the three moduli of rigidity, one in each of the principal planes longitudinal–tangential (LT), longitudinal–radial (LR) and tangential–radial (TR); and three Poisson's ratios, namely ν_{RT}, ν_{LR}, ν_{TL}. These constants, together with the three dependent Poisson's ratios ν_{RL}, ν_{TR}, ν_{LT} are presented in Table 45.4 for a selection of hardwoods and softwoods. The table illustrates the high degree of anisotropy present in timber. Comparison of E_L with either E_R or E_T, and G_{TR} with G_{LT} or G_{RL} will indicate a degree of anisotropy which can be as high as 60:1; usually the ratio of E_L to E_{HORIZ} is of the order of 40:1. Note should be taken that the values of ν_{TR} are frequently greater than 0.5.

Values of E_L for some additional timbers are to be found in Table 46.1.

Factors influencing the elastic modulus

The stiffness of timber is influenced by many factors, some of which are properties of the material while others are components of the environment.

Grain angle

Figure 45.5, in addition to illustrating the marked influence of grain angle on stiffness, shows the degree of fit between experimentally derived values and the line obtained using transformation equations to calculate theoretical values (see equation (46.7) in Section 46.6).

Density

Stiffness is related to density of the timber, a relationship which was apparent in Table 45.4 and which is confirmed by the plot of over 200 species of timber contained in *Bulletin 50* of the former Forest Products Research Laboratory

TABLE 45.4 Values of the elastic constants for five hardwoods and four softwoods determined on small clear specimens

Species	*Density (kg/m³)*	*Moisture content (%)*	E_L	E_R	E_T	v_{TR}	v_{LR}	v_{RT}	v_{LT}	v_{RL}	v_{TL}	G_{LT}	G_{LR}	G_{TR}
Hardwoods														
Balsa	200	9	6300	300	106	0.66	0.018	0.24	0.009	0.23	0.49	203	312	33
Khaya	440	11	10200	1130	510	0.60	0.033	0.26	0.032	0.30	0.64	600	900	210
Walnut	590	11	11200	1190	630	0.72	0.052	0.37	0.036	0.49	0.63	700	960	230
Birch	620	9	16300	1110	620	0.78	0.034	0.38	0.018	0.49	0.43	910	1180	190
Ash	670	9	15800	1510	800	0.71	0.051	0.36	0.030	0.46	0.51	890	1340	270
Beech	750	11	13700	2240	1140	0.75	0.073	0.36	0.044	0.45	0.51	1060	1610	460
Softwoods														
Norway spruce	390	12	10700	710	430	0.51	0.030	0.31	0.025	0.38	0.51	620	500	23
Sitka spruce	390	12	11600	900	500	0.43	0.029	0.25	0.020	0.37	0.47	720	750	39
Scots pine	550	10	16300	1100	570	0.68	0.038	0.31	0.015	0.42	0.51	680	1160	66
Douglas fir*	590	9	16400	1300	900	0.63	0.028	0.40	0.024	0.43	0.37	910	1180	79

* Listed in original as Oregon pine.

E is the modulus of elasticity in a direction indicated by the subscript (N/mm^2).
G is the modulus of rigidity in a plane indicated by the subscript (N/mm^2).
v_{ij} is the Poisson's ratios for an extensional stress in *j* direction,

$$= \frac{\text{compressive strain in } i \text{ direction}}{\text{extensional strain in } j \text{ direction}}$$

From Hearmon (1948), but with different notation for the Poisson's ratios.

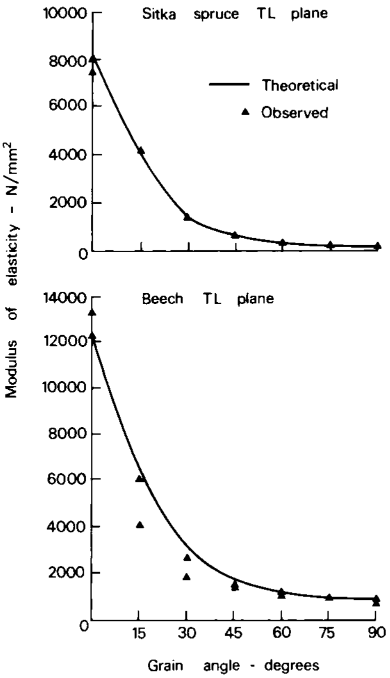

FIGURE 45.5 Effect of grain angle on the modulus of elasticity (© Building Research Establishment).

(Figure 45.6); the correlation coefficient was 0.88 for timber at 12 per cent moisture content and 0.81 for green timber and the relation is curvilinear. A high correlation is to be expected, since density is a function of the ratio of cell wall thickness to cell diameter; consequently, increasing density will result in increasing stiffness of the cell.

Owing to the variability in structure that exists between different timbers, the relation between density and stiffness will be higher where only a single species is under investigation. Because of the reduced range in density, a linear regression is usually fitted.

Similar relations with density have been recorded for the modulus of rigidity in certain species: in others, however, for example spruce, both the longitudinal-tangential and longitudinal–radial shear moduli have been found to be independent of density. Most investigators agree, however, that the Poisson's ratios are independent of density.

Knots

Since timber is anisotropic in behaviour, and since knots are characterised by the occurrence of distorted grain, it is not surprising to find that the presence of knots in timber results in a reduction in the stiffness. The relationship is difficult to quantify since the effect of the knots will depend not only on their number and size, but also on their distribution both along the length of the sample and across the faces. Dead knots, especially where the knot has fallen out, will result in larger reductions in stiffness than will green knots (see Section 44.1).

Ultrastructure

Two components of the fine or chemical structure have a profound influence on both the elastic and rigidity moduli. The first relates to the existence of a matrix material with particular emphasis on the presence of lignin. In those plants devoid of lignin, e.g. the grasses, or in wood fibres which have been delignified, the stiffness of the cells is low and it would appear that lignin, apart from its hydrophilic protective role for the cellulosic crystallites, is responsible to a considerable extent for the high stiffness found in timber.

The significance of lignin in determining stiffness is not to imply that the cellulose fraction plays no part: on the contrary, it has been shown that the angle at which the microfibrils are lying in the middle layer of the secondary cell wall, S_2, also plays a significant role in controlling stiffness (Figure 45.7).

A considerable number of mathematical models have been devised over the years to relate stiffness to microfibrillar angle. The early models were two-dimensional in approach, treating the cell wall as a planar slab of material, but later the models became much more sophisticated, taking into account the existence of cell wall layers other than the S_2, the variation in microfibrillar angle between the radial and tangential walls and consequently

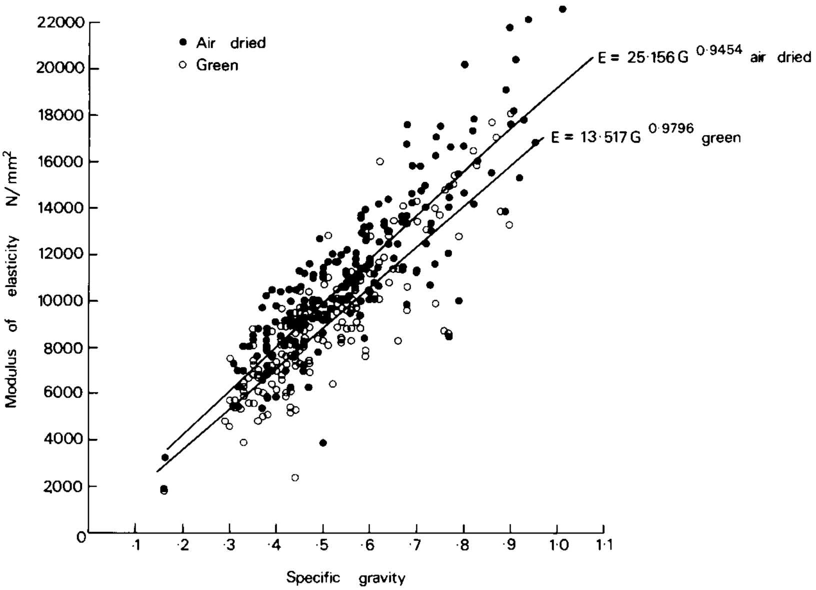

FIGURE 45.6 Effect of specific gravity on the longitudinal modulus of elasticity for over 200 species of timber tested in the green and dry states (© Building Research Establishment).

the probability that they undergo different strains, and, lastly, the possibility of complete shear restraint within the cell wall. These three-dimensional models are frequently analysed using finite element techniques. These early models were reviewed by Dinwoodie (1975).

Later modelling of timber behaviour in terms of its structure has been reviewed by Astley *et al.* (1998); it makes reference to the work of Cave (1975) who used the concept of an elastic fibre composite consisting of an inert fibre phase embedded in a water-reactive matrix. The constitutive equation is related to the overall stiffness of the composite, the volume fraction, and the stiffness and sorption characteristics of the matrix. Unlike previous models, the equation can be applied not only to elasticity, but also to shrinkage and even moisture-induced creep (Cave, 1975).

Recently, Harrington *et al.* (1998) have developed a model of the wood cell wall based on the homogenisation first, of an amorphous lignin-polyose matrix, and then of a representative volume element comprising a cellulose microfibril, its polyose-cellulose sheath and the surrounding matrix. The model predicts orthotropic elastic constants which are in good agreement with recorded values (Astley *et al.*, 1998). The predicted variation of axial stiffness with the S_2 microfibrillar angle is consistent with observed behaviour and aligned with results from other cell wall models.

Stiffness of a material is very dependent on the type and degree of chemical bonding within its structure; the abundance of covalent bonding in the longitudinal plane and hydrogen bonding in one of the transverse planes contributes considerably to the moderately high levels of stiffness characteristic of timber.

Moisture content

The influence of moisture content on stiffness is

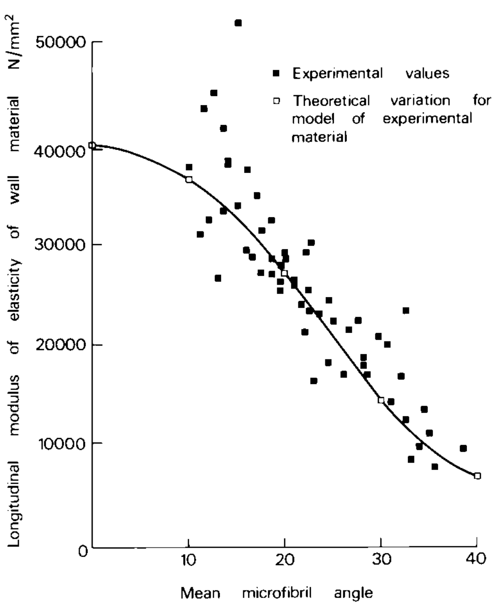

FIGURE 45.7 Effect of the mean microfibrillar angle of the cell wall on the longitudinal modulus of elasticity of the wall material in *Pinus radiata*. Calculated values from a mathematical model are also included (from Cave (1968) by permission of Springer-Verlag).

similar to, though not quite so sensitive as, that for strength which was illustrated in Figure 44.22. Early experiments in which stiffness was measured on a specimen of Sitka spruce, as it took up moisture from the dry state, clearly indicated a linear loss in stiffness as the moisture content increased to about 27 per cent, corresponding to the fibre saturation point as discussed in Chapter 44; further increase in moisture content has no influence on stiffness. These results for the variation in longitudinal moduli with moisture content under static loading have been confirmed using simple dynamic methods. Measurement of the frequency of vibration was carried out at regular intervals as samples of Sitka spruce were dried from 70 per cent to zero moisture content (Figure 45.8).

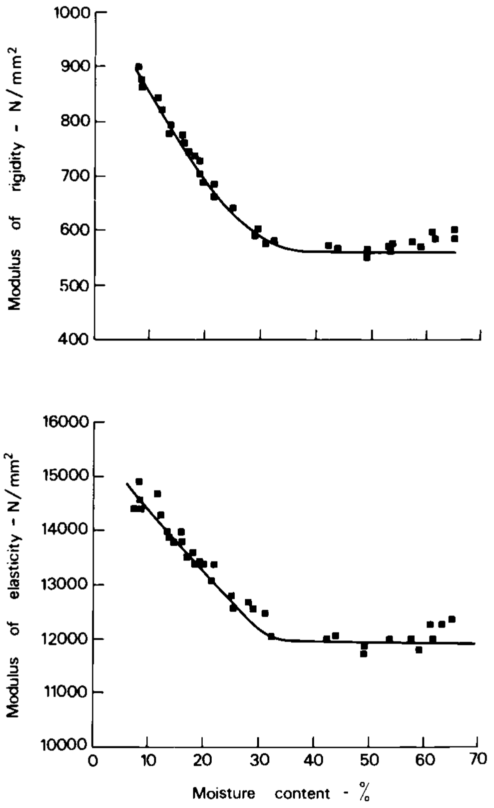

FIGURE 45.8 Effect of moisture content on the longitudinal modulus of elasticity and the modulus of rigidity in the L–R plane in Sitka spruce. Both moduli were determined dynamically (© Building Research Establishment).

Confirmation of the reduction in modulus of elasticity with increasing moisture content is forthcoming first, from Figure 45.6, in which the regression lines of elasticity against density for over 200 species of timber at 12 per cent moisture content and in the green state are presented, and second, from the review of more recent results by Gerhards (1982). The effect of moisture increase has a far greater effect on the modulus perpendicular to the grain than on the modulus along the grain (Gerhards, 1982).

Temperature

In timber, like most other materials, increasing temperature results in greater oscillatory movement of the molecules and an enlargement of the crystal lattice. These in turn affect the mechanical properties and the stiffness and strength of the material decreases.

Although the relationship between stiffness and temperature has been shown experimentally to be curvilinear, the degree of curvature is usually slight at low moisture contents and the relation is frequently treated as linear, thus:

$$E_T = E_t[1 - a(T - t)] \qquad (45.4)$$

where E is the elastic modulus, T is a higher temperature, t is a lower temperature, and a is the temperature coefficient. The value a for longitudinal modulus has been shown to lie between 0.001 and 0.007 for low moisture contents.

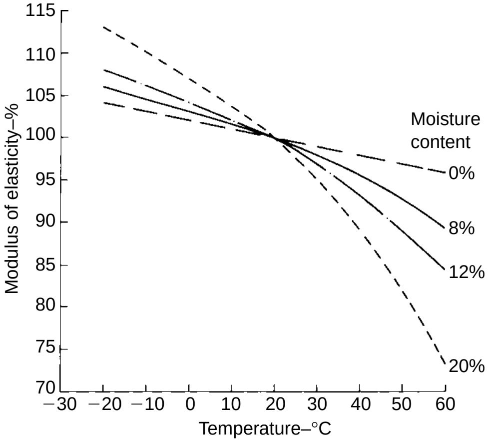

FIGURE 45.9 The interaction of temperature and moisture content on the modulus of elasticity. Results are averaged for six species of timber and the modulus at 20°C and 0 per cent moisture content is taken as unity (© Building Research Establishment).

The effect of a temperature increase is greater on the perpendicular modulus than on the longitudinal modulus (Gerhards, 1982).

At higher moisture contents the relationship of stiffness and temperature is markedly curvilinear and the interaction of moisture content and temperature in influencing stiffness is clearly shown in Figure 45.9. At zero moisture content the reduction in stiffness between −20°C and +60°C is only 6 per cent: at 20 per cent moisture content the corresponding reduction is 40 per cent. This increase in the significance of temperature with increasing moisture content has been confirmed by Gerhards (1982).

Long-term exposure to elevated temperature results in a marked reduction in stiffness as well as strength and toughness, the effect usually being greater in hardwoods than in softwoods. Even exposure to cyclic changes in temperature over long periods will result in a loss of stiffness (Moore, 1984).

45.4.2 Viscoelastic deformation

In the introduction to Section 45.4, timber was described as being neither truly elastic in its behaviour nor truly viscous, but rather a combination of both states; such behaviour is usually described as viscoelastic and, in addition to timber, materials such as concrete, bitumen and the thermoplastics are also viscoelastic in their response to stress.

Viscoelasticity infers that the behaviour of the material is time dependent; at any instant in time under load its performance wilI be a function of its past history. Now if the time factor under load is reduced to zero, a state which we can picture in concept, but never attain in practice, the material will behave truly elastically, and we have seen in Section 45.4.1 how timber can be treated as an elastic material and how the principles of orthotropic elasticity can be applied. However, where stresses are applied for a period of time, viscoelastic behaviour will be experienced and, while it is possible to apply elasticity theory with a factor covering the increase in deformation with time, this procedure is at best only a first approximation.

In a material such as timber, time-dependent behaviour manifests itself in a number of ways, of which the more common are creep, relaxation, damping capacity and the dependence of strength on duration of load. When the load on a sample of timber is held constant for a period of time, the increase in deformation over the initial instantaneous elastic deformation is called creep and Figure 45.2 illustrates not only the increase in creep with time, but also the subdivision of creep into a reversible and an irreversible component of which more will be said in a later section.

Most timber structures carry a considerable dead load and the component members of these will undergo creep; the dip towards the centre of the ridge of the roof of very old buildings bears testament to the fact that timber does creep. However, compared with thermoplastics and bitumen, the amount of creep in timber is appreciably lower.

Viscoelastic behaviour is also apparent in the form of relaxation where the load necessary to maintain a constant deformation decreases with time; in timber utilisation this has limited practical significance and the area has attracted very little research. Damping capacity is a measure of the fractional energy converted to heat compared with that stored per cycle under the influence of mechanical vibrations; this ratio is time dependent. A further manifestation of viscoelastic behaviour is the apparent loss in strength of timber with increasing duration of load; this feature is discussed in detail in Section 46.6.12 and illustrated in Figure 46.7.

Creep

Creep parameters

It is possible to quantify creep by a number of time-dependent parameters of which the two most common are *creep compliance* (known also as *specific creep*) and *relative creep* (also known as the *creep coefficient*); both parameters are a function of temperature.

Creep compliance (c_c) is the ratio of increasing strain with time to the applied constant stress, i.e.:

$$c_c(t, T) = \frac{\text{strain varying}}{\text{applied constant stress}} \tag{45.5}$$

while relative creep (c_r) is defined as either the deflection, or more usually, the increase in deflection, expressed in terms of the initial elastic deflection, i.e.:

$$c_r(t, T) = \frac{\epsilon_t}{\epsilon_0} \quad \text{or} \quad \frac{\epsilon_t - \epsilon_0}{\epsilon_0} \tag{45.6}$$

where ϵ_t is the deflection at time t, and ϵ_0 is the initial deflection.

Relative creep has also been defined as the change in compliance during the test expressed in terms of the original compliance.

Creep relationships

In both timber and timber products such as plywood or chipboard (particleboard), the rate of deflection or creep slows down progressively with time (Figure 45.10); the creep is frequently plotted against log time and the graph assumes an exponential shape. Results of creep tests can also be plotted as relative creep against log time or as creep compliance against stress as a percentage of the ultimate short-time stress.

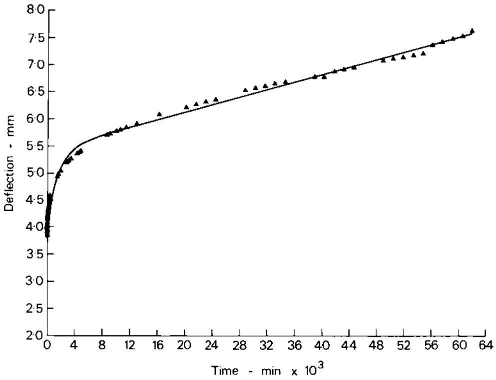

FIGURE 45.10 The increase in deformation with time of urea-formaldehyde bonded chipboard (particleboard): the regression line has been fitted to the experimental values using equation (45.10) (© Building Research Establishment).

In Section 45.4.1 it was shown that the degree of elasticity varied considerably between the horizontal and longitudinal planes. Creep, as one particular manifestation of viscoelastic behaviour, is also directionally dependent. In tensile stressing of longitudinal sections produced with the grain running at different angles, it was found that relative creep was greater in the direction perpendicular to the grain than it was parallel to the grain.

Timber- and wood-based panels, therefore, are viscoelastic materials, the time-dependent properties of which are directionally dependent. The next important criterion is whether they are linear viscoelastic in behaviour. For viscoelastic behaviour to be defined as linear, the instantaneous, recoverable and non-recoverable components of the deformation must vary directly with the applied stress. An alternative definition is that the creep compliance or relative creep must be independent of stress and not a function of it.

Timber- and wood-based panels exhibit linear viscoelastic behaviour at the lower levels of stressing, but at the higher stress levels this behaviour reverts to being non-linear. Examples of this transition in behaviour are illustrated in Figures 45.11 (a) and 45.11 (b), where for both redwood timber and UF bonded particleboard respectively, the change from linear to non-linear behaviour occurs between the 45 and 60 per cent stress level.

The linear limit for the relation between creep and applied stress varies with mode of testing, with species of timber or type of panel, and with both temperature and moisture content. In tension parallel to the grain at constant temperature and moisture content, timber has been found to behave as a linear viscoelastic material up to about 75 per cent of the ultimate tensile strength, though some workers have found considerable variability and have indicated a range from 36 to 84 per cent. In compression parallel to the grain, the onset of non-linearity appears to occur at about 70 per cent, though the level of actual stress will be much lower than in the case of tensile strength since the ultimate compression strength is only one-third that of the tensile strength. In bending, non-linearity seems to develop very much earlier at about 50–60 per cent (Figure 45.11 (a) and (b)); the actual stress levels will be very similar to those for compression.

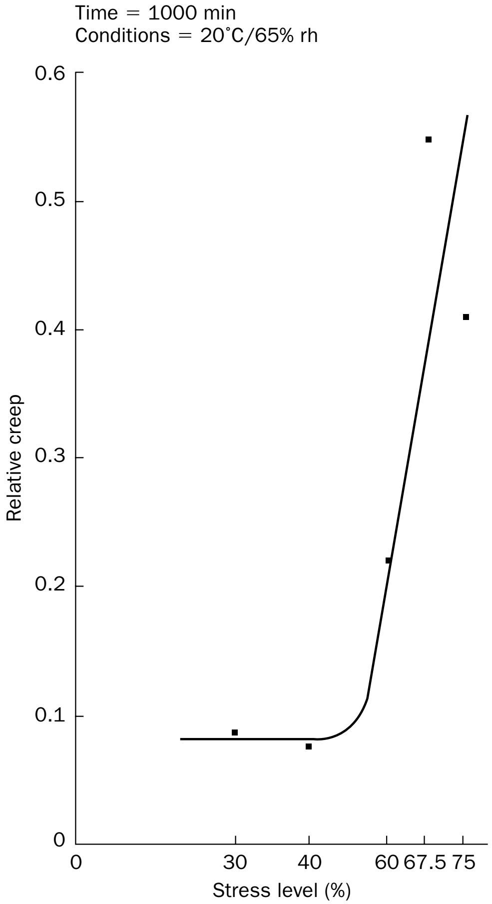

FIGURE 45.11 (a) The relation of relative creep to stress level at fixed time periods illustrating the transition from linear to non-linear viscoelastic behaviour in redwood timber (*Pinus sylvestris*) (© Building Research Establishment).

In both compression and bending, the divergence from linearity is usually greater than in the

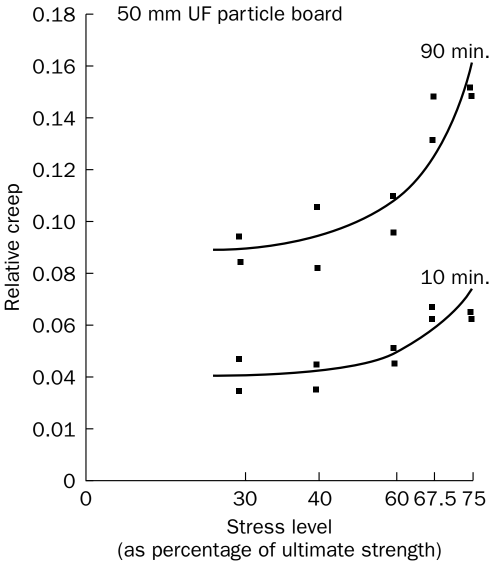

FIGURE 45.11 (b) The relation of relative creep to stress level at fixed time periods illustrating the transition from linear to non-linear viscoelastic behaviour in 50 mm UF particleboard (© Building Research Establishment).

case of tensile stressing; much of the increased deformation occurs in the non-recoverable component of creep and is associated with progressive structural changes including the development of incipient failure.

Increase not only in stress level, but also in temperature to a limited extent, and moisture content to a considerable degree, result in an earlier onset of non-linearity and a more marked departure from linearity. For most practical situations, however, working stresses are only a small percentage of the ultimate, rarely approaching even 50 per cent, and it can be safely assumed that timber, like concrete, will behave as a linear viscoelastic material under normal service conditions.

Principle of superposition

Since timber behaves as a linear viscoelastic material under conditions of normal temperature and humidity and at low to moderate levels of stressing, it is possible to apply the Boltzmann's principle of superposition to predict the response of timber to complex or extended loading sequences. This principle states that the creep occurring under a sequence of stress increments is taken as the superposed sum of the responses to the individual increments. This can be expressed mathematically in a number of forms, one of which for linear materials is:

$$\epsilon_c(t) = \sum_{1}^{n} \Delta\sigma_i c_{ci} \qquad (45.7)$$

where n is the number of load increments, $\Delta\sigma_i$ is the stress increment, c_{ci} is the creep compliance for the individual stress increments applied for differing times, $t-\tau_1, t-\tau_2, \ldots, t-\tau_n$ and $\epsilon_c(t)$ is the total creep at time t; or in integrated form

$$\epsilon_c(t) = \int_{\tau_1}^{t} c_c(t-\tau)\frac{d\sigma}{d\tau}(\tau)d\tau \qquad (45.8)$$

In experiments on timber, it has been found that in the comparison of deflections in beams loaded either continuously or repeatedly for two or seven days in every fourteen, for six months at four levels of stress, the applicability of the Boltzmann's principle of superposition was confirmed for stress levels up to 50 per cent (Nakai and Grossman, 1983).

The superposition principle has been found to be applicable even at high stresses in both shear and tension of dry samples. However, at high moisture contents, the limits of linear behaviour in shear and tension appear to be considerably lower, thereby confirming views expressed earlier on the non-linear behaviour of timber subjected to high levels of stressing and/or high moisture content.

Mathematical modelling of steady-state creep

The relationship between creep and time has been expressed mathematically using a wide range of equations. It should be appreciated that such expressions are purely empirical, none of them possessing any sound theoretical basis. Their relative merits depend on how easily their constants can be determined and how well they fit the experimental results.

One of the most successful mathematical descriptions for creep in timber under constant relative humidity and temperature appears to be the power law, of general form

$$\epsilon(t) = \epsilon_0 + at^m \qquad (45.9)$$

where $\epsilon(t)$ is the time-dependent strain, ϵ_0 is the initial deformation, a and m are material-specific parameters to be determined experimentally ($m = 0.33$ for timber), and t is the elapsed time.

The prime advantages of using a power function to describe creep is its representation as a straight line on a log/log plot, thereby making onward prediction on a time basis that much easier than using other models.

Alternatively, creep behaviour in timber, like that of many other high polymers, can be interpreted with the aid of mechanical (rheological) models comprising different combinations of springs and dashpots (piston in a cylinder containing a viscous fluid). The springs act as a mechanical analogue of the elastic component of deformation, while the dashpot simulates the viscous or flow component. When more than a single member of each type is used, these components can be combined in a wide variety of ways, though only one or two will be able to describe adequately the creep and relaxation behaviour of the material.

The simplest linear model which successfully describes the time-dependent behaviour of timber under constant humidity and temperature for short periods of time is the four-element model illustrated in Figure 45.12; the central part of the model will be recognised as a Kelvin element. To this unit has been added in series a second spring and dashpot. The strain at any time t under a constant load is given by the equation

$$Y = \frac{\sigma}{E_1} + \frac{\sigma}{E_2}\left[1 - \exp\left(\frac{-tE_2}{\eta_2}\right)\right] + \frac{\sigma t}{\eta_3} \qquad (45.10)$$

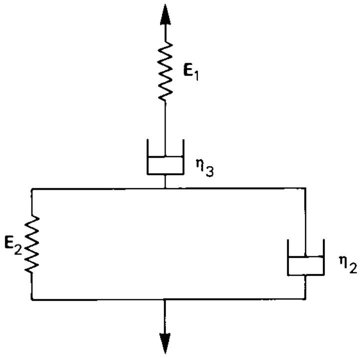

FIGURE 45.12 Mechanical analogue of the components of creep: the springs simulate elastic deformation and the dashpots viscous flow. The model corresponds to equation (45.10) (© Building Research Establishment).

where Y is the strain at time t, E_1 is the elasticity of spring 1, E_2 is the elasticity of spring 2, σ is the stress applied, η_2 is the viscosity of dashpot 2, η_3 is the viscosity of dashpot 3.

The first term on the right-hand side of equation (45.10) represents the instantaneous deformation, while the second term describes the delayed elasticity and the third term the plastic flow component. Thus, the first term describes the elastic behaviour while the combination of the second and third terms accounts for the viscoelastic or creep behaviour. The response of this particular model will be linear and it will obey the Boltzmann superposition principle.

The degree of fit between the behaviour described by the model and experimentally derived values can be exceedingly good: an example is illustrated in Figure 45.10, where the degree of correlation between the fitted line and experimental results for creep in bending of urea-formaldehyde chipboard (particleboard) beams was as high as 0.941.

A much more demanding test of any model is the prediction of long-term performance from short-term data. For timber and the various board materials, it has been found necessary to make the viscous term non-linear in these models where accurate predictions of creep (±10 per cent) are required for long periods of time (>10 years) from short-term data (6–9 months) (Dinwoodie *et al.,* 1990a). The deformation of this non-linear mathematical model is given by the equation

$$Y=\beta_1+\beta_2[1-\exp(-\beta_3 t)]+\beta_4 t^{\beta_5} \quad (45.11)$$

where β_5 is the viscous modification factor with a value $0<b<1$.

An example of the successful application of this model to predict the deflection of a sample of cement-bonded particleboard after ten years from the first nine months of data is given in Dinwoodie *et al.* (1990a).

Various non-linear viscoelastic models have been developed and tested over the years ranging from the fairly simple early approach by Ylinen (1965) in which a spring and a dashpot in his rheological model are replaced by non-linear elements, to the much more sophisticated model by Tong and Ödeen (1989a) in which the linear viscoelastic equation is modified by the introduction of a non-linear function either in the form of a simple power function, or by using the sum of an exponential series corresponding to ten Kelvin elements in series with a single spring.

All this modelling is further confirmation of the non-linear viscoelastic behaviour of timber and wood-based panels when subjected to high levels of stressing, or to lower levels at high moisture levels.

The development of models for unsteady state moisture content are described later.

Reversible and irreversible components of creep

In timber and many of the high polymers, creep under load can be subdivided into reversible and irreversible components: passing reference to this was made in Section 45.4 and the generalised relationship with time was depicted in Figure 45.2. The relative proportions of these two components of total creep appears to be related to stress level and to prevailing conditions of temperature and moisture content.

The influence of level of stress is clearly illustrated in Figure 45.13, where the total compliance at 70 per cent and 80 per cent of the ultimate stress for hoop pine in compression is subdivided into the separate components: at 70 per cent, the irreversible creep compliance accounts for about 45 per cent of the total creep compliance, while at 80 per cent of the ultimate, the irreversible creep compliance has increased appreciably to 70 per cent of the total creep compliance at the longer periods of time, though not at the shorter durations. Increased moisture content and increased temperature will also result in an enlargement of the irreversible component of total creep.

Reversible creep is frequently referred to in the literature as delayed elastic or primary creep, and in the early days was ascribed to either polymeric

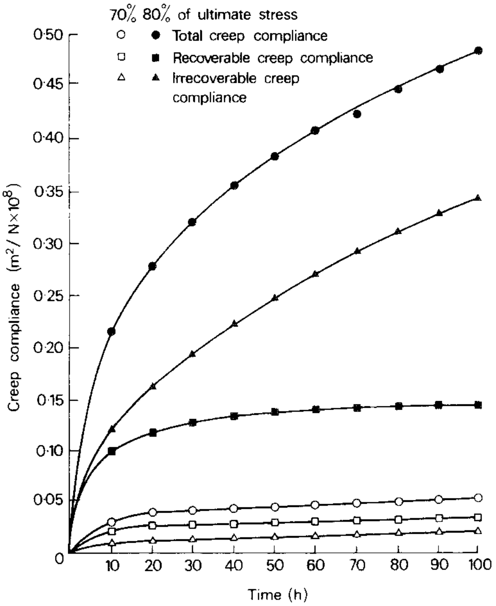

FIGURE 45.13 The relative proportions of the recoverable and irrecoverable creep compliance in samples of hoop pine (*Araucaria cunninghamii*) stressed in bending (Kingston and Budgen (1972) by permission of Springer-Verlag).

uncoiling or the existence of a creeping matrix. Owing to the close longitudinal association of the molecules of the various components in the amorphous regions, it appears unlikely that uncoiling of the polymers under stress can account for much of the reversible component of creep.

The second explanation of reversible creep utilises the concept of time-dependent, two-stage molecular motions of the cellulose, hemicellulose and the lignin constituents. The pattern of molecular motion for each component is dependent on that of the other constituents and it has been shown that the difference in directional movement of the lignin and non-lignin molecules results in considerable molecular interference such that stresses set up in loading can be transferred from one component (a creeping matrix) to another component (an attached, but non-creeping structure). It is postulated that the lignin network could act as an energy sink, maintaining and controlling the energy set up by stressing (Chow, 1973).

Irreversible creep, also referred to as viscous, plastic or secondary creep has been related to either time-dependent changes in the active number of hydrogen bonds, or to the loosening and subsequent remaking of hydrogen bonds as moisture diffuses through timber with the passage of time (Gibson, 1965). Such diffusion can result directly from stressing; thus early work indicated that when timber was stressed in tension it gained in moisture content, and conversely when stressed in compression its moisture content was lowered. It is argued, though certainly not proven, that the movement of moisture by diffusion occurs in a series of steps from one adsorption site to the next, necessitating the rupture and subsequent reformation of hydrogen bonds. The process is viewed as resulting in loss of stiffness and/or strength, possibly through slippage at the molecular level. Recently, however, it has been demonstrated that moisture movement, while affecting creep, can account for only part of the total creep obtained, and this explanation of creep at the molecular level warrants more investigation; certainly not all the observed phenomena support the hypothesis that creep is due to the breaking and remaking of hydrogen bonds under a stress bias. At moderate to high levels of stressing, particularly in bending and compression parallel to the grain, the amount of irreversible creep is closely associated with the development of kinks in the cell wall (Hoffmeyer and Davidson, 1989).

Boyd (1982) in a lengthy paper demonstrates how creep under both constant and variable relative humidity can be explained quite simply in terms of stress-induced physical interactions between the crystalline and non-crystalline components of the cell wall. Justification of his viewpoint relies heavily on the concept that the basic structural units develop a lenticular trellis format containing a water-sensitive gel which changes shape during moisture changes and load applications thereby explaining creep strains.

Attempts have been made to describe creep in terms of the fine structure of timber and it has been demonstrated that creep in the short term is highly correlated with the angle of the microfibrils in the S_2 layer of the cell wall, and inversely with the degree of crystallinity. However, such correlations do not necessarily prove any causal relation and it is possible to explain these correlations in terms of the presence or absence of moisture which would be closely associated with these particular variables.

Environmental effects on rate of creep

Temperature: steady-state

In common with many other materials, especially the high polymers, the effect of increasing temperature on timber under stress is to increase both the rate and the total amount of creep. Figure 45.14 illustrates a two-and-a-half fold increase in the amount of creep as the temperature is raised from 20°C to 54°C; there is a marked increase in the irreversible component of creep at the higher temperatures.

Various workers have examined the applicability to wood of the time/temperature superposition principle; results have been inconclusive and variable and it would appear that caution must be exercised in the use of this principle.

Temperature: unsteady-state

Cycling between low and high temperatures will

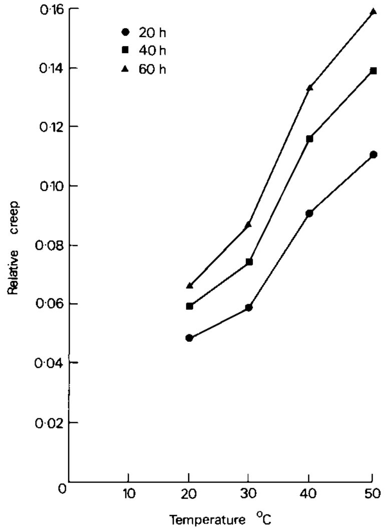

FIGURE 45.14 The effect of temperature on relative creep of samples of hoop pine (*Araucaria cunninghamii*) loaded in compression for 20, 40 and 60 hours (Kingston and B. Budgen (1972) by permission of Springer-Verlag).

induce in stressed timber and panel products a higher creep response than would occur if the temperature was held constant at the higher level; however, this effect is most likely due to changing moisture content as temperature is changed, rather than to the effect of temperature itself.

Moisture content: steady-state

The rate and amount of creep in timber of high moisture content is appreciably higher than that of dry timber; an increase in moisture content from 6 to 12 per cent increases the deflection in timber at any given stress level by about 20 per cent. It is interesting to note the occurrence of a similar increase in creep in nylon when in the wet condition.

Hunt (1999) recorded that the effect of humidity can be treated by the use of an empirical humidity-shift factor curve to be used with an empirical master creep curve. At high moisture contents this logarithmic shift factor increases rapidly; creep at 22 per cent moisture content compared with that at 10 per cent was found to be $10^{1.5}$ or 32 times as fast.

Moisture content: unsteady-state

If the moisture content of small timber beams under load is cycled from dry to wet and back to dry again, the deformation will also follow a cyclic pattern. However, the recovery in each cycle is only partial and over a number of cycles the total amount of creep is very large: the greater the moisture differential in each cycle, the higher the amount of creep (Armstrong and Kingston, 1960; Hearmon and Paton, 1964). Figure 45.15 illustrates the deflection that occurs with time in matched test pieces loaded to 3/8 ultimate short-term load where one test piece is maintained in an atmosphere of 93 per cent relative humidity, while the other is cycled between 0 and 93 per cent relative humidity. After 14 complete cycles the latter test piece had broken after increasing its initial deflection by 25 times; the former test piece was still intact having increased in deflection by only twice its initial deflection. Failure of the first test

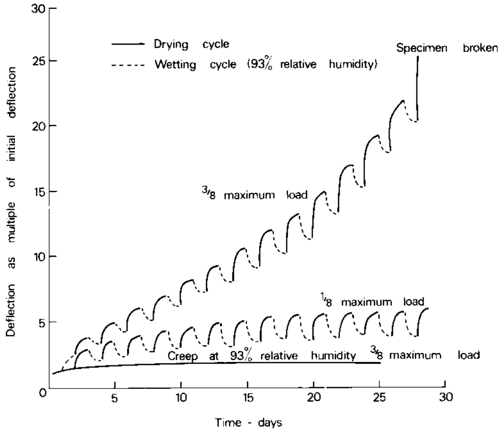

FIGURE 45.15 The effect of cyclic variations in moisture content on relative creep of samples of beech loaded to 1/8 and 3/8 of ultimate load (© Building Research Establishment).

piece occurred, therefore, after only a short period of time and at a stress equivalent to only 3/8 of its ultimate (Hearmon and Paton, 1964).

It should be appreciated that creep increased during the drying cycle and decreased during the wetting cycle with the exception of the initial wetting when creep increased. It was not possible to explain the negative deflection observed during absorption, though the energy for the change is probably provided by the heat of absorption. The net change at the end of a complete cycle of wetting and drying was considered to be a redistribution of hydrogen bonds which manifests itself as an increase in deformation of the stressed sample (Gibson, 1965).

More early work was to show that the rate of moisture change affects the rate of creep, but not the amount of creep; this appears to be proportional to the total change in moisture content (Armstrong and Kingston, 1962).

This complex behaviour of creep in timber when loaded under either cyclic or variable changes in relative humidity has been confirmed by a large number of research workers (e.g. Schniewind, 1968; Ranta-Mannus, 1973; Hunt, 1982; Mohager, 1987). However, in board materials the cyclic effect appears to be somewhat reduced (Dinwoodie, 1990b).

Later test work, covering longitudinal compression and tension stressing as well as bending, indicated that the relationship between creep behaviour and moisture change was more complex than first thought. The results of this work (e.g. Hunt, 1982) was to indicate that there are three separate components to this form of creep; these are illustrated in Figure 45.16 and are:

1. an increase in creep follows a decrease in moisture content of the sample, as described previously;
2. an increase in creep follows any increase in moisture content above the previous highest level reached after loading; three examples can be seen in the middle of the graph in Figure 45.16;
3. a decrease in creep follows an increase in moisture content below the previous highest level reached after loading as described previously.

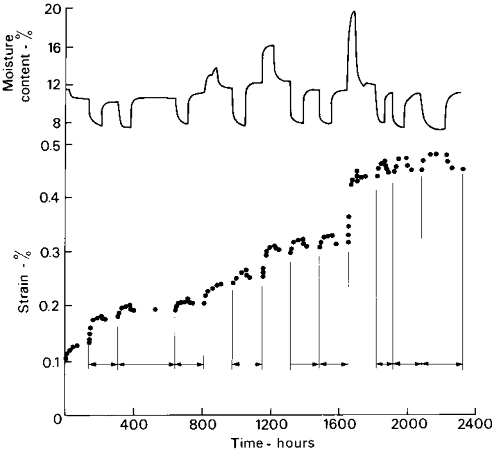

FIGURE 45.16 Creep deflection under changing moisture content levels for small samples of beech stressed in tension. Note the different responses to increasing moisture content (from Hunt (1982) by permission of the Institute of Wood Science).

It follows from points 1 and 2 above that there will always be an initial increase in creep during the initial change in moisture content, irrespective of whether adsorption or desorption is taking place.

Further experimentation has established that the amount of creep that occurs depends on the size and rate of the moisture change, and is little affected by its duration or by whether such change is brought about by one or more steps (Armstrong and Kingston, 1962). These findings were to cast doubt on the previous interpretation that such behaviour constituted true creep.

Re-inforcement of that doubt occurred with the publication of results of Arima and Grossman (1978). Small beams of *Pinus radiata* (680 × 15 × 15 mm) were cut from green timber and stressed to about 25 per cent of their short-term bending strength. While held in their deformed condition, the beams were allowed to dry for 15 days, after which the retaining clamps were removed and the initial recovery measured. The unstressed beams were then subjected to changes in relative humidity and Figure 45.17 shows the changes in recovery with changing humidity. Most important is the fact that total recovery was almost achieved; what was thought to have been viscous deformation in the post-drying and clamping stage turned out to be reversible.

These two phenomena – that creep is related to the magnitude of the moisture change and not to time, and that deformation is reversible under moisture change – cast very serious doubts on whether the deformation under changes in moisture content constituted true creep.

It was considered necessary to separate these two very different types of deformation, namely the true viscoelastic creep that occurs under constant moisture content and is directly a function of time, from that deformation which is directly related to the interaction of change in moisture content and mechanical stressing which is a function of the history of moisture change and is relatively uninfluenced by time. A term of convenience was derived to describe this latter type of deformation, namely *mechano-sorptive behaviour* (Grossman, 1976).

Changing levels of moisture content, however, will result in changes in the dimensions of timber and an allowance for this must be taken into account in the calculation of mechano-sorptive deformation. Thus,

$$\epsilon_m = \epsilon_{vc} + \epsilon_{ms} + \epsilon_s \qquad (45.11)$$

where ϵ_m = total measured strain, ϵ_{vc} is the normal time (constant moisture content) viscoelastic creep, ϵ_{ms} is the mechano-sorptive strain under changing moisture content and ϵ_s is the swelling or shrinkage strain of a matched, zero-loaded control test piece. The swelling/shrinkage strain (ϵ_s) (sometimes referred to as pseudo-creep by some workers), which is manifest during moisture cycling by an increase in deflection during desorption and a decrease during adsorption, has been ascribed to differences in the normal longitudinal swelling and shrinkage of wood: a tensile strain resulting in a smaller shrinkage coefficient and a compression strain resulting in a larger one (Hunt and Shelton, 1988).

Mechano-sorptive behaviour is linear only at

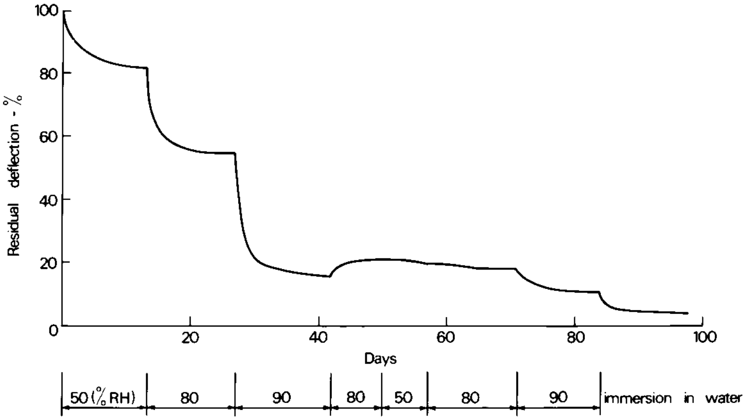

FIGURE 45.17 The amount of recovery of both viscoelastic and mechano-sorptive deflection that occurred when dried bent beams were subjected to a sequence of humidity changes (adapted from Arima and Grossman (1978) by permission of the Institute of Wood Science).

low levels of stress; in the case of compression and bending the upper limit of linear behaviour is of the order of 10 per cent, while in tension it is slightly higher (Hunt, 1980).

Susceptibility to mechano-sorptive behaviour is positively correlated with elastic compliance, microfibrillar angle of the cell wall and dimensional change rates (Hunt, 1994). Thus, both juvenile wood and compression wood have been shown to creep much more (up to five times greater) than adult wood.

Modelling of deformation under variable moisture content

The requirement for a model of mechano-sorptive behaviour was originally set out by Schniewind (1966) and later developed by Grossman (1976) and Mårtensson (1992). More recently, the list of requirements that must be satisfied for such a model has been reviewed and considerably extended by Hunt (1994); aspects of sorption are now included on the list.

Many attempts have been made over the last two decades to develop a model for mechano-sorptive behaviour. A few of these models have been explanatory or descriptive in nature-seeking relationships at the molecular, ultrastructural or microscopical levels. Most of them, however, have been either purely mathematical, with the aim of producing a generalised constitutive equation, or partly mathematical, where the derived equation is linked to some physical phenomenon, or change in structure of the timber under stress.

It will be recalled that it is 40 years since the concept of mechano-sorptive deformation was first established (Armstrong and Kingston, 1960). Since then, the concept of mechano-sorptive deformation, which is primarily a function of the amount of moisture change, has been clearly separated from that of the viscoelastic creep which is primarily a function of time. Indeed, over the last two decades the concepts have become more polarised and considerable success has been made in recent times in the derivation of effective constitutive equations for mechano-sorptive deformation.

It now appears that the thinking on creep has gone full circle and is now back to the stage where it was once thought that viscoelastic creep and mechano-sorptive behaviour were but two different manifestations of one basic relationship. The published findings by Gril (1988), Hanhijärvi (1995) and Hunt and Gril (1996) indicating that mechano-sorptive deformation may be accounted for by a coupling between creep and hygroexpansion, together with the recent findings by Hunt (1999) that time-dependent creep and mechano-sorptive behaviour are different means of reaching the same creep result, are certainly contrary to views presented over the last 20 years and give cause for a complete re-evaluation of existing concepts.

Hunt's results led him to a new way of characterising wood creep by plotting data in the form of strain rate against strain: solution of this differential equation led to the more normal relation of strain against time. It was then found that normalisation of both the ordinate and abscissa resulted in a single master creep curve for both juvenile and mature wood from a single sample and, more important, approximately also for all test humidities. The effects of humidity changes require the additional measurement of the increased activity associated with the molecular destabilisation, and its relaxation-time constraint, associated with the physical-ageing phenomenon (thermodynamic equilibrium), the application of which suggests that the speed of moisture change might be important in mechano-sorptive deformation.

More information on the parameters that should be included in these mathematical models as well as the types of models which have been developed over the years are to be found in Tong and Ödeen (1989b), Hunt (1994), Morlier and Palka (1994), Hanhijärvi (1995) and Dinwoodie (2000).

45.5 References

Arima, T. and Grossman, P.U.A. (1978) Recovery of wood after mechano-sorptive deformation. *J. Inst. Wood Sci.* 8, 2, 47–52.

Armstrong, L.D. and Kingston, R.S.T. (1960) Effect of moisture changes on creep in wood. *Nature* 185, 4716, 862–3.

Armstrong, L.D. and Kingston, R.S.T. (1962) The effect of moisture content changes on the deformation of wood under stress. *Aust. J. App. Sci.* 13, 4, 257–76.

Astley, R.J., Stol, K.A. and Harrington, J.J. (1998) Modelling the elastic constraints of softwood. Part II: The cellular microstructure. *Holz als Roh-und Werkstoff* 56, 43–50.

Barber, N.F. (1968) A theoretical model of shrinking wood. *Holzforschung* 22, 97–103.

Barber, N.F. and Meylan, B.A. (1964) The anisotropic shrinkage of wood. A theoretical model. *Holzforschung* 18, 146–56.

Boyd, J.D. (1974) Anisotropic shrinkage of wood. Identification of the dominant determinants. *Mokuzai Gakkaishi* 20, 473–82.

Boyd, J.D. (1982) An anatomical explanation for viscoelastic and mechano-sorptive creep in wood, and effects of loading rate on strength. In *New Perspectives in Wood Anatomy* (ed. P. Bass), Martinus Nijhoff/Dr W. Junk, The Hague, 171–222.

Cave, I.D. (1968) The anisotropic elasticity of the plant cell-wall. *Wood Sci. Technol.* 2, 268–78.

Cave, I.D. (1972) A theory of shrinkage of wood. *Wood Sci. Technol.* 6, 284–92

Cave, I.D. (1975) Wood substance as a water-reactive fibre-reinforced composite*, J. of Microscopy*, 104, 1, 47–52.

Cave, I.D. (1978a) Modelling moisture-related mechanical properties of wood. I. Properties of the wood constituents. *Wood Sci. and Technol.* 12, 75–86.

Cave, I.D. (1978b) Modelling moisture-related mechanical properties of wood. II. Computation of properties of a model of wood and comparison with experimental data. *Wood Sci. Technol.* 12, 127–39.

Chow, S. (1973) Molecular rheology of coniferous wood tissues. *Transactions of the Society of Rheology* 17, 109–28.

Dinwoodie, J.M. (1975) Timber – a review of the structure–mechanical property relationship. *J. of Microscopy* 104, 1, 3–32.

Dinwoodie, J.M. (2000) *Timber: Its Nature and Behaviour*, 2nd edn, E & FN Spon, London, 257 pp.

Dinwoodie, J.M., Higgins, J.A., Paxton, B.H. and Robson, D.J. (1990a) Creep in chipboard. Part 7: Testing the efficacy of models on 7–10 years data and evaluating optimum period of prediction. *Wood Sci. Technol.* 24, 181–9.

Dinwoodie, J.M., Higgins, J.A., Paxton, B.H. and Robson, D.J. (1990b) Creep research on particle board – 15 years' work at UK BRE. *Holz als Roh-und Werkstoff* 48, 5–10.

Gerhards, C.C. (1982) Effect of moisture content and temperature on the mechanical properties of wood. An analysis of immediate effects. *Wood & Fiber* 14, 1, 4–36.

Gibson, E. (1965) Creep of wood: role of water and effect of a changing moisture content. *Nature* (Lond) 206, 213–15.

Gril, J. (1988) Une modélisation du compartement hygro-rhéologique du bois à partir de sa microstructure. *Doctoral thesis, University of Paris.*

Grossman, P.U.A. (1976) Requirements for a model that exhibits mechano-sorptive behaviour. *Wood Sci. Technol.* 10, 163–8.

Hanhijärvi, A. (1995) Modelling of creep deformation mechanisms in wood. *Tech. Res. Centre of Finland Publication* 231, 143 pp.

Harington, J.J., Booker, R. and Astley, R.J. (1998) Modelling the elastic constraints of softwood. Part 1: The cell-wall lamellae. *Holz als Roh-und Werkstoff* 56, 37–41.

Hearmon, R.F.S. and Paton, J.M. (1964) Moisture content changes and creep in wood. *For. Prod. J.* 14, 357–9.

Hoffmeyer, P. and Davidson, R. (1989) Mechano-sorptive creep mechanism of wood in compression and bending. *Wood Sci. Technol.* 23, 215–27.

Hunt, D.G. (1980) A preliminary study of tensile creep of beech with concurrent moisture changes. *Proceedings of the Third International Conference on Mechanical Behaviour of Materials*, Cambridge, 1979 (eds K.J. Miller and R.F. Smith), Vol. 3, 299–308.

Hunt, D.G. (1982) Limited mechano-sorptive creep of beech wood. *J. Inst. Wood Sci.* 9 , 3, 136–8.

Hunt, D.G. (1994) Present knowledge of mechano-sorptive creep of wood. In *Creep in Timber Structures* (ed. P. Morlier), RILEM Report 8, E & FN Spon, London, 73–97.

Hunt, D.G. (1999) A unified approach to creep in wood. *Proc. Roy. Soc. London*, *A*, 455, 4077–95.

Hunt, D.G. and Gril, J. (1996) Evidence of a physical ageing phenomenon in wood. *J. Mat. Sci. Letters* 15, 80–92.

Hunt, D.G. and Shelton, C.F. (1988) Longitudinal moisture–shrinkage coefficients of softwood at the mechano-sorptive creep limit. *Wood Sci. Technol.* 22, 199–210.

Kifetew, G. (1997) Application of the early–latewood interaction theory of the shrinkage anisotropy of Scots pine. *Proc. International Conference on Wood–Water Relations*, Copenhagen (ed. P. Hoffmeyer), and published by the management committee of EC COST Action E8, 165–71.

Kingston, R.S.T. and Budgen, B. (1972) Some aspects of the rheological behaviour of wood, Part IV: Non-linear behaviour at high stresses in bending and compression. *Wood Sci. Technol.* 6, 230–8.

Mårtensson, A. (1992) Mechanical behaviour of wood exposed to humidity variations. *Report TVBK-1066*, Lund Institute of Technology, Sweden, 189 pp.

Meylan, B.A. (1968) Cause of high longitudinal shrinkage in wood. *For. Prod. J.* 18, 4, 75–8.

Mohager, S. (1987) Studier av krypning hos trä (studies of creep in wood). *Report 1987–1 of the Dept. of Building Materials*, The Royal Institute of Technology, Stockholm, 140 pp.

Moore, G.L. (1984) The effect of long term temperature cycling on the strength of wood. *J. Inst. Wood Sci.* 9 , 6, 264–7.

Morlier, P. and Palka, L.C. (1994) Basic knowledge. In *Creep in Timber Structures* (ed. P. Morlier), Rilem Report 8, E & FN Spon, London, 9–42.

Nakai, T. and Grossman, P.U.A. (1983) Deflection of wood under intermittent loading. Part 1: Fortnightly cycles. *Wood Sci. Technol.* 17, 55–67.

Ranta-Maunus, A. (1973) A theory for the creep of wood with application to birch and spruce plywood. *Technical Research Centre of Finland, Building Technology and Community Development*, Publication 4, 35 pp.

Schniewind, A.P. (1966) Uber den Einfluss von Feuchtigkeitsanderungen auf das Kriechen von Buchenholz quer zur Faser unter Berucksichtigung von Temperatur und temperaturanderungen. *Holz als Roh-und Werkstoff* 24, 87–98.

Schniewind, A.P. (1968) Recent progress in the study of rheology of wood. *Wood Sci. Technol.* 2, 189–205

Skaar, C. (1988) *Wood–Water Relations*, Springer-Verlag, Berlin, 283 pp.

Tong, L. and Ödeen, K. (1989a) A non-linear viscoelastic equation for the deformation of wood and wood structure. *Report No. 4 of the Department of Building Materials*, Royal Institute of Technology, Stockholm, 6 pp.

Tong, L. and Ödeen, K. (1989b) Rheological behaviour of wood structures. *Report No. 3 of the Department of Building Materials*, Royal Institute of Technology, Stockholm, 145 pp.

Weatherwax, R.G. and Stamm, A.J. (1946) The coefficients of thermal expansion of wood and wood products. *U.S. For. Prod. Lab.*, Madison, Report no. 1487.

Ylinen, A. (1965) Prediction of the time-dependent elastic and strength properties of wood by the aid of a general non-linear viscoelastic rheological model. *Holz als Roh und Werkstoff* 5, 193–6.

Chapter forty-six

Strength and failure in timber

46.1 Introduction

While it is easy to appreciate the concept of deformation primarily because it is something that can be observed, it is much more difficult to define in simple terms what is meant by the *strength* of a material. Perhaps one of the simpler definitions of strength is that it is a measure of the resistance to *failure*, providing of course that we are clear in our minds what is meant by failure.

Let us start therefore by defining failure. In those modes of stressing where a distinct break occurs with the formation of two fracture surfaces, failure is synonymous with rupture of the specimen. However, in certain modes of stressing, fracture does not occur and failure must be defined in some arbitrary way such as the maximum stress that the sample will endure or, in exceptional circumstances such as compression strength perpendicular to the grain, the stress at the limit of proportionality.

Having defined our end point, it is now easier to appreciate our definition of strength as the natural resistance of a material to failure. But how do we quantify this resistance? This may be done by calculating either the stress necessary to produce failure or the amount of energy consumed in producing failure. Under certain modes of testing it is more convenient to use the former method of quantification as the latter tends to be more limited in application.

46.2 Determination of strength

46.2.1 Test piece size and selection

Although in theory it should be possible to determine the strength properties of timber independent of size, in practice this is found not to be the case. A definite though small size effect has been established and in order to compare the strength of a timber sample with recorded data it is advisable to adopt the standard sizes set out in the literature.

The size of the test piece to be used will be determined by the type of information required. When this has been decided, it will determine the test procedure; standardised test procedures should always be adopted and a choice is available between National, European or International methods of test (see Figure 46.1).

Use of small clear test pieces

This size of test piece was originally used for the derivation of working stresses for timber, but in the mid-1970s it was superseded by actual structural size timber. However, the small clear test piece still remains valid for characterising new

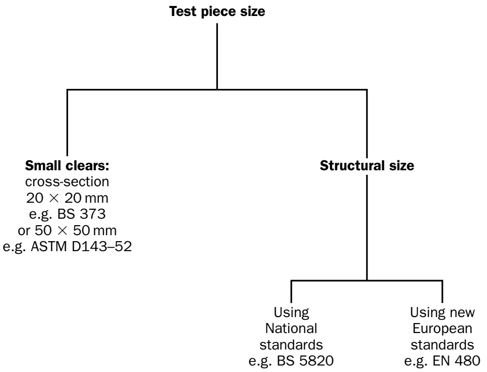

FIGURE 46.1 Alternative sizes of test piece to be used in the determination of the strength of timber.

timbers and for the strict academic comparison of wood from different trees or different species, since the use of small, knot-free, straight-grained, perfect test pieces represent the maximum quality of wood that can be obtained. As such, these test pieces are not representative of structural-size timber with all its imperfections; several arbitrarily defined reduction factors have to be used in order to obtain a measure of the working stresses of the timber, when small, clear test pieces are used (see Section 46.8.1).

Two standard procedures for testing small clear test pieces have been used internationally; the original was introduced in the USA as early as 1891 using a test sample 2 × 2 inches in cross-section; the second, European in origin, employs a test specimen 20 × 20 mm in cross-section. Prior to 1949 the former size was adopted in the UK, but after this date this larger sample was superseded by the smaller, thereby making it possible to obtain an adequate number of test specimens from smaller trees. Because of the differences in size, the results obtained from the two standard procedures are not strictly comparable and a series of conversion values has been determined (Lavers, 1969).

The early work in the UK on species characterisation employed a sampling procedure in which the test samples were removed from the log in accordance with a cruciform pattern. However, this was subsequently abandoned and a method devised applicable to the centre plank removed from a log; 20 × 20 mm sticks, from which the individual test pieces are obtained, are selected at random in such a manner that the probability of obtaining a stick at any distance from the centre of a cross-section of a log is proportional to the area of timber at that distance. Test samples are cut from each stick eliminating knots, defects and sloping grain; this technique is described fully by Lavers (1969).

Use of structural-size test pieces

The use of these larger test pieces reproduces actual service loading conditions and they are of particular value because they allow directly for defects such as knots, splits and distorted grain rather than by applying a series of reduction factors as is necessary with small clear test pieces. However, use of the large pieces is probably more costly.

46.2.2 Standardised test procedures

Europe at the present time is in a transition period in which National test procedures are being replaced by European procedures. Within the first decade of this century all National standards relating to the use of timber and panel products in construction will be withdrawn; it is uncertain at this stage whether the testing of small, clear test pieces will be retained as a National Standard provided it is not used for the derivation of characteristic values (working stresses). It is interesting to note that many of the European standards (ENs) have now been adopted as International Standards (ISOs).

46.2.3 Methods of test

Methods of test are given in Desch and Dinwoodie (1996) and Dinwoodie (2000).

46.3 Strength values

46.3.1 Derived using small clear test pieces

For a range of strength properties determined on small, clear test pieces, with the exception of tensile strength parallel to the grain, the mean values and standard deviations (see below) are presented in Table 46.1 for a selection of timbers covering the range in densities to be found in hardwoods and softwoods. Many of the timbers whose elastic constants were presented in Table 45.1 are included. All values relate to a moisture content which is in equilibrium with a relative humidity of 65 per cent at 20°C; these are of the order of 12 per cent and the timber is referred to as 'dry'. Modulus of elasticity has also been included in Table 46.1.

Table 46.1 is compiled from data presented in *Bulletin 50* of the Forest Products Research Laboratory (Lavers, 1969) which lists data for both the dry and green states for 200 species of timber. The upper line for each species provides the estimated average value while the lower line contains the standard deviation.

In Table 46.2 tensile strength parallel to the grain is listed for certain timbers and it is in this mode that timber is at its strongest.

Comparison of these values with those for compression strength parallel to the grain in Table 46.1 will indicate that, unlike many other materials, the compression strength is only about one-third that of tensile strength along the grain.

46.3.2 Derived using structural size test pieces

Structural strength values may still be recorded and used as mean values with a standard deviation where National standards are still being used in testing (e.g. BS 5820) and design (e.g. BS 5268 Pt2 1996).

An example of mean strength values derived from testing dry structural size timber to BS 5820 is given in Table 46.3 for each of the major strength modes. Not only are these mean values considerably lower than the mean values derived from small, clear test pieces (Tables 46.1 and 46.2), but the tensile strengths are now lower than the compression strengths. This is directly related to the presence of knots and associated distorted grain in the structural size test pieces.

By the year 2010, however, all structural test work and design within Europe will have to be carried out according to the new European standards by testing to EN 384 and EN 408 and designing using Eurocode 5 (ENV 1995–1–1). Within the European system, the *characteristic value* for the strength properties is taken as the 5-percentile value; for modulus of elasticity there are two characteristic values, one the 5-percentile, the other the mean or 50-percentile value.

The sample 5-percentile value is determined for each sample by the equation

$$f_{05} = f_r \qquad (46.1)$$

where f_{05} is the sample 5-percentile value, and f_r is obtained by ranking all the test values for a sample in ascending order. The 5-percentile value is the test value for which 5 per cent of the values are lower. If this is not an actual test value (i.e. the number of test values is not divisible by 20) then interpolation between the two adjacent values is permitted.

The characteristic value of strength (f_k) is calculated from the equation

$$f_k = \overline{f}_{05} k_s k_v \qquad (46.2)$$

where $\overline{f}_{05}$ is the mean (in N/mm^2) of the adjusted 5-percentile values (f_{05}) for each sample weighted according to the number of pieces in each sample, k_s is a factor to adjust for the number of samples and their size, and k_v is a factor to allow for the lower variability of f_{05} values from machine grades in comparison with visual grades; for visual grades $k_v = 1.0$, and for machine grades $k_v = 1.12$

46.4 Variability in strength values

In Chapter 44 attention was drawn to the fact that timber is a very variable material and that

TABLE 46.1 Average and standard deviation of various mechanical properties of selected timbers at 12 per cent moisture content from small, clear test pieces

	Density	Static bending*				Impact	Compression	Hardness	Shear	Cleavage	
	Dry (*kg/m*^{3})	*Modulus of rupture (N/mm*^{2}*)*	*Modulus of elasticity (N/mm*^{2}*)*	*Energy to max. load (mmN/mm*^{3}*)*	*Energy to facture (mmN/mm*^{3}*)*	*Drop of hammer (m)*	*Parallel to grain (N/mm*^{2}*)*	*On side grain (N)*	*Parallel to grain (N/mm*^{2}*)*	*Radial plane (N/mm width)*	*Tangential plane (N/mm width)*
Hardwoods											
Balsa	176	23	3200	0.018	0.035	–	15.5	–	2.4	–	–
		7.3	1060	0.007	0.017		4.43		0.62		
Obeche	368	54	5500	0.058	0.095	0.48	28.2	1910	7.7	9.3	8.4
		6.5	620	0.010	0.015	0.072	3.00	268	0.67	1.82	1.58
Mahogany	497	78	9000	0.070	0.128	0.58	46.4	3690	11.8	10.0	14.0
(*Khaya ivorensis*)		15.0	1520	0.026	0.044	0.149	8.45	816	2.56	2.08	2.90
Sycamore	561	99	9400	0.121	0.163	0.84	48.2	4850	17.1	16.8	27.3
		11.0	1160	0.028	0.049	0.136	4.83	639	2.32	2.95	3.91
Ash	689	116	11 900	0.182	0.281	1.07	53.3	6140	16.6		
		16.6	2170	0.045	0.097	0.216	7.73	1158	2.52		
Oak	689	97	10 100	0.093	0.167	0.84	51.6	5470	13.7	14.5	20.1
		16.8	1960	0.026	0.051	0.209	7.98	911	2.38	2.86	2.08
Afzelia	817	125	13 100	0.100	0.203	0.79	79.2	7870	16.6	10.5	13.3
		26.6	1760	0.043	0.087	0.215	12.02	914	2.28	2.00	2.49
Greenheart	977	181	21 000	0.213	0.395	1.35	89.9	10 450	20.5	17.5	22.2
		20.9	1990	0.047	0.088	0.207	8.49	1531	3.06	4.79	4.97
Softwoods											
Norway spruce	417	72	10 200	0.086	0.116	0.58	36.5	2140	9.8	8.4	9.1
(European)		10.2	2010	0.022	0.040	0.116	5.26	353	1.44	1.07	1.20
Yellow pine	433	80	8300	0.089	0.097	0.56	42.1	2050	9.3	8.2	11.6
(Canada)		10.9	1440	0.015	0.019	0.100	6.14	473	1.61	1.57	1.77
Douglas fir	497	91	10 500	0.097	0.172	0.69	48.3	3420	11.6	9.5	11.4
(UK)		16.9	2160	0.038	0.081	0.200	8.03	865	2.29	1.90	2.17
Scots pine	513	89	10 000	0.103	0.134	0.71	47.4	2980	12.7	10.3	13.0
(UK)		16.9	2130	0.032	0.053	0.167	9.25	697	2.45	1.82	2.47
Caribbean Pitch pine	769	107	12 600	0.126	0.253	0.91	56.1	4980	14.3	12.1	13.3
		14.5	1800	0.042	0.060	0.196	7.76	1324	2.81	1.23	1.58

*In three-point loading.

TABLE 46.2 Tensile strength parallel to the grain of certain timbers using small, clear test pieces

Timber	*Moisture content (%)*	*Tensile strength (N/mm^2)*
Hardwoods		
Ash (Home grown)	13	136
Beech (Home grown)	13	180
Yellow poplar (Imported)	15	114
Softwoods		
Scots pine (Home grown)	16	92
Scots pine (Imported)	15	110
Sitka spruce (Imported)	15	139
Western hemlock (Imported)	15	137

TABLE 46.3 Mean values for dry strength derived on structural size test pieces (approx. 97 × 47 mm) using BS 5820 (m.c. = 15–18 per cent)

Timber	*Mean values (N/mm^2)*		
	Bending	*Tension*	*Compression*
Sitka spruce (UK)	32.8	19.7	29.5
Douglas fir (UK)	35.7	21.4	32.1
Spruce/pine/fir (Canada)	43.9	26.3	39.5
Norway spruce (Baltic)	50.9	30.5	45.8

for many of its parameters, e.g. density, cell length and microfibrillar angle of the S_2 layer, distinct patterns of variation could be established within a growth ring, outwards from the pith towards the bark, upwards in the tree, and from tree to tree. The effects of this variation in structure are all too apparent when mechanical tests are performed.

Test data for small, clear test pieces are usually found to follow a normal distribution and, as described earlier an efficient estimator of the variability which occurs in any one property is the *sample standard deviation*, denoted by s. It is the square root of the variance and is derived from the formula:

$$s = \sqrt{\frac{\Sigma x^2 - \frac{(\Sigma x)^2}{n}}{n-1}} \qquad (46.3)$$

where x stands for every item successively and n is the number of items in the sample of either small, clear or structural size test pieces.

In a normal distribution, approximately 68 per cent of the results should lie, in theory, within $+1s$ and $-1s$ of the mean, and 99.87 per cent should fall within $\pm 3s$ of the mean.

As a general rule, a normal distribution curve fits the data from small, clear test pieces better than does the data from structural size test pieces, where as noted earlier, the 5-percentile characteristic value is determined simply by ranking the results.

The standard deviation provides a measure of the variability, but in itself gives little impression of the magnitude unless related to the mean. This ratio is known as the *coefficient of variation,* i.e.

$$CV = \frac{s}{\text{mean}}\% \qquad (46.4)$$

The coefficient of variation varies considerably, but is frequently under 15 per cent for many biological applications. However, reference to Table 46.1 will indicate that this value is frequently exceeded. For design purposes the two most important properties are the moduli of elasticity and rupture which have coefficients of variation typically in the range of 10–30 per cent.

46.5 Inter-relationships among the strength properties

46.5.1 Modulus of rupture and modulus of elasticity

A high correlation exists between the moduli of rupture and elasticity for a particular species: but it is doubtful whether this represents any causal relationship; rather it is more probable that the correlation arises as a result of the strong correlation that exists between density and each modulus. Whether it is a causal relationship or not, it is nevertheless put to good advantage for it forms the basis of the stress grading of timber by machine (see Section 46.8). The stiffness of a piece of timber is measured as it is deflected between rollers and this is used to predict its strength.

46.5.2 Impact bending and total work

Good correlations have been established between the height of drop in impact bending test and both *work to maximum load* and *total work*: generally the correlation is higher with the latter property.

46.5.3 Hardness and compression perpendicular to the grain

Correlation coefficients of 0.902 and 0.907 have been established between hardness and compression strength perpendicular to the grain of timber at 12 per cent moisture content and timber in the green state respectively. It is general practice to predict the compression strength from the hardness result using the following equations:

$$Y_{12} = 0.00147x_{12} + 1.103 \qquad (46.5)$$

$$Y_g = 0.00137x_g - 0.207 \qquad (46.6)$$

where Y_g and Y_{12} are compression strength perpendicular to the grain in N/mm^2 for green timber and timber at 12 per cent moisture content respectively, and x_g and x_{12} are hardness in N.

46.6 Factors affecting strength

Many of the variables noted in the previous chapter as influencing stiffness also influence the various strength properties of timber. Once again, these can be regarded as being either material dependent or manifestations of the environment.

46.6.1 Anisotropy and grain angle

The marked difference between the longitudinal and transverse planes in both shrinkage and stiffness has been discussed in previous chapters. Strength likewise is directionally dependent and the degree of anisotropy present in both tension and compression is presented in Table 46.4 for small clear test pieces of Douglas fir. Irrespective of moisture content, the highest degree of anisotropy is in tension (48:1): this reflects the fact that the highest strength of clear, straight-grained timber is in tension along the grain while the lowest is in tension perpendicularly. A similar degree of anisotropy is present in the tensile stressing of both glass-reinforced plastics and carbon-fibre-reinforced plastics when the fibre is laid up in parallel strands.

Table 46.4 also demonstrates that the degree of anisotropy in compression is an order of magnitude less than in tension. Whilst the compression strengths are markedly affected by moisture content, tensile strength appears to be relatively insensitive, reflecting the exclusion of moisture from the crystalline core of the microfibril; it is this crystalline core that imparts to timber its very high longitudinal tensile strength. The compari-

TABLE 46.4 Anisotropy in strength in small, clear test pieces

Timber	*Moisture content (%)*	*Tension*			*Compression*		
		∥ *(N/mm²)*	⊥ *(N/mm²)*	∥:⊥	∥ *(N/mm²)*	⊥ *(N/mm²)*	∥:⊥
Douglas fir	>27	131	2.69	48.7	24.1	4.14	5.82
Douglas fir	12	138	2.90	47.6	49.6	6.90	7.19

son of tension and compression strengths along the grain in Table 46.4 reveals that clear, straight-grained timber, unlike most other materials, has a tensile strength considerably greater than the compression strength. In structural timber containing knots and distorted grain, the opposite is the norm (see Table 46.3)

Anisotropy in strength is due in part to the cellular nature of timber and in part to the structure and orientation of the microfibrils in the wall layers. Bonding along the direction of the microfibrils is covalent whilst bonding between microfibrils is by hydrogen bonds. Consequently, since the majority of the microfibrils are aligned at only a small angle to the longitudinal axis, it will be easier to rupture the cell wall if the load is applied perpendicular than if applied parallel to the fibre axis.

Since timber is an anisotropic material, it follows that the angle at which stress is applied relative to the longitudinal axis of the cells will determine the ultimate strength of the timber. Figure 46.2 illustrates that over the range 0–45° tensile strength is much more sensitive to grain angle than is compression strength. However, at angles as high as 60° to the longitudinal axis both tension and compression strengths have fallen to only about 10 per cent of their value in straight-grained timber. The sensitivity of strength to grain angle in clear straight-grained timber is identical with that for fibre orientation in both glass-fibre- and carbon-fibre-reinforced plastics.

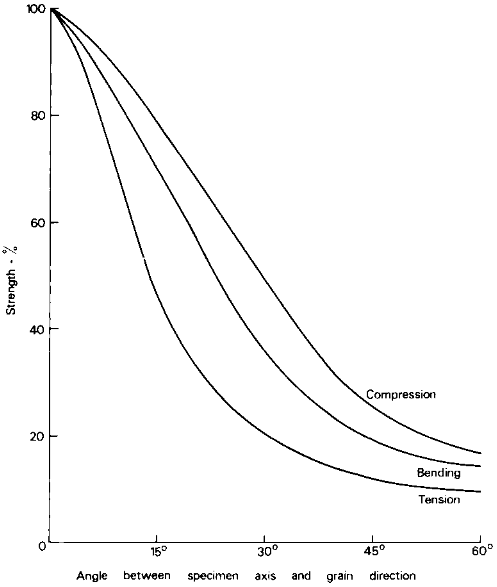

FIGURE 46.2 Effect of grain angle on the tensile, bending and compression strength of timber.

It is possible to obtain an approximate value of strength at any angle to the grain from knowledge of the corresponding values for both parallel and perpendicular to the grain using the following formula, which, in its original form, was credited to Hankinson:

$$f_\theta = \frac{f_L \times f_T}{f_L \sin^n \theta + f_T \cos^n \theta} \qquad (46.7)$$

where f_θ is the strength property at angle θ from the fibre direction, f_L is the strength parallel to the grain, f_T is the strength perpendicular to grain, and n is an empirically determined constant; in tension, $n = 1.5 - 2$ while in compression, $n = 2 - 2.5$. The equation has also been used for stiffness where a value of 2 for n has been adopted.

46.6.2 Knots

Knots are associated with distortion of the grain and since even slight deviations in grain angle reduce the strength of the timber appreciably, it follows that knots will have a marked influence on strength. The significance of knots, however, will depend on their size and distribution both along the length of a piece of timber and across its section. Knots in clusters are more important than knots of a similar size which are evenly distributed, while knots on the top or bottom edge of a beam are more significant than those in the centre; large knots are much more critical than small knots.

It is very difficult to quantify the influence of knots; one of the parameters that has been successfully used is the *knot area ratio*, which relates the sum of the cross-sectional area of the knots at a cross-section to the cross-sectional area of the piece. The loss in bending strength that occurred with increasing knot area ratio in 200 home-grown Douglas fir boards is illustrated in Figure 46.3.

The very marked reduction in tensile strength of structural size timber compared with small clear test pieces (Tables 46.2 and 46.3) is due primarily to the presence and influence of knots in the former.

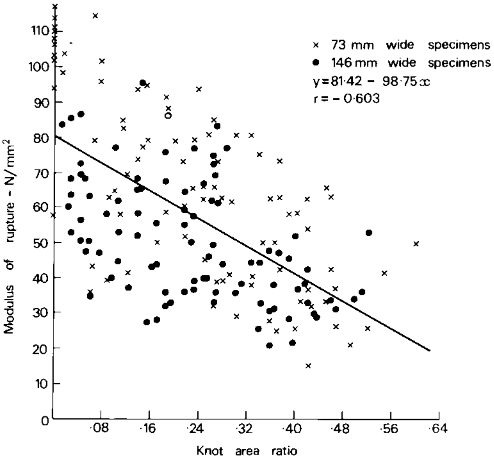

FIGURE 46.3 Effect of knot area ratio on the strength of timber (© Building Research Establishment).

46.6.3 Density

In Section 44.2 density was shown to be a function of cell wall thickness and therefore dependent on the relative proportions of the various cell components and also on the level of cell wall development of any one component. However, variation in density is not restricted to different species, but can occur to a considerable extent within any one species and even within a single tree. Some measure of the interspecific variation that occurs can be obtained from both Figure 44.20 and the limited amount of data in Tables 45.1 and 46.1. It will be observed from the latter that as density increases, so stiffness and the various strength properties increase. Density continues to be the best predictor of timber strength since high correlations between strength and density are a common feature in timber studies.

Most of the relations that have been established throughout the world between the various strength properties and timber density take the form of

$$f = kg^n \qquad (46.8)$$

where f is any strength property, g is the specific gravity, k is a proportionality constant differing for each strength property, and n is an exponent that defines the shape of the curve. An example of the use of this expression on the results of over 200 species tested in compression parallel to the grain is presented in Figure 46.4: the correlation coefficient between compression strength and density of the timber at 12 per cent moisture content was 0.902.

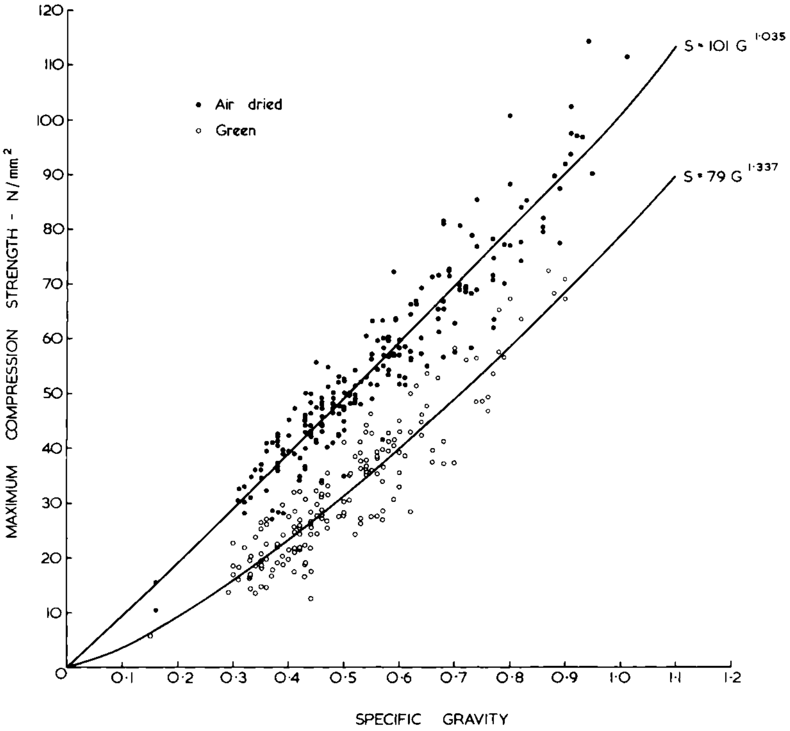

FIGURE 46.4 The relation of maximum compression strength to specific gravity for 200 species tested in the green and dry states (© Building Research Establishment).

Similar relationships have been found to hold for other strength properties, though in some the degree of correlation is considerably lower. This is the case in tension parallel to the grain where the ultrastructure probably plays a more significant role.

Over the range of density of most of the timbers used commercially, the relationship between density and strength can safely be assumed to be linear with the possible exception of shear and cleavage; similarly, within a single species, the range is low and the relationship can again be treated as linear.

46.6.4 Ring width

Since density is influenced by the rate of growth of the tree, it follows that variations in ring width will change the density of the timber and hence the strength. However, the relationship is considerably more complex than it first appears. In the ring-porous timbers such as oak and ash (see Chapter 44), increasing rate of growth (ring width) results in an increase in the percentage of the latewood which contains most of the thick-walled fibres; consequently, density will increase and so will strength. However, there is an upper limit to ring width beyond which density begins to fall owing to the inability of the tree to produce the requisite thickness of wall in every cell.

In the diffuse-porous timbers such as beech, birch and khaya, where there is uniformity in structure across the growth ring, increasing rate of growth (ring width) has no effect on density unless, as before, the rate of growth is excessive.

In the softwoods, however, increasing rate of growth results in an increased percentage of the low-density earlywood and consequently both density and strength decrease as ring width increases. Exceptionally, it is found that very narrow rings can also have very low density: this is characteristic of softwoods from the very northern latitudes where latewood development is restricted by the short summer period. Hence ring width of itself does not affect the strength of the timber: nevertheless, it has a most important indirect effect working through density.

46.6.5 Ratio of latewood to earlywood

Since the latewood comprises cells with thicker walls, it follows that increasing the percentage of latewood will increase the density and therefore the strength of the timber. Differences in strength of 150–300 per cent between the late and earlywood are generally explained in terms of the thicker cell walls of the former: however, some workers maintain that when the strengths are expressed in terms of the cross-sectional area of the cell wall, the latewood cell is still stronger than the earlywood. Various theories have been advanced to account for the higher strength of the latewood wall material; the more acceptable are couched in terms of the differences in micro-fibrillar angle in the middle layer of the secondary wall, differences in degree of crystallinity and lastly, differences in the proportion of the chemical constituents.

46.6.6 Cell length

Since the cells overlap one another, it follows that there must be a minimum cell length below which there is insufficient overlap to permit the transfer of stress without failure in shear occurring. Some investigators have gone further and have argued that there must be a high degree of correlation between the length of the cell and the strength of cell wall material, since a fibre with high strength per unit of cross-sectional area would require a larger area of overlap in order to keep constant the overall efficiency of the system.

46.6.7 Microfibrillar angle

The angle of the microfibrils in the S_2 layer has a most significant effect in determining the strength of wood. Figure 46.5 illustrates the marked reduction in tensile strength that occurs with increasing angle of the microfibrils: the effect on strength closely parallels that which occurs with changing grain angle.

46.6.8 Chemical composition

In Chapter 44 the structure of the cellulose molecule was described and emphasis was placed on

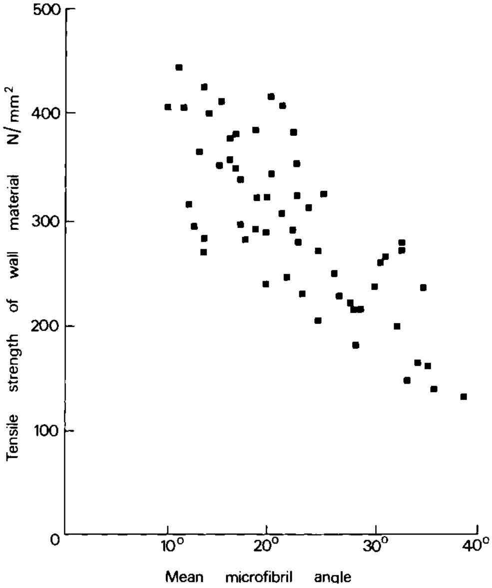

FIGURE 46.5 Effect of microfibrillar angle on the tensile strength of *Pinus radiata* blocks (from Cave (1969) by permission of Springer-Verlag).

the existence in the longitudinal plane of covalent bonds both within the glucose units and also linking them together to form filaments containing from 5000 to 10 000 units. There is little doubt that the high tensile strength of timber owes much to the existence of this covalent bonding. Certainly, experiments in which many of the β 1–4 linkages have been ruptured by gamma irradiation, resulting in a decrease in the number of glucose units in the molecule from over 5000 to about 200, have resulted in a most marked reduction in tensile strength; it has also been shown that timber with inherently low molecular lengths, e.g. compression wood, has a lower than normal tensile strength.

Until the 1970s, it had been assumed that the hemicelluloses which constitute about half of the matrix material played little or no part in determining the strength of timber. However, it has now been demonstrated that some of the hemicelluloses are orientated within the cell wall and it is now thought that these will be load-bearing.

It is known that lignin is less hydrophilic than either the cellulose or hemicelluloses and, as indicated earlier, at least part of its function is to protect the more hydrophilic substances from the ingress of water and consequent reduction in strength. Apart from this indirect effect on strength, lignin is thought to make a not too insignificant direct contribution. Much of the lignin in the cell wall is located in the primary wall and in the middle lamella. Since the tensile strength of a composite with fibres of a definite length will depend on the efficiency of the transfer of stress by shear from one fibre to the next, it will be appreciated that in timber the lignin plays a most important role. Compression strength along the grain has been shown to be affected by the degree of lignification not between the cells, but rather within the cell wall, when all the other variables have been held constant.

It would appear, therefore, that both the fibre and the matrix components of the timber composite are contributing to its strength as, in fact, they do in most composites: the relative significance of the fibre and matrix roles will vary with the mode of stressing.

46.6.9 Reaction wood

Compression wood

The chemical and anatomical properties of this abnormal wood, which is found only in the softwoods, were described in Section 44.4. When stressed, it is found that the tensile strength and toughness is lower and the compressive strength higher than that of normal timber. Such differences can be explained in terms of the changes in fine structure and chemical composition.

Tension wood

This second form of abnormal wood, which is found only in the hardwoods, has tensile strengths higher and compression strengths lower than normal wood: again this can be related to changes in fine structure and chemical composition (see Section 44.4).

46.6.10 Moisture content

The marked increase in strength on drying from the fibre saturation point to oven-dry conditions was described in detail in Section 44.7.5 and illustrated in Figure 44.22; experimentation has indicated the probability that at moisture contents of less than 2 per cent the strength of timber may show a slight decrease rather than the previously accepted continuation of the upward trend.

Confirmatory evidence of the significance of moisture content on strength is forthcoming from Figure 46.4 in which the regression line for over 200 species of compression strength of green timber against density is lower than that for timber at 12 per cent moisture content; strength data for timber are generally presented for these two levels of moisture content (Lavers, 1969).

However, reference to Table 46.4 will indicate that the level of moisture has almost no effect on the tensile strength parallel to the grain. This strength property is determined by the strength of the covalent bonding along the molecule and since, the crystalline core is unaffected by moisture (Chapter 44), retention of tensile strength

TABLE 46.5 Percentage change in strength and stiffness of Scots pine timber per 1 per cent change in moisture content (Lavers, 1983)

Property	*Moisture range (%)*		
	6–10	*12–16*	*20–24*
Modulus of elasticity (MOE: stiffness)	0.21	0.18	0.15
Modulus of rupture (MOR: bending strength)	4.2	3.3	2.4
Compression, perpendicular to the grain	2.7	2.0	1.40
Hardness	0.058	0.053	0.045
Shear, parallel to the grain	0.70	0.53	0.36

parallel to the grain with increasing moisture content is to be expected.

Within certain limits and excluding tensile strength parallel, the regression of strength, expressed on a logarithmic basis, and moisture content can be plotted as a straight line. The relationship can be expressed mathematically as:

$$\log_{10} f = \log_{10} f_s + k(\mu_s - \mu) \qquad (46.9)$$

where f is the strength at moisture content μ, f_s is the strength at the fibre saturation point, μ_s is the moisture content at the fibre saturation point, and k is a constant. It is possible, therefore, to calculate the strength at any moisture content below the fibre saturation point, assuming f_s to be the strength of the green timber and μ_s to be 27 per cent. This formula can also be used to determine the strength changes that occur for a 1 per cent increase in moisture content over certain ranges (see Table 46.5); the table illustrates for small clear test pieces how the change in strength per unit change in moisture content is non-linear.

This relation between moisture content and strength may not always apply when the timber contains defects as is the case with structural size timber. Thus, it has been shown that the effect of moisture content on strength diminishes as the size of knots increase.

The relation between moisture content and strength presented above, even for knot-free timber, does not always hold for the impact resistance of timber. In some timbers, though certainly not all, impact resistance or toughness of green timber is considerably higher than it is in the dry state; the impact resistances of green ash, cricket bat willow and teak are approximately 10 per cent, 30 per cent and 50 per cent higher respectively than the values at 12 per cent moisture content.

In the case of structural timber, several types of model have been proposed to represent moisture-property relationships; these models reflect the finding that increases in strength with drying are greater for high strength structural timber than for low strength material.

46.6.11 Temperature

At temperatures within the range +200°C to −200°C and at constant moisture content, strength properties are linearly (or almost linearly) related to temperature, decreasing with increasing temperature. However, a distinction must be made between short- and long-term effects.

When timber is exposed for short periods of time to temperatures below 95°C the changes in strength with temperature are reversible. These reversible effects can be explained in terms of the increased molecular motions and greater lattice spacing at higher temperatures. For all of the strength properties, with the possible exception of tensile parallel to the grain (Gerhards, 1982), a good rule of thumb is that an increase in temperature of 1°C produces a 1 per cent reduction in their ultimate values.

At temperatures above 95°C, or at temperatures above 65°C for very long periods of time, there is an irreversible effect of temperature due to thermal degradation of the wood substance, generally taking the form of a marked shortening of the length of the cellulose molecules and chemical changes within the hemicelluloses (see Section 47.2.3). All strength properties show a marked reduction with temperature, but toughness is particularly sensitive to thermal degrade. Repeated exposure to elevated temperature has a cumulative effect and usually the reduction is greater in the hardwoods than in the softwoods. Even exposure to cyclic changes in temperature over long periods of time has been shown to result in thermal degradation and loss in strength and especially toughness.

The effect of temperature is very dependent on moisture content, sensitivity of strength to temperature increasing appreciably as moisture content increases (Figure 46.6), as occurs also with stiffness (Figure 45.9); these early results have been confirmed by Gerhards (1982). The relationship between strength, moisture content and temperature appear to be slightly curvilinear over the range 8–20 per cent m.c. and −20° to 60°C. However, in the case of toughness, while at low moisture content it is found that toughness decreases with increasing temperature, at high moisture contents toughness actually increases with increasing temperature.

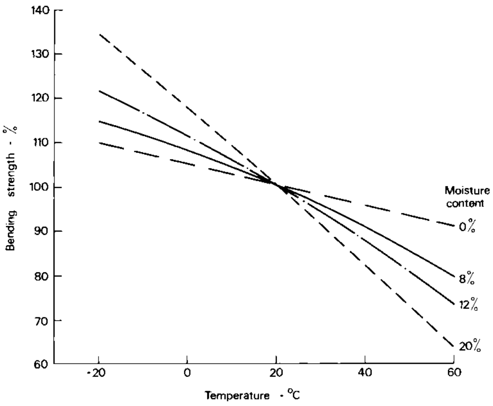

FIGURE 46.6 The effect of temperature on the bending strength of *Pinus radiata* timber at different moisture contents.

46.6.12 Time

In Chapter 45 timber was described as a viscoelastic material and as such its mechanical behaviour will be time dependent. Such dependence will be apparent in terms of its sensitivity to both rate of loading and duration of loading.

Rate of loading

Increase in the rate of load application results in increased strength values, the increase in 'green' timber being some 50 per cent greater than that of timber at 12 per cent moisture content; strain to failure, however, actually decreases. A variety of explanations have been presented to account for this phenomenon, most of which are based on the theory that timber fails when a critical strain has been reached and consequently, at lower rates of loading, viscous flow or creep is able to occur resulting in failure at lower loads.

The various standard testing procedures adopted throughout the world set tight limits on the speed of loading in the various tests: unfortunately, such recommended speeds vary throughout the world, thereby introducing errors in the comparison of results from different laboratories; the introduction of European standards (ENs) and the wider use of International standards (ISOs), should give rise to greater uniformity in the future.

Duration of load (DOL)

In terms of the practical use of timber, the duration of time over which the load is applied is perhaps the single most important variable. Many investigators have worked in this field and each has recorded a direct relationship between the length of time over which a load can be supported at constant temperature and moisture content and the magnitude of the load. This relation appears to hold true for all loading modes, but is especially important for bending strength.

The modulus of rupture (maximum bending strength) will decrease in proportion, or nearly in proportion, to the logarithm of the time over which the load is applied; failure in this particular time-dependent mode is termed *creep rupture* or *static fatigue*. Wood (1951) indicated that the relation was slightly different for ramp and constant loading, was slightly curvilinear and that there was a distinct levelling off at loads approaching 20 per cent of the ultimate short-term strength such that a critical load or stress level occurs, below which failure is unlikely to occur; the hyperbolic curve that fitted Wood's data best for both ramp and sustained loading, and which became known as the *Madison curve*, is illustrated in Figure 46.7.

Other workers have reported a linear relation, though a tendency to non-linear behaviour at very high stress levels has been recorded by some. Pearson (1972), in reviewing previous work in the field of duration of load and bending strength, plotted on a single graph the results obtained over a 30-year period and found that, despite differences in method of loading (ramp or constant), species, specimen size, moisture content, or whether the timber was solid or laminated, the results showed remarkably little scatter from a straight line described by the regression:

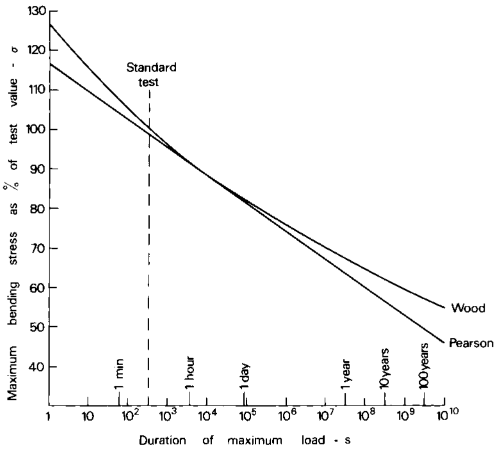

FIGURE 46.7 The effect of duration of load on the bending strength of timber (after Wood (1951) by permission of the Forest Products Laboratory, Madison, and Pearson (1972) by permission of Walter de Gruyter & Co., Berlin, New York).

$$f = 91.5 - 7\log_{10}t \tag{46.10}$$

where f is the stress level (percentage), and t is the effective duration of maximum load in hours. This regression is also plotted in Figure 46.7 for comparison with Wood's curvilinear line. Pearson's findings certainly threw doubt on the existence of a critical stress level below which creep rupture does not occur. These regressions indicate that timber beams which have to withstand a dead load for 50 years can be stressed to only 50 per cent of their ultimate short-term strength.

Although this type of log-linear relationship is still employed for the derivation of duration of load factors for wood-based panel products, this is certainly not the case with solid timber.

By the early 1970s, there was abundant evidence to indicate that the creep rupture response of structural timber beams differed considerably from the classic case for small clear test pieces described above.

Between 1970 and 1985 an extensive amount of research was carried out in America, Canada and Europe; readers desirous of following the historical development of the new concepts in DOL are referred to the comprehensive reviews by Tang (1994) and Barrett (1996). This research confirmed that the DOL effect in structural timber was different to that in small clear test pieces and was also less severe than the Madison curve predicted for loading periods up to one year: it also confirmed that high strength timber possessed a larger DOL effect than low strength timber.

The above test work clearly indicated that the DOL factors then in current use were conservative and in order to obtain a more realistic prediction of time to failure, attention moved to the possible application of reliability-based design principles for the assessment of the reliability of timber members under in-service loading conditions. In particular, this approach led to the adoption of the concept of *damage accumulation*.

It should be appreciated that in the application of this concept there does not exist any method for quantifying the actual damage; the development of damage is simply deduced from the time-to-failure data from long-term loading experiments under a given loading history. These models generally use the stress-level history as the main variable and are thus independent of material strength. In order to calculate time to failure for a given stress history under constant temperature and humidity, the damage rate is integrated from an assumed initial value of 0 to the failure value of 1 (Morlier *et al.*, 1994). Several types of damage accumulation models have been recorded, of which the most important are those listed by Morlier *et al.* (1994) and Tang (1994).

The dependence of these damage models on the stress ratio results in a logistical problem, since both the short-term and the long-term strength has to be known for the same structural test piece, but the test piece can be tested only once. This problem is usually resolved by using two side-matched test pieces and assuming equal strengths! A comparison among four of the above damage accumulation models, together with one model based on strain energy (Fridley, 1992a), is presented in Figure 46.8, from which it will be noted how large is the variability among them.

The level of both moisture content and temperature has a marked effect on time to failure. Thus, increasing levels of relative humidity result in reduced times to failure when stressed at the same stress ratios (Fridley *et al.*, 1991), while varying levels of humidity have an even greater effect in reducing times to failure (Hoffmeyer, 1990; Fridley *et al.*, 1992b).

46.7 Strength, toughness, failure and fracture morphology

There are two fundamentally different approaches to the concept of strength and failure. The first is the classical strength of materials approach, attempting to understand strength and failure of timber in terms of the strength and arrangement of the molecules, the fibrils, and the cells by thinking in terms of a theoretical strength and attempting to identify the reasons why the theory is never satisfied.

The second and more recent approach is much

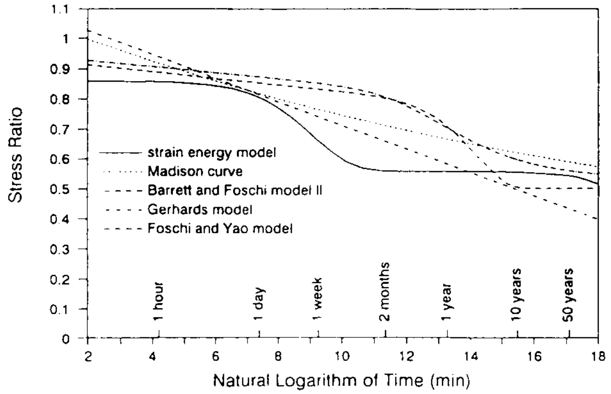

FIGURE 46.8 Comparison of duration of load predictions among four damage accumulation models and one model based on strain energy (Fridley, Tang and Soltis (1992a) with permission of the American Society of Engineers).

more practical in concept since it considers timber in its present state, ignoring its theoretical strength and its microstructure and stating that its performance will be determined solely by the presence of some defect, however small, which will initiate on stressing a small crack; the ultimate strength of the material will depend on the propagation of this crack. Many of the theories have required considerable modification for their application to the different fracture modes in an anisotropic material such as timber.

Both approaches are discussed below for the more important modes of stressing.

46.7.1 Classical approach

Tensile strength parallel to the grain

Over the years a number of models have been employed in an attempt to quantify the theoretical tensile strength of timber. In these models it is assumed that the lignin and hemicelluloses make no contribution to the strength of the timber; in the light of recent investigations, however, this may be no longer valid for some of the hemicelluloses. One of the earliest attempts modelled timber as comprising a series of endless chain molecules, and strengths of the order of 8000 N/mm^2 were obtained. More recent modelling has taken into account the finite length of the cellulose molecules and the presence of amorphous regions. Calculations have shown that the stress to cause chain slippage is generally considerably greater than that to cause chain scission irrespective of whether the latter is calculated on the basis of potential energy function or bond energies between the links in the chain; preferential breakage of the cellulose chain is thought to occur at the C—O—C linkage. These important findings have led to the derivation of minimum tensile stresses of the order of 1000–7000 N/mm^2 (Mark, 1967).

The ultimate tensile strength of timber is of the order of 100 N/mm^2, though this varies considerably between species. This figure corresponds to a value between 0.1 and 0.015 of the theoretical strength of the cellulose fraction. Since this accounts for only half the mass of the timber (Table 44.2) and since it is assumed, perhaps incorrectly, that the matrix does not contribute to the strength, it can be said that the actual strength of timber lies between 0.2 and 0.03 of its theoretical strength.

In attempting to integrate these views of molecular strength with the overall concept of failure, it is necessary to examine strength at the next order of magnitude, namely the individual cells. It is possible to separate these by dissolution of the lignin–pectin complex cementing them together (Section 44.2 and Figures 44.7 and 44.8). Using specially developed techniques of mounting and stressing, it is possible to determine their tensile strengths: much of this work has been done on softwood tracheids, and mean strengths of the order of 500 N/mm^2 have been recorded by a number of investigators. The strengths of the latewood cells can be up to three times that of the corresponding earlywood cells.

Individual tracheid strength is therefore approximately five times greater than that for solid timber. Softwood timber also contains parenchyma cells which are found principally in the rays, and lining the resin canals, and which are inherently weak; many of the tracheids tend to be imperfectly aligned and there are numerous discontinuities along the cell; consequently it is to be expected that the strength of timber is lower than that of the individual tracheids. Nevertheless, the difference is certainly substantial and it seems doubtful if the features listed above can account for the total loss in strength, especially when it is realised that the cells rupture on stressing and do not slip past one another.

When timber is stressed in tension along the grain, failure occurs catastrophically with little or no plastic deformation (Figure 45.3) at strains of about 1 per cent. Visual examination of the sample usually reveals an interlocking type of fracture which can be confirmed by optical microscopy. However, as illustrated in Figure 46.9, the degree of interlocking is considerably greater in the latewood than in the earlywood. Whereas in the former, the fracture plane is essentially vertical, in the latter the fracture plane

FIGURE 46.9 Tensile failure in spruce (*Picea abies*) showing mainly transverse cross-wall failure of the earlywood (left) and longitudinal intra-wall shear failure of the latewood cells (right) (×110, polarised light) (© Building Research Establishment).

follows a series of shallow zig-zags in a general transverse plane; it is now thought that these thin-walled cells contribute very little to the tensile strength of the timber. Thus, failure in the stronger latewood region is by shear, while in the earlywood, though there is some evidence of shear failure, most of the rupture appears to be transwall or brittle.

Examination of the fracture surfaces of the latewood cells by electron microscopy reveals that the plane of fracture occurs either within the S_1 layer or, as is more common, between the S_1 and S_2 layers. Since shear strengths are lower than tensile strengths these observations are in accord with comments made previously on the relative superiority of the tensile strengths of individual fibres compared with the tensile strength of timber. By failing in shear this implies that the shear strength of the wall layers is lower than the shear strength of the lignin–pectin material cementing together the individual cells.

Confirmation of these views is forthcoming from the work of Mark (1967) who has calculated the theoretical strengths of the various cell wall layers and has shown that the direction and level of shear stress in the various wall layers was such as to initiate failure between the S_1 and S_2 layers. Mark's treatise received a certain amount of criticism on the grounds that he treated one cell in isolation, opening it up longitudinally in his model to treat it as a two-dimensional structure; nevertheless, the work marked the beginning of a new phase of investigation into elasticity and fracture and the approach has been modified and subsequently developed. The extension of the work has explained the initiation of failure at the S_1–S_2 boundary, or within the S_1 layer, in terms of either buckling instability of the microfibrils, or the formation of ruptures in the matrix or framework giving rise to a redistribution of stress.

Thus, both the microscopic observations and the developed theories appear to agree that failure of timber under longitudinal tensile stressing is basically by shear unless density is low when transwall failure occurs. However, under certain conditions the pattern of tensile failure may be abnormal. First, at temperatures in excess of 100°C, the lignin component is softened and its shear strength is reduced. Consequently, on stressing, failure will occur within the cementing material rather than within the cell wall.

Second, transwall failure has been recorded in weathering studies where the mode of failure changed from shear to brittle as degradation progressed; this was interpreted as being caused by a breakdown of the lignin and degradation of the cellulose, both of which processes would be reflected in a marked reduction in density (Turkulin and Sell, 1997).

Finally, in timber that has been highly stressed in compression before being pulled in tension, it will be found that tensile rupture will occur along the line of compression damage which, as will be explained below, runs transversely. Consequently, failure in tension is horizontal, giving rise to a brittle type of fracture (see Figure 47.1).

In the literature a wide range of tensile failure criteria is recorded, the most commonly applied being some critical strain parameter, an approach which is supported by a considerable volume of evidence, though its lack of universal application has been pointed out by several workers.

Compression strength parallel to the grain

Few attempts have been made to derive a mathematical model for the compressive strengths of timber. One of the few, and one of the most successful is that by Easterling *et al.* (1982); in modelling the axial and transverse compressive strength of balsa, the authors found that their theory which related the axial strength linearly to the ratio of the density of the wood to the density of the dry cell wall material, and the transverse strength to the square of this ratio, was well supported by experimental evidence. It also appears that their simple theory for balsa may be applicable to timber of higher density.

Compression failure is a slow yielding process in which there is a progressive development of structural change. The initial stage of this sequence appears to occur at a stress of about 25 per cent of the ultimate failing stress (Dinwoodie, 1968), though Keith (1971) considers that these early stages do not develop until about 60 per cent of the ultimate. There is certainly a very marked increase in the amount of structural change above 60 per cent which is reflected by the marked departure from linearity of the stress–strain diagram illustrated in Figure 45.3. The former author maintains that linearity here is an artefact resulting from insensitive testing equipment and that some plastic flow has occurred at levels well below 60 per cent of the ultimate stress.

Compression deformation assumes the form of a small *kink* in the microfibrillar structure, and because of the presence of crystalline regions in the cell wall, it is possible to observe this feature using polarisation microscopy (Figure 46.10). The sequence of irreversible anatomical changes leading to failure originates in the tracheid or fibre wall at that point where the longitudinal cell is displaced vertically to accommodate the horizontally running ray. As stress and strain increase these kinks become more prominent and increase numerically, generally in a preferred lateral direction, horizontally on the longitudinal–radial plane (Figure 46.11) and at an angle to the vertical axis of from 45° to 60° on the longitudinal–tangential plane. These lines of deformation, generally called a *crease* and comprising numerous kinks, continue to develop in width and length; at failure, defined in terms of maximum stress, these creases can be observed by eye on the face of the block of timber (Dinwoodie, 1968). At this stage there is considerable buckling of the cell wall and delamination within it, usually between the S_1 and S_2 layers. Models have been produced

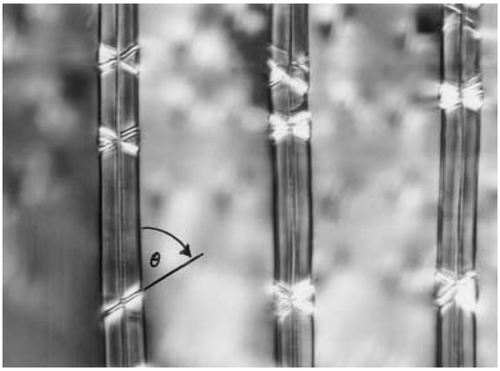

FIGURE 46.10 Formation of kinks, in the cell walls of spruce timber (*Picea abies*) during longitudinal compression stressing. The angle θ lying between the plane of shear and the middle lamella varies systematically between timbers and is influenced by temperature (×1600, polarised light) (© Building Research Establishment).

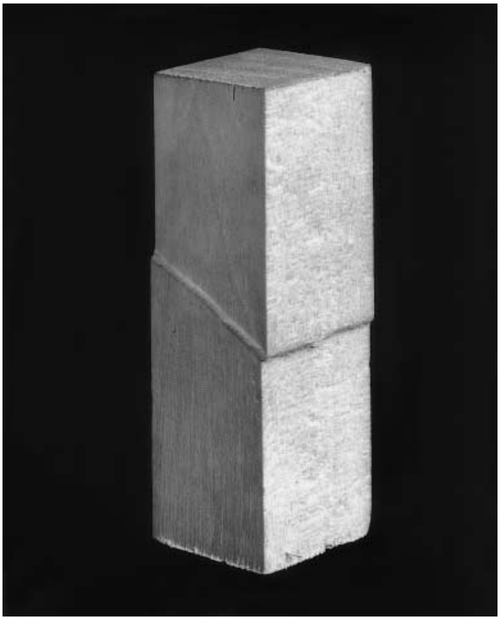

FIGURE 46.11 Failure under longitudinal compression at the macroscopic level. On the longitudinal radial plane the crease (shear line) runs horizontally, while on the longitudinal tangential plane the crease is inclined at 65° to the vertical axis (© Building Research Establishment).

to simulate buckling behaviour and calculated crease angles for instability agree well with observed angles (Grossman and Wold, 1971).

At a lower order of magnification, Dinwoodie (1974) has shown that the angle at which the kink traverses the cell wall (Figure 46.10) varies systematically between earlywood and latewood, between different species, and with temperature. Almost 72 per cent of the variation in the kink angle could be accounted for by a combination of the angle of the microfibrils in the S_2 layer and the ratio of cell wall stiffness in longitudinal and horizontal planes.

Attempts have been made to relate the size and number of kinks to the amount of elastic strain or the degree of viscous deformation; under conditions of prolonged loading, total strain and the ratio of creep strain to elastic strain (relative creep), appear to provide the most sensitive guide to the formation of cell wall deformation; the gross creases appear to be associated with strains of 0.33 per cent (Keith, 1972).

The number and distribution of kinks are dependent on temperature and moisture content: increasing moisture content, though resulting in a lower strain to failure, results in the production of more kinks, although each is smaller in size than its ‘dry’ counterpart; these are to be found in a more even distribution than they are in dry timber. Increasing temperature results in a similar wider distribution of the kinks.

Static bending

In the bending mode timber is subjected to compression stresses on the upper part of the beam and tensile on the lower part. Since the strength of clear timber in compression is only about one-third that in tension, failure will occur on the compression side of the beam long before it will do so on the tension side. In knotty timber, however, the compressive strength is often equal to and can actually exceed the tensile strength. As recorded in the previous section, failure in compression is progressive and starts at low levels of stressing: consequently, the first stages of failure in bending in clear straight-grained timber will frequently be associated with compression failure and, as both the bending stress and consequently the degree of compression failure increase, so the neutral axis will move progressively downwards from its original central position in the beam (assuming uniform cross-section) thereby allowing the increased compression load to be carried over a greater cross-section. Fracture occurs when the stress on the tensile surface reaches the ultimate strength in bending.

Toughness

Timber is a tough material, and in possessing moderate to high stiffness and strength in addition to its toughness, it is favoured with a unique combination of mechanical properties emulated only by bone, which, like timber, is a natural composite.

Toughness is generally defined as the resistance of a material to the propagation of cracks. In the comparison of materials it is usual to express toughness in terms of *work of fracture*, which is a measure of the energy necessary to propagate a crack, thereby producing new surfaces.

In timber the work of fracture, a measurement of the energy involved in the production of cracks at right angles to the grain, is about $10^4\,\mathrm{J/m^2}$; this value is an order of magnitude less than that for ductile metals, but is comparable with that for the man-made composites. Now the energy required to break all the chemical bonds in a plane cross-section is of the order of $1\text{–}2\,\mathrm{J/m^2}$; that is, four orders of magnitude lower than the experimental values. Since pull-out of the microfibrils does not appear to happen to any great extent, it is not possible to account for the high work of fracture in this way (Gordon and Jeronimidis, 1974; Jeronimidis, 1980).

One of the earlier theories to account for the high toughness in timber was based on the work of Cook and Gordon (1964) who demonstrated that toughness in fibre-reinforced materials is associated with the arrest of cracks made possible by the presence of numerous weak interfaces. As these interfaces open, so secondary cracks are initiated at right angles to the primary, thereby dissipating the energy of the original crack. This theory is applicable to timber as Figure 46.12 illustrates, but it is doubtful whether the total discrepancy in energy between experiment and theory can be explained in this way.

FIGURE 46.12 Crack-stopping in a fractured rotor blade. The orientation of the secondary cracks corresponds to the microfibrillar orientation of the middle layer of the secondary cell wall (×990, polarised light) (© Building Research Establishment).

Subsequent investigations have contributed to a better understanding of toughness in timber (Gordon and Jeronimidis, 1974; Jeronimidis, 1980). Prior to fracture it would appear that the cells separate in the fracture area; on further stressing these individual and unrestrained cells buckle inwards generally assuming a triangular shape. In this form they are capable of extending up to 20 per cent before final rupture thereby absorbing a large quantity of energy. Inward buckling of helically wound cells under tensile stresses is possible only because the microfibrils of the S_2 layer are wound in a single direction. Observations and calculations on timber have been supported by glass-fibre models and it is considered that the high work of fracture can be accounted for by this unusual mode of failure. It appears that increased toughness is possibly achieved at the expense of some stiffness, since increased stiffness would have resulted from contrawinding of the microfibrils in the S_2.

So far, we have discussed toughness in terms of only clear timber. Should knots or defects be present, timber will no longer be tough and the comments made earlier as to viewpoint are particularly relevant here. The material scientist sees timber as a tough material: the structural engineer will view it as a brittle material because of its inherent defects and this theme is developed in Section 46.7.2.

Loss in toughness, however, can arise not only on account of the presence of defects and knots, but also through the effects of acid, prolonged elevated temperatures, fungal attack, or the presence of compression damage with its associated development of cell wall deformations; these result from overstressing within the living tree, or in the handling or utilisation of timber after conversion (Section 47.2.4 and Figure 47.1) (Dinwoodie, 1971; Wilkins and Ghali, 1987). Under these abnormal conditions the timber is said to be *brash* and failure occurs in a *brittle* mode.

Fatigue

Fatigue is usually defined as the progressive damage and failure that occurs when a material is subjected to repeated loads of a magnitude smaller than the static load to failure; it is perhaps the repetition of the loads that is the significant and distinguishing feature of fatigue.

In fatigue testing the load is applied generally in the form of a sinusoidal or a square wave; minimum and maximum stress levels are usually held constant throughout the test, though other wave forms, and block or variable stress levels may be applied. In any fatigue test the three most important criteria in determining the character of the wave form are:

1. the stress range, $\Delta\sigma$, where $\Delta\sigma = \sigma_{max} - \sigma_{min}$;
2. the R-ratio, where $R = \sigma_{min}/\sigma_{max}$, which is the position of minimum stress (σ_{min}) and maximum stress (σ_{max}) relative to zero stress. This will determine whether or not reversed loading will occur; this is quantified in terms of the R-ratio, e.g. a wave form lying symmetrically about zero load will result in reversed loading and have a R-ratio $= -1$;
3. the frequency of loading.

The usual method of presenting fatigue data is by way of the *S–N* curve where logN (the number of cycles to failure) is plotted against the mean stress *S*; a linear regression is usually fitted.

Using test pieces of Sitka spruce, laminated Khaya and compressed beech, Tsai and Ansell (1990) carried out fatigue tests under load control in four-point bending. The tests were conducted in repeated and reversed loading over a range of five R-ratios at three moisture contents (Figure 46.13). Fatigue life was found to be largely species independent when normalised by static strength, but was reduced with increasing moisture content and under reversed loading. The accumulation of fatigue damage was followed microscopically in test pieces fatigued at $R = 0.1$ and was found to be associated with the formation of kinks in the cell walls and compression creases in the wood.

In related work, Bonfield and Ansell (1991) investigated the axial fatigue in constant amplitude tests in tension, compression and shear in both Khaya and Douglas fir using a wide range of R-ratios and confirmed that reversed loading is the most severe loading regime. Fatigue lives

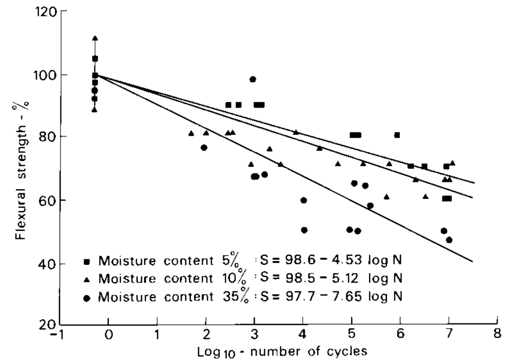

FIGURE 46.13 The effect of moisture content on sliced Khaya laminates fatigued at $R = 0$. The maximum peak stresses are expressed as a percentage of static flexural (bending) strength (from Tsai and Ansell (1990) by permission of Kluwer Academic Publishers).

measured in all-tensile tests (R = 0.1) were considerably longer than those in all-compression tests (R = 10), a result which they related to the lower static strength in compression relative to tension. *S–N* data at different R-ratios yielded a set of constant lifelines when alternating stress was plotted against mean stress; these lifelines possessed a point of inflection when loading became all compressive.

More information on fatigue in wood is to be found in Dinwoodie (2000).

46.7.2 Engineering approach to strength and fracture

The second approach to the concept of strength and failure is a more practical one and is based on the premise that all materials contain flaws or minute cracks, and that performance is determined solely by the propagation of cracks arising from these defects. The largest flaw will become self-propagating when the rate of release of strain energy exceeds the rate of increase of surface energy of the propagating crack.

The development of this concept has become known as *fracture mechanics*: its application to timber did not take place until as late as 1961. Part of the reason for this is due to the modelling of wood as an orthotropic material, and consequently there are six values of 'fracture toughness' (a material parameter, also known as the *critical stress intensity factor*, K_c) for each of the three principal modes of crack propagation. In timber, however, macroscopic crack extension almost always occurs parallel to the grain even though it is initiated in a different plane, thereby giving rise to a mixed mode type of failure.

The value of K_c (fracture toughness) is dependent not only on orientation as inferred above, but also on the opening mode, orientation, wood density, moisture content, specimen thickness and crack speed (see, e.g. Dinwoodie, 2000). Thus, the value of K_{Ic} (K_c in mode I) in the four weak parallel-to-the-grain systems is about one-tenth that in the two tough across-the-grain systems; K_{Ic} increases with increasing density and with increasing specimen thickness.

Fracture mechanics has been applied to various aspects of wood behaviour and failure, e.g. the effect of knots, splits and joints; good agreement has been found between predicted values using fracture mechanics and actual strength values. Examples are to be found in Dinwoodie (2000).

46.8 Design stresses for timber

Timber, like many other materials, is graded according to its anticipated performance in service; because of its inherent variability, distinct grades of material must be recognised.

46.8.1 Grade stresses in UK prior to 1973

These were derived from the testing of small clear test pieces (Section 46.2.1) as set out in Table 46.6 and described fully in Dinwoodie (1981), as well as in Desch and Dinwoodie (1996).

46.8.2 Grade stresses in UK from 1973 to 1995

The realisation in the 1970s that the duration of load values derived from the testing of small clear test pieces were not appropriate for structural timber led to the derivation of grade stresses directly from actual structural-size timber.

This approach necessitated the introduction of grading of the timber by either visual or mechanical means about which more is said below. In order to define these grade classes in terms of actual strength, tests on structural timber had to be performed which led to the derivation of actual grade stresses either in the form of strength classes, or as grade stresses for individual species and grades (see Table 46.6 and Desch and Dinwoodie, 1996). The advantage of the strength class system over the listing of stresses for individual species and grades is that it allows suppliers to meet a structural timber specification by supplying any combination of species and grade listed in BS 5268: Part 2 as satisfying the specified class.

Structural design using these stresses is by way of *permissible stress design* according to BS 5268: Part 2.

TABLE 46.6 Changes in the derivation of design stresses over the period before 1973 to about 2005

UK							*EUROPE*		
→1973	*1973–1995*			*1995–about 2005*			*1996→*		
Data from testing small									
clear test pieces		Structural timber			Structural timber			Structural timber	
↓		↓			↓			↓	
Mean value less 2.33s	Grading		Tests°	Grading		Tests°	Grading		Tests°
↓	↓	↓	BS 5820	↓	↓	EN 408	↓	↓	EN 408
Divided by safety	Visual	Machine	↓	Visual	Machine	EN 384	Visual	Machine	EN 384
factor* to give	BS 4978	BS 4978	↓	BS 4978	EN 519	↓	EN 518	EN 519	↓
Basic stress	(1988)	(1988)	↓	(1996)	↓	↓	↓	↓	↓
	BS 5756		↓	BS 5756		↓			↓
	(1980)		↓	(1997)		↓			↓
↓	↓	↓	↓	↓	↓	↓	↓	↓	↓
Multiplied by	*Grade* or *Strength classes*		↓	↓ →	*Strength classes and*			*Strength classes*	
strength ratio	BS 4978 (1988)		↓	↓	*Characteristic values*			*and*	
↓		↓	↓	↓	EN338			*Characteristic values*	
Derived *Grade stresses*	Stresses in standard			↓	↓			EN 338, EN 1912	
in *BS 5268 Part 2*	*BS 5268 Part 2*			↓	factored			↓	
		↓			↓				
				→	*Grade stresses*				
↓		↓			↓			↓	
Design code		*Design code*			*Design code*			*Design code*	
BS 5268 Part 2		BS 5268 Part 2			BS 5268 Part 2			ENV 1995–1–1	

s = standard deviation.

* = safety factor (1.4 for compression ∥ to the grain; 2.25 for all other modes) to cover effects of specimen size and shape, rate of loading and duration of load.

° = testing used only to derive values for inclusion in the standards.

46.8.3 Characteristic values for structural timber in Europe (including UK) from 1996

The formation of the EC as a free trade area and the production of the *Construction Products Directive* (CPD) led automatically to the introduction and implementation of new European standards and the withdrawal of conflicting National standards. Such an approach has much merit, but as far as the UK is concerned, it has led to changes in both the derivation and use of working stresses. First, test results are now expressed in terms of a *characteristic value* expressed in terms of the lower 5th percentile, in contrast to the former use in the UK of a mean value and its standard deviation. Second, in the design of timber structures the new Eurocode 5 (see below) is written in terms of *limit state design* in contrast to the former UK use of permissible stress design. Third, the number of strength classes in the new European system is greater than in the UK system thereby giving rise to mismatching of certain timbers.

However, apart from these three major changes, the grading of timber into strength classes, and the original characterisation of these by testing, adopts a similar procedure to that used in the UK after 1973 (see Table 46.6)

Characteristic values for structural timber in a range of strength classes is to be found in EN 338.

As noted above, the design of timber structures must be in accordance with Eurocode 5. The characteristic values for both timber and wood-based panel products must be reduced according to the period of loading and service class (defined in terms of level of relative humidity). Values of K_{mod} (duration of load and service class) and K_{def} (creep and service class) are set out in Eurocode 5 for each of the three service classes.

46.8.4 The UK position from 1995 to about 2005

This is the transition period for all European countries in which a choice is available between their existing National grading and design standards and the new European system. In theory both systems exist side by side, but in practice many countries, including the UK, have wisely taken advantage of this period to modify their existing standards in order to bring them nearer to the European system and reduce the magnitude of the change at the termination of this period.

The UK has already adopted machine grading of softwoods to EN 519 and has redrafted BS 4978 (1996) so that it now relates only to the visual grading of softwoods. Machine graded timber is assigned to strength classes contained in EN 338. From this standard, the characteristic value for a particular strength class and material property are read off and in turn converted (factored) to a grade stress for use in the continuing permissible stress design system set out in BS 5268: Part 2 (Anon, 1996). Visual graded timber is still assigned to grade stresses directly (see Table 46.6).

46.8.5 Visual grading

Visual grading, as the title implies, is a visual assessment of the quality of a piece of structural timber: this is carried out against the permissible defects limits given in standards BS 4978 (1996) and BS 5756 (1997) which conform to EN 518. However, visual grading is a laborious process since all four faces of the timber should be examined. Furthermore, it does not separate naturally weak from naturally strong timber and hence it has to be assumed that pieces of the same size and species containing identical defects have the same strength: such an assumption is invalid and leads to a most conservative estimate of strength.

46.8.6 Machine grading

Many of the disadvantages of visual grading can be removed by machine grading, a process which was introduced commercially in the early 1970s. The principle underlying the process is the high correlation that has been found to exist between the moduli of elasticity and rupture; this was described in Section 46.5.1. Grading machines based on this relationship usually provide higher yields of the higher grades than are achieved by visual grading. Since the above relationship varies among the different species, it is necessary to set the grading machine for each species or species group.

The equation of the regression line is only one of a number of inputs to the mathematical model used to determine the machine settings for a particular timber. These settings also depend on:

1. bandwidth (separation of the grade boundaries on the x-axis) which, in turn, is related to the grade combination being graded;
2. the overall mean and standard deviation of the modulus of elasticity of the species;
3. the interaction of bandwidth and the MOE parameters; and
4. the cross-sectional size, and whether the timber piece is sawn or planed all round (PAR).

The mathematical model can be designed to select a number of grades or strength classes.

Having established the basic relationship for each species, the grading machine can then be set up to grade the timber automatically. Depending on the type of machines, as each length of timber passes through, it is either placed under a constant load and deflection is measured, or subjected to a constant deflection and load is measured. A small computer quickly assesses the appropriate stiffness-indicating parameter every 100 to 150 mm along the length of the timber. The lowest reading of load, or the highest reading of deflection, is compared with the pre-set values stored in the computer and this determines the overall grade of the piece of timber. Grade stamps are then printed on one face of the timber towards one end of the piece.

Under the new European system this grade mark will include the specification number used in the grading (EN519):

- the species or species group;
- the timber condition (green or dry);
- the strength class;
- the grader or company name;
- the company registration number;
- the certification body (logo).

46.9 References

46.9.1 Standards and specifications

ASTM Standard D143–52 (1972) Standard methods of testing small clear specimens of timber. American Society for Testing Materials.

BS 373 (1986) Methods of testing small clear specimens of timber. BSI, London

BS 4978 (1988) Softwood grades for structural use, BSI, London.

BS 4978 (1996) Visual grading of softwood. BSI, London.

BS 5268 (1996) Structural use of timber. Part 2: Code of practice for permissible stress design, materials and workmanship. BSI, London.

BS 5756 (1996) Visual strength grading of hardwoods. BSI, London.

BS 5820 (1979) Methods of test for determination of certain physical and mechanical properties of timber in structural sizes. BSI, London.

EN 338 (1995) Structural timber – Strength classes.

EN 384 (1995) Structural timber – Determination of characteristic values on mechanical properties and density.

EN 408 (1995) Timber structures – Structural timber and glued laminated timber – Determination of some physical and mechanical properties.

EN 518 (1995) Structural timber – Grading – Requirements for visual strength grading standards.

EN 519 (1995) Structural timber – Grading – Requirements for machine strength graded timber and grading machines.

EN 1912 (1998) Structural timber – Strength classes – Assignment of visual grades and species.

ENV 1995–1–1 (1994) Eurocode 5: Design of timber structures. Part 1.1. General rules and rules for buildings.

46.9.2 Literature

Anon (1996) Specifying structural timber, Digest 416. *Building Research Establishment, Watford*, 8 pp.

Barrett J.D. (1996) Duration of load – the past, present and future. In *Proc. of International Conference on Wood Mechanics*, Stuttgart, Germany (ed. S. Aicher), and published by the management committee of EC COST 508 Action, 121–37.

Bonfield, P.W. and Ansell, M.P. (1991) Fatigue properties of wood in tension, compression and shear. *J. Mat. Sci.* 26, 4765–73.

Cave, I.D. (1969) The longitudinal Young's modulus of *Pinus radiata*. *Wood Sci. Technol.* 3, 40–8.

Cook, J. and Gordon, J.E. (1964) A mechanism for the control of crack propagation in all brittle systems. *Proc. Roy. Soc. London*, A 282, 508.

Desch, H.E. and Dinwoodie, J.M. (1996) *Timber – Structure, Properties, Conversion and Use*, 7th edn, Macmillan, Basingstoke, 306 pp.

Dinwoodie, J.M. (1968) Failure in timber, Part I: Microscopic changes in cell wall structure associated with compression failure. *J. Inst. Wood Sci.* 21, 37–53.

Dinwoodie, J.M. (1971) Brashness in timber and its significance. *J. Inst. Wood Sci.* 28, 3–11.

Dinwoodie, J.M. (1974) Failure in timber, Part II: The angle of shear through the cell wall during longitudinal compression stressing. *Wood Sci. Technol.* 8, 56–67.

Dinwoodie, J.M. (1981) *Timber: its Nature and Behaviour*, van Nostrand Reinhold, Wokingham, 190 pp.

Dinwoodie, J.M. (2000) *Timber: its Nature and Behaviour*, E & FN Spon, London, 256 pp.

Easterling, K.E., Harrysson, R., Gibson, L.J. and Ashby, M.F. (1982) The structure and mechanics of balsa wood. *Proc. Roy. Soc, London* 383, 31–41.

Fridley, K.J, Tang, R.C. and Soltis, L.A. (1991) Moisture effects on the load-duration behaviour of lumber. Part I: Effect of constant relative humidity. *Wood and Fiber Sci.* 23, 1, 114–27.

Fridley, K.C., Tang, R.C. and Soltis, L.A. (1992a) Load-duration effects in structural lumber: strain energy approach. *J. Struct. Eng., Structural Div. ASCE.* 118, 9, 2351–69.

Fridley, K.J, Tang, R.C. and Soltis, L.A. (1992b) Moisture effects on the load-duration behaviour of lumber. Part II: Effect of cyclic relative humidity. *Wood and Fiber Sci.* 24, 1, 89–98.

Gerhards, C.C. (1982) Effect of moisture content and temperature on the mechanical properties of wood: an analysis of immediate effects. *Wood and Fiber* 14, 1, 4–26.

Gordon, J.E. and Jeronimidis, G. (1974) Work of fracture of natural cellulose. *Nature* (London) 252, 116.

Grossman, P.U.A. and Wold, M.B. (1971) Compression fracture of wood parallel to the grain. *Wood Sci. Technol.* 5, 147–56.

Hoffmeyer, P. (1990) *Failure of Wood as Influenced by Moisture and Duration of Load.* State University of New York, Syracuse, New York, USA.

Jeronimidis, G. (1980) The fracture behaviour of wood and the relations between toughness and morphology. *Proc. Roy. Soc., London* B208, 447–60.

Keith, C.T. (1971) The anatomy of compression failure in relation to creep-inducing stress. *Wood Sci.* 4, 2, 71–82.

Keith, C.T. (1972) The mechanical behaviour of wood in longitudinal compression. *Wood Sci.* 4, 4, 234–44.

Lavers, G.M. (1969) The strength properties of timber. *Bulletin 50, For. Prod. Res. Lab.* (2nd edn) HMSO (3rd edn revised by G. Moore, 1983).

Mark, R.E. (1967) *Cell Wall Mechanics of Tracheids*, Yale University Press, New Haven.

Morlier, P., Valentin, G. and Toratti, T. (1994) Review of the theories on long-term strength and time to failure. *Proc. Workshop on Service Life Assessment of Wooden Structures*, Espoo, Finland (ed. S.S. Gowda), the management committee of EC COST 508 Action, 3–27.

Pearson, R.G. (1972) The effect of duration of load on the bending strength of wood. *Holzforschung* 26, 4, 153–8.

Tang, R.C. (1994) Overview of duration-of-load research on lumber and wood composite panels in North America. *Proc. Workshop on Service Life Assessment of Wooden Structures*, Espoo, Finland (ed. S.S. Gowda), published by the management committee of EC COST 508 Action, 171–205.

Tsai, K.T. and Ansell, M.P. (1990) The fatigue properties of wood in flexure. *J. Mat. Sci.* 25, 865–78.

Turkulin, J. and Sell, J. (1997) Structural and fractographic study on weathered wood. *Forschungs-und Arbeitsbericht 115/36* Abteilung Holz, EMPA, Switzerland, 4 pp.

Wilkins, A.P. and Ghali, M. (1987) Relationship between toughness, cell wall deformations and density in *Eucaluptus pilularis*. *Wood Sci. Technol.* 21, 219–26.

Wood, L.W. (1951) Relation of strength of wood to duration of load. *For. Prod. Laboratory (Madison) Report No. 1916.*

Chapter forty-seven

Durability of timber

47.1 Introduction

Durability is a term which has different concepts for many people: it is defined here in the broadest possible sense to embrace the resistance of timber to attack from a whole series of agencies whether physical, chemical or biological in origin.

By far the most important are the biological agencies, the fungi and the insects, both of which can cause tremendous havoc given the right conditions. In the absence of fire, fungal or insect attack, timber is really remarkably resistant and timber structures will survive, indeed have survived, incredibly long periods of time, especially when it is appreciated that it is a natural organic material. Examples of well-preserved timber items now over 2000 years old are to be seen in the Egyptian tombs. Both fungal and insect attack are described in Section 47.3 together with the important aspect of the natural durability of the timber.

Another important aspect of durability of timber is its reaction to fire and this is discussed in Section 47.4.

The effect of photochemical, chemical, thermal and mechanical actions are usually of secondary importance in determining durability; these will be briefly considered first in Section 47.2.

47.2 Chemical, physical and mechanical agencies affecting durability and causing degradation

47.2.1 Photochemical degradation

On exposure to sunlight the colouration of the heartwood of most timbers will lighten (e.g. mahogany, afrormosia, oak), though a few timbers will actually darken (e.g. Rhodesian teak). Indoors, the action of sunlight will be slow and the process will take several years: however, outdoors the change in colour is very rapid, taking place in a matter of months and is generally regarded as an initial and very transient stage in the whole process of *weathering*.

In weathering the action not only of light energy (photochemical degradation), but also of rain and wind results in a complex degrading mechanism which renders the timber silvery-grey in appearance: more important is the loss of surface integrity, a process which has been quantified in terms of the residual tensile strength of thin strips of wood (Derbyshire and Miller, 1981; Derbyshire *et al.*, 1995). The loss in integrity embraces the degradation of both the lignin, primarily by the action of ultraviolet light, and the cellulose by shortening of the chain length, mainly by the action of energy from the visible part of the spectrum. Degradation results in erosion of the cell wall and in particular the pit aperture and torus. Fractography using scanning electron microscopy has revealed that the progression of degradation involves initially the development of brittleness and the reduction in stress transfer capabilities through lignin degradation, followed by reductions in microfibril strength resulting from cellulose degradation (Derbyshire *et al.*, 1995).

However, the same cell walls that are attacked act as an efficient filter for those cells below and the rate of erosion from the combined effects of UV, light and rain is very slow indeed; in the absence of fungi and insects the rate of removal of the surface by weathering is of the order of only 1 mm in every 20 years. Nevertheless, because of the continual threat of biological attack, it is unwise to leave most timbers completely unprotected from the weather; it should be appreciated that during weathering, the integrity of the surface layers is markedly reduced, thereby adversely affecting the performance of an applied surface coating. In order to effect good adhesion the weathered layers must first be removed (see Section 48.4).

47.2.2 Chemical degradation

As a general rule, timber is highly resistant to a large number of chemicals and its continued use for various types of tanks and containers, even in the face of competition from stainless steel, indicates that its resistance, certainly in terms of cost, is most attractive. Timber is far superior to cast iron and ordinary steel in its resistance to mild acids and for very many years timber was used as separators in lead-acid batteries. However, in its resistance to alkalis timber is inferior to iron and steel: dissolution of both the lignin and the hemicelluloses occurs under the action of even mild alkalis.

Iron salts are frequently very acidic and in the presence of moisture result in hydrolytic degradation of the timber; the softening and darkish-blue discolouration of timber in the vicinity of iron nails and bolts is due to this effect.

Timber used in boats is often subjected to the effects of chemical decay associated with the corrosion of metallic fastenings, a condition frequently referred to as *nail sickness*. This is basically an electrochemical effect, the rate of activity being controlled by oxygen availability.

47.2.3 Thermal degradation

Prolonged exposure of timber to elevated temperatures results in a reduction in strength and a very marked loss in toughness (impact resistance). Thus, timber heated at 120°C for one month loses 10 per cent of its strength; at 140°C, the same loss in strength occurs after only one week (Shafizadeh and Chin, 1977). Tests on three softwood timbers subjected to daily cycles of 20°C to 90°C for a period of three years resulted in a reduction in toughness to only 44 per cent of its value of samples exposed for only one day (Moore, 1984). It has been suggested that degrade can occur at temperatures even as low as 65°C when exposed for many years.

Thermal degradation results in a characteristic browning of the timber with associated caramel-like odour, indicative of burnt sugar. Initially this is the result of degrade of the hemicelluloses, but with time the cellulose is also affected, with a reduction in chain length through scission of the β1–4 linkage; commensurate degrade occurs in the lignin, but usually at a slower rate (see Section 47.4).

47.2.4 Mechanical degradation

The most common type of mechanical degradation is that which occurs in timber when stressed under load for long periods of time. The concepts of duration of load (DOL) and creep are explained fully in Sections 46.6.12 and 45.4.2 respectively. Thus, it was illustrated in Figures 46.7 and 46.8 how there is a loss in strength with time under load, such that after being loaded for 50 years the strength of timber is approximately only 50 per cent. Similarly, there is a marked reduction in stiffness that manifests itself as an increase in extension or deformation with time under load, as is illustrated in Figures 45.10 and 45.13. The structural engineer, in designing his timber structure, has to take into account the loss with time of both strength and stiffness by applying two time-modification factors.

A second and less common form of mechanical degradation is the induction of compression failure within the cell walls of timber, which can arise either in the standing tree first, in the form of a *natural compression failure* due to high localised compressive stress, or second, as *brittleheart* due to the occurrence of high growth stresses in the centre of the trunk, or under service conditions where the timber is overstressed in longitudinal compression with the production of kinks in the cell wall as described in Section 46.7.1. Loss in tensile strength due to the induction of compression damage is about 10–15 per cent, but the loss in toughness can be as high as 50 per cent. An example of failure in a scaffold board in bending resulting from the prior induction of compression damage due to malpractice on site is illustrated in Figure 47.1

47.3 Natural durability and attack by fungi and insects

47.3.1 Natural durability

Generally when durability of timber is discussed, reference is being made explicitly to the resistance of the timber to both fungal and insect attack: this resistance is termed *natural durability*.

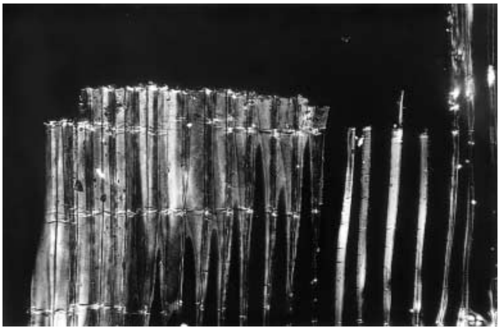

FIGURE 47.1 Kink bands and compression creases in the tension face of a scaffold board which failed in bending on site. Note how the crack pathway has followed the line of the top compression crease which had been induced some time previously (magnification × 150) (© Building Research Establishment).

In the UK, timbers have been classified into five durability groups which are defined in terms of the performance of the heartwood when buried in the ground. Examples of the more common timbers are presented in Table 47.1. Such an arbitrary classification is informative only in relative terms, though these results on 50×50 mm ground stakes can be projected linearly for increased thicknesses. Timber used externally, but not in contact with the ground, will generally have a much longer life, though quantification of this is impossible.

Recalling that timber is an organic product, it is surprising at first to find that it can withstand attack from fungi and insects for very long periods of time, certainly much greater than its herbaceous counterparts. This resistance can be explained in part by the basic constituents of the cell wall, and in part by the deposition of extractives (Sections 44.1 and 44.3.1; Table 44.2).

The presence of lignin which surrounds and protects the crystalline cellulose appears to offer a slight degree of resistance to fungal attack: certainly the resistance of sapwood is higher than that of herbaceous plants. Fungal attack can commence only in the presence of moisture and the threshold value of 20 per cent for timber is about twice as high as the corresponding value for non-lignified plants.

Timber has a low nitrogen content being of the order of 0.03–0.1 per cent by mass and, since this element is a prerequisite for fungal growth, its presence in only such a small quantity contributes to the natural resistance of timber.

The principal factor conferring resistance to biological attack is undoubtedly the presence of extractives in the heartwood. The far higher durability of the heartwood of certain species compared with the sapwood is attributable primarily to the presence in the former of toxic substances, many of which are phenolic in origin. Other factors such as a decreased moisture content, reduced rate of diffusion, density and deposition of gums and resins also play a role in determining the higher durability of the heartwood.

Considerable variation in durability can occur within the heartwood zone: in a number of

TABLE 47.1 Durability classification (resistance of heartwood to fungi in ground contact) for the more common timbers*

Durability class	*Approximate life in contact with ground (years)*	*Hardwoods*	*Softwoods*
Perishable	<5	Alder Ash, European Balsa Beech, European Birch, European Horse chestnut Poplar, black Sycamore Willow	
Nondurable	5–10	Afara Elm, English Oak, American red Obeche Poplar, grey Seraya, white	Hemlock, western Parana pine Pine, Scots (redwood) Pine, yellow Podo Spruce, European (whitewood) Spruce, Sitka
Moderately durable	10–15	Avodire Keruing Mahogany, African Oak, Turkey Sapele Seraya, dark red Walnut, European Walnut, African	Douglas fir Larch Pine, maritime
Durable	15–25	Agba Chestnut, sweet Idigbo Mahogany, American Oak, European Utile	Pine, pitch Western red cedar Yew
Very durable	>25	Afrormosia Afzelia Ekki Greenheart Iroko Jarrah Kapur Makore Opepe Purpleheart Teak	

* Note that the sapwood of all timber is perishable.

timbers the outer band of the heartwood has a higher resistance than the inner region, owing, it is thought, to the progressive degradation of toxic substances by enzymatic or microbial action.

Durability of the heartwood varies considerably among the different species, being related to the type and quantity of the extractives present: the heartwood of timbers devoid of extractives has a very low durability. Sapwood of all timbers is susceptible to attack owing not only to the absence of extractives, but also the presence in the ray cells of stored starch which constitutes a ready source of food for the invading fungus.

The sapwood and heartwood of many species of timber can have its natural durability increased by impregnation with chemicals; the preservative treatment of timber is considered in Chapter 48.

47.3.2 Nature of fungal decay

In timber, some fungi, e.g. the moulds, are present only on the surface and, although they may cause staining, they have no effect on the strength properties. A second group of fungi, the sapstain fungi, live on the sugars present in the ray cells and the presence of their hyphae in the sapwood imparts a distinctive colouration to that region of the timber when it is often referred to as 'blue-stain'. One of the best examples of sapstain is that found in recently felled Scots pine logs. In temperate countries the presence of this type of fungus results in only inappreciable losses in bending strength, though several staining fungi in the tropical countries cause considerable reductions in strength.

By far the most important group of fungi are those that cause decay of the timber by chemical decomposition; this is achieved by the digesting action of enzymes secreted by the fungal hyphae. Two main groups of timber-rotting fungi can be distinguished:

1. *The brown rots*, which consume the cellulose and hemicelluloses, but attack the lignin only slightly. During attack the wood usually darkens and in an advanced stage of attack tends to break up into cubes and crumbles under pressure. One of the best known fungi of this group is *Serpula lacrymans* which causes *dry rot.* Contrary to what its name suggests, the fungus requires an adequate supply of moisture for development.
2. *The white rots,* which attack all the chemical constituents of the cell wall. Although the timber may darken initially, it becomes very much lighter than normal at advanced stages of attack. Unlike attack from the brown rots, timber with white rot does not crumble under pressure, but separates into a fibrous mass.

In very general terms, the brown rots are usually to be found in constructional timbers, whereas the white rots are frequently responsible for the decay of exterior joinery.

Decay, of course, results in a loss of strength, but it is important to note that considerable strength reductions may arise in the very early stages of attack; toughness is particularly sensitive to the presence of fungal attack. Loss in mass of the timber is also characteristic of attack and decayed timber can lose up to 80 per cent of its air-dry mass.

The principal types of fungal attack of wood in the standing tree, of timber in felled logs, or of timber in service are set out in Table 47.2. More information on fungal attack of timber is to be found in Desch and Dinwoodie (1996).

47.3.3 Nature of insect attack

Although all timbers are susceptible to attack by at least one species of insect, in practice only a small proportion of the timber in service actually becomes infested. Some timbers are more susceptible to attack than others and generally the heartwood is much more resistant than the sapwood: nevertheless, the heartwood can be attacked by certain species, particularly when decay is also present.

In certain insects the timber is consumed by the adult form, and the best known example of this mode of attack are the *termites* where the adult, but sexually immature, workers cause most damage. Few timbers are immune to attack by

TABLE 47.2 The principal types of fungal attack

Fungus	*Location of attack*			*Effect on the timber*	
	Tree	*Logs*	*Timber*	*Gross*	*Micro*
Brown rot	✓[1]	✓	✓	Darkening of timber with cuboidal cracking.	Attacks cellulose and hemicellulose.
White rot	✓[1]	✓	✓	Bleaching of timber which turns fibrous.	Attacks cellulose, hemicellulose and lignin.
Soft rot	–	–	✓	Superficial; small cross-cracking; mostly occurring in ground contact.	Attacks cellulose of S_2 layer.
Sapstain (Blue-stain)	–	✓	✓	Stains the sapwood of timber in depth.	Stain due to colour of hyphae.
Moulds	–	✓	✓	Superficial staining due to spores.	Live on cell contents; may increase permeability of timber.
Bacteria	✓	✓	✓	Subtle changes in texture and colour.	Increases permeability; get significant decay in ground contact.

[1] Commonly as pocket rots.

these voracious eaters and it is indeed fortunate that these insects generally cannot survive the cooler weather of this country. They are to be found principally in the tropics, but certain species are present in the Mediterranean region including southern France.

In this country insect attack is mainly by the grub or larval stage of certain beetles. The adult beetle lays its eggs on the surface of the timber, frequently in surface cracks, or in the cut ends of cells; these eggs hatch to produce grubs which tunnel their way into the timber, remaining there for periods of up to three years or longer. The size and shape of the tunnel, the type of detritus left behind in the tunnel (frass) and the exit holes made by the emerging adults are all characteristic of the species of beetle.

The principal types of insect attack of wood in the standing tree, of timber in the form of felled logs, or of timber in service which may be free from decay or partially decayed are set out in Table 47.3. More information on insect attack of timber is to be found in Desch and Dinwoodie (1996).

47.3.4 Marine borers

Timber used in salt water is subjected to attack by marine-boring animals such as the shipworm (*Teredo* sp.) and the gribble (*Limnoria* sp.). Marine borers are particularly active in tropical waters; nevertheless, around the coast of Great Britain *Limnoria* is fairly active and *Teredo*, though spasmodic, has still to be considered a potential hazard. The degree of hazard will vary considerably with local conditions and there are relatively few timbers which are recognised as having heartwood resistant under all conditions: the list of resistant timbers includes ekki, greenheart, okan, opepe and pyinkado.

47.4 Performance of timber in fire

The performance of materials in fire is an aspect of durability which has always attracted much attention, not so much from the research scientist, but rather from the material user who has to conform with the legislation on safety and who is influenced by the weight of public opinion on the

TABLE 47.3 The principal types of insect attack of timber

Type of insect	*Location of attack*				*Comments*
	Tree	*Logs*	*Timber in service*		
			Sound	*Decayed*	
Pin-hole borers (Ambrosia beetle)	✓	✓	–	–	Produce galleries 1–2 mm diameter which are devoid of bore dust and are usually darkly stained; attack is frequently present in tropical hardwoods.
Forest longhorn	✓	(✓)	–	–	Galleries oval in cross-section; no bore dust but galleries may be plugged with coarse fibres; exit holes oval, 6–10 mm diameter.
Wood wasp	(✓)	✓	–	–	Galleries circular in cross-section and packed with bore dust; attacks softwoods; exit holes circular, 4–7 mm diameter.
Bark borer beetle (*Ernobius mollis*)	(✓)	✓	(✓)	–	Requires presence of bark on timber; galleries empty and mainly in bark, but will also penetrate sapwood.; exit holes circular, 1–2 mm diameter.
Powder-post beetle (*Lyctus*)	–	✓	✓	–	Attack confined to sapwood of hardwoods having large-diameter vessels; bore dust fine, talc-like; exit holes circular, 1–2 mm diameter.
Common furniture beetle (*Anobium*)	–	–	✓	–	Attacks mainly the sapwood of both softwoods and European hardwoods; bore dust like lemon-shaped pellets; exit holes circular, 1–2 mm diameter.
House longhorn beetle (*Hylotropes*)	–	–	✓	–	Attacks sapwood of softwoods mainly in the roof space of houses in certain parts of Surrey; bore dust sausage-shaped; exit holes few, oval, often ragged, 6–10 mm diameter.
Death-watch beetle (*Xestobium*)	–	–	(✓)	✓	Attacks both sap and heartwood of partially-decayed hardwoods, principally oak; bore dust bun-shaped; exit holes circular, 3 mm diameter.
Weevils (e.g. *Euophryum*)	–	–	–	✓	Attacks decayed softwoods and hardwoods in damp conditions; exit holes small, ragged about 1 mm diameter.
Wharf borer (*Narcerdes*)	–	–	–	✓	Attacks partially decayed timber to produce large galleries with 6 mm diameter oval exit hole.

✓ – main site of attack (✓) – much reduced incidence of attack.

use of only ‘safe’ materials. While various tests have been devised to assess the performance of materials in fire, there is a fair degree of agreement in the unsatisfactory nature of many of these tests, and an awareness that certain materials can perform better in practice than is indicated by these tests.

Thus, while no-one would doubt that timber is a combustible material showing up rather poorly in both the ‘spread of flame’ and ‘heat release’ tests, nevertheless in at least one aspect of performance, namely the maintenance of strength with increasing temperature and time, wood performs better than steel.

There is a critical surface temperature below which timber will not ignite. As the surface temperature increases above 100°C, volatile gases begin to be emitted as thermal degradation slowly commences; however, it is not until the temperature is in excess of 250°C that there is a sufficient build-up in these gases to cause ignition of the timber in the presence of a pilot flame. Where this is absent, the surface temperature can rise to about 500°C before the gases become self-igniting. Ignition, however, is related not only to the absolute temperature, but also to the time of exposure at that temperature, since ignition is primarily a function of heat flux.

Generally chemical bonds begin to break down at about 175°C and it is recognised that the first constituent of the timber to degrade is the lignin, and this continues slowly up to 500°C. The hemicelluloses degrade much more quickly between 200°C and 260°C as does the cellulose within the temperature range 260°C–350°C. Degradation of the cellulose results in the production of the flammable volatile gases and its marked reduction in degree of polymerisation (chain length) (Le Van and Winandy, 1990).

The performance of timber at temperatures above ignition level is very similar to that of certain reinforced thermosetting resins which have been used as sacrificial protective coatings on space-return capsules. Both timber and these ablative polymers undergo thermal decomposition with subsequent removal of mass, leaving behind enough material to preserve structural integrity.

The onset of pyrolysis in timber is marked by a darkening of the timber and the commencement of emission of volatile gases; the reaction becomes exothermic and the timber reverts to a carbonised char popularly known as charcoal (Figure 47.2). The volatiles, in moving to the surface, cool the char and are subsequently ejected into the boundary layer where they block the incoming convective heat: this most important phenomenon is known as transpirational cooling. High surface temperatures are reached and some heat is rejected by thermal radiation:

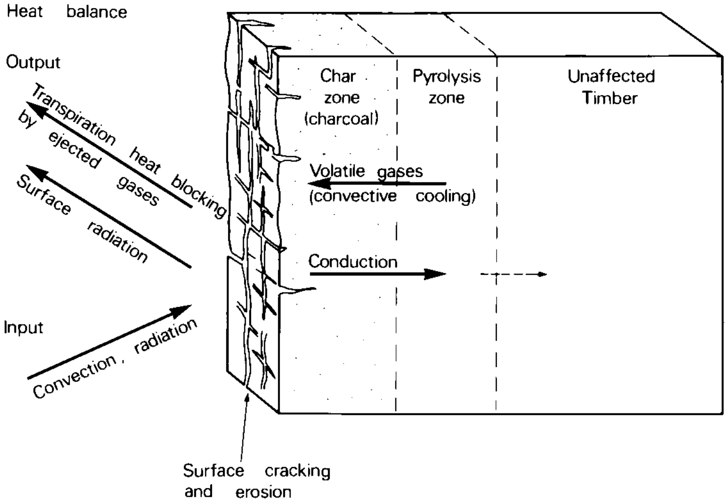

FIGURE 47.2 Diagrammatic representation of the thermal decomposition of timber (© Building Research Establishment).

the heat balance is indicated in Figure 47.2. The surface layers crack badly both along and across the grain and surface material is continually, but slowly, being lost.

A quasi-steady state is reached, therefore, with a balance between the rate of loss of surface and the rate of recession of the undamaged wood. For most softwoods and medium-density hardwoods the rate at which the front recedes is about 0.64 mm/min: for high density hardwoods the value is about 0.5 mm/min (Hall and Jackman, 1975).

The formation of the char, therefore, protects the unburnt timber which may be only a few millimetres from the surface. Failure of the beam or strut will occur only when the cross-sectional area of the unburnt core becomes too small to support the load. By increasing the dimensions of the timber above those required for structural consideration, it is possible to guarantee structural integrity in a fire for a given period of time. This is a much more desirable situation than that presented by steel, where total collapse of the beam or strut occurs at some critical temperature.

47.4.1 Methods of assessing performance

At the present time in the UK (1999), four standard tests are applicable to the evaluation of the performance of timber in fire, though this situation will change in the first few years of the new millennium with the introduction of the new European test methods to assess *reaction to fire*. These four tests assess *non-combustibility*, *ignitability*, *fire propagation* and *spread of flame*.

In three out of these four standard fire tests currently carried out, timber and board products do not fair at all well. None of the four tests demonstrates the predictability of the performance of timber in fire, nor do they indicate the guaranteed structural integrity of the material for a calculable period of time. The performance of timber in the widest sense is certainly superior to that indicated by the present set of standard tests.

Early in the first decade of the new millennium, National standards on reaction to fire will be replaced by new European standards which generally measure different aspects of the behaviour of building materials and products in fire than do the current British Standards. All construction products will be classified into one of six Euroclasses (A–F) according to their reaction-to-fire performance in fire tests. Two of these tests will be used to classify the least combustible materials (Euroclasses A_1 and A_2); these two new tests are a furnace test for *non-combustibility* (prEN ISO 1182) and an *oxygen bomb calorimeter test* (prEN ISO 1716).

At the lower end of the range of Euroclasses (classes E and F), construction products of appreciable combustibility will be assessed using a simple *ignitability test* (prEN ISO 11925–2). Products that fall into Classes A_2, B_1 C and D (and D will probably contain timber and wood-based panels) will be tested using the *single burning item test* (SBI) except where the products are used as floor coverings when the *critical flux (radiant panel) test* (prEN ISO 9239–1) will be used to determine performance in Euro classes B–E. For both floor and non-floor applications, generally only two of the above tests will be required to characterise performance of any one product. More information on the methods of assessing reaction to fire is given in Dinwoodie (2000).

The above reaction-to-fire tests relate to the product. When that product is incorporated into a building element, the *fire resistance* of that element will be determined by a whole series of other tests; most of these are still at the drafting stage, but it is anticipated that there will be at least sixty European standards (or part-standards) relating to fire resistance of parts of a building.

47.5 References

47.5.1 Standards and specifications

prEN ISO 1182. Reaction to fire tests for building products – Non-combustibility test.

prEN ISO 1716. Reaction to fire tests for building products – Determination of the gross caloric value.

prEN ISO 9239–1. Reaction to fire tests for floor coverings – Part 1: determination of the burning behaviour using a radiant heat source.

prENISO 11925–2. Reaction to fire tests for building products – Part 2: ignitability when subjected to direct impingement of flame.

prENISO 13823: 2000 Reaction to fire tests for building products – Building products excluding floorings – exposed to thermal attack by a single burning item test (SBI).

47.5.2 Literature

Derbyshire, H. and Miller, E.R. (1981) The photodegradation of wood during solar radiation. *Holz als Roh-und Werkstoff* 39, 341–50.

Derbyshire, H., Miller, E.R., Sell, J. and Turkulin, H. (1995) Assessment of wood photodegradation by microtensile testing. *Drvna Ind*. 46, 3, 123–32.

Desch, H.E. and Dinwoodie, J.M. (1996). *Timber-Structure, Properties, Conversion and Use*, 7th edn, Macmillan, Basingstoke, 306 pp.

Dinwoodie, J.M. (2000) *Timber: its Nature and Behaviour*, 2nd edn, E & FN Spon, London, 257 pp.

Hall, G.S. and Jackman, P.E. (1975) Performance of timber in fire. *Timber Trades J*. 15 Nov. 1975, 38–40.

Moore, G.L. (1984). The effect of long-term temperature cycling on the strength of wood. *J. Inst. Wood Sci*. 9, 6, 264–7.

Shafizadeh, F. and Chin, P.P.S. (1977) Thermal degradation of wood. In *Wood Technology: Chemical Aspects* (ed. I.S. Goldstein), ACS Symposium Series 4, American Chemical Society, Washington D.C., pp. 57–81.

Le Van, S.L. and Winandy, J.E. (1990) Effects of fire retardant treatments on wood strength: a review. *Wood and Fiber Sci*. 22, 1, 113–31.

Chapter forty-eight

Processing of timber

48.1 Introduction

After felling, the tree has to be processed in order to render the timber suitable for man's use. Such processing may be basically mechanical or chemical in nature or even a combination of both. On the one hand timber may be sawn or chipped, while on the other it can be treated with chemicals which markedly affect its structure and its properties. In some of these processing operations the timber has to be dried and this technique has already been discussed in Section 44.7.4 and will not be referred to again in this chapter.

The many diverse mechanical and chemical processes for timber have been described in great detail in previous publications and it is certainly not the intention to repeat such description here: readers desirous of such information are referred to the excellent and authoritative texts listed under Further Reading. In looking at processing in this chapter, the emphasis is placed on the properties of the timber as they influence or restrict the type of processing. For convenience, the processes are subdivided below into mechanical and chemical, but frequently their boundaries overlap.

48.2 Mechanical processing

48.2.1 Solid timber

Sawing and planing

The basic requirement of these processes is quite simply to produce as efficiently as possible timber of the required dimensions, having a quality of surface commensurate with the intended use. Such a requirement depends not only on the basic properties of the timber, but also on the design and condition of the cutting tool; many of the variables are inter-related and it is frequently necessary to compromise in the selection of processing variables.

In Section 44.5 the density of timber was shown to vary by a factor of ten from about 120 to 1200 kg/m^3. As density increases, so the time taken for the cutting edge to become blunt decreases: whereas it is possible to cut over 10 000 feet of Scots pine before it is necessary to resharpen, only one or two thousand feet of a dense hardwood such as jarrah can be cut. Density will also have a marked effect on the amount of power consumed in processing. When all the other factors affecting power consumption are held constant, this variable is highly correlated with timber density, as illustrated in Figure 48.1.

Timber of high moisture content never machines as well as that at lower moisture levels. There is a tendency for the thin-walled cells to be deformed rather than cut because of their

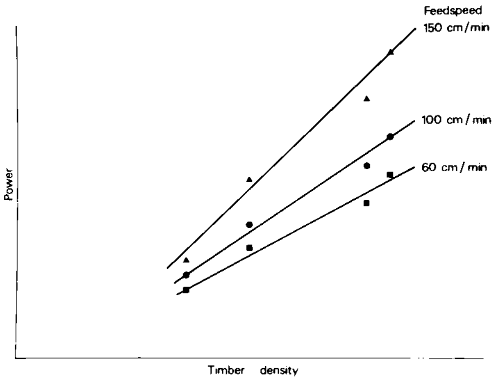

FIGURE 48.1 Effect of timber density and feedspeed on the consumption of power using a circular saw to cut along the grain *(rip-sawing)* (© Building Research Establishment).

increased elasticity in the wet condition. After the cutters have passed over, these deformed areas slowly assume their previous shape, resulting in an irregular appearance to the surface which is very noticeable when the timber is dried and painted; this induced defect is known as *raised grain.*

The cost of timber processing is determined primarily by the cost of tool maintenance, which in turn is related not only to properties of the timber, but also to the type and design of the saw or planer blade. In addition to the effect of timber density on tool life, the presence in certain timbers of gums and resins has an adverse effect because of the tendency for the gum to adhere to the tool, thereby causing overheating; in saw blades this in turn leads to loss in tension resulting in saw instability and a reduction in sawing accuracy.

A certain number of tropical hardwood timbers contain mineral inclusions which develop during the growth of the tree. The most common is *silica* which is present usually in the form of small grains within the ray cells. The abrasive action of these inclusions is considerable and the life of the edge of the cutting tool is frequently reduced to almost one-hundredth of that obtained when cutting timber of the same density, but free of silica. Timbers containing silica are frequently avoided unless they possess special features which more than offset the difficulties which result from its presence.

Moisture content of the timber also plays a significant role in determining the life of cutting tools. As moisture content decreases, so there is a marked reduction in the time interval between resharpening both saw and planer blades. The fibrous nature of tension wood (Section 44.4) will also increase tool wear.

Service life will also depend on the type and design of the tool. Although considerably more expensive than steel, the use of tungsten-carbide-tipped saws and planer blades extends the life of the cutting edge especially where timbers are either dense or abrasive. Increasing the number of teeth on the saw or the number of planer blades on the rotating stock will increase the quality of the surface, provided that the feedspeed is sufficient to provide a minimum bite per revolution; this ensures a cutting rather than a rubbing action which would accelerate blunting of the tool edge.

One of the most important tool design variables is the angle between the edge and the timber surface. As discussed in Section 44.2, timber is seldom straight-grained, tending in most cases to be in the form of a spiral of low pitch; occasionally, the grain is interlocked or wavy. Under these circumstances, there is a strong tendency for those cells which are inclined towards the direction of the rotating cutter to be pulled out rather than cut cleanly, a phenomenon known as *pick-up* or *tearing.* The occurrence of this defect can be removed almost completely by reducing the cutting angle (rake angle) of the rotating blades, though this will result in increased power consumption.

The cost of processing, though determined primarily by tool life, will be influenced also by the amount of power consumed. In addition to the effect of density of the timber previously discussed, the amount of energy required will depend on the feedspeed (Figure 48.1), tool design and, above all, on tool sharpness.

Steam bending

Steam bending of certain timbers is a long-established process which was used extensively when it was fashionable to have furniture with rounded lines. The backs of chairs and wooden hat stands are two common examples from the past, but the process is still employed at the present time, albeit on a much reduced volume. The handles for certain garden implements, walking sticks and a few sports goods are all produced by steam bending.

The mechanics of bending involves a presteaming operation to soften the lignin, swell the timber, and render the timber less stiff. With the ends restrained, the timber is usually bent round a former, and after bending the timber must be held in the restrained mode until it dries out and the bend is *set*. In broad terms the deformation is irreversible, but over a long period of time, especially with marked alternations in humidity of the atmosphere, a certain degree of recovery will arise, especially where the curve is unrestrained by some fixing. Although most timbers can be bent slightly, only certain species, principally the hardwood timbers of the temperate region, can be bent to sharp radii without cracking. When the timber is bent over a supporting, but removable strap, the limiting radius of curvature is reduced appreciably. Thus, it is possible to bend 25 mm thick ash to a radius of 64 mm and walnut to a radius of only 25 mm.

48.2.2 Board materials

The area of board materials is recognised as being the fastest growing area within the timber industry over the last two decades. Not only does this represent a greater volume of construction (particularly in the domestic area) and of consumer goods (e.g. furniture), but it also reflects a large degree of substitution of board materials for solid timber.

Production of wood-based panels in Europe in 1997 (the last year for which complete data are available) was $40.1 \times 10^6\,m^3$, of which 72.5 per cent was particleboard, 14 per cent MDF, 7.5 per cent plywood, 4.5 per cent fibreboard and 1.5 per cent OSB. Consumption would be in excess of production by about $6 \times 10^6\,m^3$ (estimate), most of which can be attributed to large imports of plywood.

In the UK, the consumption of board material in 1997 (provisional data) was $5.8 \times 10^6\,m^3$ of which 54 per cent was chipboard and OSB combined, 31 per cent was plywood, 11 per cent was MDF, 4 per cent was other fibreboards, and 0.3 per cent was CBPB. About 70 per cent of the UK consumption of chipboard and OSB combined was home produced.

As a material, timber has a number of deficiencies:

- it possesses a high degree of variability;
- it is strongly anisotropic in both strength and moisture movement;
- it is dimensionally unstable in the presence of changing humidity;
- it is available in only limited widths.

Such material deficiencies can be lowered appreciably by reducing the timber to small units and subsequently reconstituting it, usually in the form of large, flat sheets, though moulded items are also produced, e.g. trays, bowls, coffins, chair backs. The degree to which these boards assume a higher dimensional stability and a lower level of anisotropy than is the case with solid timber is dependent on the size and orientation of the component pieces of timber and the method by which they are bonded together. There are an infinite variety of board types though there are only four principal ones – plywood, chipboard (particleboard), OSB and fibreboard.

In comparison with timber, board materials possess a lower degree of variability, lower anisotropy, and higher dimensional stability: they are also available in very large sizes. The reduction in variability is due quite simply to the random repositioning of variable components, the degree of reduction increasing as the size of the components decrease. The individual board materials are discussed below in separate sections.

Plywood

Over one million cubic metres of plywood are consumed annually in the UK. Most of this is made from softwood and is imported from the United States, Canada and Finland. Less than 1 per cent of plywood is home produced.

Plywoods made from temperate hardwoods are imported mainly from Germany (beech) and Finland (birch – or birch/spruce combination) while plywoods from tropical hardwoods come predominately from South East Asia (mainly Indonesia and Malaysia) and to a lesser, but increasing, extent from South America and Africa.

Logs, the denser of which are softened by boiling in water, may be sliced into thin veneer for surface decoration by repeated horizontal or vertical cuts, or, for plywood, peeled by rotation against a slowly advancing knife to give a continuous strip. After drying, sheets of veneer for plywood manufacture are coated with adhesive and are laid up and then pressed with the grain direction at right angles in alternate layers. Plywood frequently contains an unequal number of plies so that the system is balanced around the central veneer; some plywoods, however, contain an even number of plies, but with the two central plies having the same orientation thereby ensuring that the plywood is balanced on each side of the central glue line.

As the number of plies increase, so the degree of anisotropy in both strength and movement drops quickly from the value of 40:1 for timber in the solid state. With three-ply construction and using veneers of equal thickness, the degree of anisotropy is reduced to 5:1, while for nine-ply this drops to 1.5:1. However, cost increases markedly with number of plies and for most applications a three-ply construction is regarded as a good compromise between isotropy and cost.

The common multilayered plywood is technically known as a *veneer plywood* in contrast to the range of *core plywoods* where the surface veneers overlay a core of blocks or strips of woods.

Plywood (veneer type) for use in construction in Europe must comply with the requirements of the new European specifications, the most important requirement of these being that of bond performance.

The mechanical and physical properties of the plywood, therefore, will depend not only on the type of adhesive used, but also on the species of timber selected. Both softwoods and hardwoods within a density range of 400–700 kg/m^3 are normally utilised. Plywood for internal use is produced from the non-durable species and urea–formaldehyde adhesive (UF), while plywood for external use is generally manufactured using phenol–formaldehyde (PF) resins; however, with the exception of marine grade plywood in the UK, durable timbers, or permeable non-durable timbers which have been preservative treated, are seldom used.

It is not possible to talk about strength properties of plywood in general terms since not only are there different strength properties in different grain directions, but that these are also affected by configuration of the plywood in terms of number, thickness, orientation and quality of the veneers and by the type of adhesive used. The factors which affect the strength of plywood are the same as those set out in Chapter 3 for the strength of timber, though the effects are not necessarily the same. Thus the intrinsic factors, such as knots and density, play a less significant part than they do in the case of timber, but the effect of the extrinsic variables such as moisture content, temperature and time is very similar to that for timber.

Plywood is the oldest of the timber sheet materials and for very many years has enjoyed a high reputation as a structural sheet material. Its use in the Mosquito aircraft and gliders in the 1940s, and its subsequent performance for small boat construction, for sheathing in timber-frame housing, and in the construction of web and hollow-box beams all bear testament to its suitability as a structural material.

When materials are compared in terms of their specific stiffness (stiffness per unit mass), plywood is stiffer than many other materials, including mild steel sheet; generally, plywood also has high specific strength. Another important property of plywood is its resistance to splitting, which permits nailing and screwing relatively close to the edges of the boards; this is a reflection of the removal of a line of cleavage along the grain which is a drawback of solid timber. Impact resistance (toughness) of plywood is very high and tests have shown that to initiate failure a force greater than the tensile strength of the timber species is required.

Plywoods tend to fall into three distinct groups. The first comprises those which are capable of being used structurally. Large quantities of softwood structural plywood are imported into the UK from North America, supplemented by smaller volumes from Sweden and Finland; the latter country also produces a birch/spruce structural plywood.

The use of this group of structural plywoods is now controlled in that they must first comply with the new European specification and second, the characteristic values for use in design must have been derived from semi-sized test pieces according to the new European test methods.

The second group of plywoods comprises those which are used for decorative purposes, while the third group comprises those for general-purpose use. The latter are usually of very varied performance in terms of both bond quality and strength and are frequently used indoors for infill panels and certain types of furniture.

Chipboard (particleboard)

In the UK the boards made from wood chips and resin are known as chipboards; however in most other countries the product is referred to as particleboard. The chipboard industry dates from the mid-1940s and originated with the purpose of utilising waste timber. After a long, slow start, when the quality of the board left much to be desired, the industry has grown tremendously over the last two decades, far exceeding the supplies of waste timber available and now relying to a very large measure on the use of small trees for its raw material. Such a marked expansion is due in no small part to the much tighter control in processing and the ability to produce boards with a known and reproducible performance, frequently tailor-made for a specific end use. Over 60 per cent of UK consumption is home-produced.

In the manufacture of chipboard the timber, which is principally softwood, is cut by a series of rotating knives to produce thin chips which are dried and then sprayed with adhesive. Usually the chips are blown onto flat platens in such a way that the smaller chips end up on the surfaces of the board and the coarse chips in the centre. The mat is usually first cut to length before passing into a single or multi-daylight press where it is held for 0.10–0.20 min per mm of board thickness at temperatures up to 200°C. The density of boards produced range from 450 to 750 kg/m^3, depending on end-use classification, while the resin content varies from about 9–11 per cent on the outer layers to 5–7 per cent in the centre layer, averaging out for the board at about 7–8 per cent on a dry mass basis. Over the last decade many of the new chipboard plants have installed large continuous presses; as the name implies, the mat is fed in at one end to reappear at the other distant end as a fully-cured board. This type of press has the advantage of being quick to respond to production changes in board thickness, adhesive type or board density.

Instead of using the very long continuous press, chipboard can also be made continuously using either the Mendé or an extrusion process. The former is applicable only in the manufacture of thin chipboard, i.e. 6 mm or less, and the process is analogous to that of paper manufacture in that the board is sufficiently flexible to pass between and over large heated rollers. In the extrusion process, the chipboard mat is forced out through a heated die, but this results in the orientation of the chips at right angles to the plane of the board which reduces both the strength and stiffness of the material; it is used primarily as a core in the manufacture of doors and composite panels.

The performance of chipboard, like that of plywood, is very dependent on the type of adhesive used. Much of the chipboard (particleboard) produced in Europe is made using urea–formaldehyde (UF) which, because of its sensitivity to moisture, renders this type of chipboard unsuitable for use where there is a risk of the material becoming wet, or even being subjected to marked alternations in relative humidity over a long period of time. More expensive boards possessing some resistance to the presence of moisture are manufactured using either melamine-fortified urea–formaldehyde (MUF), or phenol–formaldehyde (PF), or isocyanate (IS) adhesives: however, a true external-grade board has not yet been produced commercially.

Chipboard, like timber, is a viscoelastic material and an example of the deformation over an extended period of time has already been presented (Figure 45.10). However, the rate of creep in particleboard is considerably higher than that in timber though it is possible to reduce it by increasing the amount of adhesive or by modifying the chemical composition of the adhesive.

Within the new framework of European specifications, six grades of particleboard are specified, of which four are rated as load bearing (i.e. they can be used in structural design) and two are non-load bearing. The characteristic values for the load-bearing grades for use in structural design are given in EN 12369–1.

Particleboards are also produced from a wide variety of plant material and synthetic resin of which flaxboard and bagasse board are the best known examples.

Wet-process fibreboard

Although much smaller quantities of fibreboard are used in the UK than either chipboard or plywood, it is nevertheless a most important panel product, used extensively in the UK for insulation and the linings of doors and backs of furniture, and in Scandinavia as a cladding and roofing material.

The process of manufacture is quite different from that of the other board materials in that the timber is first reduced to chips which are then steamed under very high pressure in order to soften the lignin which is thermoplastic in behaviour. The softened chips then pass to a defibrator which separates them into individual fibres, or fibre bundles, without inducing too much damage.

The fibrous mass is usually mixed with hot water and formed into a mat on a wire mesh; the mat is then cut into lengths and, like particleboard, pressed in a multi-platen hot press at a temperature of from 180°C to 210°C; the board produced is smooth on only one side, the underside bearing the imprint of the wire mesh. By modifying the pressure applied in the final pressing, boards of a wide range of density are produced ranging from *softboard* with a density less than 400 kg/m^3, to *mediumboard* with a density range of 400–900 kg/m^3, to *hardboard* with a density exceeding 900 kg/m^3. Fibreboard, like the other board products, is moisture sensitive, but in the case of hardboard, a certain degree of resistance can be obtained by the passage of the material through a hot oil bath thereby imparting a high degree of water repellency: this material is referred to as *tempered* hardboard.

MDF (dry process fibreboard)

There has been a phenomenal increase in the production of MDF world-wide over the last two decades. In the period from 1986 to 1997 European production rose from $0.58 \times 10^6 \, m^3$ to $5.5 \times 10^6 \, m^3$. Consumption of MDF in the UK in 1997 was $0.6 \times 10^6 \, m^3$ of which $0.4 \times 10^6 \, m^3$ was home produced.

MDF is a dry process fibreboard. The fibre bundles are first dried to a low moisture content prior to being sprayed with an adhesive and formed into a mat which is hot-pressed to produce a board with two smooth faces similar to the production of particleboard; both multi-daylight and continuous presses are employed.

Various adhesive systems are employed; where the board will be used in dry conditions, a urea–formaldehyde (UF) resin is employed, while a board with improved resistance to moisture for use in humid conditions is usually manufactured using a melamine-fortified urea–formaldehyde resin (MUF), though phenol–formaldehyde (PF) or isocyanate (IS) resins are sometimes used.

The European specification for MDF includes both load-bearing and non-load-bearing grades for both dry and humid end uses. Characteristic values for structural use of the former are given in EN 12369–1; however, it should be noted that the use of the load-bearing panel under humid conditions is restricted to short periods of loading.

A very large part of MDF production is taken up in the manufacture of furniture where non-load-bearing grades for dry use are appropriate.

OSB (oriented strand board)

Like MDF, OSB manufacture is fairly new and is certainly a growth area with over 50 mills worldwide with a capacity in 1997 in excess of $16 \times 10^6\,m^3$; European capacity in 1997 was about $1 \times 10^6\,m^3$; UK production from one mill in the same year was about $240\,000\,m^3$.

Strands up to 75 mm in length with a maximum width of half its length are generally sprayed with an adhesive at a rate corresponding to about 2–3 per cent of the dry mass of the strands. It is possible to work with much lower resin concentrations than with chipboard manufacture due to the removal of dust and 'fines' from the OSB line prior to resin application: in a few mills powdered resins are used, though most manufacturers use a liquid resin. In the majority of mills a phenol–formaldehyde (PF) resin is used, but in one or two mills, a melamine-fortified urea–formaldehyde (MUF) or isocyanate (IS) resin is employed.

In the formation of the mat the strands are aligned either in each of three layers, or only in the outer two layers of the board. The extent of orientation varies among manufacturers, with property level ratios in the machine to cross direction of 1.25/1 to 2.5/1, thereby emulating plywood. Indeed, the success of OSB has been as a cheaper replacement for plywood, but it must be appreciated that its strength and stiffness are considerably lower than those of high quality structural grade plywood, though only marginally lower than those of many of the current structural softwood plywoods. It is widely used for suspended flooring, sheathing in timber-frame construction and flat roof decking.

The European specification for OSB sets out the requirements for four grades, three of which are load bearing, covering both dry and humid applications. Characteristic values for structural use of the load-bearing grades are given in EN 12369–1.

CBPB (cement bonded particleboard)

This is very much a special end-use product manufactured in relatively small quantities. It comprises by mass 70–75 per cent of Portland cement and 25–30 per cent of wood chips similar to those used in particleboard manufacture. The board is heavy with a density of about $1200\,kg/m^3$, but it is very durable (due to its high pH of 11), is more dimensionally stable under changing relative humidity (due to the high cement content), has very good performance in reaction to fire tests (again because of the high cement content) and has poor sound transmission (due to the high density). The board is therefore used in high hazard situations with respect to moisture, fire or sound.

Comparative performance of the wood-based boards

With such a diverse range of board types, each manufactured in several grades, it is exceedingly difficult to select examples in order to make some form of comparative assessment.

In general terms, the strength properties of good quality structural softwood plywood are not only considerably higher than all the other board materials, but they are usually similar to or slightly higher than that of softwood timber. Next to a good quality structural plywood in strength are the hardboards, followed by MDF and OSB. Chipboard (particleboard) is of lower strength, but still stronger than the medium boards and CBPB. Table 48.1 provides the 5th percentile strength values included in the EN product specifications, with the exception of plywood where actual test data for Douglas fir plywood have been used. In passing, it is interesting to note the reduction in anisotropy in bending strength from 4.5 for 3-ply construction to 1.8 for 7-ply layup. Other structural softwood plywoods can have strength values lower than those for Douglas fir, being similar to or only slightly above those of OSB of high quality. Actual strength values of individual manufacturer's products of non-plywood panels may be higher than these minimum specification values. It should be realised that these specification values are only for the purpose of quality control and must never be used in design calculations.

Comparison of the behaviour of these products to the effect of 24 hours' cold water soaking is also included in Table 48.1. CBPB is far superior to all other boards. Even higher swell values than those recorded in the table are to be found in 15 mm OSB/1 (general purpose board) of 25 per cent and in 3.2 mm HB.LA hardboard (loadbearing, dry) of 35 per cent. For those boards listed in the specifications for use under humid conditions that are included in Table 48.1, the table provides information on their moisture resistance in terms of their retention of internal bond strength following either the cyclic exposure test (EN 321), the boil test (EN 1087–1) or both.

48.2.3 Laminated timber

The process of cutting timber up into strips and gluing them together again has three main attractions. Defects in the original piece of timber such as knots, splits, reaction wood, or sloping grain are redistributed randomly throughout the composite member, making it more uniform in quality in comparison to the original piece of timber where the defects often result in stress raisers when load is applied. Consequently, the strength and stiffness of the laminated product will usually be higher than that of the timber from which it was made. The second attraction is the ability to create curved beams or complex shapes, while the third is the ability to use shorter lengths of timber which can be end-jointed.

Glulam, the popular term for laminated timber, has been around for many years and is to be found in the form of large curved beams in public buildings and sports halls. In manufacture, strips of timber about 20–30 mm in depth are coated with adhesive on their faces and laid up parallel to one another in a jig, the whole assembly being clamped until the adhesive has set. Generally, cold setting adhesives are used because of the size of these beams; for dry end use a urea–formaldehyde (UF) resin is employed, while for humid conditions a resorcinol–formaldehyde (RF) resin is employed. The individual laminae are end jointed using either a scarf (sloping) or finger (interlocked) joint. Structural characteristic values for glulam are determined by the strength class of the timber(s) from which it is made, factored for the number and type(s) of laminates used.

48.2.4 Mechanical pulping

The pulping industry is the single largest consumer of wood. In the UK the consumption of paper and board in 1997 was 12.2×10^6 tonnes, of which approximately half was home produced from home-grown softwood and hardwood, softwood residues, recycled fibre and imported woodpulp.

Pulp may be produced by either mechanical or chemical processes and it is the intention to postpone discussion on the latter until later in this chapter. In the original process for producing mechanical pulp, logs with a high moisture content are fed against a grinding wheel which is continuously sprayed with water in order to keep it cool and free it of the fibrous mass produced. The pulp so formed, known as stone groundwood, is coarse in texture, comprising bundles of cells rather than individual cells, and is mainly used as newsprint. To avoid the necessity to adopt a costly bleaching process, only light-coloured timbers are accepted. Furthermore, because the power consumed on grinding is a linear function of the timber density, only the low-density timbers with no or only small quantities of resin are used.

Much of the mechanical pulp now used is produced by disc-refining. Wood chips, softened in hot water, by steaming, or by chemical pretreatment, are fed into the centre of two high-speed, counter-rotating, ridged, metal plates; on passing

TABLE 48.1 Five percentile strength and stiffness and 95 percentile swell values for timber and board materials: quality control values in the EN product specifications

			EN 310				*EN 319*	*EN 317*	*Moisture resistance*	
	Thickness (mm)	*Density (kg/m^3)*	*Bending strength (N/mm^2)*		*E (N/mm^2)*		*Internal bond (N/mm^2)*	*24 hr swelling thickness (%)*	*Internal bond (N/mm^2) after*	
			Parallel	*Perpendicular*	*Parallel*	*Perpendicular*			*Cyclic EN 321*	*Boil EN 1087–1*
Solid timber – Douglas fir										
Small clear test pieces	20	590	80°	2.2°	16400°	1100°	–	–	–	–
Structural timber	100	580	22	–	8110	–	–	–	–	–
Plywood (EN 636–3)										
Douglas fir (three-ply)	4.8	520*	51*	11*	8462*	624*	–	–	–	–
Douglas fir (seven-ply)	19	600*	42*	23*	7524*	2496*	–	–	–	–
OSB/3 (EN 300)	18	670*	20	10	3500	1400	0.32	15	0.15	0.13
OSB/4	18	670*	28	15	4800	1900	0.45	12	0.17	0.15
Particleboard (EN 312)										
Type P4 (Load-bearing dry)	15	720*	15		2150		0.35	15	–	–
Type P7 (Heavy load-bearing humid)	15	740*	20		3100		0.70	8	0.36	0.23
CBPB (EN 634)	18	1000	9		4000		0.50	1.5	0.3	–
Fibreboard (EN 622)										
Part 2 hardboard (load-bearing humid) HB.HLA1	3.2	900*	38		3800		0.80	15	–	0.5
Part 3 mediumboard (load-bearing dry) MBH.LA1	10	500*	18		1800		0.10	15	–	–
Part 5 MDF (load-bearing humid) MDF.HLS	12	790*	32		2800		0.80	10	0.25	0.15

* Not in the specifications.

° Mean values.

from the centre of the plates to the periphery, the chips are reduced to fine bundles of cells or even individual cells. This process is capable of accepting a wider range of timbers than the traditional stone groundwood method.

48.3 Chemical processing

48.3.1 Treatability

The ease with which a timber can be impregnated with liquids, especially wood preservatives, is generally referred to as its *treatability*. Treatability is related directly to the permeability of timber which was discussed in some detail in Section 44.8 where the pathways of flow were described; it will be recalled that permeability was shown to be a function not only of moisture content and temperature, but also of grain direction, sapwood/heartwood, earlywood/latewood and species.

Longitudinal permeability is usually about $10^4 \times$ transverse permeability owing principally to the orientation of the cells in the longitudinal direction. Heartwood, owing to the deposition of both gums and encrusting materials, is generally much less permeable than the sapwood, while earlywood of the sapwood in the dry condition has a much lower permeability than the same tissue in the green state due to aspiration of the bordered pits in the dry state.

Perhaps the greatest variability in ease of impregnation occurs between species. Within the softwoods this can be related to the number and distribution of the bordered pits and to the efficiency of the *residual* flow paths which utilise both the latewood bordered pits and the semi-bordercd ray pits. Within the hardwoods variability in impregnation is related to the size and distribution of the vessels and to the degree of dissolution of the end walls of the vessel members.

Four arbitrary classes of treatability are recognised, different timbers being assigned to these according to the depth and pattern of penetration when treated with wood preservatives (see EN 350–2). These classes are *permeable*, *moderately resistant*, *resistant* and *extremely resistant*. This classification is equally applicable to impregnation by flame retardants, or dimensional stabilisers for, although differences in viscosity will influence degree of penetration, the treatability of the timber species will remain in the same relative order.

Artificial preservatives

Except where the heartwood of a naturally durable timber is being used, timber should always be treated with a wood preservative if there is any significant risk that its moisture content will rise above 20 per cent during its service life. At and above this moisture content, wood-destroying fungi can attack. The relationship between service environment and risk of attack by wood-destroying organisms is defined in EN 335–1 using the hazard classification of biological attack. Clearly, those timbers of greater permeability will take up preservatives more easily and are to be preferred over those that are more resistant. It is normally not necessary to protect internal woodwork which should remain dry. However, where the risk of water spillage, leakage from pipes or from the roof is seen as likely or significant, application of wood preservatives may be deemed a sensible precaution.

A variety of methods for the application of wood preservatives are available. Short-term dipping and surface treatments by brush or spray are the least effective ways of applying a preservative because of the small loading and poor penetration achieved. In these treatments only the surface layers are penetrated and there is a risk of splits occurring during service which will expose untreated timber to the risk of attack by wood-destroying organisms. Such treatments are usually confined to do-it-yourself treatments, or treatments carried out during remediation or maintenance of existing woodwork.

The most effective methods of timber impregnation are industrial methods in which changes in applied pressure ensure controlled, more uniform penetration and retention of preservative. The magnitude of the pressure difference depends on the type of preservative being used. Essentially, the timber to be treated is sealed in a pressure vessel and a vacuum drawn. While under vacuum, the vessel is filled with the preservative and then returned to atmospheric pressure during which some preservative enters the wood. At this point, an over-pressure of between zero and 13 bar is applied, depending mainly on the preservative being used, but also on the treatability of the timber. This can be held for between several minutes and many hours after which the vessel is drained of preservative. A final vacuum is often applied to recover some of the preservative and to ensure the treated timber is free of excess fluid. Details of the choice, use and application of wood preservatives can be found in BS 1282.

There are three main types of preservative in general use. The first group are the tar oils of which coal tar creosote is the most important. Its efficacy as a preservative lies not only in its natural toxicity, but also in its water repellency properties. It has a very distinctive and heavy odour and treated timber cannot be painted unless first coated with a metallic primer.

The second group are the water-borne preservatives which are suitable for both indoor and outdoor uses. The most common formulations are those containing copper, chromium and arsenic compounds, but combinations of copper/chromium and copper/chromium/boron are also used. All of these preservatives are usually applied by a vacuum high-pressure treatment; the chemicals react once in the wood and become *fixed*, i.e. they are not leached out in service.

Inorganic boron compounds are also used as water-borne preservatives, but they do not become fixed within the wood and therefore can be leached from the wood during service. Their use is therefore confined to environments where leaching cannot take place.

The third group are the solvent-type preservatives, which tend to be more expensive than those of the first two groups, but they have the advantage that machined timber can be treated without the grain being raised, as would be the case with aqueous solutions. The formulations of the solvent type are based on a variety of compounds including pentachlorophenol, tri-n-butyltin oxide, and copper and zinc naphthanates. More recently, copper and zinc versatate, zinc ocoate, and the preparations known as acypetacs zinc and acypetacs copper have been introduced. Some organic solvent preservatives include insecticides and water repellents. BS 5707 lists the standardised formulations. These preservatives find uses in the DIY and industrial sectors. Industrial treatment processes include double vacuum and immersion techniques, while DIY and on-site treatment includes dipping and brushing.

In looking at the application of these three different types of preservatives, creosote and CCA (copper-chrome-arsenic) are able to protect timber in high hazard situations, i.e. ground contact, while organic solvent preservatives are used in timber out of ground contact and preferably protected with a paint film.

Although it is not an impregnation process as defined above, it is convenient to examine here the diffusion process of preservation. The timber must be in the green state and the preservative must be water soluble. Timber is immersed for a short period in a concentrated (sometimes hot) solution of a boron compound, usually disodium octoborate tetrahydrate, and then close-stacked undercover for several weeks to allow the preservative to diffuse into the timber.

Gaseous diffusion has been examined as a method of preservative treating wood-based panels as well as timber. Treatment by trimethyl borate vapour in a sealed, evacuated chamber of material at a low moisture content results in the reaction of the gaseous trimethyl borane with the water in the wood to produce the biocide boric acid which is then deposited where the reaction occurs (Turner and Murphy, 1998).

For many years there was some difference of opinion as to whether these preservatives merely lined the walls of the cell cavity or actually entered the cell wall. However, it has been well demonstrated by electron microanalysis that whereas creosote only coats the cell walls, the water-borne preservatives do impregnate the cell wall. Although there is some evidence to show that PCP (pentachlorophenol) can penetrate the cell wall, it is doubtful whether solvent-type preservatives *in general* penetrate the wall due to their large molecular size and by being carried in a non-polar solvent.

There is considerable variation in preservative distribution in treated dry timber; in the softwoods, only the latewood tends to be treated due to aspiration of the earlywood bordered pits as described in Section 44.8.1. In the hardwoods, treatment is usually restricted to the vessels and tissue in close proximity to the vessels, again as described in Section 44.8.1.

In those timbers which can be impregnated, it is likely that the durability of the sapwood after pressure impregnation will be greater than the natural durability of the heartwood, and it is not unknown to find the heartwood of telegraph and transmission poles to be decayed while the treated sapwood is perfectly sound.

Mention has been made already of the difficulty of painting timber which has been treated with creosote. This disadvantage is not common to the other preservatives and not only is it possible to paint the treated timber, but it is also possible to glue together treated components.

Flame retardants

Flame-retardant chemicals may be applied as surface coatings or by vacuum-pressure impregnation, thereby rendering the timber less easily ignitable and reducing the rate of flame spread. Intumescent coatings will be discussed later and this section is devoted to the application of fire retardants by impregnation.

The salts most commonly employed in the UK for the vacuum pressure impregnation process are monoammonium phosphate, diammonium phosphate, ammonium sulphate, boric acid and borax. These chemicals vary considerably in solubility, hygroscopicity and effectiveness against fire. Most proprietary flame retardants are mixtures of such chemicals formulated to give the best performance at reasonable cost. Since these chemicals are applied in an aqueous solution, it means that a combined water-borne preservative and fire-retardant solution can be used which has distinct economic considerations. Quite frequently, corrosion inhibitors are incorporated where the timber is to be joined by metal connectors. Treatment of the timber involves high pressure/vacuum processes; as aqueous solutions are involved, redrying of the timber is required.

Considerable caution has to be exercised in determining the level of heating to be used in drying the timber following impregnation. The ammonium phosphates and sulphate tend to break down on heating, giving off ammonia and leaving an acidic residue which can result in degradation of the wood substance. Thus, it has been found that drying at 65°C following impregnation by solutions of these salts results in a loss of bending strength of from 10 per cent to 30 per cent. Drying at 90°C, which is adopted in certain kiln schedules, results in a loss of 50 per cent of the strength and even higher losses are recorded for the impact resistance or toughness of the timber. It is essential, therefore, to dry the timber at as low a temperature as possible and also to ensure that the timber in service is never subjected to elevated temperatures which would initiate or continue the process of acidic degradation. Most certainly, timber which has to withstand suddenly applied loads should not be treated with this type of fire retardant, and care must also be exercised in the selection of glues for construction. The best overall performance from timber treated with these flame retardants is obtained when the component is installed and maintained under cool and dry conditions.

Conscious of the limitations of flame retardants based on ammonium salts, a number of companies have developed effective retardants of very different chemical composition; these have much reduced degradation of the timber, or do not degrade the timber, and are usually non-corrosive to metal fixings. However, they are considerably more expensive than those based on ammonium salts.

Dimensional stabilisers

In Section 45.2, timber, because of its hygroscopic nature, was shown to change in dimensions as its moisture content varied in order to come into equilibrium with the vapour pressure of the atmosphere. Because of the composite nature of timber, such movement will differ in extent in the three principal axes.

Movement is the result of water adsorption or desorption by the hydroxyl groups present in all the matrix constituents. Thus it should be possible to reduce movement (i.e. increase the dimensional stability) by eliminating or at least reducing the accessibility of these groups to water. This can be achieved by either chemical changes or by the introduction of physical bulking agents.

Dimensional stability is imparted to wood by swelling of the substrate due to chemical modification, since the bonded groups occupy volume within the cell wall. At high levels of modification, wood is swollen to near its green volume, and anti-shrink efficiencies close to 100 per cent are achieved. After extended reaction, swelling in excess of the green volume can occur, which is accompanied by cell wall splitting.

Various attempts have been made to substitute the hydroxyl groups chemically by less polar groups and the most successful has been by acetylation (Rowell, 1984). In this process acetic anhydride is used as a source of acetyl groups. A very marked improvement in dimensional stability is achieved with only a marginal loss in strength. Using carboxylic acid anhydrides of varying chain length, Hill and Jones (1996) obtained good dimensional stabilisation which they attributed solely to the bulking effect. Other reagents with potential for chemical modification include isocyanates and epoxides. Readers desirous of more information on chemical modification are referred to the review by Rowell (1984) and text edited by Hon (1996).

Good stabilisation can also be achieved by reacting the wood with formaldehyde which then forms methylene bridges between adjacent hydroxyl groups. However, the acid catalyst necessary for the process causes acidic degradation of the timber.

In contrast to the above means of chemical modification, a variety of chemicals have been used to physically stabilise the cell wall; these impregnants act as bulking agents and hold the timber in a swollen condition even after water is removed, thus minimising dimensional movement.

Starting in the mid-1940s and continuing on a modest scale to the present time, some solid timber, but more usually wood veneers, are impregnated with solutions of phenol–formaldehyde. The veneers are stacked, heated and compressed to form a high-density material with good dimensional stability which still finds wide usage as a heavy-duty insulant in the electrical distribution industry.

Considerable success has also been achieved using polyethylene–glycol (PEG), a wax-like solid which is soluble in water. Under controlled conditions, it is possible to replace all the water in timber with PEG by a diffusion process, thereby maintaining it in a swollen condition. The technique has found application, among other things, in the preservation of waterlogged objects of archaeological interest, the best example of which is the Swedish wooden warship *Wasa,* which was raised from the depths of Stockholm harbour in 1961 having foundered in 1628. From 1961 the timber was sprayed continuously for over a decade with an aqueous solution of PEG which diffused into the wet timber gradually replacing the bound water in the cell wall without causing any dimensional changes.

PEG may also be applied to dry timber by standard vacuum impregnation using solution strengths of from 5 to 30 per cent. Frequently, preservative and/or fire-retardant chemicals are also incorporated in the impregnating solution. It will be noted from Figure 48.2 that following impregnation, the amount of swelling has been reduced to one-third that of the untreated timber.

Developments in the production and use of water-repellent preservatives based on resins dissolved in low-viscosity organic solvents have resulted in the ability to confer on timber a low, but nonetheless important level of dimensional stability. Their application is of considerable proven practical significance in the protection of joinery out-of-doors and these are discussed further in Section 48.4.

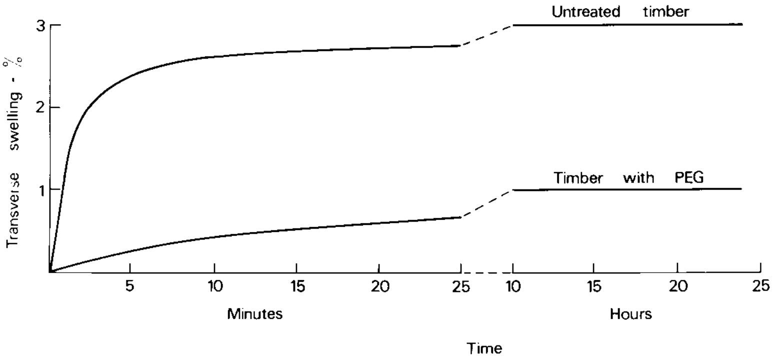

FIGURE 48.2 The comparative rates of swelling in water of untreated pine timber and timber impregnated with a 50 per cent (by mass) solution of PEG (polyethylene–glycol): this is equivalent to 22 per cent loading on a dry wood basis (adapted from R.E. Morén (1964) by permission).

48.3.2 Chemical pulping

The magnitude of the pulping industry has already been discussed, as has the production of mechanical pulp. Where paper of a higher quality than newsprint or corrugated paper is required, a pulp must be produced consisting of individual cells rather than fibre bundles. To obtain this type of pulp the middle lamella has to be removed and this can be achieved only by chemical means.

There are a number of chemical processes which are described in detail in the literature. All are concerned with the removal of lignin, which is the principal constituent of the middle lamella. However, during the pulping process lignin will also be removed from within the cell wall as well as from between the cells: this is both acceptable and desirous since lignin imparts a greyish colouration to the pulp which is unacceptable for the production of white paper.

However, it is not possible to remove all the lignin without also dissolving most of the hemicelluloses which not only add to the mass of pulp produced, but also impart a measure of adhesion between the fibres. Thus, a compromise has to be reached in determining how far to progress with the chemical reaction and the decision is dependent on the requirements of the end product. Frequently, though not always, the initial pulping process is terminated when a quarter to a half of the lignin still remains and this is then removed in a subsequent chemical operation known as bleaching, which, though expensive, has relatively little effect on the hemicelluloses. The yield of chemical pulp will vary considerably depending on the conditions employed, but it will usually be within the range of 40–50 per cent of the dry mass of the original timber.

The yield of pulp can be increased to 55–80 per cent by semi-chemical pulping. Only part of the lignin is removed in an initial chemical treatment which is designed to soften the wood chips: subsequent mechanical treatment separates the fibres without undue damage. These high-yield pulps usually find their way into card and board-liner which are extensively used for packaging where ultimate whiteness is not a prerequisite.

48.3.3 Other chemical processes

Brief mention must be made of the *destructive distillation* of timber, a process which is carried out either for the production of charcoal alone or for the additional recovery of the volatile by-products such as methanol, acetic acid, acetone and wood-tar. The timber is heated initially to 250°C, after which the process is exothermic: distillation must be carried out either in the complete absence of air, or with controlled, small amounts of air.

Timber can be softened in the presence of ammonia vapour as a result of plasticisation of the lignin. The timber can then be bent or moulded using this process, but, because of the harmful effects of the vapour, the process has never been adopted commercially.

48.4 Finishes

Finishes have a combined decorative and protective function. Indoors they are employed primarily for aesthetic reasons, though their role in resisting soiling and abrasion is also important; outdoors, however, their protective function is vital. In Section 47.2.1, the natural weathering process of timber was described in terms of the attack of the cell wall constituents by ultraviolet light and the subsequent removal of breakdown products by rain; the application of finishes is to slow down this weathering process to an acceptable level, the degree of success varying considerably among the wide range of finishes commercially available.

In Sections 44.1–44.3 the complex chemical and morphological structure of timber was described, while in Section 44.7 the hygroscopic nature of this fibre composite and its significance in determining the movement of timber was discussed. The combined effects of structure and moisture movement have a most profound effect on the performance of coatings. For example, in the softwoods the presence of distinct bands of early and latewood with their differential degree of permeability results not only in a difference in sheen or reflectance of the coating between these zones, but also in marked differences in adhesion; in Douglas fir, where the latewood is most conspicuous, flaking of paint from the latewood is a common occurrence. In addition, the radial movement of the latewood has been shown to be as high as six times that of the earlywood and consequently the ingress of water to the surface layers results in differential movement and considerable stressing of the coatings. In those hardwoods characterised by the presence of large vessels, the coating tends to sag across the vessel and it is therefore essential to apply a paste filler to the surface prior to painting; even with this, the life of a paint film on a timber such as oak (see Figure 44.6) is very short. For this reason, the use of exterior wood stains is common, as this type of finish tends not to exhibit the same degree of flaking. The presence of extractives in certain timbers (see Section 44.3.1 and Table 44.2) results in the inhibition in drying of most finishes; with iroko and Rhodesian teak, many types of finish may never dry.

Contrary to general belief, deep penetration of the timber is not necessary for good adhesion, but it is absolutely essential that the weathered cells on the surface are removed prior to repainting. Good adhesion appears to be achieved by molecular attraction rather than by mechanical keying into the cell structure.

Although aesthetically most pleasing, fully exposed varnish, irrespective of chemical composition, has a life of only a very few years, principally because of the tendency of most types to become brittle on exposure, thereby cracking and disintegrating because of the stresses imposed by the movement of the timber under changes in moisture content. Ultraviolet light can readily pass through the majority of varnish films, degrading the timber at the interface and causing adhesion failure of the coating.

A second type of natural finish which overcomes some of the drawbacks of clear varnish is the *water-repellent preservative stain* or *exterior wood stain*. There are many types available, but all consist of resin solutions of low viscosity and low solids content: these solutions are readily absorbed into the surface layers of the timber. Their protective action is due in part to the effectiveness of water-repellent resins in preventing water ingress, and in part from the presence of finely dispersed pigments which protect against photochemical attack. The higher the concentration of pigments the greater the protection, but this is achieved at the expense of loss in transparency of the finish. Easy to apply and maintain these thin films, however, offer little resistance to the transmission of water vapour into and out of the timber. Compared with a paint or varnish, the water-repellent finish will allow timber to wet up and dry out at a much faster rate, thereby eliminating problems of water accumulation which can occur behind impermeable paint systems; the presence of a preservative constituent reduces the possibility of fungal development during periods of high moisture uptake. The films do require, however, more frequent maintenance, but nevertheless have become well established for the treatment of cladding and hardwood joinery.

By far the most widely-used finish, especially for external softwood joinery, is the traditional opaque alkyd gloss or flat paint system embracing appropriate undercoats and primers; a three- or four-coat system is usually recommended. Multiple coats of oil-based paint are effective barriers to the movement of liquid and vapour water; however, breaks in the continuity of the film after relatively short exposure constitute a ready means of entry of moisture after which the surrounding, intact film will act as a barrier to moisture escape, thereby increasing the likelihood of fungal attack. The effectiveness of the paint system is determined to a considerable extent by the quality of the primer. Quite frequently window and door joinery with only a priming coat is left exposed on building sites for long periods of time. Most primers are permeable to water, are low in elasticity and rapidly disintegrate owing to stresses set up in the wet timber; it is therefore essential that only a high quality of primer is used. Emulsion-based primer/undercoats applied in two consecutive coats are more flexible and potentially more durable than the traditional resin-based primers and undercoats.

A new range of exterior quality paints has been produced in the last decade; these are either solvent-borne or water-borne formulations. Some of the formulations have a higher level of moisture permeability than conventional paint systems and have been described as *microporous*. These are claimed to resist the passage of liquid water, but to allow the passage of water vapour, thereby allowing the timber to dry out; however, there appears to be no conclusive proof for such claims.

The solvent-borne exterior paints come in many forms; for example, as a three-layer system based on flexible alkyd resins which produce a gloss finish, or a one-can system which is applied in two coats which produces a low-sheen finish.

The water-borne exterior paints are based on acrylic or alkyd-acrylic emulsions applied in either two- or three-coat systems. The water-borne system has a higher level of permeability compared with the solvent-borne system. Even more important is the high level of film extensibility of the water-borne system which is retained in ageing (Miller and Boxall, 1994), and which contributes to its better performance on-site than the solvent-borne exterior paints.

Test work has indicated that the pretreatment of surfaces to be coated with a water-repellent preservative solution has a most beneficial effect in extending the life of the complete system, first by increasing the stability of the wood surface thereby reducing the stresses set up on exposure, and second by increasing adhesion between the timber surface and the coating. This concept of an integrated system of protection employing preservation and coating, though new for timber, has long been established in certain other materials; thus, it is common practice prior to the coating of metal to degrease the surface to improve adhesion.

One specialised group of finishes for timber and timber products is that of the flame-retardant coatings. These coatings, designed only to reduce the spread of flame, must be applied fairly thickly and must neither be damaged in subsequent installation and usage of the material, nor their effect negated by the application of unsuitable coverings. Nearly all the flame retardants on the UK market intumesce on heating and the resulting foam forms a protective layer of resistant char.

48.5 References

48.5.1 Standards and specifications

BS 1282 (1975) Guide to the choice, use and application of wood preservatives. BSI, London.

BS 5707. Specification for solutions of wood preservatives in organic solvents.

Part 1: (1979) Specification for solutions for general purpose applications, including timber that is to be painted. BSI, London.

Part 2: 1976 (1986) Specification for pentachlorophenol wood preservative solution for use on timber that is not required to be painted. BSI, London.

EN 335–1 (1992) Hazard classes of wood and wood-based products against biological attack – Part 1: Classification of hazard classes.

EN 350–2 (1994) Durability of wood and wood-based products – Natural durability of solid wood – Part 2: Guide to natural durability and treatability of selected wood species of importance in Europe.

EN 12369–1 (2001) Wood-based panels – Characteristic values for use in structural design. Part 1: Particle boards, OSB and fibreboards.

48.5.2 Literature

Hill, C.A.S. and Jones, D. (1996) The dimensional stabilisation of Corsican pine sapwood by reaction with carboxylic acid anhydrides. *Holzforschung* 50, 5, 457–62.

Hon, D.N.S. (ed.) (1996) *Chemical Modification of Lignocellulosic Materials*, Marcel Dekker Inc., New York.

Miller, E.R. and Boxall, J. (1994) Water-borne coatings for exterior wood. *Building Research Establishment Information Paper* IP 4/94.

Morén, R.E. (1964) Some practical applications of polyethylene glycol for the stabilisation and preservation of wood. Paper presented to the British Wood Preserving Association annual convention.

Rowell, R.M. (1984) Chemical modification of wood. *For. Prod. Abstracts* 6, 75–8.

Turner, P. and Murphy, R.J. (1998) Treatments of timber products with gaseous borate esters. Part 2: Process improvement. *Wood Sci. Technol.* 32, 25–31.

Further reading

Barrett, J.D., Foschi, R.O., Vokey, H.P. and Varoglu, E. (eds) (1986) *Proc. International Workshop on Duration of Load in Lumber and Wood Products*. Held at Richmond, B.C., Canada, 1985, spec. pub no. SP–27, Forintek Canada Corp., 115 pp.

Barrett, J.D. and Foschi, R.O. (eds) (1979) *Proceedings of the First International Conference on Wood Fracture,* Banff, Alberta, 1978, Forintek Canada Corp., 304 pp.

Bonfield, P.W., Dinwoodie, J.M. and Mundy, J.S. (eds) (1995) *Workshop on Mechanical Properties of Panel Products*. Proc. of workshop held at Watford, 1995, and published by the management committee of EC COST Action 508, 317 pp.

Bodig, J. and Jayne, B.A. (1982) *Mechanics of Wood and Wood Composites*, Van Nostrand Reinhold, New York, 712 pp.

Bravery, A.F., Berry, R.W., Carey, J.K. and Cooper, D.E. (1987) *Recognising Wood Rot and Insect Damage in Buildings*, Building Research Establishment Report, BRE, Watford, England, 120 pp.

Desch, H.E. and Dinwoodie, J.M. (1996) *Timber – Structure, Properties, Conversion and Use*, 7th edn, Macmillan, Basingstoke, England, 306 pp.

Dinwoodie, J.M. (2000) *Timber – Its Nature and Behaviour*, E & FN Spon, London, 256 pp.

Gordon, J.E. (1976) *The New Science of Strong Materials*, 2nd edn, Penguin, 269 pp.

Hearmon, R.F.S. (1961) *An Introduction to Applied Anisotropic Elasticity*, Oxford University Press, 136 pp.

Hillis, W.E. (1987) *Heartwood and Tree Exudates*, Springer-Verlag, Berlin, 268 pp.

Hoffmeyer, P. (ed.) (1997) *International Conference on Wood–Water Relations*. Proc. of conference held in Copenhagen in 1997, published by the management committee of EC COST Action E8, 469 pp.

Jane, F.W. (1970) *The Structure of Wood*, 2nd edn, Adam & Charles Black, London, 478 pp.

Kollmann, F.F.P. and Côté, W.A. (1968) *Principles of Wood Science and Technology, I, Solid Wood*, Springer-Verlag, Berlin, 592 pp.

Kollmann, F.F.P., Kuenzi, E.W. and Stamm, A.J. (1975) *Principles of Wood Science and Technology. II, Wood-Based Materials*, Springer-Verlag, Berlin, 703 pp.

Morlier, P. (ed.) (1994) *Creep in Timber Structures*, RILEM report 8, E & FN Spon, London, 149 pp.

Morlier, P., Valentin, G. and Seoane, I. (eds) (1992) *Workshop on Fracture Mechanics in Wooden Materials*. Proc. of workshop held at Bordeaux, France, April 1992, and published by the management committee of EC COST Action 508, 203 pp.

Pizzi, A. (1983) *Wood Adhesives; Chemistry and Technology*, Marcel Dekker, New York, 364 pp.

Preston, R.D. (1974) *The Physical Biology of Plant Cell Walls*, Chapman and Hall, London, 491 pp.

Siau, J.F. (1988) *Transport Processes in Wood*, Springer-Verlag, Berlin, 245 pp.

Skaar, C. (1988) *Wood–Water Relations*, Springer-Verlag, Berlin, 283 pp.

Wise, L.E. and Jahn, E.C. (1952) *Wood Chemistry*, 2nd edn, Rheinhold Publishing Corp., New York, 688 pp.

Index

Index

Index

Index

Index